BEHIND THE SMOKE AND MIRRORS: REFLECTIONS ON IMPROVING CANNABIS PRODUCTION AND INVESTIGATING MEDICAL POTENTIAL

EDITED BY: David Meiri, Donald Lawrence Smith, Derek Stewart, Carolyn J. Baglole and Rachel G. M. Backer

PUBLISHED IN: Frontiers in Plant Science

frontiers Research Topics

ISSN 1664-8714
ISBN 978-2-83250-258-7
DOI 10.3389/978-2-83250-258-7

About Frontiers

Frontiers is more than just an open-access publisher of scholarly articles: it is a pioneering approach to the world of academia, radically improving the way scholarly research is managed. The grand vision of Frontiers is a world where all people have an equal opportunity to seek, share and generate knowledge. Frontiers provides immediate and permanent online open access to all its publications, but this alone is not enough to realize our grand goals.

Frontiers Journal Series

The Frontiers Journal Series is a multi-tier and interdisciplinary set of open-access, online journals, promising a paradigm shift from the current review, selection and dissemination processes in academic publishing. All Frontiers journals are driven by researchers for researchers; therefore, they constitute a service to the scholarly community. At the same time, the Frontiers Journal Series operates on a revolutionary invention, the tiered publishing system, initially addressing specific communities of scholars, and gradually climbing up to broader public understanding, thus serving the interests of the lay society, too.

Dedication to Quality

Each Frontiers article is a landmark of the highest quality, thanks to genuinely collaborative interactions between authors and review editors, who include some of the world's best academicians. Research must be certified by peers before entering a stream of knowledge that may eventually reach the public - and shape society; therefore, Frontiers only applies the most rigorous and unbiased reviews.
Frontiers revolutionizes research publishing by freely delivering the most outstanding research, evaluated with no bias from both the academic and social point of view. By applying the most advanced information technologies, Frontiers is catapulting scholarly publishing into a new generation.

What are Frontiers Research Topics?

Frontiers Research Topics are very popular trademarks of the Frontiers Journals Series: they are collections of at least ten articles, all centered on a particular subject. With their unique mix of varied contributions from Original Research to Review Articles, Frontiers Research Topics unify the most influential researchers, the latest key findings and historical advances in a hot research area! Find out more on how to host your own Frontiers Research Topic or contribute to one as an author by contacting the Frontiers Editorial Office: frontiersin.org/about/contact

BEHIND THE SMOKE AND MIRRORS: REFLECTIONS ON IMPROVING CANNABIS PRODUCTION AND INVESTIGATING MEDICAL POTENTIAL

Topic Editors:
David Meiri, Technion Israel Institute of Technology, Israel
Donald Lawrence Smith, McGill University, Canada
Derek Stewart, The James Hutton Institute, United Kingdom
Carolyn J. Baglole, McGill University, Canada
Rachel G. M. Backer, McGill University, Canada

Citation: Meiri, D., Smith, D. L., Stewart, D., Baglole, C. J., Backer, R. G. M., eds. (2022). Behind the Smoke and Mirrors: Reflections on Improving Cannabis Production and Investigating Medical Potential. Lausanne: Frontiers Media SA. doi: 10.3389/978-2-83250-258-7

Table of Contents

frontiers in Plant Science

REVIEW
published: 03 March 2021
doi: 10.3389/fpls.2021.627240

Medical Cannabis and Industrial Hemp Tissue Culture: Present Status and Future Potential

*Dinesh Adhikary[1], Manoj Kulkarni[2], Aliaa El-Mezawy[3], Saied Mobini[2], Mohamed Elhiti[4], Rale Gjuric[4], Anamika Ray[2], Patricia Polowick[5], Jan J. Slaski[3], Maxwell P. Jones[6] and Pankaj Bhowmik[5]**

[1] Department of Agricultural, Food, & Nutritional Sciences, University of Alberta, Edmonton, AB, Canada, [2] Canadian Cannabis Breeding Consortium, Edmonton, AB, Canada, [3] InnoTech Alberta, Vegreville, AB, Canada, [4] Farmers Business Network Inc., Winnipeg, MB, Canada, [5] National Research Council, Saskatoon, SK, Canada, [6] Department of Plant Agriculture, University of Guelph, Guelph, ON, Canada

In recent years high-THC (psychoactive) and low-THC (industrial hemp) type cannabis (*Cannabis sativa* L.) have gained immense attention in medical, food, and a plethora of other consumer product markets. Among the planting materials used for cultivation, tissue culture clones provide various advantages such as economies of scale, production of disease-free and true-to-type plants for reducing the risk of GMP-EuGMP level medical cannabis production, as well as the development and application of various technologies for genetic improvement. Various tissue culture methods have the potential application with cannabis for research, breeding, and novel trait development, as well as commercial mass propagation. Although tissue culture techniques for plant regeneration and micropropagation have been reported for different cannabis genotypes and explant sources, there are significant variations in the response of cultures and the morphogenic pathway. Methods for many high-yielding elite strains are still rudimentary, and protocols are not established. With a recent focus on sequencing and genomics in cannabis, genetic transformation systems are applied to medical cannabis and hemp for functional gene annotation via traditional and transient transformation methods to create novel phenotypes by gene expression modulation and to validate gene function. This review presents the current status of research focusing on different aspects of tissue culture, including micropropagation, transformation, and the regeneration of medicinal cannabis and industrial hemp transformants. Potential future tissue culture research strategies helping elite cannabis breeding and propagation are also presented.

Keywords: ***Cannabis sativa*, micropropagation, tissue culture, hemp, *in vitro***

OPEN ACCESS

Edited by:
Derek Stewart, The James Hutton Institute, United Kingdom

Reviewed by:
Daniel A. Jacobo-Velázquez, Monterrey Institute of Technology and Higher Education (ITESM), Mexico
Catello Di Martino, University of Molise, Italy

****Correspondence:***
Pankaj Bhowmik
Pankaj.Bhowmik@nrc-cnrc.gc.ca

Specialty section:
This article was submitted to Crop and Product Physiology, a section of the journal Frontiers in Plant Science

Received: *16 November 2020*
Accepted: *04 February 2021*
Published: *03 March 2021*

Citation:
Adhikary D, Kulkarni M, El-Mezawy A, Mobini S, Elhiti M, Gjuric R, Ray A, Polowick P, Slaski JJ, Jones MP and Bhowmik P (2021) Medical Cannabis and Industrial Hemp Tissue Culture: Present Status and Future Potential. Front. Plant Sci. 12:627240. doi: 10.3389/fpls.2021.627240

INTRODUCTION

Cannabis is a multipurpose crop with nutritional, medicinal, and industrial uses. Its leaves and flowers produce a spectrum of biologically active secondary metabolites, seeds are a source of nutritious oil and protein, and the stem contains two types of fiber serving as feedstock for the manufacturing of a variety of bio-based consumer goods (Small, 2004; Rodriguez-Leyva and Pierce, 2010; Wargent et al., 2013; Andre et al., 2016; Musio et al., 2018). The crop may have originated

and been domesticated over 5000 years ago in Asia; since then, it has been interwoven with human history. In the South Asian regions, cannabis biotypes with elevated THC levels were commonly used for medicinal and recreational purposes, building a strong connection to social and religious rituals. While in the temperate climates, low-THC types were grown initially for fiber, and later also for food (Cheng, 1963; Li, 1974; Mechoulam, 1986; Cherney and Small, 2016; Clarke and Merlin, 2016; Jiang et al., 2016). Since the discovery of two cannabinoids [cannabidiol (CBD) in 1963) and tetrahydrocannabinol (THC) in 1964] in Dr. Raphael Mechoulam's laboratory, more than 100 additional phytocannabinoids, flavonoids, and over 150 terpenes have been identified in the plant (Andre et al., 2016; Booth and Bohlmann, 2019; Rea et al., 2019). This high-value crop has built a strong foundation for a multi-billion-dollar global industry. Due to legal restrictions, research and development work has been slow and prevented researchers from investigating cannabis openly and making use of its full potential.

Recent cannabis legalization amendments in Canada, Europe, some parts of the United States, and other parts of the globe have helped promote research and use of this multipurpose crop. Commercial production increased in anticipation and response to the federal legalization of cannabis in Canada in October 2018 under the Cannabis Act (Government of Canada, 2018). Canada became the second nation after Uruguay (legalized December 2013) to legalize cannabis for recreational use at the federal level (Adinoff and Reiman, 2019). In the United States, 12 states have legalized cannabis for recreational use, with another 22 legalizing medical use (Adinoff and Reiman, 2019).

Inherently, cannabis is a dioecious species, with male and female flowers found on separate plants. Monoecious forms, which produce male and female flowers on the same plant, are very seldomly found in nature (Clarke and Merlin, 2016). Commercial monoecious cultivars of hemp have been bred for oilseed production and improved fiber yield and uniformity that cannot be achieved in dioecious forms exhibiting asynchronous maturation of the stems, as male plants commence an accelerated aging process soon after pollen shed. Due to the dioecious nature of most high THC-type cannabis and the lack of advanced breeding to produce true-to-type seed, they are propagated vegetatively and often grown indoors. Vegetative propagation maintains genetic purity and uniformity among the plants. Traditionally, indoor cannabis cultivators have depended on cuttings from a mother plant to produce genetically similar plants. While cannabis generally roots well (Caplan et al., 2018) and stem cuttings can produce large numbers of genetically similar plants, this method requires significant amounts of space. It has been observed that plants become less vigorous over time, the mother plants are susceptible to pests and diseases, and the resulting cuttings can harbor unwanted disease and serve as primary inoculum in production spaces.

As an alternative, *in vitro* techniques offer a promising approach for mass production and germplasm maintenance (Withers and Engelmann, 1997; Watt et al., 2000). Micropropagation can facilitate high throughput propagation in many species and forms the basis of disease-free plants for certified clean plant programs (Lineberger, 1983; Al-Taleb et al., 2011). Tissue culture based clean plant programs have been used in other vegetatively propagated crops such as potatoes, sweet potato, dates, sugarcane, banana, rice, tobacco, strawberry, grapes, orchids, roses, fruit trees, and some more horticulture of food and ornamental crops, helping to eradicate or prevent the spread of many plant pests, diseases, and viruses (National Clean Plant Network, 2020). Thus, developing an optimized *in vitro* method for propagating clean plants is a crucial strategy to produce large-scale genetically identical plants, retain genetic integrity, and maintain the long-term sustainability of the economically valuable crop (Conway, 2012). This review article aims to provide a comprehensive overview of the most updated available scientific research reported to date on tissue culture in cannabis, to contribute to our understanding of the cannabis tissue culture, and to assess potential applications of the optimized techniques in cannabis plant propagation, regeneration, and transformation.

INDUSTRIAL HEMP VS. MEDICAL CANNABIS (MARIJUANA)

According to Small et al. (1976), there are four groups of cannabis, 'non-intoxicant (some *C. sativa* accessions),' 'semi-intoxicant' (some *C. sativa* accessions), 'intoxicant (*C. indica*),' and 'wild' (*C. ruderalis*). *Cannabis* includes *C. indica, C. ruderalis,* and *C. sativa*. However, it has also been proposed that these three groups all belong to a single species (*C. sativa*) and the taxonomic classification among these proposed species remains a debated issue in *Cannabis* taxonomy (McPartland, 2018). For morphological and chemical characters (i.e., floral morphology and THC content), the earlier report considered them as different subspecies (Small and Cronquist, 1976), while another classified them as different species (Hillig, 2005).

Further complicating matters is the legal distinction between hemp and drug (narcotic) type cannabis. Any plant containing less than a defined concentration of the psychoactive THC is classified as hemp. In contrast, anything above the critical limit is classified as drug type cannabis. Depending upon the jurisdiction, the threshold THC concatenations in flowering plant parts differentiating between industrial hemp and drug type cannabis range from 0.2% of dry weight in most European counties, which is 0.3% in Canada, United States, and China and Brazil to 1% in Switzerland, Uruguay, Columbia, Mexico, and several Australian states. While this distinction is not based on taxonomy or genetic relationships, several studies have shown that most hemp cultivars are genetically distinct from drug-type cannabis (Rotherham and Harbison, 2011; Cascini et al., 2019). Mainly due to legal restrictions, artificial selection influenced by a decade's long black market, and insufficient knowledge of the *Cannabis* taxonomy, these sub-types are poorly defined, especially the drug type cannabis.

Hemp is generally cultivated from seed and has named cultivars similar to most other crops. In contrast, drug type cannabis is generally propagated clonally; the clones are often referred to as 'strains' but are also often referred to as cultivars. As such, any given strain/cultivar can produce various clonal

accessions with dramatically different phenotypes, making names unreliable. Further, many strains are offered by different seed companies, and the degree of genetic similarity or difference among providers has not been quantified; therefore, it is generally expected and accepted that there is significant variation within a single strain among seed companies and even within seed lots. Due to these factors, strain names in drug type cannabis are not reliable regarding a uniform phenotype.

Cannabis indica and *Cannabis sativa* are the major sources of cannabinoids, and are predominantly cultivated, while the third species, *C. ruderalis* is a wild and hardy species and is rarely grown by cultivators as there is no significant content of cannabinoids (Hilling and Mahlberg, 2004). In many lay literatures, distinction of 'indica' and 'sativa' have been mentioned and some of the earlier publications have also gathered some phenotypic differences (**Table 1** and **Figure 1**); however, there is neither solid taxonomic agreement nor genetic or chemical evidence supporting the differences (Gloss, 2015; Sawler et al., 2015; Piomelli and Russo, 2016). The use of 'indica' and 'sativa' is vaguely based on the general notion that 'sativa' originated from European hemp, while 'indica' originated from the Indian subcontinent (Small, 2015), but their exact origin is still debatable.

TRADITIONAL CLONING IN CANNABIS

For decades, seed propagation in cannabis has supported agricultural needs and facilitated genetic improvement. However, with modern horticultural practices to the cannabis industry, stem cutting or traditional cloning, and *in vitro* propagation of this high-value crop has become a common practice (Lata et al., 2009a,b, 2011; Potter, 2009). Other methods of propagation are encapsulation of axillary nodes in calcium alginate beads (Lata et al., 2009a), leaf derived callus (Lata et al., 2010c), and temporary immersion bioreactor systems (Lata et al., 2010b) but these are limited in lab experiments only. Traditional cloning involves taking stem cuttings from a healthy mother plant and providing a rooting environment for the newly cut clone (**Figure 2**). For selection as a donor, a clear indication of alternating branches with no visible sign of insects, fungus, or any mineral deficiency in a mother plant is required. Cuttings can be taken from any part of a donor; despite some suggestions that growth in the lower half is better, no difference was observed between cuttings taken from the upper and lower part of the plant (Caplan et al., 2018). However, further research is warranted to test this across more genotypes and conditions. In general, cannabis propagates readily from stem cuttings even without rooting hormones.

Stem cuttings have advantages over seed propagation, including quicker maturation, true-to-type plants, and elite genetics maintenance (**Table 2**). Along with the ease of propagation, the practice can limit unwanted gene flow (McKey et al., 2010), for example, between the hemp and drug-type, potentially retaining the proportions of active metabolites.

On the downside, space for large scale production is a concern as it can take considerable physical space, representing as much as 20–25% of production space just for cloning. Also, since it is currently manually performed, there is a low multiplication rate, and it is expensive in the long run. Therefore, this technique is more suitable for small growers requiring less than 1000 plants per growth cycle. For this reason, an adaptable, scalable, and robust high throughput tissue culture system with a high multiplication rate which preserves cannabis genetics, and produces more vigorous plants than manual clones, can prove to be more cost-effective in the long run (**Table 2**). Even small- scale growers with a small budget to use this technique to preserve genetics and test their desired strains' regenerative capacity as a proof-of-concept. Building a team of experts to develop and execute tissue culture protocols successfully can be expensive and time-intensive initially; however, in the long term, it is a promising tool that has benefited many industries, including horticulture and cereal crops (Brown and Thorpe, 1995; Hussain et al., 2012).

Stem cuttings or traditional cloning method is the widely used propagation system adopted by many growers. *In vitro* propagation is establishing in cannabis industry slowly and is expected to take over the traditional cloning method. Although stem cuttings and *in vitro* clones can be comparable in terms of vegetative growth and physiological performance (Lata et al., 2009a), *in vitro* clones provide many advantages such as faster multiplication rate, clean clones without disease or virus, cost effective etc. (**Table 1**). Considering these advantages *in vitro* propagation is expected to become method of choice for propagation as well as genetic preservation in cannabis in the near future.

CURRENT UTILIZATION AND OPPORTUNITIES FOR CANNABIS TISSUE CULTURE

The legal hemp for CBD production and the medical cannabis industry is a fast- growing market, and cultivators are turning toward advanced scientific approaches such as *in vitro* micropropagation, to reduce the production costs and offer scalable, healthy, and high-quality cannabis variety. In addition to a critical need for cost-effective propagation to meet demand, there is also a desire to establish and properly characterize cultivars equivalent to those of traditional agriculture with specific, consistent THC and cannabinoid content to match particular drug and therapeutic requirements. Legalization has opened up the options for accessing more mainstream research applications. This increases the demand for the application of some additional cell technologies applications to this crop.

In vitro Micropropagation

Although a few hemp cultivars have regenerated *in vitro* (**Figure 3**), *Cannabis* spp. have gained a wide reputation for being recalcitrant to tissue culture. At the beginning of the 1970s, along with the conventional propagation system, *in vitro* cultures of cannabis were initiated. The majority of the earlier *in vitro* studies were focused on cannabis callus culture to produce cannabinoids (Veliky and Genest, 1972; Itokawa et al.,

TABLE 1 | Phenotypic differences among *C. indica, C. sativa*, and *C. ruderalis* ecotypes.

Trait	*C. indica*	*C. sativa*	*C. ruderalis*
Climate	Tropical intense sunlight, cool arid regions (Afghanistan, Pakistan, Northern India, Nepal)	Subtropical humid climate, more rainfall, In Mexico, Colombia, Nigeria, Thailand	Northern climates, cool and hilly places, grows in wild (Russia, China)
Height	Short 1– 2 m	Tall up to 3–4 m	Very short bushy 0.6–1.0 m
Cannabis female flower	Compact and short inflorescence	Loose packed and long inflorescence	Small, compact, very short inflorescence
Habit	Shorter internode	Longer internode	Very short internodes
Leaves	Broad	Narrow	Smaller leaves
Leaf color	Dark green	Light green	Dark leaves
Stalk	Shorter woody	Taller, fibrous	Short fibrous
Maturity	Early maturity 2–3 months	Late maturity 4–6 months	Very early maturity 1.5–2 months, autoflowering
Root system	Condensed root system	Deep, expansive	Shallow smaller
Cannabinoid content	Lower THC, could be higher CBD	High THC, Lower CBD in general	Low THC and CBD
Effect	Relaxing effect, inflammation reduction (Medical use preferred)	Incite euphoria, head high (stress relief, recreational use preferred)	Not grown commercially, only for breeding earliness

Information derived from Schultes et al. (1974); Small and Cronquist (1976), Hillig (2004); Clarke and Merlin (2013), Farag and Kayser (2017), and Small (2017).

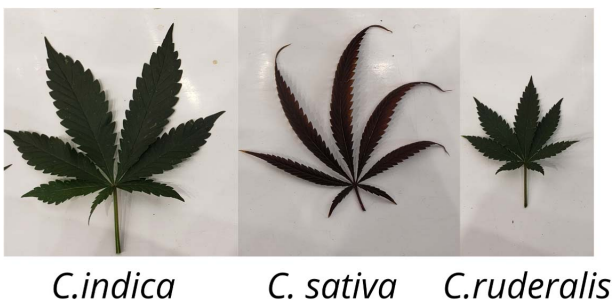

FIGURE 1 | Cannabis leaf showing morphological differences of the three different species (*C. indica, C. sativa*, and *C. ruderalis*).

1975, 1977; Hemphill et al., 1978; Hartsel et al., 1983; Loh et al., 1983; Fisse and Andres, 1985). Although there are multiple reports on shoot proliferation via micropropagation (**Table 3**), there are fewer scientific reports showing regeneration of a full plant through *de novo* regeneration (Mandolino and Ranalli, 1999; Slusarkiewicz-Jarzina et al., 2005; Wielgus et al., 2008; Chaohua et al., 2016).

The majority of regenerated strains and cultivars were monoecious, with few dioecious lines (**Table 3**). Recently, the optimization of a micropropagation and callogenesis protocol was reported for a few medical cannabis genotypes (Page et al., 2020). Although 48 years passed (**Figure 4**) since the first report of *in vitro* cell culture in cannabis, the available protocols are limited and inconsistent. *In vitro* regeneration of a cannabis plant from a single cell is still a challenge. Thus, the multi-billion-dollar cannabis industry needs an optimized tissue regeneration protocol for both industrial and medical cannabis.

It is generally understood that the most experienced cannabis companies have developed tissue culture and micropropagation techniques over the last two decades. However, most achievements in this *in vitro* field are held as a trade secret because of the competitive advantage provided within the industry. The most crucial challenges for the cannabis success micropropagation have been how to (i) reduce the length of subculture to minimize the occupied time and space, (ii) induce better root systems to increase the survival rate to >95%, (iii) optimize Plant Growth Regulators (PGRs), light (intensity and quality) and temperature required to maintain the genetically stable true-to-type clones. A generalized micropropagation workflow would require 7–8 weeks of culture transfer, 3 weeks of shoot multiplication, and 4 weeks of rooting. In terms of PGRs application, the best recommendation is optimized cytokinin and auxin for the vegetative medium and no cytokinin for the rooting medium using full MS media.

In recent years Canadian Licensed producers who are research-oriented have overcome some of these challenges. For example, the acclimatization period has been significantly reduced to less than 3 weeks. Another micropropagation challenge that the cannabis industry has recently solved is optimizing light intensity, light quality, and photoperiod in the culture room and maintaining the most effective temperature during shoot growth and root formation. Some unpublished data shows an increased propagation rate, from 3.5 to 5.8, during sub-culturing from each plantlet, through understanding and obtaining the right abiotic conditions within the culture room. As a starting point, some successful protocols are implemented with the minimum risk of somaclonal variation in cannabis (Movahedi et al., 2015; Lata et al., 2016, 2017; Grulichova et al., 2017; Page et al., 2020). These are game-changing procedures toward commercialization for cannabis micropropagation at a large-scale operation facility.

Genetic Transformation

An ability to identify, characterize, and apply the genetic variability using biotechnology is the basis of molecular breeding.

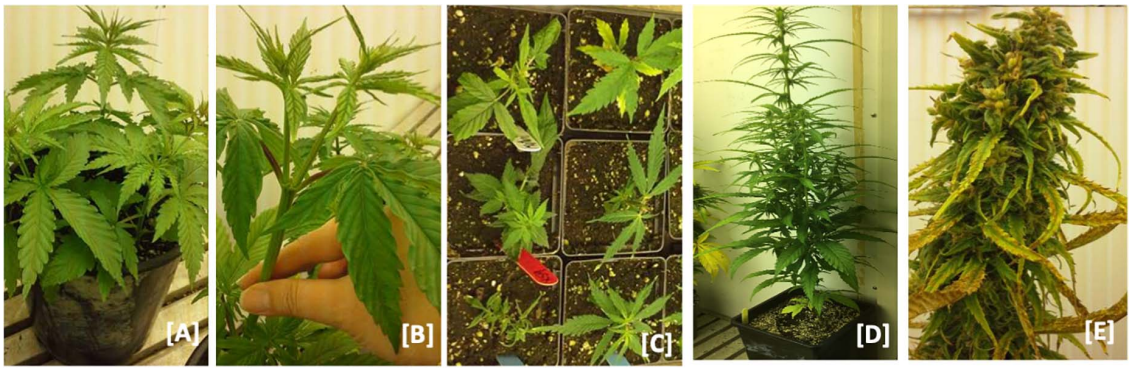

FIGURE 2 | Hemp nodal cloning. **(A)** Hemp plants at 6–8 leaf stage. **(B)** Elongated lateral branches after terminal buds removed from female plants **(C)** lateral branches planted in soil after excision from mother plants and. **(D)** Vegetative clones transferred to 7-inch pots after roots were established and grown. **(E)** Vegetative clone at maturity.

There are forward and reverse genetics approaches for genetic studies of an uncharacterized allele. With the improvement of sequencing technology, genetic transformation using reverse genetic tools has been an advantage in the molecular breeding program. While cannabis has gained a wide reputation of being recalcitrant to gene transformation and tissue culture, a few reports are describing the methods on gene transformation and regeneration (Feeney and Punja, 2003; Slusarkiewicz-Jarzina et al., 2005; Sirkowski, 2012; Wahby et al., 2013; Schachtsiek et al., 2019). Genome editing holds the potential to develop knockout mutants for significant cannabinoid biosynthesis genes such as THCA synthase, CBDA synthase, and CBGA synthase. Several varieties were tested; most were monoecious, although a few dioecious varieties were also used. In all cases, *Agrobacterium*-mediated gene transfer system was employed and exhibited successful transfer of genes, but the regeneration frequency was low to none. Feeney and Punja (2003) demonstrated the transformation success at the cellular level, but none of their treatments were successful in regeneration. Similarly, Wahby et al. (2013) applied *A. rhizogenes* strains (A4, AR10, C58, and IVIA251) and could induce hairy roots on the explants derived from hypocotyl and cotyledonary node; however, plantlet regeneration became a bottleneck for them as well. There is two patent information with the claim of successful genome modification and regeneration of cannabis with limited descriptions (Sirkowski, 2012). Thus, there is a need for an optimized protocol for the transformation and regeneration of cannabis replicable and reliable across different species.

Transient Genetic Transformation

There are various molecular tools developed for transient genetic transformation, including virus-induced gene silencing (VIGS). VIGSis an RNA mediated post-transcriptional gene silencing (PTGS) technique applied to study gene function in a relatively short period (Baulcombe, 1999; Liu et al., 2002; Senthil-Kumar and Mysore, 2014; Adhikary et al., 2019). Once a VIGS protocol is established in a species, it takes 3–6 weeks to see the loss-of-function phenotype of the tested gene/s *in vivo* (Adhikary et al., 2019). Thus, this is an ideal tool to apply, as a proof of concept, to define a target gene's function prior to creating a stable transformation. VIGS, using the Cotton leaf crumple virus (CLCrV), was recently established in *C. sativa,* demonstrating the loss-of-function phenotype of *phytoene desaturase* (*PDS)* and *magnesium chelatase subunit I* (*Chll)* genes (Schachtsiek et al., 2019). Although the loss-of-function phenotype was weak, the researchers paved a clear path to explore unknown genes' functions in the species. There are viral pathogens reported in cannabis (McPartland, 1996) and many viral vectors developed to date; tobacco rattle virus (TRV) is one of them with a broad-spectrum host range (over 400 plant species) across dicot species (Dinesh-Kumar et al., 2007). Given that TRV can also infect cannabis, potentially demonstrating a strong loss-of-phenotype than CLCrV viral vector.

Stable Genetic Transformation

Both transient and stable transformations have been incredibly beneficial for different research areas and applications in functional genomics. Stable gene transformation is preferred for many applications because once the gene modification is fixed in a plant system, it is heritable. The advantage of the altered gene function can be reaped for generations. As there are numerous reports of successful CRISPR-Cas9 mediated gene editing in many plant species, adopting this newly developed molecular tool in cannabis is vital to improving this economically important plant species. CRISPR can precisely alter a gene's function in a genome (Jinek et al., 2012). It has great potential to benefit both basic and applied plant biology research and development. Therefore, establishing the technology in the cannabis crop is essential for functional studies of thousands of unknown genes and the development of novel varieties.

Traditional genetic modification (GM) and gene editing by CRISPR method are viewed differently (Shew et al., 2018). Gene editing performed using CRISPR method is not considered to be GM organism in some regions. Conventionally, GMO crops refer to organisms that have been altered in a way that they would not have evolved naturally. Moreover, GMO involves transferring foreign DNA fragment from one species to another (transgenic) or within the same species (cisgenic). But in the

TABLE 2 | Comparison between tissue culture cloning, manual cloning, and seed propagation in cannabis.

Propagation system	Seed	Traditional cloning	*In vitro*
Roots	Tap root is prominent, grow deep, suitable for field cultivation	Adventitious roots grow from stem laterally, suitable for indoor cultivation	Adventitious roots grow from stem laterally, suitable for indoor cultivation
Genotype	In hybrids, genotype is different for each seed. In feminized seeds, genotype is close to each other	Same as mother plant	Same as mother plant
Rooting hormone	Not required	0.1% Indole-3-butyric acid (IBA) is used to promote rooting	0.1% IBA is used to promote rooting
Sexual type	Segregate in male and female (about 50% each in case of hybrid seeds); near 100% female in case of feminized seeds	All female but chances of developing hermaphrodites or mutated males	All female but chances of developing hermaphrodites or mutated males
Preferred growing	Outdoor	Indoor, hydroponic, aeroponic 18:6 h photoperiod	Indoor/hydroponic/aeroponic 18:6 h photoperiod
Preferred Light Condition	Variable between 500 – 2500 $\mu molm^2$ s^{-1}	Variable between 200 and 300 $\mu molm^2$ s^{-1}	Variable between 50 and 100 $\mu molm^2$ s^{-1}
Yield	500–600 g/plant, relatively long growing cycle and high vegetative growth	40–60 g/plant, relatively small plant, short growing cycle, flower matures within 2 months	40–60 g/plant, relatively, small, short growing cycle, flower matures within 2 months
THC%	<0.3% THC; mostly used for propagating industrial hemp	Between 4 and 30% THC depending on strain	Between 4 and 30% THC depending on strain
Growing medium	Soil/compost	Compost/vermiculite cubes/rockwool/hydrotone clay balls	Sterilized tissue culture medium
Clone health	Chances of seedling infection with mites, sucking pests, powdery mildew, Hop latent viroid (Dudding disease)	Lower chances as grown under controlled condition but could carry disease or pests if cutting come from infected mother plants. If mother plant was infected or symptomless carrier for Hop latent viroid (Dudding disease), chances to carry it forward	Lowest chances as grown under clean condition to carry disease or pests as multiplied from clean stock. Opportunity to clean for Hop Latent virus as coming from nodal clone stocks free of Hop latent viroid (Dudding disease)
Storage	2–3 years in cool dry place	In a dome for a week	For a week in controlled condition and up to 12 months at 4°C
Storage requirements	Protective cover from high sunlight, temperature, and wind; watering as necessary	Cuttings require 65–75% relative humidity; 20–23°C temperature and artificial light for growth; proper ventilation	Controlled and clean purified air HEPA filtered air in culture rooms; 45–50% relative humidity in culture rooms; 20–22°C temperature, effective ventilation
Multiplication rate	One plant can yield thousands of seeds under open pollination/between 100–200 seeds from a feminized plant	150–200 clones from one month grown vegetative plant	One to four multiplication rates in one month period but grows exponential in number with time
Hardening requirement	Not necessary	About 2–3 days; cuttings are little easier to root and acclimatize in growing environment	About a week, transition from culture tubes to soil/compost is little riskier
Cost effectiveness	Can be grown outdoor under little care	Simpler indoor setup	Tissue culture lab investment
Preferred use	Field	Recreation cannabis	Medical Cannabis

Information derived from Chandra et al. (2008, 2015), Caplan (2018), and Chandra et al. (2020).

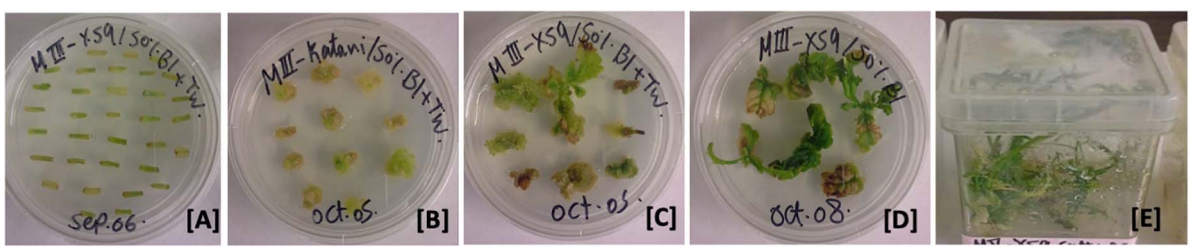

FIGURE 3 | Hemp tissue culture propagation. **(A)** Hypocotyl explants on callus-induction media. **(B)** Hypocotyl explants with the callus on callus induction media. **(C,D)** Callus and developing shoots on shoot-induction media. **(E)** Developed shoots on root-induction media.

TABLE 3 | Cannabis cell culture, transformation, and micropropagation work since 1972–2020.

Species	Cultivar	Study type	Explant	Organogenesis/Transformation	References
Cannabis sativa	Unknown	Cell suspension culture for active metabolites	Seedling tissues	No/No	Veliky and Genest, 1972
Cannabis sativa	Unknown	Assessment of cannabinoids and essential oil in callus	Seedling tissues	No/No	Itokawa et al., 1975
Cannabis sativa	Unknown	Biotransformation of cannabinoid precursors using suspension cultures	Seedling tissues	No/No	Itokawa et al., 1977
Cannabis sativa	Drug type ('152 Strain'); Fiber type ('150 Strain; TUA(2):C-71)	Cannabinoid content in callus	Bracts, calyx, and leaf tissues	No/No	Hemphill et al., 1978
Cannabis sativa	Unknown	Root development from callus	Seedling	Yes/No	Fisse et al., 1981
Cannabis sativa	Unknown	Callus culture	Seedling tissue	No/No	Heitrich and Binder, 1982
Cannabis sativa	Unknown	Assessment of metabolites inducing callus and suspension culture	Embryo, leaf, and stem	No/No	Loh et al., 1983
Cannabis sativa	Unknown	Biotransformation of cannabinoid by cell suspension culture	Seedling tissues	No/No	Hartsel et al., 1983
Cannabis sativa	Unknown	Callus induction	Stem, cotyledon, and root	No/No	Fisse and Andres, 1985
Species	**Cultivars**	**Study type**	**Explants type**	**Organogenesis/Transformation**	**References**
Cannabis sativa	Hemp type	Rooting and shooting from clone cuttings	Axillary shoots	Yes/No	Richez-Dumanois et al., 1986
Cannabis sativa	Unknown but high THCV	Biotransformation of cannabinoids using cell culture method	Leaf tissues	No/No	Braemer and Paris, 1987
Cannabis sativa	Hemp type	Preservation procedure of cannabis suspension cultures	Floral part	No/No	Jekkel et al., 1989
Cannabis sativ	Hemp	Callus formation from all the test tissues;	Leaf, hypocotyl, cotyledon, and root	Yes/No	**Mandolino and Ranalli, 1999
a		shoot regeneration from hypocotyl, cotyledon, and root			
Cannabis sativa	Fedora 19, Felina 34	Regeneration of root from callus but no shoot.	Explant not identified	Yes/Yes (Information not descriptive)	Mackinnon et al., 2000
Cannabis sativa	Hemp type	Gene transformation and Callus formation	Stem and leaf	No/Yes	Feeney and Punja, 2003
Cannabis sativa	Silesia (m), Fibrimon-24 (Potential monoecious), Novosadska, Juso-15, Fedrina-74 (m)	Full plant regeneration from callus	Petiole, axillary bud callus, and callus from internodes	Yes/No	**Slusarkiewicz-Jarzina et al., 2005

(Continued)

TABLE 3 | Continued

Species	Cultivars	Study type	Explants type	Organogenesis/Transformation	References
Cannabis sativa	Beniko (m), Bialobrzeskie (m)	Regeneration of Hemp	Roots, leaves, and stems	Yes/No (only abstract is available in the public database)	Plawuszewski et al., 2005
Cannabis sativa	Bealobrzeskie (m), Beniko (m), Silesia (m)	Callus induction and plant regeneration	Stem and cotyledon	Yes/No	** Wielgus et al., 2008
Cannabis sativa	Hemp type	Regeneration of shoot from meristems	Cotyledon, stem, and root	Yes/No	Casano and Grassi, 2009
Cannabis sativa	Hemp type	Cell suspension culture for secondary metabolites	Leaf tissues	No/No	Flores-Sanchez et al., 2009
Cannabis sativa	MX-1	Direct organogenesis using nodal segments; synthetic seed development.	Nodal segments	Yes/No	Lata et al., 2009a
Cannabis sativa	Changtu	Shoot tip culture	Shoot tip	Yes/No	Wang et al., 2009
Cannabis sativa	MX	Regeneration from leaf derived callus	Leaf tissue	Yes/No	Lata et al., 2010c
Cannabis sativa	MX	Synthetic seeds for conservation of clones	Nodal segments	Yes/No	Lata et al., 2011
Cannabis sativa	Futura77, Delta-llosa, Delta405	*Agrobacterium* infection of cannabis roots	Hypocotyls, cotyledon and cotyledonary node	Yes/Yes	Wahby et al., 2013
Cannabis sativa	unidentified	Regeneration of plants from callus	Leaf	Yes/No	** Hussain, 2014 (Thesis)
Cannabis sativa	Long-ma No. 1	Micropropagation	Internodes	Yes/No	Jiang et al., 2015
Cannabis sativa	Unidentified	Callus induction and Shoot regeneration from callus	Cotyledon and epicotyledon	Yes/No	**Movahedi et al., 2015
Cannabis sativa	Unidentified	Cell culture	Root	No/No	Farag and Kayser, 2015
Cannabis sativa	Changsa	Full Plant regeneration from callus	Cotyledon	Yes/No	Chaohua et al., 2016
Cannabis sativa	Hemp type	Direct organogenesis: in vitro root and shoot proliferation	Nodal segments	Yes/No	Lata et al., 2016
Cannabis sativa	Bialobrzeskie and Monica	Direct organogenesis (shoot and roots) using phytohormones	Shoot tips	Yes/No	Grulichova et al., 2017
Cannabis sativa	Wappa	Direct organogenesis (rooting success of stem cuttings)	Stem cuttings	Yes/No	Caplan et al., 2018
Cannabis sativa	Unknown	Cannabis transformation and regeneration	Leaf segments (for micropropagation), protoplast (transformation), and pollen (transformation)	Unclear/Yes	Flaishman et al., 2019 (Patent)
Cannabis sativa	Hemp Landrace, Futura, Canda, Joey, CFX-2 and Cherry × Workhorse	Determination of optimal hormone and mineral salts for callus induction in hemp.	Stem cuttings	Yes/No	Thacker et al., 2018
Cannabis sativa	Medicinal cannabis but strain unknown	Assessment of cannabis shoot tips for their rooting efficiency	Shoot tips and nodal cuttings	Yes/No	Kodym and Leeb, 2019

(Continued)

TABLE 3 | Continued

Species	Cultivars	Study type	Explants type	Organogenesis/Transformation	References
Cannabis sativa	High THC accessions (1KG2TF, S1525, H5458)	Regeneration of shoots from immature and mature inflorescence	Floral tissues	Yes/No	Piunno et al., 2019
Cannabis sativa	Finola and Euphoria	Callus culture; direct regeneration, and gene transformation	Leaves, petiole, and auxiliary buds	No/Yes	Schachtsiek et al., 2019
Cannabis sativa	Tygra, Monoica, Bialobrzeskie, Fibrol	Direct organogenesis (roots) from cuttings	Seedlings	Yes/no	Smýkalová et al., 2019
Cannabis sativa	Unknown	Production of phytocannabinoids from cell culture	Leaf tissue	No/No	Whitton, 2019, 2020 (Patent)
Cannabis sativa	Drug type C. sativa (BA-1)	Media optimization for callogenesis and micropropagation using explants from both male and female strains	Leaf and nodal explants	Yes/No	Page et al., 2020 (preprint)
Cannabis sativa	Hemp, Ferimon (m), Felina32 (m), Fedora17 (m), USO31 (m), and Finola	*In vitro* plant regeneration and ploidy levels of regenerated plants	Cotyledon, hypocotyl	Yes/No	**Galán-Ávila et al., 2020

*The letter 'm' indicates the monoecious cultivar. **Indicates studies with the regeneration of shoot or root or both from a single cell.*

case of CRISPR edited plants, the targeted mutation is created by using an enzyme and a small guide RNA. While the mutation continues to inherited, the CRISPR machinery can be eliminated in the next generation (Aliaga-Franco et al., 2019). This method is precise and faster than conventional breeding practices, and it is much less controversial than GMO techniques. Therefore, the establishment of CRISPR-Cas9 system in cannabis is another crucial aspect that needs to be explored.

Hairy Root Culture

Agrobacterium rhizogenes is another functional genomics tool to assess the function of a gene or developing transgenic plants. These are differentiated cultures that are induced by the infection of *Agrobacterium rhizogenes,* a soil bacterium. Hairy root culture has a high growth rate in a hormone-free medium and exhibits the potential to yield secondary metabolites comparable to the wildtype (Pistelli et al., 2010). It enables the use of stable and reproducible bioreactor-based production and extraction independent of weather conditions, regulatory hurdles, and a lower risk of microbial contamination. This is a safe approach for producing medicinal and active metabolites free of hormones/viruses and does not require pesticides or insecticides. It is also one of the critical avenues for cannabis genetic transformation and functional genomics research.

Calli or hypocotyls infected by *A. rhizogenes* respond with the emergence of hairy roots from the infected site. Hairy roots can be individually selected and tested for a higher production rate of a compound of interest and cryopreserved at –196°C as a pure culture and subculture further for commercial-scale production (Engelmann, 2004). Cannabis hairy root culture has been successfully induced by *A. rhizogenes* (Wahby et al., 2006, 2013). Hairy root cultures from cannabis callus were also reported using 4 mg/l NAA as a supplement to B5 medium under dark conditions at 25°C (Farag and Kayser, 2015). In the study, the level of THCA and CBDA was less than 2 μg/g dry weight indicating a very low level of cannabinoids present in the hairy root culture under the dark condition with a 28-day growth cycle.

While detectable levels of cannabinoids are not present in *C. sativa* hairy roots, they have been reported to contain choline, atropine, and muscarine (Wahby et al., 2006, 2017). A higher level of these compounds was observed in the *A. rhizogenes* transformed hairy roots compared to non-transformed control. Choline was the most significant compound ranged between 203 and 510 mg/L (control 66–153 mg/L); Atropine with 562–933 μg/L (control 532–553 μg/L); Muscarine with 231–367 μg/L (control undetectable) (Wahby et al., 2017). Additionally, the THCA synthase gene's heterologous expression in tobacco hairy root culture has been successful (Sirikantaramas et al., 2004; Taura et al., 2009).

Meristem Culture

The culture of indeterminate organs, especially the totipotent cells in the apical dome, is a method to obtain many virus clones in a short period (Mori, 1971; Wang and Charles, 1991). The apical dome region has no vascular connection to the developing procambium, leaf primordium, and axillary buds (Wang and Charles, 1991). This lack of vascular connection

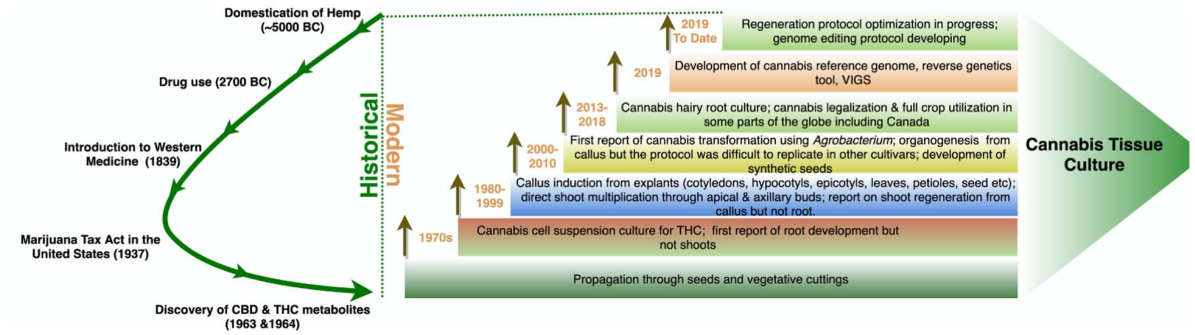

FIGURE 4 | Evolution of cannabis tissue culture research. The green curved arrow on the left shows the key events in cannabis use. Each rectangle on the right shows the major research and development activities at different years. Each brown arrow indicates that the technology is continuously developing and research work is in progress in the particular research area.

provides a basis for using the meristem for pathogen elimination as viruses readily travel through the vascular system but do not efficiently transfer from cell to cell. Uninfected cells can be isolated from the meristematic dome (Wang and Charles, 1991; Wu et al., 2020). It is a robust tool for producingvirus-free clones that can then be further multiplied at a commercial scale to produce certified virus-free plants. Characteristically, a section of tissue, mostly the apical dome, is dissected either from apical or lateral buds consisting of leaf primordia (no more than 1–2 in number) and apical meristem (0.1–0.5 mm in length) and cultured in a suitable growth medium. Upon induction of the meristem cells under a favorable combination of hormones and growth environment, the cells can continue to develop into a shoot or regenerate into plants through somatic embryogenesis or shoot organogenesis. The regeneration process occasionally gives direct shoot development from the explant, and sometimes morphogenesis occurs indirectly only after the formation of the callus.

There are well-established meristem culture protocols for different model and non-model species (Mori, 1971; Mordhorst et al., 2002; Al-Taleb et al., 2011; Spanò et al., 2018), including the closest relative of cannabis, *Humulus lupulus* (Hops), for eliminating virus infection (Grudzinska and Solarska, 2004; Grudzinska et al., 2006; Adams, 2015; Sallie and Jones, 2015). Given the importance of cannabis as a crop, the development of meristem culture for clean plant production could be useful. Unfortunately, this technique is most effective with viral diseases and would not eliminate fungal and bacterial pathogens known to infect cannabis.

Protoplast Culture

For decades, plant protoplasts have been used for genetic transformation, cell fusion, somatic mutation, and more recently, for genome editing (Lei et al., 2015). Significant progress has been made in other crop species in genetic studies using protoplasts; however, for cannabis, studies are in a development phase, with the conditions suitable for the survival of transfected protoplasts and plant regeneration are yet to be optimized. Mesophyll protoplast isolation and transformation of at least three different cannabis cultivars has been reported (Morimoto et al., 2007; Flaishman et al., 2019). Based on the recent study, only about 4% of the protoplasts survived 48 h in liquid culture and plants were not regenerated (Flaishman et al., 2019). Even in the absence of successful regeneration of a whole plant, protoplasts are of great value in confirming the effectiveness of designed guide RNA (gRNA) prior to their use for the regeneration of gene-edited plants.

Somatic Embryogenesis

Somatic embryogenesis is the regeneration of a whole plant from cultured plant cells via embryo formation, from somatic plant cells of various tissues like root, stem, leaf, hypocotyl, cotyledon or petiole (Shen et al., 2018). They morphologically resemble the zygotic embryo's bipolar structure, bear specific embryonic organs, and go through analogous development stages with similar gene expression profiles (Shen et al., 2018). Somatic embryogenesis can occur through direct regeneration. The embryos are developed directly from explant cells, or more commonly through indirect regeneration in which callus develops first, and the development of embryos occurs from callus cells (Sharp et al., 1980).

Plant regeneration via somatic embryogenesis starts with the initiation of embryogenic cultures by culturing various explants on media supplemented with only auxins or a combination of auxins and cytokinins to control cell growth and development (Osborne and McManus, 2005). One exception to this is the use of thidiazuron (TDZ), a cytokinin-like compound that is often used alone to induce somatic embryogenesis (Murthy et al., 1995). The proliferation of embryogenic cultures can occur on solid or in liquid media supplemented with auxins and cytokinins, followed by pre-maturation of somatic embryos on lower levels of PGRs or PGR free media to stimulate somatic embryo formation and development. Maturation of somatic embryos can occur by culturing on media with reduced osmotic potential or supplemented with abscisic acid (George et al., 2007). This maturation stage is critical for synthetic seed production as it allows embryos to be desiccated, stored, encapsulated, and treated like regular seeds. However, in many somatic embryogenesis systems, the maturation phase has not

been developed, and somatic embryos germinate precociously to produce plants.

Somatic embryos are used as a model system in embryology studies; however, somatic embryogenesis's main economic applications are for developing transgenic plants and large-scale virus-free vegetative propagation of elite plant genotypes. The possibility to scale up the propagation using bioreactors has been reported (Hvoslef-Eide and Preil, 2005). Somatic embryos are also ideal for genetic manipulation purposes as they develop from a single cell, thereby reducing the chances of producing chimeric plants, common when relying on shoot organogenesis or shoot proliferation (Dhekney et al., 2016). Other less common uses of somatic embryogenesis include cryopreservation of genetic materials and synthetic seed technology (George et al., 2007).

Feeney and Punja (2003) investigated the somatic embryogenesis and tissue culture propagation of hemp. Despite testing various explants and supplements, and variations in the culture medium and changes to the culture environment, there was no successful plantlet regeneration, and a reliable protocol for somatic embryogenesis in cannabis has yet to be published.

Thin Cell Layer (TCL)

Thin cell layer (TCL) culture utilizes a thin layer of tissue as the explant to allow close contact between wounded cells and nutrients and growth regulators supplied in the medium; this controls the morphogenesis of the cultures (Nhut et al., 2003). This is most useful where larger explants may also contain a high level of endogenous hormones, carbon sources, and other substances that influence and conflict with the effects of exogenous substances placed in the medium and, thus, interfere with development. In general, sterilized TCL explants are excised either longitudinally (0.5–1 mm wide, 5–10 mm long) or transversally (0.1–5 mm thick) prior to culturing (Nhut et al., 2003; Croom et al., 2016). Like other *in vitro* techniques, TCL requires an optimized protocol regarding basal media, PGRs and other added nutrients and growth conditions such as daylength, light intensity, and temperature. These conditions vary for not only the species but can be genotype-dependent. It has been widely used in different species, including bamboo, banana, citrus, tomato, rose, *Lilium ledebourii*, *Bacopa monnieri*, saffron, among others (Nhut et al., 2003; Teixeira da Silva et al., 2007; Mirmasoumi et al., 2013; Croom et al., 2016; Azadi et al., 2017). TCL's potential is yet to be explored in *Cannabis* spp.; however, it may prove to have some utility in the regeneration of genetic transformants in this high value but re calcitrant regeneration crop.

Doubled Haploid Production

Androgenesis is a biological process by which a whole plant regenerates directly from immature pollen (microspores) through the embryogenesis developmental pathway under *in vitro* conditions. While the resulting plant is haploid and inherently sterile, a diploid plant can arise either spontaneously or artificially (Gilles et al., 2017), usually with colchicine, which blocks cytokinesis without blocking chromosome doubling (Galazkajoa and Niemirowicz-Szczytt, 2013). This doubled haploid is homozygous at all loci. Doubled Haploid (DH) plants have been extensively used in plant breeding programs to increase the speed and efficiency with which homozygous lines can be obtained (Alisher et al., 2007). DH technology is traditionally used to genetically stabilize parental lines for F_1 hybrid production. This is important for the rapid integration of new traits through backcross conversion and to develop molecular mapping populations. It is also used to fix desired traits obtained through transformation or mutagenesis and simplify genomic sequencing by eliminating heterozygosity (Ferrie and Mollers, 2011). As such, this technology would be an important tool for both forward and reverse functional genomics studies.

There are two different approaches to develop haploid plants. First, *in situ* methods, using particular pollination techniques such as irradiated pollen, inter-species crosses or so-called 'inducer lines' (Ren et al., 2017); second, *in vitro* methods including the culture of haploid cells (gametes) and their development to haploid embryos and consequently haploid plants through germination. The microspores, which can be harvested in large numbers (millions), are generally isolated for culture as a uniform population. Alternatively, the culture of whole anthers is used to obtain haploid plants through the androgenesis process. The main disadvantage of another culture is the potential for developing a mix of both haploid and diploid plantlets (Elhiti et al., 2010). In this review, we will focus only on the production of doubled haploids from microspores using *in vitro* culture.

One of the most important factors affecting DH production is the microspore developmental stage. It is a complicated factor that has a strong influence on microspore culture's success. It has been reported that only microspores that are at a stage sufficiently immature have the ability to change their developmental fate from a gametophytic to embryogenic, leading to sporophytic development (Soriano et al., 2013). The most amenable stage is either the uni-nucleate stage of the microspore or the early binucleate stage, either at or just after the first pollen mitosis. At this developmental stage, the microspore's transcriptional status may still be proliferative and not yet fully differentiated (Malik et al., 2007). Although all microspores within an anther would be roughly of a similar age, not all cells have embryonic competence. Therefore, the incremental differences in the stages of development of individual microspores can be considered significant. To avoid this problem, Bhowmik et al. (2011) introduced a new treatment, discontinuous Percoll gradient centrifugation, to provide a uniform population of *B. napus* isolated microspores at the appropriate stage of development. This approach has consistently produced high embryo yields and consistent embryo development.

Hemp Microspore Culture

In 2019, an extensive hemp breeding program was introduced at Haplotech Inc.[1]. As there has been no previously reported success in the area, a hemp DH project was initiated to accelerate this program. Four different Haplotech genotypes were used for this experiment. Both male racemes and pollen-induced female colas were collected, and the buds were fractionated

[1]https://haplotech.com/

according to size into three groups (2–3, 3–4, and 4–5 mm). Each group was surface sterilized with 15% commercial bleach and washed three times with distilled-sterilized water for 5 min each. The sterilized buds were macerated in isolation media (MS basal fortified by 13% sucrose). The isolated microspores were washed by extraction medium two times or until the supernatant became clear. The isolated microspores were subjected to fractional centrifugation using Percoll, as described by Bhowmik et al. (2011). The concentration of microspores was diluted to 4×10^4cells/ml with MS basal fortified by 10% sucrose. Five ml of this diluent (4×10^4) microspores were mixed with 5 ml of induction media (MS basal, 10% sucrose supplemented with different additives for induction) in 47 mm Petri dishes. The final concentration of the culture used was 2×10^4 cells/ml. The isolated microspores in culture were observed every 3 days using an inverted microscope and a binocular microscope.

Samples of isolated microspores were stained with 4, 6-diamidino-2-phenylindole (DAPI) and observed using a fluorescence microscope to monitor their *in vitro* development, once every 3 days. Monitoring of the culture samples by DAPI staining in the first 2 weeks revealed that the microspores of all four genotypes remained uninuclear (**Figure 5A**). This developmental stage was found to be the most responsive to embryogenesis induction in many crop plants (Soriano et al., 2013). Of the factors tested, the most crucial for further development of the microspore was the induction medium formulation. Using a relatively complex medium, a few microspores responded (0.05–0.5%) and developed further, while the remainder died within 5–10 days. Microspore derived embryos initiated by a series of random divisions within the surrounding exine wall. The nucleus of uninucleate microspores (**Figure 5A**) condensed and reduced in size during the first 2 days in culture (**Figure 5B**). They then divided symmetrically within the first 5–8 days, forming two equal-sized nuclei (**Figure 5C**). This developmental stage is considered the initial stage that is often referred to as sporophytic growth (Soriano et al., 2013). Within another 3–5 days, the nuclei underwent a series of divisions resulting in the formation of multinucleate structures (**Figure 5D**). By approximately the third week of culture, globular stage embryos were observed in culture (**Figure 5E**). Early in the fourth week, these globular structures developed into heart stage embryos (**Figure 5F**). To date, growth has not progressed past this stage of embryo development. Current experiments including adjustment of the osmoticum and removal of secondary metabolites which could inhibit (microspore-derived) embryo development are running.

In vitro Mutagenesis

A mutation occurs in DNA, naturally or it can also be induced artificially. The majority of the genetic variation existing in a gene pool has occurred naturally. These genetic variations can be recombined through conventional breeding practices to develop a novel variety with desired gene traits. Although these spontaneous mutations are frequent, the desired mutation in the desired gene segment altering its biological role is extremely rare. Therefore, mutation induction tools are used in the rapid development of genetic variability in crops. For the last few decades, there were several scientific reports published assessing the impact of an induced mutation in the improvement of crops (Brock, 1971; Broertjes and Van Harten, 1988; Micke, 1999; Oladosu et al., 2016). However, in cannabis research and development is rapidly flourishing, but there are only a few reports on targeted mutation through genetic transformation (Feeney and Punja, 2003; Slusarkiewicz-Jarzina et al., 2005; Sirkowski, 2012; Wahby et al., 2013) and there is no mutant variety introduced at the commercial level. *In vitro* culture techniques, coupled with mutagenesis, has simplified the crop improvement work for both seeds and vegetatively propagated plants (Hussain et al., 2012). Little efforts have been made and published to establish DH production in cannabis, but once streamlined will open up exciting opportunities for DH mutagenesis as it has been successfully employed in canola (Szarejko, 2003).

Synthetic Seed Technology

Synthetic seeds usually refer to artificially encapsulated somatic embryos (Murashige, 1977) but have also been used in reference to encapsulated vegetative tissues that have the potential to develop into a whole plant (auxiliary buds, cell aggregates, shoot buds). Somatic embryos provide the ideal approach to developing synthetic seeds as they often have the ability to survive desiccation and can be treated in much the same way as true seeds. At the same time, other tissues lack this capacity and are less useful (Rihan et al., 2017). As shown in **Figure 6**, synthetic seeds can be successfully developed by using various explants, media, and encapsulation protocols (Bapat et al., 1987; Corrie and Tandon, 1993; Nyende et al., 2003; Chand and Singh, 2004; Rai et al., 2008; Lata et al., 2009a).

Cannabis is generally a cross-pollinating crop, and due to its allogamous nature, it is difficult to maintain existing elite varieties by seed. Typically, a minimum isolation distance of 5 km between breeding nurseries and hemp production fields is required to minimize the occurrence of nuisance pollen. Such separation is often difficult to achieve in areas with high hemp production intensity. Therefore, *in vitro* propagation using synthetic seed technology is an alternative method for large-scale clonal propagation and germplasm preservation. As the cannabis industry grows, this method may be cheaper and faster than traditional tissue culture methods. Along with the preservation of genetic uniformity, clones produced through this technique are pathogen-free, easy to handle, and transport.

Moreover, in other species, this approach has resulted in increased quality of planting material (Rihan et al., 2017). While cannabis tissue culture methods are still being optimized, Lata et al. (2009a) developed a high-frequency propagation of axillary buds of *C. sativa* encapsulated in calcium alginate gel. Calcium alginate is a hydrogel that contains nutrients, growth regulators, and sometimes antibiotics.

When directly sown on a substrate, encapsulation aids in the physical protection and establishment and growth of the explant. According to Lata et al. (2009a), gel capsule consisted of 5% sodium alginate with 50 mM $CaCl_2.2H_2O$, and full-strength MS medium supplied with 0.5 μM TDZ, and 0.075% plant preservative mixture (PPM). The optimal regrowth and

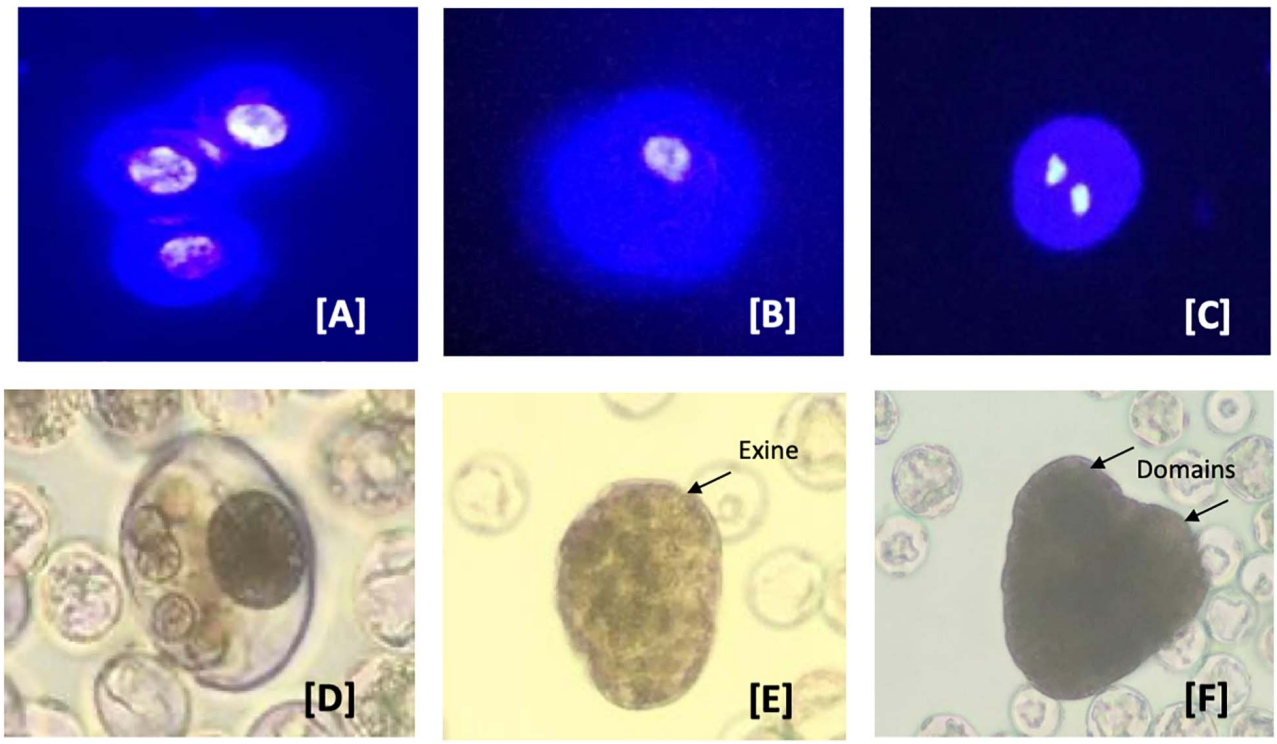

FIGURE 5 | Developmental pathways observed in *C. sativa* (industrial hemp) microspore culture. **(A–C)** Male gametophyte development in *C. sativa* during *in vitro* culture. **(A)** Uninucleate microspores; **(B)** uninucleate microspores after 3 days in culture media; **(C)** symmetrically divided microspore with two equally sized nuclei; **(D)** multinucleate structure without organization and still enclosed in exine; **(E)** globular multicellular structure with developing exine; and **(F)** heart-shape embryo with two distinct domains. The nuclei in **(A–C)** are stained with the nuclear dye 4′,6-diamidino-2-phenylindole (DAPI) to indicate viability.

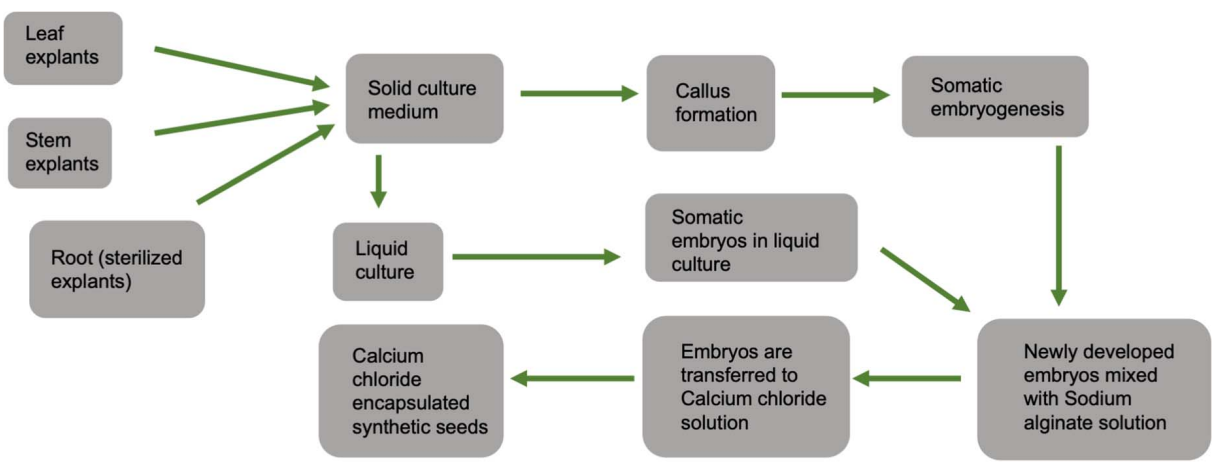

FIGURE 6 | General schematic diagram showing steps for calcium chloride encapsulated synthetic seed production.

conversion were achieved in MS medium supplemented with antimicrobial components, PPM (0.075%) and TDZ (0.5 μM) under *in vitro* conditions. Under *in vivo* condition, the optimal conversion and regrowth were exhibited on 1:1 potting mix-fertilome with coco natural growth medium supplied with MS medium containing 3% sucrose, 0.5% PPM. Clones regenerated from the explants were successfully hardened and transferred to the soil (Lata et al., 2009a).

Another hurdle to *in vitro* propagation is transporting requested strains from the tissue culture facility to the growers in a timely manner. These transportation issues become incredibly challenging for maintaining crop schedules because cannabis

crops can take more than 2 months to reach hardening stages, then spend 4 weeks in vegetative growth, then 7 or 8 weeks in flower. Greenhouse or indoor growers require a consistent supply demand to receive a high volume of plantlets every week to start over a new grow room at a very tight on-time delivery schedule, which is the most important metric in their operations. An established and cost-effective synthetic seed encapsulation technique would provide an opportunity to eliminate the transportation challenge.

CRYOPRESERVATION

Cryopreservation refers to the storage of diverse living materials at below –130°C (Engelmann, 2004). It serves as an alternative conservation approach to the conventional field and *in vitro* (i.e., slow growth) germplasm conservation and is cost-effective over extended periods with minimal space and routine maintenance requirements (Pence, 2011; Engelmann, 2014; Popova et al., 2015). It also assists current breeding programs by providing long-term storage and an easy long-distance exchange of genetic materials (e.g., pollen and meristematic apices and buds). Cryopreservation has been implemented for various plant species using different methods, the most popular and widely applicable, including controlled freezing, vitrification, encapsulation-dehydration, encapsulation-vitrification, and droplet-vitrification (Sakai and Engelmann, 2007; Popova et al., 2015). These methods follow distinct approaches to dehydrate cryopreserving living materials by converting liquid water to a glassy state to avoid the lethal formation of intracellular ice. The selection of methods and the scales of conservation using this approach are strongly determined by genotypes and tissue materials used, which contain different responses to pre- and post-cryopreservation treatments.

Conventional and *in vitro* conservation of cannabis require considerable amounts of space and routine maintenance, have genetic mutations accumulate in the plants. Conventional conservation may expose plants to virulence pathogens. The plants may eventually become susceptible to diseases. The application of cryopreservation can serve as an essential tool for the conservation of various valuable *C. sativa* genotypes with unique attributes and trading the genotypes nationally and internationally in sterile conditions. The first study on applying cryopreservation techniques in *C. sativa* was reported in 1989 using cell suspension cultures (Jekkel et al., 1989). The suspension cultures were preserved using 10% dimethyl sulfoxide (DMSO) cryoprotectant and a controlled cooling rate of 2°C/min and transfer temperature of –10°C, with a 58% survival rate after cryopreservation of the cultures. A cryopreservation protocol for *C. sativa* shoot tips was recently developed using a droplet-vitrification in liquid nitrogen for long-term conservation of this crop (Uchendu et al., 2019). The report showed that vitrified shoot tips using a cryoprotectant solution of 30% glycerol, 15% ethylene glycol, 15% DMSO in liquid MS medium with 0.4 M sucrose, pH 5.8 had 63% re-growth efficiency. Despite the promising progress made, more studies need to be done on selecting appropriate cryopreservation methods with respect to the tissue types and genotypes, increasing re-growth and survival efficiency of preserved samples, and genetic stability of regenerated plants after using different cryopreservation tools, among others.

GERMPLASM MAINTENANCE

The *in vitro* condition also raises some issues for concern, primarily when the material is maintained over a long period of time.

Clonal Stability *in vitro* Culture

In vitro mass-propagation and maintenance of elite germplasm requires genetically stable true-to-type clones. Several factors, such as the number of subcultures, changes in the relationship of auxin/cytokinin, explant type, and a high concentration of growth regulators, may influence the genetic stability of a clone under *in vitro* conditions (Joyce et al., 2003; Sato et al., 2011; Smulders and de Klerk, 2011; Nwauzoma and Jaja, 2013). While carefully selecting explant types and optimizing the conditions above, but depending on the plant species, clonal stability can be obtained during *in vitro* mass-propagation and germplasm conservation of the desired elite genotypes maintained. To date, *C. sativa* plants regenerated from nodal culture, and *in vitro* conserved synthetic seeds ('Encapsulated' nodal segments) have shown no evidence of genetic mutations; however, this has only been evaluated using low numbers of markers (Lata et al., 2010a, 2011). Despite optimizing and using properly *in vitro* conditions that limit somaclonal variations, assessment of clonal stability is required to ensure the regenerated clones are the true-to-type of the donor plants.

Somaclonal Variation

Although clonal propagation and maintenance of elite germplasm require a substantial genetic uniformity among *in vitro* regenerated plantlets, there may be a large possibility of genetic variations, called "somaclonal variation" among these plants and/or relative to the donor plants. Somaclonal variation is commonly a result of genetic alterations and changes in the new *in vitro* plants' epigenetics compared to the original source plants (Miguel and Marum, 2011; Abreu et al., 2014). The frequency and nature of somaclonal variation *in vitro* culture can be influenced by different factors, such as explant source, genotype, *in vitro* techniques, *in vitro* growth conditions, length of the culture period, and the number of subcultures. The use of *de novo* regeneration from highly differentiated tissues (i.e., roots, leaves, stems, hypocotyls, cotyledons, etc.) is generally considered to produce more somaclonal variation compared to explants with developed meristems (i.e., axillary buds and shoot tips) (Pijut et al., 2012). Most of these factors generate oxidative stress during culture initiation and subsequent subculturing. The explants and the subsequent regenerated plants exposed to the stress may retain genetic changes. For example, protoplast and callus based plant regeneration impose a high degree of oxidative stress; thus, the stress promotes a high mutation rate, whereas plants regenerated through auxiliary branching

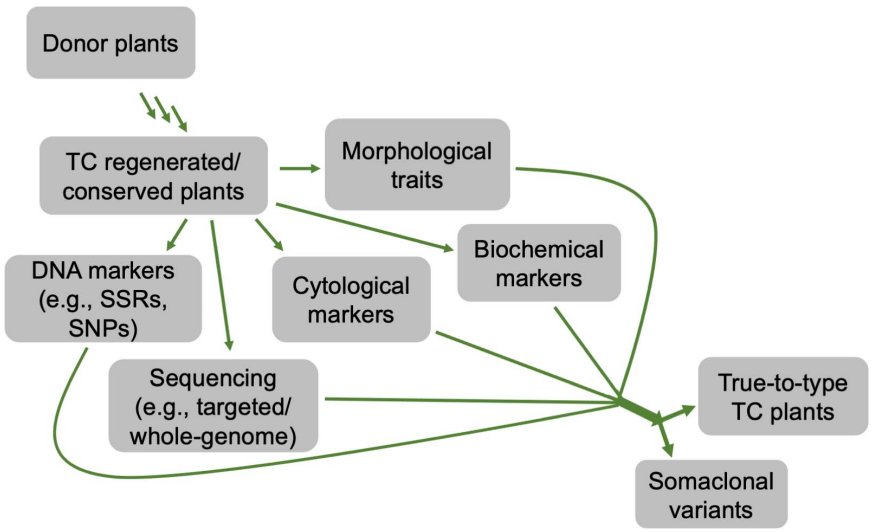

FIGURE 7 | A flow chart depicting different approaches that can be used to determine the genetic stability of *in vitro* regenerated or conserved cannabis plants, compared to its donor counterparts.

TABLE 4 | Comparison between tissue culture cloning and manual cloning in cannabis.

Parameter	Manual Cloning	Tissue culture cloning
Space to produce 1000 cuttings (square meters)	3–5	0.36
Clones processed per person per day (count)	200–250	1500–2000
Multiplication Ratio per month	1–2	4–5
Cost of Production ($)	$3–4	$0.5–1
Clone multiplication in a 3-month cycle	50–80	200–250
Cleanliness	Chances of contamination	Disease, pest, and virus free
Vigor	Chances of reduced vigor from stressed or infected mother plants	Vigor from meristematic reviving
Estimated clone production per 10,000 square feet per year (count)	200,000	2,000,000
Estimated revenue at $10 per clone	$ 2M	$ 20 M

(e.g., nodes, shoot tip) experience very low oxidative stress, normally resulting in no genetic variation (Zayova et al., 2010; Smulders and de Klerk, 2011; Krishna et al., 2016). Genetic variation can also arise from somatic mutations already present in the explants collected from the donor plant (Karp, 1994). *In vitro* regeneration of plants can also be genotype-specific, in which genotypes have different degrees of mutation risks and thus strongly determine the formation of somaclonal variation (Alizadeh et al., 2010; Eftekhari et al., 2012; Nwauzoma and Jaja, 2013). The genetic alterations strongly depend on the *in vitro* techniques used to regenerate *in vitro* plants. Additionally, despite differences across plant species, cultures maintained for a long period tend to generate high somaclonal variation, and *vice versa* (Farahani et al., 2011; Jevremovic et al., 2012; Sun et al., 2013). When cultures are getting old and continuously subcultured, the chance of generating genetically less uniform plants is increased (Zayova et al., 2010), but depends upon the plant species. For example, any more than eight subculture cycles increased somaclonal variation in banana (Khan et al., 2011), whereas over 30 subcultures did not cause any detectable somaclonal variations in *C. sativa* (Lata et al., 2010a).

Although the molecular mechanism of how somaclonal variations generated from a single plant genotype under the same *in vitro* conditions is not fully explored, several potential mechanisms causing genetic alternations and epigenetics have been proposed in different plant species. These mechanisms include changes in chromosome number, point mutations, somatic crossing over and sister chromatid exchange, chromosome breakage and rearrangement, somatic gene rearrangement, DNA replication, changes in organelle DNA, insertion or excision of transposable elements, segregation of pre-existing chimeral tissues, DNA methylation, epigenetic variation, and histone modifications and RNA interference (Sato et al., 2011; Krishna et al., 2016; references therein).

The occurrence of somaclonal variations in regenerated *in vitro* plants may be advantageous or disadvantageous, depending on *in vitro* propagation goals. If *in vitro* propagation aims to generate new variants, obtaining variations among

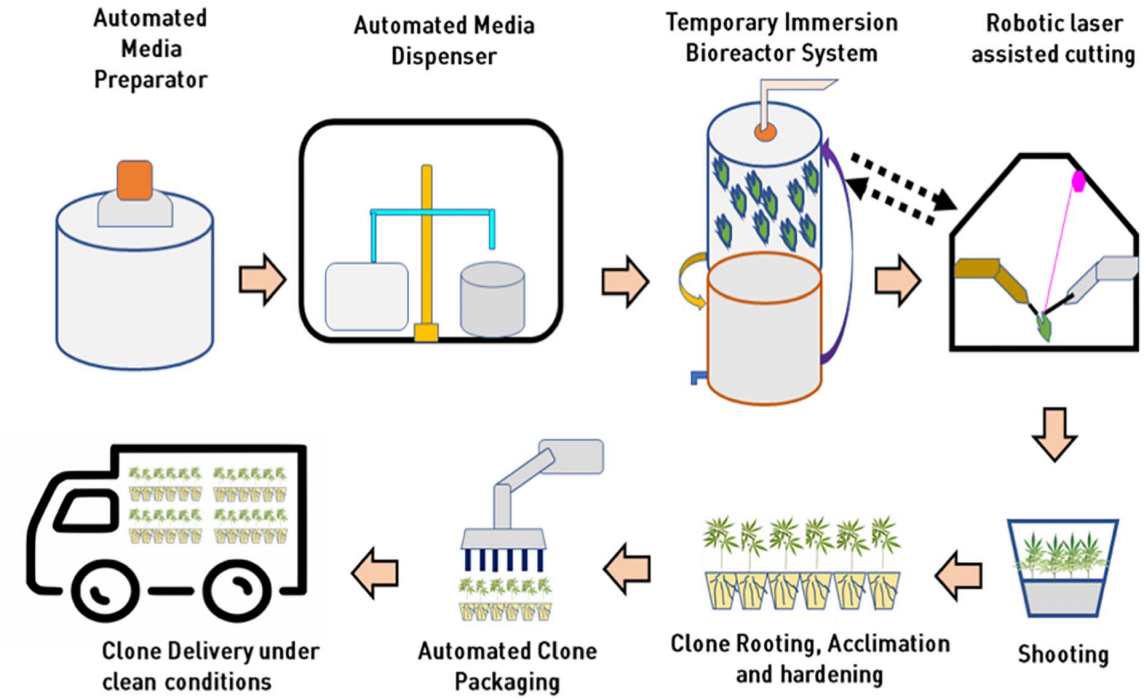

FIGURE 8 | Integration of automation and bioreactor technologies for mass propagation in cannabis for low cost clonal multiplication at *in vitro* level.

in vitro plants can be advantageous that increases genetic diversity for a genotype used. It provides an alternative tool to the breeders for obtaining genetic variability in different plant species, which are either difficult to breed or have narrow genetic bases. On the flip side, when *in vitro* propagation targets to produce multiple true-to-type *in vitro* plants and maintain elite germplasm, the occurrence of subtle somaclonal variations is a severe problem.

PHYTOCANNABINOID SYNTHESIS IN THE CANNABIS SPECIES

Nature has deftly adorned cannabis species with a spectrum of phytocannabinoids or monoterpenoids that are chemically designed with para-oriented isoprenyl and aralkyl groups (Hanus et al., 2016). Since the discovery of tetrahydrocannabinol (THC) and cannabidiol (CBD) in the early 1960s, there are over 120 cannabinoids that has been reported, and the biosynthesis pathway of these compounds has been greatly improved (Taura et al., 1995; Sirikantaramas et al., 2004; Taura et al., 2007b, 2009; Gagne et al., 2012; Stout et al., 2012; Laverty et al., 2019). Presumably, cannabigerolic acid (CBGA), the product formed by the alkylation of geranyl diphosphate and olivetol, is the key precursor compound in the synthesis of cannabinoids (Fellermeier and Zenk, 1998). The cyclization event of prenyl components of CBGA, catalyzed by three enzymes – tetrahydrocannabinolic acid synthase (THCAS) (genebank accession: AB057805), cannabidiolic acid synthase (CBDAS) (genebank accession: AB292682), and cannabichromenic acid synthase (CBCAS), lead to the formation of three major cannabinoids, THCA, CBDA, and CBCA, respectively (Sirikantaramas et al., 2004; Taura et al., 2007a). Biochemical characterization of the enzymes, THCAS and CBDAS, have demonstrated that the enzymes follow a similar reaction mechanism. In the presence of molecular oxygen, the enzymes use flavin adenine dinucleotide (FAD) cofactor to catalyze CBGA forming THCA and CBDA, and hydrogen peroxide as its chemical biproduct (Sirikantaramas et al., 2004; Taura et al., 2007b). Although it is a bit unclear, the chemical reaction for CBCAS also believed to use FAD as cofactor and molecular oxygen to complete the enzymatic activity on CBGA. The genes that encode for CBCAS and THCAS are highly similar in the nucleotide level, indicating that CBCAS is also flavoproteins, like the other two enzymes, requiring oxygen to catalyze CBGA to CBCA (Laverty et al., 2019). THCA, CBDA, and CBCA are the major cannabinoids in acidic forms that are synthesized in cannabis plant; upon decarboxylation, these compounds convert into neutral forms, THC, CBD, and CBC respectively (Wang et al., 2016).

DETERMINATION OF GENETIC FIDELITY

Variations between regenerated and donor plants can be exhibited at phenotypic, cytological, biochemical, and genetic/epigenetic levels (Hillig, 2005; Miguel and Marum, 2011; Smulders and de Klerk, 2011; Abreu et al., 2014). These variations can be determined through different approaches, such as morphological, cytological, biochemical, and molecular

analyses (**Figure 7**). For morphological traits, changes are not always observed at early developmental stages or may not entirely display the variations. By contrast, the use of cytological and molecular detection approaches determines differences at chromosomal and DNA levels, respectively, regardless of the developmental stages in various plant species (Clarindo et al., 2012; Pathak and Dhawan, 2012; Currais et al., 2013; Abreu et al., 2014; Bello-Bello et al., 2014). To date, several studies have been reported on the use of different molecular markers in *Cannabis* spp. genetic diversity, fingerprinting, etc. These markers include random amplified polymorphic DNA (RAPD), restriction fragment length polymorphisms (RFLP), amplified fragment length polymorphism (AFLP), microsatellites, inter simple sequence repeat (ISSR), short tandem repeat (STR) multiplex, and single nucleotide polymorphisms (SNPs) and PCR Allele Competitive Extension (PACE) assay (Faeti et al., 1996; Kojoma et al., 2002; Alghanim and Almirall, 2003; Gilmore and Peakall, 2003; Hakki et al., 2003; Datwyler and Weiblen, 2006; Mendoza et al., 2009; Lata et al., 2010a; Gao et al., 2014; Dufresnes et al., 2017; Henry et al., 2018). These molecular markers coupled with cytological and morphological analyses (Abreu et al., 2014) are valuable techniques to ensure the genetic stability of *in vitro* regenerated plants or *in vitro* conserved germplasm of *C. sativa*. To date, only ISSR markers have been used to confirm the genetic stability of *C. sativa* synthetic seeds during *in vitro* multiplication and storage for 6 months under different growth conditions, and *in vitro* propagated plants over 30 nodal subcultures in culture and hardening in soil for 8 months, compared to the corresponding donor plants (Lata et al., 2010a, 2011).

PROJECTED CONTRIBUTION OF TISSUE CULTURE IN THE GLOBAL CANNABIS INDUSTRY

The present global cannabis market is worth $340 B[2]. To supply cannabis (medical and recreational) to global consumers, a stable supply chain of quality production and value-added product development still needs to be established. Considering the average annual weighted usage base of 110 g per customer (Canaccord Genuity), the global cannabis demand currently could be around 19-20 M kg per year. Major cannabis consumers are in Europe, North America, South America, Asia, and Oceanic parts of the world, with an estimate of 263 million people using the drug in the previous year (European Consumer Stables Report, 2018; World Drug Report, 2019). To produce 20 M kg of cannabis every year, considering a 40-gm yield per plant, would require 500 M clones/seeds a year. An average price of $10, as, then, the overall present global expected market size for tissue culture clones/manual clones could be predicted around $5B. With intensive indoor cultivation, tissue culture clonal planting material can also reduce the risk of fungal and viral diseases, substantially reducing production cost to under $0.5 per gram to maintain a profitable cannabis production (**Table 4**). Considering these global demand scenarios, the supply of clean cannabis clones (pest free, and true to type tested) is an important supply chain component essential for the success and future growth of cannabis industry. To sustain and support the industry growth and make the production cost-effective, optimization in the cannabis tissue culture technology is vital.

The *in vitro* propagation of cannabis is superior to conventional methods because of disease-free elite plants' production and a high multiplication rate. The cannabis industry is keen to invest in *in vitro* propagation due to (i) saving footprint/production area by shifting a mother room to a tissue culture lab that will be almost 10% the size of the space needed same number of clones.

The main hurdle of *in vitro* propagation is the capital cost for the tissue culture lab setup. Setting up a massive large-scale production facility can involve a multimillion-dollar investment. Industry and technology will need to continue to improve and reduce costs so that *in vitro* propagation can be affordable for all growers.

In other plants, under a laminar flow hood setting, on an average of 100 plants per hour with 2000 working hours, 200,000 plants can be produced in a year. With an hourly labor cost of $35 per hour will cost around $0.35 per tissue culture plant (Sluis, 2005). This is around 60% of the production cost, adding another $0.15 for other costs (including electricity, resources, and marketing) makes it a baseline cost of $0.50 per plant. Scale also makes some impact on the cost of production being larger facilities can reduce the cost per plant significantly. These production costs can be as low as $0.15 per plant if the plants are produced in India, Singapore, China, or Africa where labor costs are comparatively low.

A few biotech companies recently added robotic sub-culturing technology for their cannabis plantlets and developed a fully automated micropropagation system to reduce large-scale operation costs. However, the capital investment to purchase this kind of robotic system is incredibly high at this time. Automated technologies for media preparation and dispensing, photoautotrophic bioreactor systems, robotic explant handling, and cutting, transfer laser dissected explants into fresh culture media, and automated acclimatized and hardened plant packaging in future will make cannabis tissue culture industry high throughput and extremely cost-effective for assured "*Just In Time*" supply of pest free, true-to-type cannabis clones. A conceptual model for high throughput automated cannabis *in vitro* clonal mass propagation is depicted in **Figure 8**. Robotics has the potential to bring tissue culture cost down by 25% (as low as $0.15 per plant to compete with low-cost production in some parts of the world). Tissue culture automation technology is slowly progressing, and it will not only bring high-level consistent output but also reduce the cost of production as low as 20 cents per plant.

CONCLUSION

The process of developing new varieties through conventional breeding can take 7–12 years, depending on crop species. The progress of cannabis breeding programs is limited due to the

[2]https://www.gbnews.ch/340-billion-the-global-cannabis-market/

difficulty in maintaining selected high yielding cross-pollinated elite genotypes under field or greenhouse conditions. Therefore, tissue culture techniques are advantageous for cannabis improvement because they can facilitate high multiplication rate and production of disease-free elite plants by overcoming the problems of heterozygosity from cross-pollination. The development of new industrial hemp and medical cannabis cultivars with improved traits could be further advanced using genome editing and other precision breeding tools, combined with *in vitro* techniques for regeneration. Unfortunately, hemp and cannabis plants' dioecious nature complicates the efforts toward the improvement of specific traits, such as resistance to pests and diseases. Therefore, with the recent legalization, calls for serious targeted efforts are required to advance the regeneration and transformation protocols aiming to enhance the quality and safety of the plants and end products.

AUTHOR CONTRIBUTIONS

All authors listed have made a substantial, direct and intellectual contribution to the work, and approved it for publication.

ACKNOWLEDGMENTS

We would like to thank Dr. Ayelign M. Adal from the University of British Columbia for his contribution and suggestion on composing this article.

REFERENCES

Abreu, I. S., Carvalho, C. R., and Clarindo, W. R. (2014). Massal induction of Carica papaya L. 'Golden' somatic embryos and somaclone screening by flow cytometry and cytogenetic analysis. *Cytologia* 79, 475–484. doi: 10.1508/cytologia.79.475

Adams, A. N. (2015). Elimination of viruses from the Hop (Humulus lupulus) by heat therapy and meristem culture. *J. Hortic. Sci.* 50, 152–160. doi: 10.1080/00221589.1975.11514616

Adhikary, D., Khatri-Chhetri, U., Tymm, F. J. M., Murch, S. J., and Deyholos, M. K. (2019). Virus induced gene-silencing (VIGS) system for functional genomics in betalainic species, Amaranthus tricolor. *Appl. Plant Sci.* 7:1221. doi: 10.1002/aps3.1221

Adinoff, B., and Reiman, A. (2019). Implementing social justice in thetransition from illicit to legal cannabis. *Am. J. Drug Alcohol. Abuse* 6, 673–688. doi: 10.1080/00952990.2019.1674862

Alghanim, H. J., and Almirall, J. R. (2003). Development of microsatellite markers in Cannabis sativa for DNA typing and genetic relatedness analyses. *Anal. Bioanal. Chem.* 376, 1225–1233. doi: 10.1007/s00216-003-1984-0

Aliaga-Franco, N., Zhang, C., Presa, S., Srivastava, A. K., Granell, A., Blazquez, M. A., et al. (2019). Identification of transgene-free CRISPR-edited plants of rice, tomato, and arabidopsis by monitoring DsRED fluorescence in dry seeds. *Front. Plant Sci.* 10:1150. doi: 10.3389/fpls.2019.01150

Alizadeh, M., Singh, S. K., and Patel, V. B. (2010). Comparative performance of in vitro multiplication in four grape (Vitis spp.) rootstock genotypes. *Int. J. Plant Prod.* 4, 41–50. doi: 10.22069/IJPP.2012.680

Al-Taleb, M. M., Hassawi, D. S., and Abu-Romman, S. M. (2011). Production of virus free potato plants using meristem culture from cultivars grown under Jordanian environment. *J. Agric. Environ. Sci.* 11, 467–472.

Andre, C. M., Hausman, J. F., and Guerriero, G. (2016). Cannabis sativa: The plant of the thousand and one molecules. *Front. Plant Sci.* 7:1–17. doi: 10.3389/fpls.2016.00019

Azadi, P., Bagheri, K., Gholami, M., Mirmasoumi, M., Moradi, A., and Sharafi, A. (2017). Thin cell layer, a suitable explant for in vitro regeneration of saffron (Crocus sativus L.). *J. Agric. Sci. Technol.* 19, 1429–1435.

Bapat, V. A., Mhatre, M., and Rao, P. S. (1987). Propagation of Morus indica L. (Mulberry) by encapsulated shoot buds. *Plant Cell Rep.* 6, 393–395. doi: 10.1007/BF00269570

Baulcombe, D. C. (1999). Fast forward genetics based on virus-induced gene silencing. *Curr. Opin. Plant Biol.* 2, 109–113. doi: 10.1016/S1369-5266(99)80022-3

Bello-Bello, J. J., Iglesias-Andreu, L. G., Aviles-Vinas, S. A., Gomez-Uc, E., Canto-Flick, A., and Santana-Buzzy, N. (2014). Somaclonal variation in habanero pepper (Capsicum chinense Jacq.) as assessed ISSR molecular markers. *HortScience* 49, 481–485. doi: 10.21273/HORTSCI.49.4.481

Bhowmik, P., Dirpaul, J., Polowick, P., and Ferrie, A. M. R. (2011). A high throughput Brassica napus microspore culture system: influence of percoll gradient separation and bud selection on embryogenesis. *Plant Cell Tiss Organ. Cult.* 106, 359–362. doi: 10.1007/s11240-010-9913-3

Booth, J. K., and Bohlmann, J. (2019). Terpenes in Cannabis sativa – From plant genome to humans. *Plant Sci. J.* 284, 67–72. doi: 10.1016/j.plantsci.2019.03.022

Braemer, R., and Paris, M. (1987). Biotransformation of cannabinoids by a cell suspension culture of Cannabis sativa L. *Plant Cell Rep.* 6, 150–152. doi: 10.1007/BF00276675

Brock, R. D. (1971). The role of induced mutations in plant improvement. *Environ. Exp. Bot.* 11, 181–196. doi: 10.1016/S0033-7560(71)90273-0

Broertjes, C., and Van Harten, A. M. (1988). *Applied mutation breeding for vegetatively propagated crops. Developments in crop science*. The Netherlands: Elsevier, 197–204. doi: 10.1007/BF00024972

Brown, D. C., and Thorpe, T. A. (1995). Crop improvement through tissue culture. *World J. Microbiol. Biotechnol.* 11, 409–415. doi: 10.1007/BF00364616

Caplan, D. M. (2018). *Propagation and root zone management for controlled environment Cannabis production*. Ph.D. thesis, Guelph: University of Guelph.

Caplan, D., Stemeroff, J., Dixon, M., and Zheng, Y. (2018). Vegetative propagation of cannabis by stem cuttings: effects of leaf number, cutting position, rooting hormone, and leaf tip removal. *Can. J. Plant Sci.* 98, 1126–1132. doi: 10.1139/cjps-2018-0038

Casano, S., and Grassi, G. (2009). Evaluation of media for hemp (Cannabis sativa L.) in vitro propagation. *Italus Hortus* 16, 109–112.

Cascini, F., Farcomeni, A., Migliorini, D., Baldassarri, L., Boschi, I., Martello, S., et al. (2019). Highly predictive genetic markers distinguish drug type from fiber type Cannabis sativa L. *Plants* 8:496. doi: 10.3390/plants8110496

Chand, S., and Singh, A. K. (2004). Plant regeneration from encapsulated nodal segments of Dalbergia sissoo Roxb, a timber-yielding leguminous tree species. *J. Plant Physiol.* 161, 237–243. doi: 10.1078/0176-1617-01036

Chandra, S., Lata, H., and ElSohly, M. A. (2020). Propagation of Cannabis for Clinical Research: An Approach Towards a Modern Herbal Medicinal Products Development. *Front. Plant Sci.* 11:958. doi: 10.3389/fpls.2020.00958

Chandra, S., Lata, H., Khan, I. A., and ElSohly, M. A. (2008). Photosynthetic response of Cannabis sativa L. @ to variations in photosynthetic photon flux densities, temperature and CO2 conditions. *Physiol. Mol. Biol. Plants* 14, 299–306. doi: 10.1007/s12298-008-0027-x

Chandra, S., Lata, H., Khan, I. A., Mehmedic, Z., and ElSohly, M. A. (2015). Light Dependence of Photosynthesis and Water Vapour Exchange Characteristics in Different High Δ9-THC Yielding Varieties of Cannabis sativa L. *J. Appl. Res. Med. Aromat. Plants* 2, 39–47. doi: 10.1016/j.jarmap.2015.03.002

Chaohua, C., Gonggu, Z., Lining, Z., Chunsheng, G., Qing, T., Jianhua, C., et al. (2016). A rapid shoot regeneration protocol from the cotyledons of hemp (Cannabis sativa L.). *Ind. Crop Prod.* 83, 61–65. doi: 10.1016/j.indcrop.2015.12.035

Cheng, T. K. (1963). *Archeology in China, Vol. 3 Chou China*. Cambridge: W. Heffer and Sons Ltd, 36–37.

Cherney, J. H., and Small, E. (2016). Industrial Hemp in North America: Production. *Polit. Potent. Agronomy* 6:58. doi: 10.3390/agronomy6040058

Clarindo, W. R., Carvalho, C. R., and Mendonça, M. A. C. (2012). Ploidy instability in long-term in vitro cultures of Coffea arabica L. monitored by flow cytometry. *Plant Growth Regul.* 68, 533–538. doi: 10.1007/s10725-012-9740-0

Clarke, R. C., and Merlin, M. D. (2013). *Cannabis: evolution and ethnobotany*. California: Univ of California Press.

Clarke, R. C., and Merlin, M. D. (2016). Cannabis domestication, breeding history, present-day genetic diversity, and future prospects. *Critic. Rev. Plant Sci.* 6, 293–327. doi: 10.1080/07352689.2016.1267498

Conway, G. (2012). *One billion hungry: can we feed the world?*. New York, NY: Cornell University Press.

Corrie, S., and Tandon, P. (1993). Propagation of Cymbidium giganteum wall through high frequency conversion of encapsulated protocorms under in vivo and in vitro conditions. *Ind. J. Exp. Biol.* 31, 61–64.

Croom, L., Jackson, C., Vaidya, B., Parajuli, P., and Joshee, N. (2016). Thin cell layer (TCL) culture system for herbal biomass production and genetic transformation of Bacopa monnieri L. *Wettst. Am. J. Plant Sci.* 7, 1232–1245. doi: 10.4236/ajps.2016.78119

Currais, L., Loureiro, J., Santos, C., and Canhoto, J. M. (2013). Ploidy stability in embryogenic cultures and regenerated plantlets of tamarillo. *Plant Cell Tiss. Org.* 114, 149–159. doi: 10.1007/s11240-013-0311-5

Datwyler, S. L., and Weiblen, G. D. (2006). Genetic variation in hemp and marijuana (Cannabis sativa L.) according to amplified fragment length polymorphisms. *J. Forensic Sci.* 51, 371–375. doi: 10.1111/j.1556-4029.2006.00061.x

Dhekney, S. A., Li, Z. T., Grant, T. N. L., and Gray, D. J. (2016). "Somatic embryogenesis and genetic modification of Vitis," in *In Vitro Embryogenesis in higher plants. Methods in Molecular Biology*, Vol. 1359, eds M. Germana and M. Lambardi (New York, NY: Humana Press), doi: 10.1007/978-1-4939-3061-6

Dinesh-Kumar, S., Liu, Y., and Schiff, M. (2007). *Tobacco rattle virus vectors and related compositions and methods. United States Patent US7229829B2*. Alexandria, VA: United States Patent and Trademark Office.

Dufresnes, C., Jan, C., Bienert, F., Goudet, J., and Fumagalli, L. (2017). Broad-scale genetic diversity of Cannabis for forensic applications. *PLoS One* 12:170522. doi: 10.1371/journal.pone.0170522

Eftekhari, M., Alizadeh, M., Mashayekhi, K., and Asghari, H. R. (2012). In vitro propagation of four Iranian grape varieties: influence of genotype and pretreatment with arbuscular mycorrhiza. *Vitis* 51, 175–182.

Elhiti, M., Tahir, M., Gulden, R. H., Khamiss, K., and Stasolla, C. (2010). Modulation of embryo-forming capacity in culture through the expression of Brassica genes involved in the regulation of the shoot apical meristem. *J. Exp. Bot.* 61, 4069–4085. doi: 10.1093/jxb/erq222

Engelmann, F. (2004). Plant cryopreservation: progress and prospects. *In Vitro Cell. Dev.* 40, 427–433. doi: 10.1079/IVP2004541

Engelmann, F. (2014). Cryopreservation of clonal crops: a review of key parameters. *Acta Hort.* 1039, 31–39. doi: 10.17660/ActaHortic.2014.1039.2

Faeti, V., Mandolino, G., and Ranalli, P. (1996). Genetic diversity of Cannabis sativa germplasm based on RAPD markers. *Plant Breed.* 115, 367–370. doi: 10.1111/j.1439-0523.1996.tb00935.x

Farag, S., and Kayser, O. (2015). Cannabinoids production by hairy root cultures of Cannabis sativa L. *Am. J. Plant Sci.* 6:1874. doi: 10.4236/ajps.2015.61188

Farag, S., and Kayser, O. (2017). The cannabis plant: botanical aspects. In *Handbook of Cannabis and Related Pathologies*, ed. V. Preedy (Cambridge: Academic Press), 3–12.

Farahani, F., Yari, R., and Masoud, S. (2011). Somaclonal variation in Dezful cultivar of olive (Olea europaea subsp. europaea). *Gene Conserve.* 10, 216–221.

Feeney, M., and Punja, Z. K. (2003). Tissue culture and Agrobacterium-mediated transformation of hemp (Cannabis sativa L.). *In Vitro Cell. Dev. Biol.* 39, 578–585. doi: 10.1079/IVP2003454

Fellermeier, M., and Zenk, M. H. (1998). Prenylation of olivetolate by a hemp transferase yields cannabigerolic acid, the precursor of tetrahydrocannabinol. *FEBS Lett.* 427, 283–285.

Ferrie, A. M., and Mollers, C. (2011). Haploids and doubled haploids in Brassica spp. for genetic and genomic research. *Plant Cell Tiss. Org. Cult.* 104, 375–386. doi: 10.1007/s11240-010-9831-4

Fisse, J., and Andres, J. (1985). Organogenesis and biosynthesis in an in vitro culture of Cannabis sativa L. *Boletin da Academia Galega de Ciencias* 4, 57–67.

Fisse, J., Braut, F., Cosson, L., and Paris, M. (1981). Étude in vitro des capacités organogénétiques de tissus de Cannabis sativa L.; Effet de différentes substances de croissance. *Plantes Médicinales et Phytotherapi* 15, 217–223.

Flaishman, M. A., Cohen, P. R., Cohen, O., and Bocobza, S. (2019). *Method of regenerating and transforming cannabis. WIPO/PCT Patent No WO 2019/234750 A1*. Geneva: WIPO.

Flores-Sanchez, I. J., Pec, J., Fei, J., Hae-Choi, Y., Dusek, J., and Verpoorte, R. (2009). Elicitation studies in cell suspension cultures of Cannabis sativa L. *J. Biotechnol.* 143, 157–168. doi: 10.1016/j.jbiotec.2009.05.006

Alisher, T., Forster, B. P., and Jain, S. M. (2007). *Advances in haploid production in higher plants*. Dordrecht: Springer, 35–46.

Gagne, S. J., Stout, J. M., Liu, E., Boubakir, Z., Clark, S. M., and Page, J. E. (2012). Identification of olivetolic acid cyclase from Cannabis sativa reveals a unique catalytic route to plant polyketides. *Proc. Natl. Acad. Sci.* 109, 12811–12816. doi: 10.1073/pnas.1200330109

Galán-Ávila, A., García-Fortea, E., Prohens, J., and Herraiz, F. J. (2020). Development of a Direct in vitro plant regeneration protocol From Cannabis sativa L. seedling explants: developmental morphology of shoot regeneration and ploidy level of regenerated plants. *Front. Plant Sci.* 11:645. doi: 10.3389/fpls.2020.00645

Galazkajoa, J., and Niemirowicz-Szczytt, K. (2013). Review of research on haploid production in cucumber and other cucurbits. *Folia Hort.* 25, 67–78. doi: 10.2478/fhort-2013-0008

Gao, C., Xin, P., Cheng, C., Tang, Q., Chen, P., Wang, C., et al. (2014). Diversity Analysis in Cannabis sativa Based on Large-Scale Development of Expressed Sequence Tag-Derived Simple Sequence Repeat Markers. *PLoS One* 9:e110638. doi: 10.1371/journal.pone.0110638

George, E. F., Hall, M. A., and De Klerk, G. J. (eds) (2007). *Plant propagation by tissue culture*, 3rd Edn. Dordrecht: Springer, doi: 10.1007/978-1-4020-5005-3

Gilles, L. M., Khaled, A., Laffaire, J. B., Chaignon, S., Gendrot, G., Laplaige, J., et al. (2017). Loss of pollen-specific phospholipase NOT LIKE DAD triggers gynogenesis in maize. *EMBO J.* 36, 707–717. doi: 10.15252/embj.201796603

Gilmore, S., and Peakall, R. (2003). Isolation of microsatellite markers in Cannabis sativa L. (marijuana). *Mol. Ecol. Notes* 3, 105–107.

Gloss, D. (2015). An overview of products and bias in research. *Neurotherapeutics* 12, 731–734. doi: 10.1007/s13311-015-0370-x

Government of Canada (2018). *Cannabis Act. S.C. 2018, c.16*. Canada: Government of Canada.

Grudzinska, M., and Solarska, E. (2004). The elimination of virus and Hop Latent Viroid from Hop (Humulus Lupulus L.) in Poland. *Acta Hortic.* 668, 149–152. doi: 10.17660/ActaHortic.2005.668.19

Grudzinska, M., Solarska, E., Czubacka, A., Przybys, M., and Fajbus, A. (2006). Elimination of Hop Latent Viroid from Hop plants by cold treatment and meristem tip culture. *Phytopathol. Pol.* 40, 21–30.

Grulichova, M., Mendel, P., Lalge, A. B., Slamova, N., Trojan, V., Vyhnanek, T., et al. (2017). Effect of different phytohormones on growth and development of micropropagated Cannabis sativa L. *Mendel Net.* 2017, 618–623.

Hakki, E. E., Uz, E., Sag, A., Atasoy, S., and Akkaya, S. M. (2003). Genotyping of Cannabis sativa L. accessions from Turkey using RAPD and AFLP markers. *Forensic Sci. Int.* 136:31.

Hanus, L. O., Meyer, S. M., Munoz, E., Taglialatela-Scafati, O., and Appendino, G. (2016). Phytocannabinoids: a unified critical inventory. *Nat. Prod. Rep.* 33, 1357–1392. doi: 10.1039/c6np00074f

Hartsel, S. C., Loh, W. H. T., and Robertson, L. W. (1983). Biotransformation of cannabidiol to Cannabielsoin by suspension cultures of Cannabis sativa and Saccharum officinarum. *Planta Med.* 48, 17–19. doi: 10.1055/s-2007-969870

Heitrich, A., and Binder, M. (1982). Identification of (3R,4R)-gD as an isolation artefact of cannabinoid acids formed by callus cultures of Cannabis sativa L. *Experientia* 38, 898–899. doi: 10.1007/BF01953640

Hemphill, J. K., Turner, J. C., and Mahlberg, P. G. (1978). Studies on growth and cannabinoid composition of callus derived from different strains of Cannabis sativa. *Lloydia* 41, 453–462.

Henry, P., Hilyard, A., Johnson, S., and Orser, C. (2018). Predicting chemovar cluster and variety verification in vegetative cannabis accessions using targeted single nucleotide polymorphisms. *PeerJ Prepr.* 6:e27442v1. doi: 10.7287/peerj.preprints.27442v1

Hillig, K. W. (2004). A multivariate analysis of allozyme variation in 93 Cannabis accessions from the VIR germplasm collection. *J. Ind. Hemp.* 9, 5–22. doi: 10.1300/J237v09n02_02

Hillig, K. W. (2005). Genetic evidence for speciation in Cannabis (Cannabaceae). *Genet. Resour. Crop Evol.* 52, 161–180. doi: 10.1007/s10722-003-4452-y

Hilling, K. W., and Mahlberg, P. G. (2004). A chemotaxonomic analysis of cannabinoid variationin Cannabis (Cannabaceae). *Am. J. Bot.* 91, 966–975.

Hussain, A., Qarshi, I. A., Nazir, H., and Ullah, I. (2012). Plant Tissue Culture: current status and opportunities. *InTech Open* 28:50568. doi: 10.5772/50568

Hussain, S. H. F. (2014). *Cannabinoids production in Cannabis sativa L. An in vitro approach*. Ph.D. thesis, Dortmund: Technischen Universität Dortmund, 1–138.

Hvoslef-Eide, A. K., and Preil, W. (2005). *Liquid culture systems for in vitro plant propagation*. Dordrecht: Springer, doi: 10.1007/1-4020-3200-5

Itokawa, H., Takeya, K., and Akasu, M. (1975). Studies on the constituents isolated from the callus of Cannabis sativa L. *Shoyakugaku Zasshi* 29, 106–112.

Itokawa, H., Takeya, K., and Mihashi, S. (1977). Biotransformation of Cannabinoid precursor and related alcohols by suspension cultures of callus induced from Cannabis sativa L. *Chem. Pharm. Bull.* 25, 1941–1946. doi: 10.1248/cpb.25.1941

Jekkel, Z., Heszky, L. E., and Ali, A. H. (1989). Effect of different cryoprotectants and transfer temperatures on the survival rate of hemp (Cannabis sativa L.) cell suspension in deep freezing. *Acta Biol. Hung.* 40, 127–136.

Jevremovic, S., Subotic, A., Miljkovic, D., Trifunovic, M., Petric, M., and Cingel, A. (2012). Clonal fidelity of Chrysanthemum cultivars after long term micropropagation by stem segment culture. *Acta Hortic.* 961, 211–216. doi: 10.17660/ActaHortic.2012.961.25

Jiang, H., Wang, L., Merlin, M. D., Clarke, R. C., Pan, Y., Zhang, Y., et al. (2016). Ancient Cannabis burial shroud in a Central Eurasian cemetery. *Econ. Bot.* 70, 213–221. doi: 10.1007/s12231-016-9351-1

Jiang, Y., Zunmin, X. I. A., Tang, Y., Han, Q., and Han, C. (2015). Preliminary studies on the tissue culture of Cannabis sativa L. (Industrial hemp). *Agricult. Sci Technol.* 16, 923–925.

Jinek, M., Chylinski, K., Fonfara, I., Hauer, M., Doudna, J. A., and Charpentier, E. (2012). A programmable dual-RNA–guided DNA endonuclease in adaptive bacterial immunity. *Science* 337, 816–821. doi: 10.1126/science.1225829

Joyce, S. M., Cassells, A. C., and Jain, S. M. (2003). Stress and aberrant phenotypes in vitro culture. *Plant Cell Tiss. Org.* 74, 103–121. doi: 10.1023/A:1023911927116

Karp, A. (1994). "Origins, causes and uses of variation in plant tissue cultures," in *Plant cell and tissue culture*, eds I. K. Vasil and T. A. Thorpe (Dordrecht: Kluwer Academic Publishers), 139–152. doi: 10.1007/978-94-017-2681-8

Khan, S., Saeed, B., and Kauser, N. (2011). Establishment of genetic fidelity of in vitro raised banana plantlets. *Pak. J. Bot.* 43, 233–242.

Kodym, A., and Leeb, C. J. (2019). Back to the roots: protocol for the photoautotrophic micropropagation of medicinal cannabis. *Plant Cell Tiss. Org.* 138, 399–402. doi: 10.1007/s11240-019-01635

Kojoma, M., Iida, O., Makino, Y., Sekita, S., and Satake, M. (2002). DNA fingerprinting of Cannabis sativa using inter-simple sequence repeat (ISSR) amplification. *Planta Med.* 68, 60–63. doi: 10.1055/s-2002-19875

Krishna, H., Alizadeh, M., Singh, D., Singh, U., Chauhan, N., Eftekhari, M., et al. (2016). Somaclonal variations and their applications in horticultural crops improvement. *Biotech* 6, 1–18. doi: 10.1007/s13205-016-0389-7

Lata, H., Chandra, S., Khan, I. A., and ElSohly, M. A. (2010b). Cannabis sativa L. Micropropagation in temporary immersion bioreactor system. *Planta Med.* 76:9. doi: 10.1055/s-0030-1251771

Lata, H., Chandra, S., Khan, I., and ElSohly, M. A. (2009a). Propagation through alginate encapsulation of axillary buds of Cannabis sativa L. an important medicinal plant. *Physiol. Mol. Biol. Plants* 15, 79–86. doi: 10.1007/s12298-009-0008-8

Lata, H., Chandra, S., Khan, I., and ElSohly, M. A. (2009b). Thidiazuron-induced high-frequency direct shoot organogenesis of Cannabis sativa L. *Vitr. Cell. Dev. Biol. Plant* 45, 12–19. doi: 10.1007/s11627-008-9167-5

Lata, H., Chandra, S., Khan, I., and ElSohly, M. A. (2010a). Assessment of genetic stability of micropropagated Cannabis sativa plants by ISSR markers. *Planta Med.* 76, 97–100. doi: 10.1055/s-0029-1185945

Lata, H., Chandra, S., Khan, I., and ElSohly, M. A. (2010c). High frequency plant regeneration from leaf derived callus of high D9-tetrahydrocannabinol yielding Cannabis sativa L. *Planta Med.* 76, 1629–1633. doi: 10.1055/s-0030-1249773

Lata, H., Chandra, S., Khan, I., and Elsohly, M. A. (2017). Micropropagation of Cannabis sativa L.—an update. *Cannabis sativa L. Bot. Biotechnol.* 2017, 285–297. doi: 10.1007/978-3-319-54564-6_13

Lata, H., Chandra, S., Mehmedic, Z., Khan, I., and ElSohly, M. A. (2011). In vitro germplasm conservation of high Tetrahydocannab- inol yielding elite clones of Cannabis sativa L. under slow growth conditions. *Acta Physiol. Plant.* 34, 743–750. doi: 10.1007/s11738-011-0874-x

Lata, H., Chandra, S., Techen, N., Khan, I. A., and ElSohly, M. A. (2016). In vitro mass propagation of Cannabis sativa L.: A protocol refinement using novel aromatic cytokinin meta-topolin and the assessment of eco-physiological, biochemical and genetic fidelity of micropropagated plants. *J. Appl. Res. Med. Aromat. Plants.* 3, 18–26. doi: 10.1016/j.jarmap.2015.12.001

Laverty, K. U., Stout, J. M., Sullivan, M. J., Shah, H., Gill, N., Holbrook, L., et al. (2019). A physical and genetic map of Cannabis sativa identifies extensive rearrangements at the THC/CBD acid synthase loci. *Genome Res.* 29, 146–156. doi: 10.1101/gr.242594.118

Lei, R., Qiao, W., Fan, H., and Jiang, H. (2015). A simple and effective method to encapsulate tobacco mesophyll protoplasts to maintain cell viability. *MethodX* 2, 24–32. doi: 10.1016/j.mex.2014.11.004

Li, H. (1974). An archaeological and historical account of cannabis in China. *Econ. Bot.* 28, 437–448. doi: 10.1007/BF02862859

Lineberger, R. D. (1983). Shoot proliferation, rooting, and transplant survival of tissue-culture 'Hally-Jolivette' cherry. *HortScience* 18, 182–185. doi: 10.1007/BF00044251

Liu, Y., Schiff, M., and Dinesh-Kumar, S. (2002). Virus-induced gene silencing in tomato. *Plant J.* 31, 777–786. doi: 10.1046/j.1365-313x.2002.01394.x

Loh, W. H. T., Hartsel, S. C., and Robertson, L. W. (1983). Tissue culture of Cannabis sativa L. and in vitro biotransformation of phenolics. *Zeitschrift fuer P?anzenphysiol.* 111, 395–400. doi: 10.1016/S0044-328X(83)80003

Mackinnon, L., Mcdougall, G., Aziz, N., and Millam, S. (2000). *Progress towards transformation of fibre hemp. Scottish Crop Research Institute Annual Report 2000/2001*. Dundee: Scottish Crop Research Institute.

Malik, M. R., Wang, F., Dirpaul, J. M., Zhou, N., Polowick, P. L., Ferrie, A. M., et al. (2007). Transcript profiling and identification of molecular markers for early microspore embryogenesis in Brassica napus. *Plant Physiol.* 144, 134–154.

Mandolino, G., and Ranalli, P. (1999). *Advances in biotechnological approaches for hemp breeding and industry*. Haworth: Advances in hemp research, doi: 10.1201/9781498705820

McKey, D., Elias, M., Pujol, M. E., and Duputié, A. (2010). The evolutionary ecology of clonally propagated domesticated plants. *N. Phytol.* 186, 318–332. doi: 10.1111/j.1469-8137.2010.03210.x

McPartland, J. M. (1996). A review of Cannabis diseases. *J. Int. Hemp Associat.* 3, 19–23.

McPartland, J. M. (2018). Cannabis systematics at the levels of family, genus, and species. *Cannabis Cannabinoid Res.* 3, 203–212.

Mechoulam, R. (1986). "The pharmacohistory of Cannabis sativa," in *Cannabinoids as Therapeutic Agents*, ed. R. Mechoulam (Boca Raton, FL: CRC Press), 1–19. doi: 10.1201/9780429260667-1

Mendoza, M. A., Mills, D. K., Lata, H., Chandra, S., ElSohly, M. A., and Almirall, J. R. (2009). Genetic individualization of Cannabis sativa by short tandem repeat multiplex system. *Anal. Bioanal. Chem.* 393, 719–726. doi: 10.1007/s00216-008-2500-3

Micke, A. (1999). "Mutation in plant breeding," in *Breeding in crop plants – mutations and in vitro mutation breeding*, eds B. A. Siddiqui, S. Khan (New Delhi: Kalyani Publication), 1–19. doi: 10.1007/978-1-4614-7028-1

Miguel, C., and Marum, L. (2011). An epigenetic view of plant cells cultured in vitro: somaclonal variation and beyond. *J. Exp. Bot.* 62, 3713–3725. doi: 10.1093/jxb/err155

Mirmasoumi, M., Azadi, P., Sharafi, A., Ntui, V. O., and Mii, M. (2013). Simple protocol for plant regeneration of Lilium ledebouriiusing transverse thin cell layer. *Prog. Biol. Sci.* 3, 117–122. doi: 10.22059/PBS.2013.35828

Mordhorst, A. P., Hartog, M. V., El-Tamer, M. K., Laux, T., and De Vries, S. C. (2002). Somatic embryogenesis from Arabidopsis shoot apical meristem mutants. *Planta* 214, 829–836. doi: 10.1007/s00425-001-0700-6

Mori, K. (1971). Production of virus-free carnations by means of meristem culture. *Netherl. Plant Pathol. J.* 6, 1–7. doi: 10.1007/BF02102383

Morimoto, S., Tanaka, Y., Sasaki, K., Tanaka, H., Fukamizu, T., Shoyama, Y., et al. (2007). Identification and characterization of cannabinoids that induce

cell death through mitochondrial permeability transition in Cannabis leaf cells. *J. Biol. Chem.* 282, 20739–20751. doi: 10.1074/jbc.M700133200

Movahedi, M., Ghasemi-Omran, V. O., and Torabi, S. (2015). The effect of different concentrations of TDZ and BA on in vitro regeneration of Iranian Cannabis (Cannabis sativa) using cotyledon and epicotyl explants. *J. Plant Mol. Breed.* 3, 20–27. doi: 10.22058/JPMB.2015.15371

Murashige, T. (1977). "Plant cell and organ cultures as horticultural practices," in *Proceedings of the Symposium on Tissue Culture for Horticultural Purposes*, (Ghent: ISHS), doi: 10.17660/ActaHortic.1977.78.1

Murthy, B. N. S., Murch, S. J., and Saxena, P. K. (1995). Thidiazuron-induced somatic embryogenesis in intact seedlings of peanut (Arachis hypogaeay). Endogenous growth regulator levels and significance of cotyledons. *Physiol. Plant.* 94, 268–276.

Musio, S., Müssig, J., and Amaducci, S. (2018). Optimizing hemp fiber production for high performance composite applications. *Front. Plant Sci.* 9:1702. doi: 10.3389/fpls.2018.01702

National Clean Plant Network (2020). *NCPN Factsheets, Brochures and Posters*. Auburn, AL: National Clean Plant Network.

Nhut, D. T., Teixeira, da Silva, J. A., Van Le, B., and Thanh Van, K. T. (2003). "Thin cell Layer (TCL) Morphogenesis as a powerful tool in woody plant and fruit crop micropropagation and biotechnology, floral genetics and genetic transformation," in *Micropropagation of woody trees and fruits. Forestry Sciences*, Vol. 75, eds S. M. Jain and K. Ishii (Dordrecht: Springer), 783–814. doi: 10.1007/978-94-010-0125-0_27

Nwauzoma, A. B., and Jaja, E. T. (2013). A review of somaclonal variation in plantain (Musa spp): mechanisms and applications. *J. Appl. Biosci.* 67, 5252–5260. doi: 10.4314/jab.v67i0.95046

Nyende, A. B., Schittenhelm, S., Mix-Wagner, G., and Greef, J. M. (2003). Production, storability, and regeneration of shoot tips of potato (Solanum tuberosum L.) encapsulated in calcuim alginate hollow beads. *In Vitro Cell. Dev. Biol. Plant.* 39, 540–544. doi: 10.1079/IVP2003442

Oladosu, Y., Rafii, M. Y., Abdullah, N., Hussin, G., Ramli, A., Rahim, H. A., et al. (2016). Principle and application of plant mutagenesis in crop improvement: A review. *Biotechnol. Biotechnol.* 30, 1–16. doi: 10.1080/13102818.2015.1087333

Osborne, D. J., and McManus, M. T. (2005). *Hormones signals and target cells in plant development*. Cambridge: Cambridge University Press, doi: 10.1017/CBO9780511546228

Page, L. S. R. G., Monthony, A. S., and Jones, A. M. P. (2020). Basal media optimization for the micropropagation and callogenesis of Cannabis sativa. *bioRxiv* preprint. doi: 10.1101/2020.02.07.939181

Pathak, H., and Dhawan, V. (2012). ISSR assay for ascertaining genetic fidelity of micropropagated plants of apple rootstock Merton 793. *In Vitro Cell. Dev. Biol. Plant.* 48, 137–143. doi: 10.1007/s11627-011-9385-0

Pence, V. C. (2011). Evaluating costs for the in vitro propagation and preservation of endangered plants. *In Vitro Cell. Dev. Biol. Plant.* 47, 176–187. doi: 10.1007/s11627-010-9323-6

Pijut, P. M., Beasley, R. R., Lawson, S. S., Palla, K. J., Stevens, M. E., and Wang, Y. (2012). In vitro propagation of tropical hardwood tree species—a review (2001–2011). *Propag. Ornam. Plants* 12, 25–51.

Piomelli, D., and Russo, E. B. (2016). The Cannabis sativa versus Cannabis indica debate: An interview with Ethan Russo, MD. *Cannabis Cannabinoid Res.* 1, 44–46. doi: 10.1089/can.2015.29003.ebr

Pistelli, L., Giovannini, A., Ruffoni, B., Bertoli, A., and Pistelli, L. (2010). "Hairy root cultures for secondary metabolites production," in *Bio-Farms for Nutraceuticals*, eds G. Rea, M. T. Giardi, and B. Berra (Boston, MA: Springer), 167–184. doi: 10.1007/978-1-4419-7347-4

Piunno, K. F., Golenia, G., Boudka, E. A., Downey, C., and Jones, A. M. (2019). Regeneration of shoots from immature and mature inflorescences of Cannabis sativa. *Can. J. Plant Sci.* 99, 556–559. doi: 10.1139/cjps-2018-0308

Plawuszewski, M., Lassocinski, W., and Wieglus, K. (2005). "Regeneration of polish cultivars of monoecious hemp (Cannabis sativa L.) grown in vitro," in *Renewable resources and plant biotechnology*, eds R. Kozlowski, E. Gennady, and F. Pudel (New York, NY: Nova Science Publishers Inc.), 149–154.

Popova, E., Shukla, M., and Kim, H. H. (2015). "Plant cryopreservation for biotechnology and breeding," in *Advances in plant breeding strategies: breeding, biotechnology and molecular Tools*, eds J. M. AI-Khayri, S. M. Jain, and D. V. Johnson (Berlin: Springer International Publishing).

Potter, D. J. (2009). *The propagation, characterisation and optimisation of Cannabis sativa L. as a phytopharmaceutical*. Ph.D. thesis, London: King's College London, 255.

Rai, M. K., Jaiswal, V. S., and Jaiswal, U. (2008). Encapsulation of shoot tips of guava (*Psidium guajava* L.) for short-term storage and germplasm exchange. *Sci. Hortic.* 118, 33–38. doi: 10.1016/j.scienta.2008.05.017

Rea, K. A., Casaretto, J. A., Al-Abdul-Wahid, M. S., Sukumaran, A., Geddes-McAlister, J., Rothstein, S. J., et al. (2019). Biosynthesis of cannflavins A and B from Cannabis sativa L. *Phytochem* 164, 162–171. doi: 10.1016/j.phytochem.2019.05.009

Ren, J., Wu, P., Trampe, B., Tian, X., Lübberstedt, T., and Chen, S. (2017). Novel technologies in doubled haploid line development. *Plant Biotechnol. J.* 15, 1361–1370. doi: 10.1111/pbi.12805

Richez-Dumanois, C., Braut-Boucher, F., Cosson, L., and Paris, M. (1986). Multiplication vegetative in vitro du chanvre (Cannabis sativa L.) application a la conservation des clones selectionnes. *Agronomie* 6, 487–495.

Rihan, H. Z., Kareem, F., El-Mahrouk, M. E. E., and Fuller, M. P. (2017). Artificial seeds principle, aspect, and applications. *Agronomy* 7:7040071. doi: 10.3390/agronomy7040071

Rodriguez-Leyva, D., and Pierce, G. N. (2010). The cardiac and hemostatic effects of dietary hempseed. *Nutr. Metab.* 7, 1–9. doi: 10.1186/1743-7075-7-32

Rotherham, D., and Harbison, S. A. (2011). Differentiation of drug and non-drug Cannabis using single nucleotide polymorphism (SNP) assay. *Forensic Sci. Int.* 207, 193–197. doi: 10.1016/j.forsciint.2010.10.006

Sakai, A., and Engelmann, F. (2007). Vitrification, encapsulation-vitrification and droplet-vitrification: a review. *Cryo. Lett.* 28, 151–172.

Sallie, J. V., and Jones, O. P. (2015). The culture of shoot tips of hop (Humulus lupulus L.) to eliminate viruses. *J. Hortic. Sci.* 44, 281–284. doi: 10.1080/00221589.1969.11514310

Sato, M., Hosokawa, M., and Doi, M. (2011). Somaclonal variation is induced de novo via the tissue culture process: a study quantifying mutated cells in Saintpaulia. *PLoS One* 6:23541. doi: 10.1371/journal.pone.0023541

Sawler, J., Stout, J. M., Gardner, K. M., Hudson, D., Vidmar, J., Butler, L., et al. (2015). The Genetic structure of Marijuana and Hemp. *PLoS One* 26:e0133292. doi: 10.1371/journal.pone.0133292

Schachtsiek, J., Hussain, T., Azzouhri, K., Kayser, O., and Stehle, F. (2019). Virus-induced gene silencing (VIGS) Cannabis sativa L. *Plant Methods* 15:157. doi: 10.1186/s13007-019-0542-5

Schultes, R. E., Klein, W. M., Plowman, T., and Lockwood, T. E. (1974). Cannabis: an example of taxonomic neglect. *Botanic. Museum Leaflets* 23, 337–367.

Senthil-Kumar, M., and Mysore, K. S. (2014). Tobacco rattle virus–based virus-induced gene silencing in Nicotiana benthamiana. *Nat. Protoc.* 9, 1549–1562. doi: 10.1038/nprot.2014.092

Sharp, W. R., Sondahl, M. R., Caldas, L. S., and Maraffa, S. B. (1980). The physiology of in vitro asexual embryogenesis. *Hortic. Rev.* 2, 268–310. doi: 10.1002/9781118060759.ch6

Shen, H. J., Chen, J. T., Chung, H. H., and Chang, W. C. (2018). Plant regeneration via direct somatic embryogenesis from leaf explants of Tolumnia Luise Elmore 'Elsa.'. *Bot. Stud.* 59:4. doi: 10.1186/s40529-018-0220-3

Shew, A. M., Nalley, L. L., Snell, H. A., Nayga, R. M., and Dixon, B. L. (2018). CRISPR versus GMOs: Public acceptance and valuation. *Glob. Food Secur.* 19, 71–80. doi: 10.1016/j.gfs.2018.10.005

Sirikantaramas, S., Morimoto, S., Shoyama, Y., Ishikawa, Y., Wada, Y., Shoyama, Y., et al. (2004). The gene controlling marijuana psychoactivity: molecular cloning and heterologous expression of Delta1-tetrahydrocannabinolic acid synthase from Cannabis sativa L. *J. Biol. Chem.* 279, 39767–39774. doi: 10.1074/jbc.M403693200

Sirkowski, E. (2012). *Marked Cannabis for indicating medical Marijuana. US Patent 20120311744*. Alexandria, VA: United States Patent and Trademark Office.

Sluis, C. J. (2005). "Integrating automation technologies with commercial micropropagation," in *Plant Tissue Culture Engineering*, eds S. D. Gupta and Y. Ibaraki (Berlin: Springer), 231–251. doi: 10.1007/978-1-4020-3694-1

Slusarkiewicz-Jarzina, A., Ponitka, A., and Kaczmarek, Z. (2005). Influence of cultivar, explant source and plant growth regulator on callus induction and plant regeneration of Cannabis sativa L. *Acta Biol. Craco. Ser. Bot.* 47, 145–151.

Small, E. (2004). "Narcotic Plants as sources of medicinal, nutraceuticals, and functional foods,". In *Proceedings of the International Symposium on the Development of Medicinal Plants*. Canada: Agriculture and Agri-Food, 11–67.

Small, E. (2015). Evolution and Classification of Cannabis sativa (Marijuana, Hemp) in Relation to Human Utilization. *Bot. Rev.* 81, 189–294.

Small, E. (2017). "Classification of Cannabis sativa L. in relation to agricultural, biotechnological, medical and recreational utilization," in *Cannabis sativa L. - Botany and Biotechnology*, eds S. Chandra, H. Lata, and M. ElSohly (Cham: Springer).

Small, E., and Cronquist, A. (1976). A practical and natural taxonomy for cannabis. *Taxon* 25, 405–435. doi: 10.2307/1220524

Small, E., Jul, P. Y., and Lefkovitch, L. P. (1976). A numerical taxonomic analysis of Cannabis with special reference to species. *Syst. Bot.* 1, 67–84. doi: 10.2307/2418840

Smulders, M., and de Klerk, G. (2011). Epigenetics in plant tissue culture. *Plant Growth Regul.* 63, 137–146. doi: 10.1007/s10725-010-9531-4

Smýkalová, I., Vrbová, M., Cvečková, M., Plackova, L., Zukauskaite, A., Zatloukal, M., et al. (2019). The effects of novel synthetic cytokinin derivatives and endogenous cytokinins on the in vitro growth responses of hemp (Cannabis sativa L.) explants. *Plant Cell Tiss. Org.* 139, 381–394. doi: 10.1007/s11240-019-01693

Soriano, M., Li, H., and Boutilier, K. (2013). Microspore embryogenesis: establishment of embryo identity and pattern in culture. *Plant Reprod.* 26, 181–196. doi: 10.1007/s00497-013-0226-7

Spanò, R., Bottalico, G., Corrado, A., Campanale, A., Di Franco, A., and Mascia, T. (2018). A protocol for producing virus-free artichoke genetic resources for conservation, breeding, and production. *Agriculture* 8:36. doi: 10.3390/agriculture8030036

Stout, J. M., Boubakir, Z., Ambrose, S. J., Purves, R. W., and Page, J. E. (2012). The hexanoyl-CoA precursor for cannabinoid biosynthesis is formed by an acyl-activating enzyme in Cannabis sativa trichomes. *Plant J.* 71, 353–365. doi: 10.1111/j.1365-313X.2012.04949.x

Sun, S., Zhong, J., Li, S., and Wang, X. (2013). Tissue culture-induced somaclonal variation of decreased pollen viability in torenia (Torenia fournieri Lind.). *Bot. Stud.* 54:36. doi: 10.1186/1999-3110-54-36

Szarejko, I. (2003). "Doubled haploid mutant production," in *Doubled haploid production in crop plants*, eds M. Maluszynski, K. J. Kasha, B. P. Forster, and I. Szarejko (Dordrecht: Springer), doi: 10.1007/978-94-017-1293-4_48

Taura, F., Morimoto, S., and Shoyama, Y. (1995). First direct evidence for the mechanism of Δ1-tetrahydrocannabinolic acid biosynthesis. *J. Am. Chem. Soc.* 117, 9766–9767. doi: 10.1021/ja00143a024

Taura, F., Sirikantaramas, S., Shoyama, Y., Shoyama, Y., and Morimoto, S. (2007a). Phytocannabinoids in Cannabis sativa: recent studies on biosynthetic enzymes. *Chem. Biodivers.* 4, 1649–1663. doi: 10.1002/cbdv.200790145

Taura, F., Sirikantaramas, S., Shoyama, Y., Yoshikai, K., Shoyama, Y., and Morimoto, S. (2007b). Cannabidiolic-acid synthase, the chemotype-determining enzyme in the fiber-type Cannabis sativa. *FEBS Lett.* 581, 2929–2934. doi: 10.1016/j.febslet.2007.05.043

Taura, F., Tanaka, S., Taguchi, C., Fukamizu, T., Tanaka, H., Shoyama, Y., et al. (2009). Characterization of olivetol synthase, a polyketide synthase putatively involved in cannabinoid biosynthetic pathway. *FEBS Lett.* 583, 2061–2066. doi: 10.1016/j.febslet.2009.05.024

Teixeira da Silva, J. A., Tran Thanh, Van, K., Biondi, S., Nhut, D. T., et al. (2007). Thin cell layers: developmental building blocks in ornamental biotechnology. *Floricult. Ornamental Biotech.* 1, 1–13.

Thacker, X., Thomas, K., Fuller, M., Smith, S., and DuBois, J. (2018). Determination of optimal hormone and mineral salts levels in tissue culture media for callus induction and growth of industrial hemp (Cannabis sativa L.). *J. Agric. Sci.* 9, 1250–1268. doi: 10.4236/as.2018.910088

Uchendu, E., Lata, H., Chandra, S., Khan, I., and ElSohly, M. A. (2019). Cryopreservation of shoot tips of elite cultivars of Cannabis sativa L. by droplet vitrification. *Med. Cannabis cannabinoids* 2, 29–34. doi: 10.1159/000496869

Veliky, I. A., and Genest, K. (1972). Growth and metabolites of Cannabis sativa cell suspension cultures. *Lloydia* 35, 450–456.

Wahby, I., Arráez-Román, D., Segura-Carretero, A., Ligero, F., Caba, J. M., and Fernández-Gutiérrez, A. (2006). Analysis of choline and atropine in hairy root cultures of Cannabis sativa L. by capillary electrophoresis-electrospray mass spectrometry. *Electrophoresis* 27, 2208–2215. doi: 10.1002/elps.200500792

Wahby, I., Caba, J. M., and Ligero, F. (2013). Agrobacterium infection of hemp (Cannabis sativa L.): establishment of hairy root cultures. *J. Plant Interact.* 8, 312–320. doi: 10.1080/17429145.2012.746399

Wahby, I., Caba, J. M., and Ligero, F. (2017). "Hairy root culture as a biotechnological tool in C. sativa," in *Cannabis sativa L. Botany and Biotechnology*, eds M. ElSohly, H. Lata, and C. Suman (Cham: Springer), 299–317. doi: 10.1007/978-3-319-54564-6

Wang, M., Wang, Y. H., Avula, B., Radwan, M. M., Wanas, A. S., van Antwerp, J., et al. (2016). Decarboxylation study of acidic cannabinoids: A novel approach using ultra-high-performance supercritical fluid chromatography/photodiode array-mass spectrometry. *Cannabis Cannabinoid Res.* 1, 262–271. doi: 10.1089/can.2016.0020

Wang, P. J., and Charles, A. (1991). "Micropropagation through meristem culture," in *High-Tech and Micropropagation I. Biotechnology in Agriculture and Forestry*, Vol. 17, ed. Y. P. S. Bajaj (Berlin: Springer), doi: 10.1007/978-3-642-76415-8

Wang, R., He, L. S., Xia, B., Tong, J. F., Li, N., and Peng, F. (2009). A micropropagation system for cloning of hemp (Cannabis Sativa L.) by shoot tip culture. *Pak. J. Bot.* 41, 603–608.

Wargent, E. T., Zaibi, M. S., Silvestri, C., Hislop, D. C., Stocker, C. J., Stott, C. G., et al. (2013). The cannabinoid Δ9-tetrahydrocannabivarin (THCV) ameliorates insulin sensitivity in two mouse models of obesity. *Nutr. Diabetes* 3:e68. doi: 10.1038/nutd.2013.9

Watt, M. P., Thokoane, N. L., Mycock, D., and Blakeway, F. (2000). In vitro storage of Eucalyptus grandis germplasm under minimal growth conditions. *Plant Cell Tiss. Org.* 61, 161–164. doi: 10.1023/A:1006447506869

Whitton, P. A. (2019). *Method of production of phytocannabinoids for use in medical treatments. US Patent 10,477,791 B2.* Alexandria, VA: USPTO.

Whitton, P. A. (2020). *Method of production of phytocannabinoids for use in medical treatments. US Patent US2020/0060111 A1*. Alexandria, VA: USPTO.

Wielgus, K., Luwanska, A., Lassocinski, W., and Kaczmarek, Z. (2008). Estimation of Cannabis sativa L. tissue culture conditions essential for callus induction and plant regeneration. *J. Nat. Fibers* 5, 199–207. doi: 10.1080/15440470801976045

Withers, L. A., and Engelmann, F. (1997). *In vitro conservation of plant genetic resources*. The Netherlands: Springer.

Wu, H., Qu, X., Dong, Z., Luo, L., Shao, C., Forner, J., et al. (2020). WUSCHEL triggers innate antiviral immunity in plant stem cells. *Science* 370, 227–231. doi: 10.1126/Science.abb7360

Zayova, E., Vassilevska, I. R., Kraptchev, B., and Stoeva, D. (2010). Somaclonal variations through indirect organogenesis in eggplant (Solanum melongena L.). *Biol. Divers. Conserv.* 3, 1–5.

Conflict of Interest: ME and RG were employed by the company Haplotech Inc.

The remaining authors declare that the research was conducted in the absence of any commercial or financial relationships that could be construed as a potential conflict of interest.

frontiers in Plant Science

ORIGINAL RESEARCH
published: 11 May 2021
doi: 10.3389/fpls.2021.646020

Cannabis Yield, Potency, and Leaf Photosynthesis Respond Differently to Increasing Light Levels in an Indoor Environment

*Victoria Rodriguez-Morrison†, David Llewellyn† and Youbin Zheng**

School of Environmental Sciences, University of Guelph, Guelph, ON, Canada

Since the recent legalization of medical and recreational use of cannabis (*Cannabis sativa*) in many regions worldwide, there has been high demand for research to improve yield and quality. With the paucity of scientific literature on the topic, this study investigated the relationships between light intensity (LI) and photosynthesis, inflorescence yield, and inflorescence quality of cannabis grown in an indoor environment. After growing vegetatively for 2 weeks under a canopy-level photosynthetic photon flux density (PPFD) of ≈425 $\mu mol \cdot m^{-2} \cdot s^{-1}$ and an 18-h light/6-h dark photoperiod, plants were grown for 12 weeks in a 12-h light/12-h dark "flowering" photoperiod under canopy-level PPFDs ranging from 120 to 1,800 $\mu mol \cdot m^{-2} \cdot s^{-1}$ provided by light emitting diodes. Leaf light response curves varied both with localized (i.e., leaf-level) PPFD and temporally, throughout the flowering cycle. Therefore, it was concluded that the leaf light response is not a reliable predictor of whole-plant responses to LI, particularly crop yield. This may be especially evident given that dry inflorescence yield increased linearly with increasing canopy-level PPFD up to 1,800 $\mu mol \cdot m^{-2} \cdot s^{-1}$, while leaf-level photosynthesis saturated well-below 1,800 $\mu mol \cdot m^{-2} \cdot s^{-1}$. The density of the apical inflorescence and harvest index also increased linearly with increasing LI, resulting in higher-quality marketable tissues and less superfluous tissue to dispose of. There were no LI treatment effects on cannabinoid potency, while there were minor LI treatment effects on terpene potency. Commercial cannabis growers can use these light response models to determine the optimum LI for their production environment to achieve the best economic return; balancing input costs with the commercial value of their cannabis products.

Keywords: cannabis sativa, light intensity, light response curve, cannabinoid, terpene, PPFD, sole source

OPEN ACCESS

Edited by:
Donald Lawrence Smith, McGill University, Canada

Reviewed by:
Mark Lefsrud, McGill University, Canada
Youngseok Lim, Kangwon National University, South Korea
Dhiraj Vyas, Indian Institute of Integrative Medicine (CSIR), India

***Correspondence:**
Youbin Zheng
yzheng@uoguelph.ca

†These authors have contributed equally to this work

Specialty section:
This article was submitted to Crop and Product Physiology, a section of the journal Frontiers in Plant Science

Received: *24 December 2020*
Accepted: *01 March 2021*
Published: *11 May 2021*

Citation:
Rodriguez-Morrison V, Llewellyn D and Zheng Y (2021) Cannabis Yield, Potency, and Leaf Photosynthesis Respond Differently to Increasing Light Levels in an Indoor Environment. Front. Plant Sci. 12:646020. doi: 10.3389/fpls.2021.646020

INTRODUCTION

Drug-type *Cannabis sativa* (i.e., genotypes grown for their high cannabinoid content; hereafter, cannabis) is often produced indoors to allow complete control of environmental conditions, which is important for producing consistent medicinal plants and products (United Nations Office on Drugs Crime, 2019; Zheng, 2020). Total reliance on electrical lighting for plant production gives growers the capability to manipulate crop morphology, yield, and quality using light. However, lighting-related costs comprise ≈60% of total energy used for indoor cannabis production (Mills, 2012; Evergreen Economics, 2016); making crop lighting one of the most substantial input costs

for growing cannabis indoors. With recent nationwide legalization in Canada (among many other regions worldwide), energy demand for indoor cannabis production is expected to increase rapidly as the industry intensifies production to address rising demand (Sen and Wyonch, 2018).

There are many factors that govern the cost of producing photosynthetically active radiation (PAR) for indoor cannabis production. These factors include: the capital and maintenance costs of lighting fixtures and related infrastructure, efficiency of converting electricity into PAR (usually referred to as PAR efficacy; in units of $\mu mol_{(PAR)} \cdot J^{-1}$), management of excess heat and humidity, and uniformity of PAR distribution within the plant canopy. The most common lighting technologies used for indoor cannabis production are high intensity discharge (e.g., high pressure sodium) and light emitting diodes (LED) (Mills, 2012; Evergreen Economics, 2016). These technologies have widely varying spectrum, distribution, PAR efficacy, and capital costs. However, regardless of the lighting technology used, the dominant factor that regulates the cost of crop lighting is the target canopy-level light intensity (LI).

One common precept in controlled-environment agriculture production is that crop yield responds proportionally to increasing LI; i.e., the so-called "1% rule" whereby 1% more PAR equals 1% greater yield (Marcelis et al., 2006). On a per-leaf basis, this principle is clearly limited to lower light intensities, since light use efficiency [i.e., maximum quantum yield; QY, $\mu mol_{(CO2)} \cdot \mu mol_{(PAR)}^{-1}$] of all photosynthetic tissues begins to decline at LI well below their light saturation points (LSP; i.e., the LI at peak photosynthetic rate) (Posada et al., 2012). However, in indoor-grown cannabis, it is conceivable that whole-plant photosynthesis will be maximized when LI at the upper canopy leaves are near their LSP. This is partly attributable to the inter-canopy attenuation of PAR from self-shading; allowing lower-canopy foliage to function within the range of LIs where their respective light use efficiencies are optimized (Terashima and Hikosaka, 1995). This may be especially relevant to indoor production, where relatively small changes in distance from the light source can impart substantial differences in foliar LI (Niinemets and Keenan, 2012). Further, distinguished from many other indoor-grown crops, cannabis foliage appears to tolerate very high LI, even when exposed to photosynthetic photon flux densities (PPFD) that are much higher than what they have been acclimated to Chandra et al. (2015).

There is a paucity of peer-reviewed studies that have related LI to cannabis potency and yield (e.g., mass of dry, mature inflorescence per unit area and time). Perhaps the most referenced studies reported aspects of single-leaf photosynthesis of several cultivars and under various PPFD, CO_2 concentration, and temperature regimes (Lydon et al., 1987; Chandra et al., 2011, 2015). These works have demonstrated that cannabis leaves have very high photosynthetic capacity. However, they have limited use in modeling whole canopy photosynthesis or predicting yield because single-leaf photosynthesis is highly variable; depending on many factors during plant growth such as: leaf age, their localized growing environments (e.g., temperature, CO_2, and lighting history), and ontogenetic stage (Murchie et al., 2002; Zheng et al., 2006; Carvalho et al., 2015; Bauerle et al., 2020). While lighting vendors have long relied on cannabis leaf photosynthesis studies to sell more light fixtures to cannabis growers, their models are only tangentially related to whole-canopy photosynthesis, growth, and (ultimately) yield (Kirschbaum, 2011).

Some forensic studies have utilized various methods to develop models to estimate crop yield from illicit indoor cannabis production (Toonen et al., 2006; Vanhove et al., 2011; Potter and Duncombe, 2012; Backer et al., 2019). These models used an array of input parameters (e.g., planting density, growing area, crop nutrition factors, etc.) but, they relied on "installed wattage" (i.e., $W \cdot m^{-2}$) as a proxy for LI. It is notable that reporting yield as $g \cdot W^{-1}$ (i.e., $g \cdot m^{-2}/W \cdot m^{-2}$) overlooks the instantaneous time factor inherent in power units (i.e., $W = J \cdot s^{-1}$). A more appropriate yield metric would also account for the length of the total lighting time throughout the production period (i.e., $h \cdot d^{-1} \times d$), thus factoring out the time units resulting in yield per unit energy input (e.g., $g \cdot kWh^{-1}$). Further, area-integrated power does not directly correlate to the canopy-level light environment due to myriad unknowns, such as hang height, light distribution, and fixture efficacy. It is therefore impossible to accurately ascertain canopy-level LI in these models. Eaves et al. (2020) reported linear relationships between canopy-level LI (up to 1,500 $\mu mol \cdot m^{-2} \cdot s^{-1}$) and yield; however, they had only one LI treatment above 1,000 $\mu mol \cdot m^{-2} \cdot s^{-1}$. Further, they reported substantial inter-repetition variability in their yield models, which indicates that factors other than LI may have limited crop productivity in some circumstances. While methodological deficiencies in these studies may limit the confident quantitative extrapolation of their results to production environments, it is striking that none of these studies reported evidence of saturation of inflorescence yield at very high LI.

These studies all demonstrate the exceptionally high capacity that cannabis has for converting PAR into biomass. However, there are also clear knowledge gaps in cannabis' photosynthesis and yield responses to increasing LI. Further, cannabis products are very high-value commodities relative to other crops grown in indoor environments. This means that producers may be willing to accept substantially higher lighting-related input costs in order to promote higher yields in limited growing areas. However, maximizing yield regardless of cost is not a feasible business model for most cannabis producers; rather there is a trade-off between input costs and crop productivity by selecting the optimum canopy-level LI (among other inputs) that will maximize net profits. Further complicating matters,

Abbreviations: NCER, Net CO_2 exchange rate; PPFD, photosynthetic photon flux; A_{sat}, light-saturated NCER; LSP, light saturation point; QY, maximum quantum yield; CCI, chlorophyll content index; SLW, specific leaf weight; LED, light emitting diode; DLI, daily light integral; PAR, photosynthetically active radiation; DW, dry weight; SD, standard deviation; SE, standard error; RH, relative humidity; Δ^9-THC, Δ-9-tetrahydrocannabinol; Δ^9-THCA, Δ-9-tetrahydrocannabinolic acid; TΔ^9-THC, total equivalent Δ^9-tetrahydrocannabinol; CBD, cannabidiol; TCBD, total equivalent cannabidiol; CBG, cannabigerol; CBGA, cannabigerolic acid; TCBG, total equivalent cannabigerol.

Non-Standard Abbreviations: LPPFD, localized PPFD at the measured leaf; APPFD, average PPFD at the plant apex integrated over time; LNCER, NCER at LPPFD; LI, light intensity; TLI, total light integral; LRC, light response curve; CB, deep-water culture basin; UDL, under detection limit.

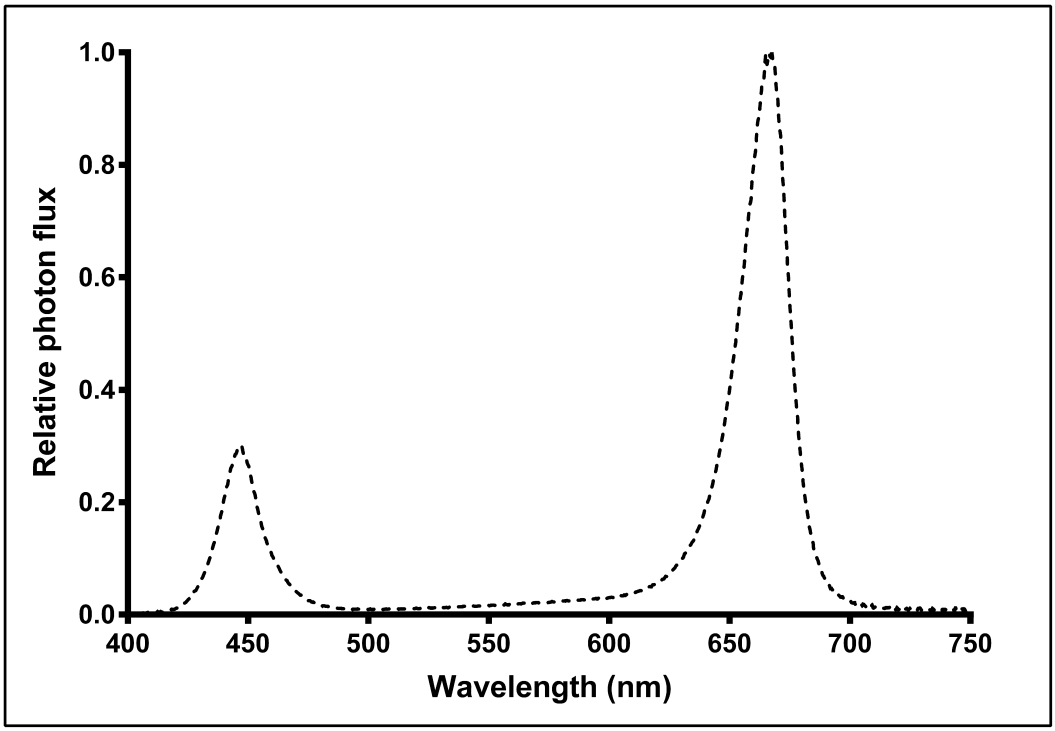

FIGURE 1 | Relative spectral photon flux distribution of Pro-650 (Lumigrow) light-emitting diode (LED) fixtures.

producers must balance fixed costs which do not vary with crop productivity (such as property tax, lease rates, building security, and maintenance, etc.) and variable costs (such as the aforementioned lighting-related costs among other crop inputs) which can have dramatic impacts on crop productivity and yield (Vanhove et al., 2014). Since indoor crop lighting is a compromise between input costs and crop productivity, it is critical for growers to select the optimum light intensity for their respective production environment and business models.

The objectives of this study were to establish the relationships between canopy-level LI, leaf-level photosynthesis, and yield and quality of drug-type cannabis. We investigated how plant growth stage and localized foliar PPFD (LPPFD; i.e., instantaneous PPFD at leaf-level) affected photosynthetic parameters and leaf morphology, and how growing cannabis at average canopy-level PPFDs (APPFD; i.e., lighting history) ranging from 120 to 1,800 $\mu mol \cdot m^{-2} \cdot s^{-1}$ affected plant morphology, yield, and quality of mature marketable inflorescence. The results of this study will assist the indoor cannabis industry to determine how much PAR cannabis growers should be providing to the crop canopy in order to maximize profits while minimizing energy use within their specific production scenarios.

MATERIALS AND METHODS

The trial area consisted of 2 adjacent deep-water culture basins (CB) located in an indoor cannabis production facility in Southern Ontario, Canada. Each CB (14.6 × 2.4 m) consisted of 24 parallel polystyrene rafts (0.6 × 2.4 m), each containing holes for 16 plant pots, oriented in 2 rows with 30-cm spacing both within- and between-rows. This spacing provided for 384 plants to be evenly spaced within each CB, at a density of 0.09 m^2/plant.

Above each CB were 3 racks of LED fixtures (Pro-650; Lumigrow, Emeryville, CA, USA), with each rack consisting 2 rows of 4 fixtures each; arranged such that all 24 fixtures were uniformly-spaced (1.2 m apart, on-center) relative to each other and centered over the footprint of the CB. Each rack of fixtures was height-adjustable via a system of pulleys and cables, such that the hang-height of the 8 fixtures in each rack could be adjusted in unison. Each fixture contained dimmable spectrum channels for blue (B, peak 455 nm), white (broad-spectrum 5,000K) and red (R, peak 660 nm) which could be individually controlled, wirelessly, through Lumigrow's SmartPAR software. The photon flux ratio of B (400–500 nm), green (G, 500–600 nm), and R (600–700 nm) was B18:G5:R77. Relative spectral photon flux distribution (**Figure 1**) was measured using a radiometrically calibrated spectrometer (UV-VIS Flame-S-XR; Ocean Optics, Dunedin, FL, USA) coupled to a CC3 cosine-corrector attached to a 1.9 m × 400 μm UV-Vis optical fiber.

Experimental Design

The experiment was conducted using a gradient design, whereby plants grown in a common environment were exposed to a broad range of canopy-level PPFDs with a high level of spatial variability across the CB. Individual plants were assigned APPFD levels based on rigorous spatial and temporal evaluations

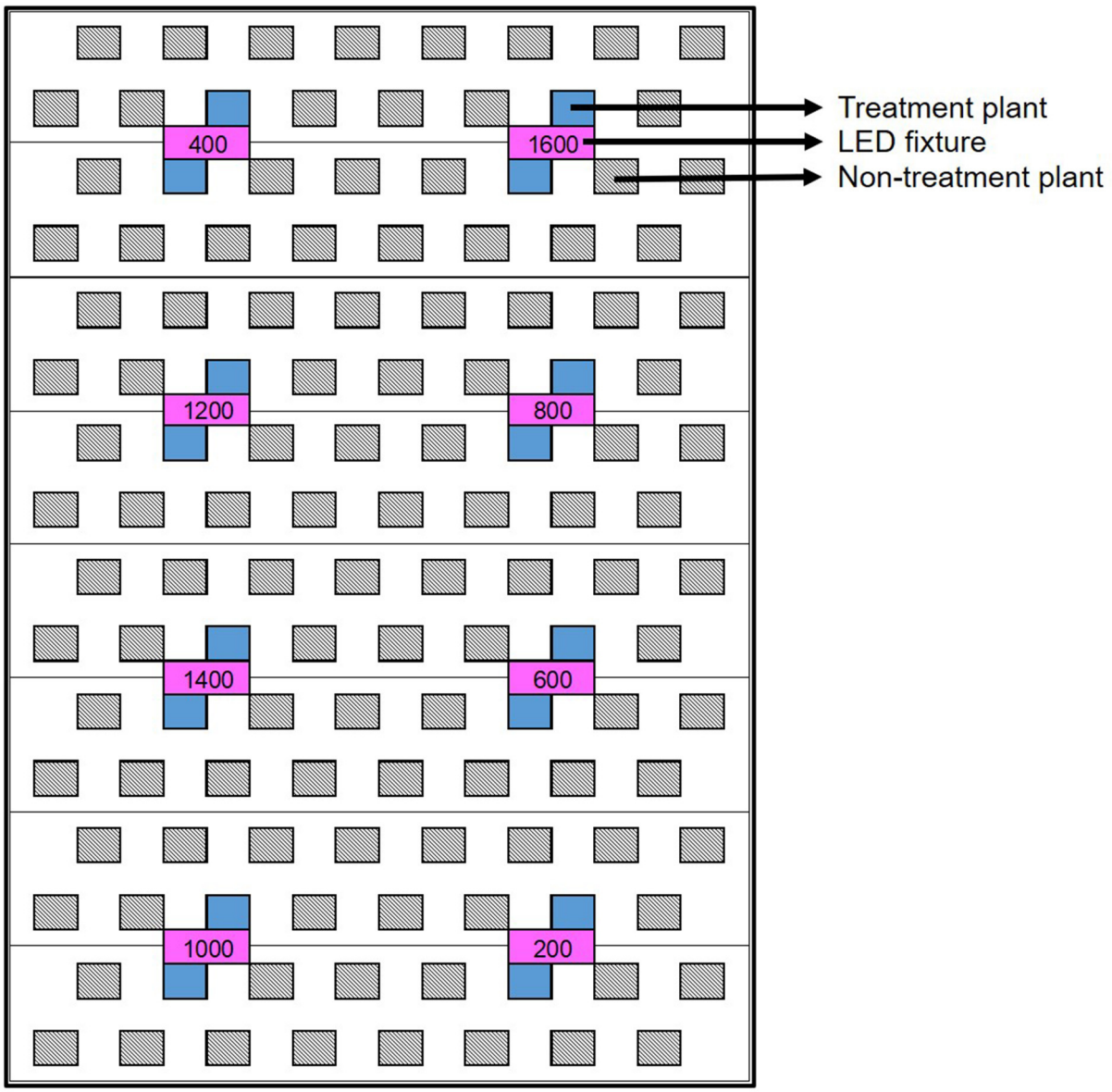

FIGURE 2 | Schematic of a single light rack (8 LED fixtures, in magenta) above one third of a deep-water culture basin (CB). The entire growing area consists of 6 of these light racks. Within each light rack, each of the 8 target PPFD levels (i.e., the "treatments") are randomly assigned to one fixture (i.e., plot). This results in a RCBD-type of experimental layout, comprised of 8 treatments × 6 replications. However, each treatment plant (in blue) was assigned an average photosynthetic photon flux density (APPFD), reflecting the average canopy-level light intensity measured throughout the trial. The APPFD levels were used as the independent variable in subsequent analyses of plant growth, physiology and harvest metrics. Each plot was surrounded by non-treatment plants (diagonal lines) to ensure uniform growing environment and normal planting density.

of LI (explained below). Gradient designs can outperform traditional "treatment × replication" experimental designs when evaluating plants' responses to a continuous variable such as LI (Kreyling et al., 2018). While they are arduous to setup and monitor, gradient designs have been successfully used to establish LI effects within other controlled-environment production scenarios (Bredmose, 1993, 1994; Jones-Baumgardt et al., 2019).

At its outset, the experiment was arranged as a randomized complete block design (RCBD) with 6 blocks of 8 PPFD target levels: 200, 400, 600, 800, 1,000, 1,200, 1,400, and 1,600 $\mu mol \cdot m^{-2} \cdot s^{-1}$, to facilitate setup. Each block consisted of a single rack of LED fixtures, with the PPFD target levels randomly assigned to individual fixtures (i.e., plots) within each rack. The two plants located most directly below each fixture were assessed experimentally (**Figure 2**). PPFD was measured at the

apex of each plant using a portable spectroradiometer (LI-180; LI-COR Biosciences, Lincoln, NE, USA). The initial hang height of each rack was determined by the maximum height whereby ≈1,600 $\mu mol \cdot m^{-2} \cdot s^{-1}$ could be achieved at the apical meristem of the tallest plant in the highest LI plot. The other treatment levels were subsequently achieved through dimming; targeting the prescribed PPFD at the apical meristem of the tallest plant in each plot while maintaining a uniform photon flux ratio of B18:G5:R77 in the entire CB. Plant height and apical meristematic PPFD were measured twice weekly until vegetative growth ceased (5 weeks after the start of the 12-h photoperiod), and weekly thereafter until harvest. The prescribed intensity levels in each block were reset each time plant height was measured, first by raising the rack of fixtures to achieve the target PPFD at the apical meristem of the tallest plant in the 1,600 $\mu mol \cdot m^{-2} \cdot s^{-1}$ plot and then adjusting the intensity settings of the remaining plots accordingly. The trial ran from the beginning of the flowering stage (i.e., when the 12-h flowering photoperiod was initiated) until harvest, for a total of 81 days (nearly 12 weeks).

While the underlying experimental arrangement was based on a RCBD organization, all analyses were performed as regressions with LI as the continuous, independent variable.

PPFD Levels

While the prescribed target PPFD levels were maintained at the apical meristem at the tallest plant within each plot on regular intervals, these values were not accurate proxies for the actual PPFD intensity dynamics experienced by each plant throughout the trial due to variability in individual plant height (on intra- and inter-plot bases), growth rates, and the lengths of the time periods between PPFD measurements. To account for these temporal dynamics in apical meristematic PPFD, total light integrals (TLIs, $mol \cdot m^{-2}$) were calculated for each plant over the total production time and then back-calculated to APPFD or daily light integral (DLI, $mol \cdot m^{-2} \cdot d^{-1}$). The TLIs were based on the product of the average PPFD level measured at the start and end of each measurement interval and the length of time the lights were on during each measurement interval. These interim light integrals were then aggregated to form a TLI for each plant and divided by the total production time in seconds (i.e., the product of the daily photoperiod and the number of days). The resulting APPFD levels were then used as the independent variable (i.e., X-axis) in regressions of LI vs. various growth, yield, and quality parameters. TLI can also be used in yield evaluations whereby the relationship between yield and TLI becomes a direct measure of production efficacy on a quantum basis (e.g., $g \cdot mol^{-1}$). This relationship can be converted to an energy-basis ($g \cdot kWh^{-1}$), if the fixture efficacy ($\mu mol \cdot J^{-1}$) and spatial distribution efficiency (i.e., proportion of photon output from fixtures that reach the target growing area) are known.

Plant Culture

Cuttings were taken from mother plants of the 'Stillwater' cultivar on 1 Aug. and 15 Aug. 2019 and rooted in stone wool cubes under 100 $\mu mol \cdot m^{-2} \cdot s^{-1}$ of fluorescent light for 14 d and then transplanted into a peat-based medium in 1-gallon plastic pots and grown under ≈425 $\mu mol \cdot m^{-2} \cdot s^{-1}$ of LED light, comprised of a mixture of Pro-325 (Lumigrow) and generic phosphor-converted white LEDs (unbranded) for an additional 14 d. The apical meristems were removed (i.e., "topped") from the first batch of clones, 10 d after transplant, and the second batch were not topped. Propagation and vegetative growth phases both had 18-h photoperiods. The first CB (CB1) was populated from the first batch of clones on 29 Aug. 2019 and the second CB (CB2) was populated from the second batch of clones on 12 Sept. 2019. In each case, 48 uniform and representative plants were selected from the larger populations of clones and placed in the plots to be evaluated experimentally. In CB1, the experimental plants initially had either 9 or 10 nodes and ranged in height (from growing medium surface to shoot apex) from 34 to 48 cm. In CB2 the experimental plants initially had either 12 or 13 nodes and ranged in height from 41 to 65 cm. Once the plants were moved to the CBs, the daily photoperiod switched to 12 h, from 06:30 HR to 18:30 HR.

Plant husbandry followed the cultivator's standard operating procedures except for the differences in canopy-level PPFD. Canopy-level air temperature, relative humidity (RH), and carbon dioxide (CO_2) concentration were monitored on 600-s intervals throughout the trial with a logger (Green Eye model 7788; AZ Instrument Corporation, Taiwan). The air temperature, RH, and CO_2 concentrations were (mean ± SD) 25.3 ± 0.4°C, 60.5 ± 4.8%, and 437 ± 39 ppm during the day (i.e., lights on) and 25.2 ± 0.3°C, 53.1 ± 3.3%, and 479 ± 42 ppm during the night. A common nutrient solution is circulated through both CBs. The nutrient concentrations in the aquaponic solution were sampled weekly and analyzed at an independent laboratory (A&L Canada; London, ON, Canada). The nutrient element concentrations ($mg \cdot L^{-1}$) in the aquaponic system were (mean ± SD, $n = 11$): 170 ± 22 Ca, 86 ± 8.2 S, 75 ± 15 N, 57 ± 5 Mg, 32 ± 4 P, 23 ± 8 K, 250 ± 32 Cl, 0.27 ± 0.1 Fe, 0.18 ± 0.07 Zn, 0.050 ± 0.02 Mn, 0.031 ± 0.006 B, and 0.028 ± 0.004 Cu. Mo was reported as below detection limit (i.e., <0.02 $mg \cdot L^{-1}$) throughout the trial. The concentrations ($mg \cdot L^{-1}$) of non-essential nutrient elements were 170 ± 18 Na and 6.7 ± 0.7 Si. The aquaponic solution was aerated with an oxygen concentrator and the pH and EC were 6.75 ± 0.2 and 1.77 ± 0.15 $mS \cdot cm^{-1}$, respectively.

Leaf Photosynthesis

Quantifications of leaf-level gas exchange of leaflets on the youngest, fully-expanded fan leaves were performed on 64 plants (32 plants per CB) each, in weeks 1, 5, and 9 after the initiation of the 12-h photoperiod using a portable photosynthesis machine (LI-6400XT; LI-COR Biosciences, Lincoln, NE, USA), equipped with the B and R LED light source (6400-02B; LI-COR Biosciences). The Light Curve Auto-Response subroutine was used to measure net carbon exchange rate [NCER; $\mu mol_{(CO2)} \cdot m^{-2} \cdot s^{-1}$] at PPFD levels of: 2,000, 1,600, 1,400, 1,200, 1,000, 800, 600, 400, 200, 150, 100, 75, 50, 25, and 0 $\mu mol \cdot m^{-2} \cdot s^{-1}$. Leaflets were exposed to 2,000 $\mu mol \cdot m^{-2} \cdot s^{-1}$ for 180 s prior to starting each light response curve (LRC) and then progressed sequentially from highest to lowest PPFD to ensure stomatal opening was not a limitation of photosynthesis (Singsaas et al., 2001). The leaf chamber setpoints were

26.7°C (block temperature), 400 ppm CO_2, and 500 $\mu mol \cdot s^{-1}$ airflow. The localized PPFD (LPPFD) at each leaflet was measured immediately prior to the LRC measurement using the LI-180. The light-saturated net CO_2 exchange rate [A_{sat}; $\mu mol_{(CO2)} \cdot m^{-2} \cdot s^{-1}$], localized NCER (LNCER; i.e., the NCER at LPPFD), maximum quantum yield [QY; $\mu mol_{(CO2)} \cdot \mu mol^{-1}_{(PAR)}$], and light saturation point [LSP; $\mu mol_{(PAR)} \cdot m^{-2} \cdot s^{-1}$] were determined for each measured leaflet using Prism (Version 6.01; GraphPad Software, San Diego, CA, USA) with the asymptotic LRC model: $y = a + b \cdot e^{(c \cdot x)}$ (Delgado et al., 1993) where y, x, a, and *e* represent NCER, PPFD, A_{sat}, and Euler's number, respectively. The LNCER of each leaflet was calculated by substituting the measured LPPFD into its respective LRC model. The QY was calculated as the slope of the linear portion of the LRC (i.e., at PPFD $\leq$200 $\mu mol \cdot m^{-2} \cdot s^{-1}$). The LSP is defined as the PPFD level where increasing LI no longer invokes a significant increase in NCER. The LSP for each LRC was determined using the methods described by Lobo et al. (2013) by evaluating the change in NCER (ΔNCER) over 50 $\mu mol_{(PAR)} \cdot m^{-2} \cdot s^{-1}$ increments, continuously along the LRC, until the ΔNCER reached a threshold value, which was determined from the prescribed measurement conditions and performance specifications of the LI-6400XT. Briefly, the minimum significant difference in CO_2 concentration between sample and reference measurements is 0.4 ppm (LI-COR Biosciences, 2012). Therefore, given the setup parameters of the leaf chamber, a ΔNCER of $\leq$0.33 $\mu mol_{(CO2)} \cdot m^{-2} \cdot s^{-1}$ over a 50 $\mu mol_{(PAR)} \cdot m^{-2} \cdot s^{-1}$ increment indicated the LSP.

The ratio of variable to maximum fluorescence (F_v/F_m) emitted from photosystem II (PSII) in dark-acclimated leaves exposed to a light-saturating pulse is an indicator of maximum quantum yield of PSII photochemistry (Murchie and Lawson, 2013). Immediately after each LRC, the leaflet was dark acclimated for $\approx$900 s and then F_v/F_m was measured with a fluorometer (FluorPen FP 100; Drasov, Czech Republic). Chlorophyll content index (CCI) was measured on three fan leaflets from leaves at the bottom and top of each plant in weeks 1, 5, and 9 using a chlorophyll meter (CCM-200; Opti-Sciences, Hudson, NH, USA). The CCI measurements from upper and lower tissues, respectively, were averaged on a per-plant basis for each measurement period.

Leaf Morphology

On day 35, one leaf from each plant was removed from node 13 (counting upwards from the lowest node) in CB1 and node 15 from CB2, ensuring that the excised leaves developed under their respective LPPFD. A digital image of each leaf was taken using a scanner (CanoScan LiDE 25; Canon Canada Inc., Brampton, ON, Canada) at 600 dpi resolution and then the leaves were oven-dried (Isotemp Oven Model 655G; Fisher Scientific, East Lyme, CT, USA), singly, to constant weight at 65°C. The images were processed using ImageJ 1.42 software (National Institute of Health; https://imagej.nih.gov/ij/download.html) to determine leaf area (LA). The dry weights (DW) of scanned leaves were measured using an analytical balance (MS304TS/A00; Mettler-Toledo, Columbus, OH, USA). Specific leaf weight (SLW; $g \cdot m^{-2}$) was determined using the following formula: DW/LA.

Yield and Quality

After 81 d, the stems of each plant was cut at substrate level and the aboveground biomass of each plant was separated into three parts: apical inflorescence, remaining inflorescence, and stems and leaves (i.e., non-marketable biomass), and weighed using a digital scale (Scout SPX2201; OHAUS Corporation, Parsippany, NJ, USA). Since the plants from CB2 had the apical meristem removed, the inflorescence from the tallest side branch was considered the apical inflorescence. The length (L) and circumference (C; measured at the midpoint) of each apical inflorescence were also measured. Assuming a cylindrical shape, the density of the apical inflorescence ($g \cdot cm^{-3}$) was calculated using the formula: apical inflorescence density = fresh weight/$\{\pi \cdot [C/(2 \cdot \pi)^2] \cdot L\}$. The apical inflorescences from 22 representative plants from CB1 were air dried at 15°C and 40% RH for 10 d until they reached marketable weight (i.e., average moisture content of $\approx$11%), determined using a moisture content analyzer (HC-103 Halogen Moisture Analyzer; Mettler-Toledo, Columbus, OH, USA). This ensured that the apical inflorescence tissues selected for analysis of secondary metabolites followed the cultivator's typical post-harvest treatment. The apical inflorescences from CB1 were homogenized on a per-plant basis and $\approx$2-g sub-samples from each plant was processed by an independent laboratory (RPC Science & Engineering; Fredericton, NB, Canada) for potency [$mg \cdot g^{-1}_{(DW)}$] using solvent extraction followed by ultra-high-performance liquid chromatography with variable wavelength detection (HPLC-VWD) for cannabinoids and gas chromatography with mass spectrometry detection (GC-MSD) for terpenes. Total equivalent Δ-9-tetrahydrocannabinol (Δ^9-THC), cannabidiol (CBD), and cannabigerol potencies were determined by assuming complete carboxylation of the acid-forms of the respective cannabinoids, whose concentrations were adjusted by factoring out the acid-moiety from the molecular weight of each compound [e.g., total Δ^9-THC = (Δ^9-THCA $\times$ 0.877) + Δ^9-THC]. The separated aboveground tissues from 16 representative plants in each CB were oven-dried (Isotemp Oven Model 655G) to constant weight at 65°C to determine LI treatment effects on moisture content, which were then used to determine DW of all harvested materials. The harvest index was calculated as the ratio of total inflorescence DW (hereafter, yield) to the total aboveground DW, on a per-plant basis.

Data Processing and Analysis

On per-CB and per-week bases, each model from the leaf photosynthesis measurements (i.e., A_{sat}, LSP, LNCER, and QY) were subjected to non-linear regression using the PROC NLMIXED procedure (SAS Studio Release 3.8; SAS Institute Inc., Cary, NC), with the LPPFD of each measured leaf as the independent variable, to determine the best-fit models after outliers were removed. In each case, best-fit models were selected based on the lowest value for the Akaike information criterion (AICc). If there were no LI treatment effects on a

given parameter, then means (± SD) were calculated. Best-fit models for F_v/F_m and CCI were similarly determined, using LPPFD and APPFD (from the start of the trial up to the time of measurement), respectively, as the independent variable. On a per-week basis, A_{sat}, LSP, LNCER, QY, F_v/F_m, and CCI data from CB1 and CB2 were pooled if the 95% CI of each element of the respective best-fit models for the two CBs overlapped, and best-fit models for pooled datasets were then recalculated. The PROC GLIMMIX Tukey-Kramer test was used ($P \leq 0.05$) on the resulting models (including means) to determine if there were differences between the measurement periods (i.e., weeks). If there were any measurement period effects on any element in the models, then weekly models for the respective parameters were reported.

Computed parameters from single-time measurements (SLW, apical inflorescence density, yield, and harvest index) were grouped per CB, using the APPFD (at the time of measurement) to define each datapoint within each CB and PROC NLMIXED was used to evaluate the best fit model for each parameter using the AICc. Parameter means were computed (on per-CB bases) when there were no LI treatment effects. If there were LI treatment effects on a given parameter, datasets from CB1 and CB2 were pooled if the 95% confidence intervals (95% CI) of each element of the respective best-fit models for the two CBs overlapped and best-fit models for pooled datasets were then recalculated. For parameters with no LI treatment effects, differences between CBs were evaluated using the 95% CI's of their respective means. For a given parameter, if the 95% CIs the parameter means for the 2 CBs overlapped, then the data was pooled and new parameter means were calculated and presented. Cannabinoids and terpenes from CB1 were modeled, with APPFD as the independent variable, using PROC NLMIXED to evaluate the best-fit model for each parameter using the AICc. Best-fit models or parameter means were reported.

RESULTS

No CB effects were found in any leaf photosynthesis, leaf morphology, and post-harvest parameters; therefore, CB1 and CB2 data were pooled for the development of all models except secondary metabolites, which were only measured in CB1. In contrast, many of the parameters that were repeated over time (i.e., in weeks 1, 5, and 9) showed differences between weeks; whereby the different weeks were modeled separately. Note also that the week-over-week ranges of LPPFD varied as the plants progressed through their ontogeny, since self-shading from upper tissues resulted in decreases in maximum LPPFD of

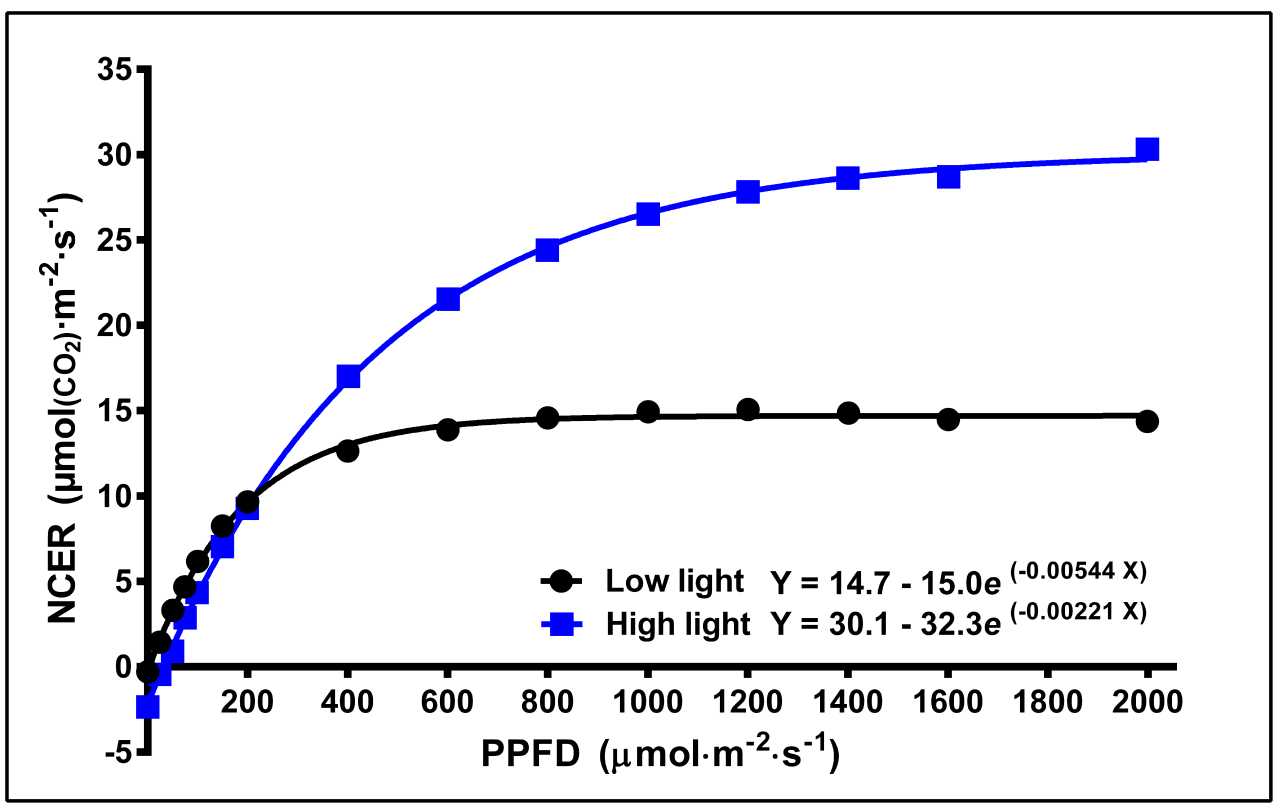

FIGURE 3 | Typical light response curves [net CO_2 exchange rate (NCER) response to light intensity] of the youngest fully-expanded fan leaves of *Cannabis sativa* 'Stillwater' grown under either low or high localized photosynthetic photon flux densities (LPPFD). The low and high LPPFD were 91 and 1,238 $\mu mol \cdot m^{-2} \cdot s^{-1}$, respectively. Measurements were made during week 5 after the initiation of the 12-h photoperiod.

leaves selected for photosynthesis measurements. Nevertheless, a consistent range of APPFDs range was maintained throughout the trial.

Leaf Photosynthesis

Leaf light response curves constructed under different LI and at different growth stages (week 1, 5, and 9) generally demonstrated the trends that the A_{sat} and LSP were higher for plants grown under high vs. low LPPFD (**Figures 3**, **4A,B**), especially after the plants had acclimated to their new lighting environments (i.e., weeks 5 and 9). There were no LPPFD effects on A_{sat} in week 1, with a mean (± SE, $n = 52$) of 23.9 ± 0.90 $\mu mol_{(CO2)} \cdot m^{-2} \cdot s^{-1}$ (**Figure 4A**). The A_{sat} in weeks 5 and 9 (**Figure 4A**) and LSP in weeks 1, 5, and 9 (**Figure 4B**) increased linearly with increasing LPPFD. At low LPPFD, the highest LSP was in week 1. The slopes of the A_{sat} and LSP models were similar in weeks 5 and 9, but the Y-intercepts for both parameters were approximately twice as high in week 5 vs. week 9. LNCER increased linearly with increasing LPPFD in weeks 1, 5, and 9 (**Figure 4C**) with the steepest and shallowest slopes coming in weeks 5 and 1, respectively. The LNCER model in week 9 had a substantially lower Y-intercept than the other 2 weeks. As evidenced by the projected intersection of the A_{sat} and LNCER models in week 5 (i.e., at LPPFD of 1,532 $\mu mol \cdot m^{-2} \cdot s^{-1}$), the maximum LPPFD in week 5 (i.e., 1,370 $\mu mol \cdot m^{-2} \cdot s^{-1}$) was nearly sufficient to saturate the photosynthetic apparatus at the top of the canopy. There were no LPPFD effects on QY, but the mean QY in weeks 1 and 5 were higher than week 9. The mean (± SE) QY were 0.066 ± 0.0013 ($n = 54$), 0.068 ± 0.0005 ($n = 60$), and 0.058 ± 0.0008 ($n = 63$) $\mu mol_{(CO2)} \cdot \mu mol^{-1}_{(PAR)}$ in weeks 1, 5, and 9 respectively. The F_v/F_m decreased linearly with increasing LPPFD in all three measurement periods (**Figure 4D**).

Chlorophyll Content Index and Plant Morphology

There were no LI treatment effects on CCI either at the top or bottom of the canopy, however within in each week, the upper canopy CCI were higher than the lower canopy. Additionally, the CCI in the upper and lower canopy was higher in week 1 vs. weeks 5 and 9. The CCI (means ± SE, $n = 91$) were 67.1 ± 0.80, 55.8 ± 2.2, and 52.0 ± 2.1 in the upper canopy and 46.3 ± 1.1, 31.1 ± 0.86, and 31.5 ± 1.1 in the lower canopy, in weeks 1, 5, and 9, respectively. The SLW increased linearly from 35.4 to 58.1 $g \cdot m^{-2}$ as APPFD (calculated based on the respective

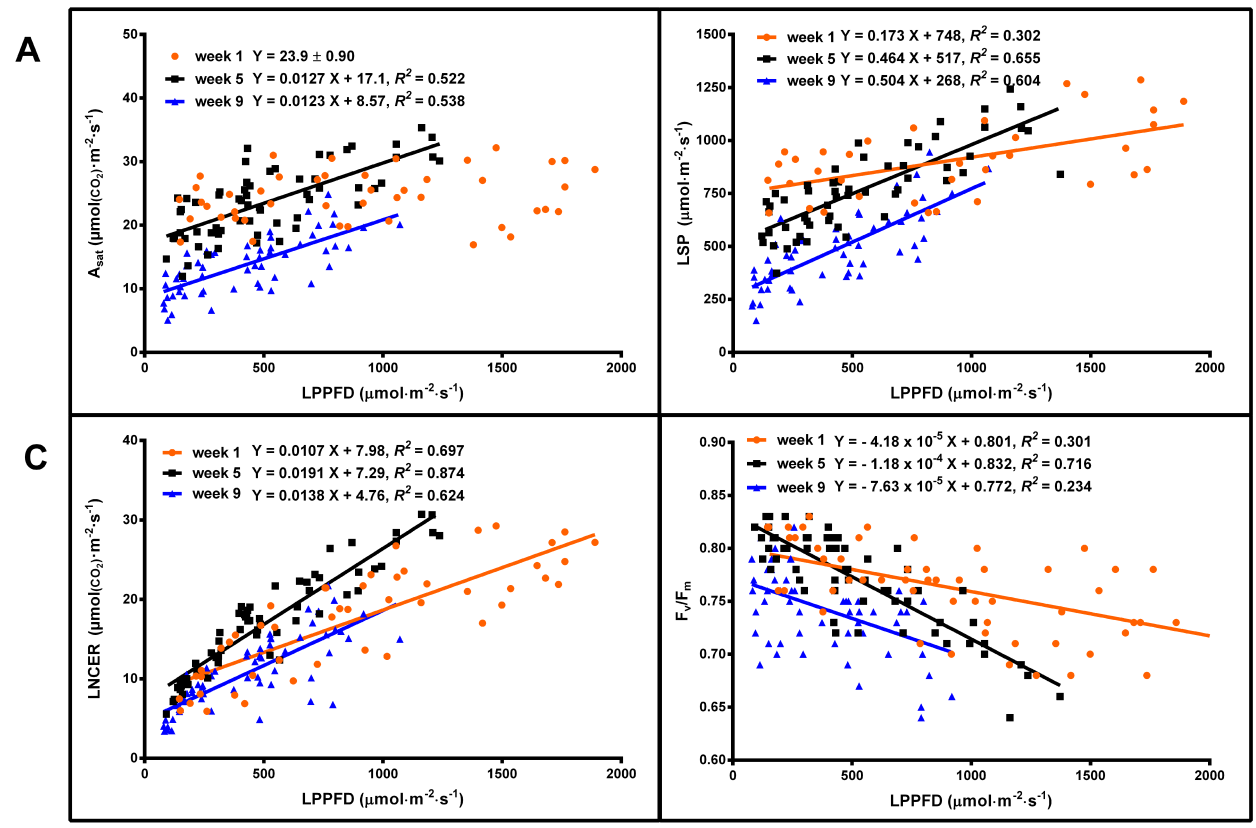

FIGURE 4 | The light-saturated net CO_2 exchange rate (A_{sat}) **(A)**, the light saturation point (LSP) **(B)**, the localized net CO_2 exchange rate (LNCER) **(C)**, and the F_v/F_m **(D)** of the youngest fully-expanded fan leaves of *Cannabis sativa* 'Stillwater' at the localized photosynthetic photon flux densities (LPPFD) that the respective leaves were growing under when the measurements were made, during weeks 1, 5, and 9 after initiation of the 12-h photoperiod. Each datum is a single plant. Regression lines are presented when $P \leq 0.05$.

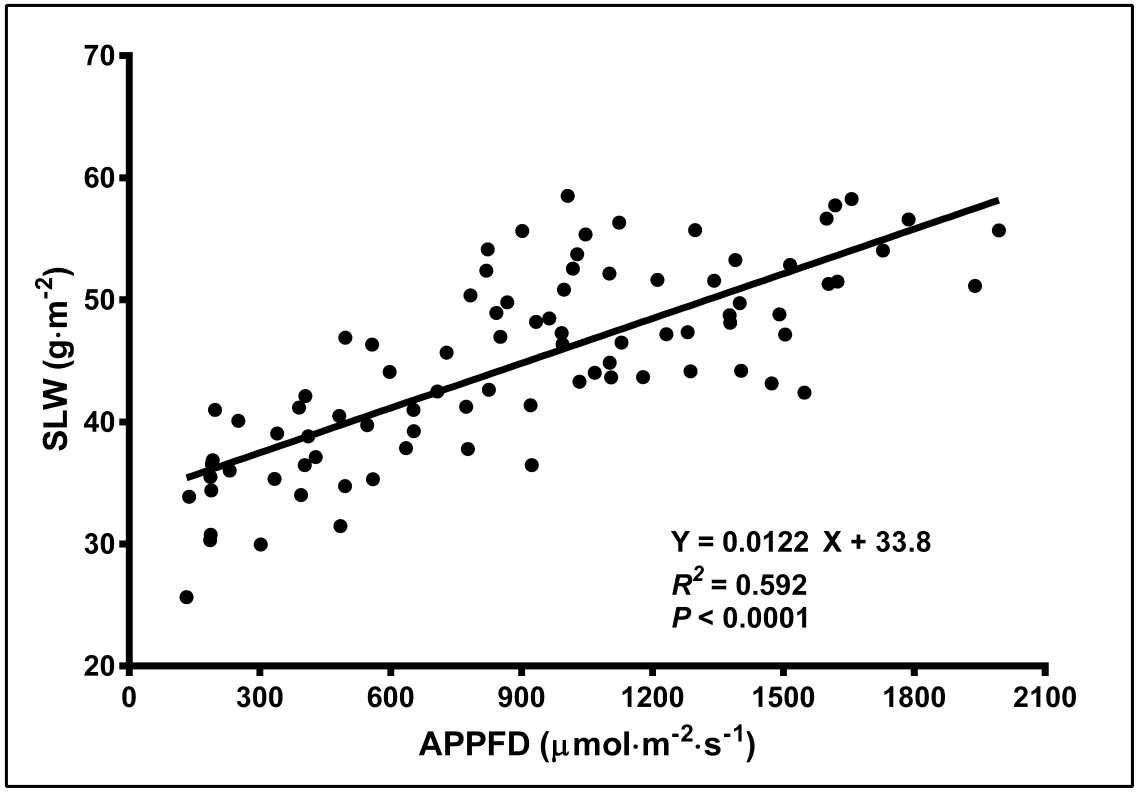

FIGURE 5 | The specific leaf weight (SLW; on a dry weight basis) of young, fully-expanded *Cannabis sativa* 'Stillwater' leaves in response to the average photosynthetic photon flux density (APPFD), measured on day 35 after initiation of the 12-h photoperiod. Each datum represents one fan leaf from a single plant.

plants' accumulated PAR exposures up to day 35 of the flowering stage) increased from 130 to 1,990 $\mu mol \cdot m^{-2} \cdot s^{-1}$ (**Figure 5**). Plants grown under low vs. high APPFD were generally shorter and wider, with thinner stems, larger leaves, and fewer, smaller inflorescences (**Figure 6**).

Yield and Quality

Cannabis yield increased linearly from 116 to 519 $g \cdot m^{-2}$ (i.e., 4.5 times higher) as APPFD increased from 120 to 1,800 $\mu mol \cdot m^{-2} \cdot s^{-1}$ (**Figure 7A**). Note that yields in the present study are true oven-DWs. Since cannabis inflorescences are typically dried to 10–15% moisture content to achieve optimum marketable quality (Leggett, 2006), dividing DW by the proportion of marketable biomass that the DW comprises (e.g., for 15% moisture, divide DW by 0.85) will estimate marketable yield. The harvest index increased linearly from 0.560 to 0.733 and (i.e., 1.3 times higher) as APPFD increased from 120 to 1,800 $\mu mol \cdot m^{-2} \cdot s^{-1}$ (**Figure 7B**). The apical inflorescence density increased linearly from 0.0893 to 0.115 $g \cdot cm^{-3}$ (i.e., 1.3 times higher) as APPFD increased from 120 to 1,800 $\mu mol \cdot m^{-2} \cdot s^{-1}$ (**Figure 7C**).

Cannabidiolic acid (CBDA) was the dominant cannabinoid in the dried inflorescences; however, there were no APPFD treatment effects on the potency of any of the measured cannabinoids (**Table 1**). Due to linear increases in inflorescence yield with increasing LI, cannabinoid yield ($g \cdot m^{-2}$) increased by 4.5 times as APPFD increased from 120 to 1,800 $\mu mol \cdot m^{-2} \cdot s^{-1}$ Myrcene, limonene, and caryophyllene were the dominant terpenes in the harvested inflorescences (**Table 2**). The potency of total terpenes, myrcene, and limonene increased linearly from 8.85 to 12.7, 2.51 to 4.90, and 1.05 to 1.60 $mg \cdot g^{-1}$ inflorescence DW (i.e., 1.4, 2.0, and 1.5 times higher), respectively, as APPFD increased from 120 to 1,800 $\mu mol \cdot m^{-2} \cdot s^{-1}$. There were no APPFD effects on the potency of the other individual terpenes.

DISCUSSION

Cannabis Inflorescence Yield Is Proportional to Light Intensity

It was predicted that cannabis yield would exhibit a saturating response to increasing LI, thereby signifying an optimum LI range for indoor cannabis production. However, the yield results of this trial demonstrated cannabis' immense plasticity for exploiting the incident lighting environment by efficiently increasing marketable biomass up to extremely high—for indoor production—LIs (**Figure 7A**). Even under ambient CO_2, the linear increases in yield indicated that the availability of PAR photons was still limiting whole-canopy photosynthesis at APPFD levels as high as ≈1,800 $\mu mol \cdot m^{-2} \cdot s^{-1}$ (i.e., DLI ≈78 $mol \cdot m^{-2} \cdot d^{-1}$). These results were generally consistent with the

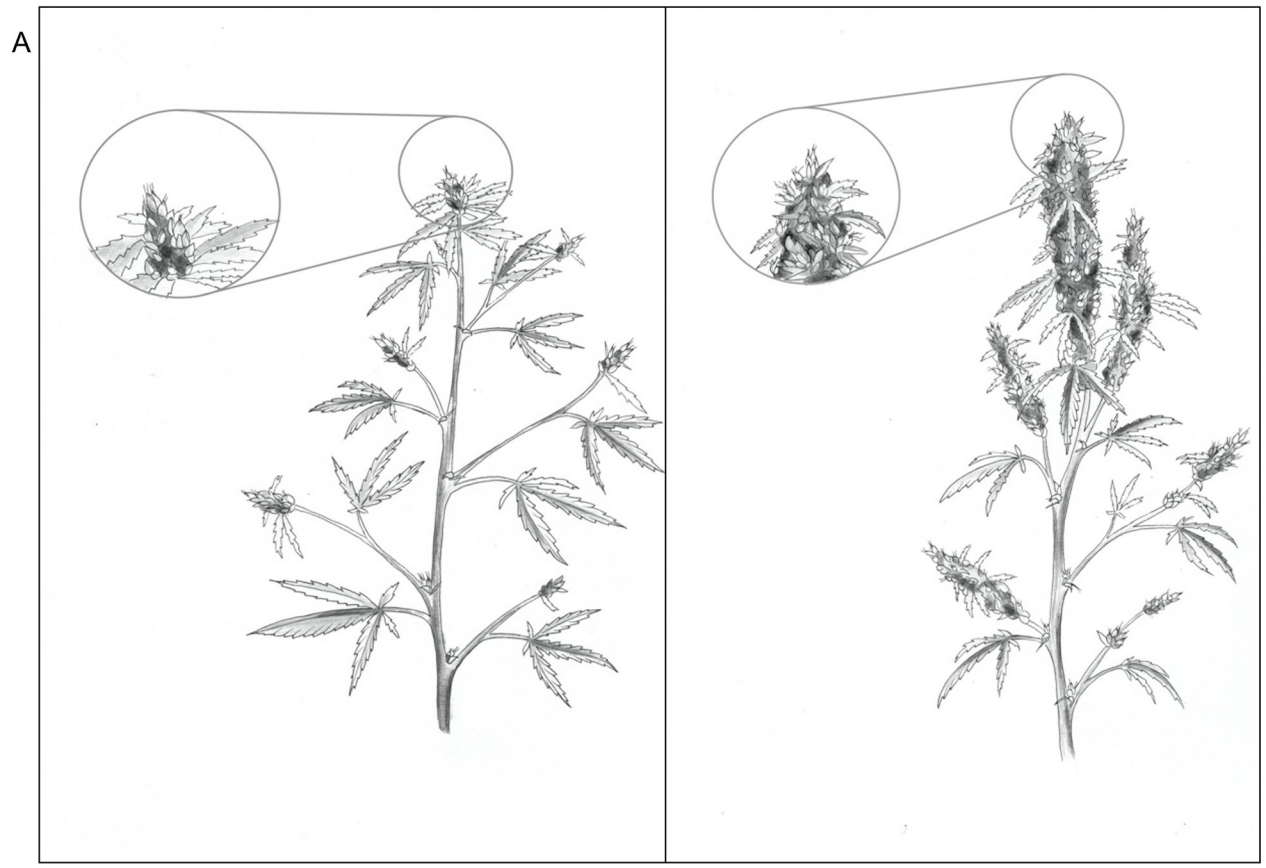

FIGURE 6 | Sketches of *Cannabis sativa* 'Stillwater' plants grown under low **(A)** and high **(B)** photosynthetic photon flux density (APPFD), 9 weeks after initiation of 12-h photoperiod (illustrated by Victoria Rodriguez Morrison).

trends of other studies reporting linear cannabis yield responses to LI (Vanhove et al., 2011; Potter and Duncombe, 2012; Eaves et al., 2020), although there is considerable variability in both relative and absolute yield responses to LI in these prior works. The present study covered a broader range of LI, and with much higher granularity, compared with other similar studies.

The lack of a saturating yield response at such high LI is an important distinction between cannabis and other crops grown in controlled environments (Faust, 2003; Beaman et al., 2009; Oh et al., 2009; Fernandes et al., 2013). This also means that the selection of an "optimum" LI for indoor cannabis production can be made somewhat independently from its yield response to LI. Effectively, within the range of practical indoor PPFD levels—the more light that is provided, the proportionally higher the increase in yield will be. Therefore, the question of the optimum LI may be reduced to more practical functions of economics and infrastructure limitations: basically, how much lighting capacity can a grower afford to install and run? This becomes a trade-off between fixed costs which are relatively unaffected by yield and profit (e.g., building lease/ownership costs including property tax, licensing, and administration) and variable costs such as crop inputs (e.g., fertilizer, electricity for lighting) and labor. Variable costs will obviously increase with higher LI but the fixed costs, on a per unit DW basis, should decrease concomitantly with increasing yield (Vanhove et al., 2014). Every production facility will have a unique optimum balance between facility costs and yield; but the yield results in the present study can help cannabis cultivators ascertain the most suitable LI target for their individual circumstances. Readers should be mindful that this study reports yield parameters as true dry weights; marketable yield can be easily determined by factoring back in the desirable moisture content of the inflorescence. For example, for a 400 $g \cdot m^{-2}$ of dry yield, the corresponding marketable yield would be 440 $g \cdot m^{-2}$ at 10% moisture content (i.e., 400 × 1.10).

It is also important to appreciate that PPFD, which represents an instantaneous LI level, does not provide a complete accounting of the total photon flux incident on the crop canopy throughout the entire production cycle. While this LI metric is ubiquitous in the horticulture industry and may be most broadly relatable to prior works, there is value in relating yield to the total photon flux received by the crop. Historically, this has been done by relating yield to installed wattage on per area bases, resulting in $g \cdot W^{-1}$ metric (Potter and Duncombe, 2012), which can be more fittingly converted to yield per unit electrical energy input ($g \cdot kWh^{-1}$) by factoring in the photoperiod and length of the production cycle (European Monitoring Centre for Drugs Drug

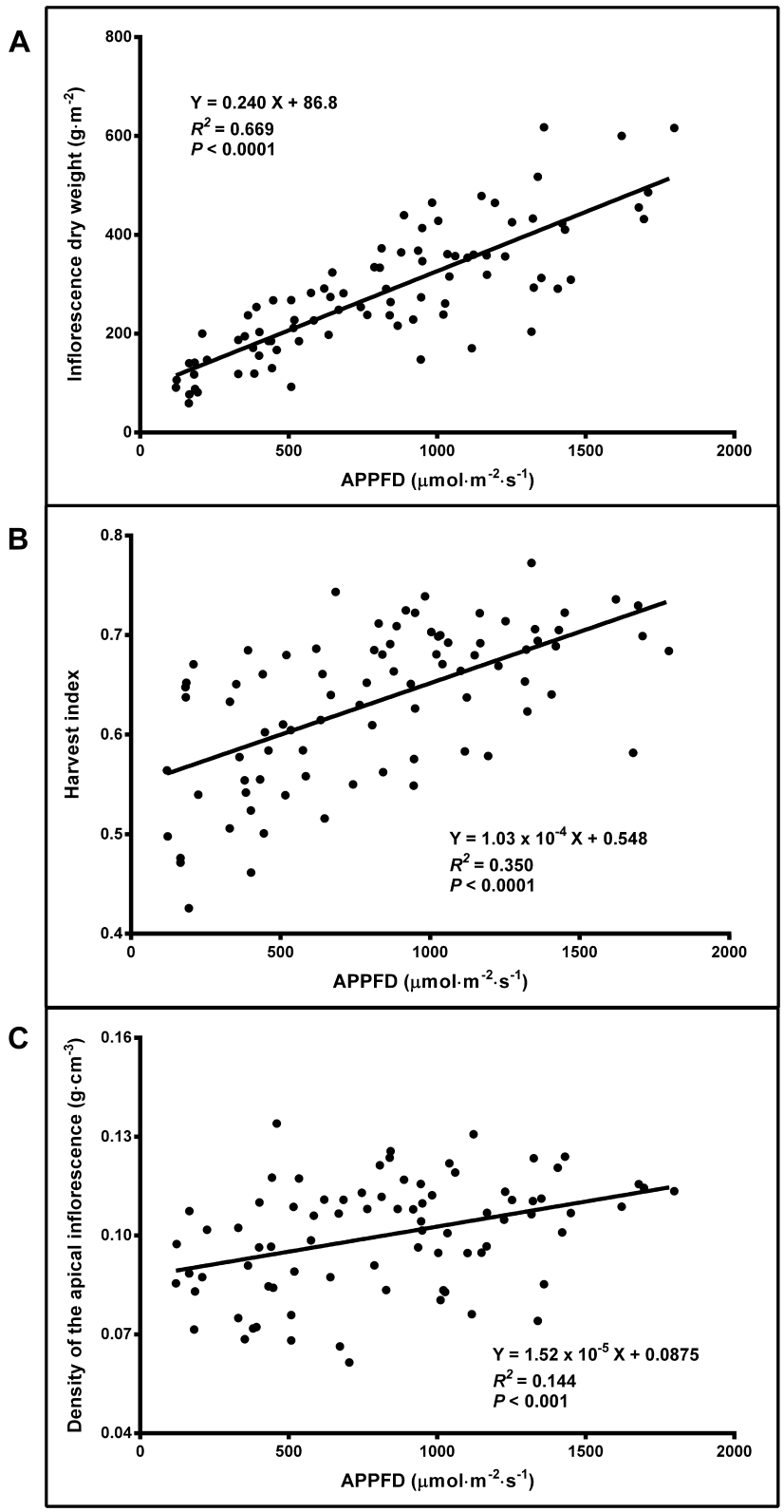

FIGURE 7 | The relationship between average apical photosynthetic photon flux density (APPFD) applied during the flowering stage (81 days) and inflorescence dry weight **(A)**, harvest index (total inflorescence dry weight / total aboveground dry weight) **(B)**, and apical inflorescence density (based on fresh weight) **(C)** of *Cannabis sativa* 'Stillwater'. Each datum is a single plant.

TABLE 1 | Cannabinoid potency in apical inflorescences of *Cannabis sativa* 'Stillwater'.

Cannabinoid	Potency ($mg \cdot g^{-1}$ of inflorescence dry weight)
Δ-9-tetrahydrocannabinol (Δ^9-THC)	UDL[z]
Δ-9-tetrahydrocannabinolic Acid (Δ^9-THCA)	12.9[y] ± 0.03
Total equivalent Δ^9-tetrahydrocannabinol (TΔ^9-THC)	11.3 ± 0.02
Cannabidiol (CBD)	5.53 ± 0.01
Cannabidiolic acid (CBDA)	214 ± 0.4
Total equivalent cannabidiol (TCBD)	193 ± 0.4
Cannabigerol (CBG)	UDL
Cannabigerolic acid (CBGA)	4.76 ± 0.01
Total equivalent cannabigerol (TCBG)	4.45 ± 0.009
Cannabinol (CBN)	UDL

[z] *Under detection limit of 0.5 $mg \cdot g^{-1}$ of inflorescence dry weight.*
[y] *Data are means ± SE (n = 22).*

Addiction, 2013). However, since photosynthesis is considered a quantum phenomenon, crop yield may be more appropriately related to incident (easily measured) or absorbed photons and integrated over the entire production cycle (i.e., TLI, $mol \cdot m^{-2}$), in a yield metric that is analogous to QY: $g \cdot mol^{-1}$. Versus using installed wattage, this metric has the advantage of negating the effects of different fixture efficacy ($\mu mol \cdot J^{-1}$), which continues its upward trajectory, especially with LEDs (Nelson and Bugbee, 2014; Kusuma et al., 2020). The present study did not directly measure lighting-related energy consumption; however, installed energy flux ($kWh \cdot m^{-2}$) can be estimated from TLI using the Lumigrow fixture's efficacy rating: 1.29 and 1.80 $\mu mol \cdot J^{-1}$, from Nelson and Bugbee (2014) and Radetsky (2018), respectively. Using the average of these values (1.55 $\mu mol \cdot J^{-1}$), the conversion from TLI to energy flux becomes: $mol \cdot m^{-2} \times 5.6 = kWh \cdot m^{-2}$. At an APPFD of 900 $\mu mol \cdot m^{-2} \cdot s^{-1}$ (i.e., TLI of 3,149 $mol \cdot m^{-2}$), the model in **Figure 7A** predicts a yield of 303 $g \cdot m^{-2}$ which corresponds to an energy use efficacy of 0.54 $g \cdot kWh^{-1}$. For comparison, doubling the LI to the highest APPFD used in this trial increases the yield by 70% but results in a ≈15% reduction in energy use efficacy. It is up to each grower to determine the optimum balance between variable (e.g., lighting infrastructure and energy costs) and fixed (e.g., production space) costs in selecting a canopy level LI that will maximize profits.

Increasing Light Intensity Enhances Inflorescence Quality

Beyond simple yield, increasing LI also raised the harvest quality through higher apical inflorescence (also called "cola" in the cannabis industry) density—an important parameter for the whole-bud market—and increased ratios of inflorescence to total aboveground biomass (**Figures 7B,C**). The linear increases in harvest index and apical inflorescence density with increasing LI both indicate shifts in biomass partitioning more in favor of generative tissues; a common response in herbaceous plants (Poorter et al., 2019) including cannabis (Potter and Duncombe, 2012; Hawley et al., 2018). The increases in these attributes under high LI may also indirectly facilitate harvesting, as there is correspondingly less unmarketable biomass to be processed and discarded, which is an especially labor-intensive aspect of cannabis harvesting.

TABLE 2 | The relationships between average photosynthetic photon flux density (APPFD) applied during the flowering stage (81 days) and terpene potency in apical inflorescences of myrcene, limonene and total terpenes, and the mean potency for terpenes with no APPFD treatment effects, of *Cannabis sativa* 'Stillwater'.

Terpene	Terpene potency ($mg \cdot g^{-1}$ of inflorescence dry weight)		
	Mean[z]	Regression equation[y]	R^2
Total terpenes		$Y = 0.00230\ X + 8.57$	0.320
Myrcene		$Y = 0.00142\ X + 2.34$	0.464
Limonene		$Y = 0.000326\ X + 1.01$	0.246
Alpha pinene	0.16[z] ± 0.01		
Beta pinene	0.22 ± 0.01		
Terpinolene	UDL[x]		
Linalool	0.53 ± 0.01		
Terpineol	0.32 ± 0.02		
Caryophyllene	2.9 ± 0.2		
Humulene	0.65 ± 0.04		
3-carene	UDL		
Cis-ocimene	UDL		
Eucalyptol	UDL		
Trans-ocimene	UDL		
Fenchol	0.22 ± 0.01		
Borneol	0.03 ± 0.01		
Valencene	UDL		
Cis-nerolidol	UDL		
Trans-nerolidol	UDL		
Guaiol	UDL		
Alpha-bisabolol	0.38 ± 0.03		
Sabinene	UDL		

[z] *When there were no APPFD treatment effects on terpene potency, the means ± SE (n = 22) are presented.*
[y] *Linear regression models for the APPFD treatment effects on terpene potency when $P \leq 0.05$.*
[x] *Under detection limit of 0.5 $mg \cdot g^{-1}$ of inflorescence dry weight.*

The terpene potency—comprised mainly of myrcene, limonene, and caryophyllene—increased by ≈25%, as APPFD increased from 130 to 1,800 $\mu mol \cdot m^{-2} \cdot s^{-1}$ (**Table 2**), which could lead to enhanced aromas and higher quality extracts (McPartland and Russo, 2001; Nuutinen, 2018). Conversely, total cannabinoid yield increased in proportion with increasing inflorescence yield since there were no LI treatment effects on cannabinoid potency (**Table 1**). Similarly, Potter and Duncombe (2012) and Vanhove et al. (2011) found no LI treatment effects on cannabinoid potency (primarily THC in those studies) and attributed increasing cannabinoid yield to enhanced biomass apportioning toward generative tissues at higher LI. Other studies had contradictory results on the effects of LI on potency. Hawley et al. (2018) did not find canopy position effects on THC or CBD potency in a subcanopy lighting (SCL) trial, but they did find slightly higher cannabigerol (CBG) potency in the

upper canopy in the control (high pressure sodium top-lighting only) and the Red-Green-Blue SCL treatment, but not in the Red-Blue SCL treatment. While it is not possible to unlink spectrum from LI in their results, the magnitude of the reported potency differences, both between canopy positions and between lighting treatments, were relatively minor. Conversely, Namdar et al. (2018) reported what appeared to be a vertical stratification on cannabis secondary metabolites, with highest potencies generally found in the most distal inflorescences (i.e., closest to the light source, PPFD ≈600 $\mu mol \cdot m^{-2} \cdot s^{-1}$). They attributed this stratification to the localized LI at different branch positions, which were reportedly reduced by ≥60% at lower branches vs. at the plant apex. However, given the lack of LI treatment effects (over a much broader range of PPFDs) on cannabinoid potency in the present study, it is likely that other factors were acting on higher-order inflorescences, such as delayed maturation and reduced biomass allocation, that reduced potency in these tissues (Hemphill et al., 1980; Diggle, 1995).

Plasticity of Cannabis Leaf Morphology and Physiology Responses to LI and Over Time

The objectives of the photosynthesis and leaf morphology investigations in this study were 2-fold: (1) to address the knowledge gap in the relationships between localized cannabis leaf photosynthesis and yield and (2) observe and report changes in physiology as the plant progresses through the flowering ontogeny.

General morphological, physiological, and yield responses of plants are well-documented across LI gradients ranging from below the compensation point to DLIs beyond 60 $mol \cdot m^{-2} \cdot d^{-1}$. Recently, the LI responses of myriad plant attributes were compiled across a tremendous range species, ecotypes and growing environments, and concisely reported them in the excellent review paper by Poorter et al. (2019). The trends in their LI models align well with primary attributes measured in the present study, including morphological parameters such as plant height and internode length (data not shown), SLW (discussed below), and physiological parameters such as F_v/F_m, LNCER (i.e., photosynthesis at growth light; Phot/A^{GL}), and A_{sat} (i.e., photosynthesis at saturating light; Phot/A^{SL}). In general, cannabis photosynthesis, and yield responses to localized LI were linear across the APPFD range of 120–1,800 $\mu mol \cdot m^{-2} \cdot s^{-1}$. While these results are in agreement with the contemporary literature on cannabis (Chandra et al., 2008, 2015; Potter and Duncombe, 2012; Bauerle et al., 2020; Eaves et al., 2020), we also showed substantial chronological dependencies on leaf photosynthetic indices.

By surveying the photosynthetic parameters of the upper cannabis canopy across a broad range of LPPFDs and over multiple timepoints during the generative phase, we saw evidence of both acclimation and early senescence as the crop progressed through its ontogeny. At the beginning of the trial, the plants were abruptly transitioned from a uniform PPFD (425 $\mu mol \cdot m^{-2} \cdot s^{-1}$) and 18-h photoperiod (i.e., 27.5 $mol \cdot m^{-2} \cdot d^{-1}$) and subjected to a much shorter photoperiod (12-h) and an enormous range of LI (120–1,800 $\mu mol \cdot m^{-2} \cdot s^{-1}$), resulting in DLIs ranging from 5.2 to 78 $mol \cdot m^{-2} \cdot d^{-1}$. Further, on a DLI-basis, ≈1/3 of the plants were exposed to lower LIs in the flowering vs. vegetative phase (i.e., APPFD <640 $\mu mol \cdot m^{-2} \cdot s^{-1}$). These sudden transitions in both LI and photoperiod resulted in substantive changes in the plants' lighting environment at the start of the trial, stimulating various morphological and physiological adaptations with differing degrees of plasticity. The leaves measured in week 1 developed and expanded during the prior vegetative phase under a different lighting regimen (LI and photoperiod). The leaves measured in week 5 were developed under their respective LPPFDs during a period characterized by slowing vegetative growth and transitioning to flower development. The leaves measured in week 9 would have also developed under their respective LPPFDs, but since cannabis vegetative growth greatly diminishes after the first 5 weeks in 12-h days (Potter, 2014), these tissues were physiologically much older than the leaves measured in week 5, with concomitant reductions in photosynthetic capacity (Bielczynski et al., 2017; Bauerle et al., 2020).

These differences in leaf physiological age, plant ontogeny, and localized lighting environments during leaf expansion vs. measurement resulted in notable temporal variability in leaf-level LI responses (**Figure 4**). In week 1, there were no LI treatment effects on A_{sat} and the slopes of the LSP, LNCER, and F_v/F_m were shallower than in weeks 5 and 9. The comparatively lower LI responses in week 1 were likely due to the reduced adaptive plasticity that mature foliar tissues have vs. leaves that developed under a new lighting regime (Sims and Pearcy, 1992). Further, Y-intercepts for the A_{sat}, LSP, and LNCER models were higher in week 1 than weeks 5 and 9, which may be partly due to the higher LI (amplified by the longer photoperiod) that the leaves developed under, during the latter part of the vegetative phase. Moreover, the A_{sat}, LSP, and LNCER models in weeks 5 and 9 have comparable slopes, but there is a vertical translation in the respective models, resulting week 9 models having substantially lower Y-intercepts (i.e., approximately half) for these parameters. The interplay of physiological age of foliage and plant ontogeny (i.e., onset of senescence) on the diminished photosynthetic capacity of the leaves in week 9 is unknown, but the dynamic temporal nature of cannabis photosynthesis (during flowering) is manifest in these models.

Given these impacts of physiological age and light history, we posit that cannabis leaf photosynthesis cannot be used as a stand-alone gauge for predicting yield. Chandra et al. (2008) and Chandra et al. (2015) provided insight into the substantial capacity for drug-type strains of indoor grown cannabis leaves to respond to LI; and the results of these trials are much lauded in the industry as evidence that maximum photosynthesis and yields will be reached under canopy-level PPFDs of ≈1,500 $\mu mol \cdot m^{-2} \cdot s^{-1}$. However, their 400–500 $\mu mol \cdot m^{-2} \cdot s^{-1}$ increments in LPPFD does not provide sufficient granularity (particularly at low LI) to reliably model the LRCs, thus no models were provided. Further, the LRCs were made on leaves of varying and unreported physiological ages, from plants exposed to a vegetative photoperiod (18-h), and acclimated to unspecified

localized LI (a canopy-level PPFD of 700 $\mu mol \cdot m^{-2} \cdot s^{-1}$ was indicated in Chandra et al., 2015). The strong associations between a tissue's light history and its photosynthesis responses to LI, demonstrated in this trial and by others (Björkman, 1981), represent a major shortcoming of using leaf LI response models to infer crop growth and yield. To illustrate, **Figure 3** shows LRCs of leaves from a single cultivar, at similar physiological ages (week 5 after transition to 12-h photoperiod) but acclimated to disparate LPPFDs: 91 and 1,238 $\mu mol \cdot m^{-2} \cdot s^{-1}$. The relative difference in LNCER at higher LIs (≈50%) between these two curves is representative of the potential uncertainty due to just one of the uncontrolled parameters (LNCER) in these prior works. Differing physiological ages of tissues at the time of measurement may have conferred an even larger degree of uncertainty in the magnitude of leaf responses to LI (Bauerle et al., 2020) than leaf light history. Consideration must also be given to the different life stages of a photoperiodic crop (i.e., vegetative vs. generative) and the inherent impact that day length imbues on the total daily PAR exposure (i.e., DLI) which can correlate better to crop yield than PPFD. Further, for a given DLI, yields are higher under longer photoperiod (Vlahos et al., 1991; Zhang et al., 2018), ostensibly due to their relative proximity to their maximum QY (Ohyama et al., 2005). A final distinction between leaf photosynthesis and whole plant yield responses to LI is the saturating LI: the LSP for leaf photosynthesis were substantially lower than the LSP for yield, which remains undefined due to the linearity of the light response model.

Newly-expanded leaves, especially in herbaceous species, are able to vary their leaf size, thickness and chlorophyll content in response to LPPFD in order to balance myriad factors such as internal and leaf surface gas exchange (CO_2 and H_2O), internal architecture of the light-harvesting complexes, and resistance to photoinhibition (Björkman, 1981). In the present study, the effects of LI on leaf morphology was only evaluated in week 5, when the crop was still actively growing vegetative biomass. Reductions in SLW (i.e., increases in specific leaf area, SLA) in response to increasing LI are abundant in the literature (Sims and Pearcy, 1992; Fernandes et al., 2013; Gratani, 2014). In particular, Poorter et al. (2019) reported a saturating response of SLW [also known as leaf mass (per) area; LMA] to LI across 520 species (36% of which were herbaceous plants), however much of their data was at DLIs lower than the minimum DLI in the present study (5.2 $mol \cdot m^{-2} \cdot d^{-1}$), which affected the shape of their SLW response model to LI. Across similar DLI ranges, the average increase in SLW across 520 species was 1.7 × in Poorter et al. (2019) vs. 1.6 × in the present study, indicating that cannabis SLW responses to LI are consistent with normal trends for this parameter.

The lack of LI treatment effects on CCI are also consistent with other studies that have shown that area-based chlorophyll content is fairly stable across a broad range of LIs (Björkman, 1981; Poorter et al., 2019), despite substantial variability in photosynthetic efficiency. However, since there were LI treatment effects on SLW, chlorophyll content on leaf volume or mass bases would likely have reduced under higher LI. The positional effects on CCI (i.e., higher in upper vs. lower canopy) were probably due to the interplay between self-shading and advancing physiological age of the lower leaves (Bauerle et al., 2020). The temporal effects on CCI, which was higher in week 1 vs. weeks 5 and 9, in both upper and lower leaves, may have been due to changes in QY over the life-cycle of the crop. Bugbee and Monje (1992) presented a similar trend; high QY during the active growth phase of a 60-d crop cycle of wheat, followed by a reduction in QY at the onset of senescence (i.e., shortly before harvest). The decline in chlorophyll content in the latter phase of the production cycle probably contributed to the reductions in the photosynthetic parameters (e.g., A_{sat}, LSP, LNCER) of the tissues measured in week 9 vs. week 5.

Overall, the impact that increasing LI had on cannabis morphology and yield were captured holistically in the plant sketches in **Figure 6**, which shows plants grown under higher LIs had shorter internodes, smaller leaves, and much larger and denser inflorescences (resulting in higher harvest index), especially at the plant apex. Like many other plant species, we have found that cannabis has immense plasticity to rapidly acclimate its morphology and physiology, both at leaf- and whole plant-levels, to changes in the growing lighting environment. Therefore, in order reliably predict cannabis growth and yield to LI, it is necessary to grow plants under a broad range of LIs through their full ontological development, as was done in this study. Without knowing the respective tissues' age and light history, instantaneous light response curves at leaf-, branch-, or even canopy-levels cannot reliably predict yield.

CONCLUSIONS

We have shown an immense plasticity for cannabis to respond to increasing LI; in terms of morphology, physiology (over time), and yield. The temporal dynamics in cannabis leaf acclimations to LI have also been explored, addressing some knowledge-gaps in relating cannabis photosynthesis to yield. The results also indicate that the relationship between LI and cannabis yield does not saturate within the practical limits of LI used in indoor production. Increasing LI also increased harvest index and the size and density of the apical inflorescence; both markers for increasing quality. However, there were no and minor LI treatment effects on potency of cannabinoids and terpenes, respectively. This means that growers may be able to vastly increase yields by increasing LI but maintain a relatively consistent secondary metabolite profile in their marketable products. Ultimately, the selection of the economic optimum canopy-level LI for a given commercial production system depends on many interrelated factors.

Future research should expand to multiple cultivars of both indica- and sativa-dominant biotypes. Further, since plant yield responses to elevated CO_2 can mirror the responses to elevated LI, the combined effects of CO_2 and LI should be investigated on cannabis yield with an in-depth cost-benefit analysis of the optimum combination of these two input parameters.

DATA AVAILABILITY STATEMENT

The raw data supporting the conclusions of this article will be made available by the authors, without undue reservation.

AUTHOR CONTRIBUTIONS

All authors contributed to the experimental design. VR-M and DL performed the experiment, collected and analyzed the data. DL, VR-M, and YZ wrote and revised the manuscript. All authors contributed to the article approved the submitted version.

FUNDING

This work was funded by Natural Sciences and Engineering Research Council of Canada (Grant# CRDPJ533527-18). Green Relief provided the research facility, cannabis plants, experimental materials, and logistical support.

ACKNOWLEDGMENTS

We thank Dr. Nigel Gale for contributing to the experimental design. We thank Derek Bravo, Tim Moffat, and Dane Cronin for technical support throughout the experiment. This article was first published as a preprint (Rodriguez-Morrison et al., 2021).

REFERENCES

Backer, R., Schwinghamer, T., Rosenbaum, P., McCarty, V., Eichhorn Bilodeau, S., Lyu, D., et al. (2019). Closing the yield gap for cannabis: a meta-analysis of factors determining cannabis yield. *Front. Plant Sci.* 10:495. doi: 10.3389/fpls.2019.00495

Bauerle, W. L., McCullough, C., Iversen, M., and Hazlett, M. (2020). Leaf age and position effects on quantum yield and photosynthetic capacity in hemp crowns. *Plants* 9:271. doi: 10.3390/plants9020271

Beaman, A. R., Gladon, R. J., and Schrader, J. A. (2009). Sweet basil requires an irradiance of 500 $\mu mol \cdot m^{-2} \cdot s^{-1}$ for greatest edible biomass production. *Hort Sci.* 44, 64–67. doi: 10.21273/HORTSCI.44.1.64

Bielczynski, L. W., Łącki, M. K., Hoefnagels, I., Gambin, A., and Croce, R. (2017). Leaf and plant age affects photosynthetic performance and photoprotective capacity. *Plant Physiol.* 175, 1634–1648. doi: 10.1104/pp.17.00904

Björkman, O. (1981). "Responses to different quantum flux densities," in *Encyclopedia of Plant Physiology: New Series: Vol. 12A, Physiological Plant Ecology 1*, eds L. Lange, P.S. Nobel, C.B. Osmond, and H. Ziegler (Heidelberg, Berlin: Springer-Verlag), 57–107. doi: 10.1007/978-3-642-68090-8_4

Bredmose, N. (1993). Effects of year-round supplementary lighting on shoot development, flowering and quality of two glasshouse rose cultivars. *Sci. Hortic.* 54, 69–85. doi: 10.1016/0304-4238(93)90084-4

Bredmose, N. (1994). Biological efficiency of supplementary lighting on cut roses the year round. *Sci. Hortic.* 59:75–82. doi: 10.1016/0304-4238(94)90094-9

Bugbee, B., and Monje, O. (1992). The limits of crop productivity. *Bioscience* 42, 494–502. doi: 10.2307/1311879

Carvalho, F. E. L., Ware, M. A., and Ruban, A. V. (2015). Quantifying the dynamics of light tolerance in *Arabidopsis* plants during ontogenesis. *Plant Cell Environ.* 38, 2603–2617. doi: 10.1111/pce.12574

Chandra, S., Lata, H., Khan, I. A., and Elsohly, M. A. (2008). Photosynthetic response of *Cannabis sativa* L. to variations in photosynthetic photon flux densities, temperature and CO_2 conditions. *Physiol. Mol. Biol. Plants* 14, 299–306. doi: 10.1007/s12298-008-0027-x

Chandra, S., Lata, H., Khan, I. A., and ElSohly, M. A. (2011). Photosynthetic response of *Cannabis sativa* L., an important medicinal plant, to elevated levels of CO_2. *Physiol. Mol. Biol. Plants* 17, 291–295. doi: 10.1007/s12298-011-0066-6

Chandra, S., Lata, H., Mehmedic, Z., Khan, I. A., and ElSohly, M. A. (2015). Light dependence of photosynthesis and water vapor exchange characteristics in different high Δ9-THC yielding varieties of *Cannabis sativa* L. *J. Appl. Res. Med. Aromat. Plants* 2, 39–47. doi: 10.1016/j.jarmap.2015.03.002

Delgado, E., Parry, M. A. J., Lawlor, D. W., Keys, A. J., and Medrano, H. (1993). Photosynthesis, ribulose-1,5-bisphosphate carboxylase and leaf characteristics of *Nicotiana tabacum* L. genotypes selected by survival at low CO_2 concentrations. *J. Exp. Bot.* 44, 1–7. doi: 10.1093/jxb/44.1.1

Diggle, P. K. (1995). Architectural effects and the interpretation of patterns of fruit and seed development. *Annu. Rev. Ecol. Syst.* 26, 531–552. doi: 10.1146/annurev.es.26.110195.002531

Eaves, J., Eaves, S., Morphy, C., and Murray, C. (2020). The relationship between light intensity, cannabis yields, and profitability. *Agron. J.* 112, 1466–1470. doi: 10.1002/agj2.20008

European Monitoring Centre for Drugs and Drug Addiction (2013). *Cannabis Production and Markets In Europe*. Lisbon: EMCDDA Insights, No. 12.

Evergreen Economics (2016). *Cannabis Agriculture Energy Demand Study Final Report*. San Diego, CA: San Diego Gas and Electric Company.

Faust, J. E. (2003). "Light," in *Ball Redbook*, ed D. Hamrick (Batabia, IL: Ball Publishing), 71–84.

Fernandes, V. F., de Almeida, L. B., da Feijó, E. V. R. S., da Silva, D. C., de Oliveira, R. A., Mielke, M. S., et al. (2013). Light intensity on growth, leaf micromorphology and essential oil production of *Ocimum gratissimum*. *Braz. J. Pharmacogn.* 23, 419–424. doi: 10.1590/S0102-695X2013005000041

Gratani, L. (2014). Plant phenotypic plasticity in response to environmental factors. *Adv. Bot.* 2014, 1–17. doi: 10.1155/2014/208747

Hawley, D., Graham, T., Stasiak, M., and Dixon, M. (2018). Improving cannabis bud quality and yield with subcanopy lighting. *HortScience* 53, 1593–1599. doi: 10.21273/HORTSCI13173-18

Hemphill, J. K., Turner, J. C., and Mahlberg, P. G. (1980). Cannabinoid content of individual plant organs from different geographical strains of *Cannabis sativa* L. *J. Nat. Prod.* 43, 112–122. doi: 10.1021/np50007a009

Jones-Baumgardt, C., Llewellyn, D., Ying, Q., and Zheng, Y. (2019). Intensity of sole-source light-emitting diodes affects growth, yield, and quality of Brassicaceae microgreens. *HortScience* 54, 1168–1174. doi: 10.21273/HORTSCI13788-18

Kirschbaum, M. U. F. (2011). Does enhanced photosynthesis enhance growth? Lessons learned from CO_2 enrichment studies. *Plant Physiol.* 155, 117–124. doi: 10.1104/pp.110.166819

Kreyling, J., Schweiger, A. H., Bahn, M., Ineson, P., Migliavacca, M., Morel-Journel, T., et al. (2018). To replicate, or not to replicate - that is the question: how to tackle nonlinear responses in ecological experiments. *Ecol. Lett.* 21, 1629–1638. doi: 10.1111/ele.13134

Kusuma, P., Pattison, P. M., and Bugbee, B. (2020). From physics to fixtures to food: Current and potential LED efficacy. *Hortic. Res.* 7:56. doi: 10.1038/s41438-020-0283-7

Leggett, T. (2006). A review of the world cannabis situation. *Bull. Narc.* 58: 1–155.

LI-COR Biosciences. (2012). *Using the LI-6400 / LI-6400XT Portable Photosynthesis System Version 6*. Lincoln, NB: LI-COR Inc.

Lobo, F. A., de Barros, M. P., Dalmagro, H. J., Dalmolin, Â. C., Pereira, W. E., de Souza, É. C., et al. (2013). Fitting net photosynthetic light-response curves with Microsoft Excel - a critical look at the models. *Photosynthetica* 51, 445–456. doi: 10.1007/s11099-013-0045-y

Lydon, J., Teramura, A. H., and Coffman, C. B. (1987). UV-B radiation effects on photosynthesis, growth and cannabinoid production of two *Cannabis sativa* chemotypes. *Photochem. Photobiol.* 46, 201–206. doi: 10.1111/j.1751-1097.1987.tb04757.x

Marcelis, L. F. M., Broekhuijsen, A. G. M., Meinen, E., Nijs, E. M. F. M., and Raaphorst, M. G. M. (2006). Quantification of the growth response to light quantity of greenhouse grown crops. *Acta Hortic.* 711, 97–103. doi: 10.17660/ActaHortic.2006.711.9

McPartland, J. M., and Russo, E. B. (2001). Cannabis and cannabis extracts: greater than the sum of their parts? *Cannabis Ther.* 1, 103–132. doi: 10.1300/J175v01n03_08

Mills, E. (2012). The carbon footprint of indoor Cannabis production. *Energy Policy* 46, 58–67. doi: 10.1016/j.enpol.2012.03.023

Murchie, E., Hubbart, S., Chen, Y., Peng, S., and Horton, P. (2002). Acclimation of rice photosynthesis to irradiance under field conditions. *Plant Physiol*. 130, 1999–2010. doi: 10.1104/pp.011098

Murchie, E., and Lawson, T. (2013). Chlorophyll fluorescence analysis: a guide to good practice and understanding some new applications. *J. Exp. Bot*. 64, 3983–3998. doi: 10.1093/jxb/ert208

Namdar, D., Mazuz, M., Ion, A., and Koltai, H. (2018). Variation in the compositions of cannabinoid and terpenoids in *Cannabis sativa* derived from inflorescence position along the stem and extraction methods. *Ind. Crops Prod*. 113, 376–382. doi: 10.1016/j.indcrop.2018.01.060

Nelson, J. A., and Bugbee, B. (2014). Economic analysis of greenhouse lighting: light emitting diodes vs. high intensity discharge fixtures. *PLoS ONE*. 9:e99010. doi: 10.1371/journal.pone.0099010

Niinemets, Ü., and Keenan, T. F. (2012). Measures of light in studies on light-driven plant plasticity in artificial environments. *Front. Plant Sci*. 3:156. doi: 10.3389/fpls.2012.00156

Nuutinen, T. (2018). Medicinal properties of terpenes found in *Cannabis sativa* and *Humulus lupulus*. *Eur. J. Med. Chem*. 157, 198–228. doi: 10.1016/j.ejmech.2018.07.076

Oh, W., Cheon, H., Kim, K. S., and Runkle, E. S. (2009). Photosynthetic daily light integral influences flowering time and crop characteristics of *Cyclamen persicum*. *Hort Sci*. 44, 341–344. doi: 10.21273/HORTSCI.44.2.341

Ohyama, K., Manabe, K., Omura, Y., Kozai, T., and Kubota, C. (2005). Potential use of a 24-hour photoperiod (continuous light) with alternating air temperature for production of tomato plug transplants in a closed system. *HortScience* 40, 374–377. doi: 10.21273/HORTSCI.40.2.374

Poorter, H., Niinemets, Ü., Ntagkas, N., Siebenkäs, A., Mäenp,ää, M., Matsubara, S., et al. (2019). A meta-analysis of plant responses to light intensity for 70 traits ranging from molecules to whole plant performance. *N. Phytol*. 223, 1073–1105. doi: 10.1111/nph.15754

Posada, J. M., Sievänen, R., Messier, C., Perttunen, J., Nikinmaa, E., and Lechowicz, M. J. (2012). Contributions of leaf photosynthetic capacity, leaf angle and self-shading to the maximization of net photosynthesis in *Acer saccharum*: a modelling assessment. *Ann. Bot*. 110, 731–741. doi: 10.1093/aob/mcs106

Potter, D. J. (2014). A review of the cultivation and processing of cannabis (*Cannabis sativa L.*) for production of prescription medicines in the UK. *Drug Test. Anal*. 6, 31–38. doi: 10.1002/dta.1531

Potter, D. J., and Duncombe, P. (2012). The effect of electrical lighting power and irradiance on indoor-grown cannabis potency and yield. *J. Forensic Sci*. 57, 618–622. doi: 10.1111/j.1556-4029.2011.02024.x

Radetsky, L. C. (2018). *LED and HID Horticultural Luminaire Testing Report Prepared For Lighting Energy Alliance Members and Natural Resources Canada*. Troy, NY: Rensselaer Polytechnic Institute.

Rodriguez-Morrison, V., Llewellyn, D., and Zheng, Y. (2021). Cannabis yield, potency, and leaf photosynthesis respond differently to increasing light levels in an indoor environment. *Preprints* 2021:2021010163. doi: 10.20944/preprints202101.0163.v1

Sen, A., and Wyonch, R. (2018). *Cannabis Countdown: Estimating the Size of Illegal Markets and Lost Tax Revenue Post-Legalization*. Toronto, ON: C.D. Howe Institute. doi: 10.2139/ssrn.3269989

Sims, D. A., and Pearcy, R. W. (1992). Response of leaf anatomy and photosynthetic capacity in *Alocasia macrorrhiza* (Araceae) to a transfer from low to high light. *Am. J. Bot*. 79, 449–455. doi: 10.1002/j.1537-2197.1992.tb14573.x

Singsaas, E. L., Ort, D. R., and DeLucia, E. H. (2001). Variation in measured values of photosynthetic quantum yield in ecophysiological studies. *Oecologia* 128, 15–23. doi: 10.1007/s004420000624

Terashima, I., and Hikosaka, K. (1995). Comparative ecophysiology of leaf and canopy photosynthesis. *Plant. Cell Environ*. 18, 1111–1128. doi: 10.1111/j.1365-3040.1995.tb00623.x

Toonen, M., Ribot, S., and Thissen, J. (2006). Yield of illicit indoor cannabis cultivation in the Netherlands. *J. Forensic Sci*. 51, 1050–1054. doi: 10.1111/j.1556-4029.2006.00228.x

United Nations Office on Drugs and Crime (2019). *World Drug Report 2019*. New York, NY: United Nations. doi: 10.18356/a4dd519a-en

Vanhove, W., Surmont, T., Van Damme, P., and De Ruyver, B. (2014). Filling in the blanks. An estimation of illicit cannabis growers' profits in Belgium. *Int. J. Drug Policy* 25, 436–443. doi: 10.1016/j.drugpo.2014.01.020

Vanhove, W., Van Damme, P., and Meert, N. (2011). Factors determining yield and quality of illicit indoor cannabis (*Cannabis* spp.) production. *Forensic Sci. Int*. 212, 158–163. doi: 10.1016/j.forsciint.2011.06.006

Vlahos, J. C., Heuvelink, E., and Martakis, G. F. P. (1991). A growth analysis study of three *Achimenes* cultivars grown under three light regimes. *Sci. Hortic*. 46, 275–282. doi: 10.1016/0304-4238(91)90050-9

Zhang, X., He, D., Niu, G., Yan, Z., and Song, J. (2018). Effects of environment lighting on the growth, photosynthesis, and quality of hydroponic lettuce in a plant factory. *Int. J. Agric. Biol. Eng*. 11, 33–40. doi: 10.25165/j.ijabe.20181102.3240

Zheng, Y. (2020). *Soilless Production of Drug-Type Cannabis sativa*. Acta Hortic (In press.).

Zheng, Y., Blom, T., and Dixon, M. (2006). Moving lamps increase leaf photosynthetic capacity but not the growth of potted gerbera. *Sci. Hortic*. 107, 380–385. doi: 10.1016/j.scienta.2005.09.004

Conflict of Interest: The authors declare that the research was conducted in the absence of any commercial or financial relationships that could be construed as a potential conflict of interest.

frontiers in Plant Science

ORIGINAL RESEARCH
published: 01 July 2021
doi: 10.3389/fpls.2021.699530

Identification of Chemotypic Markers in Three Chemotype Categories of Cannabis Using Secondary Metabolites Profiled in Inflorescences, Leaves, Stem Bark, and Roots

*Dan Jin[1,2], Philippe Henry[3,4], Jacqueline Shan[2] and Jie Chen[1,5]**

[1] Department of Biomedical Engineering, University of Alberta, Edmonton, AB, Canada, [2] PBG BioPharma Inc., Leduc, AB, Canada, [3] Egret Bioscience Ltd., West Kelowna, BC, Canada, [4] Lighthouse Genomics Inc., Salt Spring Island, BC, Canada, [5] Department of Electrical and Computer Engineering, University of Alberta, Edmonton, AB, Canada

Previous chemotaxonomic studies of cannabis only focused on tetrahydrocannabinol (THC) dominant strains while excluded the cannabidiol (CBD) dominant strains and intermediate strains (THC ≈ CBD). This study investigated the utility of the full spectrum of secondary metabolites in different plant parts in three cannabis chemotypes (THC dominant, intermediate, and CBD dominant) for chemotaxonomic discrimination. Hierarchical clustering, principal component analysis (PCA), and canonical correlation analysis assigned 21 cannabis varieties into three chemotypes using the content and ratio of cannabinoids, terpenoids, flavonoids, sterols, and triterpenoids across inflorescences, leaves, stem bark, and roots. The same clustering results were obtained using secondary metabolites, omitting THC and CBD. Significant chemical differences were identified in these three chemotypes. Cannabinoids, terpenoids, flavonoids had differentiation power while sterols and triterpenoids had none. CBD dominant strains had higher amounts of total CBD, cannabidivarin (CBDV), cannabichromene (CBC), α-pinene, β-myrcene, (−)-guaiol, β-eudesmol, α-eudesmol, α-bisabolol, orientin, vitexin, and isovitexin, while THC dominant strains had higher total THC, total tetrahydrocannabivarin (THCV), total cannabigerol (CBG), camphene, limonene, ocimene, sabinene hydrate, terpinolene, linalool, fenchol, α-terpineol, β-caryophyllene, trans-β-farnesene, α-humulene, trans-nerolidol, quercetin, and kaempferol. Compound levels in intermediate strains were generally equal to or in between those in CBD dominant and THC dominant strains. Overall, with higher amounts of β-myrcene, (−)-guaiol, β-eudesmol, α-eudesmol, and α-bisabolol, intermediate strains more resemble CBD dominant strains than THC dominant strains. The results of this study provide a comprehensive profile of bioactive compounds in three chemotypes for medical purposes. The simultaneous presence of a predominant number of identified chemotype markers (with or without THC and CBD) could be used as chemical fingerprints for quality standardization or strain identification for research, clinical studies, and cannabis product manufacturing.

Keywords: cannabis, THC, CBD, chemotypes, markers, secondary metabolites, plant parts

OPEN ACCESS

Edited by:
David Meiri,
Technion Israel Institute of Technology, Israel

Reviewed by:
David L. Joly,
Université de Moncton, Canada
Akbar Karami,
Shiraz University, Iran

***Correspondence:**
Jie Chen
jc65@ualberta.ca

Specialty section:
This article was submitted to Plant Metabolism and Chemodiversity, a section of the journal Frontiers in Plant Science

Received: *23 April 2021*
Accepted: *09 June 2021*
Published: *01 July 2021*

Citation:
Jin D, Henry P, Shan J and Chen J (2021) Identification of Chemotypic Markers in Three Chemotype Categories of Cannabis Using Secondary Metabolites Profiled in Inflorescences, Leaves, Stem Bark, and Roots. Front. Plant Sci. 12:699530. doi: 10.3389/fpls.2021.699530

INTRODUCTION

Cannabis is a complex herbal medicine containing several classes of secondary metabolites, including cannabinoids, terpenoids, flavonoids, and steroids among 545 identified compounds (Turner et al., 1980; ElSohly and Slade, 2005; Ross et al., 2005; ElSohly and Gul, 2014; Russo and Marcu, 2017; Pollastro et al., 2018; Jin et al., 2020). For medical applications, researchers widely adopt a chemotaxonomic perspective that describes three chemotypes (chemical phenotypes) based on the content of two major cannabinoids: psychoactive tetrahydrocannabinol (THC) and non-psychoactive cannabidiol (CBD) (Small and Beckstead, 1973; Turner et al., 1979; Mandolino et al., 2003; de Meijer et al., 2009). THC dominant strains have a ratio of THC/CBD > 1, intermediate strains have THC/CBD ≈ 1, and CBD dominant strains have THC/CBD < 1. Although most clinical studies focus on THC and CBD, increasing amounts of evidence show that whole plant extract has additional benefits when compared to single cannabinoids. In one study, whole cannabis extract was more effective in inducing cancer cell death than applying pure THC on cancer cell lines (Baram et al., 2019). In addition, individual cannabis extracts with similar amounts of THC produced significantly different effects on the survival of specific cancer cells, and specific cannabis extracts may selectively and differentially affect different cancer cells lines (Baram et al., 2019). In another study, extracts from five strains with similar CBD concentrations had different anticonvulsant properties in mice (Berman et al., 2018). These studies suggest that there may exist therapeutic-enhancing interactions or synergistic effects amongst cannabinoids as well as between cannabinoids and other secondary metabolites, known as the "entourage effect" (McPartland and Russo, 2001; Russo, 2011; Blasco-Benito et al., 2018). It is therefore essential to have a comprehensive, full spectrum metabolic fingerprinting of secondary metabolites in cannabis materials for research and clinical studies. Previous research also focused on female inflorescences, however, each part of the plant has a wide range of indications, primarily related with pain and inflammation, as ancient herbal medicines in various cultures (Smith and Stuart, 1911; Brand and Wiseman, 2008; Brand and Zhao, 2017; Ryz et al., 2017). Our previous study profiled cannabinoids, terpenoids, flavonoids, sterols, and triterpenoids, not only in cannabis inflorescences, but also in leaves, stem bark, and roots (Jin et al., 2020). By profiling these compounds in each cannabis plant part and associating them with therapeutic benefits, cannabis plant material that is currently treated as waste has potential to be developed into natural health products or medications.

Cannabis classification is a fundamental requirement for future medical research and applications, and it is best enabled through an overview of the class and content of potentially therapeutic secondary metabolites in each plant part. Currently, researchers attempted to discriminate and identify the chemical differences between the categories of "Sativa" (narrow-leaflet drug, NLD) and "Indica" (wide-leaflet drug, WLD) (Fischedick et al., 2010; Hazekamp and Fischedick, 2012; Hazekamp et al., 2016). Results of the chemotaxonomic separation of "Sativa" and "Indica" were mixed, and THC and CBD concentrations appeared to have no differentiation value. However, certain terpenoids were more prominent in some strains than others (Hillig, 2005b; Fischedick et al., 2010; Hazekamp and Fischedick, 2012; Fischedick, 2015, 2017; Hazekamp et al., 2016; Jin et al., 2017; McPartland and Guy, 2017). The mixed results in the current body of literature may be due to experimental design shortcomings. Firstly, the vernacular terminology ("Sativa" and "Indica") is inadequate for medical applications due to the misuse of the botanical nomenclature, extensive cross-breeding, and unreliable labeling during unrecorded hybridization (McPartland, 2017). Secondly, samples in most classification studies were collected from disparate sources (Fischedick et al., 2010; Hazekamp et al., 2016) and are subject to inconsistent environmental factors during the growth phases (Aizpurua-Olaizola, 2016) and post-harvest treatment (Jin et al., 2019). Additionally, inappropriate sample preparation and extraction procedures during laboratory analysis may affect classification results (Jin et al., 2020). All these factors contribute to the variation in chemical profiles of the final products, which in turn leads to inconsistent results and poor classification accuracy. More accurate classification results are obtainable when plants are grown in a single location, under identical environmental conditions, and uniformly processed (McPartland, 2017).

The chemical profile of CBD dominant and intermediate strains, which have gained increasing attention due to CBD's use as a therapeutic (Avraham et al., 2011; French et al., 2017; McGuire et al., 2018; Bloomfield et al., 2020), have not been studied or compared to THC dominant strains in the current literature. In this study, we used unsupervised hierarchical clustering and principal component analysis (PCA) as well as supervised canonical correlation analysis to test the goodness of fit between chemotype labeling (THC dominant, intermediate, and CBD dominant) and chemotypic variation of the full spectrum of secondary metabolites in various plant parts of 21 strains. This study also identifies chemotypic markers within each chemotype, which will facilitate strain selection for further clinical and research studies.

The objectives of this study are to:

1. investigate whether modern cannabis strains can be differentiated using a full spectrum of secondary metabolites in three chemotypes, including 14 cannabinoids, 45 terpenoids, 7 flavonoids, 3 sterols, and 3 triterpenoids, in inflorescences, leaves, stem bark, and roots;
2. investigate whether the secondary metabolites described above can differentiate strains into three chemotypes without leveraging THC and CBD data; and
3. identify chemotypic markers that can be leveraged to select and distinguish chemotypes.

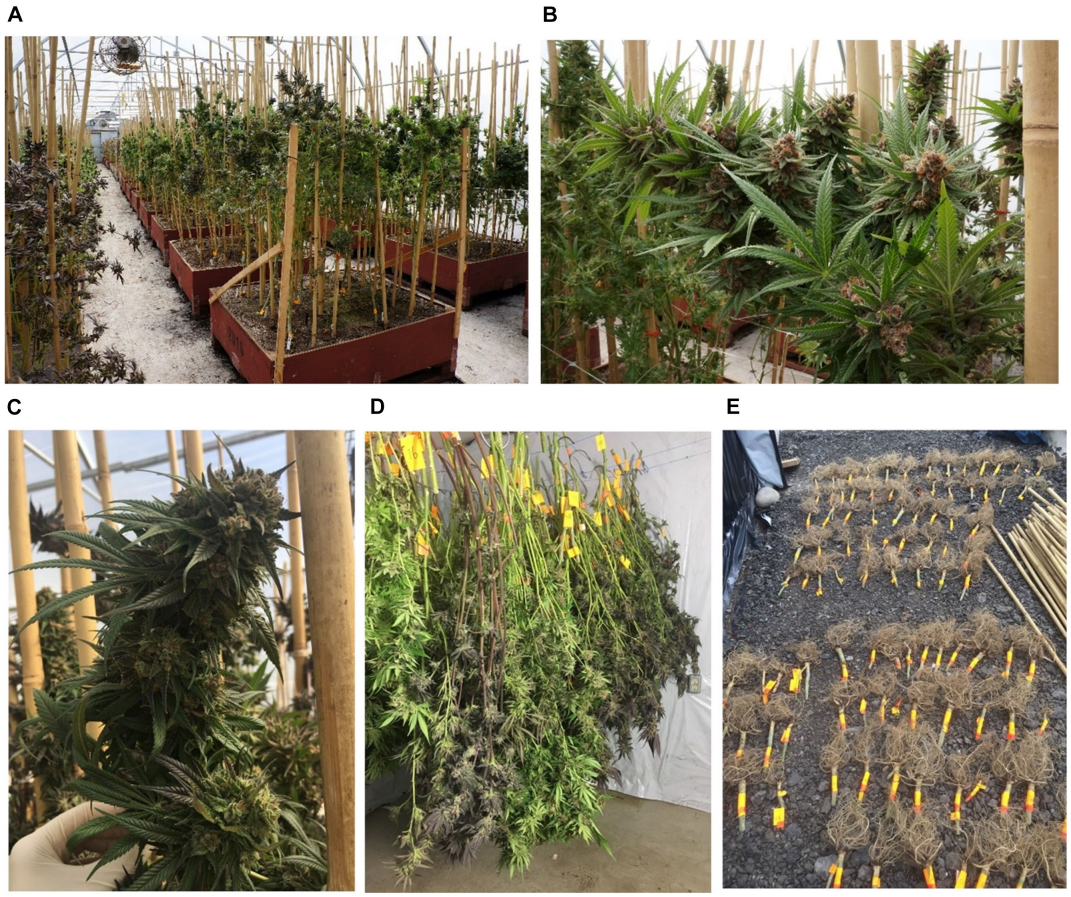

FIGURE 1 | Cannabis grown in a commercial greenhouse. **(A–C)** Cannabis plants before harvest. **(D)** Whole cannabis plants were cut above the ground and hang to dry in a drying room. **(E)** Cannabis roots were individually labeled and dried in the drying room with the other plant parts.

MATERIALS AND METHODS

Plant Material

In this project, 21 commercially available cannabis strains were grown in a commercial greenhouse (**Figure 1**) under a cannabis research license issued by Health Canada. Where possible, the reported ancestry ("Sativa-dominant," "Indica-dominant," or "hybrid") was obtained from the Leafly online database[1] or from the licensed cultivator providing the strain (**Supplementary Table 1**). Three to five cuttings per strain were rooted for 2 weeks, followed by vegetative growth under 24 h photoperiod for 2 months, and then flowered under 12 h photoperiod. After 2 months of flowering, the plants were harvested and hung to dry in a closed environment. Cannabis roots were removed and dried in the same room together with the other plant parts. Horticultural fans were used to maintain air circulation, and the temperature was kept under 35°C. The plants were dried for 7 days until the leaves and stems became brittle. At this time, the plants' moisture content is usually below 10–15% (mg/mg%) (Potter, 2009; Caplan, 2018).

[1]https://www.leafly.ca/

Sample Preparation, Extraction, and Assay

A total of 82 plants representing 21 strains were harvested. Inflorescences, leaves (fan leaves), stem bark, and roots were separately collected for each plant and analyzed for the full spectrum of secondary metabolites. Sugar leaves (small leaves extending from the inflorescences) were treated as a part of the inflorescences. Samples were prepared and analyzed according to previously developed and validated methodologies (Jin et al., 2020). Five to eight flower heads (2–4 g) of each plant were pulverized with a SPEX Geno/Grinder homogenizer (SPEX SamplePrep, Canada). Dried leaf material was crushed using a mortar and pestle and sifted through a 1.18 mm sieve. Dried stem bark and root samples were ground with the SPEX Geno/Grinder homogenizer. For cannabinoids and terpenoids extraction, 400 mg of plant material was extracted with 20 mL methanol (with 100 μg/mL tridecane as an internal standard for mono- and sesquiterpenoids) by sonication for 20 min at room temperature. For cannabinoids, the extract was spiked with Δ^9-THC-d_3 (0.5 μg/mL) as an internal standard prior to LC-MS analysis. One aliquot of the extract was used to quantify mono- and sesquiterpenoids using GC-MS. For flavonoids extraction,

250 mg of the sample was extracted with 5 mL of ethanol, water, and hydrochloric acid at a 25:10:4 volume ratio. The extract was hydrolyzed in a 100°C water bath for 135 min. The tube was then repeatedly rinsed with methanol, and the rinses were combined with the extract in a 50 mL volumetric flask, which was filled to volume with methanol. For the flavonoids assay, HPLC was used with an UV detector at 350 nm for the quantification of seven flavonoids and MS detector for compound identification. For triterpenoids and sterols extraction, 1 g of dried sample was extracted with 20 mL ethyl acetate by sonication for 1 h, followed by maceration for one day at room temperature. The extract was spiked with cholesterol (50 μg/mL) as an internal standard prior to GC-MS analysis.

Statistical Analysis

In total, 82 plants representing 21 strains were included in the following analysis. Cannabinoids were calculated as the sum of their neutral forms, metabolites (if applicable), and cannabinoid acids (multiplied by a factor converting acids into their corresponding neutral forms). For example, total THC = Δ^9 - THC + Δ^8 - THC + CBN (cannabinol, degradation product of THC) + 0.877 × tetrahydrocannabinolic acid (THCA), total CBD = CBD + 0.877 × cannabidiolic acid (CBDA), total cannabigerol (CBG) = CBG + 0.878 × cannabigerolic acid (CBGA), total cannabichromene (CBC) = CBC + 0.877 × cannabichromenic acid (CBCA), total tetrahydrocannabivarin (THCV) = THCV + 0.867 × tetrahydrocannabivarinic acid (THCVA), and total cannabidivarin (CBDV) = CBDV + 0.867 × cannabidivarinic acid (CBDVA); (Upton et al., 2014; Jin et al., 2020). Total cannabinoids was calculated as the sum of 14 cannabinoids. Total monoterpenoids (terpenoids with two isoprene units in the chemical structure) was the sum of the 29 monoterpenoids in **Supplementary Table 2.5**, and total sesquiterpenoids (terpenoids with three isoprene units) were calculated as the sum of the 16 sesquiterpenoids. Total terpenoids was the sum of total mono- and sesquiterpenoids. Total flavonoids was the sum of seven flavonoids after acid hydrolysis, including orientin, vitexin, isovitexin, quercetin, luteolin, kaempferol, and apigenin. Total sterols was the sum of campesterol, stigmasterol, and β-sitosterol. Total triterpenoids was the sum of β-amyrin, epifriedelanol, and friedelin. Compound ratios were calculated by dividing the content of one compound by the total content of that metabolite group. For example, the ratio of β-pinene was calculated as its absolute value divided by total terpenoids.

Secondary metabolites were quantified in each plant part. The following analyses were carried out only on the metabolites in the plant part where they were of highest levels among all plant parts. This distinction is made for isolating metabolites where they are present in sufficiently high concentrations (above 0.05%) to be of pharmacological interest (Russo, 2011). First, correlations were calculated between individual cannabinoids, terpenes, flavonoids, sterols, and triterpenoids. Because absolute values vary with environmental factors and relative proportions are more stable (Hillig, 2005a), compound ratios were used. Then, unsupervised (no preassigned categories as constraints) hierarchical clustering using Ward's minimum variance method (Ward, 1963) and PCA (Jolliffe, 2002) were used to check within-strain and between-cluster variation. Finally, the data were subjected to supervised (with preassigned categories as constraints) canonical correlation analysis with preassigned chemotypes in **Table 1**. The full spectrum of secondary metabolites, without THC and CBD, were subjected to hierarchical clustering, PCA, and canonical correlation analysis to investigate whether the absence of THC and CBD data would affect differentiating strains into chemotypes.

Canonical correlation analysis is also called canonical variates analysis, and is a multiple discriminant analysis that calculates the correlation between preassigned clusters and the set of covariates (chemical compounds in this study) describing the observations (Hotelling, 1936). The first canonical variable is the linear combination of the covariates that maximizes the multiple correlation between the clusters and the covariates. The second canonical variable is a linear combination uncorrelated with the first canonical variable that maximizes the multiple correlation. The analysis outputs a biplot with the first two canonical variables that provide maximum separation among the clusters. To identify marker metabolites that contribute most to the groupings, one-way ANOVA followed by Tukey honestly significant difference (HSD) *post hoc* test at the 0.05 significance level were used to determine whether significant differences exist between all clusters and each pair of clusters. Statistical analysis was performed with JMP 14.0.0.

RESULTS

Secondary Metabolites Profiled in Cannabis Inflorescences, Leaves, Stem Bark, and Roots

Secondary metabolites profiled in inflorescences, leaves, stem bark, and roots are provided in **Supplementary Table 9**. Average total cannabinoids content from 82 plants of 21 strains decreased in order of inflorescences, leaves, stem bark, and roots, as shown in **Supplementary Figure 1**. Total cannabinoids were between 7.06 and 24.42% with an average of 15.90 ± 4.02% (SD) in inflorescences, between 0.95 and 4.28% with an average of 2.17 ± 0.71% in leaves, between 0.06 and 2.33% with an average of 0.58 ± 0.28% in stem bark, and less than 0.03% in roots (**Supplementary Table 2.1**). Total average cannabinoids

TABLE 1 | Preassigned chemotypes as the working groups for canonical correlation analysis .

Clusters	Number of strains	Strain codes as chemotypes
C1 (CBD dominant)	6	3-CBD, 4-CBD, 5-CBD, 6-CBD, 8-CBD, 10-CBD
C2 (Intermediate)	3	1-Intermediate, 2-Intermediate, 9-Intermediate
C3 (THC dominant)	12	11-THC, 12-THC, 13-THC, 14-THC, 15-THC, 16-THC, 18-THC, 19-THC, 20-THC, 21-THC, 22-THC, 23-THC

content in inflorescences were 17.16 ± 4.60%, 14.98 ± 2.63%, and 13.96 ± 2.15% in THC dominant, intermediate, and CBD dominant strains, respectively (**Supplementary Table 2.2**). These values are typical for modern cannabis strains in North America and mostly agreed with reported values in the literature, which are generally between 5 and 25% (ElSohly and Gul, 2014; Fischedick, 2015; Hazekamp et al., 2016; Lynch et al., 2016; Jikomes and Zoorob, 2018; Richins et al., 2018). THC dominant strains had significantly higher concentrations of cannabinoids than the other two chemotypes ($p = 0.0035$). Total cannabinoids content in leaves and stem bark averaged from three chemotypes are summarized in **Supplementary Tables 2.3**, **2.4**.

Average total terpenoids as the sum of mono- and sesquiterpenoids in the same population decreased in order of inflorescences, leaves, stem bark, and roots (**Supplementary Figure 1**). Total terpenoids in inflorescences was between 0.753 and 3.305% with an average of 1.509 ± 0.467%, in leaves between 0.035 and 0.197% with an average of 0.103 ± 0.032%, and in stem bark and roots less than 0.03% (**Supplementary Table 2.1**). Average total terpenoids content in inflorescences and leaves for the three chemotypes are summarized in **Supplementary Tables 2.5**, **2.6**.

Average total flavonoids as the sum of orientin, vitexin, isovitexin, quercetin, luteolin, kaempferol, and apigenin was highest in leaves, lower in inflorescences, and less than 0.03% in stem bark and roots (**Supplementary Figure 1**). Total flavonoids in inflorescences were between 0.028 and 0.284% with an average of 0.091 ± 0.050%, and in leaves between 0.051 and 0.470% with an average of 0.188 ± 0.098% (**Supplementary Table 2.1**). Flavonoids exist in cannabis plants as both aglycones and conjugated glycosides and were estimated to be less than 1% in leaves (McPartland and Russo, 2001) The results of this study was congruent with this estimate, since the flavonoids were not converted to conjugated glycosides. All seven flavonoids were quantifiable in inflorescences in three chemotypes (**Supplementary Table 2.7**), while quercetin and kaempferol were below the quantification limit in leaves (**Supplementary Table 2.8**). All flavonoids identified in inflorescences and leaves were less than those reported in other studies (Flores-Sanchez and Verpoorte, 2008), possibly due to differences in strains and plant growth stage, since flavonoids content fluctuate with plant age (Vanhoenacker et al., 2002).

Total sterols content as the sum of three phytosterols, campesterol, stigmasterol, and β-sitosterol was highest in roots, lower in stem bark, and was less than 0.03% in inflorescences and leaves (**Supplementary Figure 1**). Total sterols content in roots was between 0.037 and 0.085% with an average of 0.066 ± 0.009%, and in stem bark was between 0.037 and 0.082% with an average of 0.055 ± 0.013% (**Supplementary Table 2.1**). Average total sterols content in stem bark and roots of the three chemotypes are summarized in **Supplementary Tables 2.9**, **2.10**.

Total triterpenoids as the sum of β-amyrin, epifriedanol, and friedelin was highest in roots, lower in stem bark, and was less than 0.03% in inflorescences and leaves (**Supplementary Figure 1**). Total triterpenoids in stem bark was between 0.008 and 0.136% with an average of 0.039 ± 0.023%, in roots was between 0.080 and 0.275% with an average of 0.182 ± 0.043% (**Supplementary Table 2.1**). Average total triterpenoids content in stem bark and roots in the three chemotypes are summarized in **Supplementary Tables 2.11**, **2.12**.

The distribution of secondary metabolites in each plant part agreed with conclusions from our last study (Jin et al., 2020). Correlation and classification analyses were performed only for metabolites in the plant part where they were present in the highest concentrations representative for that strain. For example, the average terpenoid content in leaves were low (0.103 ± 0.032%) compared to the levels in inflorescences (1.509 ± 0.467%), and only 15 mono- and sesquiterpenoids that were detected in inflorescences were above the quantification limit in leaves (**Supplementary Table 2.6**). In addition, the correlations between cannabinoids and terpenoids in leaves were like those in inflorescences, especially for the terpenoids that are abundant in both these two plant parts, including α-pinene, β-pinene, limonene, linalool, β-caryophyllene, trans-β-farnesene, α-humulene, trans-nerolidol, (−) guaiol, β-eudesmol, α-eudesmol, and α-bisabolol (**Supplementary Figure 2** and **Supplementary Table 8**). As such, using the terpene profile in inflorescences was adequate for clustering purposes. Flavonoids in inflorescences and leaves were included in the analysis because quercetin and kaempferol were quantifiable in inflorescences but not in leaves. For sterols, the content and ratios of three sterols are similar between stem bark and roots. Because total sterols in roots (0.064–0.068%) are slightly higher than them in stem barks (0.052–0.059%), the sterol profiles in roots were used in the data analysis. Triterpenoid profile in roots were used because the content of total triterpenoids was above the threshold for pharmacological interest in all plant parts except in roots. To summarize, the most abundant secondary metabolites in individual plant parts were used in the statistical analysis for identifying differences between the three chemotypes. These metabolites were cannabinoids, terpenes, and flavonoids in inflorescences; flavonoids in leaves; and sterols and triterpenoids in roots (**Supplementary Table 7**).

Correlation Analysis Between Secondary Metabolites

Correlations between total THC or total CBD with individual cannabinoids, terpenoids, flavonoids, sterols, and triterpenoids are plotted in **Figure 2** and summarized in **Supplementary Table 3**. Calculations were performed on quantifiable compounds using ratios. Total THC was positively correlated with two cannabinoids (total CBG and total THCV), 10 monoterpenoids (α-terpineol, limonene, camphene, fenchol, linalool, ocimene, borneol, terpinolene, β-pinene, and sabinene hydrate), four sesquiterpenoids (α-humulene, β-caryophyllene, trans-nerolidol, and trans-β-farnesene), four flavonoids (quercetin and kaempferol in flowers, luteolin and apigenin in both inflorescences and leaves), and two triterpenoids (β-amyrin and friedelin). Total CBD was positively correlated with two cannabinoids (total CBDV and total CBC), three monoterpenoids (β-myrcene, 1,8-cineole (eucalyptol), α-pinene),

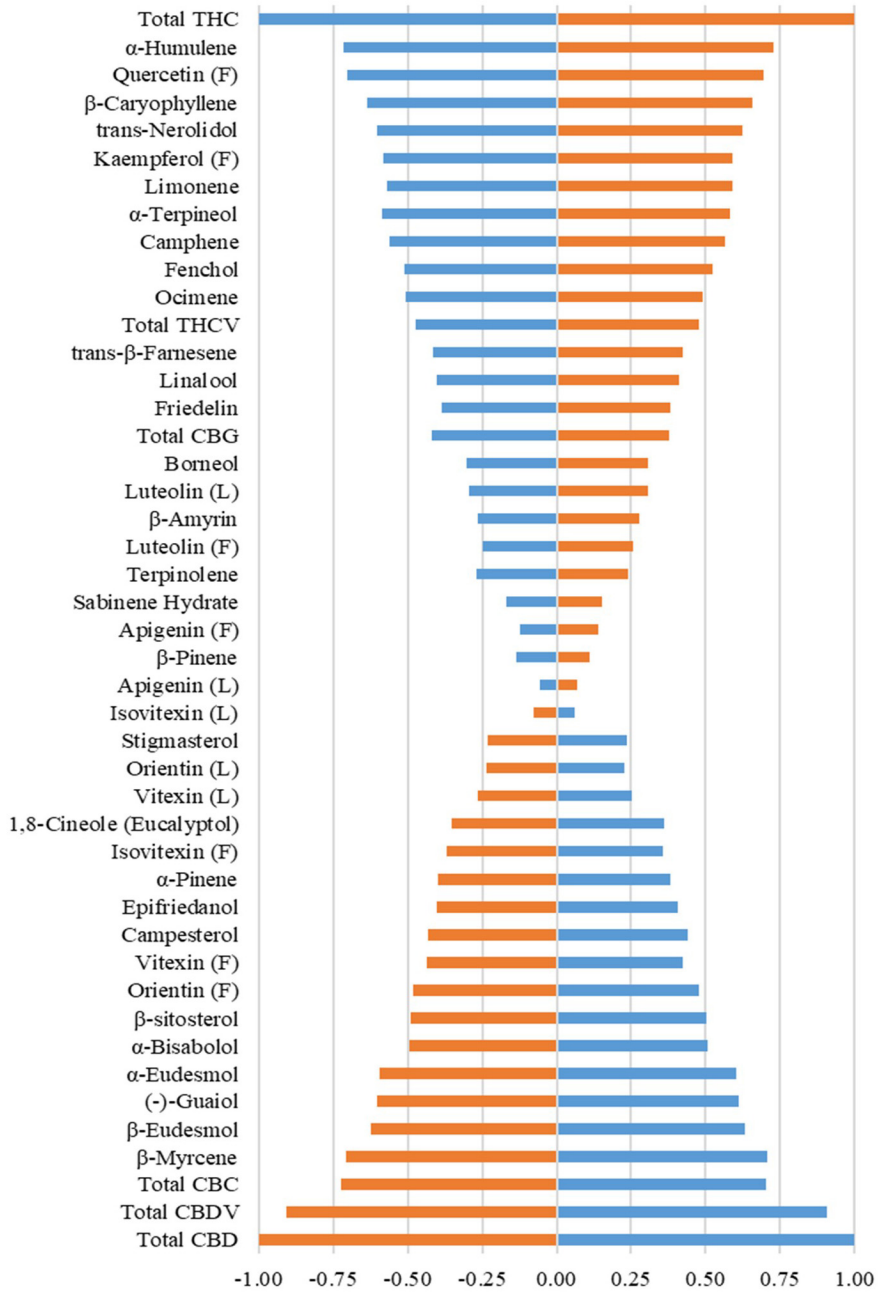

FIGURE 2 | Correlations of total THC and total CBD with cannabinoids (in inflorescences), mono- and sesquiterpenoids (in inflorescences), flavonoids (in inflorescences and leaves), sterols (in roots), and triterpenoids (in roots) on quantifiable compounds using ratios. Flavonoids quantified in inflorescences are labeled (F), and flavonoids in leaf are labeled (L).

four sesquiterpenoids (β-eudesmol, (−)-guaiol, α-eudesmol, α-bisabolol), three flavonoids (orientin, vitexin, isovitexin in both inflorescences and leaves), three sterols (campesterol, stigmasterol, β-sitosterol), and one triterpenoid (epifriedanol). Compounds that were positively correlated with THC were all negatively correlated with total CBD, and vice versa. The quantitative correlations are plotted in **Supplementary Figure 3**. Most compounds have similar correlations with total THC and total CBD when calculated using ratios and absolute values.

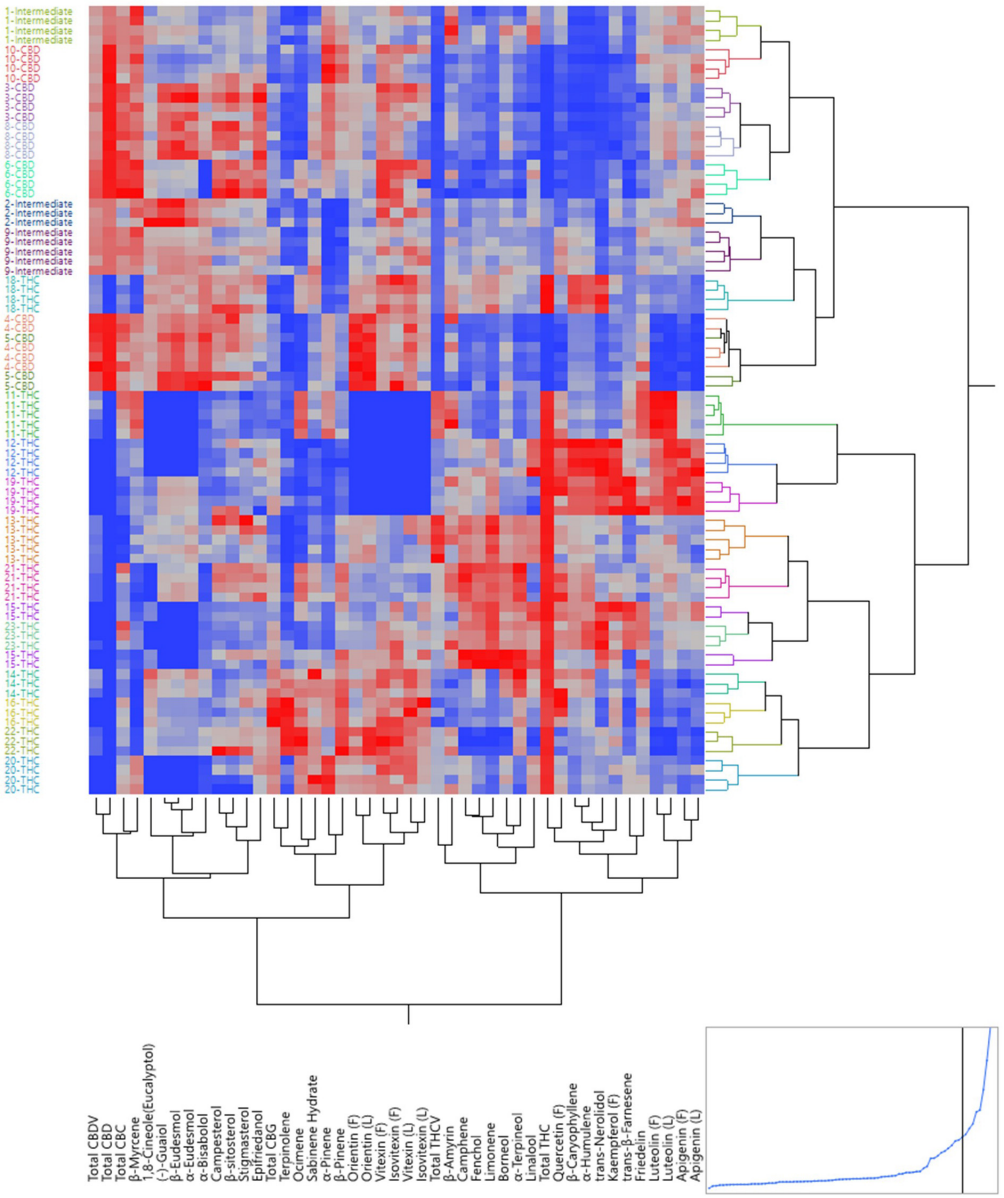

FIGURE 3 | Dendrogram by hierarchical clustering analysis using the full spectrum of secondary metabolites (in ratios) of 82 plants representing 21 strains.

Unsupervised Hierarchical Clustering

The same set of data was used to build a dendrogram of the 82 plants using hierarchical clustering, where almost all plants of the same strains were clustered together, except for one 5-CBD plant that was mixed with 4-CBD plants and plants of 15-THC that were mixed with 23-THC plants (**Figure 3**). The dendrogram shows two major branches: CBD dominant strains and intermediate strains together as one major branch, and THC dominant strains as the other. The dendrogram using absolute values of the secondary metabolites is shown in **Supplementary Figure 4**. These results both confirmed the minimum within-strain variation (between plants within each strain) and between-cluster variation (between strains within each chemotypes). The full spectrum of secondary metabolites without total THC and total CBD resulted in a dendrogram with the same grouping results (**Supplementary Figure 5**).

Unsupervised Principal Component Analysis

Figure 4 shows a scatterplot of 82 plants along two principal components (PC), where PC1 and PC2 explained 33.8 and 16.4% of the total variance, respectively. Plants of the same strains tended to occupy the same region on the plot. THC dominant strains (C3) mainly occupied the left side of the plot and CBD dominant (C1) and intermediate strains (C2) occupied the lower right quadrant. The loading matrix in **Table 2** lists the

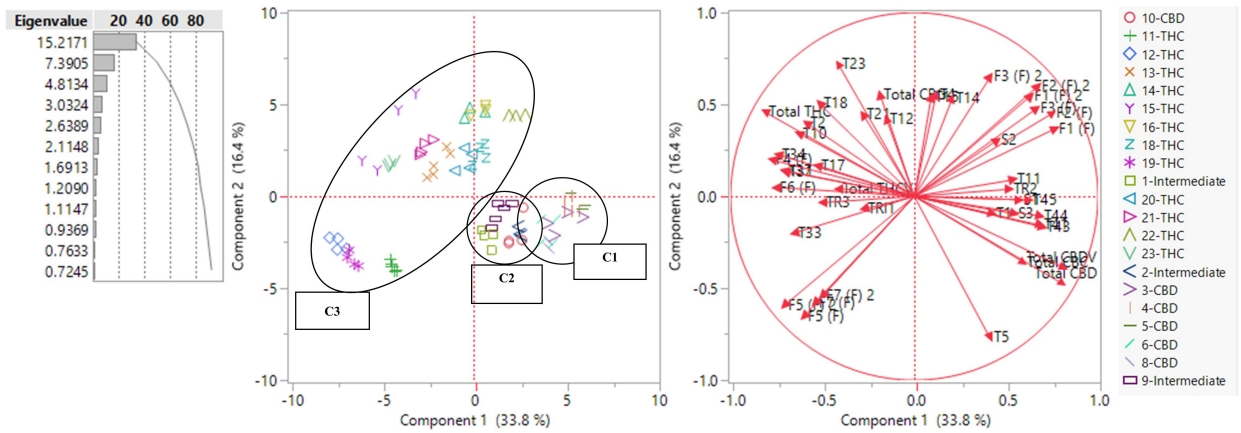

FIGURE 4 | PCA scatter plot **(left)** and loading plot **(right)** using the full spectrum of secondary metabolites (in ratios) of 82 plants representing 21 strains. Terpenoids are labeled with T and the number assigned in **Supplementary Table 2.5**. Flavonoids are labeled as F and the number assigned in **Supplementary Table 2.7**. Flavonoids quantified in inflorescences are labeled (F) and flavonoids in leaf are labeled (L). Sterols are labeled as S and the number assigned in **Supplementary Table 2.9**. Triterpenoids are labeled as TRI and the number assigned in **Supplementary Table 2.11**

compounds that contributed most to the separations along PC1 and PC2 with the absolute value of loadings equal to or greater than 0.45. PC1 was positively correlated with three cannabinoids (total CBD, total CBDV, and total CBC), one monoterpenoid (1,8-cineole (eucalyptol)), four sesquiterpenoids (β-eudesmol, (−)-guaiol, α-eudesmol, α-bisabolol), three flavonoids (orientin, vitexin, and isovitexin), three sterols (campesterol, stigmasterol, and β-sitosterol), and one triterpenoid (epifriedanol), which were compounds identified as positively correlated with total CBD. PC1 was negatively correlated with one cannabinoid (total THC), four monoterpenoids (limonene, camphene, fenchol, and linalool), four sesquiterpenoids (α-humulene, β-caryophyllene, trans-nerolidol, and trans-β-farnesene), four flavonoids (quercetin, kaempferol, and apigenin), and one triterpenoid (friedelin), which were compounds identified as positively correlated with total THC. THC dominant strains were scattered in both lower left quadrant and upper right quadrant along PC2. Compounds positively correlated with PC2 and negatively correlated with PC1 (PC1 < 0 and PC2 > 0), including total THC, total CBG, total THCV, α-terpineol, camphene, fenchol, linalool, ocimene, borneol, α-humulene, β-caryophyllene, trans-nerolidol, quercetin, and kaempferol, were more abundant in THC dominant strains than those in CBD dominant and intermediate strains. β-Myrcene was negatively correlated with PC2 and positively correlated with PC1, which means it was more abundant in CBD dominant and intermediate strains. Two flavonoids, luteolin and apigenin, were negatively correlated with PC1 and PC2, and were more abundant in THC dominant strains in the left lower quadrant than other THC dominant strains. Although some compounds were more correlated with CBD, they may be more abundant in some THC dominant strains. For example, compounds positively correlated with PC2 and positively correlated with PC1, including orientin (L), vitexin (L), and isovitexin (L), were more abundant in THC dominant strains in the upper right quadrant than strain in C1 and C2, even though these flavonoids were positively correlated with CBD. This may be the result of extensive strain crossing and hybridization. PCA using absolute values of the secondary metabolites are also shown in **Supplementary Figure 6**. The full spectrum of secondary metabolites without total THC and total CBD resulted in a similar PCA scatter plot where PC1 and PC2 explained 32.6 and 16.1% of the total variance, respectively (**Supplementary Figure 7**).

Supervised Canonical Correlation Analysis

The canonical correlation analysis of 82 plants showed good separation between the three chemotypes (**Figure 5**). Each plant was predicted to be in its originally preassigned cluster with 100% accuracy (**Supplementary Table 4**). Canonical correlation analysis using the absolute values of 45 compounds were also investigated (**Supplementary Figure 8**), with 100% accuracy in sorting each plant into its originally preassigned chemotypes. The full spectrum of secondary metabolites, absent total THC and total CBD, also predicted each plant to be in its originally preassigned cluster with 100% accuracy (**Supplementary Figure 9**). However, the distance between three clusters were smaller along two canonical axes due to reduced differences in the chemical profiles of three chemotypes after removing the THC and CBD data.

Identification of Chemotypic Markers for Three Chemotypes

Means (±SD), Tukey HSD multiple tests at the 0.05 significance level, and p value of one-way ANOVA of 45 quantifiable compounds (using ratios) for each of the three chemotypes are listed in **Supplementary Table 5** and plotted in **Figure 6**. The largest number of significant differences (Tukey HSD multiple tests at the 0.05 significance level) was 37, which was between C1 and C3. The most similar pair was C1 and C2, with 14 significant differences. The number of significant differences

TABLE 2 | Formatted loading matrix for PC1 and PC2 (only compounds with absolute loadings >0.45 are listed).

PC1				PC2			
Compound	**Positive loadings**	**Compound**	**Negative loadings**	**Compound**	**Positive loadings**	**Compound**	**Negative loadings**
Total CBDV	0.82	Total THC	−0.81	α-Terpineol	0.72	β-Myrcene	−0.77
Total CBD	0.81	Quercetin (F)	−0.77	Isovitexin (L)	0.65	Luteolin (F)	−0.65
Orientin (F)	0.77	Kaempferol (F)	−0.75	Vitexin (L)	0.60	Luteolin (L)	−0.60
Vitexin (F)	0.76	α-Humulene	−0.74	β-Pinene	0.56	Apigenin (F)	−0.58
β-Eudesmol	0.70	Luteolin (L)	−0.71	Total CBG	0.55	Apigenin (L)	−0.55
α-Eudesmol	0.69	trans-Nerolidol	−0.71	Orientin (L)	0.55	Total CBD	−0.47
(−)-Guaiol	0.68	β-Caryophyllene	−0.70	Terpinolene	0.54		
Vitexin (L)	0.68	trans-β-Farnesene	−0.65	Sabinene Hydrate	0.53		
Isovitexin (F)	0.67	Limonene	−0.63	Fenchol	0.50		
Orientin (L)	0.64	Luteolin (F)	−0.60	Isovitexin (F)	0.46		
α-Bisabolol	0.62	Camphene	−0.59	Vitexin (F)	0.45		
Total CBC	0.59	Apigenin (F)	−0.54	Borneol	0.45		
Campesterol	0.57	Linalool	−0.53				
β-sitosterol	0.55	Fenchol	−0.52				
1,8-Cineole (Eucalyptol)	0.54	Apigenin (L)	−0.50				
Epifriedanol	0.52	Friedelin	−0.50				
Stigmasterol	0.45						

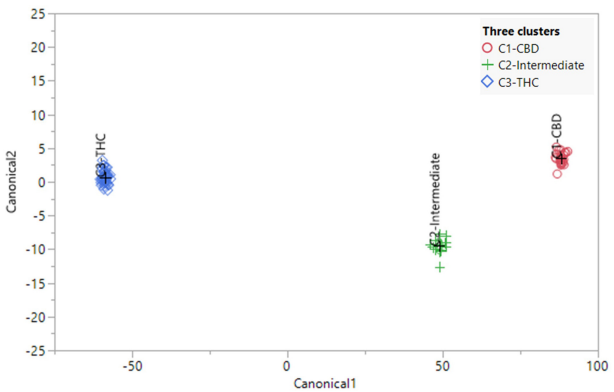

FIGURE 5 | Canonical correlation analysis using the full spectrum of secondary metabolites (using ratios) of 82 plants representing 21 strains. The plants were preassigned to three chemotypes in **Table 1**. The observations and the multivariate means of each group ("+") are represented as points on the biplot. An ellipse denoting a 50% contour is plotted for each group, that contains approximately 50% of the observations.

between C2 and C3 was 23. Strains from C1 had significant higher amount of total CBD, total CBDV, total CBC, α-pinene, β-pinene, β-myrcene, (−)-guaiol, β-eudesmol, α-eudesmol, α-bisabolol, orientin (F), vitexin (F), isovitexin (F), orientin (L), campesterol, stigmasterol, β-sitosterol, and epifriedanol than in strains of C3, which were all positively correlated with total CBD. Strains from C3 had significant higher amount of total THC, total THCV, total CBG, camphene, limonene, ocimene, linalool, fenchol, borneol, α-terpineol, β-caryophyllene, trans-β-farnesene, α-humulene, trans-nerolidol, quercetin (F), kaempferol (F), β-amyrin, and friedelin, which were all positively correlated with total THC. Most compounds in the C2 strains were at the same level with strains in C1 or C3 or at an intermediate level between C1 and C3.

Means ± SD, Tukey's HSD multiple tests at the 0.05 significance level, and p value of one-way ANOVA of the absolute values of 45 compounds for each cluster were summarized in **Supplementary Table 6**. The largest number of significant differences was 38, which was between C1 and C3. The most similar pair was C1 and C2, with 10 differences. The number of significant differences between C2 and C3 was 23. Cannabinoids, terpenoids, flavonoids, sterols, and triterpenoids that were significantly higher in C1, C2, and C3 were similar to those identified using ratios.

Although numerous significant differences in compounds were found amongst CBD dominant, intermediate, and THC dominant strains, the group means of some compounds differed by less than a factor of two. In addition, some compounds may be significantly different qualitatively in ratios but not quantitatively in absolute values. For example, all three sterols (campesterol, stigmasterol, and β-sitosterol), were significantly higher in roots of CBD dominant strains than in THC dominant strains by ratios (one-way ANOVA $p < 0.0001$, $p = 0.1279$, and $p < 0.0001$, respectively), but they were not significantly different by absolute values (one-way ANOVA $p = 0.1279$, $p = 0.0361$, and $p = 0.0169$, respectively). Compounds significantly different (one-way ANOVA $p < 0.05$) with two or more than two-fold higher in terms of both ratios and absolute values in the identified clusters than in the clusters with the lowest values were selected as chemotypic markers. These included three cannabinoids (total CBD, total CBDV, and total CBC), six terpenoids (α-pinene, β-myrcene, (−)-guaiol, β-eudesmol, α-eudesmol, and α-bisabolol), and three flavonoids (orientin, vitexin, and isovitexin) for CBD dominant strains, three cannabinoids (total THC, total

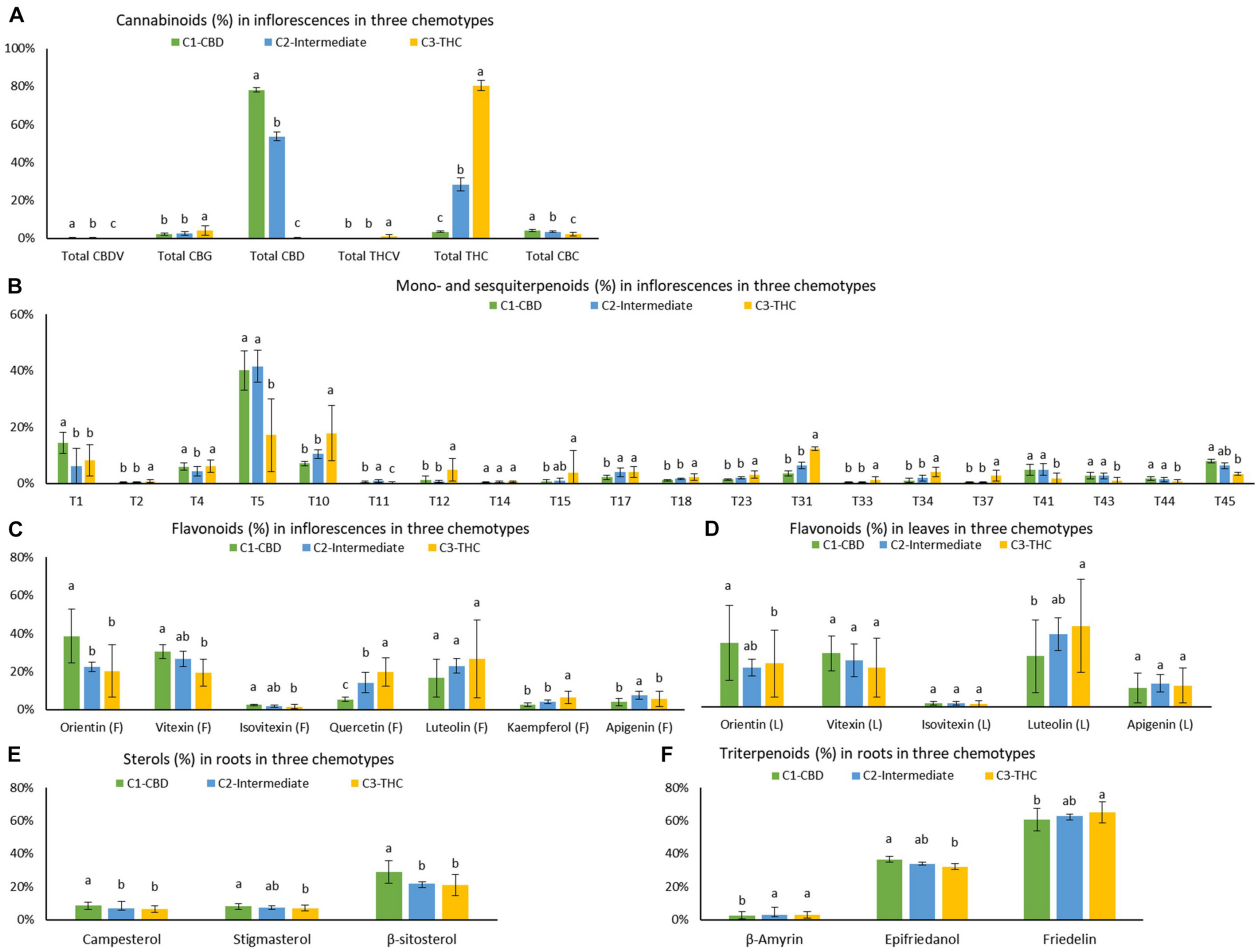

FIGURE 6 | Means and standard deviations (±SD) of **(A)** cannabinoids in inflorescences, **(B)** mono- and sesquiterpenoids in inflorescences, **(C)** flavonoids in inflorescences, **(D)** flavonoids in leaves, **(E)** sterols in roots, and **(F)** triterpenoids in roots (in ratios) for each of the three chemotypes C1 – CBD dominant, C2 – intermediate, and C3 – THC dominant. Cluster means were expressed as mean ± SD. *Levels not connected by the same letter are significantly different by Tukey HSD multiple tests at the 0.05 significance level.

THCV, and total CBG), twelve terpenoids (camphene, limonene, ocimene, sabinene hydrate, terpinolene, linalool, fenchol, α-terpineol, β-caryophyllene, trans-β-farnesene, α-humulene, and trans-nerolidol), and two flavonoids (quercetin and kaempferol) for THC dominant strains. Intermediate strains are more similar to CBD dominant strains than THC dominant strains with higher amounts of β-myrcene, (−)-guaiol, β-eudesmol, α-eudesmol, and α-bisabolol. There are more mono- and sesquiterpenoids that are significantly higher in the THC dominant cluster than in the CBD dominant and intermediate clusters. The simultaneous presence of a collection of compounds can be used to differentiate types of plants.

DISCUSSION

Cannabinoids as Chemotypic Markers

In this study, the average THC to CBD ratios in the three chemotypes were 247 ± 79, 0.5 ± 0.1, and 0.04 ± 0.01, respectively. These ratios showed that THC levels in THC dominant strains were greater than CBD levels in CBD dominant strains. This bias toward higher THC is due to the long history of extensive hybridization for recreational purposes (McPartland, 2017). A THC/CBD ratio of 247:1 in THC dominant strains matched with those in "Sativa" and "Indica" strains that were almost devoid of CBD (Fischedick et al., 2010; Hazekamp and Fischedick, 2012; Fischedick, 2015, 2017; Hazekamp et al., 2016; Jin et al., 2020). Due to CBD's therapeutic potential without psychoactive effects (Booz, 2011; Couch et al., 2017; Vallée et al., 2017; Callejas et al., 2018; Mallada Frechín, 2018), breeding for high CBD concentrations began only recently by integrating hemp-type CBD acid synthase gene clusters into a background of drug-type cannabis to elevate CBDA production (Clarke and Merlin, 2016; Grassa et al., 2018). The CBD to THC ratios in intermediate trains were similar to 1.8:1 in our previously reported values (Jin et al., 2020), and also matched with the reported cannabinoid profile of intermediate strains available in the database. These intermediate strains may have been created

by crossing purebred THC dominant types with CBD dominant types (de Meijer et al., 2003). Chemotaxonomic research in minor cannabinoids of the three chemotypes are sparse in the current literature. In this study, minor cannabinoids were mostly less than 1% in all three chemotypes and several minor cannabinoids were more abundant in one chemotypes relative to others.

Mono- and Sesquiterpenoids as Chemotypic Markers

In general, sesquiterpenoids are considered as more stable markers because monoterpenes are more volatile (McPartland, 2017). In this study, (−)-guaiol, β-eudesmol, α-eudesmol, and α-bisabolol were identified as chemotypic markers in CBD and intermediate strains. These compounds were also noted by Hillig as signature peaks on chromatograms for pre-hybridization Afghani WLD landraces (Hillig, 2005a) and modern "Indica" dominant strains (WLD), but were present in lower amounts in pre-hybridization NLD landraces and modern "Sativa" dominant strains (NLD) (Fischedick et al., 2010; Hazekamp et al., 2016). CBD dominant strains and pre-hybridization Afghani WLD landraces are similar in that they both have elevated CBD concentrations compared to their THC dominant counterparts. According to the correlation analysis in this study, these chemotypic markers for CBD dominant strains and intermediate strains may be related to CBD production. For modern "Indica" dominant strains (WLD), which are nearly devoid of CBD, even though these sesquiterpenoids were considered to be inherited from their WLD landrace ancestors despite selection for elevated THC/CBD ratios, these compounds were detected only in trace amounts (Fischedick et al., 2010; Hazekamp and Fischedick, 2012; Fischedick, 2015, 2017; Hazekamp et al., 2016). In this study, terpinolene, β-caryophyllene, and trans-β-farnesene, were identified as chemotypic markers in THC dominant strains. These compounds were also noted by Hillig as signature peaks on chromatograms for pre-hybridization NLD landraces (Hillig, 2005a) and modern "sativa" dominant strains (NLD), but were present in lower amounts in pre-hybridization WLD landraces and modern "Indica" dominant strains (WLD) (Fischedick et al., 2010; Hazekamp et al., 2016). THC dominant strains and pre-hybridization NLD landraces both have elevated THC concentrations and are almost devoid of CBD. These chemotypic markers for THC dominant strains and intermediate strains may be correlated with THC production when CBD is not produced.

Studies have shown that terpenes in cannabis are derived from two pathways: the plastidial methylerythritol phosphate (MEP) pathway and the cytosolic mevalonate (MVA) pathway (Andre et al., 2016; Booth et al., 2017; Zager et al., 2019). Geranyl diphosphate (GPP) is typically derived from the MEP pathway and is the precursor for cannabinoid and monoterpenoid biosynthesis. Farnesyl diphosphate (FPP) is commonly produced from MVA pathway and is the precursor for sesquiterpenoids, triterpenoids and sterols. Although it is hypothesized that the identified chemotypic markers may be related to CBD or THC production, currently there are no biomedical studies on these correlations. Future studies are needed on the biochemical relationship between CBD or THC production and individual terpenoid production.

Of the strains with a reported Sativa/Hybrid/Indica ancestry label, CBD dominant strains contained two "Sativa" strains, intermediate strains contained one "Sativa" strain and one "Indica" strain, and THC dominant strains contained ten "Indica" strains and one "50/50 hybrid" strain. Based on the reported ancestry, the results of this study seem to contradict other studies. The terpenoids markers in CBD dominant strains (reported as "Sativa" due to narrow leaflets) were similar to those identified in "Indica" dominant strains but different from those identified in "Sativa" dominant strains in other studies (Fischedick et al., 2010; Hazekamp and Fischedick, 2012; Fischedick, 2015, 2017; Hazekamp et al., 2016). Similarly, the terpenoids markers in THC dominant strains (reported as "Indica" due to wide leaflets) were similar to those identified in "Sativa" dominant strains but different from those identified in "Indica" dominant strains in other studies. These conflicting results reflects the unreliability of the vernacular "Sativa" and "Indica" categories, which are based on the visual determination of leaflet shape, often with no reference data for categorization (Jin et al., 2021). This may lead to mixed results in separating modern strains genetically or chemically (Elzinga et al., 2015; Sawler et al., 2015). Another explanation for the discrepancy is that instead of separating "Sativa" vs "Indica", which are often THC dominant strains, this paper focused on the differentiation between three chemotypes. Because no "Sativa" strains were reported for THC dominant strains in this study, whether (−)-guaiol, β-eudesmol, α-eudesmol, and α-bisabolol are more abundant in "Indica" dominant strains and terpinolene, β-caryophyllene, and trans-β-farnesene are more abundant in "Sativa" dominant strains as described in other studies could not be verified.

Flavonoids as Chemotypic Markers

Flavonoid variation in cannabis was investigated by Clark and Bohm (1979), the only such study that used flavonoids for chemotaxonomy and for supporting a two-species hypothesis: where luteolin was more often detected in *C. sativa* L. but not in *C. indica* Lam. (Clark and Bohm, 1979). There have yet to be chemotaxonomic studies of flavonoids across the three cannabis chemotypes. We found that orientin, vitexin, and isovitexin were the signature flavonoids of CBD dominant strains, and quercetin and kaempferol were detected only in inflorescences and tended to be higher in THC dominant strains.

Sterols and Triterpenoids as Chemotypic Markers

The role of sterols and triterpenoids in the chemotaxonomy of cannabis have not yet been investigated. In this study, CBD dominant strains had significantly higher ratios of three sterols, but they differed by less than a factor of two and may not provide a firm basis for chemotaxonomic distinction. Similarly, for triterpenoids, although the ratio of epifriedanol was higher in CBD dominant strains and friedelin was higher in THC dominant strains, the differences were

not sufficiently large for these compounds to be used as chemotype markers.

The Potential of Developing Holistic Cannabis-Based Products and Medications

Because cannabinoids are concentrated in cannabis inflorescences, cannabis leaves, stems, and roots are normally discarded by cannabis growers. However, in traditional Chinese medicine, cannabis leaves were used for treating conditions such as malaria, panting, roundworm, scorpion stings, hair loss, graying of hair. Cannabis stem bark was used for strangury and physical injury. Cannabis roots were used for gout, arthritis, joint pain, fever, skin burns, hard tumors, childbirth, and physical injury (Smith and Stuart, 1911; Brand and Wiseman, 2008; Ryz et al., 2017). Their traditional uses may serve as points of reference for investigating the medical potential of what is currently a byproduct or plant waste.

To link the traditional therapeutic uses for each part with the chemistry, we had identified the major groups of compounds in each plant part for correlation with benefits described in the literature. Cannabinoids, including THC, CBD, CBG, CBC, THCV, CBN, and CBDV, in both acid and neutral forms all have broad therapeutic potential, including anti-inflammatory (Bolognini et al., 2010; DeLong et al., 2010; De Petrocellis et al., 2012; Borrelli et al., 2013; Cascio and Pertwee, 2014; Brierley et al., 2016), analgesic (Davis and Hatoum, 1983; Evans, 1991; Cascio and Pertwee, 2014), anticonvulsant (Dwivedi and Harbison, 1975; Hill et al., 2010, 2013), antioxidant, and neuroprotective properties (Gugliandolo et al., 2018). Increasing numbers of studies have shown that minor cannabinoids significantly contribute to the variance among cannabis extract, which further alter or enhance targeted therapeutic effects comparing to pure THC or CBD alone (Berman et al., 2018; Baram et al., 2019).

Terpenoids are widely distributed in highly fragrant fruits, plants, and herbs and they have anti-inflammatory (Miguel, 2010; Xiao et al., 2018), antirheumatic (Ames-Sibin et al., 2018), pain relieving (Gouveia et al., 2018; Xiao et al., 2018), antioxidant and neuroprotective (Shahriari et al., 2018), gastroprotective (Tambe et al., 1996; Klopell et al., 2007), and larvicidal properties (Govindarajan et al., 2016). If a cannabinoid-terpenoid entourage effect exists, it may not be at the CB1 or CB2 receptor level, but rather the terpenoids may act at different molecular targets in neuronal circuits (Santiago et al., 2019).

Flavonoids share a wide range of biological effects with cannabinoids and terpenoids, including anti-inflammatory (He et al., 2016; Hayasaka et al., 2018; Sharma et al., 2018; Wang et al., 2018; Yao et al., 2018), antirheumatic (Haleagrahara et al., 2017; Chirumbolo and Bjørklund, 2018; Yang et al., 2018), analgesic (He et al., 2016; Strada et al., 2017), and antioxidant and neuroprotective properties (An et al., 2012; He et al., 2016; Ashaari et al., 2018; Tsai et al., 2018; Wang et al., 2018; Zheng et al., 2018). Ginkgo leaves are one of the prominent sources of flavonoids, with 0.4% total flavonoids in terms of total aglycones (Hasler et al., 1992). In this study, the mean of total flavonoids was $0.19 \pm 0.09\%$, which makes cannabis leaves a promising source for flavonoids extraction.

Sterols and triterpenoids are mainly present in cannabis stem bark and roots. Friedelin is the most abundant and most studied triterpenoids in cannabis, and has anti-inflammatory, antioxidant, estrogenic, anti-cancer, and liver protectant properties (Ryz et al., 2017). β-sitosterol, stigmasterol, and campesterol are the most abundant phytosterols in the human diet. Phytosterols are widely recognized as lowering the levels of low-density lipoprotein cholesterol (Gylling et al., 2014; Ras et al., 2014). They are also studied for anti-inflammatory, antioxidant, and pain relieving properties (Kozłowska et al., 2016).

These groups of identified bioactive compounds may underpin the traditional applications indicated for each plant part, but most of the therapeutic properties for these individual compounds have been studied in other herbal medicine and not in cannabis. The pharmaceutical values and the potential synergies of these bioactive compounds need to be directly investigated using cannabis material. Well-designed clinical studies are necessary to convert each part of the cannabis plant into evidence-based medicine. The chemotypic markers identified in this study will facilitate strain selection in research and clinical studies when the optimal combination of the chemical compounds is determined for treating certain conditions.

CONCLUSION

The chemical variation in CBD dominant and intermediate strains has yet to be studied or compared to THC dominant strains in the literature. This comprehensive chemotaxonomic investigation profiled cannabinoids, terpenoids, flavonoids, sterols, and triterpenoids in inflorescences, leaves, stem bark, and roots in 82 plants of 21 cannabis strains. These chemical data were subjected to correlation analysis, unsupervised clustering analysis (hierarchical clustering and PCA) and supervised canonical correlations analysis. In unsupervised clustering, 82 plants were clustered in accordance with their chemotypes. Canonical correlation analysis classified 82 plants into three chemotypes with 100% accuracy using full spectrum of secondary metabolites. Numerous significant differences that could be used as chemotypic markers were found amongst CBD dominant, intermediate, and THC dominant strains. These identified compounds were largely consistent with results from correlation analysis, hierarchical clustering, PCA, and by comparing concentration and ratio averages between chemotypes. At each step of the clustering analysis, it was found that secondary metabolites without total THC and total CBD could continue to sort strains into their defined chemotypes and achieve the same clustering results. This demonstrated that the clustering results were not solely driven by THC and CBD content or ratio, and that other metabolites can be used as chemotypic markers. However, the robustness of these markers should be tested in different growing environments to truly elucidate the chemical differences in terms of chemotypes or intra-chemotype sub-clusters. The

results of this study provide a proof-of-concept for further collaboration between academia and the industry for leveraging chemotypic markers in medical studies and clinical trials.

DATA AVAILABILITY STATEMENT

The original contributions presented in the study are included in the article/**Supplementary Material**, further inquiries can be directed to the corresponding author.

AUTHOR CONTRIBUTIONS

DJ conceived the project, designed the experiments, preformed the experiments, collected and analyzed the data, and wrote the manuscript. PH contacted the licensed cultivator for this project and proofread the manuscript. JS provided funding, provided suggestions, and proofread the manuscript. JC was the supervisory author and monitored the research progress, provided suggestions, and finalized the manuscript. All authors contributed to the article and approved the submitted version.

FUNDING

The authors are grateful to PBG BioPharma Inc. for providing financial support for travel expenses and funding for publication. The authors declare that PBG BioPharma Inc. was not involved in the study design, collection, analysis, interpretation of data, the writing of this article or the decision to submit it for publication.

ACKNOWLEDGMENTS

The authors are grateful to Labs-Mart Inc. for providing instrumentation support for chemical testing. The authors are grateful to licensed cultivator, the Emerald Flower Farm Inc., who provided cannabis strains and a commercial greenhouse to cultivate the plants. The authors are also grateful to Shengxi Jin for proofreading the manuscript.

SUPPLEMENTARY MATERIAL

The Supplementary Material for this article can be found online at: https://www.frontiersin.org/articles/10.3389/fpls.2021.699530/full#supplementary-material

Supplementary Figure 1 | Secondary metabolites profiling in cannabis roots, stem bark, leaves, and inflorescences in 82 plants of 21 strains.

Supplementary Figure 2 | Correlations of total THC and total CBD with terpenoids using content ratios (%/%) in (A) inflorescences and in (B) leaves.

Supplementary Figure 3 | Correlations of total THC and total CBD with cannabinoids (in inflorescences), mono- and sesquiterpenoids (in inflorescences), flavonoids (in inflorescences and leaves), sterols and triterpenoids (in roots) on quantifiable compounds using ratios.

Supplementary Figure 4 | Dendrogram by hierarchical clustering analysis using the full spectrum of secondary metabolites (absolute values) of 82 plants representing 21 strains.

Supplementary Figure 5 | Dendrogram by hierarchical clustering analysis using the full spectrum of secondary metabolites (using ratios) without total THC and total CBD.

Supplementary Figure 6 | PCA scatter plot (left) and loading plot (right) using the full spectrum of secondary metabolites (absolute values) of 82 plants representing 21 strains.

Supplementary Figure 7 | PCA scatter plot (left) and loading plot (right) using the full spectrum of secondary metabolites (using ratios) without total THC and total CBD.

Supplementary Figure 8 | Canonical correlation analysis using the full spectrum of secondary metabolites (absolute values) of 82 plants representing 21 strains.

Supplementary Figure 9 | Canonical correlation analysis using the full spectrum of secondary metabolites (using ratios) of 82 plants representing 21 strains.

Supplementary Table 1 | Strain information and assignment of 21 strains into three chemotypes.

Supplementary Table 2.1 | Secondary metabolites profiled in inflorescences of 82 plants of 21 strains.

Supplementary Table 2.2 | Cannabinoids profiled in inflorescences of 82 plants for three chemotypes.

Supplementary Table 2.3 | Cannabinoid profile in leaves of 82 plants for three chemotypes.

Supplementary Table 2.4 | Cannabinoid profile in stem bark of 82 plants for three chemotypes.

Supplementary Table 2.5 | Mono- and sesquiterpenoids profile in inflorescences of 82 plants for three chemotypes.

Supplementary Table 2.6 | Mono- and sesquiterpenoids profile in leaves of 82 plants for three chemotypes.

Supplementary Table 2.7 | Flavonoids profile in inflorescences for three chemotypes.

Supplementary Table 2.8 | Flavonoids profile in leaves for three chemotypes.

Supplementary Table 2.9 | Sterols profile in stem bark for three chemotypes.

Supplementary Table 2.10 | Sterols profile in roots for three chemotypes.

Supplementary Table 2.11 | Triterpenoids profile in stem bark for three chemotypes.

Supplementary Table 2.12 | Triterpenoids profile in roots for three chemotypes.

Supplementary Table 3 | Correlations of total THC and total CBD with minor cannabinoids, mono- and sesquiterpenoids, flavonoids, sterols, and triterpenoids (only positive correlations are shown).

Supplementary Table 4 | Summary prediction of 82 plants into preassigned chemotypes using Canonical correlation analysis (using ratios).

Supplementary Table 5 | Means (±SD) of the ratios of 45 secondary metabolites above quantification limit for 82 plants assigned to C1-CBD dominant, C2-intermediate, and C3-THC dominant.

Supplementary Table 6 | Means (±SD) of the absolute values of 45 secondary metabolites (mg/mg%) for 82 plants assigned to C1-CBD dominant, C2-intermediate, and C3-THC dominant.

Supplementary Table 7 | Secondary metabolites used in correlation analysis and classification analysis.

Supplementary Table 8 | Correlations of cannabinoids and terpenoids in inflorescences and leaves.

Supplementary Table 9 | Secondary metabolites in all plant parts (absolute values).

REFERENCES

Aizpurua-Olaizola, O. S. (2016). Evolution of the cannabinoid and terpene content during the growth of *Cannabis sativa* plants from different chemotypes. *J. Nat. Prod.* 79, 324–331. doi: 10.1021/acs.jnatprod.5b00949

Ames-Sibin, A. P., Barizão, C. L., Castro-Ghizoni, C. V., Silva, F. M. S., Sá-Nakanishi, A. B., Bracht, L., et al. (2018). β-Caryophyllene, the major constituent of copaiba oil, reduces systemic inflammation and oxidative stress in arthritic rats. *J. Cell. Biochem.* 119, 10262–10277. doi: 10.1002/jcb.27369

An, F., Yang, G., Tian, J., and Wang, S. (2012). Antioxidant effects of the orientin and vitexin in *Trollius chinensis* Bunge in D-galactose-aged mice. *Neural Regen. Res.* 7:2565.

Andre, C. M., Hausman, J.-F., and Guerriero, G. (2016). *Cannabis sativa*: the plant of the thousand and one molecules. *Front. Plant Sci.* 7:19. doi: 10.3389/fpls.2016.00019

Ashaari, Z., Hassanzadeh, G., Alizamir, T., Yousefi, B., Keshavarzi, Z., and Mokhtari, T. (2018). The flavone luteolin improves central nervous system disorders by different mechanisms: a review. *J. Mol. Neurosci.* 65, 491–506. doi: 10.1007/s12031-018-1094-2

Avraham, Y., Grigoriadis, N. C., Poutahidis, T., Vorobiev', L., Magen, I., Ilan, Y., et al. (2011). Cannabidiol improves brain and liver function in a fulminant hepatic failure-induced model of hepatic encephalopathy in mice. *Br. J. Pharmacol.* 162, 1650–1658. doi: 10.1111/j.1476-5381.2010.01179.x

Baram, L., Peled, E., Berman, P., Yellin, B., Besser, E., Benami, M., et al. (2019). The heterogeneity and complexity of *Cannabis* extracts as antitumor agents. *Oncotarget* 10, 4091–4106. doi: 10.18632/oncotarget.26983

Berman, P., Futoran, K., Lewitus, G. M., Mukha, D., Benami, M., Shlomi, T., et al. (2018). A new ESI-LC/MS approach for comprehensive metabolic profiling of phytocannabinoids in *Cannabis*. *Sci. Rep.* 8, 1–15.

Blasco-Benito, S., Seijo-Vila, M., Caro-Villalobos, M., Tundidor, I., Andradas, C., García-Taboada, E., et al. (2018). Appraising the "entourage effect": antitumor action of a pure cannabinoid versus a botanical drug preparation in preclinical models of breast cancer. *Biochem. Pharmacol.* 157, 285–293. doi: 10.1016/j.bcp.2018.06.025

Bloomfield, M. A. P., Green, S. F., Hindocha, C., Yamamori, Y., Yim, J. L. L., Jones, A. P. M., et al. (2020). The effects of acute cannabidiol on cerebral blood flow and its relationship to memory: an arterial spin labelling magnetic resonance imaging study. *J. Psychopharmacol. Oxf. Engl.* 34, 981–989. doi: 10.1177/0269881120936419

Bolognini, D., Costa, B., Maione, S., Comelli, F., Marini, P., Di Marzo, V., et al. (2010). The plant cannabinoid Δ9-tetrahydrocannabivarin can decrease signs of inflammation and inflammatory pain in mice. *Br. J. Pharmacol.* 160, 677–687. doi: 10.1111/j.1476-5381.2010.00756.x

Booth, J. K., Page, J. E., and Bohlmann, J. (2017). Terpene synthases from *Cannabis sativa*. *PLoS One* 12:e0173911. doi: 10.1371/journal.pone.0173911

Booz, G. W. (2011). Cannabidiol as an emergent therapeutic strategy for lessening the impact of inflammation on oxidative stress. *Free Radic. Biol. Med.* 51, 1054–1061. doi: 10.1016/j.freeradbiomed.2011.01.007

Borrelli, F., Fasolino, I., Romano, B., Capasso, R., Maiello, F., Coppola, D., et al. (2013). Beneficial effect of the non-psychotropic plant cannabinoid cannabigerol on experimental inflammatory bowel disease. *Biochem. Pharmacol.* 85, 1306–1316. doi: 10.1016/j.bcp.2013.01.017

Brand, E., and Wiseman, N. (2008). *Concise Chinese Materia Medica*. Taos, NM: Paradigm Publications.

Brand, E. J., and Zhao, Z. (2017). *Cannabis* in chinese medicine: are some traditional indications referenced in ancient literature related to cannabinoids? *Front. Pharmacol.* 8:108. doi: 10.3389/fphar.2017.00108

Brierley, D. I., Samuels, J., Duncan, M., Whalley, B. J., and Williams, C. M. (2016). Cannabigerol is a novel, well-tolerated appetite stimulant in pre-satiated rats. *Psychopharmacology* 233, 3603–3613. doi: 10.1007/s00213-016-4397-4

Callejas, G. H., Figueira, R. L., Gonçalves, F. L. L., Volpe, F. A. P., Zuardi, A. W., Crippa, J. A., et al. (2018). Maternal administration of cannabidiol promotes an anti-inflammatory effect on the intestinal wall in a gastroschisis rat model. *Br. J. Med. Biol. Res.* 51:e7132.

Caplan, D. M. (2018). *Propagation and Root Zone Management for Controlled Environment Cannabis Production*. Ph.D. Thesis. Guelph, ON: University of Guelph.

Cascio, M. G., and Pertwee, R. G. (2014). "Known pharmacological actions of nine nonpsychotropic phytocannabinoids," in *Handbook of Cannabis*, ed. R. G. Pertwee (Oxford: Oxford University Press).

Chirumbolo, S., and Bjørklund, G. (2018). Quercetin in collagen-induced arthritis. Some comments. *Int. Immunopharmacol.* 62:335. doi: 10.1016/j.intimp.2018.06.003

Clark, M. N., and Bohm, B. A. (1979). Flavonoid variation in *Cannabis* L. *Bot. J. Linn. Soc.* 79, 249–257. doi: 10.1111/j.1095-8339.1979.tb01517.x

Clarke, R. C., and Merlin, M. D. (2016). *Cannabis* domestication, breeding history, present-day genetic diversity, and future prospects. *Crit. Rev. Plant Sci.* 35, 293–327. doi: 10.1080/07352689.2016.1267498

Couch, D. G., Tasker, C., Theophilidou, E., Lund, J. N., and O'Sullivan, S. E. (2017). Cannabidiol and palmitoylethanolamide are anti-inflammatory in the acutely inflamed human colon. *Clin. Sci.* 131, 2611–2626. doi: 10.1042/cs20171288

Davis, W. M., and Hatoum, N. S. (1983). Neurobehavioral actions of cannabichromene and interactions with delta 9-tetrahydrocannabinol. *Gen. Pharmacol.* 14, 247–252. doi: 10.1016/0306-3623(83)90004-6

de Meijer, E. P. M., Bagatta, M., Carboni, A., Crucitti, P., Moliterni, V. M. C., Ranalli, P., et al. (2003). The inheritance of chemical phenotype in *Cannabis sativa* L. *Genetics* 163, 335–346. doi: 10.1093/genetics/163.1.335

de Meijer, E. P. M., Hammond, K. M., and Sutton, A. (2009). The inheritance of chemical phenotype in *Cannabis sativa* L. (IV): cannabinoid-free plants. *Euphytica* 168, 95–112. doi: 10.1007/s10681-009-9894-7

De Petrocellis, L., Orlando, P., Moriello, A. S., Aviello, G., Stott, C., Izzo, A. A., et al. (2012). Cannabinoid actions at TRPV channels: effects on TRPV3 and TRPV4 and their potential relevance to gastrointestinal inflammation. *Acta Physiol.* 204, 255–266. doi: 10.1111/j.1748-1716.2011.02338.x

DeLong, G. T., Wolf, C. E., Poklis, A., and Lichtman, A. H. (2010). Pharmacological evaluation of the natural constituent of *Cannabis sativa*, cannabichromene and its modulation by Δ9-tetrahydrocannabinol. *Drug Alcohol Depend.* 112, 126–133. doi: 10.1016/j.drugalcdep.2010.05.019

Dwivedi, C., and Harbison, R. D. (1975). Anticonvulsant activities of Δ-8 and Δ-9 tetrahydrocanabinol and uridine. *Toxicol. Appl. Pharmacol.* 31, 452–458. doi: 10.1016/0041-008x(75)90268-9

ElSohly, M. A., and Gul, W. (2014). "Constituents of *Cannabis sativa*," in *Handbook of Cannabis*, ed. R. G. Pertwee (Oxford: Oxford University Press), 3–22. doi: 10.1093/acprof:oso/9780199662685.003.0001

ElSohly, M. A., and Slade, D. (2005). Chemical constituents of marijuana: the complex mixture of natural cannabinoids. *Life Sci.* 78, 539–548. doi: 10.1016/j.lfs.2005.09.011

Elzinga, S., Fischedick, J., Podkolinski, R., and Raber, J. C. (2015). Cannabinoids and terpenes as chemotaxonomic markers in *Cannabis*. *Nat. Prod. Chem. Res.* 3:4.

Evans, F. J. (1991). Cannabinoids: the separation of central from peripheral effects on a structural basis. *Planta Med.* 57, S60–S67.

Fischedick, J. (2015). Cannabinoids and terpenes as chemotaxonomic markers in *Cannabis*. *Nat. Prod. Chem. Res.* 03:4.

Fischedick, J. T. (2017). Identification of terpenoid chemotypes among high (−)-trans-Δ9-tetrahydrocannabinol-producing *Cannabis sativa* L. cultivars. *Cannabis Cannabinoid Res.* 2, 34–47. doi: 10.1089/can.2016.0040

Fischedick, J. T., Hazekamp, A., Erkelens, T., Choi, Y. H., and Verpoorte, R. (2010). Metabolic fingerprinting of *Cannabis sativa* L., cannabinoids and terpenoids for chemotaxonomic and drug standardization purposes. *Phytochemistry* 71, 2058–2073. doi: 10.1016/j.phytochem.2010.10.001

Flores-Sanchez, I. J., and Verpoorte, R. (2008). PKS activities and biosynthesis of cannabinoids and flavonoids in *Cannabis sativa* L. *Plants Plant Cell Physiol.* 49, 1767–1782. doi: 10.1093/pcp/pcn150

French, J., Thiele, E., Mazurkiewicz-Beldzinska, M., Benbadis, S., Marsh, E., Joshi, C., et al. (2017). Cannabidiol (CBD) significantly reduces drop seizure frequency in lennox-gastaut syndrome (LGS): results of a multi-center, randomized, double-blind, placebo controlled trial (GWPCARE4)(S21.001). *Neurology* 88:S21.

Gouveia, D. N., Costa, J. S., Oliveira, M. A., Rabelo, T. K., de e Silva, A. M. O., Carvalho, A. A., et al. (2018). α-Terpineol reduces cancer pain via modulation of oxidative stress and inhibition of iNOS. *Biomed. Pharmacother.* 105, 652–661. doi: 10.1016/j.biopha.2018.06.027

Govindarajan, M., Rajeswary, M., Hoti, S. L., Bhattacharyya, A., and Benelli, G. (2016). Eugenol, α-pinene and β-caryophyllene from *Plectranthus barbatus*

essential oil as eco-friendly larvicides against malaria, dengue and Japanese encephalitis mosquito vectors. *Parasitol. Res.* 115, 807–815. doi: 10.1007/s00436-015-4809-0

Grassa, C. J., Wenger, J. P., Dabney, C., Poplawski, S. G., Motley, S. T., Michael, T. P., et al. (2018). A complete *Cannabis* chromosome assembly and adaptive admixture for elevated cannabidiol (CBD) content. *bioRxiv* [Preprint]. doi: 10.1101/458083v3

Gugliandolo, A., Pollastro, F., Grassi, G., Bramanti, P., and Mazzon, E. (2018). In vitro model of neuroinflammation: efficacy of cannabigerol, a non-psychoactive cannabinoid. *Int. J. Mol. Sci.* 19:1992. doi: 10.3390/ijms19071992

Gylling, H., Plat, J., Turley, S., Ginsberg, H. N., Ellegård, L., Jessup, W., et al. (2014). Plant sterols and plant stanols in the management of dyslipidaemia and prevention of cardiovascular disease. *Atherosclerosis* 232, 346–360. doi: 10.1016/j.atherosclerosis.2013.11.043

Haleagrahara, N., Miranda-Hernandez, S., Alim, M. A., Hayes, L., Bird, G., and Ketheesan, N. (2017). Therapeutic effect of quercetin in collagen-induced arthritis. *Biomed. Pharmacother.* 90, 38–46. doi: 10.1016/j.biopha.2017.03.026

Hasler, A., Sticher, O., and Meier, B. (1992). Identification and determination of the flavonoids from *Ginkgo biloba* by high-performance liquid chromatography. *J. Chromatogr. A* 605, 41–48. doi: 10.1016/0021-9673(92)85026-p

Hayasaka, N., Shimizu, N., Komoda, T., Mohri, S., Tsushida, T., Eitsuka, T., et al. (2018). Absorption and metabolism of luteolin in rats and humans in relation to in vitro anti-inflammatory effects. *J. Agric. Food Chem.* 66, 11320–11329. doi: 10.1021/acs.jafc.8b03273

Hazekamp, A., and Fischedick, J. T. (2012). *Cannabis* - from cultivar to chemovar. *Drug Test. Anal.* 4, 660–667. doi: 10.1002/dta.407

Hazekamp, A., Tejkalová, K., and Papadimitriou, S. (2016). *Cannabis*: from cultivar to chemovar II—a metabolomics approach to *Cannabis* classification. *Cannabis Cannabinoid Res.* 1, 202–215. doi: 10.1089/can.2016.0017

He, M., Min, J.-W., Kong, W.-L., He, X.-H., Li, J.-X., and Peng, B.-W. (2016). A review on the pharmacological effects of vitexin and isovitexin. *Fitoterapia* 115, 74–85. doi: 10.1016/j.fitote.2016.09.011

Hill, A. J., Weston, S. E., Jones, N. A., Smith, I., Bevan, S. A., Williamson, E. M., et al. (2010). Δ9-Tetrahydrocannabivarin suppresses in vitro epileptiform and in vivo seizure activity in adult rats. *Epilepsia* 51, 1522–1532. doi: 10.1111/j.1528-1167.2010.02523.x

Hill, T. D. M., Cascio, M.-G., Romano, B., Duncan, M., Pertwee, R. G., Williams, C. M., et al. (2013). Cannabidivarin-rich *Cannabis* extracts are anticonvulsant in mouse and rat via a CB1 receptor-independent mechanism. *Br. J. Pharmacol.* 170, 679–692. doi: 10.1111/bph.12321

Hillig, K. W. (2005a). *A Systematic Investigation of Cannabis*. Ph.D. thesis. Bloomington, IN: Indiana University.

Hillig, K. W. (2005b). Genetic evidence for speciation in *Cannabis* (Cannabaceae). *Genet. Resour. Crop Evol.* 52, 161–180. doi: 10.1007/s10722-003-4452-y

Hotelling, H. (1936). Relations between two sets of variates. *Biometrika* 28, 321–377. doi: 10.2307/2333955

Jikomes, N., and Zoorob, M. (2018). The cannabinoid content of legal *Cannabis* in Washington state varies systematically across testing facilities and popular consumer products. *Sci. Rep.* 8:4519.

Jin, D., Dai, K., Xie, Z., and Chen, J. (2020). Secondary metabolites profiled in *Cannabis* inflorescences, leaves, stem barks, and roots for medicinal purposes. *Sci. Rep.* 10:3309.

Jin, D., Henry, P., Shan, J., and Chen, J. (2021). Identification of phenotypic characteristics in three chemotype categories in the genus *Cannabis*. *HortScience* 1, 1–10.

Jin, D., Jin, S., and Chen, J. (2019). *Cannabis* indoor growing conditions, management practices, and post-harvest treatment: a review. *Am. J. Plant Sci.* 10, 925–946. doi: 10.4236/ajps.2019.106067

Jin, D., Jin, S., Yu, Y., Lee, C., and Chen, J. (2017). Classification of *Cannabis* cultivars marketed in canada for medical purposes by quantification of cannabinoids and terpenes using HPLC-DAD and GC-MS. *J. Anal. Bioanal. Tech.* 8:2.

Jolliffe, I. T. (2002). *Principal Component Analysis, 2nd ed, Springer Series in Statistics*. New York: Springer-Verlag.

Klopell, F. C., Lemos, M., Sousa, J. P. B., Comunello, E., Maistro, E. L., Bastos, J. K., et al. (2007). Nerolidol, an antiulcer constituent from the essential oil of *Baccharis dracunculifolia* DC (Asteraceae). *Z. Naturforschung C J. Biosci.* 62, 537–542. doi: 10.1515/znc-2007-7-812

Kozłowska, M., Gruczńska, E., Ścibisz, I., and Rudzińska, M. (2016). Fatty acids and sterols composition, and antioxidant activity of oils extracted from plant seeds. *Food Chem.* 213, 450–456. doi: 10.1016/j.foodchem.2016.06.102

Lynch, R. C., Vergara, D., Tittes, S., White, K., Schwartz, C. J., Gibbs, M. J., et al. (2016). Genomic and chemical diversity in *Cannabis*. *Crit. Rev. Plant Sci.* 35, 349–363.

Mallada Frechín, J. (2018). Effect of tetrahydrocannabinol: cannabidiol oromucosal spray on activities of daily living in multiple sclerosis patients with resistant spasticity: a retrospective, observational study. *Neurodegener. Dis. Manag.* 8, 151–159. doi: 10.2217/nmt-2017-0055

Mandolino, G., Bagatta, M., Carboni, A., Ranalli, P., and de Meijer, E. (2003). Qualitative and quantitative aspects of the inheritance of chemical phenotype in *Cannabis*. *J. Ind. Hemp.* 8, 51–72. doi: 10.1300/j237v08n02_04

McGuire, P., Robson, P., Cubala, W. J., Vasile, D., Morrison, P. D., Barron, R., et al. (2018). Cannabidiol (CBD) as an adjunctive therapy in schizophrenia: a multicenter randomized controlled trial. *Am. J. Psychiatry* 175, 225–231. doi: 10.1176/appi.ajp.2017.17030325

McPartland, J. M. (2017). "*Cannabis sativa* and *Cannabis indica* versus "Sativa" and "Indica."," in *Cannabis Sativa L.-Botany and Biotechnology*, eds S. Chandra, H. Lata, and M. A. ElSohly (Berlin: Springer), 101–121. doi: 10.1007/978-3-319-54564-6_4

McPartland, J. M., and Guy, G. W. (2017). Models of '*Cannabis* taxonomy, cultural bias, and conflicts between scientific and vernacular names. *Bot. Rev.* 4, 327–381. doi: 10.1007/s12229-017-9187-0

McPartland, J. M., and Russo, E. B. (2001). *Cannabis* and *Cannabis* extracts: greater than the sum of their parts? *J. Cannabis Ther.* 1, 103–132. doi: 10.1300/j175v01n03_08

Miguel, M. G. (2010). Antioxidant and anti-inflammatory activities of essential oils: a short review. *Molecules* 15, 9252–9287. doi: 10.3390/molecules15129252

Pollastro, F., Minassi, A., and Fresu, L. G. (2018). *Cannabis* phenolics and their bioactivities. *Curr. Med. Chem.* 25, 1160–1185. doi: 10.2174/0929867324666170810164636

Potter, D. J. (2009). *The propagation, Characterisation and Optimisation of Cannabis sativa L. as a Phytopharmaceutical*. Ph.D. Thesis. London: King's College.

Ras, R. T., Geleijnse, J. M., and Trautwein, E. A. (2014). LDL-cholesterol-lowering effect of plant sterols and stanols across different dose ranges: a meta-analysis of randomised controlled studies. *Br. J. Nutr.* 112, 214–219. doi: 10.1017/s0007114514000750

Richins, R. D., Rodriguez-Uribe, L., Lowe, K., Ferral, R., and O'Connell, M. A. (2018). Accumulation of bioactive metabolites in cultivated medical *Cannabis*. *PLoS One* 13:e0201119. doi: 10.1371/journal.pone.0201119

Ross, S. A., ElSohly, M. A., Sultana, G. N., Mehmedic, Z., Hossain, C. F., and Chandra, S. (2005). Flavonoid glycosides and cannabinoids from the pollen of *Cannabis sativa* L. *Phytochem. Anal. Int. J. Plant Chem. Biochem. Tech.* 16, 45–48. doi: 10.1002/pca.809

Russo, E. B. (2011). Taming THC: potential *Cannabis* synergy and phytocannabinoid-terpenoid entourage effects. *Br. J. Pharmacol.* 163, 1344–1364. doi: 10.1111/j.1476-5381.2011.01238.x

Russo, E. B., and Marcu, J. (2017). *Cannabis* pharmacology: the usual suspects and a few promising leads. *Cannabinoid. Pharmacol.* 80, 67–134. doi: 10.1016/bs.apha.2017.03.004

Ryz, N. R., Remillard, D. J., and Russo, E. B. (2017). *Cannabis* roots: a traditional therapy with future potential for treating inflammation and pain. *Cannabis Cannabinoid Res.* 2, 210–216. doi: 10.1089/can.2017.0028

Santiago, M., Sachdev, S., Arnold, J. C., McGregor, I. S., and Connor, M. (2019). Absence of entourage: terpenoids commonly found in *Cannabis sativa* do not modulate the functional activity of Δ9-THC at human CB1 and CB2 receptors. *Cannabis Cannabinoid Res.* 4, 165–176. doi: 10.1089/can.2019.0016

Sawler, J., Stout, J. M., Gardner, K. M., Hudson, D., Vidmar, J., Butler, L., et al. (2015). The genetic structure of marijuana and hemp. *PLoS One* 10:e0133292. doi: 10.1371/journal.pone.0133292

Shahriari, M., Zibaee, A., Sahebzadeh, N., and Shamakhi, L. (2018). Effects of α-pinene, trans-anethole, and thymol as the essential oil constituents on antioxidant system and acetylcholine esterase of *Ephestia kuehniella* Zeller (Lepidoptera: Pyralidae). *Pestic. Biochem. Physiol.* 150, 40–47. doi: 10.1016/j.pestbp.2018.06.015

Sharma, A., Kashyap, D., Sak, K., Tuli, H. S., and Sharma, A. K. (2018). Therapeutic charm of quercetin and its derivatives: a review of research and patents. *Pharm. Pat. Anal.* 7, 15–32. doi: 10.4155/ppa-2017-0030

Small, E., and Beckstead, H. D. (1973). Letter: cannabinoid phenotypes in *Cannabis sativa*. *Nature* 245, 147–148. doi: 10.1038/245147a0

Smith, F. P., and Stuart, G. A. (1911). *Chinese Materia Medica: Vegetable Kingdom*. Shanghai: American Presbyterian Mission Press.

Strada, C. L., Lima, K., da, C., da Silva, V. C., Ribeiro, R. V., Dores, E. F., et al. (2017). Isovitexin as marker and bioactive compound in the antinociceptive activity of the Brazilian crude drug extracts of *Echinodorus scaber* and *E. grandiflorus*. *Rev. Bras. Farmacogn.* 27, 619–626. doi: 10.1016/j.bjp.2017.05.011

Tambe, Y., Tsujiuchi, H., Honda, G., Ikeshiro, Y., and Tanaka, S. (1996). Gastric cytoprotection of the non-steroidal anti-inflammatory sesquiterpene, beta-caryophyllene. *Planta Med.* 62, 469–470. doi: 10.1055/s-2006-957942

Tsai, M.-S., Wang, Y.-H., Lai, Y.-Y., Tsou, H.-K., Liou, G.-G., Ko, J.-L., et al. (2018). Kaempferol protects against propacetamol-induced acute liver injury through CYP2E1 inactivation, UGT1A1 activation, and attenuation of oxidative stress, inflammation and apoptosis in mice. *Toxicol. Lett.* 290, 97–109. doi: 10.1016/j.toxlet.2018.03.024

Turner, C. E., Elsohly, M. A., and Boeren, E. G. (1980). Constituents of *Cannabis sativa* L. XVII. A review of the natural constituents. *J. Nat. Prod.* 43, 169–234. doi: 10.1021/np50008a001

Turner, C. E., Elsohly, M. A., Cheng, P. C., and Lewis, G. (1979). Constituents of *Cannabis sativa* L., XIV: intrinsic problems in classifying *Cannabis* based on a single cannabinoid analysis. *J. Nat. Prod.* 42, 317–319. doi: 10.1021/np50003a017

Upton, R., Craker, L., ElSohly, M., Romm, A., Russo, E., and Sexton, M. (2014). *Cannabis Inflorescence: Cannabis spp.; Standards of Identity, Analysis, and Quality Control*. Scotts Valley, CA: American Herbal Pharmacopoeia.

Vallée, A., Lecarpentier, Y., Guillevin, R., and Vallée, J.-N. (2017). Effects of cannabidiol interactions with Wnt/β-catenin pathway and PPARγ on oxidative stress and neuroinflammation in Alzheimer's disease. *Acta Biochim. Biophys. Sin.* 49, 853–866. doi: 10.1093/abbs/gmx073

Vanhoenacker, G., Van Rompaey, P., De Keukeleire, D., and Sandra, P. (2002). Chemotaxonomic features associated with flavonoids of cannabinoid-free *Cannabis* (*Cannabis sativa* subsp. sativa L.) in relation to hops (*Humulus lupulus* L.). *Nat. Prod. Lett.* 16, 57–63. doi: 10.1080/1057563029001/4863

Wang, J., Li, T., Feng, J., Li, L., Wang, R., Cheng, H., et al. (2018). Kaempferol protects against gamma radiation-induced mortality and damage via inhibiting oxidative stress and modulating apoptotic molecules in vivo and vitro. *Environ. Toxicol. Pharmacol.* 60, 128–137. doi: 10.1016/j.etap.2018.04.014

Ward, J. H. Jr. (1963). Hierarchical grouping to optimize an objective function. *J. Am. Stat. Assoc.* 58, 236–244. doi: 10.1080/01621459.1963.10500845

Xiao, R.-Y., Wu, L.-J., Hong, X.-X., Tao, L., Luo, P., and Shen, X.-C. (2018). Screening of analgesic and anti-inflammatory active component in Fructus Alpiniae zerumbet based on spectrum–effect relationship and GC–MS. *Biomed. Chromatogr.* 32:e4112. doi: 10.1002/bmc.4112

Yang, Y., Zhang, X., Xu, M., Wu, X., Zhao, F., and Zhao, C. (2018). Quercetin attenuates collagen-induced arthritis by restoration of Th17/Treg balance and activation of Heme Oxygenase 1-mediated anti-inflammatory effect. *Int. Immunopharmacol.* 54, 153–162. doi: 10.1016/j.intimp.2017.11.013

Yao, Z.-H., Yao, X., Zhang, Y., Zhang, S., and Hu, J. (2018). Luteolin could improve cognitive dysfunction by inhibiting neuroinflammation. *Neurochem. Res.* 43, 806–820. doi: 10.1007/s11064-018-2482-2

Zager, J. J., Lange, I., Srividya, N., Smith, A., and Lange, B. M. (2019). Gene networks underlying cannabinoid and terpenoid accumulation in *Cannabis*. *Plant Physiol.* 180, 1877–1897. doi: 10.1104/pp.18.01506

Zheng, Y.-Z., Chen, D.-F., Deng, G., Guo, R., and Fu, Z.-M. (2018). The surrounding environments on the structure and antioxidative activity of luteolin. *J. Mol. Model.* 24:149.

Conflict of Interest: DJ and JS were employed by the company PBG BioPharma Inc. PH was employed by the company Egret Bioscience and Lighthouse Genomics.

The remaining authors declare that the research was conducted in the absence of any commercial or financial relationships that could be construed as a potential conflict of interest.

frontiers in Plant Science

ORIGINAL RESEARCH
published: 15 July 2021
doi: 10.3389/fpls.2021.657323

The Highs and Lows of P Supply in Medical Cannabis: Effects on Cannabinoids, the Ionome, and Morpho-Physiology

Sivan Shiponi[1,2] *and Nirit Bernstein*[1]*

[1] *Institute of Soil Water and Environmental Sciences, Volcani Center, Rishon LeZion, Israel,* [2] *The Robert H. Smith Faculty of Agriculture, Food and Environment, The Hebrew University of Jerusalem, Rehovot, Israel*

Environmental conditions, including the availability of mineral nutrients, affect secondary metabolism in plants. Therefore, growing conditions have significant pharmaceutical and economic importance for *Cannabis sativa*. Phosphorous is an essential macronutrient that affects central biosynthesis pathways. In this study, we evaluated the hypothesis that P uptake, distribution and availability in the plant affect the biosynthesis of cannabinoids. Two genotypes of medical "drug-type" cannabis plants were grown under five P concentrations of 5, 15, 30, 60, and 90 mg L^{-1} (ppm) in controlled environmental conditions. The results reveal several dose-dependent effects of P nutrition on the cannabinoid profile of both genotypes, as well as on the ionome and plant functional physiology, thus supporting the hypothesis: (i) P concentrations $\leq$15 mg L^{-1} were insufficient to support optimal plant function and reduced photosynthesis, transpiration, stomatal conductance and growth; (ii) 30–90 mg L^{-1} P was within the optimal range for plant development and function, and 30 mg L^{-1} P was sufficient for producing 80% of the maximum yield; (iii) Ionome: about 80% of the plant P accumulated in the unfertilized inflorescences; (iv) Cannabinoids: P supply higher than 5 mg L^{-1} reduced Δ^9-tetrahydrocannabinolic acid (THCA) and cannabidiolic acid (CBDA) concentrations in the inflorescences by up to 25%. Cannabinoid concentrations decreased linearly with increasing yield, consistent with a yield dilution effect, but the total cannabinoid content per plant increased with increasing P supply. These results reveal contrasting trends for effects of P supply on cannabinoid concentrations that were highest under $<$30 mg L^{-1} P, vs. inflorescence biomass that was highest under 30–90 mg L^{-1} P. Thus, the P regime should be adjusted to reflect production goals. The results demonstrate the potential of mineral nutrition to regulate cannabinoid metabolism and optimize pharmacological quality.

Keywords: ***Cannabis*****, cannabinoids, development, efficiency, fertilization, nutrition, phosphorus, reproductive**

OPEN ACCESS

Edited by:
David Meiri,
Technion – Israel Institute of Technology, Israel

Reviewed by:
Bruce Bugbee,
Utah State University, United States
Paula Berman,
Weizmann Institute of Science, Israel

***Correspondence:**
Nirit Bernstein
Nirit@agri.gov.il

Specialty section:
This article was submitted to Crop and Product Physiology, a section of the journal Frontiers in Plant Science

Received: *22 January 2021*
Accepted: *23 April 2021*
Published: *15 July 2021*

Citation:
Shiponi S and Bernstein N (2021) The Highs and Lows of P Supply in Medical Cannabis: Effects on Cannabinoids, the Ionome, and Morpho-Physiology. Front. Plant Sci. 12:657323. doi: 10.3389/fpls.2021.657323

INTRODUCTION

Cannabis sativa is receiving commercial and academic attention globally due to its therapeutic potential for modern medicine and increasing recreational use (Small, 2018). Recent changes in regulations drive a proliferation of research efforts toward understanding the plant's medical effects (Malfait et al., 2000; Zuardi, 2006; Bonini et al., 2018). The increasing use of cannabis

as a prescription drug makes understanding the effects of environmental factors and growing conditions on the plant and its chemical composition a high priority (Decorte and Potter, 2015; Saloner and Bernstein, 2021). More than 500 secondary metabolites have been identified in cannabis plants, including terpenoids, flavonoids, and cannabinoids, which are responsible for the therapeutic qualities (Chandra et al., 2017; Gonçalves et al., 2019; Milay et al., 2020).

Secondary metabolites are involved in the interaction of plants with their environment and survival functions, such as attracting pollinators, defense against herbivores and pathogens, plant competition, symbiosis, and responses to environmental stresses (Demain and Fang, 2000; Verpoorte et al., 2002). They have been harnessed for centuries by humanity for use as pharmaceuticals, food additives and flavors (Zhao et al., 2005). These compounds biosynthesis in the plant is regulated by genetic and environmental factors; therefore, elicitation has been used for directing excelled chemical quality (Gorelick and Bernstein, 2014).

Cannabinoids are secondary metabolites produced by cannabis and stored mainly in glandular trichomes on the plant's inflorescences (Turner et al., 1978). More than 100 cannabinoids have been identified in cannabis (Berman et al., 2018; Gülck and Møller, 2020; Milay et al., 2020). The most abundant cannabinoids are the pentyl type Δ^9-tetra-hydrocannabinol (THC), cannabidiol (CBD), cannabichromene (CBC), and cannabigerol (CBG) that are present in the plant mostly in their acidic form (THCA, CBDA, CBCA, and CBGA). The precursors for cannabinoid biosynthesis in the cannabis plant are derived from two pathways, the polyketide pathway and the deoxyxylulose phosphate/methyl-erythritol phosphate (DOXP/MEP) pathway (Flores-Sanches and Verpoorte, 2008). CBGA is the direct precursor for THCA, CBDA, and CBCA, and it originates from prenylation of geranyl diphosphate (GPP) to olivetolic acid (Gülck and Møller, 2020). Δ^9-tetrahydrocannabivarin (THCV) and cannabidivarin (CBDV), propyl analogs of THC and CBD, are minor cannabinoids originating from GPP and divarinic acid that have shown important pharmacological activities (Russo, 2011; Bonini et al., 2018; Sarma et al., 2020).

The cannabinoid profile of the plant is dynamic, varies between plants and spatially within the plant (Bernstein et al., 2019a; Danziger and Bernstein, 2021a) and is affected by genetics (Turner et al., 1978; Clarke and Merlin, 2016) and growing conditions (Bernstein et al., 2019b; Danziger and Bernstein, 2021b). Environmental stresses have a potential to be used as management practices to elicit changes in the plant's secondary metabolite profile (Gorelick and Bernstein, 2014, 2017). Abiotic factors such as drought (Caplan et al., 2019), growing media (Caplan et al., 2017), salinity (Yep et al., 2020), light spectrum (Magagnini et al., 2018; Danziger and Bernstein, 2021a), nutrient supply (Bernstein et al., 2019b; Saloner and Bernstein, 2021), and stress elicitors (Jalali et al., 2019) were found to induce changes in the cannabinoid profile of *Cannabis sativa* plants.

Nutrients are essential for major plant processes such as growth, source–sink relationships, respiration, photosynthesis, photooxidation and metabolites biosynthesis, and involve in regulation and signaling in the plant cell (Engels et al., 2012). Hence, understanding the plant mineral requirements is crucial for improving yield quantity and quality (Wiesler, 2012). Phosphorus is an essential macronutrient and a key element in nucleic acids and phospholipids, as well as in energy transfer processes in the cell. It therefore participates and affects central biosynthesis pathways (White and Hammond, 2008; Shen et al., 2011; Hawkesford et al., 2012). In *Arabidopsis* plants, P deprivation reduced the concentrations of 87 primary metabolites, altered the levels of 35 secondary metabolites, and increased most organic acids, amino acids and sugar levels (Pant et al., 2015).

Understanding effects of P on medical cannabis plants at the reproductive stage is important for regulation of the secondary metabolite profile in the plant material produced for the pharmacology industry. The hypothesis guiding the study was that P uptake into the plant and its distribution and availability in vegetative and reproductive organs, affect secondary metabolism in cannabis, which is accompanied by changes to the physiological state and the ionome. To test our hypothesis, we exposed the plants to five P treatments of 5, 15, 30, 60, and 90 mg L^{-1} (ppm) P at the reproductive stage of development, and tested plant development, physiology and chemical profiling of cannabinoids and minerals within the plant. The study was conducted comparatively with two medical cannabis cultivars differing in chemovar to assess genotypic sensitivity to P nutrition. The obtained results improve our understanding of cannabis plant science, and enable to direct optimization and standardization of the medical product for the benefit of those who need it.

MATERIALS AND METHODS

Plant Material and Growing Conditions

Two commercial medicinal cannabis cultivars, "Royal Medic" (RM) and "Desert Queen" (DQ) (Teva Adir Ltd., Israel), representing two chemotypes—(i) high THC and low CBD (DQ) and (ii) balanced THC and CBD (RM)—were chosen for the study. To ensure uniformity between plants, the plants were vegetatively propagated from cuttings of the same mother plant. The rooted cuttings were cultivated under a long photoperiod of 18/6 (day/night) using metal halide bulbs. After 4 weeks, the rooted cuttings, selected for uniformity, were transplanted into 3-L pots in perlite 2 (1.2) in controlled-environment growing rooms for 10 additional days of vegetative growth under at 25°C and 60% air relative humidity. The plants of each cultivar were divided randomly into five treatment groups of six replicated plants each, and the plants were randomly arranged in the cultivation space. The plants in each group received one of five P concentrations (5, 15, 30, 60, and 90 mg L^{-1} P), and short photoperiod was applied (12/12-h light/dark) using high-pressure sodium bulbs (980 μmol $m^{-2}s^{-1}$, Greenlab by Hydrogarden, Petah Tikva, Israel) for 63 and 68 days for DQ and RM, respectively. This concentration range was chosen with the goal to target deficiency as well as over-supply of P, for identification of the optimal range of P supply for physiological

performance, as well as P stress response on yield quantity and cannabinoid production. To ensure uniform growing conditions throughout the growing room, light intensity was measured weekly, at every 50 cm^2, and adjusted so as not to exceed 10% variability. The spacing of the plants was 0.2 m^2 $plant^{-1}$, and the plants were arranged in the cultivation space such as to minimize overlapping between plants. A reflective aluminum material covered the growing room for maximum reflection and light uniformity. The nutrient solution contained (in mM): 10.42 N-NO_3^-, 2.07 N-NH_4^+, 2.56 K^+, 2.99 Ca^{+2}, 1.44 Mg^{+2}, 1.47 S-SO_4^{-2}, 0.06 Cl^-, 0.021 Fe^{+2}, 0.011 Mn^{+2}, 0.009 B^{+3}, 0.005 Zn^{+2}, 0.0008 Cu^{+2}, and 0.0003 Mo^{+2}. Routine monitoring of the irrigation solution confirmed that the P concentration remained steady and in accord with the target concentrations; pH was kept at 5.5–6.0. The leachate solution volume was ∼30% and analyzed weekly for pH and P concentration (**Supplementary Figure 3**). P concentration in the leachate solution of the lowest P treatment was lower than in the fertigation solution, and under the highest P supply treatments it was higher than in the fertigation solution, and leachate pH was similar to the pH of the fertigation solution.

Plant Architecture and Development

Biomass accumulation was measured at the experiment's termination by destructive samplings. Fresh weight of vegetative organs (leaves, stem, and roots) and reproductive organs (inflorescence and inflorescence leaves) was measured immediately following dissection from the plants. Dry weight (DW) was measured after drying at 65°C for 72 h. Morphological parameters (plant height, stem diameter, and the number of nodes on the main stem) were measured once a week throughout the experiment. Stem diameter was measured with a digital caliper (YT-7201, Signet Tools International Co., Ltd., Shengang District, Taiwan) at the location 2 cm above the plant base. All measurements were conducted on six replicated plants from each treatment in each of the two cultivars tested.

Gas Exchange Parameters (Photosynthesis, Stomatal Conductance, Transpiration Rate, and Intercellular CO_2 Concentration)

A Licor 6400 XT system (LI-COR, Lincoln, NE, United States) was used for the measurements. The youngest mature leaf on the main stem was analyzed [CO_2 concentration: 400 mg L^{-1}, PPFD: 500 μmol (m^2s) $^{-1}$]. The leaves' temperature was kept at 25°C, and the relative humidity at 60%. The measurements were conducted twice during plant development, on day 26 and 54, on six replicated plants for each treatment in each cultivar.

Photosynthetic Pigments

Five disks, 0.6 cm in diameter, were removed from the youngest mature fan leaf on the plant main stem after the leaf was washed twice in distilled water and blotted dry. The disks were placed in 0.8 ml 80% (v/v) ethanol and kept in −20°C until further analysis. For the extraction of the pigments from the tissue, the samples were heated to 95°C for 30 min, and the solution was collected. Then, 0.5 ml of 80% (v/v) ethanol was added to the remaining tissue, and the tubes were heated again for 30 min. The combined extract was mixed by vortex; 0.4 ml was diluted in 5 ml (v/v) acetone, and absorbance was measured at 663, 664, and 740 nm by Genesys 10 UV scanning spectrophotometer (Thermo Scientific, Waltham, MA, United States). Chlorophyll *a* and *b* and carotenoids were calculated according to Lichtenthaler and Welburn (1983).

Inorganic Mineral Analysis

At the termination of the experiment, the plants were separated into leaves, stems, roots, inflorescences and inflorescence leaves (that were hand-trimmed from the inflorescences), weighed, rinsed in distilled water, and dried at 65°C for 72 h. When dried, the samples were weighed again for dry weight determination, ground, and acid-digested by two different procedures and analyzed for N, P, K, Ca, Mg, Fe, Zn, and Mn as described in Saloner et al. (2019). The biomass data, the concentration of P in the various plant organs and total P in the plant were used for the calculations of P proportion in specific plant organs (Eq. 1), P utilization efficiency (Eqs. 2, 3), P acquisition efficiency (Eq. 4), and yield efficiency (Eq. 5).

$$P\ porportion\ in\ an\ organ = \frac{P\ in\ tissue\ (mg)}{P\ in\ plant\ (mg)} \quad (1)$$

$$PUE_t = \frac{Plant\ dry\ weight\ (g)}{P\ in\ the\ plant\ (mg)} \quad (2)$$

$$PUE_y = \frac{Inflorescence\ dry\ weight(g)}{P\ in\ the\ plant\ (mg)} \quad (3)$$

$$PAE = \frac{P\ in\ the\ plant(mg)}{Root\ dry\ weight\ (g)} \quad (4)$$

$$Yield\ efficiency\ (\%) = \frac{Inflorescence\ DW}{Treatment\ that\ achieved\ the\ highest\ inflorescence\ DW} * 100 \quad (5)$$

where P is phosphorus; PUEt is P utilization efficiency for total dry weight; PUE_y is P utilization efficiency for yield dry weight, and PAE is P acquisition efficiency.

Cannabinoid Analysis

Cannabinoids were analyzed in inflorescences from two locations in each plant: the apical inflorescence of the main stem (primary inflorescence) and the apical inflorescence of the lowest branch of the main stem (secondary inflorescence). The inflorescences were sampled at the end of the experiment when ∼40% of the trichomes were of amber color. The sampled inflorescences were hand-trimmed and dried in the dark at 19.5°C and 45% air humidity for 2 weeks. The dried samples were crushed manually, 50 mg was placed in a glass vial, 10 ml 100% analytical ethanol was added, and the mixture was shaken for 1 h at room temperature. One milliliter of the extract was filtered through a polyvinylidene difluoride (PVDF) membrane filter of 0.22 μm pore size (Bar-Naor Ltd., Ramat Gan, Israel). The cannabinoid concentrations were analyzed using a high-performance liquid chromatography (HPLC) system (Jasco 2000 Plus series) in a spectrum mode. The system consisted of a quaternary

pump, autosampler, column compartment, and photodiode array (PDA) detector (Jasco, Tokyo, Japan). Chromatographic separations were conducted with a Luna Omega 3 μm Polar C18 column (Phenomenex, Torrance, CA, United States), with a length of 150 mm and internal diameter of 2.1 mm, employing acetonitrile/water 75:25 (v/v) with 0.1% (v/v) formic acid, at the isocratic mode, with a flow rate of 1.0 ml/minute and run time of 20 min under 25°C. Quantification was based on analytical standards: CBC, CBD, CBDV, cannabichromenic acid (CBCA), cannabidiolic acid (CBDA), cannabidivarinic acid (CBDVA), Δ^9-tetrahydrocannabivarinic acid (THCVA), cannabicyclol (CBL), cannabinol (CBN) from Sigma-Aldrich (Germany), cannabicitran (CBT) from Cayman Chemical (Ann Arbor, MI, United States), and THC, Δ^9-tetrahydrocannabinolic acid [THCA (THCA-A)], and Δ^9-tetrahydrocannabivarin (THCV) from Restek (Bellefonte, PA, United States). For all standards, the linear R^2 of the calibration curves was >0.994 (Saloner and Bernstein, 2021). Concentrations of THCV, CBDV, CBL, CBN, and CBT were lower than the detection limits. The total amount of each cannabinoid in a plant (g/plant) was calculated as the average concentrations of the cannabinoid in the two inflorescences sampled, multiplied by the inflorescence DW yield per plant.

Statistical Analysis

The data were statistically analyzed by two-way ANOVA, followed by a *post hoc* Tukey's honest significant difference (HSD) test ($\alpha = 0.05$). Comparison of relevant means was conducted using Fisher's least significant difference test at 5% level of significance. Pearson correlation was calculated for cannabinoid concentration and yield production. The analysis was performed with the Jump software (Jump package, version 9, SAS 2015, Cary, NC, United States).

RESULTS

Morphology and Biomass

P deficiency inhibited morphological development in both varieties as was apparent by the lower values of all morphological parameters tested under low P supply (**Figure 1**). DQ plants were more sensitive to low P concentration than RM, and growth restriction was apparent in DQ under 5 and 15 mg L^{-1} P, while in RM growth restriction was greater under 5 mg L^{-1} compared with 15 mg L^{-1} P. Phosphorous supply above 30 mg L^{-1} did not induce further growth stimulation. The elongation rate decreased from the third week of exposure to the short photoperiod and was lowest under 5 mg L^{-1} P in both genotypes. Biomass accumulation increased with P in both cultivars up to 30 mg L^{-1} P (**Figure 2**). Percent DW of the leaves was highest under P deficiency in both cultivars. Plants grown under P deficiency (5–15 mg L^{-1} P) were smaller than under higher supply rates, with fewer and chlorotic leaves. Furthermore, the inflorescences appeared less dense, and the individual flowers within the inflorescence appeared smaller (**Figure 3**).

Gas Exchange and Pigments

Under P deficiency (5 and 15 mg L^{-1} P), both cultivars had lower rates of photosynthesis, transpiration rate, and stomatal conductance and higher intercellular CO_2 concentrations compared with higher supply rates (**Figure 4**). The measurements were conducted twice during plant development: at the middle and the end of the reproductive growth phase. At late maturation (second measurement), the plants were physiologically less active than earlier in development and had lower stomatal conductance, photosynthesis, and transpiration rates and higher intercellular CO_2 (**Figure 4**). Photosynthesis was highest in both cultivars at the 30–90 mg L^{-1} P range, and a small decline above 30 mg L^{-1} P was found at the first measurement in DQ (**Figures 4A,B**). Transpiration rate and stomatal conductance were highest at the first measurement under 30–60 mg L^{-1} P in RM and 30 mg L^{-1} P in DQ. At the second measurement, transpiration rate and stomatal conductance were highest at 90 mg L^{-1} P in RM and 60–90 mg L^{-1} P in DQ (**Figures 4C–F**). Intercellular CO_2 declined with the increase in P supply in both measurements; a small rise under 60 and 90 mg L^{-1} P was found at the second measurement of RM (**Figures 4G,H**). The photosynthetic pigments chlorophyll *a*, chlorophyll *b*, and carotenoids increased with the increase in P application up to 60 mg L^{-1} and did not change with further increase in P (**Supplementary Figure 1**).

Nutrient Accumulation

The distribution of the nutrients to the plant organs was nutrient specific. N, P, and K accumulated to the highest concentrations in the inflorescences. Ca and Mg concentrations were highest in the leaves in both cultivars, and high Mg accumulation was also found in RM inflorescences (**Figures 5**, **6**).

Bioaccumulation of the minerals in the plant's organs was affected by P supply (**Figures 5**, **6**). P concentration in plant tissues increased with P supply in all plant organs up to 60 mg L^{-1} (**Figures 5A**, **6A**). Interestingly, P accumulated in inflorescences to a higher proportion under P deficiency (**Figure 7**), and the relative accumulation in the vegetative organs compared to the reproductive tissue increased with the increase in P availability in the nutrient solution.

In both cultivars, N concentration in the inflorescences increased with the increase in P application up to 30 mg L^{-1} P (**Figures 5B**, **6B**) but decreased with an increase in P up to 30 mg L^{-1} in RM's leaves and stem. K concentrations in leaves, stem, and root of RM plants and DQ's stem were highest under low P supply (**Figures 5C**, **6C**). Ca concentration in the root increased with P supply in both cultivars, unlike the concentrations in the inflorescences and the stem that were highest under 5 mg L^{-1} P (**Figures 5D**, **6D**). Leaves' Ca reached a maximum concentration at 30–60 mg L^{-1} and decreased with further P supply. Like Ca, Mg concentration in DQ leaves also demonstrated a maximum response curve to P supply, while in the stem, roots, and inflorescence Mg concentrations were not affected by the level of P supplied (**Figure 6F**). However, Mg concentration in RM's stem declined with the increase in P, Mg in the leaves increased up to 30 mg L^{-1} P, and Mg in the inflorescence increased as well up to 30 mg L^{-1} P but decreased with further increase in P availability.

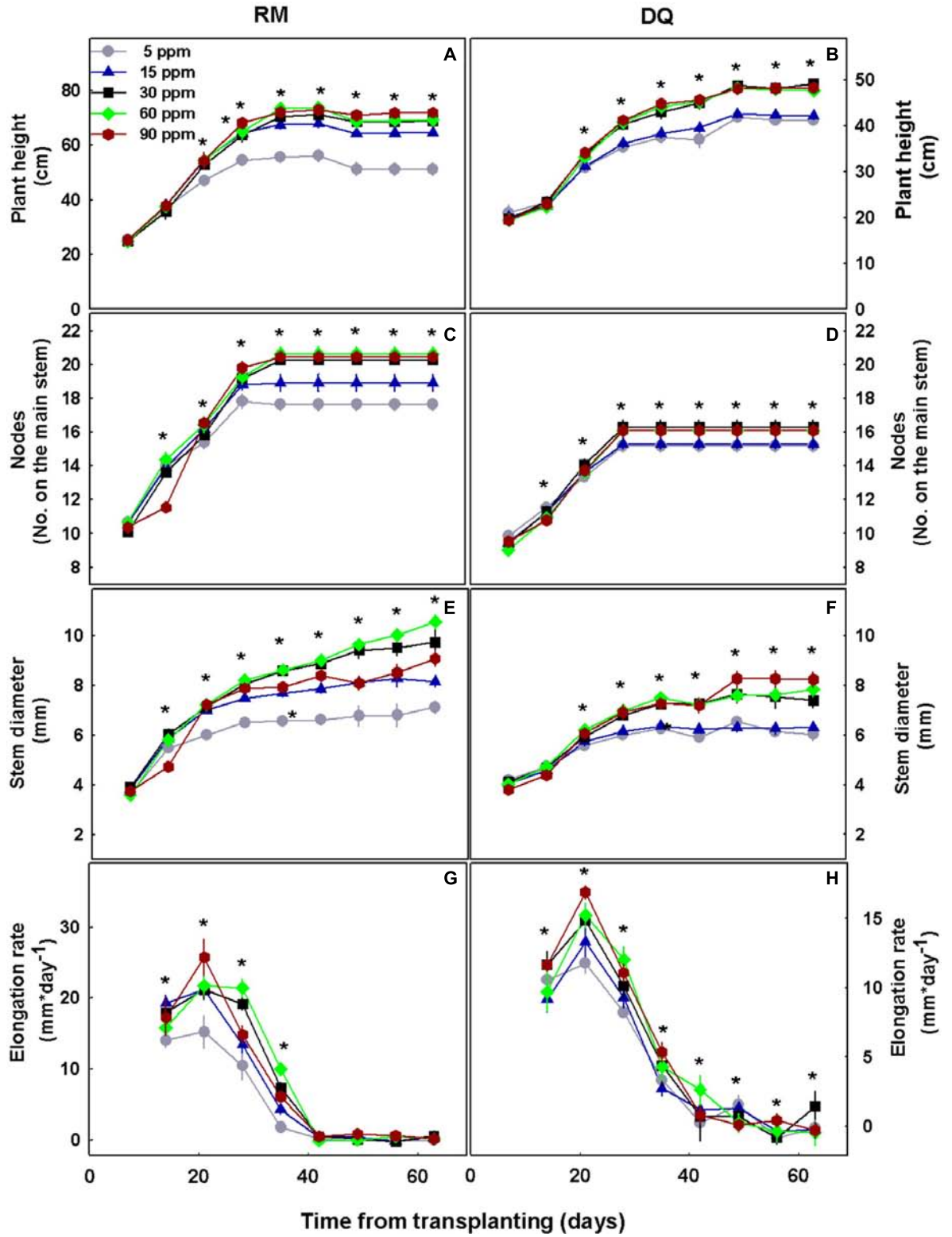

FIGURE 1 | Effect of P concentration on development of two medical cannabis cultivars, RM and DQ, at the flowering phase. Plant height **(A,B)**, number of nodes on the main stem **(C,D)**, stem diameter **(E,F)**, and elongation rate **(G,H)**. The first measurement represents the time of initiation of the P treatments, and the short photoperiod. Presented data are averages ± SD (n = 6). An asterisk above the averages represents a significant difference between treatments for a given day by Tukey's HSD test at $\alpha = 0.05$.

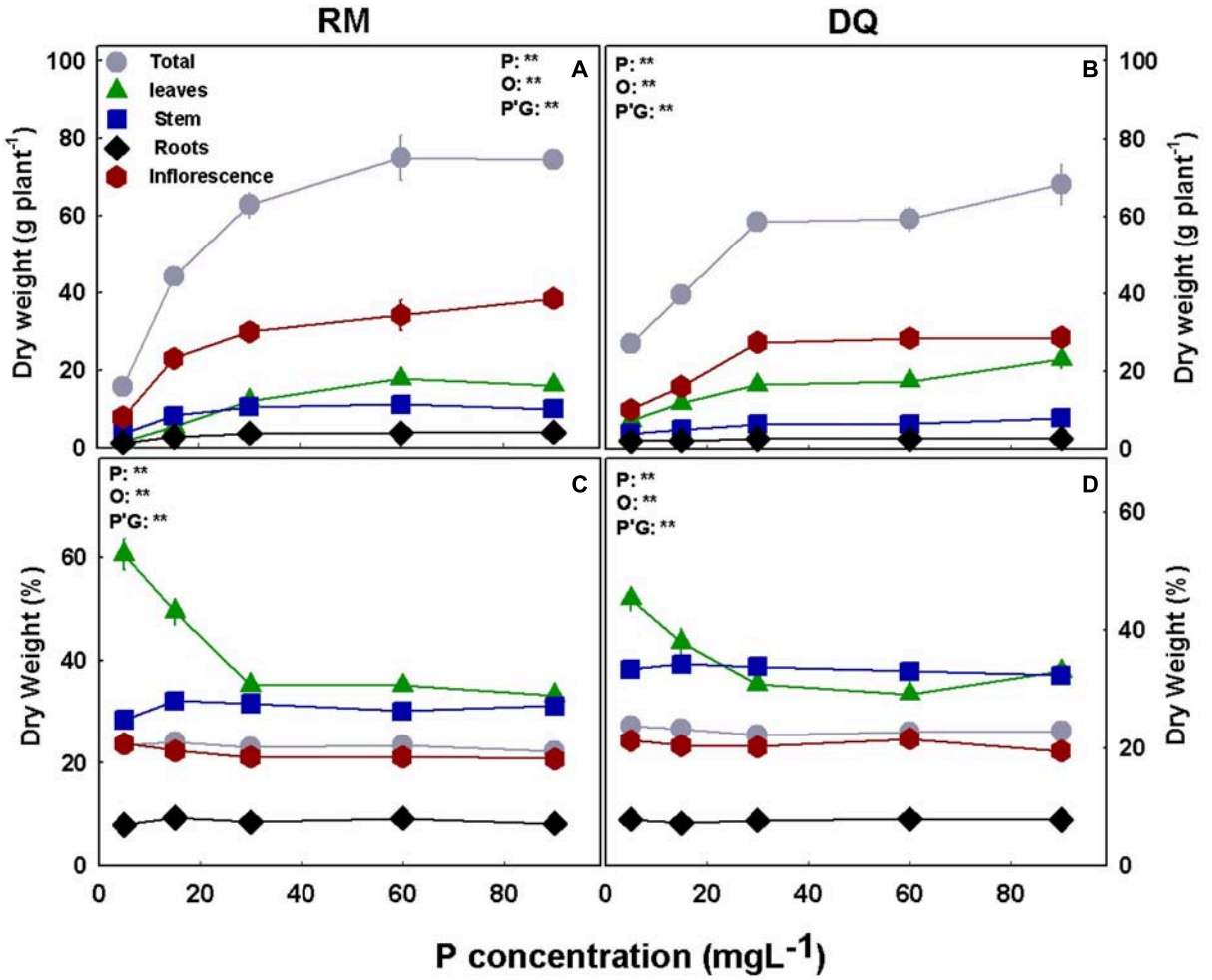

FIGURE 2 | Effect of P nutrition on biomass of the root and shoot organs in mature medical cannabis plants. Dry weight **(A,B)** and percentage of dry weight **(C,D)** of leaves, stems, roots, inflorescences, and total plant of two medical cannabis cultivars, RM **(A,C)** and DQ **(B,D)**. Presented data are averages ± SD ($n = 6$). Results of two-way ANOVA indicated as $^{**}P < 0.05$, F-test; NS, not significant $P > 0.05$, F-test. In the ANOVA results, P, phosphorus; G, genotype; and P*G, the interaction between P and G.

Manganese concentration in the leaves presented a maximum response curve to P supply in RM and increased with increasing P up to 30 mg L^{-1} in DQ (**Figures 5F**, **6F**). In the stem, Mn declined in both cultivars with the increase in P supply, and an increase in RM's stem was found at 90 mg L^{-1}. Mn in the inflorescences was not affected by the treatments in DQ and was highest under 5 mg L^{-1} P in RM, demonstrating a genotypic variability in response to P supply.

Zinc concentration was generally higher in roots and in the inflorescences compared with all other plant organs in both cultivars (**Figure 5G**, **6G**). Zn retention in roots under P scarcity (5–15 mg L^{-1} P) was observed in both genotypes. Iron concentration in DQ's leaves was not affected by the treatments and increased with P in RM (**Figures 5H**, **6H**). In the stem, Fe concentration increased with increasing P supply up to 30 mg L^{-1} P in both cultivars and was higher in DQ. The root's Fe response to the P treatments was genotype specific; it decreased with P in RM and increased in DQ. Inflorescence Fe was not affected significantly ($P > 0.05$) by the P treatments besides a slight increase at 90 mg L^{-1} P in RM.

P Efficiency

To assess P efficiency of the plant, five different parameters were calculated: (i) PUE_t (total DM/P), which analyzes the DM accumulation per P in the plant, (ii) PUE_y (flower DM/P), which analyzes the biomass of inflorescence produced per P in the plant, (iii) PAE (P/root), which calculates the P taken up by the plant per root unit, (iv) root/shoot ratio, and (v) yield efficiency (inflorescence DW/max inflorescence), which analyzes the percentage of yield in a defined treatment from the maximum yield achieved for the variety (**Figure 8**). The analyses revealed that PUE_t and PUE_y decline with the increase in P supply in both cultivars by up to 30 mg L^{-1} P and were not affected by a further increase in P supply (**Figures 8A,B**).

Phosphorus acquisition efficiency increased with the increase in P supply in both cultivars by up to 60 mg L^{-1} P

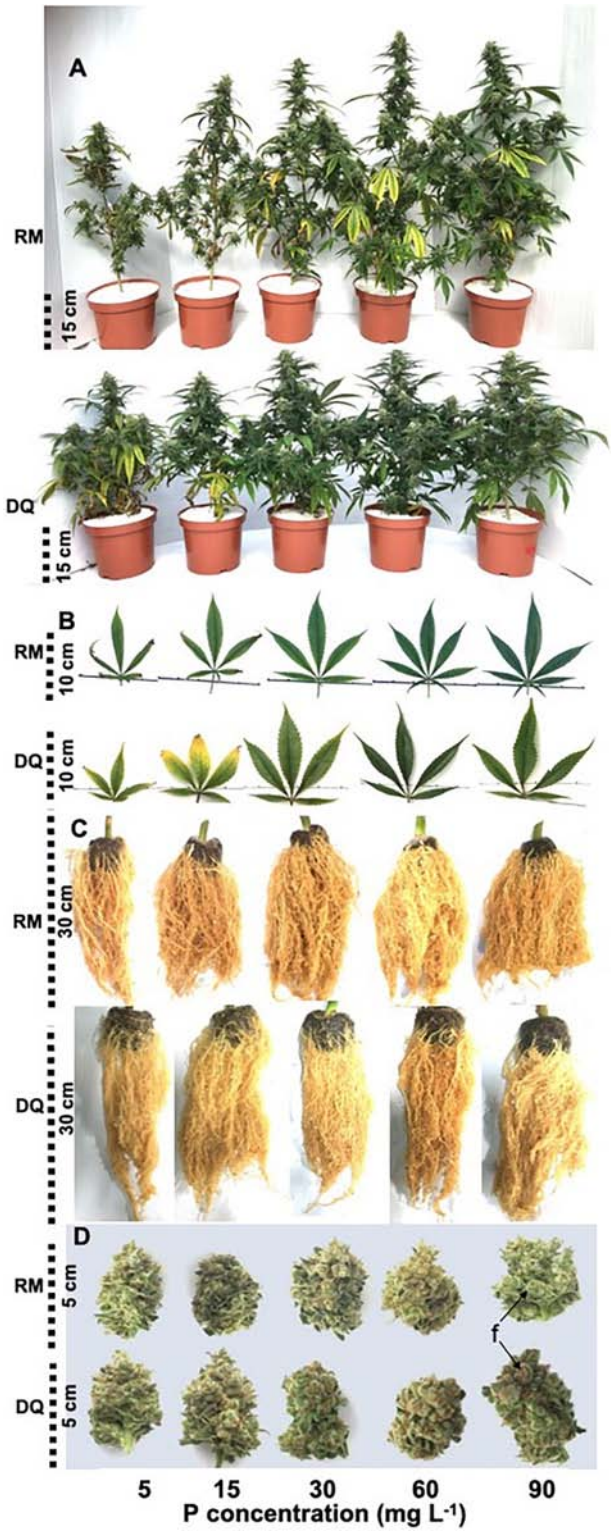

FIGURE 3 | Effect of P supply on visual appearance of whole plants **(A)**, leaves **(B)**, roots **(C)**, and trimmed inflorescences **(D)** of two medical cannabis cultivars RM and DQ. The images were taken at plant maturity. Shown are the apical inflorescence on the main stem and the youngest fully developed leaf on the main stem. "f" points at individual flowers in the inflorescence.

(**Figure 8C**). DQ had a higher PAE value than RM. The root/shoot ratio decreased with P and was significantly higher for RM (**Figure 8D**). Both cultivars reached 80% of the maximum yield at 30 mg L^{-1} P (**Figure 8E**), yet DQ reached ∼20% higher yield under 30 mg L^{-1} P supply.

Cannabinoids

Cannabinoid concentrations in the inflorescence were affected by the P treatments and overall reduced with the increase in P supply (**Figure 9**). THCA and CBDA concentrations had the most profound response to P concentrations and were reduced with P supplement in both genotypes and at both locations in the plant (i.e., in the primary and secondary inflorescences) (**Figures 9A,B**). Despite the considerable effect on THCA and CBDA, THC and CBD did not change significantly and were found at low concentrations (approximately 0.3 and 0.4% THC and 0.15% and undetected CBD in RM and DQ, respectively; **Supplementary Figure 2**). CBDVA was reduced with P in the primary inflorescence in both genotypes and demonstrated a minimum response curve in the secondary inflorescence (with a minimum at 15–30 and 30–60 mg L^{-1} in RM and DQ, respectively). THCVA concentration was reduced with P in DQ's secondary inflorescences and in RM in both inflorescences. CBCA was reduced with P in RM's upper inflorescence and was not affected in DQ. CBC concentration was low in both cultivars (RM: ∼0.03%, DQ: ∼0.003%) (**Supplementary Figure 2**).

The amount of cannabinoids produced per plant increased with P in RM for all cannabinoids tested (**Figure 10**). In DQ, such an increase was apparent only up to 30 mg L^{-1} P supply.

To understand the link between yield production and the cannabinoid concentrations, Pearson correlation coefficients were tested (**Figure 11**). In RM, CBDA, THCA, CBDVA, THCVA, and CBCA negatively correlated with yield; THCA and CBDA had the strongest negative correlation. The same results were obtained in DQ, except for CBCA which was not affected by yield in this genotype.

DISCUSSION

Phosphorus is a constituent of major compounds in the plant cells, such as nucleic acids and phospholipids, and it also plays a central role in energy transformations and as an energy carrier. It is therefore required for many key metabolic processes (Hawkesford et al., 2012). Thereby, the P status of the plant has a strong impact on plant development and metabolism (Wiesler, 2012). The present study evaluated effects of P supply on development and function of medical cannabis plants at the reproductive growth phase and on the profile of cannabinoids, the unique secondary metabolites in cannabis. The results reveal the importance of optimal P nutrition to the cannabis plant function and morpho-development as secondary metabolism was considerably affected by P supply as well as the plant gas exchange, CO_2 fixation, mineral uptake and translocation, and P use efficiency. The foremost discovery is the contrasting effect of increasing P supply to increase inflorescence yield production but to decrease the biosynthesis

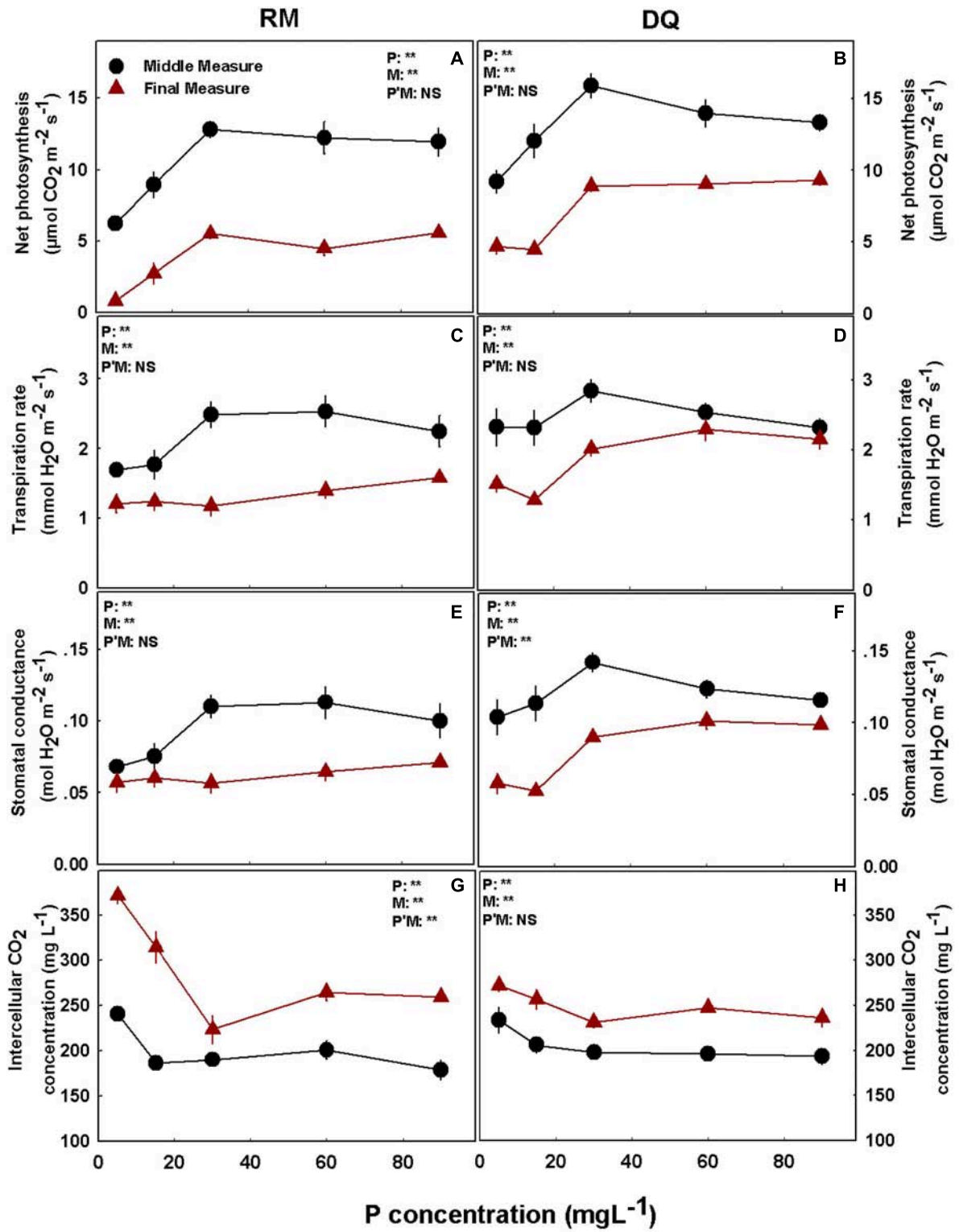

FIGURE 4 | Effect of P supply on gas exchange parameters in cannabis leaves. Net photosynthesis rate **(A,B)**, transpiration rate **(C,D)**, stomatal conductance **(E,F)**, and intercellular CO_2 **(G,H)** for two medical cannabis cultivars, RM and DQ. Results of measurements at two developmental stages, at the middle and at the end of the flowering phase. Presented data are averages ± SD ($n = 6$). Results of two-way ANOVA indicated as $^{**}P < 0.05$, F-test; NS, not significant $P > 0.05$, F-test. In the ANOVA results, P*M, the interaction between P and measurement.

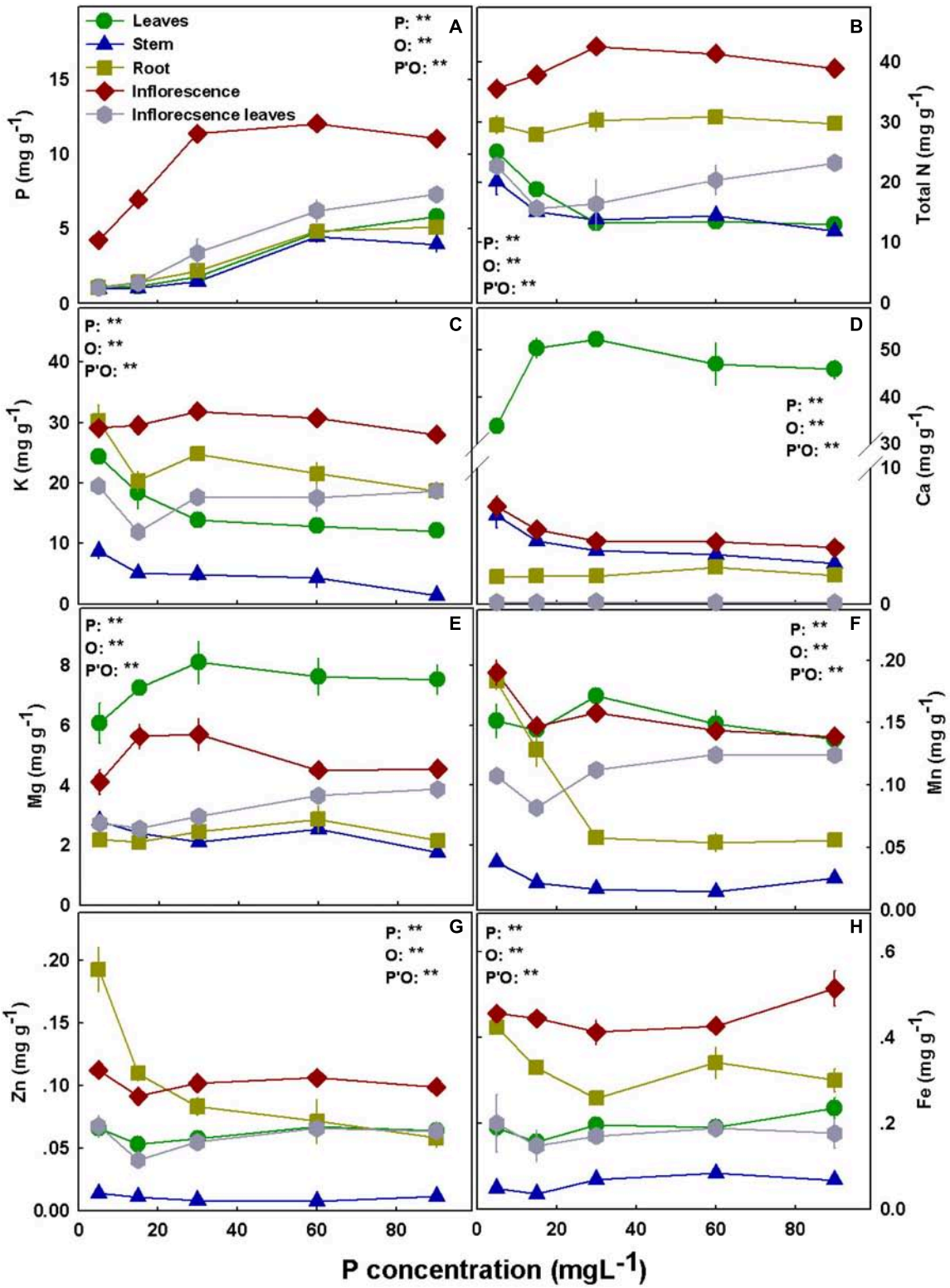

FIGURE 5 | Effect of P supply on nutrient concentrations in leaves, stems, roots, and inflorescences in the medical cannabis cultivar RM. P **(A)**, N **(B)**, K **(C)**, Ca **(D)**, Mg **(E)**, Mn **(F)**, Zn **(G)**, and Fe **(H)**. The presented data are averages ± SD ($n = 5$); the concentrations are in mg g DW^{-1}. Results of two-way ANOVA indicated as $^{**}P < 0.05$, F-test; NS, not significant $P > 0.05$, F-test. In the ANOVA results, P, phosphorus; O, organ; and P*O, the interaction between P and O.

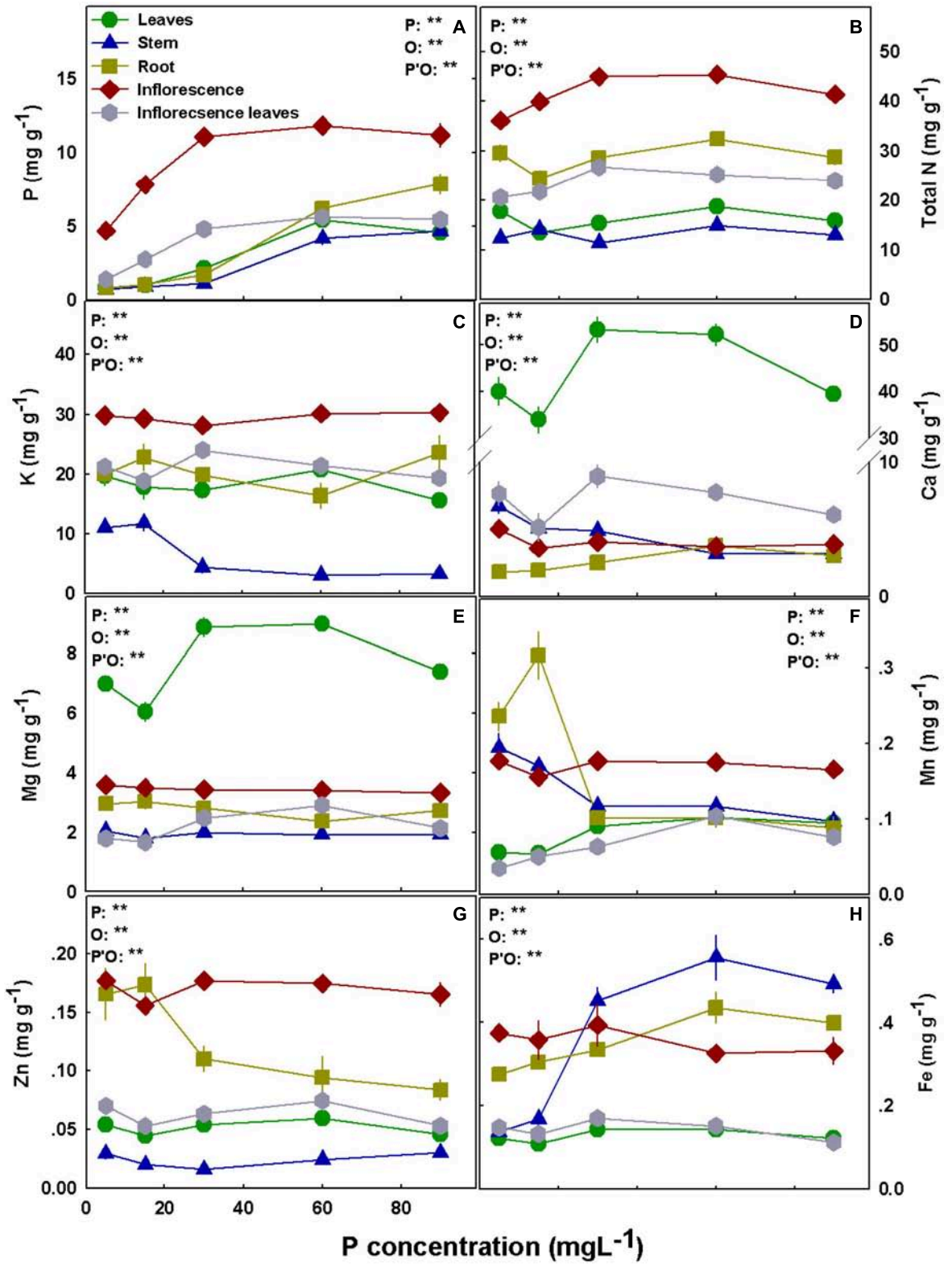

FIGURE 6 | Effect of P supply on nutrient concentrations in leaves, stems, roots and inflorescences in the medical cannabis cultivar DQ. P **(A)**, N **(B)**, K **(C)**, Ca **(D)**, Mg **(E)**, Mn **(F)**, Zn **(G)**, and Fe **(H)**. The presented data are averages ± SD ($n = 5$); the concentrations are in mg g DW^{-1}. Results of two-way ANOVA indicated as $^{**}P < 0.05$, F-test; NS, not significant $P > 0.05$, F-test. In the ANOVA results, P, phosphorus; O, organ; and P*O, the interaction between P and O.

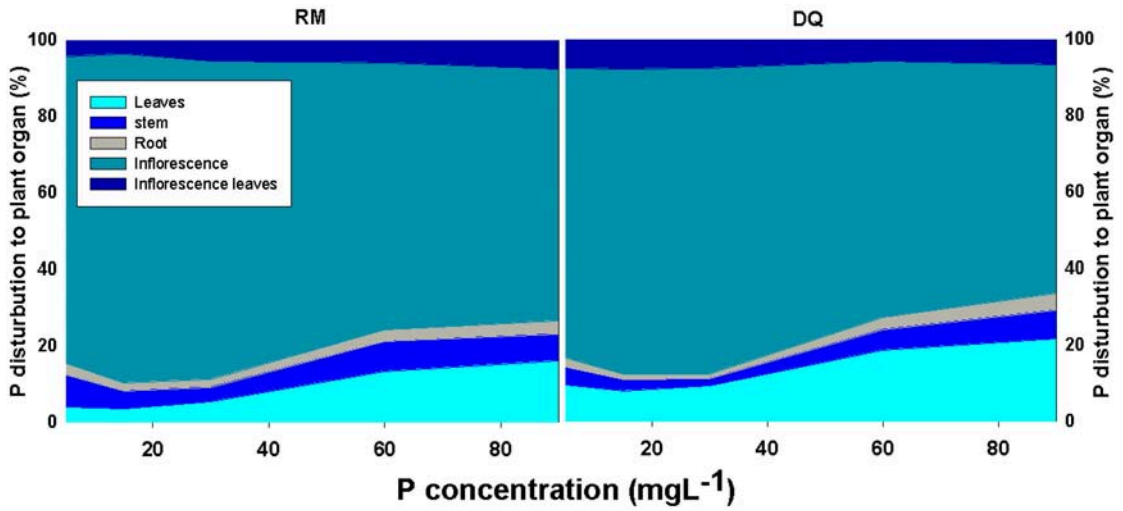

FIGURE 7 | Effect of P supply on the distribution of P in the plant to leaves, stem, roots, inflorescences, and inflorescence-leaves, in two medical cannabis cultivars, RM and DQ. The total P content in each organ is presented as the percent content of the total P in the plant. Presented data are averages (n = 5).

of major cannabinoids, demonstrating that P supply needs to be regulated to suit yield quantity vs. chemical quality goals. The revealed influence of P on the cannabinoid profile can be utilized for adjusting the cannabidiome to achieve a desirable pharmacological profile in the product for medical purposes.

The sensitivity of plant growth and development to P supply at the reproductive phase presented in this study are similar to responses we have recently reported for the vegetative phase (Shiponi and Bernstein, 2021). Responses to N and K nutrition are described in Saloner et al. (2019) and Saloner and Bernstein (2020, 2021). In both phases of growth, morphological development and biomass deposition are inhibited under P starvation, and P concentrations up to 90 mg L^{-1} P do not result in toxicity. Additionally, in both phases of plant development, DQ plants are more sensitive to low P than RM plants, demonstrating similar genotypic sensitivity. Similar to our results, stunted growth under P deficiency was obtained also for hemp, and P addition above adequate supply did not affect the plant morphology and biomass (Vera et al., 2004, 2010). P toxicity is uncommon in plants because of the plant downregulation mechanisms of P uptake (Dong et al., 1999; Hawkesford et al., 2012).

The effect of P nutrition on leaf gas exchange parameters was likewise similar for the reproductive (**Figure 4**) and the vegetative stages (Shiponi and Bernstein, 2021) as well as for the middle and end of the reproductive phase. Photosynthesis, transpiration, and stomatal conductance were lowest under low P supply and reached a maximum under 30 mg L^{-1} P (**Figure 4**). Inhibition of photosynthesis under P deficiency was reported for many plants (Brooks, 1986; Wang et al., 2018; Taliman et al., 2019), and the growth restriction we identified under P deficiency could be a result of the lower photosynthesis rate. A decline in photosynthesis, transpiration rate, and stomatal conductance under higher P application (60 and 90 mg L^{-1}) was found only in DQ plants at the first measurement. This resembles results that we have reported previously for the vegetative stage (Shiponi and Bernstein, 2021). Reduced photosynthesis as a result of P toxicity was observed in *Hakea prostrata* (Shane et al., 2004). However, the reduced photosynthesis under high P application did not affect DQ's biomass or morphology, demonstrating that carbon fixation was not a limiting factor. P impact on photosynthesis rate was found to occur *via* two pathways: by effects on stomatal conductance or by a non-stomatal pathway involving enzymes of the Calvin cycle (Brooks, 1988; Fredeen et al., 1990; Wang et al., 2018). Due to the decrease in photosynthesis rate under low P, intercellular CO_2 concentration increased in both cultivars and measurements, likely inducing the reduction in stomatal conductance (Allaway and Mansfield, 1967). The reduction in photosynthesis rate, together with the increase in intercellular CO_2 concentration, suggests a non-stomatal restriction on CO_2 assimilation under P deficiency. This result is unlike the response at the vegetative growth stage of medicinal cannabis, where a decrease in intercellular CO_2 concentration was found under low P. The reduced chlorophyll concentration under P deficiency (**Supplementary Figure 1**) could have contributed to the observed restriction of photosynthetic activity. P starvation has been reported to decrease chlorophyll concentration and photosynthesis in other plants as well (Soltangheisi et al., 2013; Frydenvang et al., 2015). The decline in photosynthesis rate, transpiration rate, and stomatal conductance with plant aging at the reproductive growth phase is probably due to the phenologically induced reduction in growth rates or the beginning of senescence at the end of the experiment that was demonstrated to occur in other plants as well (Tang et al., 2005).

Phosphorus Accumulation, Distribution, and Efficiency

Phosphorus concentration increased with the increase in P supply in all plant organs (**Figures 5A**, **6A**). In the leaves,

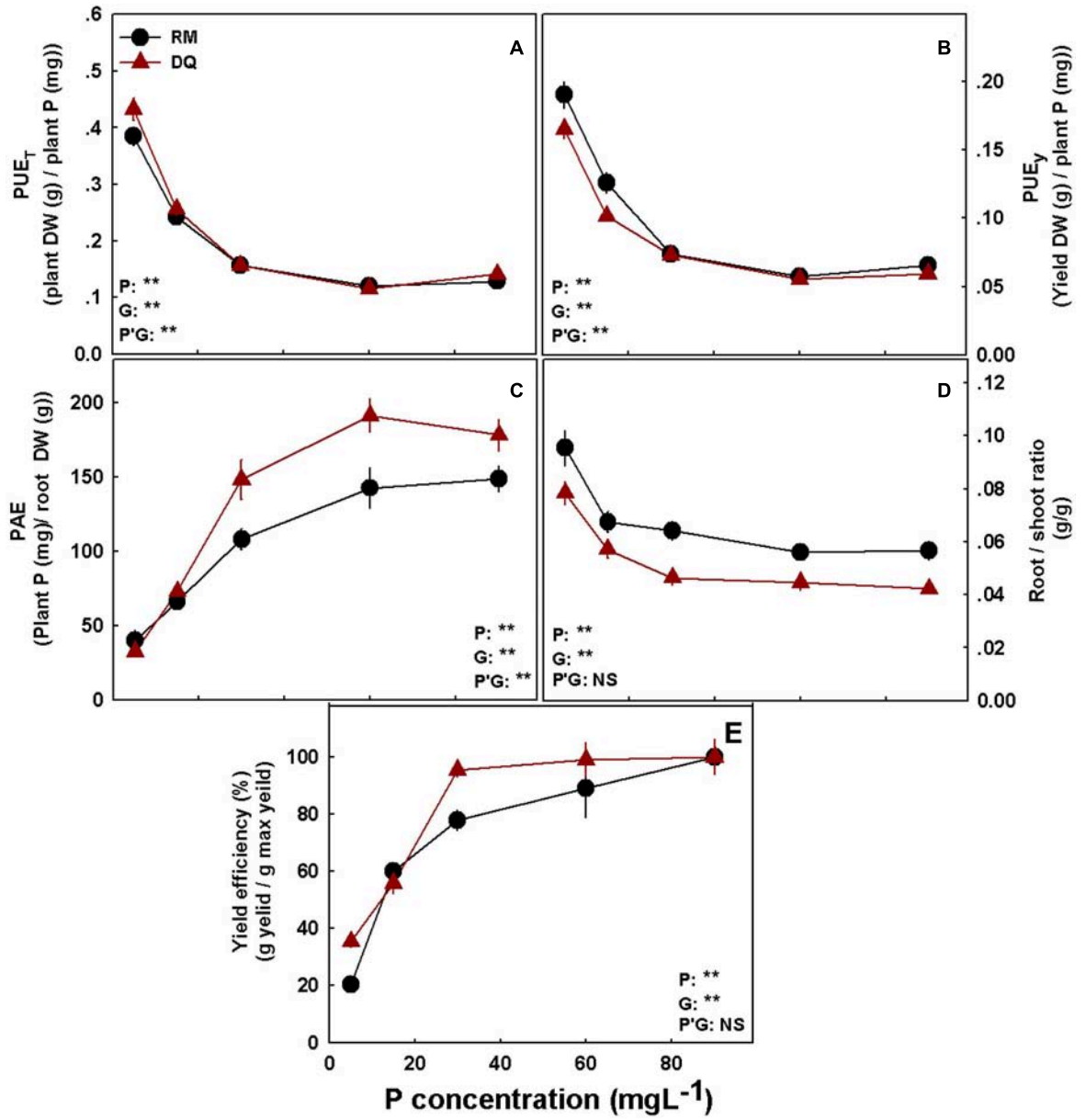

FIGURE 8 | Phosphorus efficiency parameters for two medical cannabis cultivars RM **(A)** and DQ **(B)**. P utilization efficiency for total dry weight **(A)**, P utilization efficiency for yield dry weight **(B)**, phosphorus acquisition efficiency **(C)**, Root/shoot ratio **(D)**, and yield efficiency **(E)**. Presented data are averages ± SD (n = 5). Results of two-way ANOVA indicated as $^{**}P < 0.05$, F-test; NS, not significant $P > 0.05$, F-test. In the ANOVA results, P*G, the interaction between P and genotype.

P concentration reached sufficient levels of 4.0–5.5 mg g^{-1} under 60 mg L^{-1} P supply, in accord with previous results for hemp (5–6 mg g^{-1}; Iványi and Izsáki, 2009) and for medical cannabis at the vegetative growth stage (3–4 mg g^{-1}; Shiponi and Bernstein, 2021). The leaves in P-"hungry" plants (from the 5 and 15 mg L^{-1} treatments) and leaves grown under 30 mg L^{-1} P supply contained only ∼20 and ∼40% of the P stored in leaves grown under sufficient P nutrition of 60 mg L^{-1} P, respectively, in both cultivars. Phosphorous levels in the leaves indicate that 60 mg L^{-1} P is the optimal application sufficient to support the maximum plant uptake potential. Yet, since plant uptake and accumulation potential do not necessarily support optimal plant function, additional parameters were considered, such as plant development and physiology and secondary metabolite production.

Phosphorus accumulation at the reproductive stage was substantially higher in the inflorescence than in all other plant organs, while at the vegetative growth stage, the highest accumulation was found in the roots (Shiponi and Bernstein, 2021). When biomass is taken into account, the inflorescences contained ∼80% of all plant P (**Figure 7**). An increase in P concentration in the nutrient solution decreased the proportion

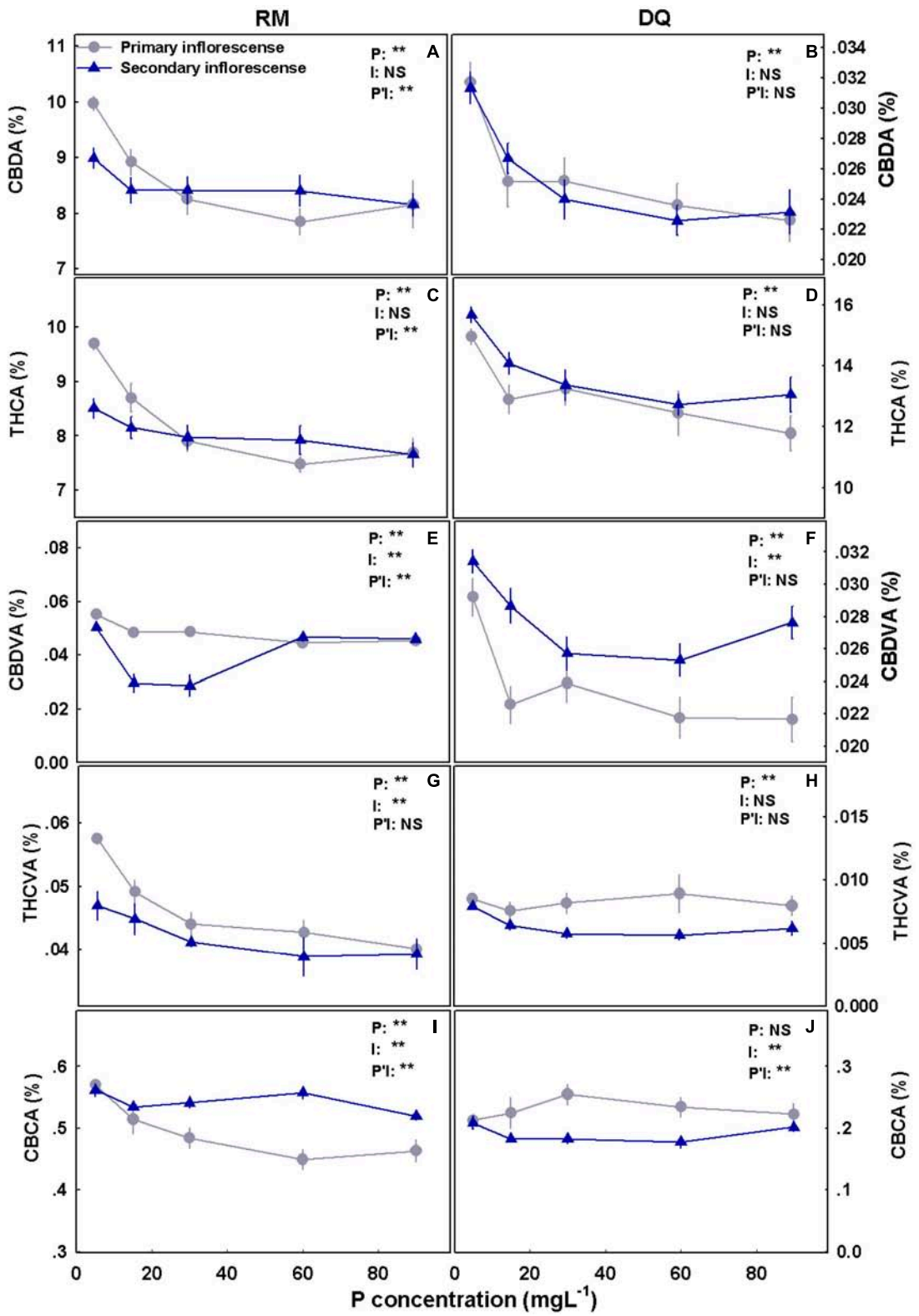

FIGURE 9 | Effect of P application on cannabinoid concentrations in primary and secondary apical inflorescences in medical cannabis plants in two cultivars, RM and DQ. Cannabidiolic acid **(A,B)**, Δ^9-tetrahydrocannabinolic acid **(C,D)**, cannabidivarinic acid **(E,F)**, Δ^9-tetrahydrocannabivarinic acid **(G,H)**, and cannabichromenic acid **(I,J)**. The presented data are averages ± SD (n = 6). Results of two-way ANOVA indicated as $^{**}P < 0.05$, F-test; NS, not significant $P > 0.05$, F-test. In the ANOVA results, P*I, the interaction between P and the inflorescence location.

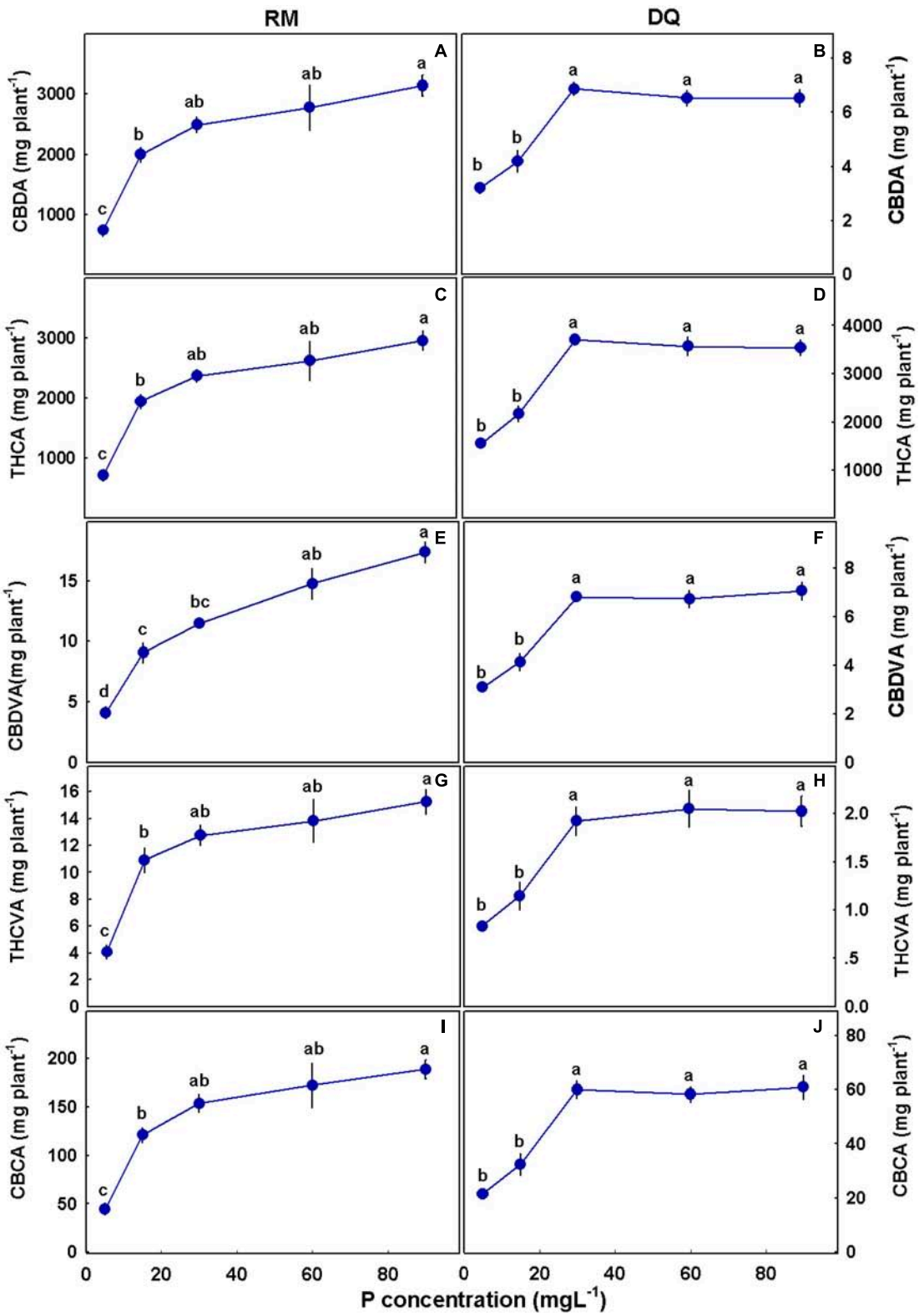

FIGURE 10 | Effect of P application on cannabinoid yield per plant for two medical cannabis cultivars, RM and DQ. Cannabidiolic acid **(A,B)**, Δ^9-tetrahydrocannabinolic acid **(C,D)**, cannabidivarinic acid **(E,F)**, Δ^9-tetrahydrocannabivarinic acid **(G,H)**, and cannabichromenic acid **(I,J)**. The presented data are averages ± SD (n = 6). Different letters above the means represent significant differences according to Tukey's honest significant difference test at α = 0.05.

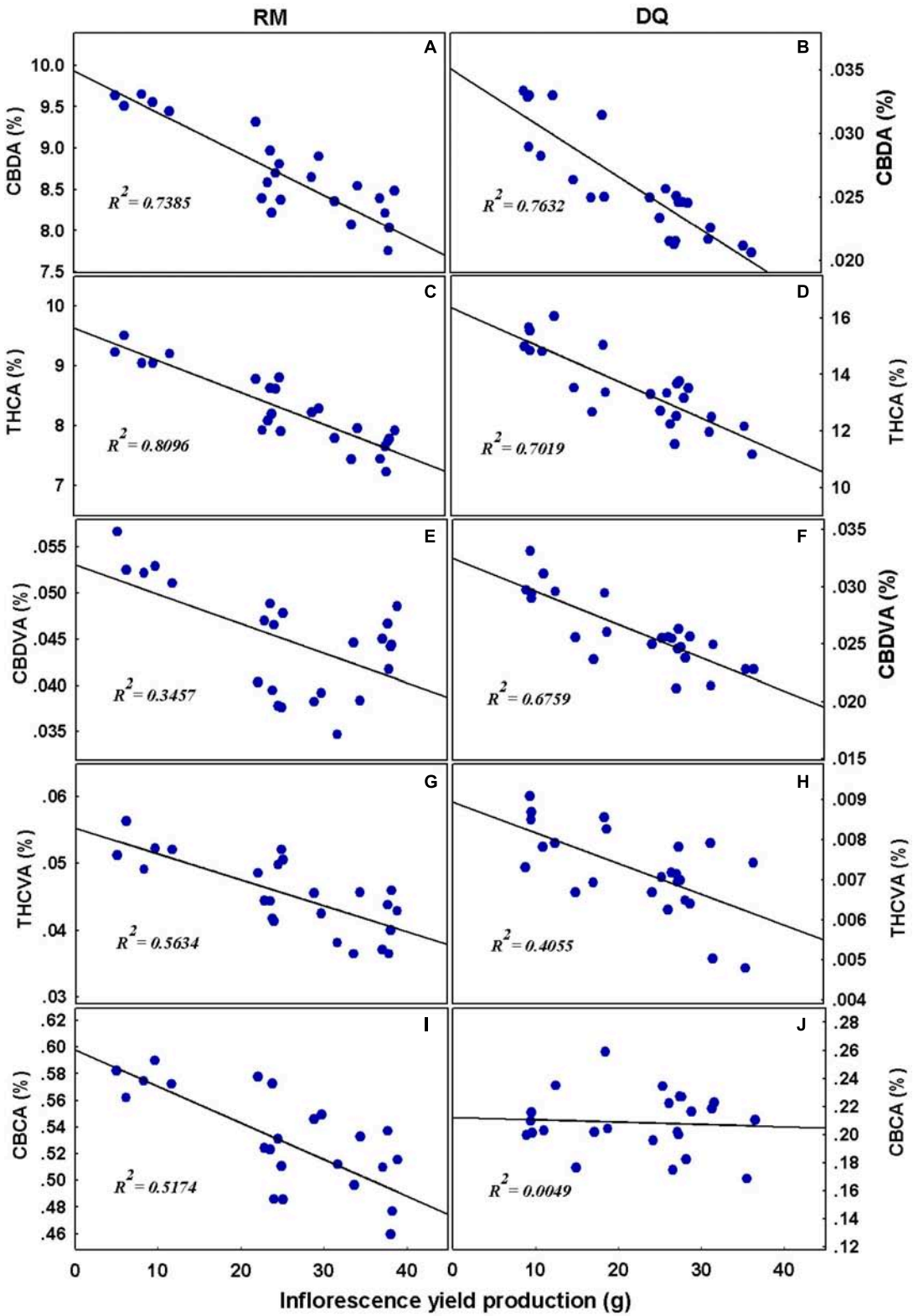

FIGURE 11 | Linear regression analysis. Relationships between cannabinoid concentrations and inflorescence yield per plant. Cannabidiolic acid **(A,B)**, Δ^9-tetrahydrocannabinolic acid **(C,D)**, cannabidivarinic acid **(E,F)**, Δ^9-tetrahydrocannabivarinic acid **(G,H)**, and cannabichromenic acid **(I,J)**. The continuous line represents the linear fit to the data.

of P accumulated in the inflorescences on account of an increased proportion of P at the vegetative tissues. Unlike the results obtained by Snapp and Lynch (1996) for beans, retention of P in roots was not apparent at the reproductive stage, and a higher proportion of P compartmentation in the root under low P was not found (**Figures 5–7**). In line with the results we obtained for cannabis at the vegetative and reproductive stages, a decline in root P concentration at maturity was found by Rose et al. (2008) for canola under high and adequate P. The enhanced translocation to the inflorescences is likely a result of breeding for excelled flower yield biomass. The reduction of the proportion of P content in the vegetative tissues under low P may imply a remobilization of P to the reproductive organs.

Distribution of minerals to plant organs is known to change with plant development, and the massive translocation of minerals to the reproductive organs supports growth of the next generation (Snapp and Lynch, 1996; Veneklaas et al., 2012). At maturity, P concentration is typically lower at the vegetative tissues compared to the grains as was found for numerous plants including lupine (Hocking and Pate, 1978), beans (Snapp and Lynch, 1996), wheat (Rose et al., 2007), canola (Rose et al., 2008), and rice (Rose et al., 2010). At the vegetative stage, root uptake is usually a more important source of P than remobilization between plant tissues. During the reproductive stage, remobilization can become a significant source for support of the new growth (Veneklaas et al., 2012). The results we obtained for cannabis suggest that uptake of P had an important role in P supply to the reproductive tissues since the accumulation of P increased with the increase in P supply. However, at the termination of the exponential growth spurt that the cannabis plant undergoes at the beginning of the reproductive phase, uptake was reduced, and remobilization played a more important role in inflorescence growth. Significant P uptake may occur post-anthesis and was suggested to be genetically related (Rose et al., 2007). Plants re-translocate at least 50% of the P contained in senescing leaves (Aerts, 1996). Remobilization of P was suggested to be part of the senescence process and pod filling in beans (Grabau et al., 1986; Snapp and Lynch, 1996), and in petunia, at the onset of flowering, the concentration of P in the vegetative organs decreased, while in the reproductive organ it gradually increased to a maximum concentration at the senescence stage (Zhang et al., 2012). P distribution in medical cannabis at the end of the cultivated plant life cycle as observed in the current study is in accord with previous knowledge on P accumulation in reproductive organs.

Phosphorus concentration in the inflorescence increased with the increase in P input up to 30 mg L^{-1} P and was not affected by further supply (**Figures 5**, **6**). Taken together with retention in roots under 90 mg L^{-1} P in DQ, the lack of increase in P accumulation in the inflorescences under higher P supply could be an indication of a defense mechanism against P toxicity. Phosphorus homeostasis is achieved by many cellular activities, among which are metabolic processes, translocation between tissues, interaction between ions, and membrane transport (Mimura, 1999). In order to maintain cellular P homeostasis, the plant coordinates between various phosphate transporters (Liu et al., 2016). For example, transporters of the PHT1 family are involved in Pi uptake and remobilization and are controlled by a complex regulation network. They are expressed in the roots for Pi uptake from the growing media and are also detected in various shoot organs such as leaves and flowers (Nussaume et al., 2011). Other phosphate transporters take part in organelle Pi transport, energy metabolism, or stress response (Liu et al., 2016). No information is so far available about P transporters in *C. sativa*, and this information is needed to shed light on P remobilization and translocation in the cannabis plant in light of the high P requirements of the plant. The vacuole functions as a primary compartment for Pi storage and remobilization and buffers Pi concentration in the cytoplasm against fluctuation. Under P deficiency, the Pi pool of the vacuole depletes, and when the Pi storage in the vacuole empties, growth ceases (Bieleski, 1973). Resupply of Pi to Pi-deficient plants results in a rapid flux of Pi into the vacuole. Compartmentation of Pi in the vacuole has an important role in Pi regulation under Pi starvation that prevents toxic levels of Pi in the cytoplasm under excess P (Liu et al., 2016). The tight Pi regulation within the cell may be the reason for the lack of visible toxicity symptoms in the current experiment.

P efficiency in the plant is gained by phosphorus utilization efficiency (PUE) and phosphorus acquisition efficiency (PAE) (Föhse et al., 1988; Wang et al., 2010a; Veneklaas et al., 2012; Wu et al., 2013). PAE is a measure of the ability of the root system to obtain P from the soil, and is an integration of many factors including root morphology and architecture, shoot/root ratio, chemical and biological conditions in the rhizosphere, and the type and density of root Pi transporters (Clarkson and Hanson, 1980; White and Hammond, 2008; George et al., 2012). PUE measures the internal P-use requirement and is commonly calculated as DM production to P concentration in the tissue (Balemi and Schenk, 2009b). PAE is frequently estimated as total P uptake/root biomass (Clarkson and Hanson, 1980). To estimate the external P requirement for optimal yield production by the cannabis plants, we calculated yield efficiency for each treatment as the percentage of yield achieved compared with the maximum yield produced. Based on previous studies, 80% of the maximum yield was defined as the threshold for the optimal P requirement (Föhse et al., 1988; Gourley et al., 1993). Both genotypes had a similar PUE response for the production of total DM and yield (**Figures 8A,B**). As described by Batten (1992), PUE in wheat was higher under P deficiency. Similar results were obtained for potato (Balemi and Schenk, 2009b), cotton (Wang et al., 2018), and lettuce (Neocleous and Savvas, 2019). PUE_t under low P supplement was significantly higher for DQ, but PUE_y was higher for RM (**Figures 8A,B**). Hence, in RM, utilization of P under deficiency is directed more toward reproductive growth than in DQ.

Phosphorus acquisition efficiency increased with P supply and was higher for DQ compared with RM under adequate P nutrition (30–90 mg L^{-1}) (**Figure 8C**). Although root/shoot ratio was higher for RM, DQ's PAE was higher, which indicates that, in this variety, parameters other than root/shoot ratio played an important part in P acquisition. Among the required traits for efficient P acquisition by plants are root elongation, increased root/shoot ratio, proliferation of root hairs and lateral roots, root secretion that affects chemical and electrochemical properties in

the rhizosphere, and membrane transport properties (White and Hammond, 2008; Wang et al., 2010a). As expected, root/shoot ratio decreased with the increase in P supply in both varieties (**Figure 8D**). Amplified root/shoot ratio under P scarcity is well known as a defense mechanism to promote P uptake (Bieleski, 1973; Shen et al., 2011; Hawkesford et al., 2012).

Wang et al. (2010a) have suggested that the plant's P efficiency depends mainly on genetic factors. Genetic variation in P efficiency was found in wheat (Ozturk et al., 2005), potato (Balemi and Schenk, 2009a), cotton (Wang et al., 2018), lettuce (Neocleous and Savvas, 2019), and soybean (Wang et al., 2010a,b). Overall, minor variations in PUE were found between the cannabis varieties tested, and PAE was significantly higher for DQ than RM.

The external requirement of P to achieve 80% of the maximum yield in both varieties was 30 mg L^{-1} (**Figure 8E**). The data presented here suggest that to achieve maximum yield, a minimum supply of 30 mg L^{-1} P, and an optimum P supply range of 30–90 mg L^{-1} P, are required in both cultivars.

Interplay Between P Nutrition and the *Cannabis* Plant Ionome

Plants require minerals for growth and development. Macroelements that are present at high concentrations in the plant as well as microelements that are accumulated at considerably lower concentrations are essential for plant function and survival (Kirkby, 2012). Interactions between minerals can affect root uptake and *in planta* translocation. Ion concentration in the root solution may therefore impose a competition between minerals, and a scarcity or an excess of minerals can have a substantial effect on plant development (White, 2012).

Similar to results for the vegetative stage (Shiponi and Bernstein, 2021), N and K concentrations in the leaves, stem, and roots did not show a consistent trend in response to P nutrition between varieties (**Figures 5**, **6**), demonstrating a genetic variability in mineral acquisition, translocation, and accumulation (Clárk, 1983). Some variations in the effect of P on mineral concentrations in the plant organs between the reproductive and the vegetative stages, such as for N and P in leaves (Shiponi and Bernstein, 2021), demonstrate also a developmental stage dependency.

An increase in Mg concentration in leaves up to 30 mg L^{-1} P supply was observed at both stages of development for both genotypes. In Shiponi and Bernstein (2021), we proposed acidification of the rhizosphere as a mechanism to induce Ca and Mg deficiency under P restriction. In support of this notion, leachate pH, in the current study for plants grown under P deficiency (5 mg L^{-1}), was lower (pH 4.5) than for plants grown under adequate P nutrition (pH 5.8) (**Supplementary Figure 3**).

Bioaccumulation of heavy metals in food crops and medicinal plants is a matter of concern worldwide due to their toxic effects on human health (Chizzola et al., 2003). Zn, Mn, Fe, Cu, Mo, and Ni are essential heavy metals that can be absorbed by plants *via* root uptake and accumulate to high concentrations (Ashfaque et al., 2016; Goyal et al., 2020). Variability in the extent of uptake and accumulation of heavy metal nutrients in plants is well documented between and within species, and *C. sativa* (hemp) was recognized as a hyper accumulator for heavy metals and is therefore considered a good candidate for soil phytoremediation (Citterio et al., 2003; Sarma et al., 2020). Hence, to maintain a safe product, data on the bioaccumulation potential of microelements in medical cannabis plant organs is required.

A decline in Mn concentration in the stem with P addition, and a maximum curve in leaves' Mn (**Figures 5F**, **6F**) were obtain also at the vegetative stage (Shiponi and Bernstein, 2021). Manganese is easily translocated from root to shoot with the transpiration stream in the xylem sap and but it moves poorly in the phloem (Loneragan, 1988; Duèiæ and Polle, 2005). Therefore, remobilization is limited, and Mn accumulates to higher concentrations in mature leaves than in young leaves. The retention of Mn in the root under low P supply in medicinal cannabis may reflect the lower transpiration rate in the 5 and 15 mg L^{-1} P treatments. When Mn levels are adequate, high concentrations of Mn can be stored in the roots and the stem and translocate to the shoot when Mn deficiency conditions develop (Clarkson, 1988; Loneragan, 1988). Generally, Mn accumulates in the root under sufficient Mn level (Loneragan, 1988), although a higher shoot/root ratio of Mn concentration is also common (Xue et al., 2004; Farzadfar et al., 2017). Baker (1981) discussed two strategies of plant response to tolerate metal toxicity: accumulators and excluders. Accumulators usually transport the metals to the aerial parts, while the excluders' response involves maintaining a low concentration in the shoot. Polechońska et al. (2013) found that the bioaccumulator plant, *Polygonum aviculare*, accumulates essential micronutrients (Zn, Mn, and Cu) in the aerial parts, unlike unessential elements that are accumulated in the root (Cd, Ni, and Pb). Xue et al. (2004) documented that in the hyperaccumulator plant *Phytolacca acinosa*, 87–95% of the Mn was translocated to the shoot. In medicinal cannabis, we found that at the vegetative-stage Mn was retained in the root, whereas at the reproductive stage the highest concentrations in the shoot were found under adequate P nutrition. *Cannabis* is known as a good bioaccumulator; thus, accumulation in the shoot is not surprising. The plant strategy can be transformed from excluder to accumulator during the plant life cycle (Baker, 1981), and it may be the reason for the differences between Mn accumulation in the plant organs at different development stages.

We identified a decrease in Zn concentrations in the root with the increase in P concentration in both the vegetative and the reproductive phase for both cultivars, and the P × Zn interaction was discussed in detail in Shiponi and Bernstein (2021). Inflorescence Zn concentration was ∼40% higher in DQ compared with RM, demonstrating a genetic variability. Genetic variability was reported before to affect heavy metal accumulation in plants (Baker and Brooks, 1989; Malik et al., 2010), and in cannabis, it can be explored for reduction of heavy metal accumulation in the pharmaceutical product.

The safety of medicinal cannabis consumption and the safe limit of heavy metal concentration in the product are not yet well researched and are topics of interest in light of the growing global demand. Thus, there is an increasing necessity for the

regulation and restriction of heavy metal concentrations in medicinal cannabis (Gauvin et al., 2018; Nie et al., 2019). Further research on the effect of the plant genotype and environmental factors in relation to heavy metal acquisition is necessary.

Cannabinoids

Cannabis is one of the oldest plant sources for medicine. It is known for centuries for its medicinal potential and has been used traditionally for thousands of years for the treatment of a wide array of ailments (Gonçalves et al., 2019). Recent changes in regulations have allowed proliferation of medical studies, and significant progress has been made toward the understanding of the potential of the plant-produced cannabinoids, and their interactions with other biologically active secondary metabolites in the plant, for modern medicine (Citti et al., 2018). Filling the medical knowledge gap, as well as knowledge concerning the influence of agro-technologies on the concentrations and ratios between the pharmacological compounds, is of high priority for optimizing the medicinal value of the product.

The production of secondary metabolites is known to be affected by environmental factors (Verpoorte et al., 2002; Ramakrishna and Ravishankar, 2011; Gorelick and Bernstein, 2014). Among other secondary metabolites, cannabis plants produce cannabinoids that are biosynthesized and stored in trichomes located mainly on the plant inflorescence. Cannabis plants differ in their cannabinoid contents due to genetic and environmental factors (Chandra et al., 2017; Danziger and Bernstein, 2021a). Abiotic stressors were found to induce changes in the cannabinoid profile in the cannabis plant (Flores-Sanches and Verpoorte, 2008; Backer et al., 2019; Caplan et al., 2019; Jalali et al., 2019; Gülck and Møller, 2020; Yep et al., 2020; Saloner and Bernstein, 2021), and in the current study, P nutrition was found to elicit changes in cannabinoid concentrations in the two genotypes tested. We found a reduction in concentrations of most tested cannabinoids with an increase in P application (**Figure 9**), which negatively correlated with yield production (**Figure 11**). Although the concentrations of many cannabinoids (especially THCA and CBDA) reduced, the amount of cannabinoids produced per plant increased with P, suggesting that the optimal P application is 30 mg L^{-1} in DQ and 30–90 mg L^{-1} in RM (**Figure 10**).

Previous studies on P effect on secondary metabolites and essential oil production found a variety of responses to increased P application. P increased essential oil production in *Cymbopogon nardus* (Ranaweera and Thilakaratne, 1992; Ranaweera et al., 1992), *Olearia phlogopappa* (Dragar and Menary, 1995), cannabis (Coffman and Gentner, 1977), dragonhead (Said-Al Ahl and Abdou, 2009), and basil (Ichimura et al., 1995). Essential oil content was not affected by P in sage (Rioba et al., 2015) and basil (Ichimura et al., 1995) and by a moderate P application in cannabis (Bernstein et al., 2019b) and was reduced in *Olearia phlogopappa* (Dragar and Menary, 1995). An increase in THCA and CBDA concentrations as a response to P deficiency are unlikely to be a direct effect of P on the biochemical pathways due to the crucial role of P in cannabinoid biosynthesis (Fellermeier et al., 2001; Flores-Sanches and Verpoorte, 2008; Sarma et al., 2020). The negative correlation between THCA and CBDA, and inflorescence yield production (**Figure 11**) indicates that a dilution effect may be a possible mechanism for the reduction in their concentration.

When Pearson correlation coefficient was performed on THCA, CBDA, and total P in the plant, the correlation was weaker compared to yield production (R^2 = RM: 0.59, 0.37 and DQ: 0.32, 0.31 for THCA and CBDA, respectively). The lower correlation with P compared with inflorescence yield suggests that the influence on the cannabinoid concentrations is probably due to yield increase and not a direct effect of P. Caplan et al. (2017) found, that in cannabis, NPK application reduced THCA, THC, and CBGA concentration and increased yield. Corresponding to our results, a negative correlation between THCA and inflorescence yield was found, and the total cannabinoids per plant increased with NPK. In our study, both genotypes analyzed responded similarly to the P treatments, and only minor changes were observed, this is despite the very different chemovars (a high THC vs. a CBD/THC balanced profile). Unlike DQ that did not show a response to P addition above 30 mg L^{-1} in total cannabinoid production, RM responded with a slight increase that might indicate a potential for yield increase with P addition for certain genotypes, which should be tested further. The reduction in THCA concentration in response to P addition was slightly higher for RM compared with DQ; THCVA was reduced with P in RM and was only slightly affected in DQ.

These results demonstrate that the effect of P nutrition on the cannabinoid profile may be genotype specific, and genetic differences should be explored for the optimization of the secondary metabolite profile by P-nutrition technologies. More research is needed on medicinal effects of cannabinoids and their interactions, in order to direct growing techniques for production of medical product with a desirable cannabinoid profile.

In Summary

Phosphorus nutrition considerably affects morpho-physiology of medicinal cannabis and its chemical profile. No signs of P toxicity were found under the concentration range tested; however, at the two lowest P supply rates (5 and 15 mg L^{-1} P), P deficiency reduced plant growth and physiological function, induced leaf chlorosis, but increased root/shoot ratio and PUE. Moreover, 80% yield efficiency was achieved under 30 mg L^{-1} P supply in both genotypes but was higher for DQ. Although both genotypes responded similarly to the P application dosages, DQ's yield production was not affected by P addition above 30 mg L^{-1}, unlike RM that responded with a small increase to P addition up to 90 mg L^{-1} P. Thereby, DQ demonstrated best performance under lower P application compared with RM that slightly increased in yield under high P supply. Taken together, our results demonstrate that the optimal P nutrition needs to be adjusted to the target product. The lowest recommended P supply for optimal yield quantity is 30 mg L^{-1} P; under higher concentrations up to 90 mg L^{-1} P, yield quantity remains optimal; and P deficiency stress (5–15 mg L^{-1} P) can be used to stimulate higher concentrations of the major cannabinoids. More research needs to be conducted on specific genotypic responses to P addition above the optimal dosage.

DATA AVAILABILITY STATEMENT

The original contributions presented in the study are included in the article/**Supplementary Material**, further inquiries can be directed to the corresponding author/s.

AUTHOR CONTRIBUTIONS

NB planned the experiments. SS carried out the experiments. NB and SS wrote the manuscript. Both authors contributed to the article and approved the submitted version.

FUNDING

This study was funded by the Chief Scientist Fund of the Ministry of Agriculture in Israel, grant no. 20-03-0018.

ACKNOWLEDGMENTS

We thank Dr. Mollie Sacks for advice concerning the design of the fertigation solutions, Yael Sade for guidance concerning cannabinoid analysis, Shiran Cohen for assistance with N and P analysis, and Dalit Morad, Guy Cohen, Geki Shoef, Ayana Neta, Eliav Shtul-Trauring, Avia Saloner, and Nadav Danziger for technical assistance. We also thank Gerry Kolin, Teva Adir, Ltd., a certified commercial growing company for the supply of the plant material for the study.

SUPPLEMENTARY MATERIAL

The Supplementary Material for this article can be found online at: https://www.frontiersin.org/articles/10.3389/fpls.2021.657323/full#supplementary-material

REFERENCES

Aerts, R. (1996). Nutrient resorption from senescing leaves of perennials: are there general patterns? *J. Ecol.* 84, 597–608. doi: 10.2307/2261481

Allaway, W. G., and Mansfield, T. A. (1967). Stomatal responses to changes in carbon dioxide concentration in leaves treated with 3-(4-chlorophenyl)-1, 1-dimethylurea. *New Phytol.* 66, 57–63. doi: 10.1111/j.1469-8137.1967.tb05986.x

Ashfaque, F., Inam, A., Sahay, S., and Iqbal, S. (2016). Influence of heavy metal toxicity on plant growth, metabolism and its alleviation by phytoremediation-a promising technology. *J. Agric. Ecol. Res. Int.* 6, 1–19. doi: 10.9734/JAERI/2016/23543

Backer, R., Schwinghamer, T., Rosenbaum, P., McCarty, V., Eichhorn Bilodeau, S., Lyu, D., et al. (2019). Closing the yield gap for cannabis: a meta-analysis of factors determining cannabis yield. *Front. Plant Sci.* 10:495. doi: 10.3389/fpls.2019.00495

Baker, A. J. M. (1981). Accumulators and excluders-strategies in the response of plants to heavy metals. *J. Plant Nutr.* 3, 643–654. doi: 10.1080/01904168109362867

Baker, A. J. M., and Brooks, R. R. (1989). Terrestrial higher plants which hyperaccumulate metallic elements. a review of their distribution, ecology and phytochemistry. *Biorecovery* 1, 81–126.

Balemi, T., and Schenk, M. K. (2009a). Genotypic difference of potato in carbon budgeting as a mechanism of phosphorus utilization efficiency. *Plant Soil* 322, 91–99. doi: 10.1007/s11104-009-9897-0

Balemi, T., and Schenk, M. K. (2009b). Genotypic variation of potato for phosphorus efficiency and quantification of phosphorus uptake with respect to root characteristics. *J. Plant Nutr. Soil Sci.* 172, 669–677. doi: 10.1002/jpln.200800246

Batten, G. D. (1992). A review of phosphorus efficiency in wheat. *Plant Soil* 146, 163–168. doi: 10.1007/BF00012009

Berman, P., Futoran, K., Lewitus, G. M., Mukha, D., Benami, M., Shlomi, T., et al. (2018). A new ESI-LC/MS approach for comprehensive metabolic profiling of phytocannabinoids in Cannabis. *Sci. Rep.* 8:14280. doi: 10.1038/s41598-018-32651-4

Bernstein, N., Gorelick, J., and Koch, S. (2019a). Interplay between chemistry and morphology in medical cannabis (*Cannabis sativa* L .). *Ind. Crop. Prod.* 129, 185–194. doi: 10.1016/j.indcrop.2018.11.039

Bernstein, N., Gorelick, J., Zerahia, R., and Koch, S. (2019b). Impact of N, P, K, and humic acid supplementation on the chemical profile of medical Cannabis (*Cannabis sativa* L). *Front. Plant Sci.* 10:736. doi: 10.3389/fpls.2019.00736

Bieleski, R. L. (1973). Phosphate pools, phosphate transport, and phosphate availability. *Annu. Rev. Plant Physiol.* 24, 225–252. doi: 10.1146/annurev.pp.24.060173.001301

Bonini, S. A., Premoli, M., Tambaro, S., Kumar, A., Maccarinelli, G., Memo, M., et al. (2018). Cannabis sativa: a comprehensive ethnopharmacological review of a medicinal plant with a long history. *J. Ethnopharmacol.* 227, 300–315. doi: 10.1016/j.jep.2018.09.004

Brooks, A. (1986). Effects of phosphorus nutrition on ribulose-1, 5-bisphosphate carboxylase activation, photosynthetic quantum yield and amounts of some Calvin-cycle metabolites in spinach leaves. *Funct. Plant Biol.* 13, 221–237. doi: 10.1071/PP9860221

Brooks, A. (1988). Effects of phosphorus nutrition on the response of photosynthesis to CO2 and O2, activation of ribulose bisphosphate carboxylase and amounts of ribulose bisphosphate and 3-phosphoglycerate in spinach leaves. *Photosynth. Res.* 15, 133–141. doi: 10.1007/BF00035257

Caplan, D., Dixon, M., and Zheng, Y. (2017). Optimal rate of organic fertilizer during the flowering stage for cannabis grown in two coir-based substrates. *HortScience* 52, 1796–1803. doi: 10.21273/HORTSCI12401-17

Caplan, D., Dixon, M., and Zheng, Y. (2019). Increasing inflorescence dry weight and cannabinoid content in medical cannabis using controlled drought stress. *HortScience* 54, 964–969. doi: 10.21273/HORTSCI13510-18

Chandra, S., Lata, H., Khan, I. A., and ElSohly, M. A. (2017). *Cannabis sativa L.-Botany and Biotechnology*. Berlin: Springer. doi: 10.1007/978-3-319-54564-6

Chizzola, R., Michitsch, H., and Franz, C. (2003). Monitoring of metallic micronutrients and heavy metals in herbs, spices and medicinal plants from Austria. *Eur. Food Res. Technol.* 216, 407–411. doi: 10.1007/s00217-003-0675-6

Citterio, S., Santagostino, A., Fumagalli, P., Prato, N., Ranalli, P., and Sgorbati, S. (2003). Heavy metal tolerance and accumulation of Cd, Cr and Ni by *Cannabis sativa* L. *Plant Soil* 256, 243–252. doi: 10.1023/A:1026113905129

Citti, C., Braghiroli, D., Vandelli, M. A., and Cannazza, G. (2018). Pharmaceutical and biomedical analysis of cannabinoids: a critical review. *J. Pharm. Biomed. Anal.* 147, 565–579. doi: 10.1016/j.jpba.2017.06.003

Clárk, R. B. (1983). Plant genotype differences in the uptake, translocation, accumulation, and use of mineral elements required for plant growth. *Genet. Aspects Plant Nutr.* 72, 49–70. doi: 10.1007/978-94-009-6836-3_5

Clarke, R. C., and Merlin, M. D. (2016). Cannabis domestication, breeding history, present-day genetic diversity, and future prospects. *Crit. Rev. Plant Sci.* 35, 293–327. doi: 10.1080/07352689.2016.1267498

Clarkson, D. T. (1988). The uptake and translocation of manganese by plant roots. *Manganese Soils Plants* 33, 101–111. doi: 10.1007/978-94-009-2817-6_8

Clarkson, D. T., and Hanson, J. B. (1980). The mineral nutrition of higher plants. *Annu. Rev. Plant Physiol.* 31, 239–298. doi: 10.1146/annurev.pp.31.060180.001323

Coffman, C. B., and Gentner, W. A. (1977). Responses of greenhouse-grown *Cannabis sativa* L. to nitrogen, phosphorus, and potassium 1. *Agron. J.* 69, 832–836. doi: 10.2134/agronj1977.00021962006900050026x

Danziger, N., and Bernstein, N. (2021a). Light matters: effect of light spectra on cannabinoid profile and plant development of medicinal cannabis (*Cannabis sativa* L.). *Indust. Crop Prod.* 194:113351. doi: 10.1016/j.indcrop.2021.113351

Danziger, N., and Bernstein, N. (2021b). Plant architecture manipulation increases cannabinoid standardization in 'drug-type' medical cannabis. *Indust. Crop Prod.* 167:113528. doi: 10.1016/j.indcrop.2021.113528

Decorte, T., and Potter, G. (2015). The globalisation of cannabis cultivation: a growing challenge. *Int. J. Drug Policy* 26, 221–225. doi: 10.1016/j.drugpo.2014.12.011

Demain, A. L., and Fang, A. (2000). "The natural functions of secondary metabolites," in *History of Modern Biotechnology I*, ed. A. Fiechter (Berlin: Springer). doi: 10.1007/3-540-44964-7_1

Dong, B., Ryan, P. R., Rengel, Z., and Delhaize, E. (1999). Phosphate uptake in Arabidopsis thaliana: dependence of uptake on the expression of transporter genes and internal phosphate concentrations. *Plant Cell Environ.* 22, 1455–1461. doi: 10.1046/j.1365-3040.1999.00500.x

Dragar, V. A., and Menary, R. C. (1995). Mineral nutrition of olearia phlogopappa: effect on growth, essential oil yield, and composition. *Commun. Soil Sci. Plant Anal.* 26, 1299–1313. doi: 10.1080/00103629509369372

Duèiæ, T., and Polle, A. (2005). Transport and detoxification of manganese and copper in plants. *Braz. J. Plant Physiol.* 17, 103–112. doi: 10.1590/S1677-04202005000100009

Engels, C., Kirkby, E., and White, P. (2012). "Mineral nutrition, yield and source – sink relationships," in *Marschner"s Mineral Nutrition of Higher Plants*, ed. P. Marschner (London: Academic Press), 85–134. doi: 10.1016/B978-0-12-384905-2.00005-4

Farzadfar, S., Zarinkamar, F., and Hojati, M. (2017). Magnesium and manganese affect photosynthesis, essential oil composition and phenolic compounds of *Tanacetum parthenium*. *Plant Physiol. Biochem.* 112, 207–217. doi: 10.1016/j.plaphy.2017.01.002

Fellermeier, M., Eisenreich, W., Bacher, A., and Zenk, M. H. (2001). Biosynthesis of cannabinoids: incorporation experiments with 13C-labeled glucoses. *Eur. J. Biochem.* 268, 1596–1604. doi: 10.1046/j.1432-1327.2001.02030.x

Flores-Sanches, J., and Verpoorte, R. (2008). Secondary metabolism in cannabis. *Phytochem. Rev.* 7, 615–639. doi: 10.1007/s11101-008-9094-4

Föhse, D., Claassen, N., and Jungk, A. (1988). Phosphorus efficiency of plants. *Plant Soil* 110, 101–109. doi: 10.1007/BF02143545

Fredeen, A. L., Raab, T. K., Rao, I. M., and Terry, N. (1990). Effects of phosphorus nutrition on photosynthesis in Glycine max (L.) Merr. *Planta* 181, 399–405. doi: 10.1007/BF00195894

Frydenvang, J., van Maarschalkerweerd, M., Carstensen, A., Mundus, S., Schmidt, S. B., Pedas, P. R., et al. (2015). Sensitive detection of phosphorus deficiency in plants using chlorophyll a fluorescence. *Plant Physiol.* 169, 353–361. doi: 10.1104/pp.15.00823

Gauvin, D. V., Zimmermann, Z. J., Yoder, J., and Tapp, R. (2018). Marijuana toxicity: heavy metal exposure through state-sponsored access to "la Fee Verte". *Pharm. Regul. Aff. Open Access* 7, 1–10. doi: 10.4172/2167-7689.1000202

George, E., Horst, W. J., and Neumann, E. (2012). "Adaptation of plants to adverse chemical soil conditions," in *Marschner"s Mineral Nutrition of Higher Plants*, ed. P. Marschner (Cambridge: Academic Press). doi: 10.1016/B978-0-12-384905-2.00017-0

Gonçalves, J., Rosado, T., Soares, S., Simão, A., Caramelo, D., Luís, Â, et al. (2019). Cannabis and its secondary metabolites: their use as therapeutic drugs, toxicological aspects, and analytical determination. *Medicines* 6:31. doi: 10.3390/medicines6010031

Gorelick, J., and Bernstein, N. (2014). Elicitation: an underutilized tool in the development of medicinal plants as a source of therapeutic secondary metabolites. *Adv. Agronomy* 124, 201–230. doi: 10.1016/B978-0-12-800138-7.00005-X

Gorelick, J., and Bernstein, N. (2017). "Chemical and physical elicitation for enhanced cannabinoid production in cannabis," in *Cannabis sativa L. - Botany and Biotechnology*, eds S. Chandra, H. Lata, and M. ElSohly (Cham: Springer). doi: 10.1007/978-3-319-54564-6_21

Gourley, C. J. P., Allan, D. L., and Russelle, M. P. (1993). Defining phosphorus efficiency in plants. *Plant Soil* 155, 289–292. doi: 10.1007/BF00025039

Goyal, D., Yadav, A., Prasad, M., Singh, T. B., Shrivastav, P., Ali, A., et al. (2020). "Effect of heavy metals on plant growth: an overview," in *Contaminants in Agriculture*, eds G. S. Naeem and A. Ansari (Cham: Springer). doi: 10.1007/978-3-030-41552-5_4

Grabau, L. J., Blevins, D. G., and Minor, H. C. (1986). P nutrition during seed development: leaf senescence, pod retention, and seed weight of soybean. *Plant Physiol.* 82, 1008–1012. doi: 10.1104/pp.82.4.1008

Gülck, T., and Møller, B. L. (2020). Phytocannabinoids: origins and biosynthesis. *Trends Plant Sci.* 25, 985–1004. doi: 10.1016/j.tplants.2020.05.005

Hawkesford, M., Horst, W., Kichey, T., Lambers, H., Schjoerring, J., Skrumsager, I., et al. (2012). "Functions of macronutrients," in *Marschner"s Mineral Nutrition of Higher Plants*, ed. P. Marschner (London: Academic Press). doi: 10.1016/B978-0-12-384905-2.00006-6

Hocking, P. J., and Pate, J. S. (1978). Accumulation and distribution of mineral elements in the annual lupins *Lupinus albus* L. and *Lupinus angustifolius* L. *Aust. J. Agric. Res.* 29, 267–280. doi: 10.1071/AR9780267

Ichimura, M., Ikushima, M., Miyazaki, T., and Kiruma, M. (1995). Effect of phosphorus on growth and concentration of mineral elements ans essensial oils of sweet basil leaves. *Hydroponics Transpl. Prod.* 396, 195–202. doi: 10.17660/ActaHortic.1995.396.23

Iványi, I., and Izsáki, Z. (2009). Effect of nitrogen, phosphorus, and potassium fertilization on nutrional status of fiber hemp. *Commun. Soil Sci. Plant Anal.* 40, 974–986. doi: 10.1080/00103620802693466

Jalali, S., Salami, A. S., Sharifi, M., and Sohrabi, S. (2019). Signaling compounds elicit expression of key genes in cannabinoid pathway and related metabolites in cannabis. *Ind. Crops Prod.* 133, 105–110. doi: 10.1016/j.indcrop.2019.03.004

Kirkby, E. (2012). "Introduction,definition and classification of nutrients," in *Marschner"s Mineral Nutrition of Higher Plants*, ed. P. Marschner (London: Academic Press). doi: 10.1016/B978-0-12-384905-2.00001-7

Lichtenthaler, K., and Welburn, A. R. (1983). Determination of total carotenoids and chlorophylls A and B of leaf extracts in different solvents. *Biochem. Soc. Trans.* 11, 591–592. doi: 10.1042/bst0110591

Liu, T. Y., Huang, T. K., Yang, S. Y., Hong, Y. T., Huang, S. M., Wang, F. N., et al. (2016). Identification of plant vacuolar transporters mediating phosphate storage. *Nat. Commun.* 7:11095. doi: 10.1038/ncomms11095

Loneragan, J. F. (1988). "Distribution and movement of manganese in plants," in *Manganese in Soils and Plants. Developments in Plant and Soil Sciences*, eds R. D. Graham, R. D. Hannam, and N. C. Uren (Dordrecht: Springer).

Magagnini, G., Grassi, G., and Kotiranta, S. (2018). The effect of light spectrum on the morphology and cannabinoid content of *Cannabis sativa* L. *Med. Cannabis Cannabinoids* 1, 19–27. doi: 10.1159/000489030

Malfait, A. M., Gallily, R., Sumariwalla, P. F., Malik, A. S., Andreakos, E., Mechoulam, R., et al. (2000). The nonpsychoactive cannabis constituent cannabidiol is an oral anti-arthritic therapeutic in murine collagen-induced arthritis. *Proc. Natl. Acad. Sci.* 97, 9561–9566. doi: 10.1073/pnas.160105897

Malik, R. N., Husain, S. Z., and Nazir, I. (2010). Heavy metal contamination and accumulation in soil and wild plant species from industrial area of Islamabad. *Pakistan. Pakistan J. Bot.* 42, 291–301.

Milay, L., Berman, P., Shapira, A., Guberman, O., and Meiri, D. (2020). Metabolic profiling of Cannabis secondary metabolites for evaluation of optimal postharvest storage conditions. *Front. Plant Sci.* 11:583605. doi: 10.3389/fpls.2020.583605

Mimura, T. (1999). "Regulation of phosphate transport and homeostasis in plant cells," in *International Review of Cytology*, ed. K. W. Jeon (Cambridge: Academic Press). doi: 10.1016/S0074-7696(08)60159-X

Neocleous, D., and Savvas, D. (2019). The effects of phosphorus supply limitation on photosynthesis, biomass production, nutritional quality, and mineral nutrition in lettuce grown in a recirculating nutrient solution. *Sci. Hortic.* 252, 379–387. doi: 10.1016/j.scienta.2019.04.007

Nie, B., Henion, J., and Ryona, I. (2019). The role of mass spectrometry in the cannabis industry. *J. Am. Soc. Mass Spectrom.* 30, 719–730. doi: 10.1007/s13361-019-02164-z

Nussaume, L., Kanno, S., Javot, H., Marin, E., Pochon, N., Ayadi, A., et al. (2011). Phosphate import in plants: focus on the PHT1 transporters. *Front. Plant Sci.* 2:83. doi: 10.3389/fpls.2011.00083

Ozturk, L., Eker, S., Torun, B., and Cakmak, I. (2005). Variation in phosphorus efficiency among 73 bread and durum wheat genotypes grown in a phosphorus-deficient calcareous soil. *Plant Soil* 269, 69–80. doi: 10.1007/s11104-004-0469-z

Pant, B. D., Pant, P., Erban, A., Huhman, D., Kopka, J., and Scheible, W. R. (2015). Identification of primary and secondary metabolites with phosphorus status-dependent abundance in Arabidopsis, and of the transcription factor PHR1 as a major regulator of metabolic changes during phosphorus limitation. *Plant Cell Environ.* 38, 172–187. doi: 10.1111/pce.12378

Polechońska, M., Zawadzki, K., Samecka-Cymerman, A., Kolon, K., Klink, A., Krawczyk, J., et al. (2013). Evaluation of the bioindicator suitability of polygonum aviculare in urban areas. *Ecol. Indic.* 24, 552–556. doi: 10.1016/j.ecolind.2012.08.012

Ramakrishna, A., and Ravishankar, G. A. (2011). Influence of abiotic stress signals on secondary metabolites in plants. *Plant Signal. Behav.* 6, 1720–1731. doi: 10.4161/psb.6.11.17613

Ranaweera, S. S., and Thilakaratne, W. P. (1992). Mineral nutrition of *Cymbopogon nardus* (L) rendle: part II. effects of magnesium and phosphorus nutrition on the fractional composition of essential oil. *Vidyodaya J. Sci.* 4, 209–219. doi: 10.4038/vjs.v4i1.6081

Ranaweera, S. S., Thilakaratne, W. P., and Thilakaratne, W. P. (1992). Mineral nutrition of *Cymbopogon nardus* (L) rendle: part I. effects of magnesium and phosphorus nutrition on growth and the yield of essential oil. *Vidyodaya J. Sci.* 4, 201–208. doi: 10.4038/vjs.v4i1.6080

Rioba, N. B., Itulya, F. M., Saidi, M., Dudai, N., and Bernstein, N. (2015). Effects of nitrogen, phosphorus and irrigation frequency on essential oil content and composition of sage (*Salvia officinalis* L.). *J. Appl. Res. Med. Aromat. Plants* 2, 21–29. doi: 10.1016/j.jarmap.2015.01.003

Rose, T. J., Pariasca-Tanaka, J., Rose, M. T., Fukuta, Y., and Wissuwa, M. (2010). Genotypic variation in grain phosphorus concentration, and opportunities to improve P-use efficiency in rice. *Field Crops Res.* 119, 154–160. doi: 10.1016/j.fcr.2010.07.004

Rose, T. J., Rengel, Z., Ma, Q., and Bowden, J. W. (2007). Differential accumulation patterns of phosphorus and potassium by canola cultivars compared to wheat. *J. Plant Nutr. Soil Sci.* 170, 404–411. doi: 10.1002/jpln.200625163

Rose, T. J., Rengel, Z., Ma, Q., and Bowden, J. W. (2008). Post-flowering supply of P, but not K, is required for maximum canola seed yields. *Eur. J. Agron.* 28, 371–379. doi: 10.1016/j.eja.2007.11.003

Russo, E. B. (2011). Taming THC: potential cannabis synergy and phytocannabinoid-terpenoid entourage effects. *Br. J. Pharmacol.* 163, 1344–1364. doi: 10.1111/j.1476-5381.2011.01238.x

Said-Al Ahl, H. A. H., and Abdou, M. A. A. (2009). Impact of water stress and phosphorus fertilizer on fresh herb and essential oil content of dragonhead. *Int. Agrophys.* 23, 403–407.

Saloner, A., and Bernstein, N. (2020). Response of medical cannabis (*Cannabis sativa* L.) to nitrogen supply under long photoperiod. *Front. Plant Sci.* 11:572293. doi: 10.3389/fpls.2020.572293

Saloner, A., and Bernstein, N. (2021). Nitrogen supply affects cannabinoid and terpenoid profile in medical cannabis (*Cannabis sativa* L.). *Ind. Crop. Prod.* 167:113516. doi: 10.1016/j.indcrop.2021.113516

Saloner, A., Sacks, M. M., and Bernstein, N. (2019). Response of medical cannabis (*Cannabis sativa* L .) genotypes to K supply under long photoperiod. *Front. Plant Sci.* 10:1369. doi: 10.3389/fpls.2019.01369

Sarma, N. D., Waye, A., Elsohly, M. A., Brown, P. N., Elzinga, S., Johnson, H. E., et al. (2020). Cannabis inflorescence for medical purposes: USP considerations for quality attributes. *J. Nat. Prod.* 83, 1334–1351. doi: 10.1021/acs.jnatprod.9b01200

Shane, M. W., McCully, M. E., and Lambers, H. (2004). Tissue and cellular phosphorus storage during development of phosphorus toxicity in *Hakea prostrata* (Proteaceae). *J. Exp. Bot.* 55, 1033–1044. doi: 10.1093/jxb/erh111

Shen, J., Yuan, L., Zhang, J., Li, H., Bai, Z., Chen, X., et al. (2011). Phosphorus dynamics: from soil to plant. *Plant Physiol.* 156, 997–1005. doi: 10.1104/pp.111.175232

Shiponi, S., and Bernstein, N. (2021). Response of medical cannabis (*Cannabis sativa* L.) genotypes to P supply under long photoperiod: functional phenotyping and the ionome. *Ind. Crops Prod.* 161:113154. doi: 10.1016/j.indcrop.2020.113154

Small, E. (2018). Dwarf germplasm: the key to giant Cannabis hempseed and cannabinoid crops. *Genet. Resour. Crop Evol.* 65, 1071–1107. doi: 10.1007/s10722-017-0597-y

Snapp, S. S., and Lynch, J. P. (1996). Phosphorus distribution and remobilization in bean plants as influenced by phosphorus nutrition. *Crop Sci.* 36, 929–935. doi: 10.2135/cropsci1996.0011183X003600040019x

Soltangheisi, A., Fauziah Ishak, C., Mohamed Musa, H., Zakikhani, H., and Abdul Rahman, Z. (2013). Phosphorus and zinc uptake and their interaction effect on dry matter and chlorophyll content of sweet com (Zea mays var. saccharata). *J. Agron.* 12, 187–192. doi: 10.3923/ja.2013.187.192

Taliman, N. A., Dong, Q., Echigo, K., Raboy, V., and Seneoka, H. (2019). Effect of phosphorus fertilization on the growth, photosynthesis, nitrogen fixation, mineral accumulation, seed yield, and seed quality of a soybean low-phytate line. *Plants* 8:119. doi: 10.3390/plants8050119

Tang, Y., Wen, X., and Lu, C. (2005). Differential changes in degradation of chlorophyll-protein complexes of photosystem I and photosystem II during flag leaf senescence of rice. *Plant Physiol. Biochem.* 43, 193–201. doi: 10.1016/j.plaphy.2004.12.009

Turner, J. C., Hemphill, J. K., and Mahlberg, P. G. (1978). Quantitative determination of cannabinoids in individual glandular trichomes of *Cannabis Sativa* L. (Cannabaceae). *Am. J. Bot.* 65, 1103–1106. doi: 10.1002/j.1537-2197.1978.tb06177.x

Veneklaas, E. J., Lambers, H., Bragg, J., Finnegan, P. M., Lovelock, C. E., Plaxton, W. C., et al. (2012). Opportunities for improving phosphorus-use efficiency in crop plants. *New Phytol.* 195, 306–320. doi: 10.1111/j.1469-8137.2012.04190.x

Vera, C. L., Malhi, S. S., Phelps, S. M., May, W. E., and Johnson, E. N. (2010). N, P, and S fertilization effects on industrial hemp in Saskatchewan. *Can. J. Plant Sci.* 90, 179–184. doi: 10.4141/CJPS09101

Vera, C. L., Malhi, S. S., Raney, J. P., and Wang, Z. H. (2004). The effect of N and P fertilization on growth, seed yield and quality of industrial hemp in the Parkland region of Saskatchewan. *Can. J. Plant Sci.* 84, 939–947. doi: 10.4141/P04-022

Verpoorte, R., Contin, A., and Memelink, J. (2002). Biotechnology for the production of plant secondary metabolites. *Phytochem. Rev.* 1, 13–25. doi: 10.1023/A:1015871916833

Wang, J., Chen, Y., Wang, P., Li, Y. S., Wang, G., Liu, P., et al. (2018). Leaf gas exchange, phosphorus uptake, growth and yield responses of cotton cultivars to different phosphorus rates. *Photosynthetica* 56, 1414–1421. doi: 10.1007/s11099-018-0845-1

Wang, X., Shen, J., and Liao, H. (2010a). Acquisition or utilization, which is more critical for enhancing phosphorus efficiency in modern crops? *Plant Sci.* 179, 302–306. doi: 10.1016/j.plantsci.2010.06.007

Wang, X., Yan, X., and Liao, H. (2010b). Genetic improvement for phosphorus efficiency in soybean: a radical approach. *Ann. Bot.* 106, 215–222. doi: 10.1093/aob/mcq029

White, P. J. (2012). "Ion uptake mechanisms of individual cells and roots: short-distance transport," in *Marschner"s Mineral Nutrition of Higher Plants*, ed. P. Marschner (London: Academic Press).

White, P. J., and Hammond, J. P. (2008). "Phosphorus nutrition of terrestrial plants," in *The Ecophysiology of Plant-Phosphorus Interactions*, eds P. J. White and J. P. Hammond (Dordrecht: Springer). doi: 10.1007/978-1-4020-8435-5

Wiesler, F. (2012). *Nutrition and Quality*, 3rd Edn. Cambridge: Academic Press. doi: 10.1016/B978-0-12-384905-2.00009-1

Wu, P., Shou, H., Xu, G., and Lian, X. (2013). Improvement of phosphorus efficiency in rice on the basis of understanding phosphate signaling and homeostasis. *Curr. Opin. Plant Biol.* 16, 205–212. doi: 10.1016/j.pbi.2013.03.002

Xue, S. G., Chen, Y. X., Reeves, R. D., Baker, A. J. M., Lin, Q., and Fernando, D. (2004). Manganese uptake and accumulation by the hyperaccumulator plant *Phytolacca acinosa* Roxb . (Phytolaccaceae). *Environ. Pollut.* 131, 393–399. doi: 10.1016/j.envpol.2004.03.011

Yep, B., Gale, N. V., and Zheng, Y. (2020). Aquaponic and hydroponic solutions modulate NaCl-induced stress in drug-type *Cannabis sativa* L. *Front. Plant Sci.* 11:1169. doi: 10.3389/fpls.2020.01169

Zhang, W., Li, X., Chen, F., and Lu, J. (2012). Accumulation and distribution characteristics for nitrogen, phosphorus and potassium in different cultivars of *Petunia hybrida* Vlim. *Sci. Hortic.* 141, 83–90. doi: 10.1016/j.scienta.2012.04.010

Zhao, J., Davis, L. C., and Verpoorte, R. (2005). Elicitor signal transduction leading to production of plant secondary metabolites. *Biotechnol. Adv.* 23, 283–333. doi: 10.1016/j.biotechadv.2005.01.003

Zuardi, A. W. (2006). History of cannabis as a medicine: a review. *Rev. Bras. Psiquiatr.* 28, 153–157. doi: 10.1590/S1516-44462006000200015

Conflict of Interest: The authors declare that the research was conducted in the absence of any commercial or financial relationships that could be construed as a potential conflict of interest.

frontiers in Plant Science

ORIGINAL RESEARCH
published: 02 August 2021
doi: 10.3389/fpls.2021.694153

Photoperiodic Flowering Response of Essential Oil, Grain, and Fiber Hemp (*Cannabis sativa* L.) Cultivars

Mengzi Zhang[1], *Steven L. Anderson*[1], *Zachary T. Brym*[2] *and Brian J. Pearson*[1]*

[1] *Department of Environmental Horticulture, Institute of Food and Agricultural Sciences, Mid-Florida Research and Education Center, University of Florida, Apopka, FL, United States,* [2] *Department of Agronomy, Institute of Food and Agricultural Sciences, Tropical Research and Education Center, University of Florida, Homestead, FL, United States*

Cultivation of hemp (*Cannabis sativa* L.) in tropical and subtropical regions can be challenging if the flowering behavior of a given cultivar is unknown, poorly understood, or not accurately selected for the photoperiod. Identifying cultivars adapted to local environmental conditions is key to optimizing hemp vegetative and flowering performance. We investigated the effects of varying light cycles in regulating extension growth and flowering response of 15 essential oil and 12 fiber/grain hemp cultivars both indoors and outdoors. Plants were subjected to 11 photoperiods in the controlled rooms ranging from 12 to 18 h, and natural day length in the field. The critical photoperiod threshold was identified for seven essential oil cultivars and two fiber/grain cultivars. "Cherry Wine-CC," "PUMA-3," and "PUMA-4" had the shortest critical day length between 13 h 45 min and 14 h. The flowering of essential oil cultivars was generally delayed by 1–2 days when the photoperiod exceeded 13 h compared with 12 h, and flowering was further delayed by 7–8 days when the photoperiod exceeded 14 h. In fiber/grain cultivars, flowering was generally delayed by 1–3 days when the day length exceeded 14 h. Flowering for most essential oil cultivars was delayed by 5–13 days under a 14-h photoperiod compared with 13 h 45 min, suggesting a photoperiod difference as little as 15 min can significantly influence the floral initiation of some essential oil cultivars. Cultivars represented by the same name but acquired from different sources can perform differently under the same environmental conditions, suggesting genetic variation among cultivars with the same name. Average days to flower of fiber/grain cultivars was correlated with reported cultivar origin, with faster flowering occurring among northern cultivars when compared with southern cultivars. Plant height generally increased as the day length increased in essential oil cultivars but was not affected in fiber/grain cultivars. In addition, civil twilight of ~2 $\mu mol \cdot m^{-2} \cdot s^{-1}$ was discovered to be biologically effective in regulating hemp flowering. Collectively, we conclude that most of the essential oil cultivars and some southern fiber/grain cultivars tested express suitable photoperiods for tropical and sub-tropical region cultivation.

Keywords: critical photoperiod, twilight, subtropical, cultivar, extension growth, genetic variation, origin, sex

OPEN ACCESS

Edited by:
Derek Stewart,
The James Hutton Institute,
United Kingdom

Reviewed by:
Gerhard Buck-Sorlin,
Agrocampus Ouest, France
Izabela Michalak,
Wrocław University of Science and Technology, Poland

***Correspondence:**
Brian J. Pearson
bpearson@ufl.edu

Specialty section:
This article was submitted to Crop and Product Physiology, a section of the journal Frontiers in Plant Science

Received: *12 April 2021*
Accepted: *28 June 2021*
Published: *02 August 2021*

Citation:
Zhang M, Anderson SL, Brym ZT and Pearson BJ (2021) Photoperiodic Flowering Response of Essential Oil, Grain, and Fiber Hemp (Cannabis sativa L.) Cultivars. Front. Plant Sci. 12:694153. doi: 10.3389/fpls.2021.694153

INTRODUCTION

Cultivation of hemp (*Cannabis sativa* L.) within the USA was restricted in 1937 following the passage of the Marihuana Tax Act. Similarly, hemp cultivation was prohibited throughout the western world during most of the twentieth century (Cherney and Small, 2016; Congressional Research Service, 2019). With the legal status of *Cannabis* production shifting in the USA following the passage of the 2014 and 2018 farm bills (Agricultural Act of 2014, P.L. 113-79; Agriculture Improvement Act of 2018, P.L. 115-334), restrictions on hemp production were relaxed and interest in hemp cultivation thereafter rapidly increased. Within the USA, the classification of *Cannabis* is based upon the concentration of Δ9-tetrahydrocannabinol (THC) present in plant tissue. Plants with a concentration of $\leq$ 0.3% THC on a dry weight basis are legally recognized as industrial hemp, whereas plants containing >0.3% are recognized as marijuana, a Schedule I drug as defined by the Controlled Substances Act of 1967 (Congressional Research Service, 2019). Industrial hemp is commercially cultivated for its fiber, seed, and secondary metabolites [such as cannabidiol (CBD) and cannabigerol (CBG)]. Hemp is used to produce a wide variety of industrial and consumer products including food and beverages, personal care products, nutritional supplements, therapeutic products, fabrics and paper, and construction materials (Congressional Research Service, 2019). In 2016, the global fiber hemp market was valued at nearly $700 million with an expected growth rate of 10–20%, whereas the hemp-derived CBD market in 2022 is expected to be more than 2-fold greater than it was in 2018 to become a $1.3 billion-dollar market (Hemp Business Journal, 2018; Anderson et al., 2019).

Hemp fiber quality can be largely influenced by flowering time, sex characteristics, and other environmental factors independent of heritable genetic variation (Petit et al., 2020). "Technical maturity" for fiber production of monoecious hemp is reached at peak flowering of male plants (Mediavilla et al., 2001). At the onset of flowering, the nutrient flow is shifted from the development of stem and leaves to flower and seeds (Salentijn et al., 2019). High primary bast fiber content with a low secondary bast fiber content in fiber hemp is considered advantageous for textile production. However, the primary bast fiber layer experiences a proportional decrease during the flowering stage, whereas the secondary bast fiber fraction increase along the stems (Mediavilla et al., 2001; Salentijn et al., 2019). Harvest after the flowering of the male hemp plant will result in fiber loss and reduction of fiber fineness (Keller et al., 2001). Thus, precise prediction of flowering time is essential for determining fiber hemp harvest time and maximizing fiber quality. On the other hand, hemp is naturally dioecious (male and female flowers on separate plants) with monoecious (male and female flowers on the same plant) cultivars existing. Male plants in dioecious genotypes have a finer fiber and superior for textile production, whereas monoecious genotypes are more uniform in plant height and better for the dual harvest of fiber and seed (Salentijn et al., 2019). Understanding the sex composition of fiber/grain hemp cultivars is beneficial for breeding purposes and is critical for selecting the ideal cultivar for a specific production purpose.

Hemp can be challenging to cultivate in tropical and subtropical regions, given high temperatures, high humidity, and ample presence of disease and pests. However, relatively short daylengths experienced in tropical and subtropical environments arguably present the greatest challenge to the successful cultivation of hemp at lower latitudes. Hemp is considered an annual, dioecious, short-day plant (SDP) originating from temperate regions of Central Asia. Most hemp varieties are photoperiodic, and thus flowering of hemp is dependent upon day length or photoperiod. *Cannabis* has adapted to a wide range of climates and latitudes (23–52°N) and thus can possess large variability in its sensitivity to day length (Zhang et al., 2018). Timing of transition from vegetative growth to flowering is key for high yield and acceptable fiber quality of hemp (Amaducci et al., 2012). Earlier seasonal planting under critical daylength can extend the vegetative growth period before late-summer flowering, which is expected to occur generally 4–5 weeks after the summer solstice in the northern hemisphere, dependent upon hemp variety and latitude (Cherney and Small, 2016; Anderson et al., 2019). Relatively short day length experienced in tropical and subtropical regions result in reduced vegetative growth and early seasonal transition to flowering that ultimately limits stem elongation and fiber biomass yield, key factors for successful commercial cultivation of industrial hemp (Cosentino et al., 2012; Hall et al., 2014). Thus, genotypes of hemp adapted to higher latitudes would be expected to perform poorly when cultivated in tropical and subtropical environments due to premature flowering and the negative influence it has on plant growth and yield (Amaducci et al., 2008; Cosentino et al., 2012; Hall et al., 2012).

Hemp expresses broad genetic diversity in hemp photoperiod requirements for vegetative-to-reproductive transition requirements, similar to that seen in other major crops (e.g., maize; Navarro et al., 2017). Identifying plant genotypes adapted to light conditions of a region is key to the successful cultivation of photoperiod crops, such as hemp (Jung and Müller, 2009; Cho et al., 2017). Zhang et al. (2018) discovered that *Cannabis* could be generally categorized in three northern hemispheric haplogroups distinguished by geographical location (north of 40°N, 30 to 40°N, and south of 30°N); however, a myriad of photoperiod responses can be observed when breeding among haplogroups. Hemp selected for fiber production is generally believed to be a quantitative SDP with a relatively long photoperiod, around 14 h (dependent upon the origin of the plant material). Excluding European varieties, the photoperiod response of most industrial hemp is poorly documented. "Kompolti" (Hungarian variety) and "Futura 77" (French variety) have an estimated maximal optimum photoperiod of 13.8 and 14 h, respectively (Heslop-Harrison and Heslop-Harrison, 1969). An estimated photoperiod of roughly 14 h was identified by Amaducci et al. (2008) for five European hemp cultivars as the most important single factor controlling flowering date. Flowering was increasingly delayed at longer photoperiods, but a 24-h photoperiod did

not prevent "Fedrina 74" (French variety) and "Kompolti Hybrid TC" (Hungarian variety) from flowering (Van der Werf et al., 1994; Lisson et al., 2000). A Portuguese fiber variety was reported to have a maximum optimal photoperiod of 9 h, although the critical photoperiod is somewhere between 20 and 24 h (Heslop-Harrison and Heslop-Harrison, 1972; Lisson et al., 2000). In contrast to European hemp, the flowering of Chilean and US Kentucky hemp varieties occurred promptly under a photoperiod of 14 h or fewer but was considerably delayed or failed to flower when photoperiod exceeded 16 h (Borthwick and Scully, 1954). A subtropical Australian variety, "BundyGem," had a critical photoperiod between 13 h 40 min and 14 h 40 min, and plant maturity was significantly delayed when day length exceeded 14 h 40 min (Hall et al., 2014). A photoperiod of 11–12 h has been reported to induce flowering of Thai hemp (Sengloung et al., 2009). While most of the studies on hemp have been conducted in the field or greenhouses, plant responses to environmental factors in a more strictly controlled environment, such as growth chambers, are very limited.

Until recently, *Cannabis* plants grown for recreational use have largely been cultivated indoors using artificial lighting. Given that most of these cultivation operations were conducted before the legalization of marijuana and were thus illegal, critical photoperiods of these types of *Cannabis* plants are not documented in the literature, and information is limited. A day length of 12 and 18 h are common practices to induce flowering or keep plants vegetative, respectively (Potter, 2014). Moher et al. (2020) indicated that *C. sativa* "802," although not categorized as hemp given its 15–20% THC content, had a critical photoperiod between 15 and 16 h. Growth chamber environments are ideal for investigating the photoperiodism of hemp. With artificial lighting (typically from light-emitting diodes) being the only radiation source indoors, the photoperiod is strictly controlled by the hours of light operation. In tropical and subtropical regions, the vegetation of hemp under long days can be achieved in protected environments, such as greenhouses, by manipulating photoperiod utilizing end-of-day extension lighting and night interruption techniques that have been utilized in the production of other common SDPs (Lane et al., 1965; Vince-Prue and Canham, 1983; Runkle et al., 1998; Zhang and Runkle, 2019). However, since hemp is often cultivated outdoors to reduce production costs, it is imperative that it is germinated or transplanted at timing with respect to natural photoperiod. Prediction of flowering time in response to a specific, known photoperiod is thus critical to support successful production both outdoors and indoors and optimize select hemp varieties for a diverse range of growing regions. To directly address these needs, we investigated 15 cultivars of essential oil hemp, and 12 cultivars of fiber/grain hemp with seven growth rooms to (i) empirically define critical photoperiod thresholds to induce vegetative to floral transition in diverse hemp cultivars; (ii) compare critical photoperiod thresholds to flowering dates within a subtropical field environment; and (iii) quantify the physiological response of hemp cultivars under different photoperiod treatments.

MATERIALS AND METHODS

Expt. 1: Photoperiod Trial for Essential Oil Cultivars

Seedling Preparation and Vegetative Stage

Seeds, cuttings, or plants of all essential oil cultivars were obtained from three different sources (**Supplementary Table 1**). Cultivars were selected based on commercial interest and availability. Seeds of five essential oil cultivars, "Cherry Wine-BS," "Cherry Blossom-BS," "Cherry*T1-BS," "Berry Blossom-BS," and "Cherry Blossom-Tuan-BS," were sown in 72 round cell propagation sheets (DPS72, The HC Companies, Twinsburg, OH) within Pro-Mix soilless substrate (HP Mycorrhizae Pro-Mix; Premier Tech Horticulture Ltd., Quakertown, PA) containing 65–75% peat, 8–35% perlite, dolomite limestone, and mycorrhizae on November 19, 2019. Cuttings of the other 10 essential oil cultivars, "ACDC-AC," "Super CBD-AC," "Cherry-AC," "Wife-AC," "Cherry Blossom-BC," "JL Baux-CC," "ACDC-CC," "Cherry Wine-CC," "Cherry-CC," and "Wife-CC," were propagated on November 25, 2019. Each cultivar was propagated from identical mother stock plants to reduce potential genetic diversity among replicates. Stems of plant propagules were dipped into rooting hormone (Dip'N Grow; Dip'N Grow Inc., Clackamas, OR) containing 1,000 mg/L indole-3-butyric acid (IBA)/500 mg/L naphthaleneacetic acid (NAA) and then inserted into 3.8 cm Rockwool cubes (Grodan; ROXUL Inc., Milton, Canada) that were pre-soaked with water exhibiting a pH of 5.8 as per manufacturer recommendations. Both seeded trays and cuttings were grown at 25°C under 24-h photoperiod and were hand irrigated daily as needed.

After roots were well-established (∼21 days), the most uniform rooted propagules of each cultivar were selected and transplanted into 1.1 L containers (SVD-450, T.O. Plastics, Clearwater, MN) filled with Pro-Mix soilless substrate and top-dressed with 5 g of Osmocote Plus 15-9-12 5-6 month slow-release fertilizer (Everris NA, Inc.; Dublin, OH) containing 7% ammoniacal and 8% nitrate nitrogen, 9% phosphate and 12% soluble potash on December 17, 2019. Plants were randomly assigned to seven identical controlled rooms with 10 replicates per cultivar in each room and were cultivated at 25°C under a photoperiod of 18 h (0600–2400 HR) for vegetative growth. Plants were irrigated for 4 min every 5 days for the first 2 weeks and 4 min every 3 days thereafter as controlled by an automatic irrigation system.

Lighting Treatments During the Flowering Stage

After 3 weeks of vegetative growth following transplant, seven lighting treatments were randomly assigned to each controlled room on January 7, 2020. Ten plants of each hemp cultivar were grown at 25°C under the photoperiod of 12 h (0600–1800 HR), 12 h 30 min (0600–1830 HR), 13 h (0600–1900 HR), 13 h 30 min (0600–1930 HR), 13 h 45 min (0600–1945 HR), 14 h (0600–2000 HR), and 18 h (0600–2400 HR) provided by light-emitting diodes (LEDs) (VYPR 2p; Fluence Bioengineering, Inc., Austin, TX). Lighting treatments were maintained until the termination of the experiment 5 weeks following the vegetative growth period.

Environmental Conditions During Seedling, Vegetative, and Flowering Stage

Propagation of cuttings and germination of seeds was conducted indoors in an environmentally controlled propagation room at the Mid-Florida Research and Education Center (Apopka, FL). Air temperatures were maintained in all indoor grow rooms utilizing air conditioners set to 25°C. Air temperature and relative humidity data were collected by thermocouples installed at plant canopy height, and data was recorded using a wireless data logging station (HOBO RX3000; Onset Computer Corporation, Bourne, MA) every 10 min. The average temperature in the propagation room was 24.9 ± 0.04°C. Within the propagation room, a 24-h photoperiod was provided by fluorescent lamps (E-conolight; Sturtevant, WI) as sole-source lighting. The photosynthetic photon flux density (PPFD) on the propagation bench was measured by a quantum sensor (MQ-500; Apogee Instruments Inc., Logan, UT) at 10 representative positions at seedling canopy level. The average PPFD that cuttings and seedlings received was 53.9 ± 3.02 and 73.5 ± 3.61 $\mu mol \cdot m^{-2} \cdot s^{-1}$, respectively, with a daily light integral of ∼4.7 and 6.4 $mol \cdot m^{-2} \cdot d^{-1}$, respectively.

Following the transplant, all plants were cultivated in seven identical environmentally controlled rooms. Each room was equipped with two sole-source LEDs (VYPR 2p; Fluence Bioengineering, Inc., Austin, TX) regulated by a timer (Titan Controls Apollo 8; Hawthorne Gardening Company, Vancouver, WA) to provide varying controlled photoperiod treatments. A PPFD of ∼300 and 330 $\mu mol \cdot m^{-2} \cdot s^{-1}$ was maintained at plant canopy height at the onset of the vegetative and flowering stages, respectively. Average temperature, relative humidity, and light intensity for vegetative and flowering stages for each lighting treatment are reported in **Supplementary Table 2**.

Plant Measurements and Data Collection

The flowering of female hemp plants is defined as the appearance of dual, fork-shaped stigmas protruding from tubular bracts (Hall et al., 2012) being visible at the apical meristem or decimal code of 2201 defined by Mediavilla et al. (1998). The flowering of male hemp plants is defined when five radial segments of the first pointed male bud open and start to release pollen (Hall et al., 2012) or decimal code of 2101 (Mediavilla et al., 1998). Plant height (from the substrate surface to the tallest meristem) was measured at the initiation of lighting treatments and flowering. Extension growth was calculated by subtracting initial plant height from height at flowering. Days to flower and plant sex were recorded when plants initiated flowering. Boolean evaluation of plant flowering status (flowering percentage) was conducted at the end of week 5 following the initiation of lighting treatments.

Experimental Design and Data Analysis

The experiment was conducted using a complete randomized design with seven lighting treatments and multiple replicates. Each plant was considered an experimental unit. Data were pooled from multiple replicates and were analyzed with a restricted maximum likelihood mixed model analysis in JMP® Pro 15 (SAS Institute, Inc., Cary, NC) with *post hoc* mean separation tests performed using Tukey's honest significant difference test at $P \leq 0.05$. Normality of the residuals was evaluated with QQ-plots and the Anderson-Darling A2 statistic goodness of fit test in JMP. Homogenous variances were tested using Levene's test.

Expt. 2: Photoperiod Trial for Fiber and Grain Cultivars

Seedling Preparation and Vegetative Stage

Twelve fiber/grain hemp cultivars from seven different source origins were purchased, including Canada cultivars— "CFX-1" and "Joey;" Poland cultivar— "Tygra"; Serbia cultivar— "Helena"; Italy cultivars— "Carmagnola Selezionata," "Fibranova," and "Eletta Campana"; North China cultivar— "HAN-FN-H;" Central China cultivars— "HAN-NE" and "HAN-NW"; and South China cultivars— "PUMA-3" and "PUMA-4." Seeds were sown in 72 round cell propagation sheets (DPS72, The HC Companies, Twinsburg, OH) filled with Pro-Mix HP soilless substrate on February 18, 2020. They were placed under a mist bench in a greenhouse and grown at 25°C under natural daylight supplemented with 1,000 W metal halide lighting to maintain an 18-h photoperiod. Seedlings were misted for 1 min at 8 a.m., 12 p.m., and 5 p.m. each day.

Seedlings possessing the most uniform height were selected three weeks after germination when roots were well-established and transplanted into 1.1 L containers, as described above, with Fafard 4P potting media (Sun Gro Horticulture Canada Ltd., Agawam, MA) containing 48% peat, 30% pine bark, 10% perlite, and 12% vermiculite, top-dressed with 5 g of Osmocote Plus slow-release fertilizer as described above. Plants were randomly assigned to seven identical environmentally controlled rooms with 10 replicates for "CFX-1," "Tygra," "Helena," "Eletta Campana," "HAN-FN-H," and "HAN-NE"; 9 replicates for "PUMA-3;" 7 replicates for "Joey" and "Fibranova;" 6 replicates for "PUMA-4"; and 4 replicates for "Carmagnola Selezionata" and "HAN-NW" due to poor germination rates. Plants were grown at 25°C under an 18-h photoperiod (0600–2400 HR) for vegetative growth until the initiation of photoperiod treatments.

Lighting Treatments During the Flowering Stage

Seven lighting treatments were randomly assigned to each controlled room after 2 weeks of plant vegetative growth on March 23, 2020. Twelve fiber/grain hemp cultivars were subjected to seven photoperiod treatments: 12 h (0600–1800 HR), 13 h 30 min (0600–1930 HR), 13 h 45 min (0600–1945 HR), 14 h (0600–2000 HR), 14 h 30 min (0600–2030 HR), 14 h 45 min (0600 HR−2045 HR), and 18 h (0600–2400 HR) provided by LEDs. Treatments were selected based on the common photoperiod range of fiber/grain cultivars documented in the literature and the expected photoperiod of tropical and subtropical regions. Lighting treatments were maintained for 5 weeks before the termination of the experiment.

Environmental Conditions During Seedling, Vegetative, and Flowering Stage

Germination of seedlings was conducted in a research greenhouse under a mist bench. Greenhouse heaters and fans were controlled by an environmental control system

(Wadsworth Control System, Arvada, CO) and operated when greenhouse temperature was $\leq$ 16°C or $\geq$ 24°C, respectively. Seedlings were misted for a duration of 1 min three times per day utilizing a programmable irrigation controller (Sterling 12; Superior Controls Co., Inc., Valencia, CA) and subjected to an 18-h photoperiod (from 0700 HR to 0100 HR) with 11 h of ambient solar radiation (from 0700 HR to 1800 HR) and 8 h of supplemental metal halide 7,500°K lamps (UltraSun 1,000 W; Hawthorne Hydroponics LLC., Vancouver, WA) that operated from 1700 HR to 0100 HR. Greenhouse environmental conditions were recorded every 15 min by a weather station data logger (WatchDog 2475; Spectrum Technologies, Inc., Aurora, IL). Average air temperature, relative humidity, photosynthetic active radiation, and daily light integral was 24.0 ± 0.08°C, 60.1 ± 0.45%, 261.6 ± 5.07 $\mu mol \cdot m^{-2} \cdot s^{-1}$, and 22.6 ± 0.44 $mol \cdot m^{-2} \cdot d^{-1}$, respectively.

After transplant in 1.1 L containers, all plants were cultivated in seven identical environmentally controlled rooms, as described previously. Average air temperature, relative humidity, and light intensity for the vegetative stage and flowering stage for each lighting treatment were also reported in **Supplementary Table 2**.

Plant Measurements and Data Collection

Plant height, recorded from the substrate surface to the tallest meristem, was measured at the initiation of lighting treatments and at flowering. Days to flower and plant sex were recorded when plants started to flower, as defined previously. The flowering of monoecious plants was defined when a female or male flowering occurred as defined previously or by decimal code of 2301 and 2304, respectively (Mediavilla et al., 1998). Boolean evaluation of plant flowering status (flowering percentage) was conducted at the end of week 5 after the initiation of the lighting treatments. Experimental design and data analysis were conducted as described for Expt. 1.

Expt. 3: Expanded Photoperiod Trial for Selected Essential Oil and Fiber/Grain Cultivars

Based on results of Expts. 1 and 2, an expanded photoperiod trial was designed with select essential oil, fiber, and grain cultivars to better understand the effect of photoperiodism on a broader scale.

Seedling Preparation and Vegetative Stage

Six fiber/grain hemp cultivars, "Carmagnola Selezionata," "Helena," "Eletta Campana," "HAN-FN-H," "PUMA-3," and "PUMA-4," were propagated as described in Expt. 2 on May 24, 2020. Cuttings of 10 essential oil cultivars, "ACDC-AC," "Super CBD-AC," "Cherry-AC," "Cherry Blossom-BC," "Cherry Wine-BS," "Cherry Blossom-BS," "Cherry*T1-BS," "JL Baux-CC," "ACDC-CC," and "Cherry-CC," were propagated as described in Expt. 1 on June 18, 2020. Both cuttings and seeded trays were placed under a mist bench that misted 8 s every 20 min in a greenhouse and grown at 25°C under natural daylight with supplemental metal halide lamps as described in Expt. 2 maintaining an 18-h photoperiod. Plants grew vegetatively under the mist bench in the greenhouse for 3–4 weeks before being transplanted into 1.1 L containers and assigned to lighting treatments.

Seedlings or clones of the 10 essential oil cultivars were thinned and transplanted as described in Expt. 2 with Pro-Mix HP soilless substrate on June 18, 2020, for fiber cultivars, and July 11, 2020, for essential oil cultivars. Slow-release fertilizer was applied as described in Expt. 1. All plants were cultivated for vegetative growth for 7 days and then randomly assigned to identical environmentally controlled rooms under different lighting treatments with five replicates per cultivar.

Lighting Treatments During the Flowering Stage

Six lighting treatments were randomly assigned to each controlled room as proposed: 12 h 30 min (0600–1830 HR), 13 h (0600–1900 HR), 14 h 30 min (0600–2030 HR), 14 h 45 min (0600–2045 HR), 15 h (0600–2100 HR), and 15 h 30 min (0600–2130 HR). Different photoperiods were provided by LEDs as described previously. Photoperiod lighting treatments were maintained for 5 weeks before the termination of the experiment. Ten essential oil cultivars were selected based on the results from Expt. 1 and were evaluated from 14 h 30 min to 15 h 30 min.

A Boolean evaluation of flowering status (flowering percentage) was conducted as described previously. Environmental conditions of the greenhouse during the vegetative stage were as described in Expt. 2, and the environmental conditions of the controlled rooms during the flowering stage were as described in Expt. 1 and provided in **Supplementary Table 2**. Experimental design and data analysis were conducted as described for Expt. 1.

Expt. 4: Flowering Time Trial Under Natural Daylengths Within a Field-Grown Subtropical Central Florida Environment

Seedling Preparation and Vegetative Stage

Fourteen essential oil and 12 fiber/grain cultivars were evaluated for flowering response time under natural daylength, field-grown conditions following seedling establishment of fiber/grain cultivars and rooting of clonally propagated essential oil cultivars. Fiber/grain seeds were sown in 72-cell trays within Pro-Mix HP soilless substrate on April 30, 2020, and propagated as described in Expt. 2. Seedlings were watered daily by hand as needed. Fourteen essential oil cultivars were clonally propagated as described in Expt. 2 on May 1, 2020. Rooted plants were transplanted into the field on June 3, 2020.

Field Trial Set Up

The field trial was designed using plasticulture production techniques with Chapin Turbulent Flow-Deluxe drip tape (Catalog # 11714142N, Jain Irrigation USA, Watertown, NY) placed below the plastic emitting 0.76 L h^{-1} per dripper at 68.9 kPa spaced 0.10 m between drippers. Plants were spaced 0.9 m apart within rows, and rows were spaced 1.5 m apart between row centers. Total plot lengths were 3.7 m, including walking allies. The total trial area was 0.9 ha. Trials received 2 h of drip irrigation per day. A soluble fertilizer with micronutrients (Peter 20-20-20; ICL Specialty Fertilizers, Dorchester County, SC, USA) was

applied every 14 days at 8.8 kg N ha^{-1} for an accumulated rate of 48 kg N ha^{-1} (six applications total).

Experimental Design and Data Collection

The experiment was conducted using a complete randomized block design comprised of an essential oil trial and a fiber/grain trial. Both trials contain three replicates of each cultivar. Each plot/replicate within the trial consisted of three plants. Flowering time was measured as defined previously. During the civil twilight period (sun 6–0° below the horizon), light intensity was recorded every 2 min manually in an open field with a quantum sensor (MQ-500; Apogee Instruments Inc., Logan, UT) for 3 days. A restricted maximum likelihood mixed model analysis in JMP® Pro 15 (SAS Institute, Inc., Cary, NC) was performed to estimate genetic means of flowering time.

RESULTS AND DISCUSSIONS

Identifying Critical Photoperiod Thresholds

Critical photoperiod differed significantly among essential oil cultivars (**Table 1**). In addition, a significant effect was observed on flowering percentages of the essential oil cultivars. As expected, all essential oil cultivars in Expt. 1 flowered in response to 12-h photoperiod, and no plants flowered in response to 18 h (**Table 1**). One cultivar, "Cherry Wine-CC," was identified with a critical photoperiod below 14 h, with no flowers developed above 14 h. Four cultivars expressed 100% floral initiation at the longest photoperiod (14 h, excluding 18 h control), with an additional six cultivars that demonstrated a complete floral initiation (>50%) when cultivated under 14 h of light. For this reason, expanded photoperiod treatments of up to 15 h 30 min were evaluated for select essential oil cultivars (Expt. 3). Of the 10 essential oil cultivars evaluated within Expt. 3, five cultivars expressed a majority (>50%) of floral initiation between 15 h and 15 h 30 min. Four of them, including "Cherry-AC," "Cherry Blossom-BS," "ACDC-CC," and "Cherry-CC," have been identified with a critical photoperiod within this range. In addition, "Cherry Wine-CC" had the shortest, critical photoperiod identified between 13 h 45 min and 14 h. The critical photoperiod for "Super CBD-AC" and "Cherry Blossom-BC" occurred between 14 h 45 min and 15 h. For the rest of the cultivars, "ACDC-AC" had a significant flowering reduction when the photoperiod was extended from 15 h to 15 h 30 min. "Wife-AC" flowered significantly less under 13 h 30 min compared with 13 h, but the critical photoperiod is likely >14 h. Similarly, the percentage flowering of "Berry Blossom-BS," "Cherry Blossom-Tuan-BS," and "Wife-CC" decreased when photoperiod was increased from 13 h 45 min to 14 h. Our results suggest that a photoperiod difference of as little as 15 min could significantly influence floral initiation and development of some essential oil hemp cultivars. Moreover, floral initiation can occur at varying rates when the photoperiod is close to the critical threshold of some cultivars.

Less variation in critical photoperiod thresholds was observed for fiber/grain hemp than essential oil cultivars. Like essential oil cultivars, all fiber/grain cultivars flowered in response to a 12-h photoperiod (**Table 1**). For the majority of the fiber cultivars (8 of 12), plants did not flower under an 18-h photoperiod. "CFX-1," "Joey," "Tygra," and "Helena" flowered in response to a photoperiod of 18 h and did not remain vegetative like the majority of the other fiber hemp cultivars evaluated in this study, thus suggesting their critical photoperiod could be above 18 h. The critical photoperiod of PUMA 3 and 4 was identified between 13 h 45 min and 14 h, but the floral initiation was greatly reduced by more than 70% when day length exceeded 13 h. Similarly, the flowering of HAN-NE and HAN-NW was also greatly reduced when day length exceeded 14 h 30 min. To verify the critical photoperiod of "CFX-1," "Joey," "Tygra," and "Helena," seeds were germinated on February 18, 2020, and placed under a 24-h photoperiod in a greenhouse. All four cultivars flowered on April 20, 2020, under a 24-h photoperiod. This observation was consistent with previous reports where a 24-h photoperiod did not prevent the flowering of "Fedrina 74" and "Kompolti Hybrid TC" and that the critical photoperiod of a Portuguese fiber hemp variety from Coimbra is between 20 and 24 h (Heslop-Harrison and Heslop-Harrison, 1972; Van der Werf et al., 1994). In addition, "CFX-1" and "Joey" formed flower buds during the 3-week propagation stage in the greenhouse in Expt. 2. Available literature supports that primordium formation in hemp varieties occurs in response to quantitative short days, and the photoperiod inductive phase is jointly affected by photoperiod and temperature (Lisson et al., 2000; Hall et al., 2012). However, Spitzer-Rimon et al. (2019) argued that *Cannabis* could enter the reproductive phase under both long-day and short-day conditions because "solitary flowers," which are developed in the axil of each stipulate leaf, are differentiated under such conditions. Flower induction of "solitary flowers" is likely age-dependent and is controlled not by photoperiod but rather internal signals. Therefore, they reported that *Cannabis* could be considered a day-neutral plant where floral initiation is not dependent upon photoperiod requirements. These "solitary flowers," which can be referred to as sex-indicating flowers or pre-flowers, are believed to be the start of calyx development in hemp and are not photoperiod dependent (Green, 2017; Williams, 2020). In our study, long-day conditions did not prevent the floral initiation of "CFX-1," "Joey," "Tygra," and "Helena." Thus, they are likely day-neutral cultivars given floral initiation occurred in response to a 24-h photoperiod.

Hall et al. (2012) suggested that the hemp juvenile phase was not affected by photoperiod, and the length of the juvenile phase is either determined by the development of reproductive organs or the apical meristem, which is independently timed to produce flowering signals. In our study, the length of the juvenile phase was observed to be cultivar-specific, with "CFX-1" being the shortest and "Helena" is the longest among the four day-neutral cultivars (**Figure 2**). Traits, such as days to maturity and cannabinoid production, have been identified to be nearly entirely controlled by genetics. However, the environment can play a significant role in other traits, such as yield and plant height, and thus the influence of environment and genetics are likely needed to be considered collectively (Campbell et al., 2019). Different hemp cultivars have been suggested to have different lengths of juvenile phase and photosensitive phase, largely in association with geographic origin. Cultivars adapted to northern latitudes tend to have a short life cycle and grow and flower

TABLE 1 | Flowering percentage of essential oil and fiber/grain hemp from Expt. 1, 2, and 3.

Cultivar	Treatments											Critical photoperiod
	18 h (%)	15 h 30 min (%)	15 h (%)	14 h 45 min (%)	14 h 30 min (%)	14 h (%)	13 h 45 min (%)	13 h 30 min (%)	13 h (%)	12 h 30 min (%)	12 h (%)	
Essential oil cultivars												
ACDC-AC	0	40*	100*	100*	100*	100	100	100	100	100	100	>15 h
Super CBD-AC	0	0*	0*	100*	100*	100	100	100	100	100	100	14 h 45 min–15 h
Cherry-AC	0	0*	20*	100*	100*	80	100	100	100	100	100	15 h–15 h 30 min
Wife-AC	0	—	—	—	—	10	20	22	80	100	100	>14 h
Cherry Blossom-BC	0	0*	0*	80*	100*	70	90	100	100	100	100	14 h 45 min–15 h
Cherry Wine-BS	0	—	—	100*	100*	70	89	100	100	100	100	>14 h 45 min
Cherry Blossom-BS	0	0*	60*	100*	100*	78	100	89	100	100	100	15 h–15 h 30 min
Cherry*T1-BS	0	—	—	100*	100*	43	100	90	100	100	100	>14 h 45 min
Berry Blossom-BS	0	—	—	—	—	30	80	80	90	100	100	> 14 h
Cherry Blossom-Tuan-BS	0	—	—	—	—	60	90	100	100	100	100	> 14 h
JL Baux-CC	0	60*	100*	100*	100*	100	88	100	100	100	100	>15 h 30 min
ACDC-CC	0	0*	100*	100*	100*	100	100	100	100	100	100	15 h–15 h 30 min
Cherry Wine-CC	0	—	—	—	—	0	60	50	70	100	100	13 h 45 min–14 h
Cherry-CC	0	0*	100*	100*	100*	80	100	100	100	100	100	15 h–15 h 30 min
Wife-CC	0	—	—	—	—	30	60	50	90	100	100	> 14 h
Fiber/grain cultivars												
CFX-1	100	—	—	100	100	100	100	100	—	—	100	> 18 h or DN[z]
Joey	100	—	—	100	100	100	100	100	—	—	100	> 18 h or DN
Tygra	100	—	—	100	100	100	100	100	—	—	100	> 18 h or DN
Carmagnola Selezionata	0	100*	100*	100	100	100	100	100	—	—	100	> 15 h 30 min
Helena	22	100*	100*	100	100	100	100	100	—	—	100	> 18 h or DN
Fibranova	0	—	—	100	100	100	100	100	—	—	100	> 14 h 45 min
Eletta Campana	0	80*	40*	100	100	100	100	100	—	—	100	> 15 h 30 min
HAN-FN-H	0	100*	80*	100	100	100	100	100	—	—	100	> 15 h 30 min
HAN-NE	0	—	—	20	100	100	100	100	—	—	100	> 14 h 45 min
HAN-NW	0	—	—	25	100	100	100	100	—	—	100	> 14 h 45 min
PUMA-3	0	—	—	0	0	0	22	11	50*	100*	100	13 h 45 min–14 h
PUMA-4	0	—	—	0	0	0	17	17	60*	100*	100	13 h 45 min–14 h

The Boolean evaluation was conducted at week 5 of flowering after the treatment initiation, excluding dead plants.

[*] Data from Expt. 3. Values were calculated based on five replicates.

—Data not available.

[z] DN = day-neutral.

faster within their limited growing seasons, whereas cultivars adapted to southern latitudes and closer to the equator tend to flower later to ensure sufficient vegetative growth before short days occur (Amaducci et al., 2008; Small, 2015; Zhang et al., 2018). This theory is supported by our study results where cultivars of northern origin ("CFX," "Joey," "Tygra," etc.) responded to a longer photoperiod and flowered faster than southern cultivars ("PUMA-3," "PUMA-4," "HAN-NW," etc.) having a shorter critical day length threshold (**Figure 2**). Thus, understanding the juvenile phase and photosensitivity is essential for selecting the right hemp cultivar for a target region.

Some plant species can respond to light even at a very low intensity and are thus considered highly photosensitive. For these species of plants, civil twilight, or the period that occurs shortly before sunrise and after sunset when the sun is between 0 and 6° below the horizon, may still be biologically effective to the plant's photoperiodism response (Salisbury, 1981; Kishida, 1989). For example, rice (*Oryza sativa*) is light-insensitive to twilight both at dusk and dawn; perilla (*Perilla frutescens*) and Biloxi soybean (*Glycine max*) are light-insensitive at dusk but more light-sensitive at dawn; and cocklebur (*Xanthium saccharatum*) is both light-sensitive at dusk and dawn (Takimoto and Ikeda, 1961). For hemp, Borthwick and Scully (1954) suggested that 0.12 ft-candle or more would sufficiently prevent hemp from flowering, suggesting hemp is extremely sensitive to light. In our experience, light intensity as little as 2 $\mu mol \cdot m^{-2} \cdot s^{-1}$ can cause

light pollution and disrupt the flowering for "Cherry Blossom-BS" in the greenhouse. To evaluate the effect of twilight on hemp, we conducted field trials (Expt. 4) to investigate the performance of essential oil, fiber, and grain hemp cultivars under natural day light conditions. The average light intensity during civil twilight period in our study was 2.4 ± 0.54 $\mu mol \cdot m^{-2} \cdot s^{-1}$, which is within the light range reported by Kishida (1989). By comparing plant response and photoperiod to sunrise to sunset daylengths and civil twilight lengths, our results support the hypothesis that flowering performance of hemp is affected by civil twilight (**Figure 1**). Most flowering data from the field trial were in alignment with our trials from the controlled rooms (Expt. 1 to 3) and plants flowered around the critical photoperiod we tested, with a few exceptions. "Cherry Wine-BS", "Cherry Blossom-BS", "Cherry-AC", "Super CBD", and "ACDC-AC" flowered later and slower in the field compared with the controlled rooms (**Figure 1**). It is possible that the day length changes under the natural conditions are slower to occur and not as drastic compared with conditions imposed in the controlled rooms and therefore plants would respond to day length changes slower under natural conditions. On the contrary, "Cherry Wine-CC" and "PUMA-4" flowered earlier, suggesting that these cultivars might be more sensitive to the dark period. In addition, differences in individual perception of flowering initiation may have led to the reduced correlation between field and growth chamber floral initiation dates collected for these cultivars. Additional years of field trials will aid in the importance of civil twilight's effect on *Cannabis* flowering. Collectively, we believe that civil twilight length and the slow progression of day length changes under natural conditions should be taken into consideration for the biologically effective photoperiod for hemp flowering. Additional rigorous experiments involving artificial dawn and dusk regimes in controlled rooms is needed to further verify the hypothesis.

Days to Flower

Flowering response was delayed as flowering photoperiod increased. In both essential oil and fiber/grain cultivars, plants subjected to 12-h photoperiod had an average flowering time of 13–14 days (**Figure 2**). This is supported by Borthwick and Scully (1954) where 10–14 days of short-day photoperiod was sufficient for flower induction in at least some of the Chilean and Kentucky varieties.

Among essential oil cultivars, flowering was generally delayed by 1–2 days when photoperiod exceeded 13 h compared with 12 h, and flowering was significantly delayed by 7–8 days when photoperiod exceed 14 h (**Figure 2**). Across cultivars and regardless of sources, "ACDC" and "Super CBD" flowered the fastest, with an average flowering time of 13 days after initiation of the critical photoperiod. "Wife-AC," "Wife-CC," and "Cherry Wine" had an average flowering time of 21 d, suggesting these cultivars took longer to either perceive the photoperiod or to complete flower formation and initiation.

Essential oil hemp cultivars demonstrated delayed floral initiation at longer photoperiods and significant genetic variation in floral initiation across photoperiod treatments. Variance in observed photosensitivity is likely a result of genetic variation that influenced floral initiation response to light cues. Flowering for most essential oil cultivars was delayed by 5–13 days under a 14-h photoperiod compared with 13 h 45 min (**Figure 3** and **Supplementary Figure 1**). Flowering of "ACDC-AC" and "Cherry*T1-BS" was significantly delayed by 4 and 6 days, respectively, under 13 h 45 min compared with 12 h. Moreover, the delayed flowering of "Cherry-CC" started at 13 h 30 min and in "Wife-CC," 13 h. This suggests that floral initiation of these cultivars was more sensitive to photoperiod than others. In contrast, no significant differences were observed in days to flower among different treatments of "Wife-AC," "Berry Blossom-BS," and "Cherry Blossom-Tuan-BS," suggesting the flowering formation and initiation were rather similar under different day lengths, as long as they were below the critical photoperiod.

Cultivars represented by the same name acquired from different sources performed differently in days to flower. A photoperiod of 13 h 30 min significantly delayed the flowering of "ACDC-CC" but not "ACDC-AC," whereas 13 h 45 min delayed the flowering of "ACDC-AC" but not "ACDC-CC" (**Figure 3**). Delay of flowering in "Cherry-CC" started under a photoperiod of 13 h 30 min. In comparison, flowering occurred 30 min later at 14 h for "Cherry-AC." A photoperiod of 13 h delayed flowering of "Wife-CC" by 8 days compared with 12 h, but not in "Wife-AC." Similarly, flowering of "Cherry Wine-BS" was significantly delayed by 7 days under a 13-h photoperiod compared with a 12-h photoperiod. However, no differences in flowering were observed in "Cherry Wine-CC." In conjunction with Sawler et al. (2015), these results indicated that plants with the same cultivar names from different sources could have varying genetics and subsequently performed differently.

Most fiber/grain cultivars tested did not flower under an 18-h photoperiod (**Table 1**). Flowering was delayed by 1–3 days if the photoperiod exceeded 14 h, and no differences were observed among treatments beyond 14 h (**Figure 2**). This is consistent with the theory that hemp is a quantitative SDP and has a photoperiod of roughly 14 h where flowering would occur promptly below 14 h and flowering would be delayed under a longer photoperiod (Borthwick and Scully, 1954; Heslop-Harrison and Heslop-Harrison, 1969; Amaducci et al., 2008; Hall et al., 2014). When subjected to the critical photoperiod, average days to flower was shortest among cultivars from northern latitudes and longest among those from southern latitudes with a gradient response correlated to the cultivar's genetic origin. More specifically, Canada/Northern Europe cultivars flowered 4–11 days after lighting transition. Cultivars from comparatively lower latitudinal regions (North China/Italy) flowered from 12 to 16 days, whereas South China cultivars flowered 21–25 days (**Figure 2** and **Supplementary Figure 2**). Moreover, different photoperiod treatments did not affect the flowering of "CFX-1," "Joey," "Tygra," "Carmagnola Selezionata," and "Helena" (**Supplementary Figure 2**). Collectively, considering that 24-h day length did not prevent "CFX-1," "Joey," "Tygra," and "Helena" from flowering and their flowering process was not influenced by imposed photoperiods (**Table 1** and **Supplementary Figure 2**), these four fiber cultivars are likely photoperiod insensitive or day-neutral.

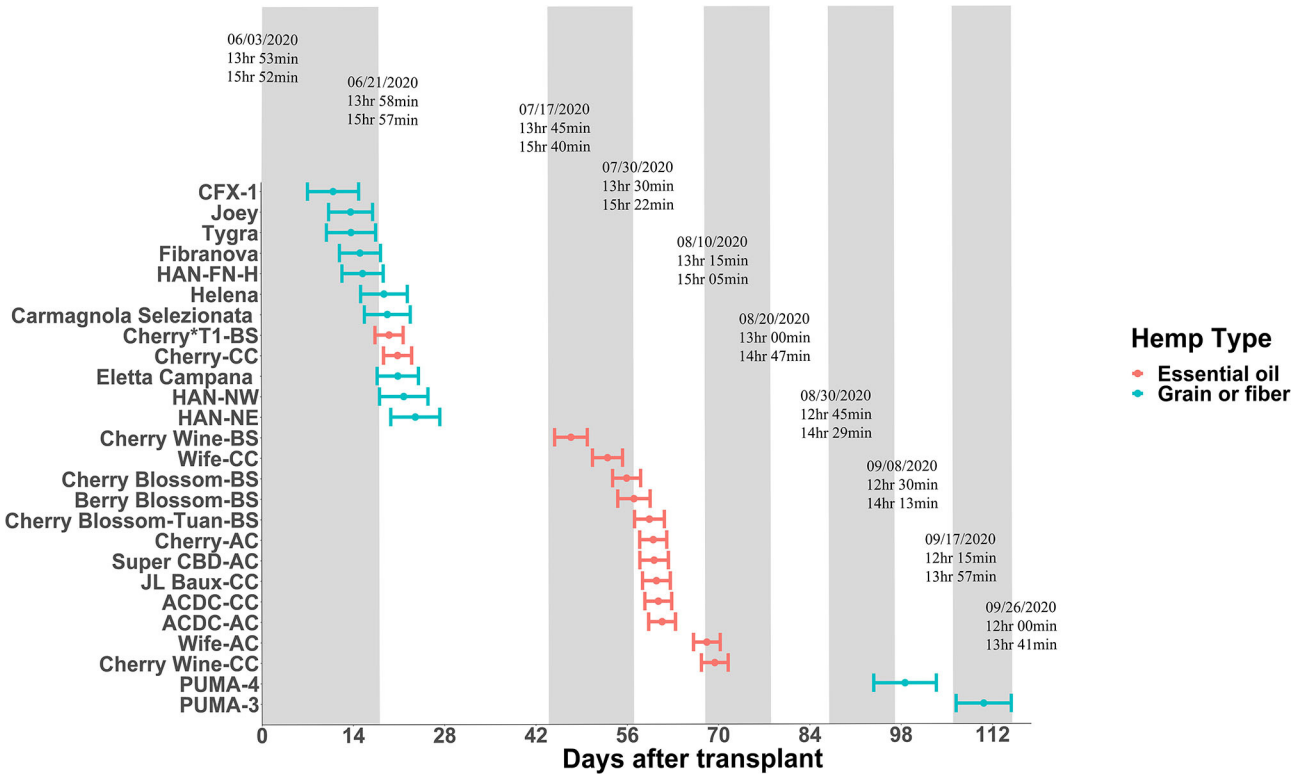

FIGURE 1 | Flowering date of essential oil, grain, and fiber cultivars after transplanting from greenhouse to field conditions on June 3, 2020. Points depict genetic means, and error bars represent 95% confidence intervals. The floating text depicts dates of 15-min daylength intervals (top), sunrise to sunset daylengths (middle), and civil twilight lengths (bottom).

Temperature differences and other stresses such as nutrient deficiencies can result in differences in flowering time (Amaducci et al., 2008; Hall et al., 2012). Amaducci et al. (2008) indicated that high temperature would accelerate flowering by decreasing the duration between the formation of flower primordia and full flowering, and thus modeling had been used to predict flowering time based on day length and temperature. Hall et al. (2012) also indicated that the photoperiod inductive phase of hemp is jointly influenced by air temperature and photoperiod. In our study, growing conditions including air temperature and nutrient fertility are nearly identical in each environmentally controlled room and thus did not contribute to differences in plant flowering performances. As recorded in this study, the flowering response was, therefore, free from the confounding influence of temperature and nutrient deficiency (excluding Expt. 4) and thus provides an enhanced foundational understanding of relationships between photoperiod and flowering response in hemp.

Collectively, based upon study findings and available literature, we believe the hemp juvenile phase to be controlled by genetics rather than photoperiod or temperature. The pre-flowering of the single sex-indicating flower at the axillary is photo insensitive. The response to photoperiod from pre-flowering to flowering at the apical meristem is affected by both photoperiod and temperature and can be either quantitative (most cultivars) or day-neutral (such as "CFX-1," "Joey," "Tygra," and "Helena"), dependent upon cultivar.

Extension Growth

Hemp cultivated within northern latitudes generally has a longer stem and greater biomass due to the late flowering and prolonged vegetative phase (Hall et al., 2014; Tang et al., 2016; Salentijn et al., 2019). The highest stem yield is usually obtained by late-maturing cultivars (Höppner and Mange-Hartmann, 2007). Generally, plant height increased as day length increased, as would be expected from increased photosynthesis. In our study, plant height extension growth was 47–102% greater under a 14-h day length compared with the 12-h day length, the control group in nine essential oil cultivars, while the imposed photoperiods did not affect the remaining six cultivars (**Figure 2**). The longer stem could have resulted from a longer vegetative stage caused by the delay in floral initiation, which has been reported on a variety of crops (Craig and Runkle, 2013; Zhang and Runkle, 2019). This is also supported by Höppner and Mange-Hartmann (2007), where stem length is positively correlated with the vegetative phase duration. However, under certain photoperiod treatments, flowering was delayed, but the height extension growth was not affected; this included "Cherry Wine-BS," "Cherry Wine-CC," and "Wife-CC" under 13 h, "ACDC-CC" under 13 h 30 min, "ACDC-AC" and "Cherry*T1-BS" under

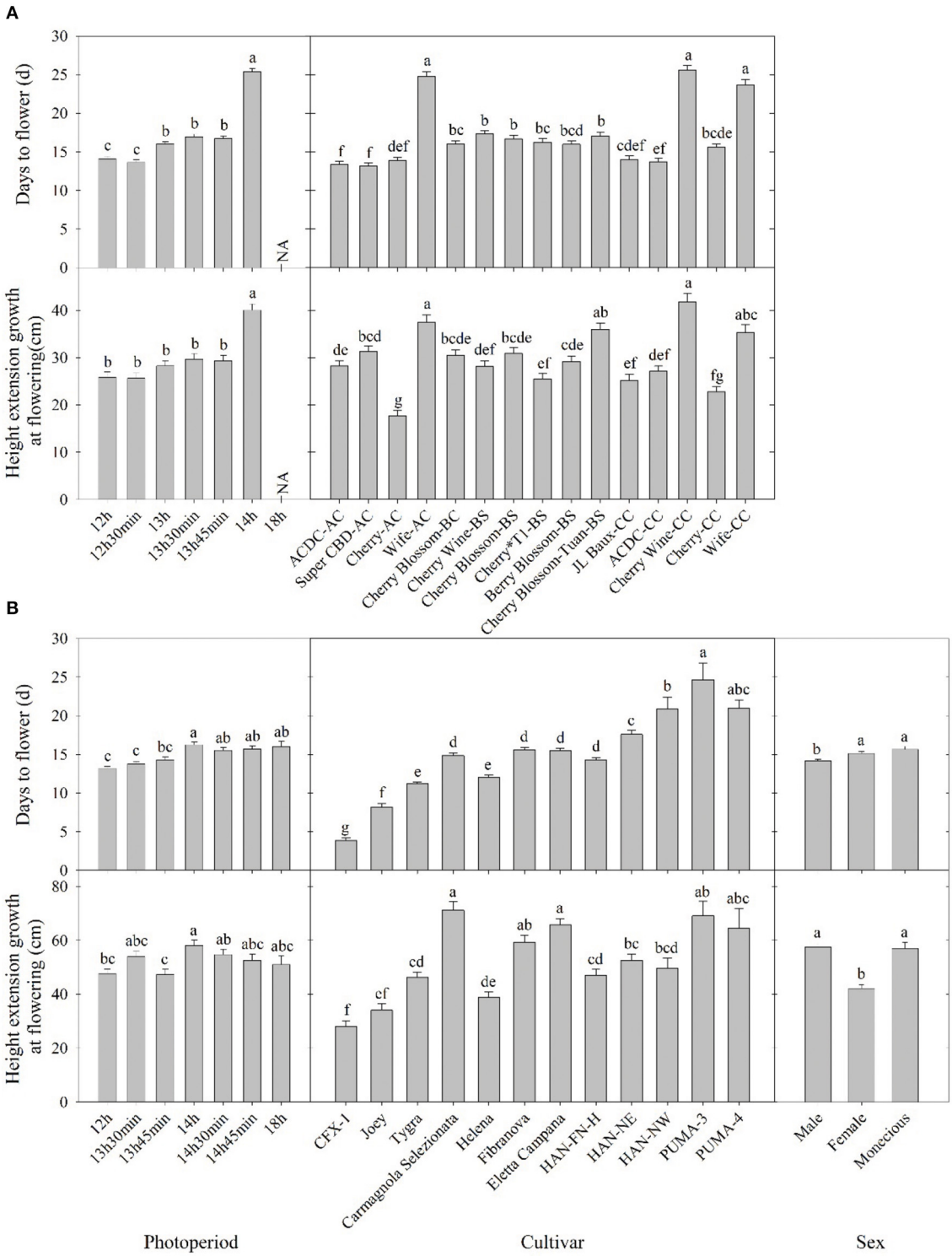

FIGURE 2 | Days to flower after lighting treatment initiated and height extension growth at the flowering of **(A)** essential oil and **(B)** fiber/grain cultivars under different photoperiods, cultivars, and/or sex from Expt. 1 and 2. Means sharing a letter are not statistically different by Tukey's honest significance difference test at $P \leq 0.05$. Error bars indicate standard error.

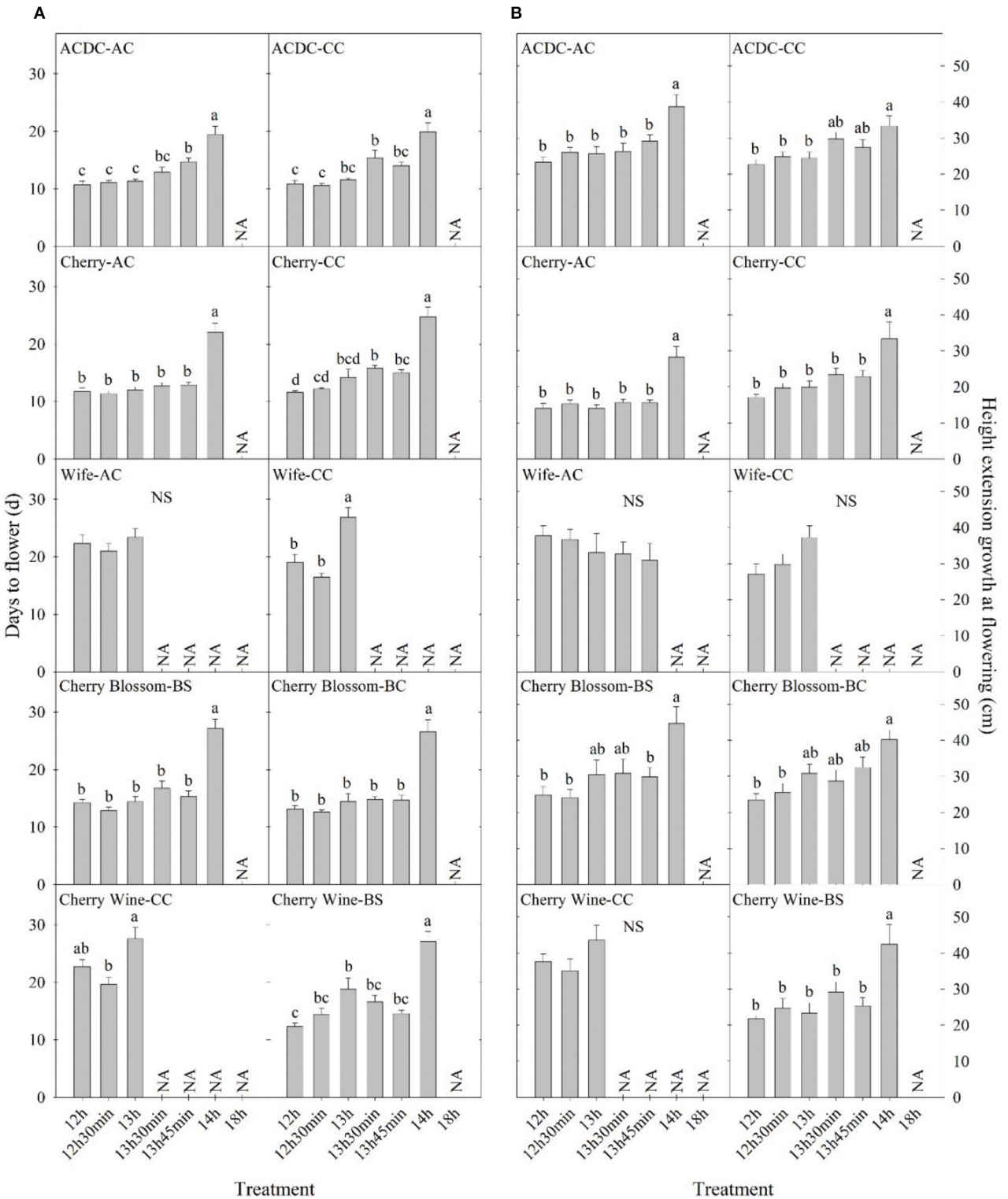

FIGURE 3 | Comparison of **(A)** days to flower and **(B)** height extension growth at flowering of 10 essential oil cultivars with the same name but different sources in Expt. 1. All data were pooled from 10 replications except "ACDC-AC" ($n = 9$). NS indicates insignificant treatment effects. NA indicates less than four valid data under such treatment. Means sharing a letter are not statistically different by Tukey's honest significance difference test at $P \leq 0.05$. Error bars indicate standard error.

TABLE 2 | Origin and sex status of fiber/grain hemp cultivars in Expt. 2.

Cultivar	Origins	Male (%)	Female (%)	Monoecious (%)	Unknown (%)
CFX-1	Canada	17.1	82.9	0.0	0.0
Joey	Canada	45.7	34.8	19.5	0.0
Tygra	Poland	40.0	4.3	55.7	0.0
Helena	Serbia	50.7	10.2	33.3	5.8
Carmagnola Selezionata	Italy	48.1	33.3	3.7	14.9
Fibranova	Italy	32.7	46.9	6.1	14.3
Eletta Campana	Italy	35.7	47.1	2.9	14.3
HAN-FN-H	North China	32.8	48.6	4.3	14.3
HAN-NE	Central China	37.1	37.1	0.0	25.8
HAN-NW	Central China	25.0	50.0	0.0	25.0
PUMA-3	South China	14.3	7.9	1.6	76.2
PUMA-4	South China	7.3	12.2	0.0	80.5

13 h 45 min, and "Cherry-CC" under both 13 h 30 min and 13 h 45 min (**Figure 3** and **Supplementary Figure 1**). Results indicated that flowering initiation of essential oil hemp was more sensitive than extension growth in response to photoperiods. In addition, unlike flowering, extension growth of essential oil cultivars with the same name but from different sources generally responded similarly, except "Cherry Wine." Campbell et al. (2019) indicated that plant height was collectively influenced by both environment (e.g., irrigation) and genetics, accounting for 38 and 36% of the variance, respectively. We concluded that similar height extension growth among essential oil cultivars under different treatments was due to similar irrigation applications.

In contrast to essential oil cultivars, extension growth of fiber/grain cultivars was not affected by photoperiod, except "CFX-1" and "HAN-NE" (**Supplementary Figure 3**). Height extension of "HAN-NE" was 58–64% greater when day length exceeds 14 h due to the later flower initiation development. Interestingly, stem extension of "CFX-1" was shorter under an 18-h photoperiod compared with a 13 h 30 min photoperiod. We believe "CFX-1" is photo insensitive, and individual variances caused this difference.

Sex

Plant sex was recorded and calculated across the lighting treatments for fiber/grain hemp cultivars (**Table 2**). Among all the fiber/grain hemp cultivars tested, most cultivars had a relatively equal proportion of male and female plants in general with a small occurrence of monoecious plant development, which is consistent with Hall et al. (2012). "Tygra" had the highest proportion of monoecious plants (55.7%) with a small proportion of female plant development (4.3%). "Helena" was one-third monoecious. Most of "CFX-1" were female plants with no monoecious plants that developed. The sex of more than 25% of "HAN-NE," "HAN-NW," "PUMA-3," and "PUMA-4" could not be determined due to a lack of flowering response throughout our experiment.

Overall, the flowering of female and monoecious plants was delayed by 1–2 days compared with male plants (**Figure 3**). Our observations were supported by Borthwick and Scully (1954) findings where the greater flowering delay occurred in male plants compared with female plants under long photoperiods. Hall et al. (2012) and Van der Werf et al. (1994) suggested extending the day length would alter the sex proportion of flowering hemp plants and that male and monoecious plants would fail to flower when photoperiod exceeded the optimal day length. Additionally, Van der Werf et al. (1994) suggested that unlike male hemp plants, female flowering would be less influenced by photoperiod. We did not observe such trends in fiber hemp cultivars, and no flowering pattern or changes in flowering percentage were identified when the photoperiod exceeded the optimal 14 h. Female hemp also has a significantly shorter extension growth than male and monoecious plants at flowering (**Figure 3**).

CONCLUSION

This research reported flowering and growth of 27 hemp cultivars in response to different photoperiods under both indoor controlled and outdoor natural environments. Most of the essential oil cultivars and some southern fiber/grain cultivars (such as "PUMA-3" and "PUMA-4") tested express suitable photoperiods for tropical and sub-tropical region cultivation. Pre-flowering of hemp is photo insensitive, but the response to photoperiod from pre-flowering to flowering can be either quantitative or day neutral. Depending on photosensitivity, a photoperiod difference of as little as 15 min significantly influenced the floral initiation of some essential oil cultivars. Northern fiber/grain hemp cultivars had a shorter juvenile phase and faster flowering than cultivars from southern latitudes. Cultivar name may not be enough to finely estimate photoperiod response for essential oil cultivars. The flowering performance of hemp appears to be influenced by civil twilight, and thus this should be considered when attempting to time cultivation to maximize vegetative and flowering response. Male plants flower

faster than female and monoecious plants. Plant height generally increased as the day length increased in essential oil cultivars but not in fiber/grain cultivars.

DATA AVAILABILITY STATEMENT

The raw data supporting the conclusions of this article will be made available by the authors, without undue reservation.

AUTHOR CONTRIBUTIONS

MZ performed the conceptualization, data curation, formal analysis, investigation, methodology, original draft, review and editing (lead), supervision, validation, and visualization. SA performed the conceptualization, data curation, formal analysis, investigation, methodology, supervision, validation, visualization, and review and editing (supporting). ZB performed funding acquisition, project administration, supervision, resources, and review and editing (supporting). BP performed the conceptualization, methodology, project administration, supervision, resources, and review and editing (supporting). All authors contributed to the article and approved the submitted version.

FUNDING

This project was made possible by financial support from Green Roads LLC, Roseville Farms LLC, and the UF/IFAS Office of the Dean and Research.

ACKNOWLEDGMENTS

We would like to acknowledge Brandon White and Chris Halliday for their technical support; James Johnston and Dillan Raab for their hard work and effort in maintaining experimental plants and collecting phenotypic data; Jerry Fankhauser and Sandra Alomar for administrative assistance; Green Point Research, ANO Colorado LLC, and Green Roads LLC for donating the cultivars used in this research; and all members of the University of Florida IFAS Industrial Hemp Pilot Project for their collaboration.

SUPPLEMENTARY MATERIAL

The Supplementary Material for this article can be found online at: https://www.frontiersin.org/articles/10.3389/fpls.2021.694153/full#supplementary-material

REFERENCES

Amaducci, S., Colauzzi, M., Bellocchi, G., Cosentino, S. L., Pahkala, K., Stomph, T. J., et al. (2012). Evaluation of a phenological model for strategic decisions for hemp (*Cannabis Sativa* L.) biomass production across European sites. *Ind. Crops Prod.* 37, 100–110. doi: 10.1016/j.indcrop.2011.11.012

Amaducci, S., Colauzzi, M., Bellocchi, G., and Venturi, G. (2008). Modelling post-emergent hemp phenology (*Cannabis sativa* L.): theory and evaluation. *Eur. J. Agron.* 28, 90–102. doi: 10.1016/j.eja.2007.05.006

Anderson, E., Baas, D., Thelen, M., Burns, E., Chilvers, M., Thelen, K., et al. (2019). *Industrial Hemp Production in Michigan*. Available online at: https://www.canr.msu.edu/hemp/uploads/files/industrialhempinfosheet_2019-05-24.pdf (accessed February 20, 2021).

Borthwick, H. A., and Scully, N. J. (1954). Photoperiodic responses of hemp. *Botanical Gazette* 116, 14–29. doi: 10.1086/335843

Campbell, B. J., Berrada, A. F., Hudalla, C., Amaducci, S., and McKay, J. K. (2019). Genotype× environment interactions of industrial hemp cultivars highlight diverse responses to environmental factors. *Agrosyst. Geosci. Environ.* 2, 1–11. doi: 10.2134/age2018.11.0057

Cherney, J. H., and Small, E. (2016). Industrial hemp in North America: production, politics and potential. *Agronomy* 6:58. doi: 10.3390/agronomy6040058

Cho, L. H., Yoon, J., and An, G. (2017). The control of flowering time by environmental factors. *Plant J.* 90, 708–719. doi: 10.1111/tpj.13461

Congressional Research Service (2019). *Defining Hemp: A Fact Sheet*. Available online at: https://www.everycrsreport.com/files/20190322_R44742_1b0195c6aa7e2cad29256c85a8574347c1ee833d.pdf (accessed October 18, 2020).

Cosentino, S. L., Testa, G., Scordia, D., and Copani, V. (2012). Sowing time and prediction of flowering of different hemp (*Cannabis sativa* L.) genotypes in southern Europe. *Ind. Crops Prod.* 37, 20–33. doi: 10.1016/j.indcrop.2011.11.017

Craig, D. S., and Runkle, E. S. (2013). A moderate to high red to far-red light ratio from light-emitting diodes controls flowering of short-day plants. *J. Am. Soc. Hort. Sci.* 138, 167–172. doi: 10.21273/JASHS.138.3.167

Green, G. (2017). *The Cannabis Grow Bible. 3rd Edn.* Green Candy Press.

Hall, J., Bhattarai, S. P., and Midmore, D. J. (2012). Review of flowering control in industrial hemp. *J. Natural Fibers* 9, 23–36. doi: 10.1080/15440478.2012.651848

Hall, J., Bhattarai, S. P., and Midmore, D. J. (2014). Effect of industrial hemp (*Cannabis sativa* L.) planting density on weed suppression, crop growth, physiological responses, and fibre yield in the subtropics. *Renew. Bioresources* 2, 1–7. doi: 10.7243/2052-6237-2-1

Hemp Business Journal (2018). *Farm Bill Effect: Impact on U.S. and Global Hemp Markets*. Available online at: https://www.hempbizjournal.com/farm-bill-effect-impacts-on-us-hemp-market-and-global-hemp-market/ (accessed July 10, 2020).

Heslop-Harrison, J., and Heslop-Harrison, Y. (1969). *Cannabis sativa L.* The induction of flowering. Some case studies. MacMillan Co. Pty. Ltd.

Heslop-Harrison, J., and Heslop-Harrison, Y. (1972). *Sexuality of Angiosperms. Physiology of Development: From Seeds to Sexuality*. New York, NY: Academic Press.

Höppner, F., and Mange-Hartmann, U. (2007). Yield and quality of fibre and oil of fourteen hemp cultivars in Northern Germany at two harvest dates. *Landbauforschung Volkenrode* 57, 219–232.

Jung, C., and Müller, A. E. (2009). Flowering time control and applications in plant breeding. *Trends in Plant Sci.* 14, 563–573. doi: 10.1016/j.tplants.2009.07.005

Keller, A., Leupin, M., Mediavilla, V., and Wintermantel, E. (2001). Influence of the growth stage of industrial hemp on chemical and physical properties of the fibres. *Ind. Crops Prod.* 13, 35–48. doi: 10.1016/S0926-6690(00)00051-0

Kishida, Y. (1989). Changes in light intensity at twilight and estimation of the biological photoperiod. *Jpn. Agr. Res. Qrtly.* 22, 247–252.

Lane, H. C., Cathey, M., and Evans, L. T. (1965). The dependence of flowering in several long-day plants on the spectral composition of light extending the photoperiod. *Amer. J. Bot.* 52, 1006–1014. doi: 10.1002/j.1537-2197.1965.tb07278.x

Lisson, S. N., Mendham, N. J., and Carberry, P. S. (2000). Development of a hemp (*Cannabis sativa* L.) simulation model 2. The flowering response of two hemp cultivars to photoperiod. *Austr. J. Exp. Agr.* 40, 413–417. doi: 10.1071/EA99059

Mediavilla, V., Jonquera, M., Schmid-Slembrouck, I., and Soldati, A. (1998). Decimal code for growth stages of hemp (*Cannabis sativa* L.). *J. Intl. Hemp Assn.* 5:65.

Mediavilla, V., Leupin, M., and Keller, A. (2001). Influence of the growth stage of industrial hemp on the yield formation in relation to certain fibre quality traits. *Ind. Crops Prod*. 13, 49–56. doi: 10.1016/S0926-6690(00)00052-2

Moher, M., Jones, M., and Zheng, Y. (2020). Photoperiodic response of *in vitro Cannabis sativa* plants. *Hort Sci*. 56, 108–113. doi: 10.21273/HORTSCI15452-20

Navarro, J. A. R., Willcox, M., Burgueño, J., Romay, C., Swarts, K., Trachsel, S., et al. (2017). A study of allelic diversity underlying flowering-time adaptation in maize landraces. *Nat. Genet*. 49, 476–480. doi: 10.1038/ng.3784

Petit, J., Salentijn, E. M., Paulo, M. J., Thouminot, C., van Dinter, B. J., Magagnini, G., et al. (2020). Genetic variability of morphological, flowering, and biomass quality traits in hemp (*Cannabis sativa* L.). *Front. Plant Sci*. 11:102. doi: 10.3389/fpls.2020.00102

Potter, D. J. (2014). "Cannabis horticulture," in *Handbook of Cannabis* (Oxford: Oxford University Press). doi: 10.1093/acprof:oso/9780199662685.003.0004

Runkle, E. S., Heins, R. D., Cameron, A. C., and Carlson, W. H. (1998). Flowering of herbaceous perennials under various night interruption and cyclic lighting treatments. *HortScience* 33, 672–677. doi: 10.21273/HORTSCI.33.4.672

Salentijn, E. M., Petit, J., and Trindade, L. M. (2019). The complex interactions between flowering behavior and fiber quality in hemp. *Front. Plant Sci*. 10:614. doi: 10.3389/fpls.2019.00614

Salisbury, F. B. (1981). Twilight effect: initiating dark measurement in photoperiodism of Xanthium. *Plant Physiol*. 67, 1230–1238. doi: 10.1104/pp.67.6.1230

Sawler, J., Stout, J. M., Gardner, K. M., Hudson, D., Vidmar, J., Butler, L., et al. (2015). The genetic structure of marijuana and hemp. *PLoS ONE* 10:e0133292. doi: 10.1371/journal.pone.0133292

Sengloung, T., Kaveeta, L., and Nanakorn, W. (2009). Effect of sowing date on growth and development of Thai hemp (*Cannabis sativa* L.). *Kasetsart J*. 43, 423–431.

Small, E. (2015). Evolution and classification of *Cannabis sativa* (marijuana, hemp) in relation to human utilization. *Bot. Rev*. 81, 189–294. doi: 10.1007/s12229-015-9157-3

Spitzer-Rimon, B., Duchin, S., Bernstein, N., and Kamenetsky, R. (2019). Architecture and florogenesis in female *Cannabis sativa* plants. *Front. Plant Sci*. 10:350. doi: 10.3389/fpls.2019.00350

Takimoto, A., and Ikeda, K. (1961). Effect of twilight on photoperiodic induction in some short day plants. *Plant Cell Physiol*. 2, 213–229. doi: 10.1093/oxfordjournals.pcp.a077680

Tang, K., Struik, P. C., Yin, X., Thouminot, C., Bjelkova, M., Stramkale, V., et al. (2016). Comparing hemp (*Cannabis sativa* L.) cultivars for dual- purpose production under contrasting environments. *Ind. Crop. Prod*. 87, 33–44. doi: 10.1016/j.indcrop.2016.04.026

Van der Werf, H. M. G., Haasken, H. J., and Wijlhuizen, M. (1994). The effect of daylength on yield and quality of fibre hemp (*Cannabis sativa* L.). *Eur. J. Agron*. 3, 117–123. doi: 10.1016/S1161-0301(14)80117-2

Vince-Prue, D., and Canham, A. (1983). "Horticultural significance of photmorphogenesis," in *Photomorphogenesis. Photomorphogenesis*, eds W. Shropshire and H. Mohr (Heidelberg: Springer-Verlag), 518–544. doi: 10.1007/978-3-642-68918-5_20

Williams, A. (2020). *Hemp Breeding and the Uses of Photoperiod Manipulation*. Creative Components 560.

Zhang, M., and Runkle, E. S. (2019). Regulating flowering and extension growth of poinsettia using red and far-red light-emitting diodes for end-of-day lighting. *HortScience* 54, 323–327. doi: 10.21273/HORTSCI13630-18

Zhang, Q., Chen, X., Guo, H., Trindade, L. M., Salentijn, E. M., Guo, R., et al. (2018). Latitudinal adaptation and genetic insights into the origins of *Cannabis sativa* L. *Front. Plant Sci*. 9:1876. doi: 10.3389/fpls.2018.01876

Conflict of Interest: The authors declare that the research was conducted in the absence of any commercial or financial relationships that could be construed as a potential conflict of interest.

Publisher's Note: All claims expressed in this article are solely those of the authors and do not necessarily represent those of their affiliated organizations, or those of the publisher, the editors and the reviewers. Any product that may be evaluated in this article, or claim that may be made by its manufacturer, is not guaranteed or endorsed by the publisher.

frontiers in Plant Science

ORIGINAL RESEARCH
published: 13 September 2021
doi: 10.3389/fpls.2021.729261

Genome-Wide Characterization of the *MLO* Gene Family in *Cannabis sativa* Reveals Two Genes as Strong Candidates for Powdery Mildew Susceptibility

*Noémi Pépin[1†], Francois Olivier Hebert[1,2†] and David L. Joly[1]**

[1] Centre d'Innovation et de Recherche sur le Cannabis, Université de Moncton, Département de biologie, Moncton, NB, Canada, [2] Institut National des Cannabinoïdes, Montréal, QC, Canada

Cannabis sativa is increasingly being grown around the world for medicinal, industrial, and recreational purposes. As in all cultivated plants, cannabis is exposed to a wide range of pathogens, including powdery mildew (PM). This fungal disease stresses cannabis plants and reduces flower bud quality, resulting in significant economic losses for licensed producers. The *Mildew Locus O* (*MLO*) gene family encodes plant-specific proteins distributed among conserved clades, of which clades IV and V are known to be involved in susceptibility to PM in monocots and dicots, respectively. In several studies, the inactivation of those genes resulted in durable resistance to the disease. In this study, we identified and characterized the *MLO* gene family members in five different cannabis genomes. Fifteen *Cannabis sativa MLO* (*CsMLO*) genes were manually curated in cannabis, with numbers varying between 14, 17, 19, 18, and 18 for CBDRx, Jamaican Lion female, Jamaican Lion male, Purple Kush, and Finola, respectively (when considering paralogs and incomplete genes). Further analysis of the *CsMLO* genes and their deduced protein sequences revealed that many characteristics of the gene family, such as the presence of seven transmembrane domains, the MLO functional domain, and particular amino acid positions, were present and well conserved. Phylogenetic analysis of the MLO protein sequences from all five cannabis genomes and other plant species indicated seven distinct clades (I through VII), as reported in other crops. Expression analysis revealed that the *CsMLOs* from clade V, *CsMLO1* and *CsMLO4*, were significantly upregulated following *Golovinomyces ambrosiae* infection, providing preliminary evidence that they could be involved in PM susceptibility. Finally, the examination of variation within *CsMLO1* and *CsMLO4* in 32 cannabis cultivars revealed several amino acid changes, which could affect their function. Altogether, cannabis *MLO* genes were identified and characterized, among which candidates potentially involved in PM susceptibility were noted. The results of this study will lay the foundation for further investigations, such as the functional characterization of clade V MLOs as well as the potential impact of the amino acid changes reported. Those will be useful for breeding purposes in order to develop resistant cultivars.

Keywords: *Cannabis*, powdery mildew, fungal disease, susceptibility genes, plant–pathogen interactions, *MLO*

OPEN ACCESS

Edited by:
Donald Lawrence Smith, McGill University, Canada

Reviewed by:
Michele Wiseman, Oregon State University, United States
Kevin McKernan, Medicinal Genomics Corporation, United States

****Correspondence:***
David L. Joly
david.joly@umoncton.ca

† These authors have contributed equally to this work

Specialty section:
This article was submitted to Plant Symbiotic Interactions, a section of the journal Frontiers in Plant Science

Received: *22 June 2021*
Accepted: *19 August 2021*
Published: *13 September 2021*

Citation:
Pépin N, Hebert FO and Joly DL (2021) Genome-Wide Characterization of the MLO Gene Family in Cannabis sativa Reveals Two Genes as Strong Candidates for Powdery Mildew Susceptibility. Front. Plant Sci. 12:729261. doi: 10.3389/fpls.2021.729261

INTRODUCTION

Cannabis sativa is a dicotyledonous plant belonging to the Cannabaceae family, and it is considered a socially and economically important crop as it is increasingly being grown and cultivated around the world. In Canada alone, the sales from cannabis stores in 2020 reached over 2.6 billion dollars (Statistics Canada, 2021), and the number of licensed cultivators, processors, and sellers quadrupled from 2018 to 2020 (Health Canada, 2020). It is used as a source of industrial fiber, seed oil, food, as well as for medicinal, spiritual, and recreational purposes (Small, 2015). As in all cultivated plants, cannabis is exposed to numerous pathogens, and the resulting diseases play a limiting role in its production.

Powdery mildew (PM) is a widespread plant disease caused by ascomycete fungi of the order Erysiphales, for which more than 800 species have been described (Braun and Cook, 2012). They are obligate biotrophs that form invasive structures in epidermal cells for nutrient uptake, called haustoria (Glawe, 2008). These pathogens can infect nearly 10,000 monocotyledonous and dicotyledonous plant species and cause significant damage to crops and ornamental plants (Braun et al., 2002). The PM disease in cannabis, caused by *Golovinomyces ambrosiae* emend. (including *Golovinomyces spadiceus*), has been reported on indoor- and greenhouse-grown plants in Canada and in the United States, where the enclosed conditions provide an ideal environment for the germination and propagation of the fungal spores (Pépin et al., 2018; Szarka et al., 2019; Farinas and Peduto Hand, 2020; Weldon et al., 2020; Wiseman et al., 2021). An analysis of cannabis buds revealed *Golovinomyces* sp. in 79% of tested samples (Thompson et al., 2017), highlighting its ubiquity among licensed producers. The symptoms initially appear as white patches on leaves, and eventually, the mycelia progress to cover the entire leaf surface, the flower bracts, and buds, resulting in stressed and weakened plants, reduced yield, and reduced flower buds quality. Fungicides are widely used to prevent and control this disease in agricultural settings. However, a scarce amount of such products are currently approved by Health Canada as the presence of fungicide residues in the inflorescences raises concerns (Punja, 2021). Besides, they are costly, and fungicide resistance in PM has been observed and documented in other plant species in recent years (Vielba-Fernández et al., 2020). Alternative approaches to managing this disease have been described, such as the use of biological control (e.g., *Bacillus subtilis* strain QST 713), reduced risk products (e.g., potassium bicarbonate, knotweed extract), and physical methods (e.g., de-leafing, irradiation) (Punja, 2021). Nonetheless, some of these methods increase production costs, are labor-intensive, and necessitate further research. Therefore, identifying sources of genetic resistance to PM in cannabis and ultimately breeding or developing resistant cultivars offer the most effective and sustainable approach to controlling PM.

A common strategy used in resistance breeding relies on the exploitation of resistance genes in plants, which encodes for cytoplasmic receptors such as nucleotide-binding leucine-rich repeat proteins or surface receptors such as receptor-like kinases and receptor-like proteins. These immune receptors can detect specific proteins or molecules produced by the pathogen and subsequently induce plant defense responses (Dangl and Jones, 2001). While useful, most resistance genes confer race-specific resistance and are therefore frequently overcome by the emergence of a pathogen's new virulent race within a few years. An alternative approach in resistance breeding is to exploit susceptibility genes (*S-genes*) in plants. *S-genes* are defined as genes that facilitate infection and support compatibility for a pathogen (van Schie and Takken, 2014). The alteration of such genes can limit the pathogen's ability to infect the plant and therefore provide a durable type of resistance (van Schie and Takken, 2014). Such PM resistance was initially observed in an X-ray irradiated barley (*Hordeum vulgare*) population in the 1940s (Freisleben and Lein, 1942). It was discovered later that the immunity was attributable to a mutated *S-gene* named *Mildew Locus O* (*MLO*), which was recessively inherited. Complete resistance to all known isolates of PM, caused by *Blumeria graminis* f. sp. *hordei* was conferred in barley by these loss-of-function mutations when present in the homozygous state. This type of resistance has been durable under field conditions and has been used for over 40 years in barley breeding programs, without any break in the resistance (Jørgensen, 1992; Büschges et al., 1997; Lyngkjær and Carver, 2000; Piffanelli et al., 2002).

Since discovering *MLO* genes in barley, many *MLO* homologs have been identified in several plant species, especially in monocots and eudicots, as the PM disease affects angiosperms solely. For instance, *MLO* genes were identified in Rosaceae [roses (Kaufmann et al., 2012), apple, peach, strawberry and apricot (Pessina et al., 2014)], Cucurbitaceae [cucumber (Zhou et al., 2013), melon, watermelon, zucchini (Iovieno et al., 2015) and pumpkin (Win et al., 2018)], Solanaceae [tomato (Bai et al., 2008), pepper (Zheng et al., 2013), tobacco, potato and eggplant (Appiano et al., 2015)], Fabaceae [pea (Humphry et al., 2011; Pavan et al., 2011), soybean (Shen et al., 2012; Deshmukh et al., 2014), barrel medic, chickpea, narrow-leaf lupin, peanut, pigeon pea, common bean, mungbean (Rispail and Rubiales, 2016) and lentil (Polanco et al., 2018)], Brassicaceae [thale cress (Devoto et al., 1999, 2003)], Vitaceae [grapevine (Feechan et al., 2008)], and Poaceae [rice (Liu and Zhu, 2008), wheat (Konishi et al., 2010), sorghum (Singh et al., 2012), maize (Devoto et al., 2003; Kusch et al., 2016), foxtail millet (Kusch et al., 2016) and stiff brome (Ablazov and Tombuloglu, 2016)]. Furthermore, thorough phylogenetic analyses of land plants revealed that *MLO* genes were not only present in monocots and eudicots but also in basal angiosperms, gymnosperms, lycophytes, and bryophytes (Jiwan et al., 2013; Kusch et al., 2016; Shi et al., 2020). Many MLO-like proteins were also identified in algae and other unicellular eukaryotes, suggesting that *MLO* is an ancient eukaryotic protein (Jiwan et al., 2013; Kusch et al., 2016; Shi et al., 2020).

The *MLO* gene family is described as a medium-sized plant-specific gene family, with a varying number of members between 7 in wheat to 39 in soybean, depending on the species (Acevedo-Garcia et al., 2014). The resulting MLO proteins are characterized by the presence of seven transmembrane domains integral to the plasma membrane with an extracellular N-terminus and an intracellular C-terminus (Devoto et al., 1999). They are also characterized by the presence of a calmodulin-binding domain

in the C-terminal region that is likely implicated in sensing calcium influx and mediating various signaling cascades (Kim et al., 2002a,b). MLO protein sequences identified across land plants also possess several highly conserved amino acids, some of which have been deemed essential for the structure, functionality, and stability of the protein (Devoto et al., 2003; Elliott et al., 2005; Reinstädler et al., 2010; Kusch et al., 2016). Mutations in these residues could affect the accumulation, maturation, and function of the protein and are therefore attractive targets for breeding programs (Elliott et al., 2005; Reinstädler et al., 2010).

Throughout land plant evolution, the MLO protein family diversified into subfamilies, or clades, which have been demonstrated in several phylogenetic analyses. MLO proteins are usually grouped into seven defined clades (I to VII), among which clades IV and V appear to host MLO proteins associated with PM susceptibility in monocots and dicots, respectively (Acevedo-Garcia et al., 2014; Kusch et al., 2016). It has been documented in many species, such as barley, tomato, and apple, that *MLO* genes from these two clades (IV and V in monocots and dicots, respectively) are up-regulated upon PM infection (Piffanelli et al., 2002; Zheng et al., 2013; Pessina et al., 2014). It has also been demonstrated that the overexpression of these genes results in enhanced susceptibility to the pathogen (Zheng et al., 2013). Furthermore, the inactivation of these genes in many species by gene silencing, genome editing, or TILLING has resulted in increased or complete resistance to PM (Wang et al., 2014; Acevedo-Garcia et al., 2017; Nekrasov et al., 2017; Ingvardsen et al., 2019; Wan et al., 2020). Besides the implication of clade V and IV MLOs in PM susceptibility, recent studies have suggested that *MLO* genes from other clades are implicated in various physiological and developmental processes. For example, it was demonstrated that in *Arabidopsis thaliana*, *AtMLO4* and *AtMLO11* from clade I are involved in root thigmomorphogenesis (Chen et al., 2009; Bidzinski et al., 2014), while *AtMLO7* from clade III is involved in pollen tube reception by the embryo sac (Kessler et al., 2010). In rice (*Oryza sativa*), *OsMLO12* from clade III mediates pollen hydration (Yi et al., 2014). Interestingly, barley *HvMLO1* has been shown to differentially regulate the establishment of mutualistic interactions with the endophyte *Serendipita indica* and the arbuscular mycorrhizal fungus *Funneliformis mosseae* (Hilbert et al., 2020). Indeed, another study clearly showed barley *HvMLO1*, wheat *TaMLO1,* and barrel medic *MtMLO8* from clade IV to be involved in the establishment of symbiotic relationships with beneficial mycorrhizal fungi (Jacott et al., 2020). These findings suggest that PMs might have appropriated and exploited these genes as an entryway to successful pathogenic colonization (Jacott et al., 2020). However, in pea, no evidence was found for the implication of *PsMLO1*, a clade V gene, in the establishment of relationships with mycorrhizal and rhizobial symbionts (Humphry et al., 2011).

Although *MLO* genes have been studied in many monocot and dicot species, they have only been preliminarily studied in cannabis (McKernan et al., 2020). The growing interest in cannabis research has led to the publication of several genomes in recent years, thus providing an opportunity to conduct a comprehensive analysis of the *MLO* gene family in cannabis. In this study, we manually curated and characterized the members of the *MLO* gene family in cannabis from five different available genomes: Purple Kush and Finola (Laverty et al., 2019), CBDRx (Grassa et al., 2021), and Jamaican Lion (female, McKernan et al., 2018; male, McKernan et al., 2020). Through phylogenetic analysis, we identified candidate *MLO* genes likely to be involved in PM susceptibility in cannabis, observed their subcellular localization by confocal microscopy, and monitored their expression profile in cannabis leaves during infection. We also searched for potential naturally occurring resistant mutants by investigating amino acid changes in 32 cultivars. A better understanding of cannabis *MLOs* offers enormous opportunities to breed PM-resistant cultivars and develop new control methods, thereby increasing productivity and yield.

MATERIALS AND METHODS

In silico Identification and Manual Curation of the Cannabis *MLO* Genes

Cannabis *MLO* genes in CBDRx were initially identified (also named 'cs10,' NCBI accession GCA_900626175.2) using TBLASTN from the BLAST+ suite (Camacho et al., 2009) with *Arabidopsis thaliana* amino acid sequences as queries (*AtMLO1-AtMLO15*, NCBI accession numbers: NP_192169.1, NP_172598.1, NP_566879.1, NP_563882.1, NP_180923.1, NP_176350.1, NP_179335.3, NP_565416.1, NP_174980.3, NP_201398.1, NP_200187.1, NP_565902.1, NP_567697.1, NP_564257.1, NP_181939.1). In parallel, all official gene models were extracted from the NCBI CBDRx annotation report (NCBI Annotation Release 100[1]) with an InterPro (IPR004326) and/or Pfam (PF03094) identification number related to the *MLO* gene family (Blum et al., 2021; Mistry et al., 2021). These two sequence datasets were merged together, and multiple sequence alignments were performed using MUSCLE v.3.8.31 (Edgar, 2004) with the genomic and the amino acid versions of each *MLO* gene model. Only unique sequences were kept, and all *MLO* gene models that were retained but incomplete were further manually curated. The full genomic sequences were aligned and manually compared with their corresponding full-length mRNA transcripts using BLASTN from the BLAST+ suite (Camacho et al., 2009). Each gene was characterized based on total length, chromosome localization, strand, START and STOP positions, as well as number and size of exons and introns (**Figure 1** and **Table 1**). The resulting streamlined and manually curated *MLO* gene models for CBDRx were considered the definitive reference set for this genome.

The reference set of CBDRx *MLO* genes were used as queries to search for the presence of homologs in four other cannabis genomes (Purple Kush – GCA_000230575.5, Finola – GCA_003417725.2, Jamaican Lion female – GCA_012923435.1, Jamaican Lion male – GCA_013030025.1), using TBLASTN. Manual curation of each set of *MLO* genes was performed in each of these genomes, using the same approach described previously for CBDRx. In the process, several frameshifts (mostly small

[1]https://www.ncbi.nlm.nih.gov/genome/annotation_euk/Cannabis_sativa/100/

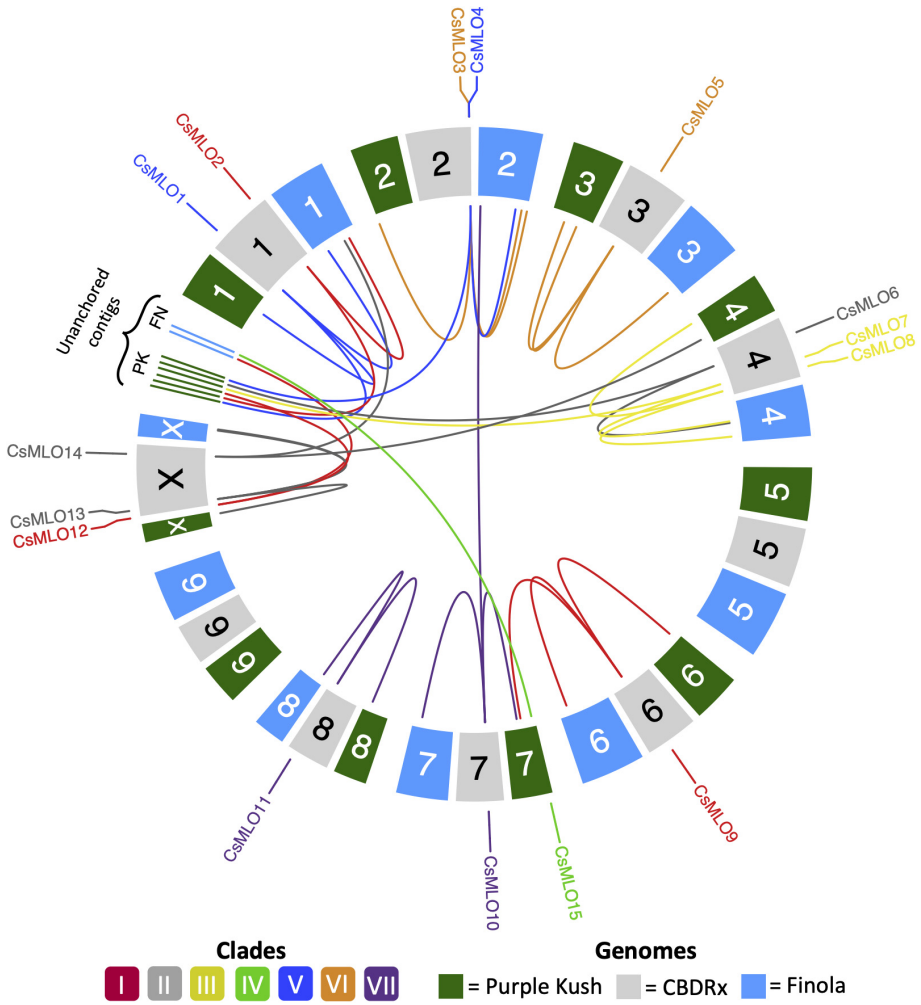

FIGURE 1 | Circular map of *CsMLO* genes identified in the chromosome-level assemblies of CBDRx, Finola, and Purple Kush. All 10 haploid chromosomes (9 autosomes + X chromosome) from each genome are displayed as colored boxes labeled with their respective chromosome number. Homologous chromosomes are grouped together, while unanchored contigs are located between chromosome 1 and chromosome X, grouped per genome. Chromosome numbers represent the "standardized" chromosome numbers, according to whole genome alignments with the CBDRx reference. Color indicate MLO clades, from I to VII. Homology relationships between the three genomes are displayed with solid lines of colors corresponding to each MLO clade. Clade IV *CsMLO* (herein named *CsMLO15*) is absent from the CBDRx assembly.

insertions and deletions) were noted and manually corrected in the coding sequence of multiple *MLOs* in Finola (13 genes) and Purple Kush (7 genes). None of the homologs for these genes showed any frameshift in any other genome. All the frameshifts identified in Finola and Purple Kush were thus examined by comparing their respective coding sequence with available transcriptomic data from the CanSat3 assembly project[2], using BLASTN. Based on evidence from mRNA sequences, all these frameshifts were manually corrected. All of the manually curated *MLO* genes for all five cannabis genomes were ultimately considered as our reference and final set of *Cannabis sativa MLO* (*CsMLO*) genes (**Table 1**, **Supplementary Tables 1–5**, and **Supplementary Files 1–3**). The structure of our final *CsMLO* gene models was compared to their respective genome annotation available on NCBI (CBDRx, Jamaican Lion male and female) (**Supplementary Tables 1–3**).

Chromosomal localization of each manually curated *CsMLO* gene in the chromosome-level genome assemblies, i.e., CBDRx, Finola, and Purple Kush, was displayed on a chromosomal map (**Figure 2**) with the R package Circlize (Gu et al., 2014). As chromosome information is not available for Jamaican Lion female and Jamaican Lion male, those were not considered for this analysis. Chromosome numbers in Finola and Purple Kush were standardized to match the official chromosome numbers in the CBDRx reference genome, using whole genome alignments on the D-Genies platform[3]. This analysis served as a preliminary assessment of synteny for *CsMLO* genes.

[2]http://genome.ccbr.utoronto.ca/downloads.html

[3]http://dgenies.toulouse.inra.fr/

TABLE 1 | Members of the *CsMLO* gene family as predicted and manually curated in the CBDRx genome.

Gene	Clade	Chr.	Strand	Start position	End position	Genomic length (bp)	Exons	Protein length (aa)	TMs[b]	Subcellular localization[c]	Conserved aa/30[d]	Conserved aa/58[e]
CsMLO1-CBDRx	V	1	+	21,631,499	21,636,477	4,979	15	555	7	Cell membrane	28	57
CsMLO2-CBDRx	I	1	–	84,421,095	84,415,528	5,568	15	551	7	Cell membrane	30	58
CsMLO3-CBDRx	VI	2	–	92,590,377	92,584,053	6,325	15	547	7	Cell membrane	25	52
CsMLO4-CBDRx	V	2	+	92,612,089	92,622,483	10,395	15	631	7	Cell membrane	30	56
CsMLO5-CBDRx	VI	3	–	42,556,462	42,507,454	49,009	15	515	7	Cell membrane	30	58
CsMLO6-CBDRx	II	4	–	29,809,460	29,799,903	9,558	14	520	7	Cell membrane	30	57
CsMLO7-CBDRx	III	4	–	65,440,972	65,435,678	5,295	15	549	7	Cell membrane	29	57
CsMLO8-CBDRx	III	4	+	79,070,668	79,074,427	3,760	15	542	7	Cell membrane	30	57
CsMLO9-CBDRx	I	6	+	49,150,225	49,156,766	6,542	15	568	7	Cell membrane	30	57
CsMLO10-CBDRx	VII	7	–	23,870,119	23,830,282	39,838	14	535	7	Cell membrane	30	57
CsMLO11-CBDRx	VII	8	–	51,420,983	51,416,370	4,614	14	583	7	Cell membrane	30	58
CsMLO12-CBDRx	I	X	+	443,359	447,357	3,999	14	558	7	Cell membrane	29	55
CsMLO13-CBDRx	II	X	+	10,840,654	10,844,220	3,567	14	508	7	Cell membrane	30	58
CsMLO14-CBDRx	II	X	+	89,459,459	89,463,372	3,914	12	516	7	Cell membrane	30	56
CsMLO15-CBDRx[a]	IV	N/A	N/A	N/A	N/A	N/A	N/A	N/A	N/A	N/A	N/A	N/A

[a] *CsMLO15-CBDRx is not predicted in the CBDRx genome, as compared to the other four genomes analyzed.*
[b] *Number of transmembrane domains (TMs) in the predicted protein, as determined by the CCTOP online prediction server (Dobson et al., 2015).*
[c] *Subcellular localization as predicted by three online prediction servers: Plant-mPLoc (Chou and Shen, 2010), YLoc-HighRes (Briesemeister et al., 2010), and DeepLoc 1.0 (Almagro Armenteros et al., 2017).*
[d] *Number of conserved amino acids out of the 30 identified in Elliott et al. (2005).*
[e] *Number of conserved amino acids out of the 58 identified in Kusch et al. (2016).*

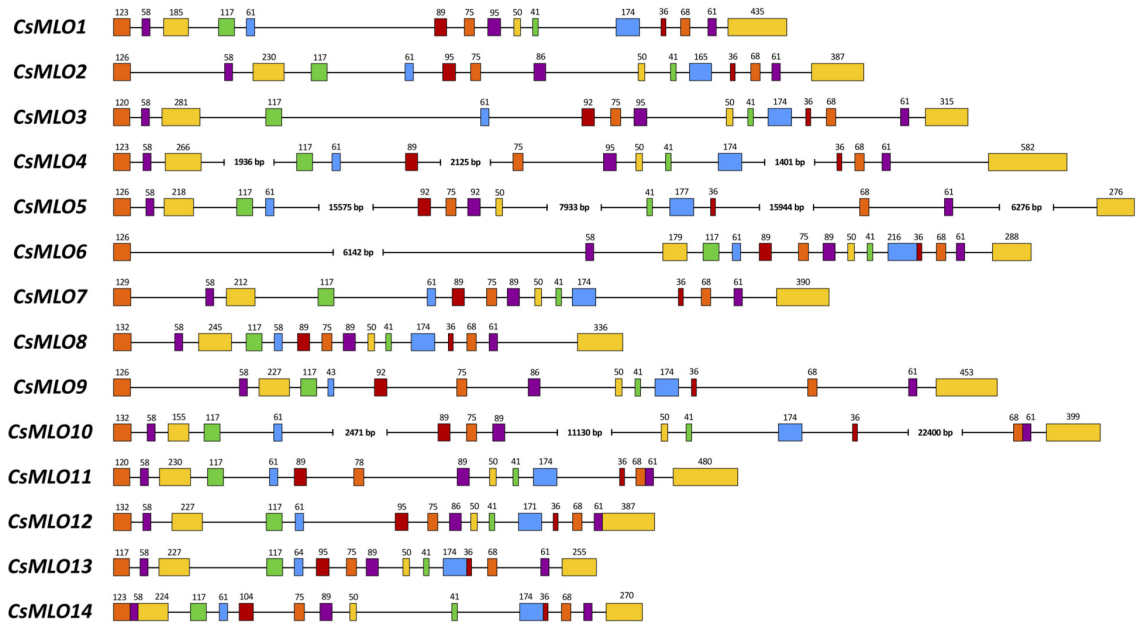

FIGURE 2 | Intron–exon organization of the 14 manually curated *CsMLO* genes identified in the CBDRx genome. Exons are shown as rectangles and introns as lines. The exon color code simply allows demonstrating exon conservation across all sequences. The numbers above exons indicate the exon's length (bp). Note that the STOP codon (3 bp) is included in the last exon's length. Sequences exhibiting one or several large introns are severed where necessary (i.e., *CsMLO4*, *CsMLO5*, *CsMLO6*, and *CsMLO10*) and are therefore not drawn to scale.

Gene and Protein Characterization

The protein sequences from the five genomes were analyzed through several online prediction servers in order to identify functional domains (InterProScan, Jones et al., 2014), transmembrane domains (CCTOP, Dobson et al., 2015), subcellular localizations (Plant-mPLoc, Chou and Shen, 2010; DeepLoc 1.0, Almagro Armenteros et al., 2017; YLoc-HighRes, Briesemeister et al., 2010), signal peptide (SignalP 5.0, Almagro Armenteros et al., 2019a), calmodulin-binding domains (CaMELS, Abbasi et al., 2017) as well as mitochondrial,

chloroplast, and thylakoid luminal transit peptide (TargetP 2.0, Almagro Armenteros et al., 2019b). Conserved amino acids described in Elliott et al., 2005 (30 invariant amino acids) and Kusch et al., 2016 (58 highly conserved amino acids) were screened in all *CsMLO* sequences using our final protein alignment (**Supplementary File 3**). Our manually curated *MLO* gene models in the five cannabis genomes were also screened for conserved *cis*-acting elements in the promoter regions. A homemade Python script (v.3.7.3, Van Rossum and Drake, 2009) was used to extract a 2 kb upstream region of each *CsMLO* gene, and these promoter regions were used as search queries in the plantCARE database (Lescot et al., 2002).

Phylogenetic Analysis

Amino acid sequences for all manually curated CsMLOs from CBDRx, Jamaican Lion female and male, Purple Kush and Finola were aligned together with MLO sequences previously identified in *Arabidopsis thaliana* (AtMLOs, as indicated in Devoto et al., 2003), *Vitis vinifera* (grapevine: VvMLOs, as indicated in Feechan et al., 2008), *Prunus persica* (peach: PpMLOs, as indicated in Pessina et al., 2014), *Hordeum vulgare* (barley: HvMLOs, as indicated in Kusch et al., 2016) and *Zea mays* (maize: ZmMLOs, as indicated in Kusch et al., 2016). *Chlamydomonas reinhardtii* MLO (XP_001689918) was used as an outgroup. Alignment of protein sequences was performed using MAFFT v7.407_1 (Katoh and Standley, 2013) with default parameters within NGPhylogeny.fr (Lemoine et al., 2019) and used to construct phylogenetic trees. A first tree was constructed using PhyML+SMS v1.8.1_1 (Lefort et al., 2017) with default parameters within NGPhylogeny.fr (**Figure 3**), and a second tree was constructed using MrBayes v3.2.6_1 (Huelsenbeck and Ronquist, 2001) with default parameters within NGPhylogeny.fr (**Supplementary Figure 1**). PhyML+SMS implements SMS (Smart Model Selection) that uses a heuristic approach for model selection. The trees were interpreted and visualized using iTOL (Letunic and Bork, 2019). All MLO proteins identified were classified into clades based on previous phylogenetic analyses (Kusch et al., 2016).

Transcriptional Activity of *CsMLOs* in Response to Powdery Mildew Infection

Sampling and RNA Sequencing

An RNA-seq time series analysis of the infection of cannabis by PM was performed to characterize the transcriptional response of *CsMLO* genes. The experiment was conducted in a controlled environment at Organigram Inc., a Health Canada approved licensed producer (Moncton, New-Brunswick, Canada). Cannabis fan leaves from 4-week-old vegetative plants ('Pineapple Express,' drug-type I) were manually inoculated with *G. ambrosiae* emend. (including *G. spadiceus*) spores. Heavily infected leaves, loaded with fungal spores, were scraped against the surface of the leaves from the 4-week-old plants to induce infection. Leaf samples (punch holes) were taken at five time points during the infection (n = 3 per time point): day zero (T0), 6 h post-inoculation (6H), 1 day post-inoculation (1D), 3 days post-inoculation (3D) and 8 days post-inoculation (8D). RNA samples were extracted from leaf tissues using the RNeasy® Plant Mini Kit (QIAGEN, Hilden, Germany) following the standard manufacturer's protocol. Each mRNA extraction was treated with QIAGEN's RNase-Free DNase Set (QIAGEN, Hilden, Germany), involving a first round of the TURBO DNA-free™ DNA Removal Kit through the extraction protocol and then two rounds of the DNA-free™ Kit (Life Technologies, Carlsbad, CA, United States). Fifteen individual RNA-seq libraries were generated for the five time points sampled (n = 3 per time point). cDNA libraries were sequenced on a total of six lanes, using the Illumina HiSeq v4 technology (PE 125 bp) at the Centre d'expertise et de services Génome Québec (Montreal, QC, Canada). In total, ∼200 Gb of raw sequencing data were generated, which represents 1.728 billion of 2 × 125 bp paired-end sequences distributed across all 15 libraries (BioProject accession: PRJNA738505, SRA accessions: SRR14839036-50).

Short-Read Alignment on the Reference Genome and Differential Gene Expression

Raw sequencing reads were cleaned, trimmed, and aligned on the same reference genome as the one initially used to find our final *MLO* gene models (CBDRx) to estimate changes in transcript-specific levels of expression over the course of the infection. Specifically, mild trimming thresholds were applied to clean and trim all raw reads, using Trimmomatic v.0.34 (Bolger et al., 2014) with the following parameters: ILLUMINACLIP:$VECTORS:2:30:10, SLIDINGWINDOW:20:2, LEADING:2, TRAILING:2, MINLEN:60. The cleaned reads from our 15 individual libraries were aligned on the CBDRx reference genome using STAR v.2.7.6 (Dobin et al., 2013) in genome mode with default parameters and the official NCBI Cannabis annotation release 100 associated with the genome. Genome-wide raw read counts were obtained for each library using htseq-count v.0.11.1 (Anders et al., 2015) with the 'intersection-non-empty' mode.

Downstream analyses of differential gene expression patterns were conducted using the R packages 'limma-voom' (Law et al., 2014) and edgeR (Robinson et al., 2010) in RStudio v.1.3.1073 (RStudio Team, 2020). Reference sequences with insufficient sequencing depth were filtered out by keeping only the ones with more than five Counts Per Million (CPM) in at least three samples. This mild CPM threshold allowed the filtering of very low coverage genes without losing too much information in the dataset. This filtered dataset was normalized using the Trimmed Mean of M-values (TMM) method implemented in edgeR. A transformation of the data was then performed using the 'limma-voom' function, which estimates the mean-variance relationship for each transcript, allowing for better and more robust comparisons of gene expression patterns across RNA-seq libraries (Law et al., 2014). Each transcript was finally fitted to an independent linear model with $\log_2$(CPM) values as the response variable and the time point (0, 6 h, 24 h, 3 days, and 8 days post-infection) as the explanatory variable. All linear models were treated with limma's empirical Bayes analysis pipeline (Law et al., 2014). Differentially expressed genes were chosen based on a False Discovery Rate (FDR, Benjamini–Hochberg procedure) < 0.05. Genomic regions corresponding to the curated CBDRx *MLO*

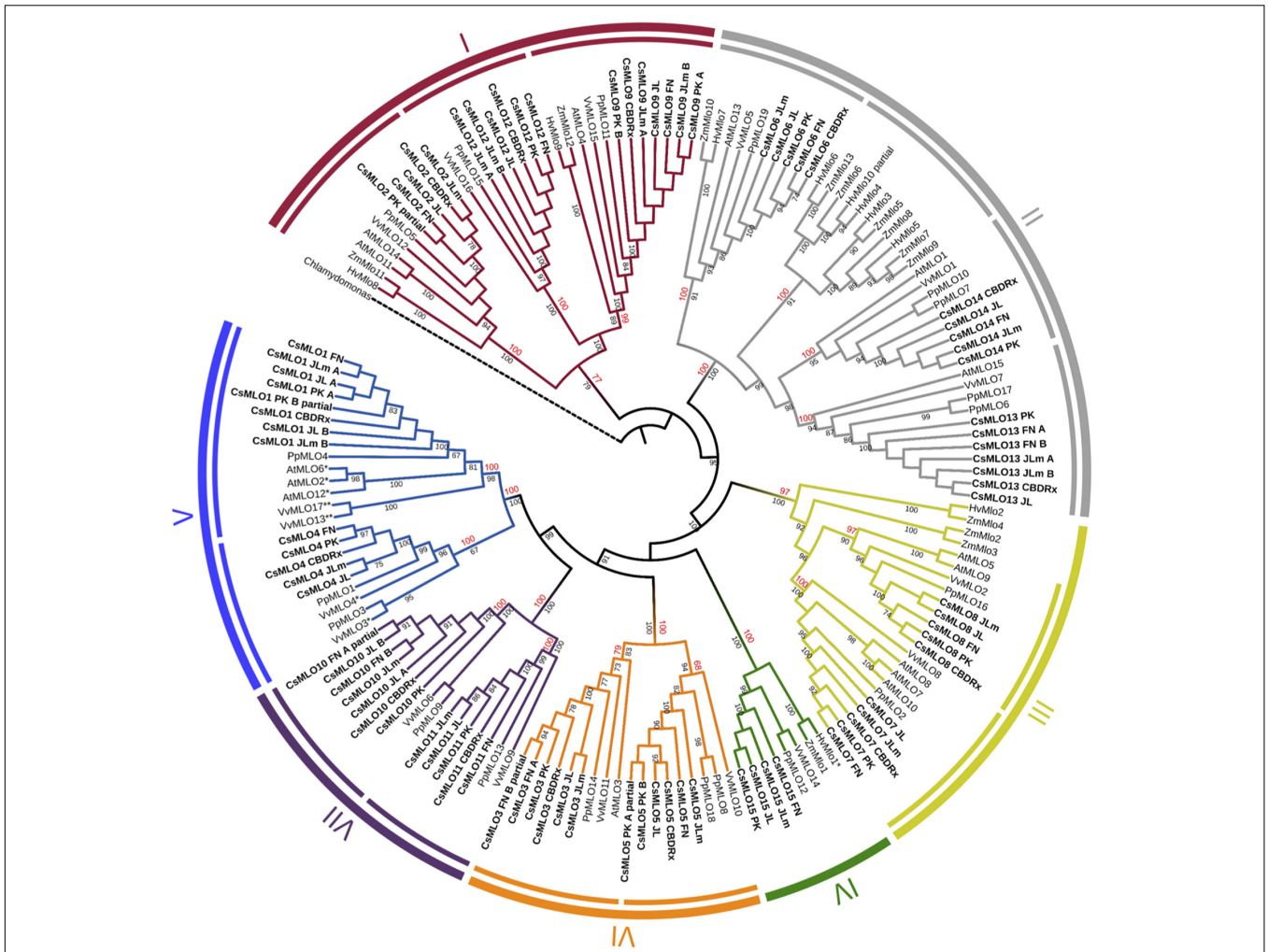

FIGURE 3 | Phylogenetic relationships of CsMLOs based on maximum likelihood analysis. Phylogenetic tree of manually curated CsMLO proteins (bold) with MLO proteins from selected species (*Arabidopsis thaliana*, *Prunus persica*, *Vitis vinifera*, *Hordeum vulgare*, and *Zea mays*). *Chlamydomonas reinhardtii* was used as an outgroup. Phylogenetic relationships were estimated using the maximum likelihood method implemented in PhyML + SMS with 1,000 bootstrap independent replicates. The seven defined clades are indicated, as well as potential subclades identified in this study (inner circles). Number on a node indicates the percentage of bootstrap when higher than 65% (black), or the posterior probabilities of major clades and subclades, according to a Bayesian phylogenetic inference performed on the same alignment (red) (**Supplementary Figure 1**). MLOs with one asterisk (*) have been experimentally demonstrated to be required for PM susceptibility (Büschges et al., 1997; Feechan et al., 2008; Wan et al., 2020), while MLOs with two asterisks (**) have been identified as main probable candidates for PM susceptibility (Pessina et al., 2016).

gene models were extracted from the output of edgeR/limma-voom for each comparison made (i.e., each time point compared to T0) and looked for significant gene expression differences among *MLO* genes (FDR < 0.05). These expression differences in *MLOs* over the course of the infection were visualized in RStudio v.1.3.1073 (RStudio Team, 2020) on a scatter plot using CPM values (**Figure 4** and **Supplementary Figure 2**).

Cloning of Clade V *CsMLOs* for Transient Expression in *Nicotiana benthamiana* and Confocal Microscopy

The two selected *MLO* gene sequences (*CsMLO1* and *CsMLO4*) were synthesized commercially into the Gateway-compatible vector pDONR^{TM}/Zeo (Invitrogen, Carlsbad, CA, United States) (Hartley et al., 2000). The entry vectors were inserted into *Escherichia coli* OneShot® TOP10 cells (Invitrogen, Carlsbad, CA, United States) by chemical transformation according to the manufacturer's instructions. Positive colonies were selected, and plasmid DNA was extracted with the EZ-10 Spin Column Plasmid DNA Miniprep Kit (Bio Basic Inc., Markham, ON, Canada). The extracted entry vectors were confirmed by PCR with the primers M13-F (5′-GTAAAACGACGGCCAGT-3′) and M13-R (5′-CAGGAAACAGCTATGAC-3′) as well as M13-F and MLO1_1-R (5′-ATGTGCCATTATAAATCCATGCCT-3′, this study).

The Gateway-compatible destination vector chosen was pB7FWG2.0, which is under the regulation of the 35S Cauliflower

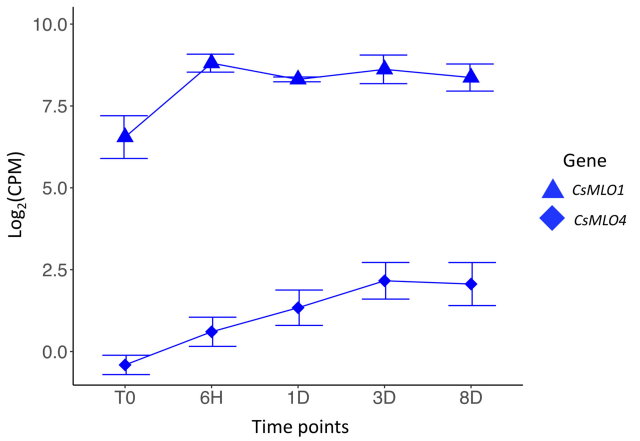

FIGURE 4 | Transcriptomic response of clade V *CsMLO* genes following inoculations with powdery mildew. Time series analysis of the infection of *Cannabis sativa* leaves by PM, showing average gene expression for *CsMLO1* (blue triangles) and *CsMLO4* (blue diamonds). Gene expression is displayed on the *y*-axis as the average logarithmic value of the Counts Per Million [$\log_2$(CPM)] at each time point (displayed on the *x*-axis, $n = 3$ per time point). Time points: no infection/control (T0), 6 h post-inoculation (6H), 24 h post-inoculation (1D), 3 days post-inoculation (3D), and 8 days post-inoculation (8D). Error bars at each time point represent the standard deviation (SD).

Mosaic Virus (CaMV) promoter and harbors the plant selectable marker gene *bar* (bialaphos acetyltransferase), which confer resistance against glufosinate ammonium. It also possesses a streptomycin and spectinomycin resistance gene for plasmid selection, and an EGFP-fusion in C-terminal, for visualization by confocal microscopy (Karimi et al., 2002). According to the manufacturer's instructions, the destination vector was inserted into *Escherichia coli* One Shot® ccdB Survival™ cells (Life Technologies) by chemical transformation. Positive colonies were selected, and plasmid DNA was extracted with the EZ-10 Spin Column Plasmid DNA Minipreps Kit (Bio Basic Inc., Markham, ON, Canada). The extracted destination vectors were confirmed by PCR with the primers T-35S-F (5′-AGGGTTTCTTATATGCTCAACACATG-3′, Debode et al., 2013) and EGFP-C (5′-CATGGTCCTGCTGGAGTTCGTG-3′).

The two synthesized MLO gene sequences were then inserted into the vector pB7FWG2.0 through an LR clonase reaction following the manufacturer's instructions (Invitrogen, Carlsbad, CA, United States). Plasmids were then transferred to *E. coli* OneShot® TOP10 cells (Invitrogen, Carlsbad, CA, United States) by chemical transformation according to the manufacturer's instructions. Positive colonies were selected, and plasmid DNA was extracted with the EZ-10 Spin Column Plasmid DNA Minipreps Kit (Bio Basic Inc., Markham, ON, Canada). The extracted expression vectors were amplified by PCR with the primers 35S Promoter (5′-CTATCCTTCGCAAGACCCTTC-3′) and MLO1_1-R as well as MLO2_3-F (5′-TCTTTCAGAATGCATTTCAACTTGC-3′, this study) and EGFP-N (5′-CGTCGCCGTCCAGCTCGACCAG-3′). Sequencing of the PCR products above was performed to confirm the junction between the plasmid and the inserted gene and the junction between the inserted gene and the GFP, respectively.

The recombinant vectors were then transferred to *Agrobacterium tumefaciens* ElectroMAX™ LBA4404 cells by electroporation (Invitrogen, Carlsbad, CA, United States). The expression vector in *A. tumefaciens* was confirmed by PCR using the primers 35S Promoter and MLO1_1R and MLO2_3-F + EGFP-N. Cultures of transformed *A. tumefaciens* (*CsMLO1* and *CsMLO4*) were incubated with agitation at 28°C in LB broth containing spectinomycin (100 mg/mL) for 24 h. The cultures were then centrifuged at 5,000 × *g* for 5 min, the supernatant was discarded, and the pellet was resuspended in $MgCl_2$ (10 mM). The cells were brought to an OD_{600} of 0.5 and incubated at room temperature for 2 h with acetosyringone (200 μM). *Nicotiana benthamiana* plants, about 2 weeks old, were watered a few hours before infiltration, and the bacterial suspensions were administered using sterile 1 mL syringes (without needles) on the abaxial surface of the leaves. The plants were then returned to growth chambers, and the observation of epidermal cells was performed 3 days after infiltration using a confocal laser scanning microscope. Leaves were observed under a Leica TCS SP8 confocal laser scanning microscopy (Leica Microsystems). Images were observed through an HC PL APO CS2 40X/1.40 oil immersion objective at excitation/emission wavelengths of 488/503–521 nm.

In silico Screening of Clade V *CsMLO* Sequence Variants in 32 Cannabis Cultivars

Thirty-one distinct drug-type *Cannabis sativa* cultivars from Organigram Inc. (Moncton, NB, Canada) and one industrial hemp variety ('Anka,' UniSeeds, obtained from Céréla, Saint-Hughes, Québec, Canada) were screened to identify potential polymorphisms in clade V *CsMLOs* that could be associated with increased susceptibility or resistance to PM. Raw sequencing files (Illumina paired-end 125 bp) from these 32 cultivars (BioProject accession: PRJNA738519, SRA accessions: SRR14857079-110) were aligned on the reference CBDRx genome using 'speedseq' v.0.1.2 (Chiang et al., 2015). 'bcftools view' v.1.10.2 (Li, 2011) was used on the raw BAM alignment files to extract the genomic regions corresponding to the two clade V *CsMLO* genes, based on the positions of our manually curated CBDRx *MLO* gene models. Genotypes in these two *CsMLOs* were called for Single Nucleotide Polymorphisms (SNPs) and small insertions and deletions (INDELs) across the 32 cannabis cultivars using 'bcftools mpileup' v.1.10.2 (Li, 2011). Variants with a mapping quality <20 and/or with a read depth >500× were filtered out, and allelic frequencies for each variant were extracted using an in-house Python script (v.3.7.3, Python Software Foundation, 2020). Next, SNPGenie v.1.0 (Nelson et al., 2015) was used to estimate the ratio of non-synonymous to synonymous polymorphisms in the two clade V *CsMLO* genes across all 32 cultivars. Based on the output from SNPGenie, genomic positions of all non-synonymous polymorphisms found in the two genes were extracted using an in-house Python script (v.3.7.3, Python Software Foundation, 2020). Visual representations of these

polymorphisms at the gDNA and amino acid levels were prepared using Microsoft© PowerPoint v.16.49 (Microsoft Corporation, Redmond, WA, United States).

RESULTS

CsMLO Gene Identification and Genomic Localization

Through careful manual curation, we were able to identify a total of 14, 17, 19, 18 and 18 distinct *CsMLO* genes in the genomes of CBDRx, Jamaican Lion female, Jamaican Lion male, Purple Kush, and Finola, respectively. Our final manually curated *CsMLO* genes were numbered 1–15 based on chromosomal positions in CBDRx, from chromosome 1 through chromosome X (**Table 1**, **Supplementary Tables 1–5**, and **Supplementary Files 1–3**). *CsMLO* gene numbers and IDs in all four other genomes (Finola, Jamaican Lion female, Jamaican Lion male, Purple Kush) were based on homology relationships, supported by our phylogenetic and orthology analyses (see the section "Materials and Methods" for details). We also physically located each set of *CsMLO* genes on the chromosomes of CBDRx, Finola and Purple Kush (**Figure 1**). Our results show that eight of the 10 chromosomes harbor evenly spaced *CsMLO* genes, chromosomes 5 and 9 being the only ones not carrying *MLO* genes. We were able to anchor all 14 CBDRx *CsMLO* genes on their respective chromosomes, while two (*CsMLO12-FN*, *CsMLO15-FN*) and six (*CsMLO1-PK_B*, *CsMLO2-PK*, *CsMLO4-PK*, *CsMLO6-PK*, *CsMLO7-PK*, *CsMLO12-PK*) *MLO* genes were located on unanchored contigs in Finola and Purple Kush, respectively (**Supplementary Figure 1**, **Table 1**, and **Supplementary Tables 1, 4, 5**). The CBDRx genome showed an absence of *MLO15*, while this gene was present in all other cannabis genomes. We identified homology and paralogy relationships among all *CsMLO* sequences, which revealed potential duplication patterns in certain genomes. Overall, we detected paralogs for *CsMLO1*, *CsMLO5*, *CsMLO9*, *CsMLO10*, *CsMLO12* and *CsMLO13* in the genomes of Finola, Purple Kush, Jamaican Lion male and Jamaican Lion female (*CsMLO* paralogs were designated with A/B suffixes, see **Table 1** and **Supplementary Tables 1–5**). CBDRx remained the only genome in which we did not identify *CsMLO* paralogs. Most of the *CsMLO* genes had syntenic positions across all three chromosome-level genome assemblies, with the exception of *CsMLO9*, *CsMLO10* and *CsMLO14* (**Figure 1**). *CsMLO14* was the only *CsMLO* gene identified across all five genomes that had three different locations in the three genomes, i.e., chromosome X in CBDRx, chromosome 1 in Finola and chromosome 4 in Purple Kush. Partial/incomplete genes were also noted in the genomes of Finola (*CsMLO3-FN-B* and *CsMLO10-FN-A*) and Purple Kush (*CsMLO1-PK-B*, *CsMLO2-PK* and *CsMLO5-PK-A*).

CsMLO Gene Structure and Protein Characterization

Manually curated *CsMLO* genes identified in CBDRx ranged in size between 3,567 bp (*CsMLO14-CBDRx*) and 49,009 bp (*CsMLO5-CBDRx*), with an average size of 11,240 bp and a median size of 5,431 bp (**Table 1** and **Supplementary Tables 1–5**). The structural organization of these *CsMLO* genes is depicted in **Figure 2**. The number of exons varied between 12 and 15, with some of the exons showing signs of fusion in certain genes (**Figure 2**). The number of amino acid residues in these *CsMLO* gene sequences varied between 509 and 632. Intron size varied considerably, with 11 introns belonging to four different *CsMLO* genes (*CsMLO4*, *CsMLO5*, *CsMLO6*, *CsMLO10*) exhibiting a length greater than 1,000 bp. *CsMLO5* had the longest introns: intron 5 (15.6 kb), intron 9 (7.9 kb), intron 12 (15.9 kb), and intron 14 (6.3 kb) (**Figure 2**). The *CsMLO* genes that we characterized in the four other genomes (Finola, Jamaican Lion female and male, Purple Kush) were consistently similar to the ones identified in CBDRx in terms of length, intron and exon structural organization and genomic localization (**Supplementary Files 1–3**). The longest *CsMLO* gene characterized among all our manually curated gene models belonged to Jamaican Lion (female), with a total length of 49,673 nucleotides (*CsMLO5-JL*).

Proteins encoded by all identified *CsMLO* genes comprised seven transmembrane domains (TMs) of similar lengths (**Table 1** and **Supplementary Tables 1–5**). The only exceptions were found in the genomes of Finola and Purple Kush in which we identified a total of four partial *CsMLO* genes, for which encoded proteins harbored less than seven TMs: CsMLO3-FN-B (five TMs), CsMLO10-FN-A (three TMs), CsMLO1-PK-B (four TMs), CsMLO5-PK-A (six TMs). Similarly, all identified CsMLO proteins were predicted to be localized in the cell membrane by several online prediction servers, such as Plant-mPLoc (Chou and Shen, 2010), DeepLoc 1.0 (Almagro Armenteros et al., 2017), and YLoc-HighRes (Briesemeister et al., 2010; **Table 1** and **Supplementary Tables 1–5**). Three partial/incomplete sequences were also predicted to localize elsewhere, such as the chloroplasts and nucleus by Plant-mPLoc for CsMLO1-PK-B, and the endoplasmic reticulum by DeepLoc 1.0 for CsMLO5-PK-A and CsMLO3-FN-B. We assumed that these three predictions were unreliable as they were made using incomplete sequences and not present unanimously throughout all prediction servers. No signal peptide (SignalP 5.0, Almagro Armenteros et al., 2019a), mitochondrial transit peptide, chloroplast transit peptide, or thylakoid luminal transit peptide (TargetP 2.0, Almagro Armenteros et al., 2019b) were predicted in any of the CsMLO protein sequences (results not shown). The invariable 30 amino acid residues previously described in Elliott et al. (2005) were identified in all CsMLOs (**Table 1** and **Supplementary Tables 1–5**). Across all identified CsMLOs (excluding the five partial sequences), the amount of conserved amino acids varied between 25 and 30, and 74.1% (60/81) of CsMLO sequences possessed all 30 amino acids. In Kusch et al. (2016), a larger dataset of MLO proteins was analyzed and thus identified 58 highly conserved amino acids, rather than invariant, showing that substitutions are possible. These 58 amino acid residues were also screened in all CsMLOs (**Table 1** and **Supplementary Tables 1–5**). Across all identified CsMLOs (excluding the five partial sequences), the amount of conserved amino acids varied between 52 and 58, and only

23.5% (19/81) of CsMLO sequences possessed all 58 amino acids. However, 74.1% (60/81) possessed 57 or more of the conserved amino acids.

Phylogenetic Analysis of CsMLOs

We performed a phylogenetic analysis on the curated cannabis MLO proteins identified among the five genomes (CsMLOs). The dataset was completed with the MLO protein family from *Arabidopsis thaliana* (AtMLOs, Devoto et al., 2003), *Prunus persica* (PpMLOs, Pessina et al., 2014), *Vitis vinifera* (VvMLOs, Feechan et al., 2008), *Hordeum vulgare* and *Zea mays* (HvMLOs and ZmMLOs, Kusch et al., 2016), using the *Chlamydomonas reinhardtii* MLO as the outgroup. Phylogenetic tree construction was performed using the PhyML + SMS algorithm, which confirmed the seven known clades of MLO proteins (**Figure 3**), with bootstrap values equal or greater than 97% (except for clade I, supported with a bootstrap value of 77%). Clade numbers from I to VII were assigned according to the previous study of Kusch et al. (2016). Previous studies have reported the presence of an eighth clade (e.g., Pessina et al., 2014), clustering with clade VII in other papers. Here, we followed the seven clades nomenclature, but this potential eighth clade would correspond to one of the two clade VII subclades. Indeed, potential subclades were also identified in our study, indicated as separate lines in the inner circle of **Figure 3**, which were also supported with high values of bootstrap (equal or greater than 83%, with the exception of one clade V subclade, supported with a value of 67%). The same clades and subclades were also found to be supported by high posterior values equal or greater than 77% (indicated in red), following phylogenetic tree construction using MrBayes (also see **Supplementary Figure 1**). Apart from one clade II subclade that appeared monocot-specific, all subclades depicted here included CsMLOs, as well as PpMLOs and VvMLOs. In each subclade, all CsMLOs clustered together with bootstrap values of 100. Two subclades were found in the phylogenetic clade V, containing all the dicot MLO proteins experimentally shown to be required for PM susceptibility (Acevedo-Garcia et al., 2014). In one of those clade V subclades, three of the cannabis genomes were found to harbor two near-identical genes. All cannabis genomes except CBDRx were found to include one *MLO* gene grouping with clade IV, which contains all monocot MLO proteins acting as PM susceptibility factors (**Figure 3**).

Transcriptional Reprogramming of Cannabis *MLOs* in Response to *Golovinomyces ambrosiae* Infection

We conducted an RNA-seq analysis to look at the transcript abundance of *CsMLO* genes in leaves of the susceptible cannabis cultivar "Pineapple Express" during infection by *G. ambrosiae* emend. (including *G. spadiceus*). Five time points were investigated, corresponding to key stages of the infection: 0 (control), 6 h post-inoculation (hpi) (conidia germination and appressoria formation), 24 hpi (haustoria formation), 3 days post-inoculation (dpi) (secondary hyphae formation), and 8 dpi (secondary haustoria, secondary appressoria and conidiophore/conidia formation). No significant expression was detected at any time point for *CsMLO6*, *CsMLO8*, *CsMLO11*, and *CsMLO15* (in this particular case, reads were aligned to the genome of Jamaican Lion male, as the CBDRx genome is devoid of *CsMLO15*). While *CsMLO3* and *CsMLO11* were expressed, no up- or down-regulation was observed under our conditions. Nine genes, namely *CsMLO1*, *CsMLO2*, *CsMLO4*, *CsMLO5*, *CsMLO7*, and *CsMLO9* were found to be significantly differentially expressed (FDR < 0.05) after inoculation with the pathogen (**Figure 4** and **Supplementary Figure 2**). In the case of clade V genes, *CsMLO1* showed a peak of 2.23-fold up-regulation at 6 hpi (FDR = 2.83×10^{-4}), and remained somewhat constant for the remaining of the infection, while the expression of *CsMLO4* increased steadily between T0 and 3 dpi, reaching a peak of 2.02-fold up-regulation (when compared to T0) and remained constant at 8 dpi (FDR = 7.87×10^{-4}).

An analysis of the 2 kb upstream region of all *CsMLO* genes identified through the five cannabis genomes revealed the presence of key regulatory motifs with functions related to environmental/hormonal response (e.g., ABRE, AuxRR-core, ERE, GARE, P-box, TATC-box, TGA-element, GT1-motif, G-box, light response elements), stress and defense response (TC-rich repeats, MBS, ARE, GC-motif, LTR element), developmental regulation (circadian, HD-Zip, CCAAT-box, MSA-like), seed-specific metabolism (O2-site, RY-element) and wound response (WUN-motif). In total, 82 (95%) *CsMLO* genes had at least one motif related to environmental/hormonal response, while 80 (93%) *CsMLO* genes had a MYB-related sequence, a motif typically involved in development, metabolism and responses to biotic and abiotic stresses (Dubos et al., 2010; **Supplementary Table 6**). We found the presence of at least one *cis*-acting element involved in gene overexpression by biotic and abiotic factors (ABRE, CGTCA, TGACG, TCA) in 100% of the 13 *CsMLO* genes from clade V identified in all five genomes. The analysis of protein domains, their location in the protein and the overall topology of each gene ultimately revealed a consistent pattern among all *CsMLO* genes.

Subcellular Localization of Clade V *CsMLOs*

The subcellular localization of clade V MLOs, such as CsMLO1 and CsMLO4, was first analyzed using online tools. As mentioned previously, these analyses predicted that CsMLO1 and CsMLO4 possessed seven transmembrane domains and were localized in the plasma membrane (**Table 1** and **Supplementary Tables 1–5**). To determine the subcellular localization of CsMLO1 and CsMLO4 *in planta*, we constructed two vectors under the control of the CaMV 35S promoter where the coding sequences of CsMLO1 and CsMLO4 were fused to enhanced green fluorescent protein (EGFP) in C-terminal (*35S::CsMLO1-EGFP* and *35S::CsMLO4-EGFP*). The agroinfiltration-based transient gene expression system was used to transform *Nicotiana benthamiana* leaves with each construct. The epidermal cells were observed 3 days after transformation for GFP signal using confocal laser scanning microscopy. The CsMLO1-EGFP fusion protein was observed in the cell periphery as well as throughout

the cell forming networks in a punctuate pattern, while the CsMLO4-EGFP fusion protein was observed solely in the cell periphery in a defined way (**Figure 5**).

Polymorphism Analysis of Clade V *CsMLOs* Among 32 Cultivars

Comparison of 32 distinct cannabis cultivars to the CBDRx reference genome to detect polymorphisms in *CsMLO* clade V genes revealed a total of 337 (*CsMLO1*, 101 indels and 236 SNPs) and 852 (*CsMLO4*, 154 indels and 698 SNPs) polymorphisms, mainly located in the last cytosolic loop of the protein, near the C-terminus. Among these polymorphic loci, we identified 14 and 12 non-synonymous SNPs for *CsMLO1* and *CsMLO4*, respectively (**Supplementary Table 7**). The only SNP that was not located near the C- or N-terminus was found in *CsMLO1*, in the second cytoplasmic loop. All other SNPs in *CsMLO1* were distributed in the first cytoplasmic loop (three non-synonymous SNPs), the second extracellular loop (four non-synonymous SNPs) and the last cytoplasmic loop, near the C-terminus (six non-synonymous SNPs, **Figure 6**). The scenario for *CsMLO4* is slightly different, with a single non-synonymous SNP identified in the second extracellular loop and the remaining 11 SNPs all located in the last cytoplasmic loop, near the C-terminus (**Figure 6**). About half of these non-synonymous SNPs in both genes induced a change in amino acid charges or polarity, with seven (50%) and five (42%) SNPs having a change in electric charges in *CsMLO1* and *CsMLO4*, respectively. None of the SNPs identified in either of the two *CsMLO* clade V genes had an impact on conserved amino acids in the proteins (Elliott et al., 2005; Kusch et al., 2016). Overall, allele frequencies associated with these SNPs in *CsMLO1* and *CsMLO4* showed an even distribution of reference and alternate alleles throughout the 32 cultivars. There was one exception with 'Ultra Sour,' which was identified as the only homozygous cultivar for the alternate allele in three non-synonymous SNPs found in exons 1 (G40E) and 3 (P96Q, P111T).

DISCUSSION

Considering the role of specific *MLO* genes in flowering plants' susceptibility to PM, one of the most prevalent pathogens in indoor cannabis productions (Punja et al., 2019), our primary goal was to structurally and functionally characterize this gene family at a manual-curation level in multiple cannabis genomes. In order to develop mitigation strategies aimed at reducing the deleterious impacts of the pathogen on cannabis production, and in an attempt to better understand other functional roles of *CsMLOs*, the first step consisted in identifying the exact number and structure of these genes in different genetic backgrounds. Our results first showed that *CsMLO* numbers are variable across different cannabis types. Second, they showed that two distinct clade V genes were present in all genomes (with paralogs in

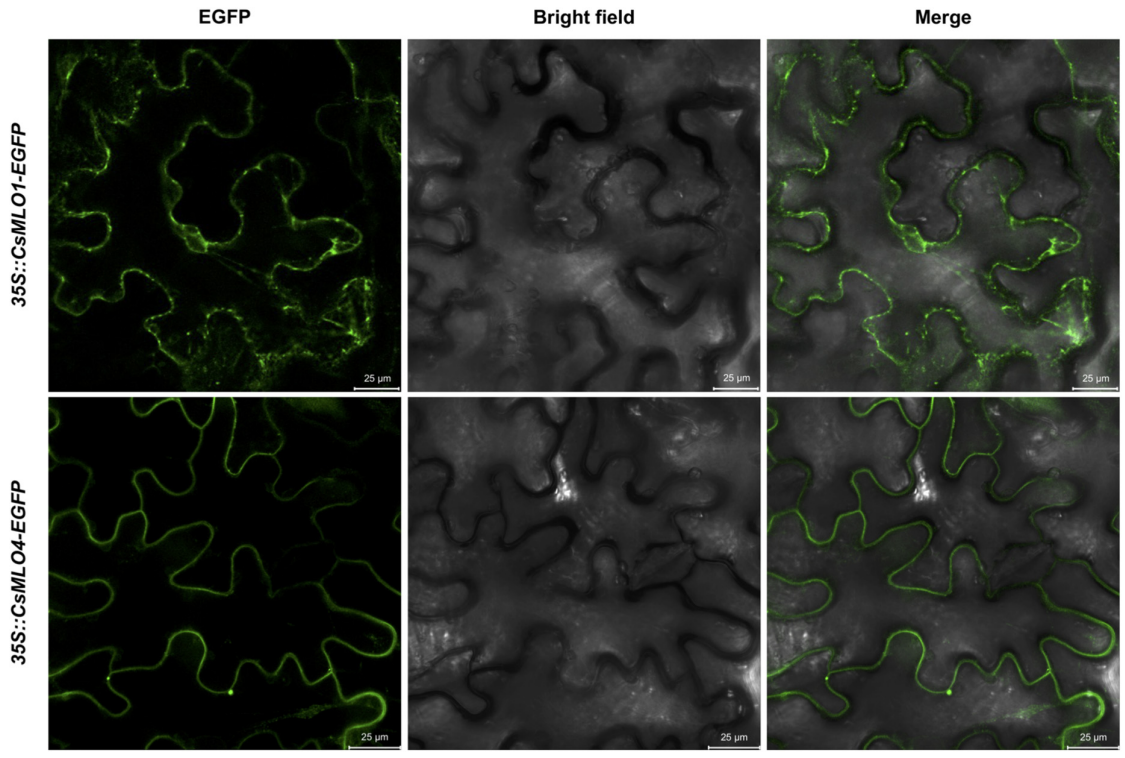

FIGURE 5 | Subcellular localization of *CsMLO1* and *CsMLO4* as observed by confocal laser scanning microscopy. Transient expression of *35S::CsMLO1-EGFP* and *35S::CsMLO4-EGFP* constructs in *Nicotiana benthamiana* leaf epidermal cells shown 3 days after agro-infiltration. Scale bars = 25 µm.

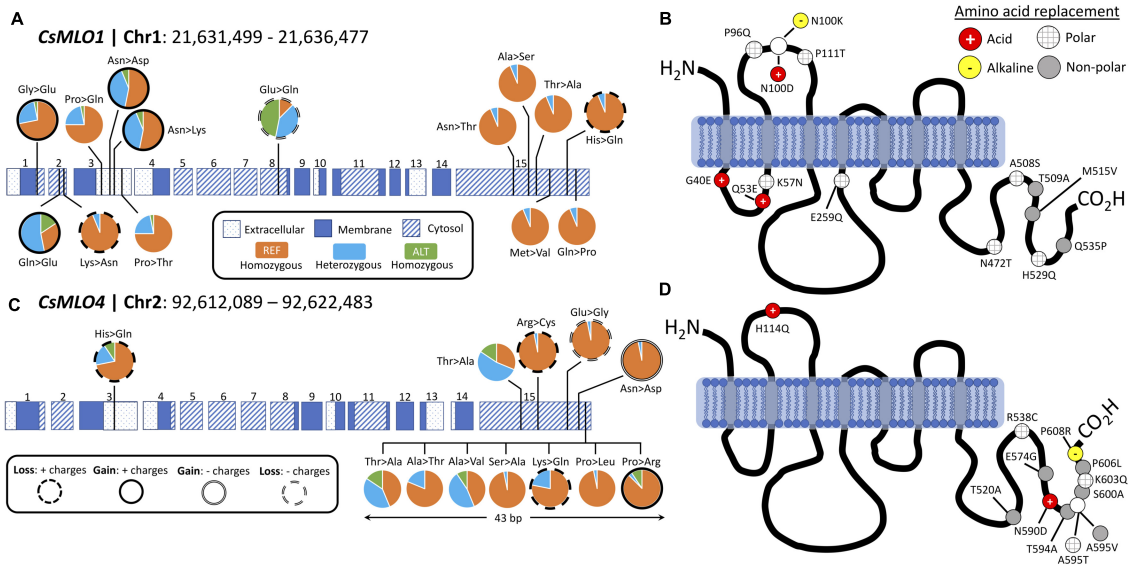

FIGURE 6 | Protein structure and polymorphism analysis of the two clade V genes (*CsMLO1* and *CsMLO4*) in 32 distinct cannabis cultivars aligned against the CBDRx reference genome. Panels A and B exhibit all non-synonymous nucleic acid substitutions **(A)** and amino acid replacements **(B)** identified in *CsMLO1* (located on chromosome 1) from 32 hemp and drug-type cannabis cultivars. Panels **(C,D)** exhibit all non-synonymous nucleic acid substitutions **(C)** and amino acid replacements **(D)** identified in *CsMLO4* (located on chromosome 2) from the same 32 hemp and drug-type cannabis cultivars as shown on panels **(A,B)**. On panels **(A,C)** (gDNA), pie charts display, for each SNP along the coding sequence, the genotype frequencies calculated among the 32 cultivars. Colored horizontal rectangles on panels **(A,C)** represent the exons, numbered from 1 to 15: dotted rectangles represent extracellular domains of the resulting protein, while blue and striped rectangles represent membrane and cytoplasmic domains, respectively. Genotype frequency color code on panels **(A,C)**: samples called as homozygous for the reference allele are depicted in orange, samples called as heterozygous are depicted in light blue, and samples called as homozygous for the alternate allele are depicted in green. On panels **(B,D)** (amino acid sequence), the gray vertical rectangles depict transmembrane domains and the solid black curves depict cytoplasmic and extracellular loops. Resulting amino acid replacements on panels **(B,D)** are color-coded according to the gain or loss of polarity: red circles with white cross display a replacement with an acidic amino acid, yellow circles with black hyphen represent a replacement with an alkaline amino acid, gray circles display a replacement with a non-polar amino acid, and gray-striped white circles represent a replacement with a polar amino-acid.

certain cultivars) and that these clade V genes possessed *cis*-acting elements typically overexpressed by biotic and abiotic factors. These specific elements in the promoter regions of clade V *CsMLOs* allow them to be responsive to experimental PM infection, which we validated in the context of an infection time point experiment.

CsMLOs and the Importance of Manual Curation

We used 15 *Arabidopsis thaliana* MLO protein sequences to mine the genomes of five cannabis cultivars of four different types (THC-dominant, balanced THC:CBD, CBD-dominant, food-oil hemp), yielding a sum of 86 *CsMLOs* across all genomes (**Table 1** and **Supplementary Tables 1–5**). According to our data, these genes are organized into 15 *CsMLO* homologs in total (**Figures 1**, **3** and **Supplementary Tables 1–5**). We were not able to retrieve *CsMLO15* in CBDRx, making this genome devoid of clade IV *MLO*. Whether this is an artifactual gene loss resulting from the genome assembly and cleaning process or a biological reality in this specific cultivar remains to be verified with additional sequencing data. If this is a biological reality, it could suggest that these genes potentially have redundant and similar functions or are imbricated into functional networks buffered by redundancy (Tully et al., 2014; AbuQamar et al., 2017). The loss of a gene in the genome of CBDRx in this context could potentially be phenotypically less detrimental. Gene length also varied with a 14-fold difference between the shortest and longest sequence, with two genes (*CsMLO5* and *CsMLO10*) exhibiting multiple unusually long introns (>10,000 nucleotides, **Figure 2**). Intron length distribution across the 15 *CsMLOs* showed considerable variability, which explained the significant variations observed in gene length across all *CsMLOs*. Plant introns are typically relatively short and rarely extend beyond 1 kb, making these large *CsMLO* introns up to 10 times longer than typical plant exons (Wu et al., 2013). However, the numbers and positions of exons and introns for the same homologs across the five genomes were highly conserved. We found that cannabis genes tend to have on average five introns (median number of introns across the genome = 4), indicating that *CsMLOs* have three times the number of introns found in a typical gene from the cannabis genome. This could indicate that those introns are likely to play an important functional role and, thus, may be a significant aspect of gene regulation (Seoighe and Korir, 2011). On the other hand, selection against intron size could be counterbalanced in *CsMLOs* by a selective preference for larger introns which correlates with more regulatory elements and a more complex transcriptional control (e.g., in *Vitis vinifera*, Jiang and Goertzen, 2011). Even though the complete *CsMLO* gene catalog could be retrieved in each genome through gene

prediction algorithms combined with targeted BLAST searches, the precise characterization of each gene structure (i.e., start/stop codons, coding sequence, exon–intron boundaries) could not be achieved without multiple efforts of manual curation.

Automated gene structure prediction algorithms are often considered sufficiently reliable to recover the complete genome-wide repertoire of genes of a given sample. However, as repeat content, size, and structural complexity of those genes increase (i.e., numerous small exons delimited by long introns, as observed in *CsMLOs*), errors are increasingly likely to occur and thus impair the accuracy of automated annotations (Guigó et al., 2000; Pilkington et al., 2018). Because 13% of the *CsMLOs* identified here had introns larger than 10 kb (*CsMLO5* and *CsMLO10*), and two additional genes (*CsMLO4* and *CsMLO6*) had introns larger than 1,000 bp, most of these *CsMLOs* were mispredicted by automated gene prediction algorithms (**Supplementary Tables 1–3**). These algorithms typically have 10 kb as the default maximum intron length (e.g., in MAKER2, Holt and Yandell, 2011). In comparison, *Arabidopsis thaliana* genome annotation version 10 indicates that there are 127,854 introns in the nuclear genes, and of these, 99.23% are less than 1,000 bp, while only 16 introns are larger than 5 kb (NCBI accession: GCF_000001735.4, TAIR10.1). Long multi-exon genes having long introns end up fragmented into several shorter "genes" by these programs, thus inflating the actual number of genes within the family. The severity of such errors is influenced by various factors such as the quality of the assembly (Treangen and Salzberg, 2012; Yandell and Ence, 2012) and the availability and quality of extrinsic evidence (e.g., RNA-seq, orthologous sequences). While assembly quality is influenced by genome size and repeat content (Tørresen et al., 2019; Whibley et al., 2021), the disparity in the number of mispredicted genes observed in this study is also likely to be related to differences in sequencing technology (Oxford Nanopore vs. Pacific Biosciences), sequencing depth, algorithms used for *de novo* assembly, and simple base calling accuracy. Overall, these results revealed that cannabis possesses an extensive repertoire of *MLOs* characterized by significant gene size variations across all family members. These results also demonstrate the importance of manual curation when working with automatically generated gene models. Identifying the complete and detailed set of *CsMLOs* for each genome allowed the possibility to assess synteny and evolutionary patterns among *Cannabis sativa* and other plant species.

Evolutionary Dynamics of *CsMLOs*, Gene Duplications and Potential Implications

The vast majority of studies investigating phylogenetic relationships within the *MLO* gene family usually classifies its members in seven clades. A few times, an extra clade has been proposed, or various subclades have been identified, but no consensus has been reached yet. In our study, we classified genes according to the seven clades, and identified some potential subclades presented in **Figure 3**, most of which appear concordant with results from other studies. In two previous studies (Rispail and Rubiales, 2016; Polanco et al., 2018), clade I is divided in two subclades (Ia and Ib). Subclade Ia would correspond in our tree to the two subclades respectively including *CsMLO12* and *CsMLO9*, while subclade Ib would correspond to the subclade that includes *CsMLO2*. However, Iovieno et al. (2016) divided clade I in three subclades (Ia, Ib, and Ic). Subclade Ia from Iovieno et al. (2016) appears to correspond to subclade Ib from Polanco et al. (2018), and in our tree is represented by the subclade including *CsMLO2*. Subclades Ib and Ic from Iovieno et al. (2016) would correspond to subclade Ia from Polanco et al. (2018) and would be represented by the subclades including *CsMLO12* and *CsMLO9*, respectively. In Iovieno et al. (2016), clade II is divided into 15 subclades (named from IIa to IIq excluding IIj). Subclades IIa and IIb would be represented in our tree by the subclade including *CsMLO6*; subclades IIc, IId, and IIe would be represented by the monocot-specific subclade; subclades IIf, IIg and IIh would be represented by the subclade including *CsMLO13*; and subclades IIi to IIq would be represented by the subclade including *CsMLO14*. Still in Iovieno et al. (2016), clade III is divided into three subclades (IIIa, IIIb, and IIIc), subclades IIIb and IIIc corresponding in our tree to the subclades including *CsMLO8* and *CsMLO7*, respectively. Subclade IIIa would correspond to the two immediate outlying monocot sequences (*ZmMlo2* and *ZmMlo3*), while our two next outlying monocot sequences (*HvMlo2* and *ZmMlo4*) would correspond to clade VIII (in Iovieno et al., 2016, as there is no consensus on clade VIII). Clade IV has also been divided into two subclades (IVa and IVb) which are grouped together in our tree, subclade IVa from their study simply corresponding to monocot sequences and subclade IVb corresponding to dicot sequences. Clade V has been divided into three subclades (Va, Vb, and Vc), for which subclade Va corresponds in our tree to the subclade including *CsMLO1*, while subclade Vb would correspond to the two outlying sequences from the other subclade from our tree (*PpMLO3* and *VvMLO3*), and subclade Vc would correspond to the remaining of this subclade that includes *CsMLO4*. Clade VI is not divided into subclades in this paper, while we clearly identified two subclades in our tree, one including *CsMLO5* and one including *CsMLO3*. Clade VII has been divided into two subclades in Iovieno et al. (2016), and the same division can be found in our tree, with Iovieno's subclade VIIa corresponding to the subclade that includes *CsMLO11*, while subclade VIIb would correspond to the subclade including *CsMLO10*. In Zheng et al. (2016), a different clade VIII had been defined, which would correspond to Iovieno et al. (2016) subclade VIIa, while Zheng et al. (2016) clade VII would correspond to Iovieno et al. (2016) subclade VIIb. In most studies, this eighth clade has been merged within clade VII, which is also the case here. As described above, a distinct clade VIII was also defined as a monocot-specific clade in Iovieno et al. (2016), making the use of an 8-clades system confusing. In our opinion, the clade VIII described by Iovieno et al. (2016) could be considered as a subclade of clade III, represented in our tree by the most "diverged" sequences in this clade, *HvMlo2* and *ZmMlo4*.

Manual curation of *CsMLOs* across the five studied genomes revealed with exactitude their respective genomic localization, showing an overall conserved syntenic pattern, except for two genomes, Finola and Purple Kush, which exhibited distinct chromosome localizations for specific *CsMLO* orthologs, as

compared to the rest of the genomes. The number of *CsMLOs* per genome, ranging from 14 to 18, was comparable to other plant genomes, such as *Arabidopsis thaliana* (15, Chen et al., 2006), *Vitis vinifera* (14, Feechan et al., 2008), *Cucumis sativus* (13, Zhou et al., 2013), *Solanum lycopersicum* (15, Chen et al., 2014), *Hordeum vulgare* (11, Kusch et al., 2016), *Medicago truncatula* (14, Rispail and Rubiales, 2016), *Cicer arietinum* (13, Rispail and Rubiales, 2016), *Lupinus angustifolius* (15, Rispail and Rubiales, 2016), *Arachis* spp. (14, Rispail and Rubiales, 2016), *Cajanus cajan* (20, Rispail and Rubiales, 2016), *Phaseolus vulgaris* (19, Rispail and Rubiales, 2016) and *Vigna radiata* (18, Rispail and Rubiales, 2016). The genomes of Finola and Purple Kush, however, exhibited certain anomalies. Firstly, we found a greater proportion of genes located on unanchored contigs in Finola (11%) and Purple Kush (33%) as compared to CBDRx (0%). Secondly, two paralog pairs, one in Finola (*CsMLO10-FN-A* and *CsMLO10-FN-B*) and one in Purple Kush (*CsMLO9-PK-A* and *CsMLO9-PK-B*), had one of the two paralogs located on a different chromosome (**Figure 1**).

The genome-wide distribution of *CsMLOs* described here did not suggest the involvement of tandem duplications as a predominant mechanism of emergence for *MLOs* in cannabis, as suggested in other taxa (e.g., Liu and Zhu, 2008; Pessina et al., 2014; Rispail and Rubiales, 2016). Indeed, recent bioinformatic analyses suggested that segmental and tandem duplications were a widespread mechanism for the expansion of the *MLO* gene family in diverse plant species, spanning from algae to dicots (Shi et al., 2020). For example, clear evidence of tandem duplication events have been detected in *P. vulgaris* and *V. radiata*, and in *M. domestica*, respectively (Pessina et al., 2014; Rispail and Rubiales, 2016). We did not find evidence that tandem duplications were widespread in *CsMLOs*, as most of the genes were evenly spread out in the genomes, with multiple other unrelated genes in between these *CsMLOs*. Some of the *CsMLOs* were located physically close to one another and they were genetically related, but not similar enough (<85%) to be considered as tandem duplicates. In this case, segmental duplication appears to be a more likely mechanism of emergence for *CsMLOs*, although we did not specifically search for segmental duplications in the present study. In total, four (4.7%) *CsMLOs* across the five genomes were located in tandem duplications (**Figure 1**). These four putative tandem gene duplications were located in Finola only, on chromosome X (*CsMLO13-FN-A* and *CsMLO13-FN-B*) and on chromosome 2 (*CsMLO3-FN-A* and *CsMLO3-FN-B*). Other *CsMLOs* that could represent potential tandem gene duplications in Jamaican Lion male (*CsMLO1-JLm*, *CsMLO12-JLm, CsMLO13-JLm*) and female (*CsMLO1-JL*, *CsMLO10-JL*) all had the two paralogs located on different contigs that were, on average, longer than 2 Mb each. These different contigs containing two *CsMLO* paralogs typically harbored large sequences (>10 kb) of high homology (>95% similarity), which could suggest that they are either the result of segmental duplications, or that they represent two copies of highly polymorphic loci (Fan et al., 2008; Lallemand et al., 2020). We did not find evidence of tandem duplications in the genome of Purple Kush, indicating that this genome is potentially more fragmented than the others. The duplication of *CsMLO13* (clade II) on chromosome X is of potential interest as it was duplicated in the male genomes only (Finola and Jamaican Lion male, **Supplementary Tables 3, 5**). *MLO* clade II genes originally evolved in ancient seed-producing plants, suggesting that genes from this clade could have sex-related functions (Feechan et al., 2008; Jiwan et al., 2013; Zhou et al., 2013). On the other hand, this male-specific duplication could represent a technical artifact caused by the fact that the sequence of *CsMLO13* on chromosome Y was concatenated with its homologous version on chromosome X, thus producing a false tandem duplication. To our knowledge, no studies have documented in detail the structure and evolutionary relationships between orthologous *MLOs* in a group of genomes from the same species. Plus, information on sex-specific distribution of *MLOs* in comparable heterogametic sex plant systems is scarce, which makes the interpretation of this finding difficult. This could ultimately indicate that clade II *MLOs* may not be solely related to seed production or development, as suggested in other systems (Kusch et al., 2016). Recently, a clade II *MLO* was shown to be dictating PM susceptibility in mungbean (Yundaeng et al., 2020). However, apart from this example, only clade V *MLOs* have been shown to be involved in this trait in dicots. In this study, one cannabis clade V *MLO*, *CsMLO1*, appears to be duplicated in three different genomes (three out of the four THC-producing cultivars). If not an assembly artifact, the presence of such an additional copy of a clade V *MLO* would make it tedious to obtain complete immunity to PM. In other plants such as *Arabidopsis*, inactivation of all clade V *MLOs* is required to achieve complete immunity, even though these genes unevenly contribute to susceptibility, with *AtMLO2* playing a major role (Consonni et al., 2006). The presence of a single copy of *CsMLO1* in the industrial hemp variety Finola and the CBD-dominant CBDRx (which ancestry has been suggested to be 11% hemp, Grassa et al., 2021) could suggest that hemp is *de facto* less susceptible or that attaining this target in hemp could be easier to achieve. On the other hand, both Jamaican Lion cultivars investigated here have been described as being highly resistant to PM (McKernan et al., 2020), even though both have this extra, apparently functional, *CsMLO1* copy. In this particular case, resistance to PM is likely due to other genetic factors than a loss-of-susceptibility that would have been obtained through deletion/mutation of clade V *MLOs* (see below).

Upregulation of Clade V *MLOs* Triggered by Powdery Mildew Infection

The transcriptomic response of *Cannabis sativa* to PM performed here revealed that clade V *CsMLOs* are rapidly triggered, at least 6 h post-inoculation, upon infection by the pathogen (**Figure 4**). Our results revealed that the two clade V *CsMLO* genes responded with different activation patterns, potentially suggesting specific roles. As described above, all three clade V *MLO* genes need to be inactivated in order to achieve complete immunity against PM in *Arabidopsis* (Consonni et al., 2006). However, in other plants, not all members of clade V are *S*-genes, and the inactivation of only a subset of the clade V *MLO* genes is required (Bai et al., 2008; Pavan et al., 2011). In those cases, the

precise identification of the exact genes involved in susceptibility needs to rely on additional criteria. A shared element of all *MLO* genes involved in PM susceptibility is that they respond to fungal penetration, showing significant upregulation as soon as 6 h after inoculation (Piffanelli et al., 2002; Bai et al., 2008; Zheng et al., 2013), and candidate genes can thus be identified based on increased expression (Feechan et al., 2008; Pessina et al., 2014). Indeed, being an *S*-gene, the expression of *MLO* is necessary for the successful invasion of PM (Freialdenhoven et al., 1996; Lyngkjær et al., 2000; Zellerhoff et al., 2010). For instance, in watermelon, upregulation was only observed for one clade V *MLO* (out of five), *ClMLO12*, and only at time points corresponding to nine and 24 h after inoculation with *Podosphaera xanthii*, making it the prime candidate dictating PM susceptibility (Iovieno et al., 2015). In apple, three genes (including two out of the four clade V *MLOs*, *MdMLO11* and *MdMLO19*) were found to be significantly up-regulated after inoculation with PM, reaching about 2-fold compared to non-inoculated plants (Pessina et al., 2014). Similarly, three out of four grapevine clade V *MLOs* (*VvMLO3*, *VvMLO4*, and *VvMLO17*) were induced during infection by *Erysiphe necator* (Feechan et al., 2008). Interestingly, in both apple and grapevine, a clade VII *MLO* was also found to respond to PM, but the significance of this finding is unclear. In our case, both clade V *CsMLOs* (*CsMLO1* and *CsMLO4*) appeared responsive to PM infection, showing a 2-fold upregulation (FDR < 0.05). Even though our experimental design was limited, both clade V *CsMLOs* were induced following inoculation with PM, while it was not the case for other *CsMLOs*. Validating the expression of clade V *CsMLOs* using a different approach and/or more importantly using different cultivars would be important to confirm our findings. It is interesting to note that analyzing similar time points (5 and 8 days after inoculation) from a similar RNA-seq experiment (BioProject PRJNA634569), using the same method as the one used in this study, showed a significantly higher expression of both *CsMLO1* and *CsMLO4* at both time points, when compared with mock-inoculated controls (*t*-tests, $P < 0.05$). This was further supported by the presence of *cis*-acting elements involved in gene overexpression by biotic and abiotic stresses in all of the clade V *CsMLOs* characterized in this study. These combined results suggest that cannabis is in a similar situation to that observed in *A. thaliana*, where all clade V genes could be involved in susceptibility.

As of now, *VrMLO12* in mungbean (*Vigna radiata*), which clusters with clade II genes, is the sole report of an *MLO* gene outside of clade V being clearly involved in PM susceptibility in dicots (Yundaeng et al., 2020). In rice, a clade II *MLO* (*OsMLO3*) was also found to have an expression pattern similar to clade V *MLOs* from *Arabidopsis* (Nguyen et al., 2016) and could partially restore PM susceptibility in barley mutants, suggesting an involvement in plant defense (Elliott et al., 2002). According to our results, clade II *CsMLOs* should not be considered candidates, as none showed an induction following inoculation with *G. ambrosiae* emend. (including *G. spadiceus*). However, other *CsMLOs* outside of clade V were found to be differentially expressed, a situation not different from previous findings in apple (Pessina et al., 2014), grapevine (Feechan et al., 2008), and tomato (Zheng et al., 2016). Interestingly, while only one out of four clade V *MLO* showed pathogen-dependent upregulation in tomato (*SlMLO1*), there is some overlap between non-clade V genes that respond to PM in tomato and cannabis. The pathogen-triggered response is, however, not always in the same direction. In tomato, three clade I *MLOs* (*SlMLO10*, *SlMLO13* and *SlMLO14*) were induced following an infection challenge with *Oidium neolycopersici*. While the cannabis orthologs of the last two (*CsMLO9* and *CsMLO2*, respectively) were also differentially expressed after inoculation with PM, their expression levels rather decreased over time (**Supplementary Figure 2**). Similarly, the expression of the tomato clade III *SlMLO4* significantly increased during infection, while that of its cannabis ortholog *CsMLO7* decreased (**Supplementary Figure 2**). The sole tomato clade VI gene, *SlMLO16*, was also found to be induced (Zheng et al., 2016). While its direct cannabis ortholog *CsMLO3* was not found to be up-regulated, it was the case for the other cannabis clade VI gene, *CsMLO5*, for which no ortholog exists in tomato or *Arabidopsis*. This particular gene was the only *CsMLO* to be induced following a challenge with *G. ambrosiae* emend. (including *G. spadiceus*) outside of clade V.

Following our attempt to further characterize the two clade V CsMLOs and determine their subcellular localization *in planta* using confocal laser scanning microscopy, we observed that CsMLO4 was located in the plasma membrane while CsMLO1 was located in endomembrane-associated compartments, including the plasma membrane, the endoplasmic reticulum and the Golgi apparatus (**Figure 5**). In plants, the presence of a reticulate and network-looking pattern and bright spots, as observed for CsMLO1, are typically associated with the endoplasmic reticulum and Golgi stacks, respectively (Bassham et al., 2008). A time-series performed using confocal microscopy demonstrated that the CsMLO1-EGFP fusion protein was extremely dynamic compared to the CsMLO4-EGFP fusion protein (results not shown), supporting its implication in intracellular trafficking through the endomembrane system. Many studies have demonstrated that MLOs are localized in the plasma membrane (Devoto et al., 1999; Kim and Hwang, 2012; Nie et al., 2015), supporting our observations with regards to CsMLO4. Other studies have indicated that MLOs are associated with the plasma membrane and/or other endomembrane compartments, such as the endoplasmic reticulum and the Golgi apparatus (Chen et al., 2009; Jones and Kessler, 2017; Qin et al., 2019) and thus supporting our observations with regards to CsMLO1. To further support our findings and to determine precise subcellular localization of CsMLOs, subcellular fractionation studies as well as fluorescence colocalization with specific organelle markers should be performed.

Genetic Variation Within Clade V *CsMLOs*: A Quest Toward Durable Resistance

Several natural or induced loss-of-function mutations have been identified in *MLO* genes that reduce susceptibility to PM (Büschges et al., 1997; Consonni et al., 2006; Bai et al., 2008; Pavan et al., 2011; Wang et al., 2014). Barley *HvMlo1*

is probably the most studied *MLO* gene, and most mutations leading to loss-of-function (and thus, resistance to PM) in this gene appear to cluster in the second and third cytoplasmic loops (Reinstädler et al., 2010). The functional importance of those loops is still unclear, but evidence in other plants also points toward this particular region (Fujimura et al., 2016; Acevedo-Garcia et al., 2017). Outside of this region, the integrity of transmembrane domains, as well as certain invariant cysteine and proline residues, are critical for the function and accumulation of MLO proteins (Elliott et al., 2005; Reinstädler et al., 2010). Examination of polymorphisms among 32 cannabis cultivars (including one hemp variety) identified only a single SNP in the second cytoplasmic loop of *CsMLO1*. No mutations were identified among those invariant cysteine and proline residues, and no mutations were found either in any of the strictly conserved residues or within transmembrane domains. This suggests that loss-of-function mutations in *CsMLOs* could be rare or non-existent among commercial cultivars, complicating future breeding efforts. The potential lack of diversity among the cultivars included in our analysis might also have impeded our ability to find causative loss-of-function mutations, which could be a scenario likely generalizable to a significant part of the cannabis production industry. Nevertheless, it is possible that mutations identified outside of those previously identified regions could inactivate *CsMLOs*. Three mutations causing amino acid replacements were identified in the first cytoplasmic loop of *CsMLO1*, and five mutations (four in *CsMLO1* and one in *CsMLO4*) were identified in the first extracellular loop. The proximal part of the C-terminus of MLO proteins contains a binding site for the cytoplasmic calcium sensor, calmodulin (Kim et al., 2002a,b). In barley MLO, binding of calmodulin to this domain appears to be required for full susceptibility. Unfortunately, even though a high number of polymorphisms were identified in the cytoplasmic C-terminus of both *CsMLO1* (six mutations) and *CsMLO4* (10 mutations), those mutations are not found within the calmodulin-binding domain but rather at the distal end of the C-terminus. This might not be surprising, as this region is intrinsically disordered (Kusch et al., 2016). Intrinsically disordered regions, i.e., regions lacking stable secondary structures, usually exhibit greater amounts of non-synonymous mutations and other types of polymorphisms because of the lack of structural constraints (Nilsson et al., 2011; Kusch et al., 2016). Another study conducted on clade V *MLOs* had also revealed that both the first extracellular loop and the C-terminus were under strong positive selection (Iovieno et al., 2015), which seems in agreement with our observations.

The fact that potential loss-of-function mutations in clade V *MLOs* were not identified among the 32 investigated genomes suggests that complete resistance to PM might be hard to find among existing commercial cultivars. Nevertheless, such mutations might be present at a very low frequency, especially in "wild" populations or in landraces that have infrequently been used in breeding programs. For example, natural *mlo* alleles exist in barley but have only been found in landraces from Ethiopia and Yemen (Reinstädler et al., 2010). Similarly, the natural loss-of-function mutations in pea and tomato originated from wild accessions (Bai et al., 2008; Humphry et al., 2011). This should reinforce the importance of preserving cannabis wild populations and encourages efforts to establish germplasm repositories. However, *MLO*-based resistance to PM being a recessive trait, and assuming that both *CsMLO1* and *CsMLO4* are involved, this would mean that loss-of-function mutations would need to be bred as homozygous recessive for both genes into elite plants (not considering that multiple copies of a given *CsMLO* might exist, as suggested here for *CsMLO1*). In the absence of natural mutants, or to accelerate the implementation of *mlo*-based resistance in breeding programs, induced mutagenesis and genome editing might be interesting alternatives. While such approaches have not been optimized for cannabis, loss-of-function mutations have been obtained through those in other crops, such as barley (Reinstädler et al., 2010), wheat (Wang et al., 2014; Acevedo-Garcia et al., 2017), or tomato (Nekrasov et al., 2017).

There might also be other routes to combating PM than MLO. In crops where gene-for-gene interactions exist with PM (e.g., in cereals), a series of functional alleles confer complete resistance against distinct sets of PM isolates (Bourras et al., 2019). Since a similar situation has been observed between hop (*Humulus lupulus*, the closest relative of cannabis) and *Podosphaera macularis* (Henning et al., 2011), it is likely that such gene-for-gene interactions exist between cannabis and PM. Indeed, the first gene conferring complete resistance to an isolate of PM has recently been identified in cannabis (Mihalyov and Garfinkel, 2021). In grapevine, resistance is usually considered polygenic, and there appears to be a diverse range of responses to invasion by *Erysiphe necator*, from penetration resistance to the induction of plant cell death (Feechan et al., 2011). Because cannabis has been excluded from scientific research for decades, very little is known about the biology of PM infection (i.e., genetic diversity, histology, host range), and no data on resistance levels among cultivars has been published as of now. Still, a recent study observed higher copy numbers of a thaumatin-like protein in several cannabis cultivars reported to be resistant to PM, and similar correlations were identified with copy number variations of endochitinases and *CsMLOs* (McKernan et al., 2020). Thaumatin-like proteins and endochitinases might thus represent additional targets potentially involved in quantitative resistance to PM.

CONCLUSION

Genome-wide characterization of *CsMLOs* performed in this study indicated that genes from clade V, which are immediately triggered upon infection by PM, are likely involved as early actors in the fungal infection process by the plant. Polymorphism data generated for clade V *CsMLOs* in multiple commercial cultivars suggested that loss-of-function mutations, required to achieve a resistance phenotype, are rare events and potentially challenging to assemble, especially when considering their recessive nature and the genetic redundancy of multiple clade V *CsMLOs*. Preserving a diversified collection of feral and, ideally, landrace cannabis genetic backgrounds while establishing coherent germplasm repositories could represent efficient strategies to compose with this complex biological reality. This will allow the

creation of novel and valuable knowledge on the fundamental biology supporting the interaction between PM and cannabis, ultimately leading to more sustainable horticultural and agro-industrial practices.

DATA AVAILABILITY STATEMENT

The original contributions presented in the study are publicly available. This data can be found here: National Center for Biotechnology Information (NCBI) BioProject database under accession number PRJNA738505, SRA accessions: SRR14839036-SRR14839050. Python and Shell BASH scripts (total of 3) are provided as a compressed archive file (**Supplementary File 4**).

AUTHOR CONTRIBUTIONS

NP, FOH, and DLJ contributed to the conception and design of the study. NP performed the experiments. NP, FOH, and DLJ analyzed the data and drafted the manuscript. DLJ contributed reagents, equipment, and funds. All authors revised the manuscript, read, and approved the submitted version.

FUNDING

TRICHUM (Translating Research into Innovation for Cannabis Health at Université de Moncton) is supported by grants from Genome Canada (Genome Atlantic NB-RP3), the Atlantic Canada Opportunity Agency (project 212090), and the New Brunswick Innovation Foundation (RIF2018-036), Mitacs and Organigram.

ACKNOWLEDGMENTS

We greatly thank François Sormany and Alex J. Cull for their help generating the RNA-seq and genomic datasets, respectively, Hugo Germain and his team for sharing their expertise with confocal microscopy, and Organigram for their continued support and for providing biomaterials.

SUPPLEMENTARY MATERIAL

The Supplementary Material for this article can be found online at: https://www.frontiersin.org/articles/10.3389/fpls.2021.729261/full#supplementary-material

Supplementary Figure 1 | Phylogenetic relationships of CsMLOs based on Bayesian inference analysis. Phylogenetic tree of manually curated CsMLO proteins (bold) with MLO proteins from selected species (*Arabidopsis thaliana*, *Prunus persica*, *Vitis vinifera*, *Hordeum vulgare*, and *Zea mays*). *Chlamydomonas reinhardtii* was used as an outgroup. Phylogenetic relationships were estimated using the MrBayes tool implemented on NGPhylogeny.fr, using default parameters. The seven defined clades are indicated, as well as potential subclades identified in this study (inner circles). Number on a node indicates the posterior probabilities of major clades and subclades. MLOs with one asterisk (*) have been experimentally demonstrated to be required for PM susceptibility (Büschges et al., 1997; Feechan et al., 2008; Wan et al., 2020), while MLOs with two asterisks (**) have been identified as main probable candidates for PM susceptibility (Pessina et al., 2016).

Supplementary Figure 2 | Transcriptomic response of *CsMLO* genes from all clades, except from clade V, following inoculations with powdery mildew. *CsMLO* genes from clades I, II, III, VI, and VII are displayed in clade-specific plots with different colors depicting the different clades: red (clade I), gray (clade II), yellow (clade III), orange (clade VI), and purple (clade VII). Gene expression is displayed on the *y*-axis as the average logarithmic value of the counts per million [$\log_2$(CPM)] at each time point (displayed on the *x*-axis, *n* = per time point). Time points: no infection/control (T0), 6 h post-inoculation (6H), 24 h post-inoculation (1D), 3 days post-inoculation (3D), and 8 days post-inoculation (8D). Error bars at each time point represent the standard deviation (SD).

Supplementary Table 1 | Members of the *CsMLO* gene family as predicted and manually curated in the CBDRx genome.

Supplementary Table 2 | Members of the *CsMLO* gene family as predicted and manually curated in the Jamaican Lion (female) genome.

Supplementary Table 3 | Members of the *CsMLO* gene family as predicted and manually curated in the Jamaican Lion (male) genome.

Supplementary Table 4 | Members of the *CsMLO* gene family as predicted and manually curated in the Purple Kush genome.

Supplementary Table 5 | Members of the *CsMLO* gene family as predicted and manually curated in the Finola genome.

Supplementary Table 6 | Plant *cis*-acting regulatory elements identified in *CsMLOs* across five distinct cultivars.

Supplementary Table 7 | Non-synonymous SNPs identified in *CsMLO1* and *CsMLO4* of 32 cannabis cultivars with their respective amino acid change in the resulting protein.

Supplementary File 1 | Nucleotide alignment of the genomic sequences from all 86 *CsMLOs*. Exons and introns are separated by multiple gaps in the alignment, as is the case for the insertion in the first exon of *CsMLO5-JLm*.

Supplementary File 2 | Nucleotide alignment of the coding sequences from all 86 *CsMLOs*.

Supplementary File 3 | Amino acid alignment of the protein sequences from all 86 *CsMLOs*.

Supplementary File 4 | Python and Bash scripts used to parse SNP data and RNA-seq results (archive file).

REFERENCES

Abbasi, W. A., Asif, A., Andleeb, S., and Minhas, F. U. A. A. (2017). CaMELS: *in silico* prediction of calmodulin binding proteins and their binding sites. *Proteins* 85, 1724–1740. doi: 10.1002/prot.25330

Ablazov, A., and Tombuloglu, H. (2016). Genome-wide identification of the mildew resistance locus O (*MLO*) gene family in novel cereal model species *Brachypodium distachyon*. *Eur. J. Plant Pathol.* 145, 239–253. doi: 10.1007/s10658-015-0833-2

AbuQamar, S., Moustafa, K., and Tran, L. S. (2017). Mechanisms and strategies of plant defense against *Botrytis cinerea*. *Crit. Rev. Biotechnol.* 37, 262–274. doi: 10.1080/07388551.2016.1271767

Acevedo-Garcia, J., Kusch, S., and Panstruga, R. (2014). Magical mystery tour: *MLO* proteins in plant immunity and beyond. *New Phytol.* 204, 273–281. doi: 10.1111/nph.12889

Acevedo-Garcia, J., Spencer, D., Thieron, H., Reinstädler, A., Hammond-Kosack, K., Phillips, A. L., et al. (2017). *mlo*-based powdery mildew resistance in hexaploid bread wheat generated by a non-transgenic TILLING approach. *Plant Biotechnol. J.* 15, 367–378. doi: 10.1111/pbi.12631

Almagro Armenteros, J. J., Salvatore, M., Emanuelsson, O., Winther, O., von Heijne, G., Elofsson, A., et al. (2019a). Detecting sequence signals in targeting peptides using deep learning. *Life Sci. Alliance* 2:e201900429. doi: 10.26508/lsa.201900429

Almagro Armenteros, J. J., Sønderby, C. K., Sønderby, S. K., Nielsen, H., and Winther, O. (2017). DeepLoc: prediction of protein subcellular localization using deep learning. *Bioinformatics* 33, 3387–3395. doi: 10.1093/bioinformatics/btx431

Almagro Armenteros, J. J., Tsirigos, K. D., Sønderby, C. K., Petersen, T. N., Winther, O., Brunak, S., et al. (2019b). SignalP 5.0 improves signal peptide predictions using deep neural networks. *Nat. Biotechnol.* 37, 420–423. doi: 10.1038/s41587-019-0036-z

Anders, S., Pyl, P. T., and Huber, W. (2015). HTSeq-A Python framework to work with high-throughput sequencing data. *Bioinformatics* 31, 166–169. doi: 10.1093/bioinformatics/btu638

Appiano, M., Pavan, S., Catalano, D., Zheng, Z., Bracuto, V., Lotti, C., et al. (2015). Identification of candidate *MLO* powdery mildew susceptibility genes in cultivated Solanaceae and functional characterization of tobacco *NtMLO1*. *Transgenic Res.* 24, 847–858. doi: 10.1007/s11248-015-9878-4

Bai, Y., Pavan, S., Zheng, Z., Zappel, N. F., Reinstädler, A., Lotti, C., et al. (2008). Naturally occurring broad-spectrum powdery mildew resistance in a Central American tomato accession is caused by loss of *Mlo* function. *Mol. Plant Microbe Interact.* 21, 30–39. doi: 10.1094/MPMI-21-1-0030

Bassham, D. C., Brandizzi, F., Otegui, M. S., and Sanderfoot, A. A. (2008). The secretory system of *Arabidopsis*. *Arabidopsis Book* 6:e0116. doi: 10.1199/tab.0116

Bidzinski, P., Noir, S., Shahi, S., Reinstädler, A., Gratkowska, D. M., and Panstruga, R. (2014). Physiological characterization and genetic modifiers of aberrant root thigmomorphogenesis in mutants of *Arabidopsis thaliana MILDEW LOCUS O* genes. *Plant Cell Environ.* 37, 2738–2753. doi: 10.1111/pce.12353

Blum, M., Chang, H. Y., Chuguransky, S., Grego, T., Kandasaamy, S., Mitchell, A., et al. (2021). The InterPro protein families and domains database: 20 years on. *Nucleic Acids Res.* 49, D344–D354. doi: 10.1093/nar/gkaa977

Bolger, A. M., Lohse, M., and Usadel, B. (2014). Trimmomatic: a flexible trimmer for illumina sequence data. *Bioinformatics* 30, 2114–2120. doi: 10.1093/bioinformatics/btu170

Bourras, S., Kunz, L., Xue, M., Praz, C. R., Müller, M. C., Kälin, C., et al. (2019). The *AvrPm3-Pm3* effector-NLR interactions control both race-specific resistance and host-specificity of cereal mildews on wheat. *Nat. Commun.* 10:2292. doi: 10.1038/s41467-019-10274-1

Braun, U., and Cook, R. T. A. (2012). *Taxonomic Manual of the Erysiphales* (Powdery Mildews). CBS Biodiversity Series No. 11. Utrecht: CBS-KNAW Fungal Biodiversity Centre.

Braun, U., Cook, R. T. A., Inman, A. J., and Shin, H. D. (2002). "The taxonomy of the powdery mildew fungi," in *The Powdery Mildews: A Comprehensive Treatise*, eds R. R. Bélanger, W. R. Bushnell, A. J. Dik, and T. L. W. Carver (Saint Paul, MN: APS Press), 13–55.

Briesemeister, S., Rahnenführer, J., and Kohlbacher, O. (2010). YLoc-an interpretable web server for predicting subcellular localization. *Nucleic Acids Res.* 38, 497–502. doi: 10.1093/nar/gkq477

Büschges, R., Hollricher, K., Panstruga, R., Simons, G., Wolter, M., Frijters, A., et al. (1997). The barley *Mlo* gene: a novel control element of plant pathogen resistance. *Cell* 88, 695–705. doi: 10.1016/S0092-8674(00)81912-1

Camacho, C., Coulouris, G., Avagyan, V., Ma, N., Papadopoulos, J., Bealer, K., et al. (2009). BLAST+: architecture and applications. *BMC Bioinformatics* 10:421. doi: 10.1186/1471-2105-10-421

Chen, Y., Wang, Y., and Zhang, H. (2014). Genome-wide analysis of the mildew resistance locus o (*MLO*) gene family in tomato (*Solanum lycopersicum* L.). *Plant Omics* 7, 87–93.

Chen, Z., Hartmann, H. A., Wu, M.-J., Friedman, E. J., Chen, J.-G., Pulley, M., et al. (2006). Expression analysis of the *AtMLO* gene family encoding plant-specific seven-transmembrane domain proteins. *Plant Mol. Biol.* 60, 583–597. doi: 10.1007/s11103-005-5082-x

Chen, Z., Noir, S., Kwaaitaal, M., Hartmann, H. A., Wu, M. J., Mudgil, Y., et al. (2009). Two seven-transmembrane domain MILDEW RESISTANCE LOCUS O proteins cofunction in *Arabidopsis* root thigmomorphogenesis. *Plant Cell* 21, 1972–1991. doi: 10.1105/tpc.108.062653

Chiang, C., Layer, R. M., Faust, G. G., Lindberg, M. R., David, B., Garrison, E. P., et al. (2015). SpeedSeq: ultra-fast personal genome analysis and interpretation. *Nat. Methods* 12, 966–968. doi: 10.1038/nmeth.3505

Chou, K. C., and Shen, H. B. (2010). Plant-mPLoc: a top-down strategy to augment the power for predicting plant protein subcellular localization. *PLoS One* 5:e11335. doi: 10.1371/journal.pone.0011335

Consonni, C., Humphry, M. E., Hartmann, H. A., Livaja, M., Durner, J., Westphal, L., et al. (2006). Conserved requirement for a plant host cell protein in powdery mildew pathogenesis. *Nat. Genet.* 38, 716–720. doi: 10.1038/ng1806

Dangl, J. L., and Jones, J. D. G. (2001). Plant pathogens and integrated defence responses to infection. *Nature* 411, 826–833. doi: 10.1038/35081161

Debode, F., Janssen, E., and Berben, G. (2013). Development of 10 new screening PCR assays for GMO detection targeting promoters (pFMV, pNOS, pSSuAra, pTA29, pUbi, pRice actin) and terminators (t35S, tE9, tOCS, tg7). *Eur. Food Res. Technol.* 236, 659–669. doi: 10.1007/s00217-013-1921-1

Deshmukh, R., Singh, V. K., and Singh, B. D. (2014). Comparative phylogenetic analysis of genome-wide *Mlo* gene family members from *Glycine max* and *Arabidopsis thaliana*. *Mol. Genet. Genomics* 289, 345–359. doi: 10.1007/s00438-014-0811-y

Devoto, A., Hartmann, H. A., Piffanelli, P., Elliott, C., Simmons, C., Taramino, G., et al. (2003). Molecular phylogeny and evolution of the plant-specific seven-transmembrane *MLO* family. *J. Mol. Evol.* 56, 77–88. doi: 10.1007/s00239-002-2382-5

Devoto, A., Piffanelli, P., Nilsson, I. M., Wallin, E., Panstruga, R., von Heijne, G., et al. (1999). Topology, subcellular localization, and sequence diversity of the *Mlo* family in plants. *J. Biol. Chem.* 274, 34993–35004. doi: 10.1074/jbc.274.49.34993

Dobin, A., Davis, C. A., Schlesinger, F., Drenkow, J., Zaleski, C., Jha, S., et al. (2013). STAR: ultrafast universal RNA-seq aligner. *Bioinformatics* 29, 15–21. doi: 10.1093/bioinformatics/bts635

Dobson, L., Reményi, I., and Tusnády, G. E. (2015). CCTOP: a consensus constrained topology prediction web server. *Nucleic Acids Res.* 43, W408–W412. doi: 10.1093/nar/gkv451

Dubos, C., Stracke, R., Grotewold, E., Weisshaar, B., Martin, C., and Lepiniec, L. (2010). MYB transcription factors in *Arabidopsis*. *Trends Plant Sci.* 15, 573–581. doi: 10.1016/j.tplants.2010.06.005

Edgar, R. C. (2004). MUSCLE: multiple sequence alignment with high accuracy and high throughput. *Nucleic Acids Res.* 32, 1792–1797. doi: 10.1093/nar/gkh340

Elliott, C., Müller, J., Miklis, M., Bhat, R. A., Schulze-Lefert, P., and Panstruga, R. (2005). Conserved extracellular cysteine residues and cytoplasmic loop-loop interplay are required for functionality of the heptahelical *MLO* protein. *Biochem. J.* 385, 243–254. doi: 10.1042/BJ20040993

Elliott, C., Zhou, F., Spielmeyer, W., Panstruga, R., and Schulze-Lefert, P. (2002). Functional conservation of wheat and rice *Mlo* orthologs in defense modulation to the powdery mildew fungus. *Mol. Plant Microbe Interact.* 15, 1069–1077. doi: 10.1094/MPMI.2002.15.10.1069

Fan, C., Chen, Y., and Long, M. (2008). Recurrent tandem gene duplication gave rise to functionally divergent genes in *Drosophila*. *Mol. Biol. Evol.* 25, 1451–1458. doi: 10.1093/molbev/msn089

Farinas, C., and Peduto Hand, F. (2020). First report of *Golovinomyces spadiceus* causing powdery mildew on industrial hemp (*Cannabis sativa*) in Ohio. *Plant Dis.* 104:2727. doi: 10.1094/PDIS-01-20-0198-PDN

Feechan, A., Jermakow, A. M., Torregrosa, L., Panstruga, R., and Dry, I. B. (2008). Identification of grapevine *MLO* gene candidates involved in susceptibility to powdery mildew. *Funct. Plant Biol.* 35, 1255–1266. doi: 10.1071/FP08173

Feechan, A., Kabbara, S., and Dry, I. B. (2011). Mechanisms of powdery mildew resistance in the Vitaceae family. *Mol. Plant Pathol.* 12, 263–274. doi: 10.1111/j.1364-3703.2010.00668.x

Freialdenhoven, A., Peterhänsel, C., Kurth, J., Kreuzaler, F., and Schulze-Lefert, P. (1996). Identification of genes required for the function of non-race-specific *mlo* resistance to powdery mildew in barley. *Plant Cell* 8, 5–14. doi: 10.1105/tpc.8.1.5

Freisleben, R., and Lein, A. (1942). Über die Auffindung einer mehltauresistenten Mutante nach Röntgenbestrahlung einer anfälligen reinen Linie von Sommergerste. *Naturwissenschaften* 30:608. doi: 10.1007/BF01488231

Fujimura, T., Sato, S., Tajima, T., and Arai, M. (2016). Powdery mildew resistance in the Japanese domestic tobacco cultivar Kokubu is associated with aberrant splicing of *MLO* orthologues. *Plant Pathol.* 65, 1358–1365. doi: 10.1111/ppa.12498

Glawe, D. A. (2008). The powdery mildews: a review of the world's most familiar (yet poorly known) plant pathogens. *Annu. Rev. Phytopathol.* 46, 27–51. doi: 10.1146/annurev.phyto.46.081407.104740

Grassa, C. J., Weiblen, G. D., Wenger, J. P., Dabney, C., Poplawski, S. G., Timothy Motley, S., et al. (2021). A new *Cannabis* genome assembly associates elevated cannabidiol (CBD) with hemp introgressed into marijuana. *New Phytol.* 230, 1665–1679. doi: 10.1111/nph.17243

Gu, Z., Gu, L., Eils, R., Schlesner, M., and Brors, B. (2014). Circlize implements and enhances circular visualization in R. *Bioinformatics* 30, 2811–2812. doi: 10.1093/bioinformatics/btu393

Guigó, R., Agarwal, P., Abril, J. F., Burset, M., and Fickett, J. W. (2000). An assessment of gene prediction accuracy in large DNA sequences. *Genome Res.* 10, 1631–1642. doi: 10.1101/gr.122800

Hartley, J. L., Temple, G. F., and Brasch, M. A. (2000). DNA cloning using *in vitro* site-specific recombination. *Genome Res.* 10, 1788–1795. doi: 10.1101/gr.143000

Health Canada (2020). *Licensed Cultivators, Processors and Sellers of Cannabis Under the Cannabis Act*. Available online at: https://www.canada.ca/en/health-canada/services/drugs-medication/cannabis/industry-licensees-applicants/licensed-cultivators-processors-sellers.html (accessed December 1, 2020)

Henning, J. A., Townsend, M. S., Gent, D. H., Bassil, N., Matthews, P., Buck, E., et al. (2011). QTL mapping of powdery mildew susceptibility in hop (*Humulus lupulus* L.). *Euphytica* 180, 411–420. doi: 10.1007/s10681-011-0403-4

Hilbert, M., Novero, M., Rovenich, H., Mari, S., Grimm, C., Bonfante, P., et al. (2020). *MLO* differentially regulates barley root colonization by beneficial endophytic and mycorrhizal fungi. *Front. Plant Sci.* 10:1678. doi: 10.3389/fpls.2019.01678

Holt, C., and Yandell, M. (2011). MAKER2: an annotation pipeline and genome-database management tool for second-generation genome projects. *BMC Bioinformatics* 12:491. doi: 10.1186/1471-2105-12-491

Huelsenbeck, J. P., and Ronquist, F. (2001). MRBAYES: Bayesian inference of phylogenetic trees. *Bioinformatics* 17, 754–755. doi: 10.1093/bioinformatics/17.8.754

Humphry, M., Reinstädler, A., Ivanov, S., Bisseling, T., and Panstruga, R. (2011). Durable broad-spectrum powdery mildew resistance in pea *er1* plants is conferred by natural loss-of-function mutations in *PsMLO1*. *Mol. Plant Pathol.* 12, 866–878. doi: 10.1111/j.1364-3703.2011.00718.x

Ingvardsen, C. R., Massange-Sánchez, J. A., Borum, F., Uauy, C., and Gregersen, P. L. (2019). Development of *mlo*-based resistance in tetraploid wheat against wheat powdery mildew. *Theor. Appl. Genet.* 132, 3009–3022. doi: 10.1007/s00122-019-03402-4

Iovieno, P., Andolfo, G., Schiavulli, A., Catalano, D., Ricciardi, L., Frusciante, L., et al. (2015). Structure, evolution and functional inference on the *Mildew Locus O* (*MLO*) gene family in three cultivated Cucurbitaceae *spp*. *BMC Genomics* 16:1112. doi: 10.1186/s12864-015-2325-3

Iovieno, P., Bracuto, V., Pavan, S., Lotti, C., Ricciardi, L., and Andolfo, G. (2016). Identification and functional inference on the *Mlo*-family in Viridiplantae. *J. Plant Pathol.* 98, 587–594. doi: 10.4454/JPP.V98I3.027

Jacott, C. N., Charpentier, M., Murray, J. D., and Ridout, C. J. (2020). *Mildew Locus O* facilitates colonization by arbuscular mycorrhizal fungi in angiosperms. *New Phytol.* 227, 343–351. doi: 10.1111/nph.16465

Jiang, K., and Goertzen, L. R. (2011). Spliceosomal intron size expansion in domesticated grapevine (*Vitis vinifera*). *BMC Res. Notes* 4:52. doi: 10.1186/1756-0500-4-52

Jiwan, D., Roalson, E. H., Main, D., and Dhingra, A. (2013). Antisense expression of peach mildew resistance locus O (*PpMlo1*) gene confers cross-species resistance to powdery mildew in *Fragaria x ananassa*. *Transgenic Res.* 22, 1119–1131. doi: 10.1007/s11248-013-9715-6

Jones, D. S., and Kessler, S. A. (2017). Cell type-dependent localization of *MLO* proteins. *Plant Signal. Behav.* 12:e1393135. doi: 10.1080/15592324.2017.1393135

Jones, P., Binns, D., Chang, H. Y., Fraser, M., Li, W., McAnulla, C., et al. (2014). InterProScan 5: genome-scale protein function classification. *Bioinformatics* 30, 1236–1240. doi: 10.1093/bioinformatics/btu031

Jørgensen, I. H. (1992). Discovery, characterization and exploitation of *Mlo* powdery mildew resistance in barley. *Euphytica* 63, 141–152. doi: 10.1007/BF00023919

Karimi, M., Inzé, D., and Depicker, A. (2002). GATEWAY^{TM} vectors for *Agrobacterium*-mediated plant transformation. *Trends Plant Sci.* 7, 193–195. doi: 10.1016/s1360-1385(02)02251-3

Katoh, K., and Standley, D. M. (2013). MAFFT multiple sequence alignment software version 7: improvements in performance and usability. *Mol. Biol. Evol.* 30, 772–780. doi: 10.1093/molbev/mst010

Kaufmann, H., Qiu, X., Wehmeyer, J., and Debener, T. (2012). Isolation, molecular characterization, and mapping of four rose *MLO* orthologs. *Front. Plant Sci.* 3:244. doi: 10.3389/fpls.2012.00244

Kessler, S. A., Shimosato-Asano, H., Keinath, N. F., Wuest, S. E., Ingram, G., Panstruga, R., et al. (2010). Conserved molecular components for pollen tube reception and fungal invasion. *Science* 330, 968–971. doi: 10.1126/science.1195211

Kim, D. S., and Hwang, B. K. (2012). The pepper *MLO* gene, *CaMLO2*, is involved in the susceptibility cell-death response and bacterial and oomycete proliferation. *Plant J.* 72, 843–855. doi: 10.1111/tpj.12003

Kim, M. C., Lee, S. H., Kim, J. K., Chun, H. J., Choi, M. S., Chung, W. S., et al. (2002a). *Mlo*, a modulator of plant defense and cell death, is a novel calmodulin-binding protein: isolation and characterization of a rice *Mlo* homologue. *J. Biol. Chem.* 277, 19304–19314. doi: 10.1074/jbc.M108478200

Kim, M. C., Panstruga, R., Elliott, C., Möller, J., Devoto, A., Yoon, H. W., et al. (2002b). Calmodulin interacts with *MLO* protein to regulate defence against mildew in barley. *Nature* 416, 447–450. doi: 10.1038/416447a

Konishi, S., Sasakuma, T., and Sasanuma, T. (2010). Identification of novel *Mlo* family members in wheat and their genetic characterization. *Genes Genet. Syst.* 85, 167–175. doi: 10.1266/ggs.85.167

Kusch, S., Pesch, L., and Panstruga, R. (2016). Comprehensive phylogenetic analysis sheds light on the diversity and origin of the *MLO* family of integral membrane proteins. *Genome Biol. Evol.* 8, 878–895. doi: 10.1093/gbe/evw036

Lallemand, T., Leduc, M., Landès, C., Rizzon, C., and Lerat, E. (2020). An overview of duplicated gene detection methods: why the duplication mechanism has to be accounted for in their choice. *Genes* 11:1046. doi: 10.3390/genes11091046

Laverty, K. U., Stout, J. M., Sullivan, M. J., Shah, H., Gill, N., Holbrook, L., et al. (2019). A physical and genetic map of *Cannabis sativa* identifies extensive rearrangements at the *THC/CBD acid synthase* loci. *Genome Res.* 29, 146–156. doi: 10.1101/gr.242594.118

Law, C. W., Chen, Y., Shi, W., and Smyth, G. K. (2014). Voom: precision weights unlock linear model analysis tools for RNA-seq read counts. *Genome Biol.* 15:R29. doi: 10.1186/gb-2014-15-2-r29

Lefort, V., Longueville, J. E., and Gascuel, O. (2017). SMS: smart model selection in PhyML. *Mol. Biol. Evol.* 34, 2422–2424. doi: 10.1093/molbev/msx149

Lemoine, F., Correia, D., Lefort, V., Doppelt-Azeroual, O., Mareuil, F., Cohen-Boulakia, S., et al. (2019). NGPhylogeny.fr: new generation phylogenetic services for non-specialists. *Nucleic Acids Res.* 47, W260–W265. doi: 10.1093/nar/gkz303

Lescot, M., Déhais, P., Thijs, G., Marchal, K., Moreau, Y., Van De Peer, Y., et al. (2002). PlantCARE, a database of plant *cis*-acting regulatory elements and a portal to tools for *in silico* analysis of promoter sequences. *Nucleic Acids Res.* 30, 325–327. doi: 10.1093/nar/30.1.325

Letunic, I., and Bork, P. (2019). Interactive tree of life (iTOL) v4: recent updates and new developments. *Nucleic Acids Res.* 47, W256–W259. doi: 10.1093/nar/gkz239

Li, H. (2011). A statistical framework for SNP calling, mutation discovery, association mapping and population genetical parameter estimation from sequencing data. *Bioinformatics* 27, 2987–2993. doi: 10.1093/bioinformatics/btr509

Liu, Q., and Zhu, H. (2008). Molecular evolution of the *MLO* gene family in *Oryza sativa* and their functional divergence. *Gene* 409, 1–10. doi: 10.1016/j.gene.2007.10.031

Lyngkjær, M. F., and Carver, T. L. W. (2000). Conditioning of cellular defence responses to powdery mildew in cereal leaves by prior attack. *Mol. Plant Pathol.* 1, 41–49. doi: 10.1046/j.1364-3703.2000.00006.x

Lyngkjær, M. F., Newton, A. C., Atzema, J. L., and Baker, S. J. (2000). The barley *mlo*-gene: an important powdery mildew resistance source. *Agronomie* 20, 745–756. doi: 10.1051/agro:2000173

McKernan, K. J., Helbert, Y., Kane, L. T., Ebling, H., Zhang, L., Liu, B., et al. (2018). Cryptocurrencies and zero mode wave guides: an unclouded path to a more contiguous *Cannabis sativa* L. genome assembly. *OSF* [Preprint] Available online at: https://osf.io/7d968/ (accessed June 3, 2021).

McKernan, K., Helbert, Y., Kane, L., Ebling, H., Zhang, L., Liu, B., et al. (2020). Sequence and annotation of 42 *Cannabis* genomes reveals extensive copy number variation in cannabinoid synthesis and pathogen resistance genes. *Biorxiv* [Preprint] doi: 10.1101/2020.01.03.894428

Mihalyov, P. D., and Garfinkel, A. R. (2021). Discovery and genetic mapping of PM1, a powdery mildew resistance gene in *Cannabis sativa* L. *Front. Agron.* 3:720215. doi: 10.3389/fagro.2021.720215

Mistry, J., Chuguransky, S., Williams, L., Qureshi, M., Salazar, G. A., Sonnhammer, E. L. L., et al. (2021). Pfam: the protein families database in 2021. *Nucleic Acids Res.* 49, D412–D419. doi: 10.1093/nar/gkaa913

Nekrasov, V., Wang, C., Win, J., Lanz, C., Weigel, D., and Kamoun, S. (2017). Rapid generation of a transgene-free powdery mildew resistant tomato by genome deletion. *Sci. Rep.* 7:482. doi: 10.1038/s41598-017-00578-x

Nelson, C. W., Moncla, L. H., and Hughes, A. L. (2015). SNPGenie: estimating evolutionary parameters to detect natural selection using pooled next-generation sequencing data. *Bioinformatics* 31, 3709–3711. doi: 10.1093/bioinformatics/btv449

Nguyen, V. N. T., Vo, K. T. X., Park, H., Jeon, J. S., and Jung, K. H. (2016). A systematic view of the *MLO* family in rice suggests their novel roles in morphological development, diurnal responses, the light-signaling pathway, and various stress responses. *Front. Plant Sci.* 7:1413. doi: 10.3389/fpls.2016.01413

Nie, J., Wang, Y., He, H., Guo, C., Zhu, W., Pan, J., et al. (2015). Loss-of-function mutations in *CsMLO1* confer durable powdery mildew resistance in cucumber (*Cucumis sativus* L.). *Front. Plant Sci.* 6:1155. doi: 10.3389/fpls.2015.01155

Nilsson, J., Grahn, M., and Wright, A. P. H. (2011). Proteome-wide evidence for enhanced positive Darwinian selection within intrinsically disordered regions in proteins. *Genome Biol.* 12:R65. doi: 10.1186/gb-2011-12-7-r65

Pavan, S., Schiavulli, A., Appiano, M., Marcotrigiano, A. R., Cillo, F., Visser, R. G. F., et al. (2011). Pea powdery mildew *er1* resistance is associated to loss-of-function mutations at a *MLO* homologous locus. *Theor. Appl. Genet.* 123, 1425–1431. doi: 10.1007/s00122-011-1677-6

Pépin, N., Punja, Z. K., and Joly, D. L. (2018). Occurrence of powdery mildew caused by *Golovinomyces cichoracearum sensu lato* on *Cannabis sativa* in Canada. *Plant Dis.* 102:2644. doi: 10.1094/PDIS-04-18-0586-PDN

Pessina, S., Lenzi, L., Perazzolli, M., Campa, M., Dalla Costa, L., Urso, S., et al. (2016). Knockdown of *MLO* genes reduces susceptibility to powdery mildew in grapevine. *Hortic. Res.* 3:16016. doi: 10.1038/hortres.2016.16

Pessina, S., Pavan, S., Catalano, D., Gallotta, A., Visser, R. G. F., Bai, Y., et al. (2014). Characterization of the *MLO* gene family in Rosaceae and gene expression analysis in *Malus domestica*. *BMC Genomics* 15:618. doi: 10.1186/1471-2164-15-618

Piffanelli, P., Zhou, F., Casais, C., Orme, J., Jarosch, B., Schaffrath, U., et al. (2002). The barley *MLO* modulator of defense and cell death is responsive to biotic and abiotic stress stimuli. *Plant Physiol.* 129, 1076–1085. doi: 10.1104/pp.010954

Pilkington, S. M., Crowhurst, R., Hilario, E., Nardozza, S., Fraser, L., Peng, Y., et al. (2018). A manually annotated *Actinidia chinensis* var. *chinensis* (kiwifruit) genome highlights the challenges associated with draft genomes and gene prediction in plants. *BMC Genomics* 19:257. doi: 10.1186/s12864-018-4656-3

Polanco, C., Sáenz de Miera, L. E., Bett, K., and de la Vega, M. P. (2018). A genome-wide identification and comparative analysis of the lentil *MLO* genes. *PLoS One* 13:e0194945. doi: 10.1371/journal.pone.0194945

Punja, Z. K. (2021). Emerging diseases of *Cannabis sativa* and sustainable management. *Pest Manag. Sci.* 77, 3857–3870. doi: 10.1002/ps.6307

Punja, Z. K., Collyer, D., Scott, C., Lung, S., Holmes, J., and Sutton, D. (2019). Pathogens and molds affecting production and quality of *Cannabis sativa* L. *Front. Plant Sci.* 10:1120. doi: 10.3389/fpls.2019.01120

Python Software Foundation (2020). *Python Language Reference, Version 3.7.3*. Wilmington, DE: Python Software Foundation.

Qin, B., Wang, M., He, H.-X., Xiao, H.-X., Zhang, Y., and Wang, L.-F. (2019). Identification and characterization of a potential candidate *MLO* gene conferring susceptibility to powdery mildew in rubber tree. *Phytopathology* 109, 1236–1245. doi: 10.1094/PHYTO-05-18-0171-R

Reinstädler, A., Müller, J., Czembor, J. H., Piffanelli, P., and Panstruga, R. (2010). Novel induced *mlo* mutant alleles in combination with site-directed mutagenesis reveal functionally important domains in the heptahelical barley *Mlo* protein. *BMC Plant Biol.* 10:31. doi: 10.1186/1471-2229-10-31

Rispail, N., and Rubiales, D. (2016). Genome-wide identification and comparison of legume *MLO* gene family. *Sci. Rep.* 6:32673. doi: 10.1038/srep32673

Robinson, M. D., McCarthy, D. J., and Smyth, G. K. (2010). edgeR: a bioconductor package for differential expression analysis of digital gene expression data. *Bioinformatics* 26, 139–140. doi: 10.1093/bioinformatics/btp616

RStudio Team (2020). *RStudio: Integrated Development for R.* Boston, MA: RStudio, PBC. Available online at: http://www.rstudio.com/

Seoighe, C., and Korir, P. K. (2011). Evidence for intron length conservation in a set of mammalian genes associated with embryonic development. *BMC Bioinformatics* 12(Suppl. 9):S16. doi: 10.1186/1471-2105-12-S9-S16

Shen, Q., Zhao, J., Du, C., Xiang, Y., Cao, J., and Qin, X. (2012). Genome-scale identification of *MLO* domain-containing genes in soybean (*Glycine max* L. Merr.). *Genes Genet. Syst.* 87, 89–98. doi: 10.1266/ggs.87.89

Shi, J., Wan, H., Zai, W., Xiong, Z., and Wu, W. (2020). Phylogenetic relationship of plant *MLO* genes and transcriptional response of *MLO* genes to *Ralstonia solanacearum* in tomato. *Genes* 11:487. doi: 10.3390/genes11050487

Singh, V. K., Singh, A. K., Chand, R., and Singh, B. D. (2012). Genome wide analysis of disease resistance *MLO* gene family in sorghum [*Sorghum bicolor* L. Moench]. *J. Plant Genomics* 2, 18–27.

Small, E. (2015). Evolution and classification of *Cannabis sativa* (Marijuana, Hemp) in relation to human utilization. *Bot. Rev.* 81, 189–294. doi: 10.1007/s12229-015-9157-3

Statistics Canada (2021). *T20Table 20-10-0008-01 Retail Trade Sales by Province and Territory (x 1,000)*. Ottawa, ON: Statistics Canada.

Szarka, D., Tymon, L., Amsden, B., Dixon, E., Judy, J., and Gauthier, N. (2019). First report of powdery mildew caused by *Golovinomyces spadiceus* on industrial hemp (*Cannabis sativa*) in Kentucky. *Plant Dis.* 103:1773. doi: 10.1094/PDIS-01-19-0049-PDN

Thompson, G. R., Tuscano, J. M., Dennis, M., Singapuri, A., Libertini, S., Gaudino, R., et al. (2017). A microbiome assessment of medical marijuana. *Clin. Microbiol. Infect.* 23, 269–270. doi: 10.1016/j.cmi.2016.12.001

Tørresen, O. K., Star, B., Mier, P., Andrade-Navarro, M. A., Bateman, A., Jarnot, P., et al. (2019). Tandem repeats lead to sequence assembly errors and impose multi-level challenges for genome and protein databases. *Nucleic Acids Res.* 47, 10994–11006. doi: 10.1093/nar/gkz841

Treangen, T. J., and Salzberg, S. L. (2012). Repetitive DNA and next-generation sequencing: computational challenges and solutions. *Nat. Rev. Genet.* 13, 36–46. doi: 10.1038/nrg3117

Tully, J. P., Hill, A. E., Ahmed, H. M. R., Whitley, R., Skjellum, A., and Mukhtar, M. S. (2014). Expression-based network biology identifies immune-related functional modules involved in plant defense. *BMC Genomics* 15:421. doi: 10.1186/1471-2164-15-421

Van Rossum, G., and Drake, F. L. (2009). *Python 3 Reference Manual*. Scotts Valley, CA: CreateSpace.

van Schie, C. C. N., and Takken, F. L. W. (2014). Susceptibility genes 101: how to be a good host. *Annu. Rev. Phytopathol.* 52, 551–581. doi: 10.1146/annurev-phyto-102313-045854

Vielba-Fernández, A., Polonio, Á, Ruiz-Jiménez, L., de Vicente, A., Pérez-García, A., and Fernández-Ortuño, D. (2020). Fungicide resistance in powdery mildew fungi. *Microorganisms* 8, 1–34. doi: 10.3390/microorganisms8091431

Wan, D. Y., Guo, Y., Cheng, Y., Hu, Y., Xiao, S., Wang, Y., et al. (2020). CRISPR/Cas9-mediated mutagenesis of *VvMLO3* results in enhanced resistance to powdery mildew in grapevine (*Vitis vinifera*). *Hortic. Res.* 7:116. doi: 10.1038/s41438-020-0339-8

Wang, Y., Cheng, X., Shan, Q., Zhang, Y., Liu, J., Gao, C., et al. (2014). Simultaneous editing of three homoeoalleles in hexaploid bread wheat confers

heritable resistance to powdery mildew. *Nat. Biotechnol.* 32, 947–951. doi: 10.1038/nbt.2969

Weldon, W. A., Ullrich, M. R., Smart, L. B., Smart, C. D., and Gadoury, D. M. (2020). Cross-infectivity of powdery mildew isolates originating from hemp (*Cannabis sativa*) and Japanese Hop (*Humulus japonicus*) in New York. *Plant Heal. Prog.* 21, 47–53. doi: 10.1094/PHP-09-19-0067-RS

Whibley, A., Kelley, J. L., and Narum, S. R. (2021). The changing face of genome assemblies: guidance on achieving high-quality reference genomes. *Mol. Ecol. Resour.* 21, 641–652. doi: 10.1111/1755-0998.13312

Win, K. T., Zhang, C., and Lee, S. (2018). Genome-wide identification and description of *MLO* family genes in pumpkin (*Cucurbita maxima* Duch.). *Hortic. Environ. Biotechnol.* 59, 397–410. doi: 10.1007/s13580-018-0036-9

Wiseman, M. S., Bates, T., Garfinkel, A., Ocamb, C. M., and Gent, D. H. (2021). First report of powdery mildew caused by *Golovinomyces ambrosiae* on *Cannabis sativa* in Oregon. *Plant Dis.* doi: 10.1094/PDIS-11-20-2455-PDN

Wu, J. Y., Xiao, J. F., Wang, L. P., Zhong, J., Yin, H. Y., Wu, S. X., et al. (2013). Systematic analysis of intron size and abundance parameters in diverse lineages. *Sci. China Life Sci.* 56, 968–974. doi: 10.1007/s11427-013-4540-y

Yandell, M., and Ence, D. (2012). A beginner's guide to eukaryotic genome annotation. *Nat. Rev. Genet.* 13, 329–342. doi: 10.1038/nrg3174

Yi, J., An, S., and An, G. (2014). *OsMLO12*, encoding seven transmembrane proteins, is involved with pollen hydration in rice. *Plant Reprod.* 27, 169–180. doi: 10.1007/s00497-014-0249-8

Yundaeng, C., Somta, P., Chen, J., Yuan, X., Chankaew, S., Srinives, P., et al. (2020). Candidate gene mapping reveals *VrMLO12* (*MLO* Clade II) is associated with powdery mildew resistance in mungbean (*Vigna radiata* [L.] Wilczek). *Plant Sci.* 298:110594. doi: 10.1016/j.plantsci.2020.110594

Zellerhoff, N., Himmelbach, A., Dong, W., Bieri, S., Schaffrath, U., and Schweizer, P. (2010). Nonhost resistance of barley to different fungal pathogens is associated with largely distinct, quantitative transcriptional responses. *Plant Physiol.* 152, 2053–2066. doi: 10.1104/pp.109.151829

Zheng, Z., Appiano, M., Pavan, S., Bracuto, V., Ricciardi, L., Visser, R. G. F., et al. (2016). Genome-wide study of the tomato *SlMLO* gene family and its functional characterization in response to the powdery mildew fungus *Oidium neolycopersici*. *Front. Plant Sci.* 7:380. doi: 10.3389/fpls.2016.00380

Zheng, Z., Nonomura, T., Appiano, M., Pavan, S., Matsuda, Y., Toyoda, H., et al. (2013). Loss of function in *Mlo* orthologs reduces susceptibility of pepper and tomato to powdery mildew disease caused by *Leveillula taurica*. *PLoS One* 8:e70723. doi: 10.1371/journal.pone.0070723

Zhou, S. J., Jing, Z., and Shi, J. L. (2013). Genome-wide identification, characterization, and expression analysis of the *MLO* gene family in *Cucumis sativus*. *Genet. Mol. Res.* 12, 6565–6578. doi: 10.4238/2013.December.11.8

Conflict of Interest: The authors declare that the research was conducted in the absence of any commercial or financial relationships that could be construed as a potential conflict of interest.

Publisher's Note: All claims expressed in this article are solely those of the authors and do not necessarily represent those of their affiliated organizations, or those of the publisher, the editors and the reviewers. Any product that may be evaluated in this article, or claim that may be made by its manufacturer, is not guaranteed or endorsed by the publisher.

frontiers in Plant Science

ORIGINAL RESEARCH
published: 14 September 2021
doi: 10.3389/fpls.2021.668315

Genomic Evidence That Governmentally Produced *Cannabis sativa* Poorly Represents Genetic Variation Available in State Markets

Daniela Vergara[1], Ezra L. Huscher[1†], Kyle G. Keepers[1†], Rahul Pisupati[2], Anna L. Schwabe[3], Mitchell E. McGlaughlin[3] and Nolan C. Kane[1]**

[1] Kane Laboratory, Department of Ecology and Evolutionary Biology, University of Colorado Boulder, Boulder, CO, United States, [2] Austrian Academy of Sciences, Vienna Biocenter, Gregor Mendel Institute, Vienna, Austria, [3] School of Biological Sciences, University of Northern Colorado, Greeley, CO, United States

OPEN ACCESS

Edited by:
Derek Stewart,
The James Hutton Institute,
United Kingdom

Reviewed by:
Pan Liao,
Purdue University, United States
Wajid Waheed Bhat,
Michigan State University,
United States

***Correspondence:**
Daniela Vergara
daniela.vergara@colorado.edu
Nolan C. Kane
nolan.kane@colorado.edu

† These authors have contributed equally to this work

Specialty section:
This article was submitted to Plant Metabolism and Chemodiversity, a section of the journal Frontiers in Plant Science

Received: 16 February 2021
Accepted: 28 June 2021
Published: 14 September 2021

Citation:
Vergara D, Huscher EL, Keepers KG, Pisupati R, Schwabe AL, McGlaughlin ME and Kane NC (2021) Genomic Evidence That Governmentally Produced Cannabis sativa Poorly Represents Genetic Variation Available in State Markets. Front. Plant Sci. 12:668315. doi: 10.3389/fpls.2021.668315

The National Institute on Drug Abuse (NIDA) is the sole producer of *Cannabis* for research purposes in the United States, including medical investigation. Previous research established that cannabinoid profiles in the NIDA varieties lacked diversity and potency relative to the *Cannabis* produced commercially. Additionally, microsatellite marker analyses have established that the NIDA varieties are genetically divergent form varieties produced in the private legal market. Here, we analyzed the genomes of multiple *Cannabis* varieties from diverse lineages including two produced by NIDA, and we provide further support that NIDA's varieties differ from widely available medical, recreational, or industrial *Cannabis*. Furthermore, our results suggest that NIDA's varieties lack diversity in the single-copy portion of the genome, the maternally inherited genomes, the cannabinoid genes, and in the repetitive content of the genome. Therefore, results based on NIDA's varieties are not generalizable regarding the effects of *Cannabis* after consumption. For medical research to be relevant, material that is more widely used would have to be studied. Clearly, having research to date dominated by a single, non-representative source of *Cannabis* has hindered scientific investigation.

Keywords: cannabinoids, copy number variation, genome diversity, HEMP, repetitive genomic content, marijuana, NIDA, THC

INTRODUCTION

Public perception of recreational and medicinal *Cannabis sativa* L. (marijuana, hemp) use has shifted, with *Cannabis* derived products quickly becoming a multibillion-dollar legal industry. However, the National Institute on Drug Abuse (NIDA), a United States governmental agency, continues to be the sole producer of *Cannabis* for research. Additionally, high-tetrahydrocannabinol (THC) producing *Cannabis* continues to be classified as a Schedule I drug, along with heroin, LSD, and ecstasy, according to the DEA (DEA, 2020). This Schedule I classification restricts the acquisition of *Cannabis* from the private markets, making NIDA the only federally legal source for research. In addition to this limitation, research on *Cannabis* requires a multitude of permits and supervision (Nutt et al., 2013; Hutchison et al., 2019). However, the

medical and recreational *Cannabis* industry in North America are predicted to grow to 7.7 and 14.9 billion dollars, respectively, by late 2021 (Hutchison et al., 2019).

Cannabis sativa (marijuana, hemp) is an angiosperm member of the family Cannabaceae (Bell et al., 2010). It appears to be one of the oldest domesticated plants, utilized by numerous ancient cultures, including Egyptians, Chinese, Greeks, and Romans (Li, 1973, 1974; Russo, 2007). This versatile plant has many known uses, including fiber for paper, rope and clothing, oil for cooking and consumption, and numerous medicinal applications. The plant produces secondary metabolites known as cannabinoids that interact with the human body in physiological (Russo, 2011; Swift et al., 2013; Volkow et al., 2014) and psychoactive (Russo and John, 2003; ElSohly and Desmond, 2005) ways. The cannabinoids compounds are manufactured in the trichomes, which are abundant on the female flowers (Sirikantaramas et al., 2005). The remarkable properties of cannabinoids are partly responsible for driving the growth of the thriving *Cannabis* industry. Two of the main cannabinoids— Δ-9-tetrahydrocannabinolic acid (THCA) and cannabidiolic acid (CBDA)—when heated are converted to the neutral forms Δ-9 THC and cannabidiol (CBD), respectively (Russo, 2011). Two well-characterized enzymes, Δ-9-tetrahydrocannabinolic acid synthase (THCAS) and cannabidiolic acid synthase (CBDAS), are responsible for the production of these cannabinoids in the plant.

Despite the regulatory hurdles and the limited scope of contributions from the United States government, *Cannabis* research is growing at a rapid pace (Vergara et al., 2016; Kovalchuk et al., 2020) and United States scientists have made significant advances in *Cannabis* research from multiple disciplines. Researchers in the United States have produced one of the most complete publicly available *Cannabis* genome assemblies to date, along with the locations of the cannabinoid family of genes in the genome (Grassa et al., 2018). However, oversight is needed to assure the quality and consistency of *Cannabis* testing across laboratories (Jikomes and Zoorob, 2018). Regulation and supervision will allow for a deeper understanding of all the compounds produced by the plant, particularly minor cannabinoids which are not always measured (Vergara et al., 2020) and are produced using multiple genes with complex interactions (Vergara et al., 2019). This is particularly important because medical *Cannabis* use has outpaced its research (Hutchison et al., 2019). Collaborative research between American academic institutions and private companies has shown that the cannabinoid content and genetic profile of *Cannabis* provided by NIDA is not reflective of what consumers have access to from the private markets (Vergara et al., 2017; Schwabe et al., 2019). Therefore, research with these varieties may not reflect the physiological effects of *Cannabis* consumed by the general public.

In 2017, we compared the cannabinoid chemotypes from the *Cannabis* produced in the private market to the chemotypes from the governmentally produced *Cannabis* for NIDA by the University of Mississippi (Vergara et al., 2017). We found that NIDA's *Cannabis* lacked potency and chemotypic variation and had an excess of cannabinol (CBN), which is a degradation product of THC. The cannabinoid diversity from the governmentally produced *Cannabis* was a fraction (only 27% of the THC) of that from the private markets. A study using microsatellite markers also showed that NIDA's *Cannabis* was genetically different from commercially available recreational and medical varieties. This study concluded that results from research using flower material supplied by NIDA may not be comparable to consumer experiences with *Cannabis* from legal private markets (Schwabe et al., 2019).

Here, we present results of analysis to further examine the genetic diversity in governmentally produced *Cannabis*. We acquired DNA from two NIDA-produced samples which had been previously analyzed using ten variable microsatellite regions (Schwabe et al., 2019). After sequencing, we compared their overall genomic diversity to that of previously sequenced varieties including hemp- and marijuana-types (Lynch et al., 2016; Vergara et al., 2019). We report here the genomic characteristics of the two NIDA samples, including overall genetic variation, as well as genetic variation within the cannabinoid family of genes, the maternally inherited organellar genomes (mitochondrial and chloroplast), and the repetitive genomic content. We compare this diversity to the publicly available genomes from other *Cannabis* lineages within the species, to characterize the relationships with other well-studied lineages.

MATERIALS AND METHODS

NIDA's Samples

Bulk *Cannabis* supplied for research purposes is referred to as "research grade marijuana" by NIDA and is characterized by the level of THC and CBD (NIDA, 2016). They offer 12 different categories of *Cannabis* for research that vary in the levels of THC (low < 1%, medium 1–5%, high 5–10%, and very high > 10%) and CBD (low < 1%, medium 1–5%, high 5–10%, and very high > 10%)". The high THC NIDA sample (**Supplementary Table 1**) has an RTI log number 13494–22, reference number SAF 027355 and the high THC/CBD has an RTI log number 13784-1114-18-6, reference number SAF 027355. DNA from both samples was extracted by Schwabe et al. (2019) and provided to the University of Colorado Boulder. These two samples were sequenced using standard Illumina multiplexed library preparation protocols as described in Lynch et al. (2016) which yielded to an approximate coverage of 17–20x (**Supplementary Table 1**).

Genome Assembly, Whole Genome Libraries, and Nuclear Genome Exploration

We aligned sequences from 73 different *Cannabis* plants to the previously developed CBDRx assembly Cs10 (Grassa et al., 2018). These genomes were sequenced using the Illumina platform by different groups (**Supplementary Table 1**) and are, or will be, publicly available on GenBank. For detailed information on sequencing and the library preparation of the 57 genomes sequenced by our group at the University of Colorado Boulder please refer to Lynch et al., 2016. The remaining 16 genomes were

sequenced and provided by different groups (**Supplementary Table 1**), however, most of these genomes have been previously used in other studies (Lynch et al., 2016; Vergara et al., 2019).

We aligned the 73 libraries to the CBDRx assembly using Burrows-Wheeler alignment (ver. 0.7.10-r789; Li and Durbin, 2009), then calculated the depth of coverage using SAMtools (ver. 1.3.1-36-g613501f; Li et al., 2009) as described in Vergara et al. (2019). We used GATK (ver. 3.0) to call single nucleotide polymorphisms (SNPs). We filtered for SNPs lying in the single-copy portion of the genome (Lynch et al., 2016) which resulted in 7,738,766 high-quality SNPs. The single-copy portion of the genome does not include repetitive sequences such as transposable elements or microsatellites. Subsequently, we were then able to estimate the expected coverage at single-copy sites as in Vergara et al. (2019). We performed a STRUCTURE analysis (ver. 2.3.4; Pritchard et al., 2000) with $K = 3$ in accordance with previous research (Sawler et al., 2015; Lynch et al., 2016). With these STRUCTURE results, we then classified the different varieties into four different groupings: Broad-leaf marijuana-type (BLMT), Narrow-leaf marijuana-type (NLMT), Hemp, and Hybrid (**Supplementary Table 2**). Hybrid individuals had less than 60% population assignment probability to a particular group. We found 12 individuals in the BLMT group, 16 in the Hemp group, 14 in the Hybrid group, and 31 in the NLMT group. We then used SplitsTree (ver. SplitsTree4; Huson, 1998) to visualize relationships among the 73 individuals, VCFtools (ver. 4.0; Danecek et al., 2011) to calculate genome-wide heterozygosity as measures of overall variation, and PLINK (ver. 1.07; Purcell et al., 2007) for a principal component analysis (PCA).

Cannabinoid Gene Pathway Exploration

Using BLAST, we found 12 hits for putative CBDA/THCA synthase genes in the CBDRx assembly (**Supplementary Table 3**) with more than 80% identity and an alignment length of greater than 1,000 bp. For this BLAST analysis, we used the CBCA synthase (Page and Stout, 2017), the THCA synthase with accession number KP970852.1, and the CBDA synthase with accession number AB292682.1.

We estimated the gene copy-number (CN) for the cannabinoid genes (Vergara et al., 2019) and calculated summary statistics of the CN for each of the 12 genes by variety (**Supplementary Table 1**). Differences in the estimated gene CN between the cultivars for each of the 12 cannabinoid synthases gene family were determined using one-way ANOVAs on the CN of each gene as a function of the lineages (BLMT, Hemp, Hybrid, and NLMT), with a later *post hoc* analysis to establish one-to-one group differences using the R statistical platform (R Core Team, 2013).

We used BLAST to search for the two enzymes upstream in the cannabinoid pathway using the methodology from Vergara et al. (2019). We found 1 hit to olivetolate geranyltransferase enzyme, and two hits to olivetolic acid synthase (**Supplementary Table 1**).

Maternally Inherited Genomes

We used the publicly available chloroplast (Vergara et al., 2015) and mitochondrial (White et al., 2016) genome assemblies to construct haplotype networks using PopART (ver. 1.7; Leigh and Bryant, 2015) using only variants with a high quality score in the variant call file. The chloroplast and mitochondrial haplotype networks comprised 508 and 1,929 SNPs, respectively.

Repetitive Genomic Content

We used RepeatExplorer (ver.2; Novák et al., 2010) to determine the repetitive content in 71 of the 73 genomes (Pisupati et al., 2018). We excluded "Jamaican Lion" (NLMT) and "Feral Nebraska" (hemp) genomes due to low-quality reads that led to dubious results. We estimated the repetitive content of the genome and annotating repeat families using custom python scripts[1].

RESULTS

Nuclear Genome Exploration

Our analysis of the nuclear genome used 7,738,766 high-quality SNPs from the inferred single-copy portion of the genome. STRUCTURE analysis (**Figure 1A**) shows the population assignment probabilities for all 73 different varieties including both of NIDA's varieties. This analysis established that NIDA's samples cluster with both the hemp and NLMT groupings, with less than 60% in either group, and therefore we categorized them as Hybrid (**Supplementary Table 2**). The individuals that are part of the Hemp (orange, $n = 16$), NLMT (blue, $n = 31$), or BLMT (purple, $n = 12$) groups had a population assignment probability of more than 60% to that particular group. However, those individuals with a probability of less than 60% to a particular population were assigned to the Hybrid group (gray, $n = 14$), which includes both of NIDAs samples.

In addition to clustering probability results (**Figure 1B**) from STRUCTURE, we colored the varieties in the PCA (**Figure 1B**) and SplitsTree (**Figure 2**) according to their color scheme from the STRUCTURE analysis. The first two principal components in the PCA explain 28.71% of the variation (**Figure 1** bottom panel), and the two NIDA varieties cluster together, also seen in the SplitsTree analysis (**Figure 2**). Both the PCA and SplitsTree indicate high genetic similarity between the NIDA samples and neither of them cluster with any other strains.

The Hybrid group which contains NIDA's samples show the widest range of heterozygosity ($\mu = 0.131$, s.d = 0.0545) in the single-copy portion of the genome. However, it is not significantly different from any other group (**Figure 3**). This wide range of heterozygosity in the hybrid group is expected given that we are grouping individuals that do not belong to one particular genetic group but rather have some assignment probability to two or three genetic groups. Therefore, varieties which are not related to each other, or that belong to more than one group are found in the hybrid category. This may explain why the Hybrid group has the highest mean heterozygosity in this study (Hemp: $\mu = 0.0817$, s.d = 0.0352; BLMT $\mu = 0.0959$, s.d = 0.0405; and NLMT $\mu = 0.112$, s.d = 0.0411).

[1]https://github.com/rbpisupati/nf-repeatexplorer.git

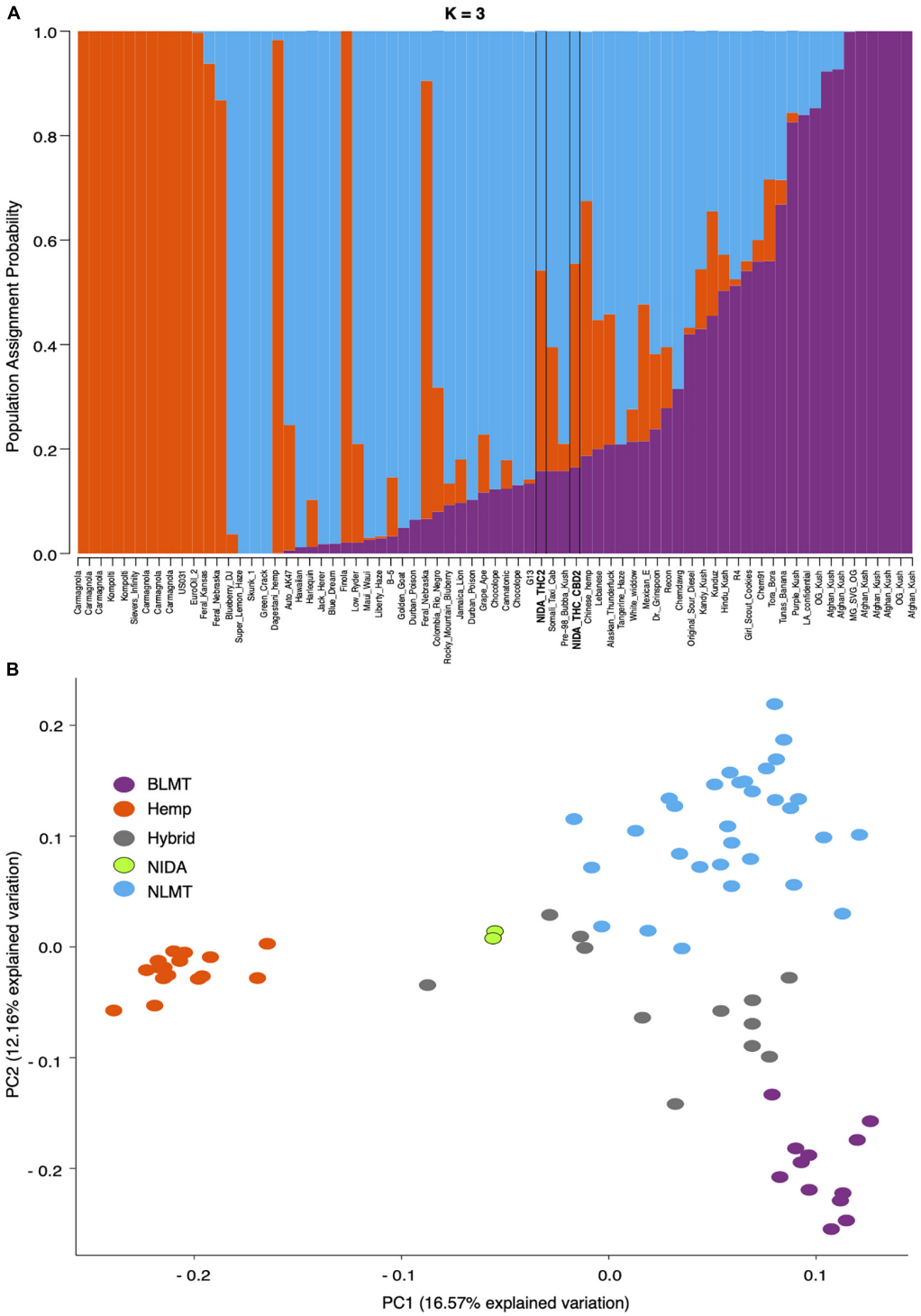

FIGURE 1 | STRUCTURE and Principal Component Analyses. Proportion of each color in the bar indicates the probability of assignment to Hemp (orange), NLMT (blue), or BLMT (purple), groups. Both of NIDA's strains outlined with black margins are assigned to both NLMT and Hemp groups with less than 60% probability, and therefore we assigned them to the Hybrid group **(A)**. The two NIDA samples in green cluster with each other and away from other varieties **(B)**.

Cannabinoid Gene Pathway Exploration

Independent of which synthase we used for the BLAST analysis (either THCA, CBDA, or CBCA), the BLAST results delivered the same hits on the CBDRx assembly with different percent identities. Based on percent-identity scores, our BLAST results identified a hit in the CBDRx assembly that appears to code

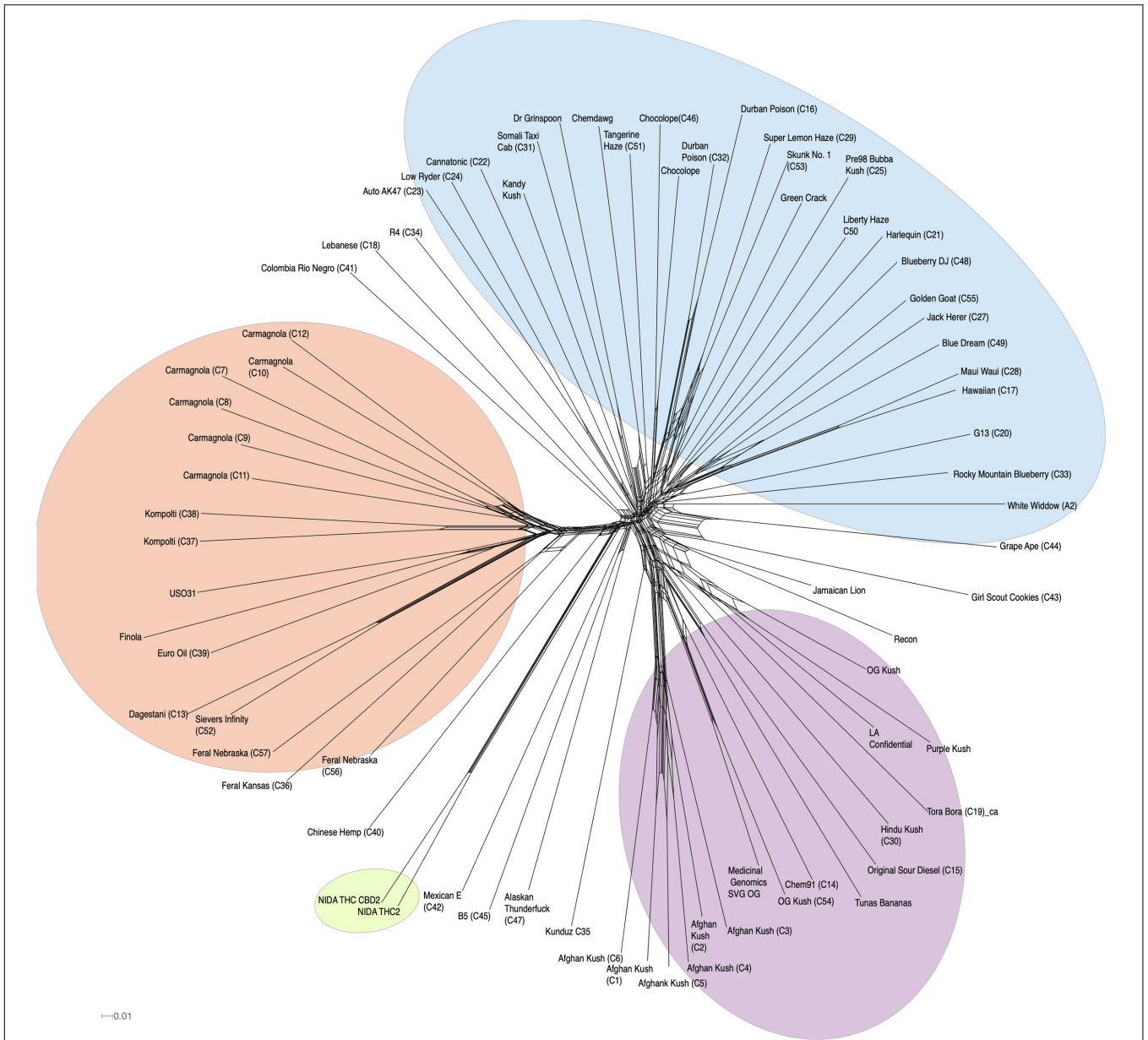

FIGURE 2 | SplitsTree graph. Genetically similar individuals cluster together, such as the NIDA cluster, "Afghan Kush" cluster, and "Carmagnola" cluster. NIDA samples are highlighted in green. Hemp, NLMT, and BLMT shown in orange, blue, and purple, respectively.

for cannabichromenic acid synthase (CBCAS), and one that possibly codes for CBDAS, but we did not find a hit for THCAS (**Supplementary Table 3**). After calculating the copy number variation, we found that most groups have one copy of the CBCAS gene (BLMT μ = 1.38, s.d = 1.1; Hemp μ = 1.88, s.d = 2.15; Hybrid μ = 1.56, s.d = 1.33; and NLMT μ = 1.44, s.d = 2.57). Despite the hemp group having the widest range, no group significantly differed from the others (**Figure 4A**). For the CBCAS genes, the NIDA samples had estimated copy numbers of 0.37 and 0.34. These values are on the lower side of the copy number distribution, with values ranging from 0.016 to 8.75. We include the copy number variation of an unknown cannabinoid, which was the only other locus that had significant differences between groups (**Figure 4B**).

The copy number variation for the CBDAS gene was higher, ranging from 1 to 3 or more copies (BLMT μ = 3.24, s.d = 1.23; Hemp μ = 1.57, s.d = 1.04; Hybrid μ = 2.59, s.d = 1.17; and NLMT μ = 2.97, s.d = 3.15). The Hemp group on average has a lower copy number of these genes, which is significantly different from every other group (**Figure 4C**). For the CBDAS genes, the NIDA samples had an estimated copy number of 2.35 and 2.55. These copy number estimates are close to the mean and median values of the whole dataset (μ = 2.64; median = 2.55).

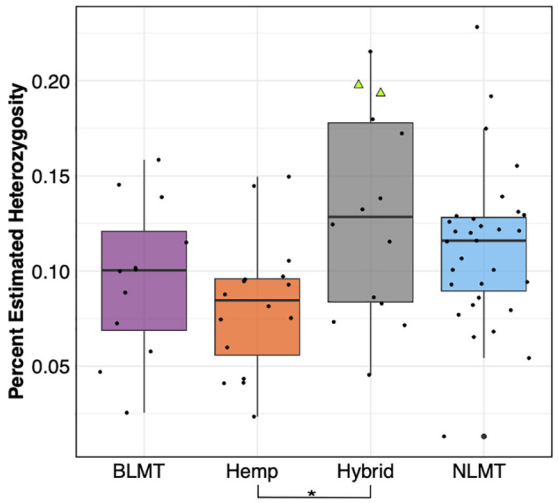

FIGURE 3 | Genome wide heterozygosity. The Hemp lineage differs significantly from the Hybrid grouping with a $P < 0.03$. The two NIDA samples are presented within the Hybrid grouping by two green triangles.

The copy number estimates for the two enzymes upstream in the cannabinoid olivetolate geranyltransferase, and olivetolic acid synthase (**Supplementary Table 1**) were not significantly different between groups. The approximate copy number for olivetolate geranyltransferase was one gene (BLMT $\mu = 1.51$, s.d = 0.89; Hemp $\mu = 1.06$, s.d = 0.70; Hybrid $\mu = 1.32$, s.d = 0.89; and NLMT $\mu = 1.89$, s.d = 5.53). The approximate copy number for the two copies of olivetolic acid synthase was higher, ranging from 1 to 2 copies (BLMT $\mu = 0.98$, s.d = 0.73; Hemp $\mu = 0.64$, s.d = 0.55; Hybrid $\mu = 0.57$, s.d = 0.46; NLMT $\mu = 1.24$, s.d = 4.41 for the first gene, and BLMT $\mu = 1.47$, s.d = 0.74; Hemp $\mu = 1.33$, s.d = 1.03; Hybrid $\mu = 1.39$, s.d = 0.93; and NLMT $\mu = 2.00$, s.d = 5.79 for the second gene).

Maternally Inherited Genomes

We analyzed both the chloroplast (**Figure 5A**) and mitochondrial (**Figure 5B**) haplotype networks. The chloroplast haplotype network (**Figure 5A**) contains eight haplotypes, with a common haplotype (I) that comprises 58 individuals (79%). Most of the individuals in the haplotypes that diverge from the main haplotype (haplotypes II, V, and VI) are hemp types. Both NIDA samples possess the main chloroplast haplotype (I).

The mitochondrial haplotype network contains a common haplotype with 60 individuals (82%), and five additional haplotypes which are mostly comprised of hemp individuals (**Figure 5B**). As with the chloroplast, both the NIDA samples possess the common haplotype. The haplotype group for each individual for both the chloroplast and mitochondria is given in columns 11 and 12 in **Supplementary Table 1**.

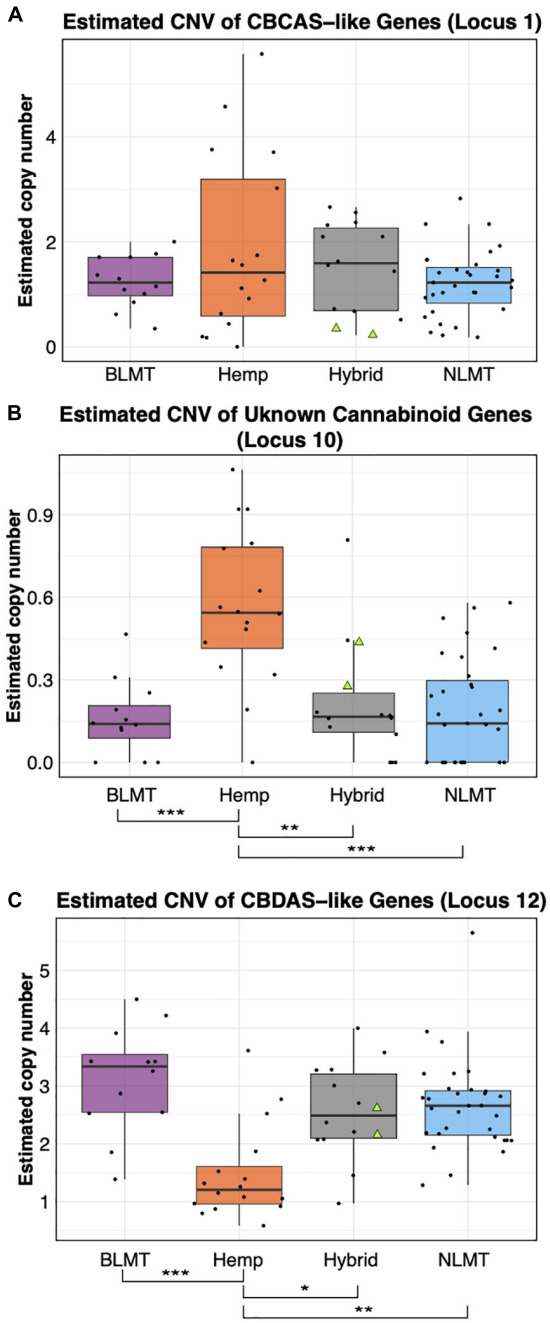

FIGURE 4 | Copy Number Variation in cannabinoid genes. The estimated copy number of the CBCAS-like genes **(A)** is not different between groups despite the Hemp lineage having the widest range. Another unknown cannabinoid locus **(B)** shows significant differences between Hemp and the other groups at the $P < 0.001$ level. The Hemp lineage also differs significantly with a $P < 0.01$ from the other lineages in the estimated copy number of CBDAS-like genes **(C)**. The two NIDA samples are presented within the Hybrid grouping by two green triangles.

Repetitive Genomic Content

We found that the 71 genomes analyzed had similar repetitive content in their genomes (BLMT $\mu = 62.9\%$, s.d = 2%; Hemp $\mu = 61.2\%$, s.d = 2.6%; Hybrid $\mu = 62.8\%$, s.d = 2%; and NLMT $\mu = 62.9\%$, s.d = 3%) with few outliers (**Figure 6**). The NLMT had the most variation in the fraction of genomes containing repetitive content, ranging from 58.6 to 70%. Both NIDA samples

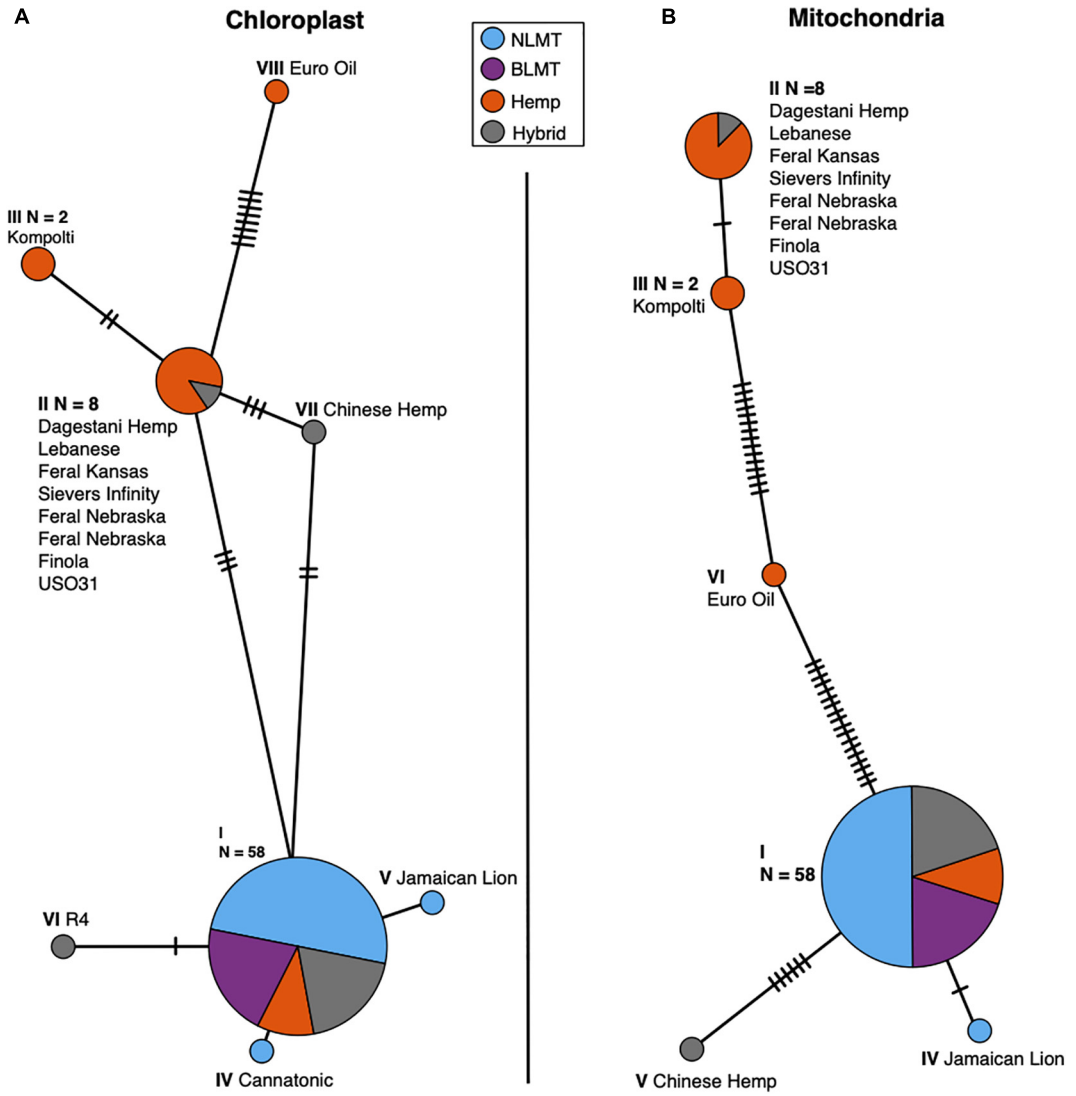

FIGURE 5 | Chloroplast **(A)** and Mitochondrial **(B)** haplotype networks. Both haplotype networks are similar with a common haplotype shared by most individuals (79 and 82% for the chloroplast and mitochondria, respectively) and smaller haplotypes that differ slightly, mostly comprised of Hemp individuals.

(showed as triangles in **Figure 6**) had 61.1% of their genomes as repetitive content. As shown in Pisupati et al. (2018), the majority of repetitive content in *Cannabis* is composed of Long Terminal Repeats (LTR) elements (Ty1 copia and Ty3 gypsy; **Supplementary Figure 1**).

DISCUSSION

In this study, we analyzed the genomes of two *Cannabis* samples produced by the sole legal provider of *Cannabis* for research in the United States, the NIDA. We compared these two samples to the genomes of 71 commercially available varieties, many of which are medicinally or recreationally available on the legal market for sale to the general public. A previous study has shown that *Cannabis* provided by NIDA lacks diversity and cannabinoid potency compared to commercially available *Cannabis* (Vergara et al., 2017), and microsatellite marker analysis also shows that these differences extend to the genetic level (Schwabe et al., 2019). The results of this study concur with previous studies that NIDA-produced *Cannabis* fundamentally differs from *Cannabis* consumed by the public.

Our whole-genome exploration suggests that the samples from NIDA are very similar to each other, and not divergent to all other varieties in our analysis (**Figures 1**, **2**), including the varieties commonly used for recreational and medical purposes (**Figure 2**). Therefore, the samples from NIDA seem to be distantly related to those that are publicly available for consumption.

Even though the two samples supplied by NIDA have high heterozygosity (**Figure 3** and **Supplementary Table 1**), they are comparable to other varieties from the Hybrid group

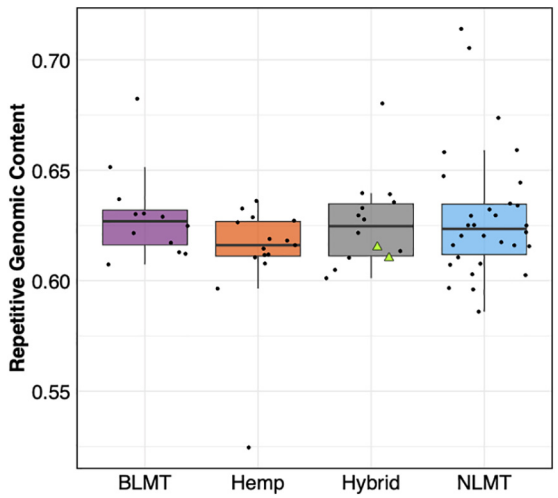

FIGURE 6 | Repetitive Genomic content. The estimated repetitive genomic content by group which does not differ significantly between groups. The two NIDA samples are presented within the hybrid grouping by two green triangles.

and from the NLMT group. The high heterozygosity of both samples from NIDA could be due to recent outcrossing, and perhaps a recent hybrid origin. However, because we only sampled two individuals, this may not represent the overall heterozygosity of all varieties produced for NIDA. Still, as already stated, previous research on the chemotypic variation of NIDA's varieties show their limited cannabinoid diversity (Vergara et al., 2017), supporting the possibility that these two samples are recent hybrids and not bred for their chemotypic profiles including cannabinoids.

The copy number of the cannabinoid genes from the NIDA samples in some cases fall under the median (**Figure 4A**), above the median (**Figure 4B**), or near the median (**Figure 4C**). However, there are some varieties that have up to 13 copies of some genes (**Supplementary Table 1**), in agreement with previous reports (Vergara et al., 2019). Gene copy number may have implications in cannabinoid production (Vergara et al., 2019), and in gene expression influencing several phenotypes that are also relevant to other plant systems (Stranger et al., 2007; Gaines et al., 2010; Ollivier et al., 2016). Furthermore, since gene expression is correlated with enzymatic activity (Li and Yi, 2012; Xu et al., 2014), it is crucial to understand how gene copy number in the cannabinoid genes is related to enzymatic activity and to cannabinoid production, particularly because varieties and individuals within varieties differ in the number (Vergara et al., 2019) and type of cannabinoid genes (van Velzen and Schranz, 2020). Therefore, future studies once legalization allows for proper *Cannabis* material to be studied at academic research institutions could focus on the expression differences of key cannabinoid genes at the mRNA and proteins levels through transcriptomic and proteomic analyses. However, the observations from this genomic study may be one of the reasons that account for the differences in chemotype between different cannabis varieties, and our study presents evidence that substantiates, at the genomic level, previous findings that the NIDA strains differ chemotypically from *Cannabis* available to the public (Vergara et al., 2017).

Regarding the analysis of the maternally inherited genomes, both NIDA samples have common haplotypes compared to other varieties in the analysis, supporting recent research on the mitochondrial genome diversity in *Cannabis* (Attia et al., 2020). The repetitive content in the samples from NIDA is comparable to that from other varieties (**Figure 6**), which is mostly still unknown (**Supplementary Figure 1**). However, NIDA's samples are in the lower end of the range of repetitive content with 61%. The lack of genetic similarity between NIDA and other strains, as apparent in the genetic clustering illustrated in **Figure 1**, may explain why the chemotype of NIDA material is different from *Cannabis* from the legal market (Vergara et al., 2017). Other factors contributing to NIDA's aberrant chemotype could be differences in cultivation, storage, and processing.

One of the caveats of this investigation is that the Hybrid group is not a lineage of truly related individuals, but a grouping of individuals whose population assignment probability is less than 60% to any of the other groups, and hence is somewhat arbitrary. Had we chosen a higher Hybrid assignment probability value, there would be fewer individuals in the NLMT, BLMT, or Hemp groupings and more individuals in the Hybrid group. Had we chosen a lower value, there would be fewer individuals in the Hybrid category and more individuals in the other groupings. However, there are individuals with 100% assignment probability to one group, for example, "Carmagnola" has 100% genetic assignment to the Hemp group, "Afghan Kush" has 100% genetic assignment to the BLMT group, and "Super Lemon Haze" has 100% genetic assignment to the NLMT group. If we had chosen a value of 40% instead of 60%, both the NIDA varieties would have grouped with the NLMT group (see **Supplementary Table 2** for assignment probability proportions).

In addition to limiting the research capacity on genetic and chemotypic variation by restricting investigation to only *Cannabis* supplied by NIDA, medical research using this material is also limited. Given that NIDA's samples do not represent the genomic or phenotypic variation found in *Cannabis* provided by the legal market, consumer experiences may be different from that which is published in the scientific literature. Therefore, medical research is hindered by using varieties that are not representative of what people are consuming, making medical research less predictive. The use of NIDA's *Cannabis* may be one of the reasons why a recent review found therapeutic support for only three medical conditions (Abrams, 2018), while efficacy as an appetite stimulant, as a relaxant, or to treat epilepsy were not supported despite numerous patient reports (Mattes et al., 1994; Gloss and Vickrey, 2014; Detyniecki and Hirsch, 2016).

Limiting *Cannabis* types available for study creates an obstacle for scientific discovery. It has been proposed that *Cannabis* may be evolving dioecy from monoecious populations (Divashuk et al., 2014; Razumova et al., 2016; Prentout et al., 2019) and cytonuclear interactions, which could be involved in this transition to dioecy, may be also taking place. To understand processes like these, scientists need access to a diverse and

growing variety of *Cannabis* plants which are not available through NIDA. Important discoveries in other plant groups, such as transposable elements (McClintock, 1950), genes related to pathogen resistance (Leister et al., 1996), or genes related to yield (Sakamoto and Matsuoka, 2008) would have not been possible had there been similar restrictions on their research.

This limitation also affects the untapped possibilities of using *Cannabis* to treat a multitude of illnesses, with enough anecdotal evidence from consumers to merit rigorous scientific investigation, using strains that are reflective of those used by consumers claiming medicinal and/or therapeutic effects.

Cannabis is the most widely consumed illicit substance in both in the United States and worldwide (Gloss, 2014), and therefore it is a matter of public health and safety to provide honest and accurate information. This information is also crucial to policy officials who rely on facts for laws and regulation. In conclusion, scientists must be allowed to use all publicly available forms of *Cannabis* for research purposes to maximize scientific, economic, and medicinal benefit to society.

DATA AVAILABILITY STATEMENT

The genomic libraries for NIDA1 and NIDA2 are available on NCBI (Accessions SAMN19677471 and SAMN19677472, respectively). The datasets generated and analyzed for this study can be found in the Dryad repository https://doi.org/10.5061/dryad.3n5tb2rgm.

AUTHOR CONTRIBUTIONS

DV analyzed the single-copy portion of the genome, made figures, wrote the first draft of the manuscript, and conceived and led the project. EH analyzed the single-copy portion of the genome including STRUCTURE and SplitsTree analyses and wrote the pertinent bioinformatic pipelines. KK wrote bioinformatic pipelines for the single-copy portion analysis and PCA. RP analyzed the repetitive content of the genome. AS and MM acquired DNA samples. NK conceived and directed the project. All authors contributed to manuscript preparation.

FUNDING

This research was supported by donations to the University of Colorado Foundation gift fund 13401977-Fin8 to NK and to the Agricultural Genomics Foundation and is part of the joint research agreement between the University of Colorado Boulder and Steep Hill Inc. which made possible the sequencing of the two NIDA genomes.

ACKNOWLEDGMENTS

We thank B. Holmes of Centennial Seeds; D. Liles, C. Casad, A. Ledden, and J. Cole of The Farm; MMJ America, Medicinal Genomics, A. Rheingold and M. Rheingold of Headquarters; and D. Salama, Nico Escondido, Sunrise Genetics, and B. Sievers for providing DNA samples or sequence information.

SUPPLEMENTARY MATERIAL

The Supplementary Material for this article can be found online at: https://www.frontiersin.org/articles/10.3389/fpls.2021.668315/full#supplementary-material

REFERENCES

Abrams, D. I. (2018). The therapeutic effects of *Cannabis* and cannabinoids: an update from the National academies of sciences, engineering and medicine report. *Eur. J. Intern. Med.* 49, 7–11. doi: 10.1016/j.ejim.2018.01.003

Attia, Z., Pogoda, C. S., Vergara, D., and Kane, N. C. (2020). Variation in mtDNA haplotypes suggests a complex history of reproductive strategy in *Cannabis sativa*. *bioRxiv* [Preprint]. doi: 10.1101/2020.12.28.424591

Bell, C. D., Soltis, D. E., and Soltis, P. S. (2010). The age and diversification of the angiosperms re-revisited. *Am. J. Bot.* 97, 1296–1303. doi: 10.3732/ajb.0900346 doi: 10.3732/ajb.0900346

Danecek, P., Auton, A., Abecasis, G., Albers, C. A., Banks, E., DePristo, M. A., et al. (2011). The variant call format and VCFtools. *Bioinformatics* 27, 2156–2158. doi: 10.1093/bioinformatics/btr330

DEA (2020). *Title 21 Code of Federal Regulations*. Available online at: https://www.deadiversion.usdoj.gov/21cfr/cfr/1308/1308_11.htm

Detyniecki, K., and Hirsch, L. J. (2016). Cannabidiol for epilepsy: trying to see through the haze. *Lancet Neurol.* 15, 235–237. doi: 10.1016/s1474-4422(16)00002-8

Divashuk, M. G., Alexandrov, O. S., Razumova, O. V., Kirov, I. V., and Karlov, G. I. (2014). Molecular cytogenetic characterization of the dioecious *Cannabis sativa* with an XY chromosome sex determination system. *PLoS One* 9:e85118. doi: 10.1371/journal.pone.0085118

ElSohly, M. A., and Desmond, S. (2005). Chemical constituents of marijuana: the complex mixture of natural cannabinoids. *Life Sci.* 78, 539–548.

Gaines, T. A., Zhang, W., Wang, D., Bukun, B., Chisholm, S. T., Shaner, D. L., et al. (2010). Gene amplification confers glyphosate resistance in *Amaranthus palmeri*. *Proc. Natl. Acad. Sci. U.S.A.* 107, 1029–1034. doi: 10.1073/pnas.0906649107

Gloss, D. (2014). *Management of Substance Abuse: Cannabis*. Geneva: World Health Organization.

Gloss, D., and Vickrey, B. (2014). Cannabinoids for epilepsy. *Cochrane Database Syst. Rev.* 2014:CD009270.

Grassa, C. J., Wenger, J. P., Dabney, C., Poplawski, S. G., Motley, S. T., Michael, T. P., et al. (2018). A complete *Cannabis* chromosome assembly and adaptive admixture for elevated cannabidiol (CBD) content. *bioRxiv* [Preprint]. doi: 10.1101/458083

Huson, D. H. (1998). SplitsTree: analyzing and visualizing evolutionary data. *Bioinformatics (Oxf. Engl.)* 14, 68–73.

Hutchison, K. E., Bidwell, L. C., Ellingson, J. M., and Bryan, A. D. (2019). *Cannabis* and health research: rapid progress requires innovative research designs. *Value Health* 22, 1289–1294. doi: 10.1016/j.jval.2019.05.005

Jikomes, N., and Zoorob, M. (2018). The cannabinoid content of legal cannabis in Washington state varies systematically across testing facilities and popular consumer products. *Sci. Rep.* 8:4519.

Kovalchuk, I., Pellino, M., Rigault, P., van Velzen, R., Ebersbach, J., Ashnest, J. R., et al. (2020). The genomics of *Cannabis* and its close relatives. *Ann. Rev. Plant Biol.* 71, 713–739.

Leigh, J. W., and Bryant, D. (2015). Popart: full−feature software for haplotype network construction. *Methods Ecol. Evol.* 6, 1110–1116.

Leister, D., Ballvora, A., Salamini, F., and Gebhardt, C. (1996). A PCR–based approach for isolating pathogen resistance genes from potato with potential for wide application in plants. *Nat. Genet.* 14, 421–429. doi: 10.1038/ng1296-421

Li, H., and Durbin, R. (2009). Fast and accurate short read alignment with Burrows–Wheeler transform. *Bioinformatics* 25, 1754–1760. doi: 10.1093/bioinformatics/btp324

Li, H. L. (1973). An archaeological and historical account of cannabis in China. *Econom. Bot.* 28, 437–448.

Li, H. L. (1974). Origin and use of cannabis in Eastern Asia; linguistic-cultural implications. *Econom. Bot.* 28, 293–301. doi: 10.1007/bf02861426

Li, H., Handsaker, B., Wysoker, A., Fennell, T., Ruan, J., Homer, N., et al. (2009). The sequence alignment/map format and SAMtools. *Bioinformatics* 25, 2078–2079. doi: 10.1093/bioinformatics/btp352

Li, L., and Yi, H. (2012). Effect of sulfur dioxide on ROS production, gene expression and antioxidant enzyme activity in *Arabidopsis* plants. *Plant Physiol. Biochem.* 58, 46–53. doi: 10.1016/j.plaphy.2012.06.009

Lynch, R. C., Vergara, D., Tittes, S., White, K., Schwartz, C. J., Gibbs, M. J., et al. (2016). Genomic and chemical diversity in *Cannabis*. *Crit. Rev. Plant Sci.* 35, 349–363. doi: 10.1080/07352689.2016.1265363

Mattes, R. D., Engelman, K., Shaw, L. M., and Elsohly, M. A. (1994). Cannabinoids and appetite stimulation. *Pharmacol. Biochem. Behav.* 49, 187–195. doi: 10.1016/0091-3057(94)90475-8

McClintock, B. (1950). The origin and behavior of mutable loci in maize. *Proc. Natl. Acad. Sci. U.S.A.* 36, 344–355. doi: 10.1073/pnas.36.6.344

NIDA (2016). *Marijuana Plant Material Available from the NIDA Drug Supply Program*. Available online at: *https://www.drugabuse.gov/researchers/research-resources/nida-drug-supply-program-dsp/marijuana-plant-material-available-nida-drug-supply-program* (accessed on January 2021).

Novák, P., Neumann, P., and Macas, J. (2010). Graph-based clustering and characterization of repetitive sequences in next-generation sequencing data. *BMC Bioinformatics* 11:378. doi: 10.1186/1471-2105-11-378

Nutt, D. J., King, L. A., and Nichols, D. E. (2013). Effects of schedule I drug laws on neuroscience research and treatment innovation. *Nat. Rev. Neurosci.* 14, 577–585. doi: 10.1038/nrn3530

Ollivier, M., Tresset, A., Bastian, F., Lagoutte, L., Axelsson, E., Arendt, M.-L., et al. (2016). Amy2B copy number variation reveals starch diet adaptations in ancient European dogs. *R. Soc. Open Sci.* 3:160449. doi: 10.1098/rsos.160449

Page, J. E., and Stout, J. M. (2017). *Cannabichromenic Acid Synthase from Cannabis sativa*. U.S. Patent no 20170211049A1. Ottawa, ON: National Research Council Canada.

Pisupati, R., Vergara, D., and Kane, N. C. (2018). Diversity and evolution of the repetitive genomic content in *Cannabis sativa*. *BMC Genomics* 19:156. doi: 10.1186/s12864-018-4494-3

Prentout, D., Razumova, O., Rhoné, B., Badouin, H., Henri, H., Feng, C., et al. (2019). A high-throughput segregation analysis identifies the sex chromosomes of *Cannabis sativa*. *bioRxiv* [Preprint]. bioRxiv:721324,

Pritchard, J. K., Stephens, M., and Donnelly, P. (2000). Inference of population structure using multilocus genotype data. *Genetics* 155, 945–959. doi: 10.1093/genetics/155.2.945

Purcell, S., Neale, B., Todd-Brown, K., Thomas, L., Ferreira, M. A., Bender, D., et al. (2007). PLINK: a tool set for whole-genome association and population-based linkage analyses. *Am. J. Hum. Genet.* 81, 559–575. doi: 10.1086/519795

R Core Team (2013). *R: A language and Environment for Statistical Computing*. Vienna: R Foundation for Statistical Computing.

Razumova, O. V., Alexandrov, O. S., Divashuk, M. G., Sukhorada, T. I., and Karlov, G. I. (2016). Molecular cytogenetic analysis of monoecious hemp (*Cannabis sativa* L.) cultivars reveals its karyotype variations and sex chromosomes constitution. *Protoplasma* 253, 895–901. doi: 10.1007/s00709-015-0851-0

Russo, E. B. (2007). History of cannabis and its preparations in saga, science, and sobriquet. *Chem. Biodiver.* 4, 1614–1648. doi: 10.1002/cbdv.200790144 doi: 10.1002/cbdv.200790144

Russo, E. B. (2011). Taming THC: potential cannabis synergy and phytocannabinoid-terpenoid entourage effects. *Br. J. Pharmacol.* 163, 1344–1364. doi: 10.1111/j.1476-5381.2011.01238.x

Russo, E. B., and John, M. M. (2003). Cannabis is more than simply Δ9-tetrahydrocannabinol. *Psychopharmacology* 165, 431–432.

Sakamoto, T., and Matsuoka, M. (2008). Identifying and exploiting grain yield genes in rice. *Curr. Opin. Plant Biol.* 11, 209–214. doi: 10.1016/j.pbi.2008.01.009

Sawler, J., Stout, J. M., Gardner, K. M., Hudson, D., Vidmar, J., Butler, L., et al. (2015). The genetic structure of marijuana and hemp. *PLoS One* 10:e0133292. doi: 10.1371/journal.pone.0133292

Schwabe, A. L., Hansen, C. J., Hyslop, R. M., and McGlaughlin, M. E. (2019). Research grade marijuana supplied by the National institute on drug abuse is genetically divergent from commercially available *Cannabis*. *bioRxiv* [Preprint]. doi: 10.1101/592725

Sirikantaramas, S., Taura, F., Tanaka, Y., Ishikawa, Y., Morimoto, S., and Shoyama, Y. (2005). Tetrahydrocannabinolic acid synthase, the enzyme controlling marijuana psychoactivity, is secreted into the storage cavity of the glandular trichomes. *Plant Cell Physiol.* 46, 1578–1582. doi: 10.1093/pcp/pci166

Swift, W., Wong, A., Li, K. M., Arnold, J. C., and McGregor, I. S. (2013). Analysis of cannabis seizures in NSW, Australia: cannabis potency and cannabinoid profile. *PLoS One* 8:e70052. doi: 10.1371/journal.pone.0070052

Stranger, B. E., Forrest, M. S., Dunning, M., Ingle, C. E., Beazley, C., Thorne, N., et al. (2007). Relative impact of nucleotide and copy number variation on gene expression phenotypes. *Science* 315, 848–853. doi: 10.1126/science.1136678

van Velzen, R., and Schranz, M. E. (2020). Origin and evolution of the cannabinoid oxidocyclase gene family. *bioRxiv* [Preprint]. doi: 10.1101/2020.12.18.423406

Vergara, D., Baker, H., Clancy, K., Keepers, K. G., Mendieta, J. P., Pauli, C. S., et al. (2016). Genetic and genomic tools for *Cannabis sativa*. *Crit. Rev. Plant Sci.* 35, 364–377. doi: 10.1080/07352689.2016.1267496

Vergara, D., Bidwell, L. C., Gaudino, R., Torres, A., Du, G., Ruthenburg, T. C., et al. (2017). Compromised external validity: federally produced cannabis does not reflect legal markets. *Sci. Rep.* 7:46528.

Vergara, D., Gaudino, R., Blank, T., and Keegan, B. (2020). Modeling cannabinoids from a large-scale sample of *Cannabis sativa* chemotypes. *bioRxiv* [Preprint]. doi: 10.1101/2020.02.28.970434

Vergara, D., Huscher, E. L., Keepers, K. G., Givens, R. M., Cizek, C. G., Torres, A., et al. (2019). Gene copy number is associated with phytochemistry in *Cannabis sativa*. *AoB Plants* 11:lz074.

Vergara, D., White, K. H., Keepers, K. G., and Kane, N. C. (2015). The complete chloroplast genomes of *Cannabis sativa* and *Humulus lupulus*. *Mitochondrial DNA A DNA Mapp. Seq. Ana.l* 27, 3793–3794. doi: 10.3109/19401736.2015.1079905

Volkow, N. D., Baler, R. D., Compton, W. M., and Weiss, S. R. B. (2014). Adverse health effects of marijuana use. *New Engl. J. Med.* 370, 2219–2227. doi: 10.1056/NEJMra1402309

White, K. H., Vergara, D., Keepers, K. G., and Kane, N. C. (2016). The complete mitochondrial genome for *Cannabis sativa*. *Mitochondrial DNA B Resour.* 1, 715–716. doi: 10.1080/23802359.2016.1155083

Xu, F., Cao, S., Shi, L., Chen, W., Su, X., and Yang, Z. (2014). Blue light irradiation affects anthocyanin content and enzyme activities involved in postharvest strawberry fruit. *J. Agricult. Food Chem.* 62, 4778–4783. doi: 10.1021/jf501120u

Conflict of Interest: DV is the founder and president of the non-profit organization Agricultural Genomics Foundation, and the sole owner of CGRI, LLC. NK is a board member of the non-profit organization Agricultural Genomics Foundation.

The remaining authors declare that the research was conducted in the absence of any commercial or financial relationships that could be construed as a potential conflict of interest.

Publisher's Note: All claims expressed in this article are solely those of the authors and do not necessarily represent those of their affiliated organizations, or those of the publisher, the editors and the reviewers. Any product that may be evaluated in this article, or claim that may be made by its manufacturer, is not guaranteed or endorsed by the publisher.

frontiers in Plant Science

MINI REVIEW
published: 20 September 2021
doi: 10.3389/fpls.2021.721986

Cannabis Glandular Trichomes: A Cellular Metabolite Factory

*Cailun A. S. Tanney, Rachel Backer, Anja Geitmann and Donald L. Smith**

Department of Plant Science, Macdonald Campus, McGill University, Montreal, QC, Canada

Cannabis has been legalized for recreational use in several countries and medical use is authorized in an expanding list of countries; markets are growing internationally, causing an increase in demand for high quality products with well-defined properties. The key compounds of *Cannabis* plants are cannabinoids, which are produced by stalked glandular trichomes located on female flowers. These trichomes produce resin that contains cannabinoids, such as tetrahydrocannabinolic acid and cannabidiolic acid, and an array of other secondary metabolites of varying degrees of commercial interest. While growers tend to focus on improving whole flower yields, our understanding of the "goldmines" of the plant – the trichomes – is limited despite their being the true source of revenue for a multi-billion-dollar industry. This review aims to provide an overview of our current understanding of cannabis glandular trichomes and their metabolite products in order to identify current gaps in knowledge and to outline future research directions.

Keywords: *Cannabis*, trichome, flower, metabolite, cannabinoid, terpene, inflorescence

OPEN ACCESS

Edited by:
Gea Guerriero, Luxembourg Institute of Science and Technology, Luxembourg

Reviewed by:
Felix Stehle, Technical University Dortmund, Germany
Milton Brian Traw, Nanjing University, China
Nirit Bernstein, Agricultural Research Organization (ARO), Israel

****Correspondence:***
Donald L. Smith
Donald.Smith@McGill.Ca

Specialty section:
This article was submitted to Plant Metabolism and Chemodiversity, a section of the journal Frontiers in Plant Science

Received: *08 June 2021*
Accepted: *16 August 2021*
Published: *20 September 2021*

Citation:
Tanney CAS, Backer R, Geitmann A and Smith DL (2021) Cannabis Glandular Trichomes: A Cellular Metabolite Factory. Front. Plant Sci. 12:721986. doi: 10.3389/fpls.2021.721986

INTRODUCTION

Trichomes are formed on the plant surface across a range of taxonomically disparate species, providing a variety of functions and benefits to the plant. These can include simple tasks, such as affecting leaf temperature and photosynthesis, or more complicated functions, such as pest-deterrence *via* their physical structures or production of compounds (Wagner, 1991; Hare et al., 2003). Glandular trichomes are of particular commercial interest as they are one of the key plant structures that produce essential oils – an industry valued at 18.62 billion USD in 2020 (Grand View Research, 2020). Other oil-producing plant structures are internal glands and other trichome types, some of which are capable of producing resinous secretions. Trichome morphology is highly variable both among plant species and within the plant itself (Sangwan et al., 2001). In *Cannabis sativa* L. (hereafter, cannabis), stalked glandular trichomes are the trichome morph that produces substances of economic value (Fairbairn, 1972; Sirikantaramas et al., 2005). These trichomes develop a secretory cavity between secretory disk cells and the cuticle where secondary metabolites, including cannabinoids and terpenes, are deposited and stored (Kim and Mahlberg, 1991, 1997; Sirikantaramas et al., 2005; Marks et al., 2009). Though there are a variety of other trichome morphs found across the cannabis plant, they are beyond the scope of this review.

While male plants produce small amounts of cannabinoids, in cannabis cultivation, the primary products are the female flowers clustered in inflorescences (Ohlsson et al., 1971). Stalked glandular trichomes are primarily concentrated on the calyces and bracts (**Figure 1A**; Spitzer-Rimon et al., 2019; Leme et al., 2020) with populations extending to the inflorescence

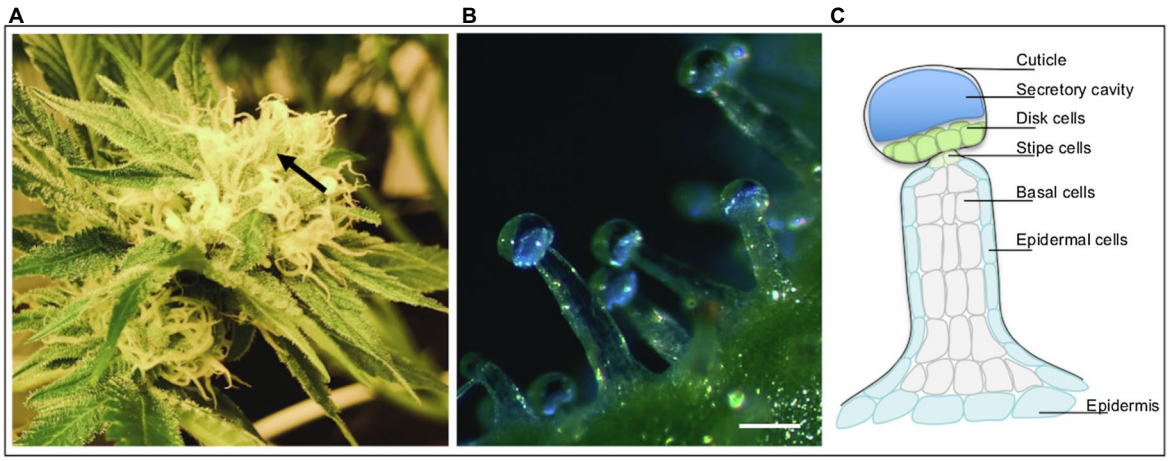

FIGURE 1 | Cannabis (*Cannabis sativa* L.) inflorescence and trichomes. **(A)** An individual inflorescence, with majority of the organs covered in stalked glandular trichomes. Arrow indicates cluster of calyces and bracts covered with trichomes. **(B)** Dark field micrograph of stalked glandular trichomes protruding from calyx epidermis. Biosynthesis of secondary metabolites occurs in the secretory disk cells lining the base of the globular trichome head. The metabolites are stored in the clear subcuticular cavity above the secretory disk cells; this cavity will turn milky white to dark brown over the course of flower maturity. **(C)** Graphic illustration of stalked glandular trichome structure.

"sugar leaves"; these are the sites of accumulation for secreted metabolic products. These valuable secretions include tetrahydrocannabinolic acid (THCA), cannabidiolic acid (CBDA), terpenes, and flavonoids (ElSohly and Slade, 2005; Flores-Sanchez and Verpoorte, 2008). Cannabis plant morphology and cannabinoid profiles are influenced by genetics and the cultivation environment, highlighting the importance of controlled conditions for cannabis cultivation (Magagnini et al., 2018; Danziger and Bernstein, 2021a, b). With the gradual global increase in social and legal acceptance of cannabis, there has been considerable interest in producing consistent high-quality yields. In addition, as medicinal uses for cannabinoids are supported by peer-reviewed research and clinical trials, the global demand for medicinal cannabis products will continue to increase. This will create further pressure on growers to improve control over the concentration of specific cannabis metabolites and the associated cannabis genotypes. However, the genotypes and environmental conditions needed to obtain this level of precision remain poorly characterized. Ultimately, these elusive methods need to be centered around trichomes as the "factories" of the plant. Current efforts have focused on the effects of breeding and cultivar selection, industrial growing conditions, and fertilization methods on flower yield and cannabinoid profiles (Vanhove et al., 2011; Campiglia et al., 2017; Tang et al., 2017; Hawley et al., 2018; Janatová et al., 2018; Burgel et al., 2020; Saloner and Bernstein, 2021). However, as undefined cannabis plant material in pioneering research papers formed the backbone for future cannabis/cannabinoid research, comparing data with uniform standards is impossible. Thus, the need for systematically validating results of these papers and cannabis production "folklore" is paramount yet challenging due to the impact of genotype and growing environment. Regardless of these challenges, since trichomes are ultimately responsible for yield and quality control, it is necessary to advance our understanding of how they, specifically, are affected by these efforts, as well as to investigate new approaches to broaden the scope of possible cost-effective applications for improving yield.

TRICHOME PROFILES

Trichomes Across the Plant Kingdom

Trichomes are found across the plant kingdom, displaying a stunning variety of shapes and properties. Glandular trichomes, which arise from the epidermis on vegetative and reproductive organs, can be generally divided into secretory and non-secretory types with the former being able to secrete substances (Tian et al., 2017). Both the morphologies and metabolic secretions of trichomes are consistent within a plant species, and some species have different trichome morphs on the same plant organ (Muravnik, 2020). Secreted compounds, including THCA (Sirikantaramas et al., 2005), can be toxic to plant cells; therefore, metabolite storage in the cavity of the glandular head affords protection to the plant (Sirikantaramas et al., 2008). While different glandular trichome morphs invoke different storage strategies, the architecture of the morph and cavity position in relation to the secretory cells determine secretion direction (Tissier et al., 2017). The molecular details surrounding the development of glandular trichomes and their secretions are beyond the scope of this article, and we refer to in-depth reviews by Muravnik (2020) and Tian et al. (2017).

Genomic studies are imperative to investigate the factors that influence trichome development in cannabis, both within and between cultivars. Trichome differentiation mechanisms have been investigated in *Arabidopsis thaliana*, with transcription factor (TFs) groups playing key roles in the transcriptional networks for trichome production and patterns (Tian et al., 2017).

While genomic studies are available for other economic plants, including *Humulus lupulus* which belongs to the Cannabaceae family (Matoušek et al., 2016; Mishra et al., 2020), similar studies for cannabis are lacking despite their potentially important impacts for precise cannabis trichome control. Taking advantage of the genetic libraries available for related species with similar resin secretions will help guide these much-need studies (Braich et al., 2019; Zager et al., 2019; Liu et al., 2021).

Key Cannabis Metabolites

The decades-long stigma surrounding cannabis has led to a variety of misconceptions surrounding the plant and its products regarding cannabinoid biosynthesis. While THCA and CBDA are the major cannabinoids produced by the plant, their degradation products, THC and CBD, are of great interest for their psychoactive and therapeutic effects. Additional cannabinoids are gradually gaining interest as their effects on the human body are beginning to be understood (ElSohly and Slade, 2005; Aizpurua-Olaizola et al., 2016; Andre et al., 2016). Fresh cannabis flower tissue contains relatively low levels of THC and CBD and higher levels of THCA and CBDA as the acid forms are converted to neutral forms *via* decarboxylation in post-harvest processing and storage; the rate of conversion is primarily dependent on temperature and light (Yamauchi et al., 1967). Metabolites, including cannabinoids, terpenes, and flavonoids, are formed within secretory disk cells that line the base of the glandular trichome head and stored in the subcuticular cavity (**Figure 1B,C**; Kim and Mahlberg, 1991, 1997). Within the cells, cannabinoid biosynthesis starts in the cytosol, moves to the plastid, and finishes with oxidocyclization in the apoplastic space; transport between these areas is not yet resolved (Gülck and Møller, 2020). A plethora of cannabinoids have been identified in recent years, bringing the total known number to just over 110, which can be divided into 11 subclasses (ElSohly and Gul, 2014; Andre et al., 2016; Hanuš et al., 2016; Berman et al., 2018). The biosynthesis pathways of the key cannabinoids, in particular THC and CBD, are described in detail in previous reviews (Gülck and Møller, 2020; Desaulniers Brousseau et al., 2021).

To date, over 120 terpenes have been identified in cannabis, which are broadly classified as monoterpenes and sesquiterpenes based on differences in their carbon skeletons (ElSohly and Slade, 2005; Degenhardt et al., 2009). Terpenes have a biosynthesis pathway similar to cannabinoids, and this process has been extensively reviewed (Booth et al., 2017; Desaulniers Brousseau et al., 2021). Terpenes impart floral aroma and flavor, making them important components for plant product applications, like essential oils, from many plant species. Terpene profiles vary among cannabis cultivars (Booth et al., 2017) and hemp oils containing more monoterpenes score better on olfactory evaluations than oils containing more sesquiterpenes while an oil containing a mix of both scored highest on scent tests (Mediavilla and Steinemann, 1997). Thus, the terpene composition of cannabis flowers at maturity can directly affect the olfactory quality of flower-based products and extracts, including essential oil-based goods.

Flavonoids are an additional major cannabis phytochemical group; however, this group of compounds has received less research focus compared to cannabinoids and terpenes. Similar to terpenes, flavonoids are found across a wide range of plant genera with a broad range of roles and benefits for the plant (Panche et al., 2016). There are over 20 identified flavonoids for cannabis, with three relatively unique compounds known as cannflavin A, B, and C (Bautista et al., 2021). The potential pharmaceutical uses of flavonoids, spanning from anti-inflammatories to anti-cancer therapies, are boosting interest in these compounds particularly as the entourage effects afforded by cannabis metabolite profiles become better understood (Tomko et al., 2020; Bautista et al., 2021). As flavonoids are produced primarily in cannabis leaves, not the inflorescences (Jin et al., 2020), the present article will focus on cannabinoids and terpenes.

CANNABIS GLANDULAR TRICHOMES

Previously, three types of glandular trichomes on cannabis flowers were described – referred to as capitate-sessile, capitate-stalked, and bulbous – based on structural assessments by scanning electron microscopy (Hammond and Mahlberg, 1973). The trichomes were differentiated based on their morphology, where bulbous trichomes were small and low, sessile trichomes were comprised of a globular head on a very short stalk, and stalked trichomes had a larger globular head on a long stalk; of the three trichome types, stalked trichomes produce the greatest amount of cannabinoids (Hammond and Mahlberg, 1973; Mahlberg and Kim, 2004; Livingston et al., 2020). Unfortunately, this non-specific differentiation between trichome types led to misidentification of trichomes due to the similar appearance of sessile and stalked morphs (Dayanandan and Kaufman, 1976; Livingston et al., 2020). However, a recent study on trichome anatomy revealed that sessile trichomes on vegetative leaves consistently have exactly eight secretory disk cells while stalked glandular trichomes on mature flowers have 12–16; these numbers were consistent across hemp and drug-type varieties (Livingston et al., 2020). As sessile-presenting trichomes on immature cannabis flowers can contain more than eight disk cells and emit fluorescence at intermediate wavelengths, which true sessile trichomes cannot, sessile-presenting trichomes are now thought to be a precursor developmental stage of immature stalked trichomes (Livingston et al., 2020). These discoveries allow for improved accuracy of trichome classification during plant development, may provide more precise estimates of plant maturity and allow for identification of optimal points of metabolite production. This understanding further allows for greater accuracy when assessing the density of stalked glandular trichomes and the ability to predict mature flower trichome densities.

The causes of variable metabolite profiles found among varieties/genotypes and plant organs are genetic and environmental. For example, flowers sampled from the upper region of the plant produce significantly greater quantities of cannabinoids and terpenes than lower positions; light source

and plant maturity are believed to be important factors influencing the concentration and/or amounts (Namdar et al., 2018; Eichhorn Bilodeau et al., 2019). Abiotic factors that influence cannabis growth are the same as those affecting other plant species, such as temperature, fertilization, photoperiod, and light intensity (Taschwer and Schmid, 2015; Conant et al., 2017; Pagnani et al., 2018; Bernstein et al., 2019; Eichhorn Bilodeau et al., 2019; Taghinasab and Jabaji, 2020). However, knowledge regarding how these factors influence growth and trichome formation is limited, with much work needed to produce scientific evidence to support links between metabolite production and environmental factors (Taghinasab and Jabaji, 2020). Research on cannabis is in the early stages, and future work is necessary to investigate signaling pathways that mediate the effect of external factors on metabolite production. Attention toward developing this area of cannabis research is increasing (Mudge et al., 2019; Aliferis and Bernard-Perron, 2020; Conneely et al., 2021).

Potential Benefits of Cannabis Trichomes to the Plant

The exact benefit of cannabinoids and terpenes for the plant has yet to be discovered but several findings point to defense-related functions. This is consistent with a common role of trichomes in many plant species (Levin, 1973). Early studies have also hypothesized that THC protects against ultraviolet (UV) radiation, as cannabis plants produce significantly elevated levels of THC when exposed to higher levels of UVB radiation, possibly resulting in the development of geographical chemotypes (Pate, 1983). A recent study found that CBD could be a potential sunscreen additive as its application to human keratinocyte and melanocyte cells led to improved cell viability after exposure to UVB radiation, suggesting that cannabinoids protect cells against this type of potentially DNA-damaging radiation and supporting the geographical chemotype hypothesis (Gohad et al., 2020). These findings indicate that cannabinoids may be secreted and concentrated around flowers to protect the reproductive organs – and thereby the next generation – from the effects of sun damage; genotypes that originate from closer to the equator will produce higher levels of cannabinoids due to the higher incidence of UVB radiation in that region.

Terpenes may act as deterrents against herbivory, as the monoterpenes α-pinene and limonene repel insects are present in higher concentrations in flowers while sesquiterpenes, which are bitter to mammals, have greater concentrations in the lower leaves (Potter, 2009; Nerio et al., 2010; Russo, 2011). This apparent range of terpene profiles, dependent on organ and position, is in line with probable causes of damage, as insects would be more likely to damage the flowers and herbivorous mammals are likely to focus on the larger fan leaves. In addition, cannabinoids and terpenes can complement each other to provide plants with a complex defense mechanism against insects. The ratio of monoterpenes to sesquiterpenes determines cannabis resin viscosity while CBGA and THCA are toxic to insects. Altering the ratio of terpene types to increase viscosity can trap insects while CBGA and THCA induce apoptosis as shown on cultured insect cell lines, thus protecting the plant and critical tissues like flowers as they develop (Sirikantaramas et al., 2005; Russo, 2011). Terpenes and cannabinoids also interact after ingestion by animals as terpenes were shown to contribute to the affinity of THC to cannabinoid receptor 1 receptors in humans, among other effects (Russo and McPartland, 2001; Andre et al., 2016). The interactions between terpenes and cannabinoids are thus subject to ongoing investigations, not only to gain insight into the role of terpenes for plants, but also due to the potential therapeutic benefits which the medicinal cannabis sector could leverage.

The role of cannabinoids in biotic stress tolerance is consistent with their elevated concentration in flowers where trichome densities are highest. In addition to reducing the risk of pest-related damage, cannabinoids also have antimicrobial properties. Five key compounds [THC, CBD, cannabichromene (CBC), cannabigerol (CBG), and cannabinol (CBN)] and their acid precursor forms have significant antibacterial activity against several methicillin-resistant *Staphylococcus aureus* strains through bacterial membrane targeting (van Klingeren and ten Ham, 1976; Appendino et al., 2008; Farha et al., 2020). This suggests that cannabinoids, including those that are typically secreted in low concentrations, have a broad range of benefits, acting both within and outside the plant, particularly with regards to cannabinoid production in flowers when compared to the rest of the plant (Farha et al., 2020). However, while there is an increasing understanding of the defensive properties of the major metabolic products produced by cannabis, the lesser-known compounds must also be given attention. As there have been over 200 identified cannabinoid and terpene compounds combined, the costs for producing this vast number of secondary metabolites must be investigated to elucidate their individual benefits and roles in plant function. Transcriptomic studies into these lesser-known compounds and their expression in response to common stressors could provide an important start into answering these questions.

Overall, the range of potential benefits of these secondary metabolites strongly suggests that they play a key role in the general health and survival of cannabis plants and their progeny through a combination of factors. To corroborate this, genomics, transcriptomics, and metabolomics studies must be conducted to confirm hypothesized characteristics associated with various trichome morphs, their development patterns across different tissues, and their non-uniform metabolite secretions. Evidence is required to prove that these compounds are not simply by-products of other biological processes but truly have a primary role in defense mechanisms. To be meaningful, these studies should not only include cannabis cultivars that are the result of centuries of breeding, but also naturally occurring types that are not products of human selection activity, though these are rarely available. One hundred ten whole genomes of cannabis cultivars, from wild plants and historical varieties to modern hybrids, with a focus on Asian sources to account for the likely domestication origin, were recently sequenced and analyzed to provide an invaluable genetic framework for the history of the plant; the resulting information can be applied to secondary metabolite investigations (Ren et al., 2021). With time, the validity of these hypotheses is sure to be determined

thanks to this new genomic information, along with valuable insight into the impressive complexity seen within them.

CONCLUSION AND FUTURE PROSPECTS

Cannabis was left behind in the agricultural research boom of the last century because of its illegal status in most jurisdictions. While many of the advancements in plant science for a wide range of other species are applicable to cannabis, multiple species-specific traits require dedicated research both to gain fundamental insights and to provide evidence-based data to the growing industry. Since industrial agriculture practices became globally established and genomic studies became possible in the 20th century, researchers have been able to elucidate novel agricultural applications derived from molecular-scale understanding, while cannabis applications remain centered on breeding and environmental conditions; cultivation protocols were largely based on anecdotal rather than scientific evidence. For example, the soybean genome has been unraveled to identify genetic markers related to nematode resistance and this has been exploited to support precise breeding strategies (Kim et al., 2016); meanwhile, the simple taxonomy of cannabis remains controversial (Koren et al., 2020). The cannabis research field is slowly catching up to the level of investigation that is observed for other valuable crop species, with one example being a recent study demonstrating a high-throughput assay using genetic markers to identify sex and chemotype of cannabis germplasm (Toth et al., 2020). However, this study was primarily focused on THC:CBD ratios to determine chemotype and when modeling "total potential cannabinoids" only THC, CBD, CBG, and CBC were included, highlighting the limits of current genetic studies (Toth et al., 2020). Regardless of their limitations, these studies signal the beginning of cannabis truly entering 21st century agricultural research.

Trichomes and essential oils in other plant species have been well characterized in recent decades, and it is important that our understanding of cannabis trichomes reach similar levels of comprehension. The increasingly widespread legalization and public acceptance of cannabis suddenly brings a once-shunned plant into a position of intense interest and high demand in a time of exceptional experimental standards, raising expectations that questions surrounding it be answered much more quickly than for previous crops. Simple breeding and agricultural production techniques for influencing metabolite profiles are not precise nor always consistent, leading to a host of potential complications for both producer and consumer. An example of this complication is the growing medicinal and recreational consumer demand for products with greater THC levels, causing a trend referred to as "lab shopping" that is observed where producers will test their products at several laboratories until they receive the desired cannabinoid concentration analysis for their products (Swider, 2021; Zoorob, 2021). The resulting lack of reliability in the identification might potentially lead to health complications and distrust by those who use cannabis for pain mitigation and as an appetite stimulant/anti-emetic. These issues highlight the need for not just a more reliable and ethical approach to cannabis product quality, but also for methods to reliably tailor metabolite production at the trichome source. New approaches, such as phytomicrobiome manipulation and exploitation, present interesting possibilities, as root inoculums have demonstrated similar effects on THC and CBD contents to nitrogen application (Pagnani et al., 2018; Lyu et al., 2019). If methods can be developed to consistently replicate specific metabolite concentrations and combinations within small ranges across cannabis plants at the trichome level, and if these methods were to become standard across the industry, the benefits for both producers, medical practitioners, and consumers would be great.

From a scientific perspective, multiple interesting questions are associated with the glandular trichomes. Primarily, these questions center around differences related to genotype and growing conditions. How changes to soil composition, light, nutrients, water levels, and other environmental factors affect trichome densities remain largely unknown for cannabis. Our knowledge on how the metabolite profiles themselves differ among varieties is limited and primarily based on poor reporting from growers that are incomplete beyond the major cannabinoids and terpenes, leaving 100 of metabolites unknown. Our lack of knowledge in these areas of cannabis metabolism and composition make it difficult to directly hypothesize exactly where and how differences occur, stressing the need for rigorous uniform standards to allow unbiased and scientifically sound data comparisons. The more we understand about trichomes, the more applicable our knowledge of this plant will be to those along the chain of production and consumption.

AUTHOR CONTRIBUTIONS

CT compiled the literature and prepared the manuscript. AG and DS provided the conceptual context. RB, DS, and AG provided the revision and feedback. All authors contributed to the article and approved the submitted version.

FUNDING

Funding for this work was provided by the NSERC (CREATE 543319-2020) and the RGPIN/04714-2018, RGPIN-2020-07047.

ACKNOWLEDGMENTS

The authors would like to acknowledge the editor and reviewers for their constructive feedback on the first version of this review.

REFERENCES

Aizpurua-Olaizola, O., Soydaner, U., Öztürk, E., Schibano, D., Simsir, Y., Navarro, P., et al. (2016). Evolution of the cannabinoid and terpene content during the growth of *Cannabis sativa* plants from different Chemotypes. *J. Nat. Prod.* 95, 207–217. doi: 10.1021/acs.jnatprod.5b00949

Aliferis, K. A., and Bernard-Perron, D. (2020). Cannabinomics: application of metabolomics in cannabis (*Cannabis sativa* L.) Research and Development. *Front. Plant Sci.* 11:554. doi: 10.3389/fpls.2020.00554

Andre, C. M., Hausman, J. F., and Guerriero, G. (2016). *Cannabis sativa*: the plant of the thousand and one molecules. *Front. Plant Sci.* 7:19. doi: 10.3389/fpls.2016.00019

Appendino, G., Gibbons, S., Giana, A., Pagani, A., Grassi, G., Stavri, M., et al. (2008). Antibacterial cannabinoids from *Cannabis sativa*: A structure-activity study. *J. Nat. Prod.* 71, 1427–1430. doi: 10.1021/np8002673

Bautista, J. L., Yu, S., and Tian, L. (2021). Flavonoids in *Cannabis sativa*: biosynthesis, bioactivities, and biotechnology. *ACS Omega* 6, 5119–5123. doi: 10.1021/acsomega.1c00318

Berman, P., Futoran, K., Lewitus, G. M., Mukha, D., Benami, M., Shlomi, T., et al. (2018). A new ESI-LC/MS approach for comprehensive metabolic profiling of phytocannabinoids in cannabis. *Sci. Rep.* 8:14280. doi: 10.1038/s41598-018-32651-4

Bernstein, N., Gorelick, J., Zerahia, R., and Koch, S. (2019). Impact of N, P, K, and humic acid supplementation on the chemical profile of medical cannabis (*Cannabis sativa* L). *Front. Plant Sci.* 10:736. doi: 10.3389/fpls.2019.00736

Booth, J. K., Page, J. E., and Bohlmann, J. (2017). Terpene synthases from *Cannabis sativa*. *PLoS One* 12:e073911. doi: 10.1371/journal.pone.0173911

Braich, S., Baillie, R. C., Jewell, L. S., Spangenberg, G. C., and Cogan, N. O. I. (2019). Generation of a comprehensive transcriptome atlas and transcriptome dynamics in medicinal cannabis. *Sci. Rep.* 9:16583. doi: 10.1038/s41598-019-53023-6

Burgel, L., Hartung, J., Pflugfelder, A., and Graeff-Hönninger, S. (2020). Impact of growth stage and biomass fractions on cannabinoid content and yield of different hemp (*Cannabis sativa* L.) genotypes. *Agronomy* 10:372. doi: 10.3390/agronomy10030372

Campiglia, E., Radicetti, E., and Mancinelli, R. (2017). Plant density and nitrogen fertilization affect agronomic performance of industrial hemp (*Cannabis sativa* L.) in Mediterranean environment. *Ind. Crop. Prod.* 100, 246–254. doi: 10.1016/j.indcrop.2017.02.022

Conant, R. T., Walsh, R. P., Walsh, M., Bell, C. W., and Wallenstein, M. D. (2017). Effects of a microbial biostimulant, mammoth PTM, on *Cannabis sativa* bud yield. *J. Hortic.* 4:191. doi: 10.4172/2376-0354.1000191

Conneely, L. J., Mauleon, R., Mieog, J., Barkla, B. J., and Kretzschmar, T. (2021). Characterization of the *Cannabis sativa* glandular trichome proteome. *PLoS One* 16:e0242633. doi: 10.1371/journal.pone.0242633

Danziger, N., and Bernstein, N. (2021a). Light matters: effect of light spectra on cannabinoid profile and plant development of medical cannabis (*Cannabis sativa* L.). *Ind. Crop. Prod.* 164:113351. doi: 10.1016/j.indcrop.2021.113351

Danziger, N., and Bernstein, N. (2021b). Plant architecture manipulation increases cannabinoid standardization in 'drug-type' medical cannabis. *Ind. Crop. Prod.* 167:113528. doi: 10.1016/j.indcrop.2021.113528

Dayanandan, P., and Kaufman, P. B. (1976). Trichomes of *Cannabis sativa* L. (Cannabaceae). *Am. J. Bot.* 63, 578–591. doi: 10.1002/j.1537-2197.1976.tb11846.x

Degenhardt, J., Köllner, T. G., and Gershenzon, J. (2009). Monoterpene and sesquiterpene synthases and the origin of terpene skeletal diversity in plants. *Phytochemistry* 70, 1621–1637. doi: 10.1016/j.phytochem.2009.07.030

Desaulniers Brousseau, V., Wu, B. S., MacPherson, S., Morello, V., and Lefsrud, M. (2021). Cannabinoids and terpenes: how production of photo-protectants can be manipulated to enhance *Cannabis sativa* L. Phytochemistry. *Front. Plant Sci.* 12:620021. doi: 10.3389/fpls.2021.620021

Eichhorn Bilodeau, S., Wu, B. S., Rufyikiri, A. S., MacPherson, S., and Lefsrud, M. (2019). An update on plant photobiology and implications for cannabis production. *Front. Plant Sci.* 10, 296. doi: 10.3389/fpls.2019.00296

ElSohly, M. A., and Gul, W. (2014). "Constituents of *cannabis sativa*," in *Handbook of Cannabis*. ed. R. Pertwee (Oxford: Oxford University Press), 3–22. doi: 10.1093/acprof:oso/9780199662685.003.0001

ElSohly, M. A., and Slade, D. (2005). Chemical constituents of marijuana: the complex mixture of natural cannabinoids. *Life Sci.* 78, 539–548. doi: 10.1016/j.lfs.2005.09.011

Fairbairn, J. W. (1972). The trichomes and glands of Cannabis sativa L. *BULL. STUPEF* 24, 29–33.

Farha, M. A., El-Halfawy, O. M., Gale, R. T., Macnair, C. R., Carfrae, L. A., Zhang, X., et al. (2020). Uncovering the hidden antibiotic potential of cannabis. *ACS Infect. Dis.* 6, 338–346. doi: 10.1021/acsinfecdis.9b00419

Flores-Sanchez, I. J., and Verpoorte, R. (2008). Secondary metabolism in cannabis. *Phytochem. Rev.* 7, 615–639. doi: 10.1007/s11101-008-9094-4

Gohad, P., McCoy, J., Wambier, C., Kovacevic, M., Situm, M., Stanimirovic, A., et al. (2020). Novel cannabidiol sunscreen protects keratinocytes and melanocytes against ultraviolet B radiation. *J. Cosmet. Dermatol.* 20, 1350–1352. doi: 10.1111/jocd.13693

Grand View Research (2020). Essential Oils Market Size, Share & Trends Analysis Report by Application (Food & Beverages, Spa & Relaxation), By Product (Orange, Peppermint), By Sales Channel, And Segment Forecasts, 2020–2027. *San Francisco, CA*. Available at: https://www.grandviewresearch.com/industry-analysis/essential-oils-market#:~:text=The%20global%20essential%20oils%20market%20size%20was%20estimated%20at%20USD,USD%2018.6%20billion20in202020.&text=The%20global%20essential%20oils%20market%20is%20expected%20to%20grow%20at,USD%2033.3%20billion20by202027 (Accessed 05 June, 2021)

Gülck, T., and Møller, B. L. (2020). Phytocannabinoids: origins and biosynthesis. *Trends Plant Sci.* 25, 985–1004. doi: 10.1016/j.tplants.2020.05.005

Hammond, C. T., and Mahlberg, P. G. (1973). Morphology of glandular hairs of *Cannabis sativa* from scanning electron microscopy. *Am. J. Bot.* 60, 524–528. doi: 10.1002/j.1537-2197.1973.tb05953.x

Hanuš, L. O., Meyer, S. M., Muñoz, E., Taglialatela-Scafati, O., and Appendino, G. (2016). Phytocannabinoids: a unified critical inventory. *Nat. Prod. Rep.* 33, 1357–1392. doi: 10.1039/C6NP00074F

Hare, J. D., Elle, E., and Van Dam, N. M. (2003). Costs of glandular trichomes in Datura wrightii: a three-year study. *Evolution* 57, 793–805. doi: 10.1111/j.0014-3820.2003.tb00291.x

Hawley, D., Graham, T., Stasiak, M., and Dixon, M. (2018). Improving cannabis bud quality and yield with subcanopy lighting. *HortScience* 53, 1593–1599. doi: 10.21273/HORTSCI13173-18

Janatová, A., Fraňková, A., Tlustoš, P., Hamouz, K., Božik, M., and Klouček, P. (2018). Yield and cannabinoids contents in different cannabis (*Cannabis sativa* L.) genotypes for medical use. *Ind. Crops Prod.* 112, 363–367. doi: 10.1016/j.indcrop.2017.12.006

Jin, D., Dai, K., Xie, Z., and Chen, J. (2020). Secondary metabolites profiled in cannabis inflorescences, leaves, stem barks, and roots for medicinal purposes. *Sci. Rep.* 10:3309. doi: 10.1038/s41598-020-60172-6

Kim, E. S., and Mahlberg, P. G. (1991). Secretory cavity development in glandular Trichomes of *Cannabis sativa* L. (Cannabaceae). *Am. J. Bot.* 78, 220–229. doi: 10.1002/j.1537-2197.1991.tb15749.x

Kim, E. S., and Mahlberg, P. G. (1997). Immunochemical localization of tetrahydrocannabinol (THC) in cryofixed glandular trichomes of cannabis (Cannabaceae). *Am. J. Bot.* 84, 336–342. doi: 10.2307/2446007

Kim, K. S., Vuong, T. D., Qiu, D., Robbins, R. T., Grover Shannon, J., Li, Z., et al. (2016). Advancements in breeding, genetics, and genomics for resistance to three nematode species in soybean. *Theor. Appl. Genet.* 129, 2295–2311. doi: 10.1007/s00122-016-2816-x

Koren, A., Sikora, V., Kiprovski, B., Brdar-Jokanović, M., Aćimović, M., Konstantinović, B., et al. (2020). Controversial taxonomy of hemp. *Genetika* 52, 1–13. doi: 10.2298/GENSR2001001K

Leme, F. M., Schönenberger, J., Staedler, Y. M., and Teixeira, S. P. (2020). Comparative floral development reveals novel aspects of structure and diversity of flowers in Cannabaceae. *Bot. J. Linn. Soc.* 193, 64–83. doi: 10.1093/botlinnean/boaa004

Levin, D. A. (1973). The role of Trichomes in plant defense. *Q. Rev. Biol.* 48, 3–15. doi: 10.1086/407484

Liu, Y., Zhu, P., Cai, S., Haughn, G., and Page, J. E. (2021). Three novel transcription factors involved in cannabinoid biosynthesis in *Cannabis sativa* L. *Plant Mol. Biol.* 106, 49–65. doi: 10.1007/s11103-021-01129-9

Livingston, S. J., Quilichini, T. D., Booth, J. K., Wong, D. C. J., Rensing, K. H., Laflamme-Yonkman, J., et al. (2020). Cannabis glandular trichomes alter

morphology and metabolite content during flower maturation. *Plant J.* 101, 37–56. doi: 10.1111/tpj.14516

Lyu, D., Backer, R., Robinson, W. G., and Smith, D. L. (2019). Plant growth-promoting Rhizobacteria for cannabis production: yield, cannabinoid profile and disease resistance. *Front. Microbiol.* 10:1761. doi: 10.3389/fmicb.2019.01761

Magagnini, G., Grassi, G., and Kotiranta, S. (2018). The effect of light Spectrum on the morphology and cannabinoid content of *Cannabis sativa* L. *Med. Cannabis Cannabinoids* 1, 19–27. doi: 10.1159/000489030

Mahlberg, P. G., and Kim, E. S. (2004). Accumulation of cannabinoids in glandular trichomes of cannabis (Cannabaceae). *J. Ind. Hemp* 9, 15–36. doi: 10.1300/J237v09n01_04

Marks, M. D., Tian, L., Wenger, J. P., Omburo, S. N., Soto-Fuentes, W., He, J., et al. (2009). Identification of candidate genes affecting Δ9-tetrahydrocannabinol biosynthesis in *Cannabis sativa*. *J. Exp. Bot.* 60, 3715–3726. doi: 10.1093/jxb/erp210

Matoušek, J., Kocábek, T., Patzak, J., Bříza, J., Siglová, K., Mishra, A. K., et al. (2016). The "putative" role of transcription factors from HlWRKY family in the regulation of the final steps of prenylflavonid and bitter acids biosynthesis in hop (*Humulus lupulus* L.). *Plant Mol. Biologicals* 92, 263–277. doi: 10.1007/s11103-016-0510-7

Mediavilla, V., and Steinemann, S. (1997). Essential oil of *Cannabis sativa* L. strains. *J. Ind. Hemp* 4, 80–82.

Mishra, A. K., Kocábek, T., Nath, V. S., Awasthi, P., Shrestha, A., Killi, U. K., et al. (2020). Dissection of dynamic transcriptome landscape of leaf, bract, and lupulin gland in hop (*Humulus lupulus* L.). *Int. J. Mol. Sci.* 21:233. doi: 10.3390/ijms21010233

Mudge, E. M., Brown, P. N., and Murch, S. J. (2019). The terroir of cannabis: terpene metabolomics as a tool to understand *Cannabis sativa* selections. *Planta Med.* 85, 781–796. doi: 10.1055/a-0915-2550

Muravnik, L. E. (2020). "The structural peculiarities of the leaf glandular Trichomes: A review," in *Plant Cell and Tissue Differentiation and Secondary Metabolites. Reference Series in Phytochemistry*. eds. K. Ramawat, H. Ekiert and S. Goyal (Cham: Springer), 1–35.

Namdar, D., Mazuz, M., Ion, A., and Koltai, H. (2018). Variation in the compositions of cannabinoid and terpenoids in *Cannabis sativa* derived from inflorescence position along the stem and extraction methods. *Ind. Crop. Prod.* 113, 376–382. doi: 10.1016/j.indcrop.2018.01.060

Nerio, L. S., Olivero-Verbel, J., and Stashenko, E. (2010). Repellent activity of essential oils: A review. *Bioresour. Technol.* 101, 372–378. doi: 10.1016/j.biortech.2009.07.048

Ohlsson, A., Abou-Chaar, C. I., Agurell, S., Nilsson, I. M., Olofsson, K., and Sandberg, F. (1971). Cannabinoid constituents of male and female Cannabis sativa. *Bull Narc.* 23, 29–32.

Pagnani, G., Pellegrini, M., Galieni, A., D'Egidio, S., Matteucci, F., Ricci, A., et al. (2018). Plant growth-promoting rhizobacteria (PGPR) in *Cannabis sativa* 'Finola' cultivation: An alternative fertilization strategy to improve plant growth and quality characteristics. *Ind. Crop. Prod.* 123, 75–83. doi: 10.1016/j.indcrop.2018.06.033

Panche, A. N., Diwan, A. D., and Chandra, S. R. (2016). Flavonoids: An overview. *J. Nutr. Sci.* 5:e47. doi: 10.1017/jns.2016.41

Pate, D. W. (1983). Possible role of ultraviolet radiation in evolution of cannabis chemotypes. *Econ. Bot.* 37, 396–405. doi: 10.1007/BF02904200

Potter, D. J. (2009). The propagation, characterisation and optimisation of *Cannabis sativa* L. as a phytopharmaceutical. Doctoral thesis. London, England: King's College London.

Ren, G., Zhang, X., Li, Y., Ridout, K., Serrano-Serrano, M. L., Yang, Y., et al. (2021). Large-scale whole-genome resequencing unravels the domestication history of *Cannabis* sativa. *Sci. Adv.* 7:eabg2286. doi: 10.1126/sciadv.abg2286

Russo, E. B. (2011). Taming THC: potential cannabis synergy and phytocannabinoid-terpenoid entourage effects. *Br. J. Pharmacol.* 163, 1344–1364. doi: 10.1111/j.1476-5381.2011.01238.x

Russo, E. B., and McPartland, J. M. (2001). Cannabis and cannabis extracts: greater than the sum of their parts? *J. Cannabis Ther.* 1, 103–132.

Saloner, A., and Bernstein, N. (2021). Nitrogen supply affects cannabinoid and terpenoid profile in medical cannabis (*Cannabis sativa* L.). *Ind. Crop. Prod.* 167:113516. doi: 10.1016/j.indcrop.2021.113516

Sangwan, N. S., Farooqi, A. H. A., Shabih, F., and Sangwan, R. S. (2001). Regulation of essential oil production in plants. *Plant Growth Regul.* 34, 3–21. doi: 10.1023/A:1013386921596

Sirikantaramas, S., Taura, F., Tanaka, Y., Ishikawa, Y., Morimoto, S., and Shoyama, Y. (2005). Tetrahydrocannabinolic acid synthase, the enzyme controlling marijuana psychoactivity, is secreted into the storage cavity of the glandular trichomes. *Plant Cell Physiol.* 46, 1578–1582. doi: 10.1093/pcp/pci166

Sirikantaramas, S., Yamazaki, M., and Saito, K. (2008). Mechanisms of resistance to self-produced toxic secondary metabolites in plants. *Phytochem. Rev.* 7:467. doi: 10.1007/s11101-007-9080-2

Spitzer-Rimon, B., Duchin, S., Bernstein, N., and Kamenetsky, R. (2019). Architecture and florogenesis in female *Cannabis sativa* plants. *Front. Plant Sci.* 10:350. doi: 10.3389/fpls.2019.00350

Swider, J.. (2021). Lab Shopping: Highlighting the Need for Checks and Balances in Cannabis. Available at: https://cannabisindustryjournal.com/column/lab-shopping-highlighting-the-need-for-checks-and-balances-in-cannabis/ (Accessed 6 May, 2021).

Taghinasab, M., and Jabaji, S. (2020). Cannabis microbiome and the role of endophytes in modulating the production of secondary metabolites: an overview. *Microorganisms* 8:355. doi: 10.3390/microorganisms8030355

Tang, K., Struik, P. C., Yin, X., Calzolari, D., Musio, S., Thouminot, C., et al. (2017). A comprehensive study of planting density and nitrogen fertilization effect on dual-purpose hemp (*Cannabis sativa* L.) cultivation. *Ind. Crop. Prod.* 107, 427–438. doi: 10.1016/j.indcrop.2017.06.033

Taschwer, M., and Schmid, M. G. (2015). Determination of the relative percentage distribution of THCA and δ9-THC in herbal cannabis seized in Austria - Impact of different storage temperatures on stability. *Forensic Sci. Int.* 254, 167–171. doi: 10.1016/j.forsciint.2015.07.019

Tian, N., Liu, F., Wang, P., Zhang, X., Li, X., and Wu, G. (2017). The molecular basis of glandular trichome development and secondary metabolism in plants. *Plant Gene* 12, 1–12. doi: 10.1016/j.plgene.2017.05.010

Tissier, A., Morgan, J. A., and Dudareva, N. (2017). Plant volatiles: going 'In' but not 'Out' of Trichome cavities. *Trends Plant Sci.* 22, 930–938. doi: 10.1016/j.tplants.2017.09.001

Tomko, A. M., Whynot, E. G., Ellis, L. D., and Dupré, D. J. (2020). Anti-cancer potential of cannabinoids, terpenes, and flavonoids present in cannabis. *Cancers* 12:1985. doi: 10.3390/cancers12071985

Toth, J. A., Stack, G. M., Cala, A. R., Carlson, C. H., Wilk, R. L., Crawford, J. L., et al. (2020). Development and validation of genetic markers for sex and cannabinoid chemotype in *Cannabis sativa* L. *GCB Bioenergy* 12, 213–222. doi: 10.1111/gcbb.12667

van Klingeren, B., and ten Ham, M. (1976). Antibacterial activity of Δ9-tetrahydrocannabinol and cannabidiol. *Antonie Van Leeuwenhoek* 42, 9–12. doi: 10.1007/BF00399444

Vanhove, W., Van Damme, P., and Meert, N. (2011). Factors determining yield and quality of illicit indoor cannabis (cannabis spp.) production. *Forensic Sci. Int.* 212, 158–163. doi: 10.1016/j.forsciint.2011.06.006

Wagner, G. J. (1991). Secreting glandular trichomes: more than just hairs. *Plant Physiol.* 96, 675–679. doi: 10.1104/pp.96.3.675

Yamauchi, T., Shoyama, Y., Aramaki, H., Azuma, T., and Nishioka, I. (1967). Tetrahydrocannabinolic acid, a genuine substance of tetrahydrocannabinol. *Chem. Pharm. Bull.* 15, 1076–1079. doi: 10.1248/cpb.15.1075

Zager, J. J., Lange, I., Srividya, N., Smith, A., and Markus Lange, B. (2019). Gene networks underlying cannabinoid and terpenoid accumulation in cannabis. *Plant Physiol.* 180, 1877–1897. doi: 10.1104/pp.18.01506

Zoorob, M. J. (2021). The frequency distribution of reported THC concentrations of legal cannabis flower products increases discontinuously around the 20% THC threshold in Nevada and Washington state. *J. Cannabis Res.* 3:6. doi: 10.1186/s42238-021-00064-2

Conflict of Interest: The authors declare that the research was conducted in the absence of any commercial or financial relationships that could be construed as a potential conflict of interest.

Publisher's Note: All claims expressed in this article are solely those of the authors and do not necessarily represent those of their affiliated organizations, or those of the publisher, the editors and the reviewers. Any product that may

be evaluated in this article, or claim that may be made by its manufacturer, is not guaranteed or endorsed by the publisher.

frontiers in Plant Science

ORIGINAL RESEARCH
published: 21 September 2021
doi: 10.3389/fpls.2021.732344

Variables Affecting Shoot Growth and Plantlet Recovery in Tissue Cultures of Drug-Type *Cannabis sativa* L.

*Janesse E. Holmes, Samantha Lung, Danielle Collyer and Zamir K. Punja**

Department of Biological Sciences, Simon Fraser University, Burnaby, BC, Canada

Tissue culture approaches are widely used in crop plants for the purposes of micropropagation, regeneration of plants through organogenesis, obtaining pathogen-free plantlets from meristem culture, and developing genetically modified plants. In this research, we evaluated variables that can influence the success of shoot growth and plantlet production in tissue cultures of drug-type *Cannabis sativa* L. (marijuana). Various sterilization methods were tested to ensure shoot development from nodal explants by limiting the frequency of contaminating endophytes, which otherwise caused the death of explants. Seven commercially grown tetrahydrocannabinol (THC)-containing cannabis genotypes (strains) showed significant differences in response to shoot growth from meristems and nodal explants on Murashige and Skoog (MS) medium containing thidiazuron (1 μM) and naphthaleneacetic acid (0.5 μM) plus 1% activated charcoal. The effect of Driver and Kuniyuki Walnut (DKW) or MS basal salts in media on shoot length and leaf numbers from nodal explants was compared and showed genotype dependency with regard to the growth response. To obtain rooted plantlets, shoots from meristems and nodal explants of genotype Moby Dick were evaluated for rooting, following the addition of sodium metasilicate, silver nitrate, indole-3-butyric acid (IBA), kinetin, or 2,4-D. Sodium metasilicate improved the visual appearance of the foliage and improved the rate of rooting. Silver nitrate also promoted rooting. Following acclimatization, plantlet survival in hydroponic culture, peat plugs, and rockwool substrate was 57, 76, and 83%, respectively. The development of plantlets from meristems is described for the first time in *C. sativa* and has potential for obtaining pathogen-free plants. The callogenesis response of leaf explants of 11 genotypes on MS medium without activated charcoal was 35% to 100%, depending on the genotype; organogenesis was not observed. The success in recovery of plantlets from meristems and nodal explants is influenced by cannabis genotype, degree of endophytic contamination of the explants, and frequency of rooting. The procedures described here have potential applications for research and commercial utility to obtain plantlets in stage 1 tissue cultures of *C. sativa*.

Keywords: meristems, nodal explants, shoot growth, rooting, plantlet recovery, micropropagation, callogenesis, *Cannabis sativa* L.

OPEN ACCESS

Edited by:
David Meiri,
Technion Israel Institute of Technology, Israel

Reviewed by:
Laura Pistelli,
University of Pisa, Italy
Alessandro Nicolia,
Council for Agricultural and Economics Research (CREA), Italy

****Correspondence:***
Zamir K. Punja
punja@sfu.ca

Specialty section:
This article was submitted to Crop and Product Physiology, a section of the journal Frontiers in Plant Science

Received: *28 June 2021*
Accepted: *10 August 2021*
Published: *21 September 2021*

Citation:
Holmes JE, Lung S, Collyer D and Punja ZK (2021) Variables Affecting Shoot Growth and Plantlet Recovery in Tissue Cultures of Drug-Type Cannabis sativa L. Front. Plant Sci. 12:732344. doi: 10.3389/fpls.2021.732344

INTRODUCTION

Cannabis sativa L., a member of the Cannabaceae family, is a dioecious, annual flowering plant that has been cultivated for thousands of years for its fiber (as hemp) and medicinal and psychotropic properties (as cannabis or marijuana). Vegetative cuttings are the conventional method for commercial propagation of cannabis to ensure rapid propagation of desired genotypes without the introduction of genetic variability resulting from sexual reproduction as *C. sativa* is allogamous (Punja and Holmes, 2020). However, vegetative cuttings can lose vigor, since donor (mother or stock) plants can be affected by fungal pathogens and viruses that can reduce their growth and quality (Punja et al., 2019; Punja, 2021). However, maintaining donor plants to be used as a source of vegetative cuttings can be time-consuming and space-intensive. Hence, there is interest in using tissue culture methods to propagate cannabis, as it is recognized as a means to potentially increase plant numbers of desired genotypes (micropropagation), and maintain them in a controlled and stable environment (preservation) (Monthony et al., 2021). In addition, callus production (callogenesis) from explants in tissue culture can potentially be used to increase plant numbers through organogenesis (Page et al., 2021). However, there are still many challenges remaining in establishing a micropropagation and callusing system for cannabis plants (Monthony et al., 2021). The quality of source (donor) plants, genotype or strain used, surface sterilization methods, explant type, and tissue culture medium and growth regulators can all influence the success rate of recovery of plantlets in stage 1 of tissue culture (the introduction of explant material for establishment of cultures). Rooting and acclimatization of plantlets are challenging aspects to tissue culture of hemp and cannabis as well. Lata et al. (2009) reported successful propagation of strain MX-1 of cannabis in tissue culture, but it is not known whether this method can be applied to other genotypes of cannabis. Monthony et al. (2021) described a procedure for the micropropagation of six cannabis genotypes, but rooting and plantlet recovery were not addressed. The success of a tissue culture method for cannabis is contingent upon obtaining a high frequency of plantlets growing independently in growth media.

In this research, we investigated various factors that can influence the recovery of plantlets of cannabis in tissue culture. The objectives of this study were to (1) assess the efficacy of sterilization methods to reduce the frequency of contaminants originating from donor plants; (2) recover and identify the various microbes present as contaminants in tissue cultures; (3) evaluate shoot growth from meristems of five different genotypes; (4) determine the responses of seven different genotypes to shoot growth from nodal explants; (5) evaluate the response of 11 different genotypes to callus development; (6) develop a rooting method for plantlets derived from tissue culture; and (7) evaluate acclimatization responses in different growth substrates (peat, rockwool, and hydroponic system) to achieve a high frequency of plantlet recovery.

MATERIALS AND METHODS

Genotypes

The genotypes used were Moby Dick (MBD), Space Queen (SPQ), Copenhagen Kush (CPH), Cheesequake (CHQ), Pennywise (PWE), Girl Scout Cookie (GSC), Death Bubba (DEB), Afghan Kush (AFK), Island Honey (ISH), Pink Kush (PNK), Pure CBD (CBD), and White Rhino (WHR). Various combinations of genotypes were used in experiments, depending on their availability. Donor plants of the various genotypes were grown by a licensed producer according to Health Canada requirements in a controlled-environment room or under commercial greenhouse conditions The growing medium for the donor plants was either pure coco fibers or a coco fiber:vermiculite mix (3:1). The plants in the controlled-environment room were placed under two Sunblaster brand 54-watt 6400 k T5HO lights with a 24-h photoperiod. The plants were watered as needed with a solution of 1 ml/L Sensi Grow Coco pH Perfect A+B (Advanced Nutrients, Los Angeles, CA, Untied States) and 1 ml/L CALiMAGIc (General Hydroponics, Santa Rosa, CA, United States) adjusted to a pH of 5.8–6.2 using pH-Down (Advanced Nutrients, Los Angeles, CA, Untied States) (Scott and Punja, 2021). The plants in the commercial greenhouse were grown according to the standards for the industry and kept under a 16-h photoperiod to maintain vegetative growth. Explants were taken as needed for the tissue culture experiments described.

Explants

The explants tested included meristems, nodal segments, leaves, and petiole tissues. Meristems were dissected from terminal and lateral shoots from donor plants (**Figure 1A**). The external tissue was cut away with a scalpel, and two sets of primordial leaves were left to protect the meristem from excessive damage from sterilization. Nodal segments with axillary buds were removed from lateral stems of the plants and trimmed to a 1-cm length (**Figure 2A**). Leaves were trimmed from the plants and used for leaf explants in callus induction experiments. They were cut into pieces measuring 0.5 to 1 cm^2. Petiole segments from young leaves were cut into 1-cm long pieces for callus induction.

Sterilization

The standard sterilization protocol involved placing explants in a stainless steel tea strainer and immersing them in 70% EtOH in a glass beaker for 1 min while stirring with a magnetic stir bar. The explants were transferred to a 10% bleach solution (0.625% NaOCl) with 0.1% Tween 20 for 20 min, followed by three rinses in sterile distilled water, 3 min each. In some of the experiments, the bleach concentration, length of sterilization, and length of rinsing were adjusted according to explant type and source. The explants were blotted dry on sterile filter paper placed in a laminar flow hood and used immediately for tissue culture experiments.

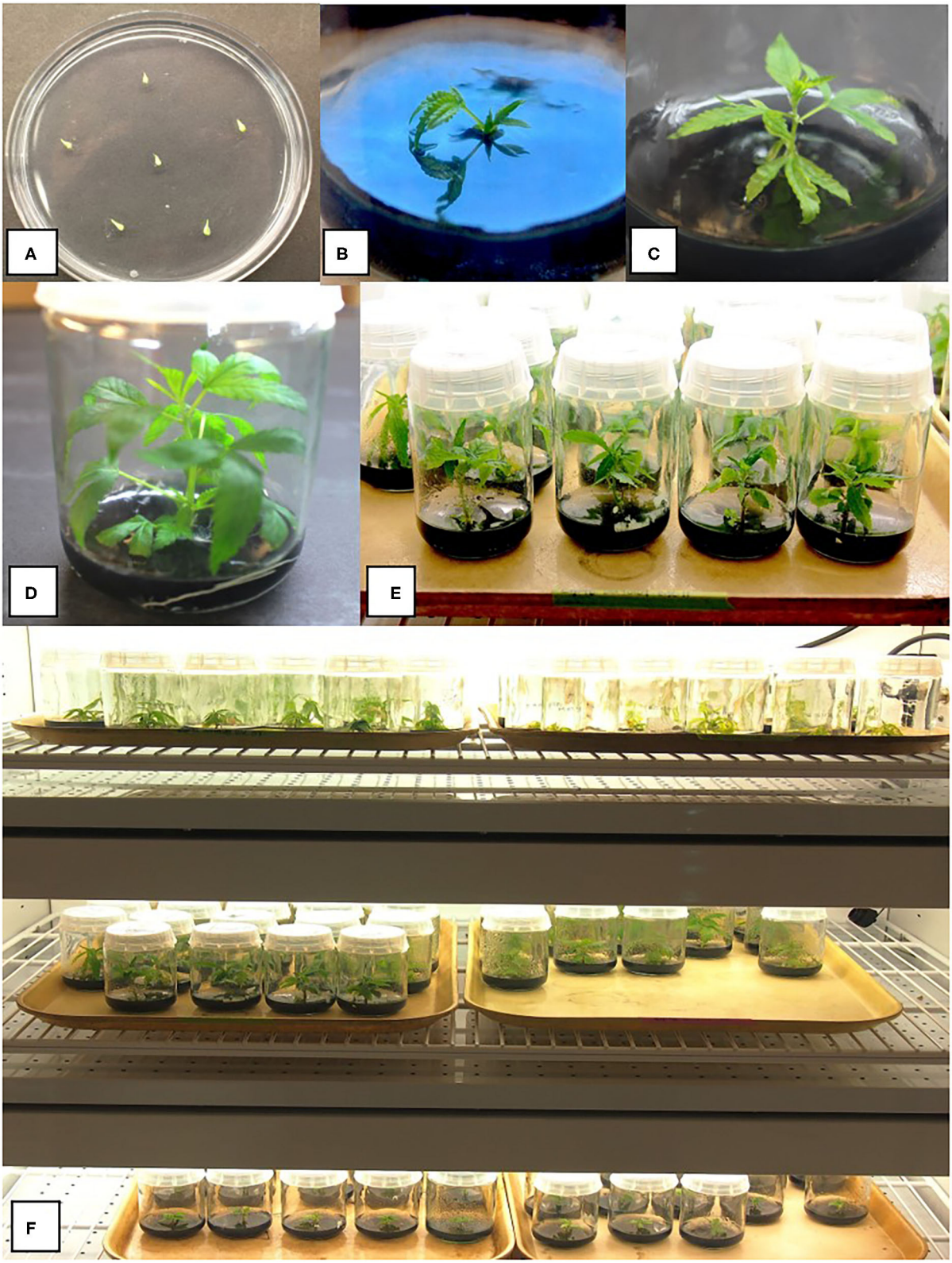

FIGURE 1 | Various stages of growth of shoots derived from meristems of drug-type cannabis genotypes grown on a multiplication medium (MM) containing activated charcoal. **(A)** Meristem explants placed on an agar medium in a 90-mm Petri dish to show their small size. **(B)** Early shoot growth after 4 weeks in culture from a meristem. **(C)** Shoot growth after 8 weeks. **(D,E)** Shoot growth after 10 weeks from meristems. **(F)** Baby food jars containing meristem explants at different stages of development in a controlled environment growth chamber. A number of different strains are shown. Conditions of incubation are described in the Methods section.

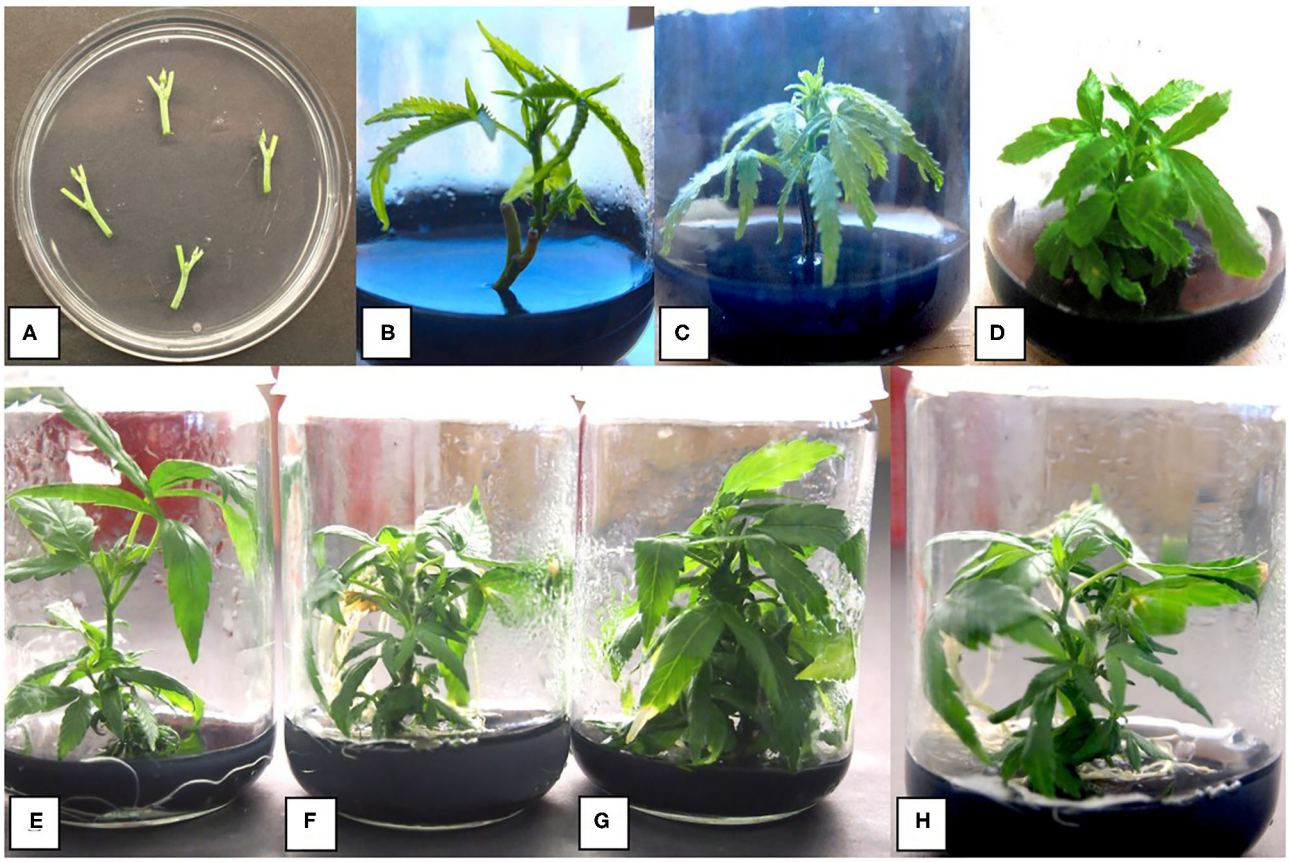

FIGURE 2 | Stages of growth of shoots derived from nodal segments of drug-type cannabis genotypes grown on MM containing activated charcoal. **(A)** Nodal stem explants placed on an agar medium in a 90-mm Petri dish to show their size. **(B)** Shoot growth after 4 weeks from a nodal stem explant. The rate of growth is greater than that from a meristem. **(C)** Shoot growth after 6 weeks. **(D)** Shoot growth after 8 weeks. **(E)** Shoot growth after 8 weeks of genotype Death Bubba (DEB) from nodal explants. **(F)** Shoot growth after 8 weeks of genotype Pink Kush (PNK) from nodal explants. **(G)** Shoot growth after 8 weeks of genotype White Rhino (WHR) from nodal explants. **(H)** Shoot growth after 8 weeks of genotype Moby Dick (MBD) from nodal explants.

Media

The medium containing Murashige and Skoog basal salts, as described by Lata et al. (2009), was used in initial tissue culture experiments. The medium was supplemented with myo-inositol (0.1 g/L) and activated charcoal (1 g/L). The growth regulators added were thidiazuron (TDZ, 1 μM) and naphthaleneacetic acid (NAA, 0.5 μM). This combination of ingredients constitutes a multiplication medium, referred to as MM. All the chemical reagents were from Sigma-Aldrich (St. Louis, MO). The medium was adjusted to pH 6.6 ± 0.01 before autoclaving for 20 min at 121°C. Following autoclaving, the pH dropped to ∼5.8. The medium was dispensed into 220 ml culture jars C1770 with Magenta B caps (Phytotechnology Laboratories®, Lenexa, KS, United States), and each jar received ∼25 ml of the medium. A single meristem or nodal explant was placed inside each jar. For callus induction, MM without activated charcoal (MM-AC) was used. Each 90-mm Petri dish received ∼25 ml of the medium onto which four to five leaves or petiole segments were placed.

Meristem and Nodal Explant Growth

For meristems, genotypes Cheesequake, Pure CBD, Moby Dick, Pennywise, and Space Queen were used. Jars containing meristem explants prepared as described above were placed inside a Conviron A1000 growth chamber (Conviron Environments Ltd., Manitoba, Canada) under T5 fluorescent lights with an 18-h photoperiod and a light intensity of 102 μmoles m^{-2} s^{-1} (**Figure 1**). The temperature range was 25 ± 2°C. The meristems were left in culture for 6 weeks and transferred to fresh MM medium and incubated for another 4 weeks (**Figure 1**). At this time, shoot height, number of axillary buds developing, and number of shoots that formed were evaluated (**Table 1**). There was a minimum of 10 replicate jars, each containing a meristem for each genotype, and the experiment was conducted three times (n = 30) using different sources of explants of the same genotype. The shoots were maintained in culture for a maximum of 3 months by monthly transfer to fresh MM medium.

TABLE 1 | Comparison of growth of shoots from meristems and nodal explants of five genotypes of drug-type *Cannabis sativa*.

Explant type							
Meristems[a]				Nodal segments[a]			
Genotype[b]	Shoot height (cm)	No. of buds	No. of shoots	Genotype[b]	Shoot height (cm)	No. of buds	No. of shoots
CBD	3.6 (0.37) a,d	8.0 (1.38) a	1.9 (0.32) a	BLD	4.9 (0.51) a	4.6 (0.4) a	0.4 (0.13) a
CHQ	1.5 (0.08) b,c	6.2 (0.69) a,c	0.5 (0.18) c	SWD	3.8 (0.27) a	3.8 (0.38) a,b	0.4 (0.17) a
MBD	4.5 (0.42) a	6.9 (0.84) a	1.9 (0.27) a	MBD	2.2 (0.27) b	2.9 (0.28) b	0.3 (0.11) a
SPQ	1.9 (0.15) b	3.4 (0.37) c	0.2 (0.07) b	SPQ	1.5 (0.11) c	1.2 (0.11) c	0.0 (0.0) b
PWE	3.1 (0.25) c,d	5.6 (0.53) a,c	2.0 (0.31) a	–	–	–	–

[a] *Data for meristems were collected after 10 weeks in culture and for nodal explants after 6 weeks in culture.*

[b] *Within each explant type, genotypes were compared with each other for shoot height, number of buds produced, and number of shoots. Data presented are from 10 explants, and the experiment was conducted three times (n = 30). Means were compared following ANOVA, and means separation was achieved by Tukey's honestly significant difference (HSD) test. Means within a column followed by the same letter are not significantly different at P < 0.05.*

For nodal segments, genotypes BLD, SPQ, MBD, and SWD were used. Jars containing a segment each were incubated under T5 fluorescent lights with an 18-h photoperiod and a light intensity of 102 μmoles m^{-2} s^{-1} and a temperature range of 21–27°C for 2 weeks. The shoots were transferred to fresh MM medium and allowed to grow for another 4 weeks (**Figure 2**). The percentage of explants surviving, shoot height, number of shoots per explant, number of buds developing, and number of leaves were recorded (**Table 1**). For each genotype tested, there was a minimum of 10 replicate jars, each containing a nodal explant, and the experiment was conducted three times ($n = 30$) using different explant sources of the same genotype. To determine if there were differences between the genotypes, the data were analyzed using Statplus version 2.21 and R systems (version 3.3.3). ANOVA was performed followed by Tukey's honestly significant difference (HSD) test to determine significance at $P < 0.05$.

Comparison of DKW and MS Salts

Two basal salts media, Driver and Kuniyuki Walnut (cat.#D190; Phytotechnology Laboratories®, Lenexa, KS, United States) and Murashige and Skoog (cat.#M5524; Sigma Aldrich, Saint Louis, MO, United States), were compared for nodal explant growth using genotypes CPH and PWE. The composition of DKW medium, as used in this study, is as follows: 5.22 g/L DKW basal salts, 20 g/L sucrose, 0.1 g/L myo-inositol, 1 ml/L Gamborg B5 vitamins, 0.5 uM NAA, 1 uM TDZ, 1 g/L activated charcoal, and 3 g/L Phytagel. Explants were sterilized as described above but rinsed for 1 min instead of 3 min. They were transferred to either DKW or MM. Twenty jars, each containing a nodal explant, were placed under the lighting conditions described above. The initial height of the nodal explants was measured 4 days after placement on each medium to account for differences between initial explant size. The explants were transferred to the respective fresh media after 2 weeks, and 2 weeks later, the heights of the shoot from the base where it attached to the original explant to the top were measured using ImageJ. The height differences from the start to the end of the experiment represented the shoot height for each explant. The number of leaves on nodal explants on each medium was also assessed (**Figure 3**). The experiment was conducted twice. Only data from nodal stem segments that grew were included in the statistical analysis. The shoot height data for CPH on both media were compared by an unpaired two-sample *t*-test. For the data on leaf numbers for CPH and the shoot length data and number of leaves data for PWE, Wilcoxon Rank Sum non-parametric tests were performed as the data did not meet the "normality" assumptions of the unpaired two-sample *t*-test.

Internal Contaminants in Nodal Explants

In many nodal explants derived from donor plants used in tissue culture experiments, contamination by fungi, bacteria, and yeasts was frequently observed on the agar medium, in some cases up to 50%. This caused many of the explants to die (**Figure 4**). To reduce the level of microbial contamination, the following treatments were assessed by adding them to MM by filter sterilization after autoclaving: (1) the fungicide captan (Maestro 8-DF) was added at 0.01 and 0.02 g/L; (2) streptomycin sulfate was added at 100 mg/L; (3) Plant Preservative Mixture (PPM) (Plant Cell Technology, Washington, DC, United States) was added at 2 mg/L. For all treatments, 10 nodal stem segments of genotype CHQ were used for each of the treatments, and the experiment was conducted twice ($n = 20$). Assessments of the extent of microbial contamination were made after 4 weeks. To assess the effect of fungicides on endophytic contamination, the fungicide Luna (fluopyram) was applied to donor plants of genotypes CPH and PWE at 5 ml/L as a foliar spray until run-off. Plants were grown for 3 weeks before nodal stem segments were collected. Nodal stem segments from treated and control plants were dissected and sterilized with ethanol:bleach as described previously and rinsed with sterile distilled three times for 1 min each. The nodal stem segments were transferred to MM and grown under a 16-h photoperiod for 4 weeks, after which the proportion of jars with microbial contamination was evaluated. A total of 20 explants were included for each treatment group. The data obtained from the CPH genotype met the requirements for a chi-square test, but the data from PWE did not, so Fisher's Exact test was performed. The experiment was conducted once. The sample size was $n = 20$ for each group.

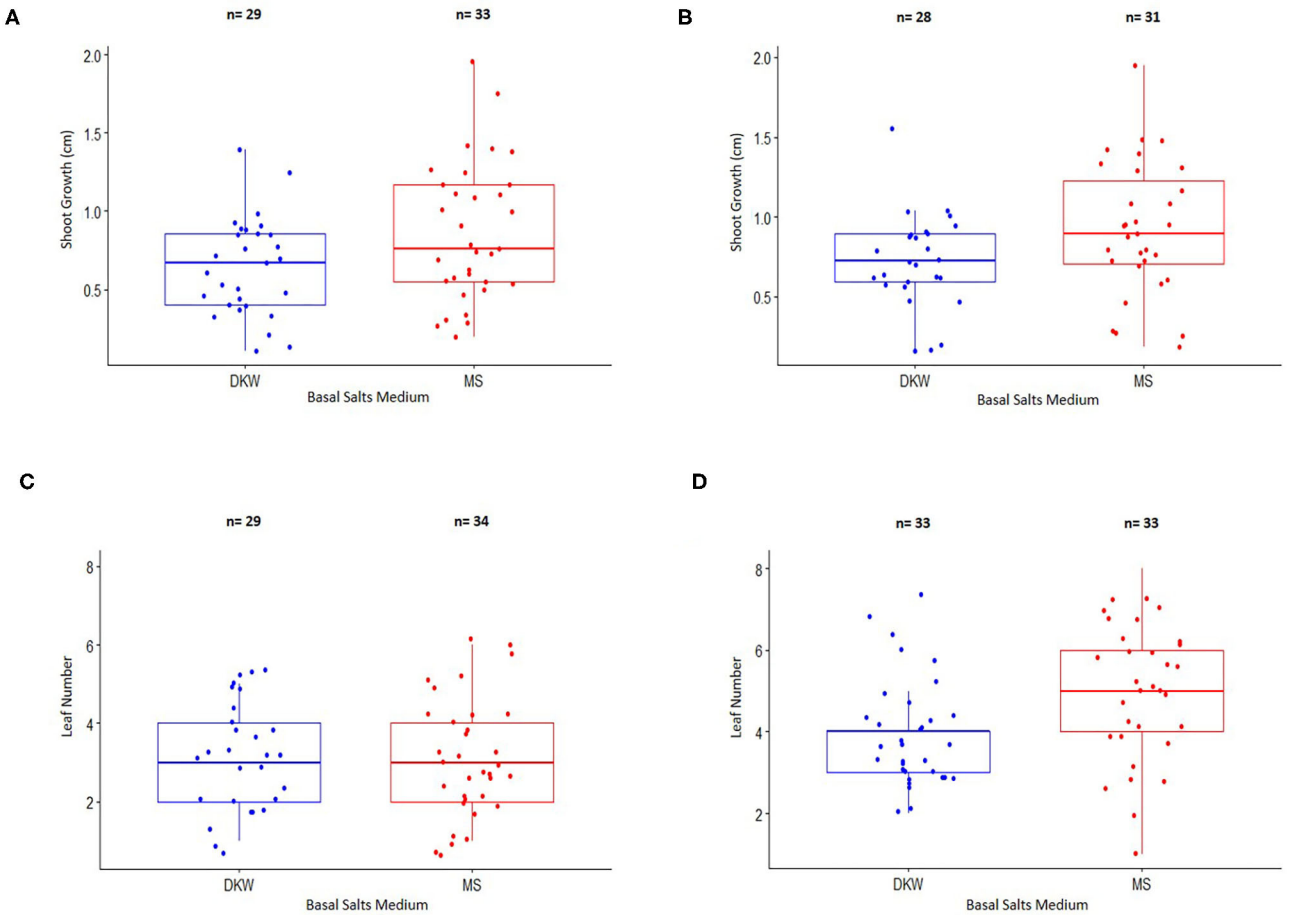

FIGURE 3 | Comparison of shoot growth and leaf number from nodal stem explants of two cannabis genotypes placed on a basal salt medium containing either Driver and Kuniyuki Walnut (DKW) or Murashige and Skoog (MS) salts. **(A)** Shoot length of genotype Copenhagen Kush (CPH). **(B)** Shoot length of genotype Pennywise (PWE). **(C)** Leaf number of genotype Copenhagen Kush (CPH). **(D)** Leaf numbers of genotype Pennywise (PWE). The box of each dataset represents the interquartile range (IQR), which contains the third quartile (Q3–top side of the box), the median value of all of the data (the middle line), and the first quartile (Q1–bottom side of the box). The bars represent the maximum (Q3 + 1.5*IQR) and minimum (Q1–1.5*IQR) of the data. The numbers (*n*) above the bars depict explant numbers used.

Identification of Tissue Culture Contaminants

Colonies representing the most common contaminants seen in tissue culture were transferred to potato dextrose agar + streptomycin (130 mg/L) for 2 weeks and then to potato dextrose broth placed on a shaker at 125 rpm at room temperature for 7 days. The mycelium was harvested, and DNA was extracted using the DNeasy Plant Mini Kit (cat. No. 69104; QIAGEN, Hilden, Germany). For PCR, the internal transcribed spacer regions (ITS1 and ITS2) as well as the 5.8S gene of ribosomal rDNA were amplified using the universal eukaryotic primers UN-UP18S42 (5′-CGTAACAAGGTTTCCG TAGGTGAAC-3′) and UN-LO28S576B (5′-GTTTCTTTTCC TCCGCTTATTAATATG-3′) to produce a DNA template for sequencing. PCR conditions were as follows: initial denaturation at 94°C for 3 min, followed by 40 cycles of denaturation at 94°C for 30 s, annealing at 55°C for 45 s, and extension at 72°C for 2 min, and a final extension at 72°C for 7 min, followed by 4°C hold. PCR products were cut and sent to Eurofins Genomics (Eurofins MWG Operon LLC 2016, Louisville, KY, United States) for sequencing. The resulting sequences were compared with the corresponding ITS1-5.8S-ITS2 sequences from the National Center for Biotechnology Information (NCBI) GenBank database to confirm species identity using only sequence identity values above 99%. Once the identity of the cultured microbes was determined, random samples of nodal explants were obtained from the same donor plants (genotypes CPH and MBD), and 10–50 mg of fresh tissue was used for total DNA extraction and PCR following the conditions described above for fungal cultures. For examination of the nodal explants under a scanning electron microscope for potential microbes that could be present in internal tissues, samples were taken from donor plants known to be contaminated based on isolation in culture. They were processed following the procedure described by Punja et al. (2019).

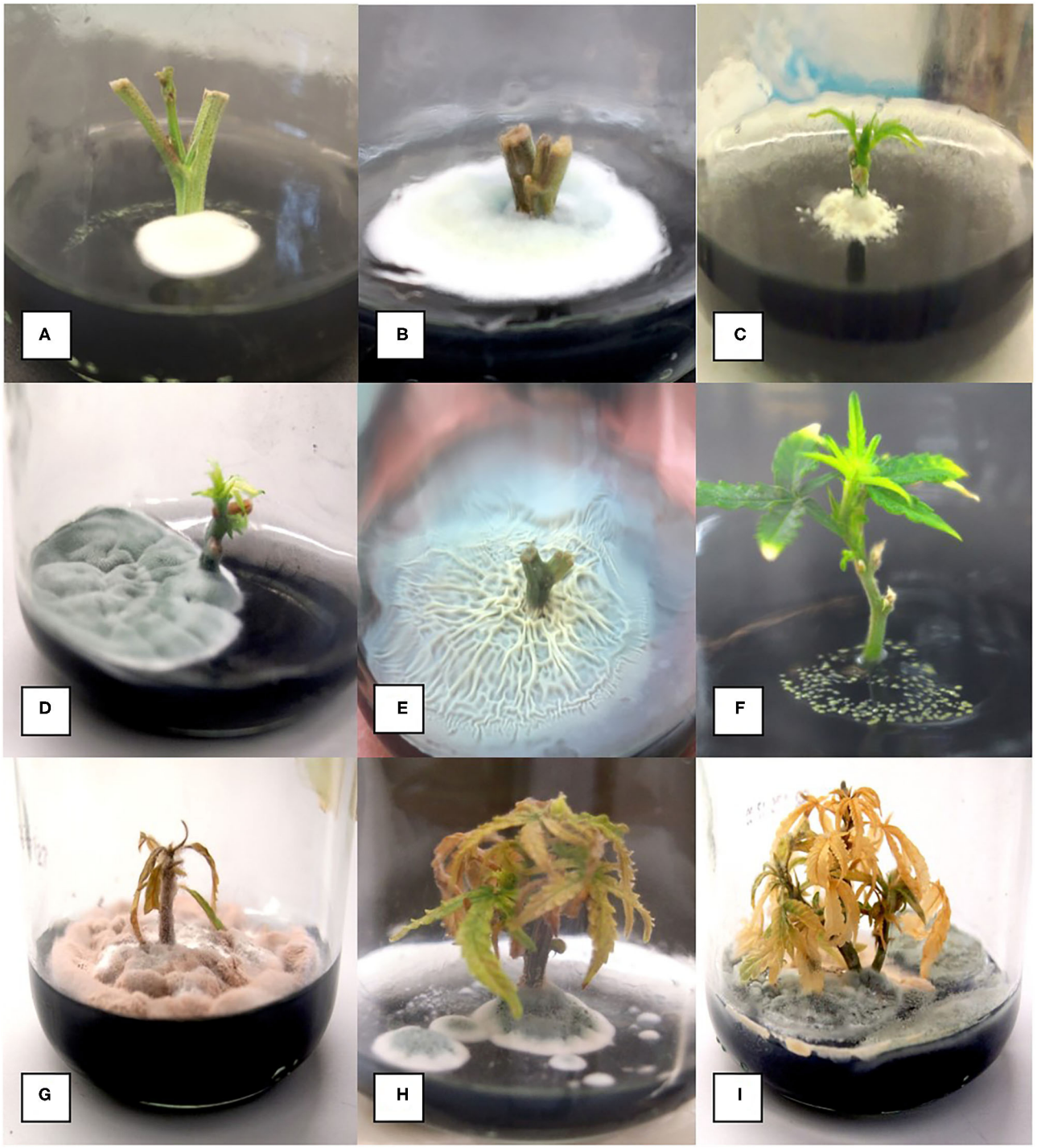

FIGURE 4 | Range of microbial contaminants emerging from surface-sterilized nodal stem explants at various times after placement on MM containing activated charcoal. **(A)** Early emergence of *Penicillium* species. **(B)** Large colony of *Penicillium* growing from a nodal explant. **(C)** Colony of *Chaetomium* emerging from a nodal explant. **(D)** Large colony of *Penicillium* growing out of a nodal stem explant. **(E)** Extensive *Bacillus* growth emerging from a nodal stem explant. **(F)** Growth of *Pseudomonas* from a stem explant. **(G–I)** Death of established shoots from nodal stem segments due to contamination by microbes appearing later during plantlet growth.

Rooting of Shoots From Nodal Explants

Genotype Moby Dick was used for root induction. Following the 8-week growth period for nodal segments, shoots measuring 2 cm in height were transferred to MS basal salts medium with the following amendments to induce rooting. The amendments were silver nitrate (40 μM), sodium metasilicate (6 and 9

mg/L), indole-3-butyric acid (5, 12.3, 37, and 42 μM), 2,4-dichlorophenoxyacetic acid (5 μM), and kinetin (1 μM). The shoots were incubated for 4 weeks on media containing these additives and rated for rooting frequency. Each treatment had a minimum of 10 explants, and the experiment was repeated three times ($n = 30$). The data were analyzed using Statplus version 2.21 and R systems (version 3.3.3). ANOVA was performed followed by Tukey's HSD test to determine significance at $P < 0.05$.

Acclimatization for Plantlet Recovery

Shoots of genotype Moby Dick derived from either meristems or nodal explants that had formed roots were selected at random and transferred to one of the following growing substrates: peat plugs (Jiffy-7® peat pellets), rockwool cubes (2.5 × 2.5 × 3.8 cm, Grodan) or placed in a Turboklone (T-24 turbo-mini) (https://turboklone.com) containing a hydroponic nutrient solution with 1 ml/L of pH Perfect® Sensi Grow A&B and CALiMAGIc (General Hydroponics, Santa Rosa, CA, United States) and 0.25 ml/L of Rapid Start Rooting Enhancer (General Hydroponics, Santa Rosa, CA, United States) ∼pH 5.8. Every 3 days, a nutrient mixture (without Rapid Start) was added to top up the system. The peat plugs/rockwool cubes were soaked for a minimum of 20 min in the same nutrient solution used for hydroponic growth. The plugs containing shoots were then placed in a sterilized tray (28 × 56 cm) and covered with a plastic dome (http://www.jiffypot.com/). The domes were misted with water every 2 days, and the vents were opened halfway after 7 days and fully opened after 9 days. Domes were removed 2 weeks post transfer. The percentage of survival of plantlets was assessed 4 weeks after transfer. Each treatment had a minimum of 10 replicates, and the experiment was conducted twice. The data were analyzed using Statplus version 2.21 and R systems (version 3.3.3). ANOVA was performed followed by Tukey's HSD test to determine significance at $P < 0.05$.

Callus Growth

Genotypes Girl Scout Cookie, Space Queen, Moby Dick, and Pennywise were tested. After sterilization, leaf and petiole explants were placed on MM-AC. Petri dishes with leaf and petiole explants were kept on wire rack shelves under ambient conditions (temperature range of 21–25°C). One-half of the dishes were wrapped in aluminum foil to exclude light, and the remainder was left under the same conditions of supplemental lighting as for the nodal explants. Callus development was first observed after 4 weeks. Dishes were incubated for 6–10 weeks before measurements were taken. The percentage of explants that developed callus as well as the surface area of callus was measured. For the latter, an Alvin TD 1204 Circle Master Template (Alvin & Company, Bloomfield, CT, USA) was used to estimate the circle corresponding to the size that matched the callus, and the measurement was converted to cm^2.

In a subsequent experiment, the following eight genotypes were compared: AFK, CPH, DEB, ISH, PWE, PNK, CBD, and WHR. Leaf segments from greenhouse-grown plants were sterilized in the bleach solution for 15 min and rinsed 3 times for 1 min in sterile ddH_2O then placed on MM-AC. The dishes were wrapped in Al foil and incubated at 21–23°C for a maximum of 8 weeks. The callus area was measured using the "freehand" tool in ImageJ from photos taken of the Petri dishes that included a ruler for measurement. If the data did not meet the assumptions of parametric tests (i.e., ANOVA, unpaired two-sample *t*-test, etc.), then non-parametric tests were used (i.e., Welch's ANOVA, and Wilcoxon Rank Sum test). If the data met the assumptions of the ANOVA test, then they were used followed *post-hoc* by Tukey's HSD test.

RESULTS

Shoot Growth From Meristem and Nodal Explants

Placement of meristems on MM medium (with 1% activated charcoal) resulted in shoot growth after 4 weeks in culture (**Figure 1B**), which continued to elongate after 8–10 weeks (**Figures 1C,D**). Baby food jars containing meristem explants at different stages of development were placed in a controlled environment growth chamber to allow for a comparison of growth of different genotypes (**Figure 1E**). Meristems of five different cannabis genotypes were assessed for their shoot regeneration response. After 10 weeks of growth, shoot height, number of axillary buds, and number of axillary shoots were measured (**Table 1**). The genotype with the greatest shoot height value was MBD, with an average height of 4.5 cm, which was significantly greater compared with genotypes CHQ, SPQ and PWE ($P < 0.001$). The average shoot growth across genotypes was 2.92 cm (**Table 1**). The number of axillary buds present on the shoots from meristems ranged from 8.5 for CBD to 3.4 for SPQ. The number of axillary buds produced per plantlet was not significantly different ($P > 0.05$) among CBD, CHQ, MBD, and PWE. SPQ had the lowest number of buds compared with the other genotypes ($P < 0.05$). Across genotypes, plantlets from meristems produced 6.38 axillary buds on average and 1.4 shoots (**Table 1**). Genotype SPQ showed poor growth for all parameters compared with the four other genotypes. While CBD plantlets were generally shorter, they had a higher number of buds that resulted in a bushier appearance. Genotypes MBD and PWE had similar shoot growth, but MBD was significantly taller than PWE (**Table 1**). Genotype SPQ generally showed the poorest growth among all the genotypes.

Measurements of height, number of axillary buds, and number of axillary shoots were obtained from nodal stem explants after 6 weeks (**Table 1**). The genotypes tested were BLD, SWD, MBD, and SPQ. The average shoot height ranged from 1.5 to 4.9 cm for SPQ and BLD, respectively (**Table 1**). BLD and SWD were significantly ($P < 0.001$) taller than MBD and SPQ at 4.9 and 3.8 cm, respectively. The average height across genotypes after 4 weeks was 3.075 cm. The average number of axillary buds across strains was 2.98, and the average number of shoots across genotypes was 0.3 (**Table 1**).

Comparison of DKW and MS Salts

Shoot length and leaf numbers from nodal stem segments were evaluated for genotypes CPH and PWE after 4 weeks of growth on DKW or MM salts (**Figure 3**). For CPH, 78.4% of

explants on DKW and 89.2% on MM basal salts grew and were included in a statistical comparison by an unpaired two-sample *t*-test. For PWE, 70% of explants on DKW and 77.5% on MM grew and were included in a statistical comparison by the Wilcoxon Rank Sum test. The data showed that there was a significant difference between DKW and MS basal salts in shoot length for CPH ($p = 0.02947$; **Figure 3A**). The average CPH shoot length on DKW and MM was 6.44 and 8.63 mm, respectively. In comparing shoot length for PWE on DKW and MM, there was no significant difference ($p = 0.08354$). The average PWE shoot length on DKW and MS was 7.66 and 9.2 mm, respectively (**Figure 3B**). For CPH leaf number, there was no difference between DKW and MM ($p = 0.6882$; **Figure 3C**). The average number of leaves on DKW and MM was 3.31 and 3.12, respectively. For PWE leaf number, there was a significant difference between DKW and MM ($p = 0.04468$; **Figure 3D**). The average number of leaves on DKW and MM was 4.13 and 5.64, respectively.

Internal Contaminants and Alternative Sterilization Methods

In general, an average of 50% of nodal stem explants were found to be contaminated by microbes (a range of 10 to 80%), despite the rigorous sterilization methods used, and these had to be discarded. These contaminants included fungi, bacteria, and yeasts (**Figure 4**). Due to the high frequency of microbial contaminants from nodal stem explants when grown in a tissue culture medium, the addition of fungicides and antibiotics was assessed. The addition of a fungicide (captan) at 0.01 and 0.02 g/L to the tissue culture medium post-sterilization did not significantly reduce the contamination frequency on genotype CHQ ($P = 0.05$). The addition of streptomycin sulfate at 100 mg/L caused stunting and chlorosis of the tissue culture shoots (data not shown). Plant preservative mixture (PPM) at 2 ml/L appeared to delay the onset of contamination, but microbial growth would appear 1 to 3 weeks later. Nodal stem explants sterilized with 5% PPM + 3x basal salt solution or 70% EtOH and 10% bleach +0.1% Tween 20 showed no differences in microbial contamination on genotype CPH (60.5 vs. 60%, chi-square test $p > 0.05$). For CPH donor plants treated with Luna fungicide, a chi-square test was significant at $p < 0.05$, which suggests that fungicide treatment of donor plants could reduce the endophytic contamination observed in tissue culture. The CPH control group showed 88.2% contamination, and the Luna treatment group showed 31.8% contamination. However, the PWE plants treated with Luna did not differ significantly from the untreated control as overall contamination rates were much lower (12.5 vs. 16.7%, Fisher's exact test $p > 0.05$). These results indicate that genotypes may differ in terms of the extent of microbial contamination.

Identification of Tissue Culture Contaminants

The contaminants observed growing on agar media consisted of bacteria, which were identified to genus level as *Bacillus* and *Pseudomonas*, yeasts that were not identified, and many fungi. In an attempt to better categorize the fungal contaminants, which represented the majority of contaminants present in nodal stem tissues, a PCR-based method was utilized. Cultures of 11 fungi recovered from nodal explants each produced a band size of about 650 bp after PCR. After sequencing and comparing the results in BlastN, a range of fungi were identified. This was followed by using naturally contaminated nodal explants, in which the frequency of detection of fungal contamination was 16/19 samples (**Figures 5A,B**). The plant DNA band was at 750 bp, as the universal primers used amplified both fungal and plant DNA. The genus and species of fungi present in cannabis stem tissues are shown in **Figure 5**. The PCR test could detect fungal contaminants present at DNA concentrations of 1 ng/ul (qPCR data not shown). Sections of stem segments when plated onto potato dextrose agar yielded colonies of *Penicillium* that emerged directly from the pith tissues (**Figure 5C**). When pith tissues were examined under a scanning electron microscope (**Figure 5D**), a close-up showed that fungal spores could be seen growing in and around pith cells (**Figures 5E,F**).

Rooting of Shoots From Nodal Explants

Representative plantlets from sodium metasilicate treatments of 0, 6, and 9 mg/L are shown in **Figures 6A–C**. The addition of sodium metasilicate caused visible differences in plant growth and leaf morphology, recorded on a scale of 1–3, as shown in **Figures 6D–F**. A rating of 1 shows thin curled leaves, while a rating of 3 shows dark green, flat, and toothed margins. The addition of sodium metasilicate at 6 mg/L significantly ($p < 0.05$) improved the leaf morphology rating compared with MM and MM + Na_2SiO_3 at 9 mg/L according to Tukey's HSD test (**Figure 6G**). On the MM + 6 mg/L Na_2SiO_3, the leaf morphology rating was comparable with the leaf rating of plants grown on the MM without Na_2SiO_3. The addition of Na_2SiO_3 at 6 mg/L produced the greatest proportion of rooted plantlets according to Tukey's HSD test ($p < 0.05$; **Figure 6H**). The proportion of rooted plants was 0.4 (40%) for MM + Na_2SiO_3 at 6 mg/L compared with 0.1, 0.1, and 0.2 for treatments MM, MM + 9 mg/L Na_2SiO_3, and MM without phytohormones (MMC). The addition of sodium metasilicate did not significantly affect any of the growth parameters measured for nodal stem segments or meristems: height, number of buds, and number of shoots (data not shown).

The addition of indole-3-butyric acid, 2,4-dichlorophenoxyacetic acid (2,4-D), and kinetin (KIN) was tested as alternatives to TDZ and NAA in rooting media. KIN and 2,4-D were tested at 1 and 5 μM, respectively, alone and in combination. Neither hormone alone or in combination performed significantly better than the MM (data not shown). The combination of KIN and 2,4-D produced an average of 63% rooted plants, while the MM produced an average of 44% rooted plants. The MMC was used as the basal medium in the indole-3-butyric acid experiments. IBA was tested at 5, 12.3, 37, and 42 μM. While there was a trend toward decreased rooting as more IBA was added, the only statistically significant difference ($p < 0.05$ by Tukey's HSD test) was between 5 and 42 μM (**Figure 7A**). The MM (listed as C in **Figure 7A**) was

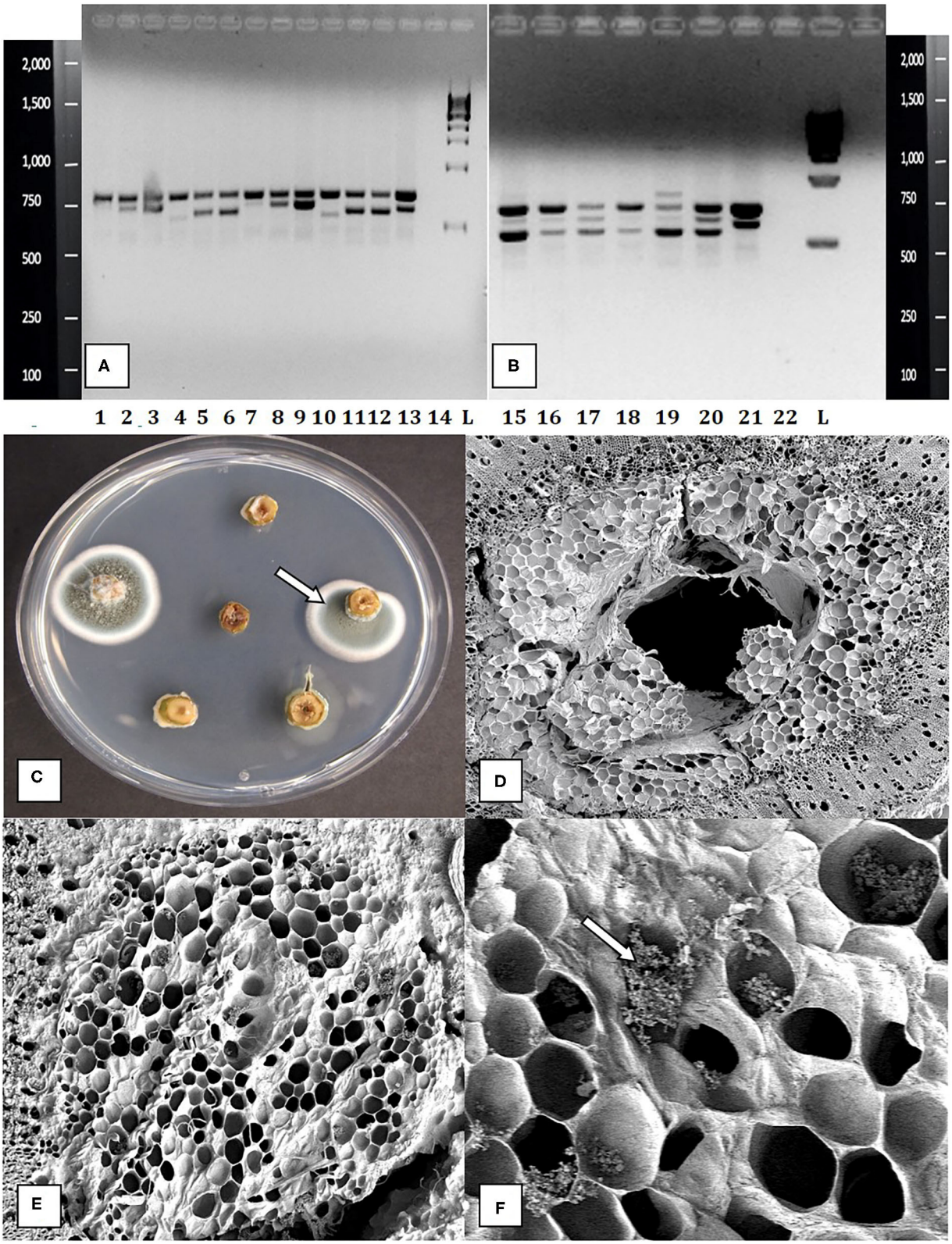

FIGURE 5 | Molecular detection and identification of tissue culture contaminants. **(A,B)** PCR detection of fungal DNA present in naturally contaminated nodal explants. Upper bands at 750 bp size are plant DNA. Lower bands at ca. 650 bp are fungal DNA. These bands were cut and sequenced to determine the corresponding fungus present. Lanes 1–13 (lower bands) are as follows: clean, *Simplicillium lasoniveum*, *Trichoderma harzianum*. Clean, *Beauveria bassiana*,

(Continued)

FIGURE 5 | *Fusarium oxysporum.* Clean, *Trametes versicolor*, *Lecanicillium fungicola*, *Chaetomium globosum*, *F. oxysporum*, *F. oxysporum*, *L. fungicola*. Lane 14 = water control. L = molecular weight standards. Lanes 15–21 (lower bands) = *Penicillium chrysogenum*, *Penicillium copticola*, *C. globosum*, *Penicillium olsonii*, *P. olsonii*, *T. versicolor.* Lane 22 = water control, L= molecular weight standards. **(C)** Growth of *Penicillium* colonies emerging from the center of pith tissues in cut nodal segments. **(D)** Cross-section of a cannabis nodal stem explant showing the central pith surrounded by pith cells. **(E)** Close-up of pith cells as viewed in the scanning electron microscope. **(F)** Magnified view of pith cells in the scanning electron microscope showing fungal sporulation inside pith cells, likely of *Penicillium* sp. (arrow).

not significantly different from any of the IBA concentrations; however, it averaged 44% rooted plants, while IBA at 5 μM produced 83% rooting.

Silver nitrate was added at 40 μM to the MM and MMC containing IBA at 37 μM instead of TDZ and NAA. The IBA with added silver nitrate had significantly more roots than IBA at 37 μM alone according to Tukey's HSD test ($p < 0.05$; **Figure 7B**). The $AgNO_3$ did not significantly increase the proportion of roots produced when added to the MM.

Rooting and Acclimatization for Plantlet Recovery

Spontaneous rooting was observed on some of the nodal explants (**Figures 8A,B**). Rooted plantlets were carefully removed from the tissue culture jars, rinsed of excess medium (**Figure 8C**), and transferred to a coco fiber growing medium. For comparison of rockwool, peat, or hydroponic system (**Figures 8D,E**), at least 10 plantlets were used per acclimatization substrate, and the experiment was repeated twice for different batches of plants ($n = 20$). The plantlets were of genotype MBD. Acclimatization success was calculated based on the number of healthy surviving plants after 2 weeks divided by the total number of plants that had been transferred for acclimatization. The survival success rate after acclimatization was 57, 76, and 83% for hydroponic, peat, and rockwool, respectively, which was not statistically different. **Figures 8F,G** show plants grown in coco growing substrate where they grew normally and produced more shoots. However, plants grown in rockwool appeared more vigorous and grew faster (**Figure 8H**).

Callus Growth

Callus development from leaves, measured as callus diameter, was genotype-dependent (**Figure 9A**). Genotypes GSC and SPQ readily developed callus, while for genotypes MBD and PWE, callus diameter was <2 mm. In this experiment, one-way ANOVA was performed followed by Tukey's HSD test ($p < 0.05$). In the follow-up experiment, the mean callus area for the eight genotypes was compared by Welch's one-way ANOVA ($p < 0.05$). A Games–Howell non-parametric *post-hoc* test was then performed and identified that the following genotype comparisons were significantly different from one another: AFK vs. PNK, CPH vs. PNK, DEB vs. PNK, DEB vs. PWE, PNK vs. PWE, and PNK vs. WHR (**Figure 9B**). Leaf and petiole explants on media placed in the dark produced more callus than explants grown under light conditions (**Figure 9C**). Callus development from leaves and petioles showed genotype dependence. In SPQ, leaves developed more callus than petioles ($p < 0.05$), while on GSC, there was no significant difference between the explant types ($p < 0.05$; **Figure 9D**). The appearance of callus derived from leaf explants is shown in **Figure 10**. Within 4 to 8 weeks in culture, extensive callus growth could be observed from leaf segments (**Figures 10A–D**). The appearance of the callus was similar on leaf explants and petiole explants (**Figures 10E,F**). None of the calli showed evidence of differentiation toward shoot development or somatic embryo development. Further transfers of calli to new media eventually resulted in browning and death.

DISCUSSION

The results from this study conducted on drug-type cannabis (marijuana) show that the response to tissue culture conditions is first and foremost influenced by the genetic background (genotype) of the plants tested. The findings also indicated that both meristems and nodal explants were responsive to the tissue culture conditions tested, and that measurements of shoot growth could be used to determine the response of genotypes and quantify effects of media amendments on growth. Lastly, the findings show that the recovery of rooted plantlets is influenced by the degree of internal contamination of nodal explants and the extent to which rooting and acclimatization of the plantlets could be achieved using different treatments. Knowledge of these variables can enhance the successful recovery of plantlets from tissue cultures of *C. sativa*, which was the main objective of this study. This study focused on stage 1 of the micropropagation process as described by Page et al. (2021). This phase is equivalent to an initiation phase (establishment of cultures) and did not involve repeated cycles of subcultures and multiplication of shoots as observed in stage 2, the multiplication phase that increases plant numbers through micropropagation (Monthony et al., 2021; Page et al., 2021). Research on stage 1 is valuable to establish the genotypic response of a range of cannabis strains to initial tissue culture conditions and to rapidly recover plantlets from meristems or nodal explants for a first cycle of propagation.

Many previous reports of tissue culture of *Cannabis sativa* L. have utilized hemp varieties because of legal restrictions placed on the cultivation of drug-type cannabis in most regions of the world (Adhikary et al., 2021; Monthony et al., 2021). However, Lata et al. (2009) and Page et al. (2021) researched some of the variables that can influence the response of drug-type *C. sativa* to tissue culture conditions. In these studies, nodal segments with axillary buds were used for direct regeneration of shoots in stage 1 micropropagation (Lata et al., 2009, 2016; Page et al., 2021). The differential response of various genotypes to tissue culture conditions, as reported in this study, was also noted by Monthony et al. (2021). Prior research has shown that the response to tissue culture conditions in other plant species is affected by genotype (Islam et al., 2005; Martínez et al., 2017). If cannabis micropropagation is to be successful, an assessment of

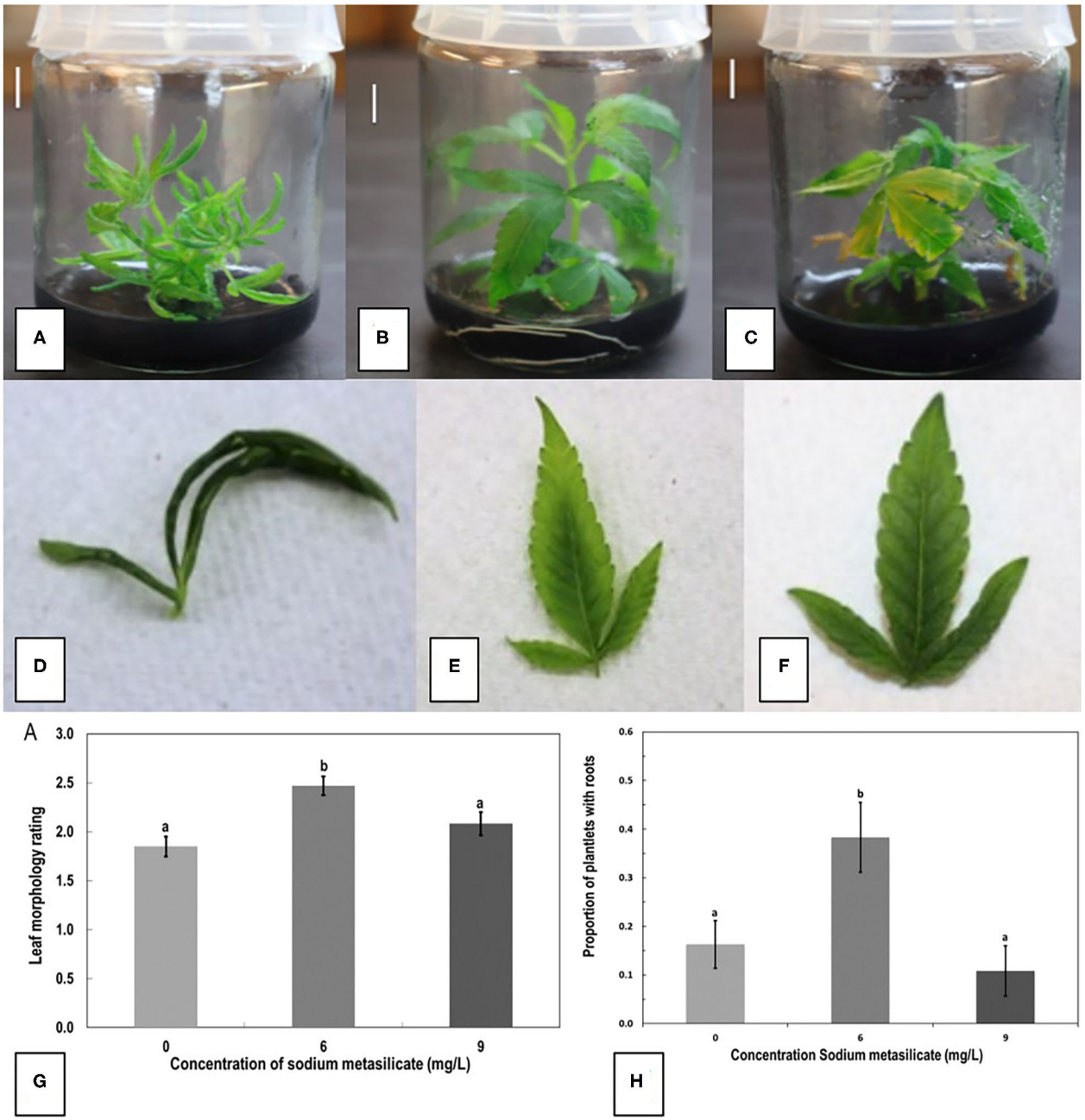

FIGURE 6 | The effect of sodium metasilicate at 0 **(A)**, 6 **(B)**, and 9 **(C)** mg/L in the MM on shoot growth of genotype MBD from nodal segments. Optimal growth and rooting can be seen on 6 mg/L. **(D–F)** Leaf morphology rating scale applied to plantlets during growth in tissue culture as an indication of plantlet health. **(D)** A rating of 1 shows thin curled leaves, light green in color. **(E)** A rating of 2 shows leaves light green in color with some curling. **(F)** A rating of 3 shows dark green, flat leaves with serrated margins. **(G)** Average leaf morphology rating after 4 weeks of growth on MM with added sodium metasilicate. **(H)** Proportion of plantlets that developed roots on MM supplemented with sodium metasilicate at 6 mg/L was significantly different to the proportion of roots that developed from plantlets on MM, MM + sodium metasilicate 9 mg/L, and MMC. Bars followed by different letters indicate significant differences.

the response of genotypes of interest to tissue culture conditions would first need to be established before a full-scale tissue culture method could be developed for commercial use. In this study, some of the cannabis genotypes, e.g., MBD, produced shoots over 4.5 cm in height and formed multiple shoots and buds, while the other genotypes (SPQ and CHQ) grew poorly. Strain MBD was selected for a further study on plantlet recovery. A higher frequency of shoots and buds can potentially give rise to more plantlets during stage 2 micropropagation and can enhance plantlet numbers.

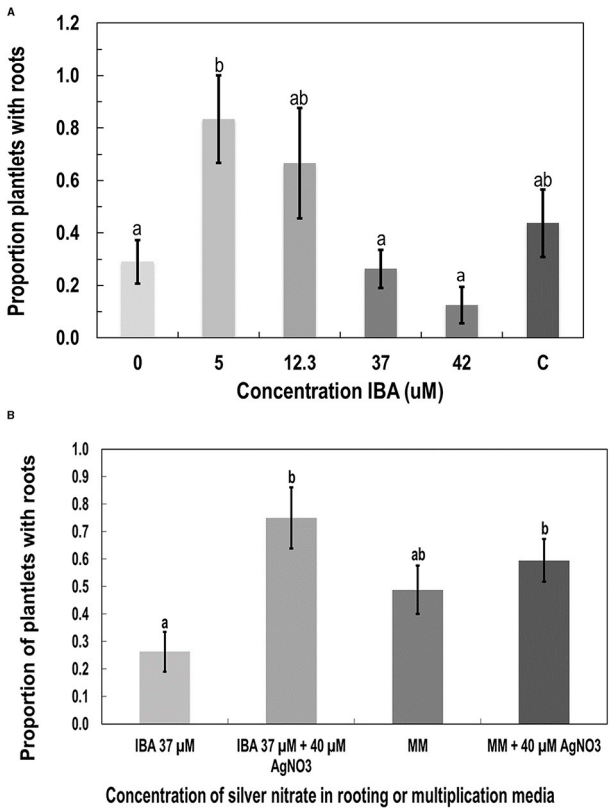

FIGURE 7 | The effect of additives to the MS salts medium on root development in plantlets of genotype MBD derived from nodal stem segments after 4 weeks of growth. Additives were **(A)** indole-3-butyric acid IBA, **(B)** silver nitrate ($AgNO_3$), compared with MM as a control. Statistical analysis was performed by Tukey's HSD test with significance at $p < 0.05$. Bars followed by different letters indicate significant differences.

Meristems and axillary buds have both been used as starting explant sources for shoot induction in tissue culture experiments of various plant species. For example, axillary buds are commonly used for the propagation of fruit and nut trees, while meristems have been used for sweet potato and strawberry propagation (Hussain et al., 2012). Growth of axillary buds in tissue culture has been studied in mint (*Mentha* species) (Rech and Pires, 1986), Cancer tree (*Camptotheca acuminate*) (Liu and Li, 2001), hops (*Humulus lupus*) (Roy et al., 2001), Andean blueberry (*Vaccinium floribundum*) (Cobo et al., 2018), and other woody plants (Sahoo and Chand, 1998). In order to obtain plants free from pathogens, particularly viruses, meristem tip culture is a preferred method. Successful eradication of viruses using tissue culture techniques alongside a secondary method, such as thermotherapy, has been demonstrated in sugarcane (Cheong et al., 2012), *Lilium* spp. (Chinestra et al., 2015), dahlias (Nerway et al., 2020), artichoke (Spanò et al., 2018), and many others. We compared meristem and nodal explant types in this study and successfully obtained plantlets from both, with the meristems showing significantly lower microbial contamination rates compared with the nodal explants bearing axillary buds. However, shoot production from the meristems required a longer time in culture (10 weeks) compared with the axillary buds (6 weeks).

Meristems have not been previously tested as an explant source in either hemp or cannabis, although shoot tips were used for direct regeneration of hemp (Wang et al., 2009), and stem tips were used for micropropagation and retipping studies on hemp (Lubell-Brand et al., 2021). Meristems are important starting material, as they contain a lower frequency of internally-borne microbes and viruses (Wang and Hu, 1980). Since *C. sativa* L. is reported to harbor fungi and bacteria internally as endophytes (Scott et al., 2018; Punja et al., 2019), consequently, explants taken from mother plants that naturally carry endophytes or pathogens have a higher risk of becoming contaminated after transfer to tissue culture media, as observed in this study. Monthony et al. (2021) circumvented this problem by first establishing *in vitro* plants in stage 1 that were subsequently used to provide an explant material for studies on micropropagation and callogenesis in stage 2. While this approach is advantageous to provide clean explants and maintain desired genotypes *in vitro*, the explants used in the present study were derived from donor plants grown under commercial greenhouse conditions, as they provided unlimited quantities of tissues, and the plants could be evaluated for commercially desired traits prior to introduction into the tissue culture environment. To avoid higher contamination rates from these tissues, we evaluated a range of decontamination methods. Following reports of the addition of fungicides to tissue culture media to reduce fungal contamination (Nagy et al., 2005; Panathula et al., 2014), we added captan at 0.02 g/L, but it did not show any effect. We also tested a widely used broad spectrum product, Plant Presrvative Mixture™ (PPM; Plant Cell Technology, Washington, DC, United States), which reduced initial contamination in tissue culture but not beyond 2 weeks. Similarly, nodes that had been surface-sterilized in 5% PPM for 4 h showed no difference in contamination levels compared with nodes sterilized with 10% bleach +0.1% Tween 20. Interestingly, the application of a systemic fungicide (Luna) to the indoor-grown donor plants, followed 3 weeks later by the removal of nodal explants, showed reduced contamination levels in tissue cultures of one strain by almost 3-fold.

The contaminating microbes in cannabis explants appear to reside within the central pith tissues, as shown in this study using scanning electron microscopy and reported elsewhere (Punja et al., 2019). This could explain the difficulty in eradicating them with surface-sterilization methods. Donor plants of some genotypes, e.g., CPH appeared to have a higher background level of contamination compared with other genotypes, e.g., PWE. Most of the contaminants emerged after several weeks in the tissue culture environment and originated from the central pith of the nodal explants (see **Figure 5**). Axillary buds may contain pathogens or endophytes living internally, which can easily be transferred into tissue culture (Wang and Hu, 1980). Internal contamination is less of a concern for meristems, as the vascular dome and first primordial leaves are generally free of bacteria, fungi, and viruses (Ramgareeb et al., 2010). Previous studies have demonstrated that an extensive array of fungal and bacterial endophytes can colonize hemp and cannabis plants (Kusari et al., 2013; Scott et al., 2018; Punja et al., 2019).

FIGURE 8 | Root development on shoots after 8–10 weeks of growth in tissue culture and acclimatization to produce plants. **(A,B)** Spontaneous development of roots on nodal explants. **(C)** Plantlets were removed from tissue culture and transferred to coco growth media and placed under high humidity conditions for 2 weeks. **(D,E)** Acclimatization of plantlets from meristems of genotype MBD in different growth substrates. Plantlets were removed from tissue culture jars after 12 weeks of growth on the MM and placed into rockwool or peat under humid conditions for 14 days. Rockwool or peat plugs were soaked in a fertilizer mix of 1 ml/L of pH Perfect® Sensi Grow A&B and CALiMAGIc (General Hydroponics, Santa Rosa, CA, United States) in ~pH 5.8 water. **(F,G)** Growth of plants on a coco potting medium under ambient conditions following successful acclimatization. **(H)** Hydroponic system filled with 8 L of the fertilizer mix with vigorous growth of plants derived from meristem tissue cultures.

Kusari et al. (2013) found 30 different species of fungal endophytes, of which P*enicillium copticola* was the most prevalent. Scott et al. (2018) found 134 bacterial and 54 fungal strains in three hemp cultivars. The most abundant fungal genera were *Aureobasidium*, *Alternaria*, and *Cochliobolus*, and the most abundant bacterial genera were *Pseudomonas*, *Pantoea*, and *Bacillus*. Punja et al. (2019) showed that endophytic and pathogenic fungi, such as species of *Chaetomium*, *Trametes*, *Trichoderma*, *Penicillium*, and *Fusarium*, could colonize cannabis plants internally. Previous tissue culture studies on

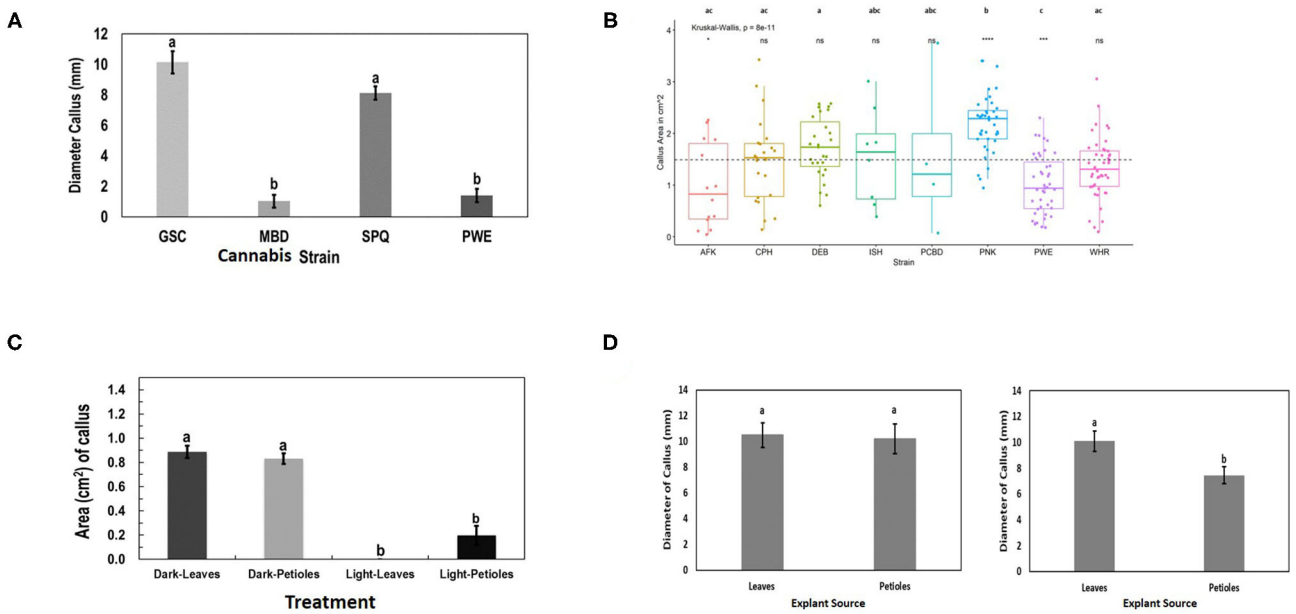

FIGURE 9 | Response of cannabis genotypes to callus development on MM without activated charcoal (MM-AC). **(A)** Callus diameter of four genotypes developing from 1 cm^2 leaf explants. **(B)** Callus area from leaf explants of 8 cannabis genotypes compared with the mean callus area across all strains (represented by the dotted line). The "*"represents significance level and "ns" represents not significant relationships between each genotype and across all genotype means (dotted line). A Kruskal–Wallis test resulting in a p of 8×10^{-11} and a Games–Howell *post-hoc* test were performed. Significant differences identified in the Games–Howell *post-hoc* test are shown using letters above the boxplots of each strain. **(C)** Growth of Cheesequake (CHQ) callus from leaf and petiole explants after 1 month under 24-h dark and 24-h light conditions on MM. Statistical analysis was performed by Tukey's HSD test with significance at $p < 0.05$. Bars followed by different letters indicate significant differences. **(D)** Growth of callus from leaves and petioles of genotype Girl Scout Cookie (GSC) (left) and Space Queen (SPQ) (right). Measurements of diameter were made after 4 weeks. Statistical analysis was performed by Tukey's HSD test with significance at $p < 0.05$. Bars followed by different letters indicate significant differences.

hemp and cannabis have not described problems with tissue culture contaminants. It is likely that the coco fiber used as a substrate for growing plants in this study harbored microbes that eventually colonized the internal tissues of the stems and became established (Punja et al., 2019). Other growing media, such as rockwool, may contain lower levels of contaminating microbes. Donor plants grown in a coco fiber substrate over prolonged periods of time in indoor environments, e.g., for up to a year, such as CPH, showed much higher background levels of contaminants. Recent microbiome studies have demonstrated that the bulk soil and rhizosphere of cannabis and hemp plants are the most influential in determining the subsequent composition of internal microbes in other regions of the plant (Barnett et al., 2020; Comeau et al., 2021). Therefore, attention should be given to the condition of donor plants with regard to the substrate they are grown in and their duration in the growing environment. Young plants grown in relatively sterile growth substrates should be selected for tissue culture studies.

A polymerase chain reaction-based assay showed conclusively that cannabis stem tissues contained a range of fungi. The method allowed the detection of 1 ng/ml of genomic DNA and could be used to screen donor plants to determine the background level of microbial contamination. Similar PCR-based methods have been used to screen mother plants and tissue-cultured plants such as strawberries, sweet potatoes, and roses to ensure they are free of bacteria and fungi (Moreno-Vázquez et al., 2014; University of California Davis, 2008). This approach can be applied to cannabis plants before they are deployed in tissue culture. In addition, if meristem culture of cannabis is used to obtain pathogen-free plantlets, it would have to be accompanied by a similar PCR-based assay to test for the absence of these pathogens. Nodal explant cultivation is unlikely to be free of pathogens given the high levels of internal contamination observed in this study. Therefore, shoots derived from nodal cultures should be avoided because of the potential for contaminants. Meristems represent the explant of choice to obtain pathogen-free plantlets from tissue cultures of *C. sativa*.

The tissue culture medium used for growth of plant tissues can influence the success in initiation and multiplication of shoot growth and elongation. Following shooting, a second medium with a higher concentration of auxin can be used to induce rooting (Lata et al., 2009; Wang et al., 2009; Chandra et al., 2017). We used the multiplication medium described by Lata et al. (2009) containing Murashige and Skoog (MS) basal salts supplemented with myo-inositol and activated charcoal. The growth regulators added were thidiazuron (TDZ, 1.0 μM) and naphthaleneacetic acid (NAA, 0.5 μM). On this medium, both explant types responded favorably, and shoots were produced in the initiation phase and could be transferred to subsequent media of the same composition for measurements to be made.

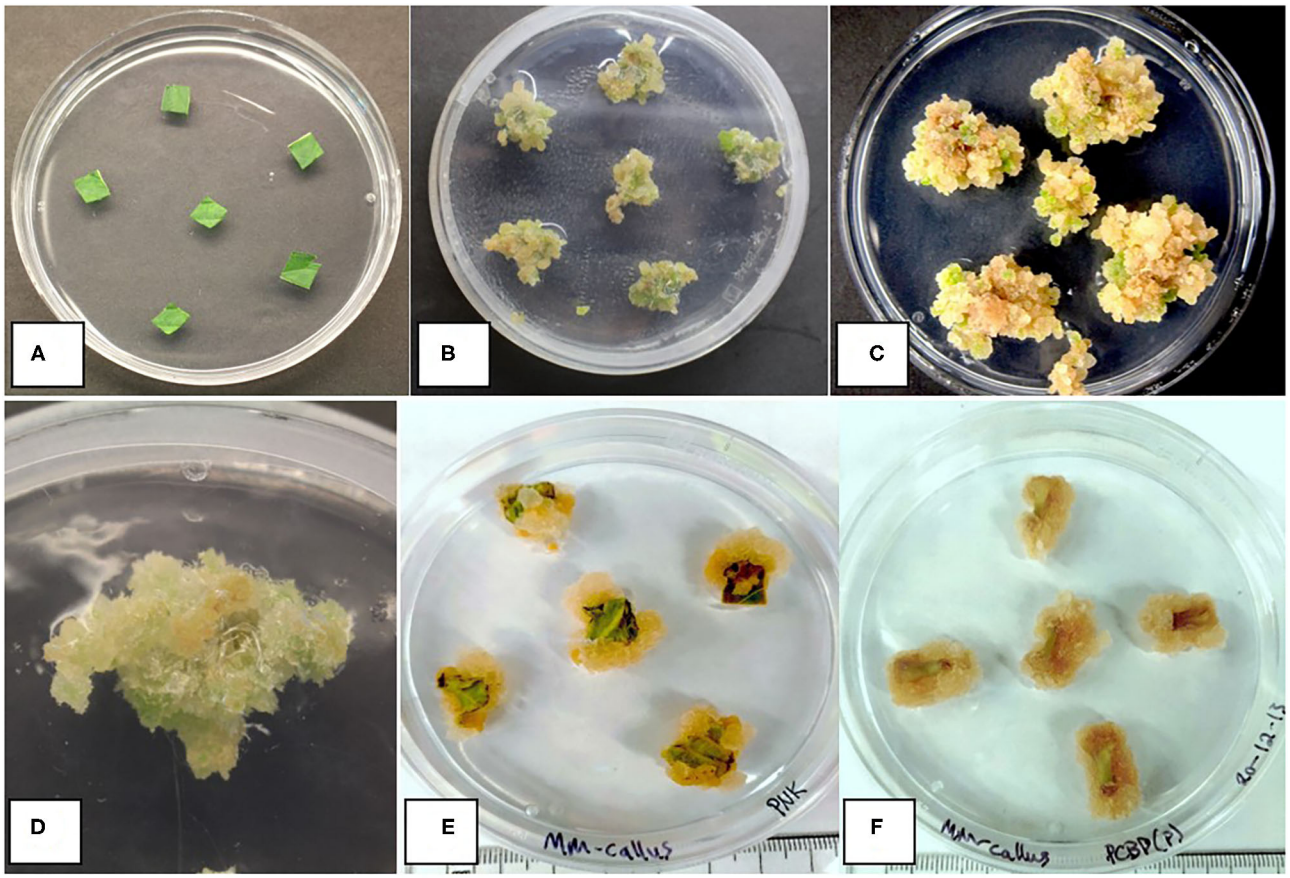

FIGURE 10 | Callus development on leaf and petiole explants of different cannabis genotypes on MM-AC. **(A)** Leaf explants at the start of the experiment from a donor plant. **(B)** Callus from leaf explants of genotype SPQ after 8 weeks of growth. Variation in callus growth between explants can be seen. **(C)** Callus growth of genotype GSC from leaf explants after 8 weeks of growth. **(D)** Callus from leaf explants of genotype SPQ after 8 weeks of growth. **(E)** Callus from leaf explants of cannabis genotype Pink Kush after 8 weeks in the dark. **(F)** Callus from petiole explants of cannabis genotype Pure CBD after 8 weeks in the dark. No evidence of shoot development was observed in any of the callus cultures.

However, continuous subcultures over extended time periods on MS salts medium tended to produce shoots that displayed hyperhydricity and developed signs of nutrient deficiency with low multiplication rates (authors, unpublished observations). These symptoms were also described by Page et al. (2021) on MS salts medium. The addition of activated charcoal appeared to improve growth on the MS medium; therefore, MS salts plus 1% activated charcoal was used in most of the experiments in this study. Activated charcoal, when added to tissue culture media, can absorb or bind some of the toxic waste compounds released from growing plants, in particular phenolic compounds, thereby improving *in vitro* plant tissue growth (Wang and Huang, 1976; Thomas, 2008; Chandra et al., 2017). This would be particularly useful in stage 1 micropropagation. Page et al. (2021) reported that a tissue culture medium based on DWK basal salts supported better canopy growth than MS basal salts from nodal explant segments that were intended for stage 2 micropropagation. They compared five cannabis genotypes and used two-node explants originating from micro-propagated plantlets grown on a DWK salts medium. Their results showed that explants grown on DKW produced a larger canopy area and had a higher multiplication rate than explants grown on MS. In this study, comparisons between the two basal salts media using two cannabis genotypes did not show consistent differences in shoot growth that could be attributed to the effect of medium composition during stage 1 micropropagation. Wang et al. (2009) used an MS basal salts medium with 30 g/L sucrose, 6.8 g/L phytagel, and 1 μM of TDZ to produce axillary buds from shoot tips of hemp during micropropagation. Lubell-Brand et al. (2021) used an MS salts medium described by Lata et al. (2016) in which TDZ was replaced with the growth regulator meta-topolin (mT). They reported that hyperhydricity was reduced by modifying the agar content of the medium, coupled with improved vessel ventilation and enhanced nitrogen levels. Therefore, both DKW and MS salts media can support short-term growth in tissue culture media during the initiation of cultures. However, continuous subcultures and multiplication on a DKW-based medium appear to yield healthier and more vigorous plants (Page et al., 2021) or on an MS medium supplemented with enhanced levels of nitrogen (Lubell-Brand et al., 2021).

Rooting is often the most challenging step in micropropagation (equivalent to Stage 3 micropropagation according to Page et al., 2021), especially in woody plant species (Ranaweera et al., 2013). IBA, a naturally occurring auxin, has previously been shown to induce rooting in cannabis plants at 5 μM (Lata et al., 2009), which was confirmed in this study. However, since the rooting frequency with IBA was not significantly different from that with MM, further rooting experiments with sodium metasilicate and silver nitrate were conducted on MM. KIN and 2,4-D were also tested for promotion of rooting. In callus cultures, these hormones induced rooting (Feeney and Punja, 2003). When added to MMC, neither KIN nor 2,4-D alone or in combination induced rooting in plantlets to the extent reported from callus. To promote root induction, sodium metasilicate (containing 22.9% silicon) was added to MM. Silicon was included because of its reported positive impact on rooting seen in other plant species (Zhuo, 1995; Soares et al., 2011). Previous research has also shown a positive effect of the addition of silicon to tissue culture media on leaf morphology of banana (*Musa acuminata*) (Luz et al., 2012). In this study, a significant increase in rooting and improved leaf morphology were observed when sodium metasilicate was added to MM at 6 mg/L. Sodium metasilicate has not been previously used in tissue culture of *C. sativa*. In this study, silver nitrate ($AgNO_3$) increased the number of rooted plants when added with IBA, but had no significant effect when added to MM. $AgNO_3$ could be combined with a lower concentration of IBA (5 instead of 37 μM) or with sodium metasilicate to determine the effects on plantlet recovery. However, the use of $AgNO_3$ may alter the sex expression toward male flower formation (Punja and Holmes, 2020).

The final step in tissue culture propagation is acclimatization of plantlets (Stage 4). At this stage, plantlets are removed from the jars/containers and acclimatized to external environmental conditions. When removing plantlets from the medium, roots should be carefully washed to avoid damage, and the agar should be washed off to prevent fungal growth from the residual sucrose. In this study, plantlets were transferred directly to rockwool, peat, and hydroponic substrates for a comparison of survival following acclimatization. Rockwool, peat, and coco fiber are the most common soilless growing media used worldwide for the production of fruits, vegetables, and cut flowers (Savaas and Gruda, 2018). In the present study, the plantlets generally grew better in rockwool during acclimatization, followed by peat and the hydroponic system, although the substrate response was not statistically different. The plantlets exhibiting a bushy morphology with long thin curled leaves acclimatized poorly. The addition of sodium metasilicate improved the morphology of the plants and was a contributing factor to improved acclimatization. Lata et al. (2016) acclimatized and hardened well-rooted cannabis plantlets with a 100% survival rate by 10-day pre-incubation on a coconatural medium before transfer into potting mix-fertilome. A mixed approach of using tissue culture medium with sterile rockwool cubes for multiplication and rooting of cannabis (Kodym and Leeb, 2019) may be a good option for improving acclimatization. Rooting can also be done *ex vitro*, i.e., outside the tissue culture environment. For example, a peat-based medium and high humidity conditions were used successfully for tea plants (*Camellia sinensis* L.) (Ranaweera et al., 2013). When compared with conventionally propagated tea plants using tissue culture, the *ex vitro* rooted micro shoots produced superior plants. Similarly, an *in vitro–ex vitro* micropropagation system was recently described for hemp (Lubell-Brand et al., 2021).

In addition to direct regeneration of shoots from axillary buds or meristems, efforts have been made toward indirect regeneration of shoots from callus cultures of hemp and cannabis. These have not been successful because of the recalcitrant nature of this species (Monthony et al., 2021). Differences in callus growth from petioles and leaves were attributed to different genetic backgrounds of the plants tested. Slusarkiewicz-Jarzina et al. (2005) and Wielgus et al. (2008) studied the effect of plant growth regulators on the development of callus and subsequent regeneration in five hemp genotypes. Their results showed that genotype was an important and determining factor for callus growth and regeneration. The hemp cultivar Fibrimon-24 produced the most calluses (83%), while a different cultivar, Silesia, had a regeneration rate of only 2.5%. In previous studies, callus formation has been induced from both hemp and cannabis explant tissues using combinations of the auxins 2,4-dichlorophenoxyacetic acid (2,4-D), naphthaleneacetic acid (NAA), and indole-3-butyric acid (IBA), and the cytokinins kinetin (KIN) and thidiazuron (TDZ) (Braemer and Paris, 1987; Feeney and Punja, 2003; Lata et al., 2009; Wahby et al., 2013; Movahedi et al., 2015). Various explants have been studied for callus induction in hemp and cannabis, such as cotyledons and epicotyls (Wielgus et al., 2008; Movahedi et al., 2015), leaves (Mandolino and Ranalli, 1999; Page et al., 2021), and petioles (Slusarkiewicz-Jarzina et al., 2005). In this study and in that of Page et al. (2021), the genotype was shown to influence the extent of callus formation. Page et al. (2021) found that the addition of 2,4-dichlorophenoxyacetic acid to media was required for callus production, and that media containing DWK salts yielded healthier and faster-growing calluses than the MS medium. We did not test callus growth on the DWK salts medium. Interestingly, genotype SPQ, which responded poorly for shoot growth from meristems and nodal explants, responded well to callus production in this study. In contrast, genotype MDB, which responded very well to shoot growth, produced the least callus. The interest in deriving calluses from cannabis explants followed by regeneration of shoots is to allow genetic transformation studies to succeed (Feeney and Punja, 2003). In addition, there are numerous applications of tissue culture methods for cannabis and hemp improvement, and these have been described elsewhere (Adhikary et al., 2021). To date, however, there are few reports describing the successful utility of tissue culture approaches for *C. sativa* on a large and cost-effective scale.

The interest in micropropagation through tissue culture is to produce genetically identical, pathogen-free plants year-round

in a limited amount of space (Yancheva and Kondakova, 2018; Lubell-Brand et al., 2021; Monthony et al., 2021). The results of this study, and those of previous investigators (Lata et al., 2009; Wang et al., 2009; Page et al., 2021) show that it is possible to obtain plantlets from tissue cultures of drug-type *C. sativa*, but the process requires a detailed assessment of the genotypic response, evaluation of the effect of basal salts medium, establishment of conditions promoting shoot growth and rooting frequency, and achievement of success in acclimatization. In addition, distinguishing between the requirements of stage 1 micropropagation (initiation of tissue cultures) verses stage 2 micropropagation (multiplication of shoots), as pointed out by Page et al. (2021), may result in differing protocols being developed. In contrast to the vegetative clonal propagation method that is widely used in the cannabis industry, tissue culture approaches will still play a minor role in commercial production until research efforts have resolved many of the remaining challenges and the cost-effectiveness of this approach is proven. This study has attempted to assess the variables that can affect success in plantlet recovery from stage 1 micropropagation using meristems and nodal stem explants in order to provide future directions in this area.

DATA AVAILABILITY STATEMENT

The raw data supporting the conclusions of this article will be made available by the authors, without undue reservation.

AUTHOR CONTRIBUTIONS

All the authors contributed in the formulation of concepts of the research and designed the experiments, collected the data, wrote the manuscript, and prepared the figures.

FUNDING

Funding was provided through a Collaborative Research and Development (CRD) grant from Agrima Botanicals and the Natural Sciences and Engineering Research Council of Canada (NSERC).

ACKNOWLEDGMENTS

We thank S. Chen, C. Scott, and L. Ni for providing assistance in various aspects of the study.

REFERENCES

Adhikary, D., Kulkarni, M., El-Mezawy, A., Mobini, S., Elhiti, M., Gjuric, R., et al. (2021). Medical cannabis and industrial hemp tissue culture: present status and future potential. *Front. Plant Sci.*12:275. doi: 10.3389/fpls.2021.627240

Barnett, S. E., Cala, A. R., Hansen, J. L., Crawford, J., Viands, D. R., Smart, L. B., et al. (2020). Evaluating the microbiome of hemp. *Phytobiomes J.* 4, 351–363. doi: 10.1094/PBIOMES-06-20-0046-R

Braemer, R., and Paris, M. (1987). Biotransformation of cannabinoids by a cell suspension culture of *Cannabis sativa* L. *Plant Cell Rep*. 6, 150–152.

Chandra, S., Lata, H., Khan, I. A., and ElSohly, M. A. (2017). "*Cannabis sativa* L.: botany and horticulture," in *Cannabis sativa L. Botany and Biotechnology,* eds S. Chandra, H. Lata, M. ElSohly M (Cham: Springer). doi: 10.1007/978-3-319-54564-6

Cheong, E. J., Mock, R., and Li, R. (2012). Elimination of five viruses from sugarcane using *in vitro* culture of axillary buds and apical meristems. *Plant Cell Tissue Organ. Cult.*109, 439–445. doi: 10.1007/s11240-011-0108-3

Chinestra, S. C., Curvetto, N. R., and Marinangeli, P. A. (2015). Production of virus-free plants of *Lilium* spp. from bulbs obtained *in vitro* and *ex vitro*. *Sci. Horticult.* 194, 304–312. doi: 10.1016/j.scienta.2015.08.015

Cobo, M., Gutiérrez, B., and Torres, M. (2018). Regeneration of Mortiño (*Vacciniumfloribundum* Kunth) plants through axillary bud culture. *In Vitro Cell Dev. Biol. Plant* 54, 112–116. doi: 10.1007/s11627-018-9884-3

Comeau, D., Novinscak, A., Joly, D. L., and Filion, M. (2021). Spatio-temporal and cultivar-dependent variations in the cannabis microbiome. *Front. Microbiol.* 11:491. doi: 10.3389/fmicb.2020.00491

Feeney, M., and Punja, Z. K. (2003). Tissue culture and *Agrobacterium*-mediated transformation of hemp (*Cannabis sativa* L.). *In Vitro Cell Dev. Biol. Plant* 39, 578–585. doi: 10.1079/IVP2003454

Hussain, A., Qashi, I., Nazir, H., and Ullah, I. (2012). "Plant tissue culture: current status and opportunities," in *Recent Advances in Plant in vitro Culture,* eds A. Leva and L. Rinaldi, 2–28. doi: 10.5772/50568

Islam, M. M., Ahmed, M., and Mahaldar, D. (2005). *In vitro* callus induction and plant regeneration in seed explants of rice (*Oryza sativa* L.). *Res. J. Agri. Biol. Sci.* 1, 72–75.

Kodym, A., and Leeb, C. (2019). Back to the roots: Protocol for the photoautotrophic micropropagation of medicinal *Cannabis*. *Plant Cell Tiss. Org. Cult.*138, 399–402. doi: 10.1007/s11240-019-01635-1

Kusari, P., Kusari, S., Spiteller, M., and Kayser, O. (2013). Endophytic fungi harbored in *Cannabis sativa* L.: diversity and potential as biocontrol agents against host plant-specific phytopathogens. *Fung. Div.* 60, 137–151. doi: 10.1007/s13225-012-0216-3

Lata, H., Chandra, S., Khan, I., and ElSohly, M. A. (2009). Thidiazuron-induced high-frequency direct shoot organogenesis of *Cannabis sativa* L. *In Vitro Cell. Dev. Biol. Plant* 45, 12–19. doi: 10.1007/s11627-008-9167-5

Lata, H., Chandra, S., Techen, N. Z., Khan, I. A., and ElSohly, M. A. (2016). *In vitro* mass propagation of*Cannabis sativa* L.: a protocol refinement using novel aromatic cytokinin meta-topolin and the assessment of eco-physiological, biochemical and genetic fidelity of micropropagated plants. *J. Appl. Res. Med. Aromat. Plants* 3, 18–26. doi: 10.1016/j.jarmap.2015.12.001

Liu, Z., and Li, Z. (2001). Micropropagation of *Camptothecaacuminata*Decaisne from axillary buds, shoot tips, and seed embryos in a tissue culture system. *In Vitro Cell. Dev. Biol. Plant* 37, 84–88. doi: 10.1007/s11627-001-0016-z

Lubell-Brand, J., Kurtz, L. E., and Brand, M. H. (2021). An *in vitro-ex vitro* micropropagation system for hemp. *Hort Technology* 31, 199–207. doi: 10.21273/HORTTECH04779-20

Luz, J., Abreu Asmar, S., Pasqual, M., Gomes de Araujo, A., Pio, L. A. S., and Ferreira Resende, R. (2012). Modification in leaf anatomy of banana plants cultivar "Maçã" subjected to different silicon sources *in vitro*. *Acta Hort.* 961, 239–243. doi: 10.17660/ActaHortic.2012.961.30

Mandolino, G., and Ranalli, P. (1999). Advances in biotechnological approaches for hemp breeding and industry. *Adv. Hemp Res*. 9, 185–212.

Martínez, M. T., Corredoira, E., Vieitez, A. M., Cernadas, M. J., Montenegro, R., Ballester, A., et al. (2017). Micropropagation of mature *Quercus ilex* L. trees by axillary budding. *Plant Cell Tiss. Organ Cult.* 131, 499–512. doi: 10.1007/s11240-017-1300-x

Monthony, A. S., Page, S. R., Hesami, M., and Jones, A. M. P. (2021). The past, present, and future of *Cannabis sativa* tissue culture. *Plants* 10:185. doi: 10.3390/plants10010185

Moreno-Vázquez, S., Larrañaga, N., Uberhuaga, E. C., Braga, E. J. B., and Pérez-Ruíz, C. (2014). Bacterial contamination of *in vitro* plant cultures: confounding effects on somaclonal variation and detection of contamination in plant tissues. *Plant Cell Tiss. Organ Cult*. 119, 533–541. doi: 10.1007/s11240-014-0553-x

Movahedi, M., Ghasemi-Omran, V. O., and Torabi, S. (2015). The effect of different concentrations of TDZ and BA on *in vitro* regeneration of Iranian cannabis (*Cannabis sativa*) using cotyledon and epicotyl explants. *J. Plant Mol. Breed*. 3, 20–27. doi: 10.22058/JPMB.2015.15371

Nagy, J. K., Sule, S., and Sampaio, J. P. (2005). Apple tissue culture contamination by *Rhodotorula* spp.: identification and prevention.

In Vitro Cell Dev. Bio Plant. 41, 520–524. doi: 10.1079/IVP2005647

Nerway, Z. A. A., Duhoky, M. M. S., and Kassim, N. A. (2020). *In vitro* elimination of dahlia mosaic virus by using meristem culture, electrotherapy and chemotherapy. *Iraqi J. Agr. Sci.* 51, 665–674. doi: 10.36103/ijas.v51i2.994

Page, S. R. G., Monthony, A. S., and Jones, A. M. P. (2021). DKW basal salts improve micropropagation andcallogenesis compared to MS basal salts in multiple commercial cultivars of *Cannabis sativa*. *Botany* 99, 269–279. doi: 10.1139/cjb-2020-0179

Panathula, C. S., Mahadev, M. D. N., and Naidu, C. V. (2014). The stimulatory effects of the antimicrobial agents bavistin, cefotaxime and kanamycin on *in vitro* plant regeneration of *Centellaasiatica* (L.) -an important antijaundice medicinal plant. *Am. J. Plant Sci.* 5, 279–285. doi: 10.4236/ajps.2014.53038

Punja, Z. K. (2021). Emerging diseases of *Cannabis sativa* and sustainable management. *Pest Manag. Sci.* 77, 3857–72. doi: 10.1002/ps.6307

Punja, Z. K., Collyer, D., Scott, C., Lung, S., Holmes, J., and Sutton, D. (2019). Pathogens and molds affecting production and quality of *Cannabis sativa* L. *Front. Plant Sci.* 10:1120. doi: 10.3389/fpls.2019.01120

Punja, Z. K., and Holmes, J. E. (2020). Hermaphroditism in marijuana (*Cannabis sativa* L.) inflorescences – Impact on floral morphology, seed formation, progeny sex ratios, and genetic variation. *Front. Plant Sci.* 11:718. doi: 10.3389/fpls.2020.00718

Ramgareeb, S., Snyman, S. J., van Antwerpen, T., and Rutherford, R. S. (2010). Elimination of virus and rapid propagation of disease-free sugarcane (*Saccharum* spp. cultivar NCo376) using apical meristem culture. *Plant Cell Tiss. Organ. Cult.* 100, 175–181. doi: 10.1007/s11240-009-9634-7

Ranaweera, K. K., Gunasekara, M. T. K., and Eeswara, J. P. (2013). *Ex vitro* rooting: a low cost micropropagation technique for tea [*Camellia sinensis* (L.) O. Kuntz] hybrids. *Sci. Horti.* 155, 8–14. doi: 10.1016/j.scienta.2013.03.001

Rech, E., and Pires, J. (1986). Tissue culture propagation of *Mentha* spp. by the use of axillary buds. *Plant Cell Rep.* 5, 17–18. doi: 10.1007/BF00269708

Roy, A. T., Leggett, G., and Koutoulis, A. (2001). Development of a shoot multiplication system for hop (*Humuluslupulus* L.). *In Vitro Cell. Dev. Biol. Plant*. 37, 79–83. doi: 10.1007/s11627-001-0015-0

Sahoo, Y., and Chand, P. K. (1998). Micropropagation of *Vitexnegundo* L., a woody aromatic medicinal shrub, through high-frequency axillary shoot proliferation. *Plant Cell. Rep*. 18, 301–307. doi: 10.1007/s002990050576

Savaas, D., and Gruda, N. (2018). Application of soilless culture technologies in the modern greenhouse industry – a review. *Eur. J. Hort. Sci*. 83, 280–293. doi: 10.17660/eJHS.2018/83.5.2

Scott, C., and Punja, Z. K. (2021). Evaluation of disease management approaches for powdery mildew on *Cannabis sativa* L. (marijuana) plants. *Can. J. Plant Pathol.* 43, 394–412. doi: 10.1080/07060661.2020.1836026

Scott, M., Rani, M., Samsatly, J., Charron, J. B., and Jabaji, S. (2018). Endophytes of industrial hemp (*Cannabis sativa* L.) cultivars: identification of culturable bacteria and fungi in leaves, petioles, and seeds. *Can. J. Microbiol*. 64, 664–680. doi: 10.1139/cjm-2018-0108

Slusarkiewicz-Jarzina, A., Ponitka, A., and Kaczmarek, Z. (2005). Influence of cultivar, explant source and plant growth regulator on callus induction and plant regeneration of *Cannabis sativa* L. *Acta Biol. Cracov. Bot*. 47, 145–151.

Soares, J. D. R., Pasqual, M., Rodrigues, F. A., Villa, F., and Araujo, A. G. (2011). Silicon sources in the micropropagation of the cattleya group orchid. *Acta Sci. Agron*. 33, 503–507. doi: 10.4025/actasciagron.v33i3.6281

Spanò, R., Bottalico, G., Corrado, A., Campanale, A., Di Franco, A., and Mascia, T. (2018). A protocol for producing virus-free artichoke genetic resources for conservation, breeding, and production. *Agri. Basel* 8:36. doi: 10.3390/agriculture8030036

Thomas, T. D. (2008). The role of activated charcoal in plant tissue culture. *Biotechnol. Adv*. 26, 618–631. doi: 10.1016/j.biotechadv.2008.08.003

University of California Davis (2008). *Guide to the Strawberry Clean Plant Program*. Retrieved from https://fps.ucdavis.edu/strawberry.cfm

Wahby, I., Caba, J., and Ligero, F. (2013). Agrobacterium infection of hemp (*Cannabis sativa* L.): establishment of hairy root cultures. *J. Plant Interact*. 8, 312–320. doi: 10.1080/17429145.2012.746399

Wang, P. J., and Hu, C. Y. (1980). "Regeneration of virus-free plants through *in vitro* culture," in *Advances in Biomedical Engineering*, *Vol. 18*, ed A. Fiechter A (Berlin, Springer Press), 61–99.

Wang, P. J., and Huang, L. C. (1976). Beneficial effects of activated charcoal on plant tissue and organ cultures. *In VitroCell Dev. Biol. Plant* 12, 260–262. doi: 10.1007/BF02796447

Wang, R., He, L.-S., Xia, B., Tong, J.-F., Li, N., and Peng, F. (2009). A micropropagation system for cloning of hemp (*Cannabis sativa* L.) by shoot tip culture. *Pak. J. Bot*. 41, 603–608.

Wielgus, K., Luwanska, A., Lassocinski, W., and Kaczmarek, Z. (2008). Estimation of *Cannabis sativa* L. tissue culture conditions essential for callus induction and plant regeneration. *J. Nat. Fib*. 5, 199–207. doi: 10.1080/15440470801976045

Yancheva, S., and Kondakova, V. (2018). "Plant tissue culture technology: present and future development," in *Bioprocessing of Plant In Vitro Systems, Reference Series in Phytochemistry*, eds A. Pavlov, T. Bley (Springer International Publishing), 39–63.

Zhuo, T. S. (1995). The detection of the accumulation of silicon in *Phalaenopsis* (*Orchidaceae*). *Ann. Bot.* 75, 605–607. doi: 10.1006/anbo.1995.1065

Conflict of Interest: The authors declare that the research was conducted in the absence of any commercial or financial relationships that could be construed as a potential conflict of interest.

Publisher's Note: All claims expressed in this article are solely those of the authors and do not necessarily represent those of their affiliated organizations, or those of the publisher, the editors and the reviewers. Any product that may be evaluated in this article, or claim that may be made by its manufacturer, is not guaranteed or endorsed by the publisher.

frontiers in Plant Science

ORIGINAL RESEARCH
published: 29 September 2021
doi: 10.3389/fpls.2021.675770

Comparative Genetic Structure of *Cannabis sativa* Including Federally Produced, Wild Collected, and Cultivated Samples

Anna L. Schwabe[1], Connor J. Hansen[1,2], Richard M. Hyslop[2] and Mitchell E. McGlaughlin[1]**

[1]School of Biological Sciences, University of Northern Colorado, Greeley, CO, United States, [2]Department of Chemistry and Biochemistry, University of Northern Colorado, Greeley, CO, United States

Currently in the United States, the sole licensed facility to cultivate *Cannabis sativa* L. for research purposes is the University of Mississippi, which is funded by the National Institute on Drug Abuse (NIDA). Studies researching *Cannabis* flower consumption rely on NIDA-supplied "research grade marijuana." Previous research found that cannabinoid levels of NIDA-supplied *Cannabis* do not align with commercially available *Cannabis*. We sought to investigate the genetic identity of *Cannabis* supplied by NIDA relative to common categories within the species. This is the first genetic study to include "research grade marijuana" from NIDA. Samples (49) were assigned as Wild Hemp (feral; 6) and Cultivated Hemp (3), NIDA (2), CBD drug type (3), and high THC drug type subdivided into Sativa (11), Hybrid (14), and Indica (10). Ten microsatellites targeting neutral non-coding regions were used. Clustering and genetic distance analyses support a division between hemp and drug-type *Cannabis*. All hemp samples clustered genetically, but no clear distinction of Sativa, Hybrid, and Indica subcategories within retail marijuana samples was found. Interestingly, the two analyzed "research grade marijuana" samples obtained from NIDA were genetically distinct from most drug-type *Cannabis* available from retail dispensaries. Although the sample size was small, "research grade marijuana" provided for research is genetically distinct from most retail drug-type *Cannabis* that patients and patrons are consuming.

Keywords: *Cannabis sativa*, NIDA, genotype, marijuana, microsatellite, phenotype, strains, hemp (*Cannabis sativa* L.)

OPEN ACCESS

Edited by:
Derek Stewart, The James Hutton Institute, United Kingdom

Reviewed by:
Gordon J. McDougall, The James Hutton Institute, United Kingdom
Michael Benjamin Kantar, University of Hawaii, United States

***Correspondence:**
Anna L. Schwabe
schw0701@bears.unco.edu
Mitchell E. McGlaughlin
mitchell.mcgalughlin@unco.edu

Specialty section:
This article was submitted to Crop and Product Physiology, a section of the journal Frontiers in Plant Science

Received: *03 March 2021*
Accepted: *01 September 2021*
Published: *29 September 2021*

Citation:
Schwabe AL, Hansen CJ, Hyslop RM and McGlaughlin ME (2021) Comparative Genetic Structure of Cannabis sativa Including Federally Produced, Wild Collected, and Cultivated Samples. Front. Plant Sci. 12:675770. doi: 10.3389/fpls.2021.675770

INTRODUCTION

Humans have a long history with *Cannabis sativa*, with evidence of cultivation dating back as far as 10,000 years (Abel, 2013). The World Health Organization reports *Cannabis* as the most widely cultivated, trafficked and abused illicit drug, and it constitutes over half of worldwide drug seizures (World Health Organization, 2018). The United States is currently experiencing drastic changes in patterns of *Cannabis* use associated with widespread relaxation of laws that previously limited both medical and recreational consumption (Cousijn et al., 2018), as well as hemp cultivation. This has led to a need for extensive research into the basic biology and

taxonomy of *Cannabis sativa* (Hillig, 2005; Clarke and Merlin, 2013; Lynch et al., 2016; Vergara et al., 2016; Small, 2017).

Cannabis sativa is the only described species in the genus *Cannabis* (Cannabaceae) but there are several commonly described subcategories that are widely recognized. There are two primary groups, which are well-supported by genetic analyses (Sawler et al., 2015; Lynch et al., 2016; Dufresnes et al., 2017; Soler et al., 2017): (1) hemp or hemp type which is legally defined in the United States as *Cannabis* containing no more than 0.3% THC, and (2) marijuana, drug type, or drug type which encompasses all *Cannabis* with THC concentrations >0.3% THC. The term marijuana is controversial, so unless referencing "research grade marijuana" as defined by the US government, we utilize the term "drug type," as there is no acceptable widely used term for *Cannabis* that does not classify as hemp. It is important to note that much of the confusion around *Cannabis* groups is related to the fact that hemp and drug types are distinguished based on % THC content, which is a variable trait that has been selected for or against in the two groups. Hemp types tend to have higher concentrations of CBD than drug types (de Meijer et al., 1992). High THC drug types generally contain >12% THC and average ~10–23% THC in dispensaries (Potter et al., 2008; Vergara et al., 2017; Jikomes and Zoorob, 2018). Within the two major groups, *Cannabis* can be further divided into varietals or strains. High THC drug types are often categorized further in the commercial marketplace: Sativa, Indica, and Hybrid strains, which reportedly have different intoxicating effects (Heilig, 2011; Hazekamp and Fischedick, 2012; Smith, 2012; McPartland, 2017; Leafly, 2018). There is continuing debate among experts surrounding the appropriate taxonomic treatment of *Cannabis* groups, which is confounded by colloquial usage of these terms vs. what researchers suggest is more appropriate nomenclature (Small et al., 1976; Emboden, 1977, 1981; Clarke and Merlin, 2015; Small, 2015, 2016; McPartland, 2017; McPartland and Guy, 2017). Genetic analyses have not shown clear and consistent differentiation among the three commonly described high THC drug strain categories (Sawler et al., 2015; Lynch et al., 2016), but both the recreational and medical *Cannabis* communities maintain that there are distinct differences in effects between Sativa and Indica strains (Smith, 2012; Leafly, 2018).

Although *Cannabis* has been federally controlled in the United States since 1937, as of February 2021, 36 states and the District of Columbia (DC) allow regulated medical use, and 16 states and Washington DC allow adult recreational use (ProCon, 2018a). However, because the DEA lists THC as a Schedule I substance (United States Congress, 1970), research on all aspects of this plant has been limited. In the United States, a Schedule I substance is described as a drug with no accepted medical use and a high potential for abuse (United States Congress, 1970). Surgeon General Jerome Adams recently expressed concern that the current scheduling in the most restrictive category is inhibiting research on *Cannabis* as a potentially therapeutic plant (Jaeger, 2018). The University of Mississippi, funded through the National Institutes of Health/National Institute on Drug Abuse (NIH/NIDA), currently holds the only license issued by the Drug Enforcement Administration (DEA) for the cultivation of *Cannabis* for research purposes (Drug Enforcement Administration and Department of Justice, 2016). As such, NIDA serves as the sole legal provider of drug-type *Cannabis* for federally funded medical research in the United States. NIDA does not grow or distribute hemp-type *Cannabis*.

Medical research on *Cannabis* has primarily focused on isolated THC and CBD (Borgelt et al., 2013; Maa and Figi, 2014; Backes and Weil 2014; National Institute on Drug Abuse, 2016a, 2019, 2020; Baron, 2018; Citti et al., 2018; Cousijn et al., 2018) but there are hundreds of other chemical constituents in *Cannabis* (ElSohly, 2007), including cannabinoids and terpenes (Baron, 2018). Recent research has documented that NIDA-provided *Cannabis* has distinctly different cannabinoid profiles than commercially available *Cannabis* (Vergara et al., 2017). Specifically, Vergara et al. (2017) found that NIDA-reported THC and CBD concentrations were only 27 and 48%, respectively, of the mean values of commercially available drug-type *Cannabis* samples in the four US cities (Vergara et al., 2017). Due to the growing evidence that chemical constituents in various combinations and abundances in the whole plant work in concert to create the suite of reported physiological effects (Baron, 2018; Nahler et al., 2019; Russo, 2019; Ferber et al., 2020), it is important to know how strains vary in all relevant components. The chemical makeup of each variant of *Cannabis* is influenced by environmental conditions (e.g., light, water, nutrients, soil, airflow, etc.) and the underlying genetic makeup. Since genotype does not change, genetic data is essential baseline information for understanding *Cannabis* diversity, consistency, and potential effects.

In the current study, we investigated the genetic relationship of two types of NIDA-obtained *Cannabis* to commercially available drug-type *Cannabis*, as well as wild (feral) and cultivated hemp. Since *Cannabis* has been under heavy artificial selection for different traits such as THC content or industrial uses, we focused solely on genetic data. We assessed ten variable nuclear microsatellite loci targeting non-coding regions of the genome to examine genetic differentiation among our samples independent of recent human selection. Included in the present study were samples from NIDA (high THC and high THC/CBD), high THC drug type, low THC/high CBD drug type, wild growing hemp (presumed escapees from cultivation), and cultivated hemp. This study aimed to investigate where research grade *Cannabis* supplied by NIDA falls on the genetic spectrum of *Cannabis* groups.

MATERIALS AND METHODS

Cannabinoid concentrations were not measured for any of the samples, as this was a genetic study. Samples were categorized based on the information provided at the time of acquisition. A total of 49 *Cannabis* samples acquired in the United States were used in this research (**Supplementary Table 1**), including Wild (feral) hemp (6), Cultivated hemp (3), NIDA samples (2), high CBD drug type (3), and high THC drug type (35). The wild

collected hemp was sampled from herbaria collections and is presumed to represent feral specimens that escaped from cultivation. NIDA "research grade marijuana" was limited to two samples obtained *via* another study: "high THC" defined by NIDA as containing >5–10% THC (RTI log number 13494-22, reference number SAF 027355) and "high THC/CBD" defined by NIDA as containing 5–10% of both THC and CBD (RTI log number 13784-1114-18-6, reference number SAF 027355: National Institute on Drug Abuse, 2016b). NIDA has limited the access of "research grade marijuana" for non-medical research, so we did not have access to a wider sampling of the types they provide. High THC drug-type samples were further subdivided into three frequently used colloquial strain categories: Sativa (11), Hybrid (14), and Indica (10) based on information available online (Leafly, 2018; PotGuide.com, 2018; Wikileaf, 2018; Seedfinder, 2020). *Cannabis* is genetically diverse and based on our research which included 122 samples (Schwabe and McGlaughlin, 2019), and other published research (Gao et al., 2014; Sawler et al., 2015; Lynch et al., 2016; Dufresnes et al., 2017; Soler et al., 2017; Pisupati et al., 2018), the sampling used here adequately captures the genetic diversity within and among the groups.

DNA was extracted using a CTAB extraction protocol (Doyle, 1987) modified to use 0.035–0.100 g of dried flower tissue per extraction. Ten variable microsatellite loci developed by Schwabe & McGlaughlin (Schwabe and McGlaughlin, 2019) were used in this study following their previously described procedures.

GENALEX ver. 6.4.1 (Peakall and Smouse, 2006, 2012; 59, 60) was used to calculate pairwise genetic differentiation (F_{ST}) and Nei's genetic distance (D) between each of the seven groups and to determine the presence of private alleles. PCoA eigenvalues calculated in GENALEX were used to plot the PCoA in RStudio with the ggplot package (R Studio Team, 2015) with 95% confidence interval ellipses.

Genotypes were analyzed using the Bayesian cluster analysis program STRUCTURE ver. 2.4.2 (Pritchard et al., 2000). Burn-in and run-lengths of 50,000 generations were used with ten independent replicates for each STRUCTURE analysis, testing K = 1–10. The number of genetic groups for the data set was determined by STRUCTURE HARVESTER (Earl and vonHoldt, 2012), which implements the method of Evanno et al. (2005).

Maverick v1.0.5 (Verity and Nichols, 2016) was used as an additional verification of Bayesian clustering analysis using thermodynamic integration to determine the appropriate number of genetic groups. The following parameters were used: admixture parameter (alpha) of 0.03 with a standard deviation (alphaPropSD) of 0.008, ten replicates (mainRepeats), 1,000 Burn-in iterations (mainBurnin), 5,000 sample iterations (mainSamples), 100 TI rungs (thermodynamicRungs), 500 TI Burn-in iterations (thermodynamicBurnin), and 1,000 TI iterations (thermodynamicSamples).

RESULTS

Our analyses examined the genetic differentiation and structure of samples from seven *Cannabis* groups (**Supplementary Table 1**): (1) **Wild hemp** – feral wild collected hemp; (2) **Cultivated hemp** – obtained from hemp cultivators; (3) **NIDA** – "research grade marijuana" samples obtained from NIDA classified as high THC or high THC/CBD; (4) **high CBD** – drug-type *Cannabis* with relatively high levels of CBD and low levels of THC; and commercially available high THC drug-type *Cannabis* described as (5) **Sativa**, (6) **Hybrid**, or (7) **Indica**. With the exception of genetic distance statistics, the analyses were performed on samples at the individual level, where the genetic placement of each sample is determined independent of its' putative *Cannabis* group. Conducting analyses at an individual level controls for biases that might arise due to the artificial nature of named groups and varying group sample sizes. Clustering (PCoA) and proportion of genetic assignment (STRUCTURE) analyses are presented first by assigning each sample by color to either hemp type or drug type (**Figures 1, 2**; Supplementary Figure 1), as these have previously been shown to separate well using genetic data (Datwyler and Weiblen, 2006; Piluzza et al., 2013; Sawler et al., 2015; Lynch et al., 2016; Dufresnes et al., 2017). The same analyses are then presented by color assignment to one of the seven subcategories to determine further possible relationships within and among these groups (**Figures 3, 4**).

Genetic Analyses: Individual Level

Hemp V. Drug Types

Principal coordinate analysis (PCoA) with 95% confidence interval ellipses around the hemp-type (red) and drug-type (blue) groups shows clear separation of hemp samples from the drug types. NIDA samples are indicated in green and cluster within the hemp confidence interval (**Figure 1**). Coordinate 1 explains 13.02% of the genetic variation, and an additional 11.17% of the genetic variation is explained by coordinate 2.

STRUCTURE was used to examine sample assignment to genetic groups while allowing admixture. The appropriate number of STRUCTURE groups from K = 1–10 was validated using STRUCTURE HARVESTER (Earl and vonHoldt, 2012), which had high support for two genetic groups (K = 2, $\Delta K = 61.35$). An additional genetic structure analysis (MAVERICK 1.0.5: Verity and Nichols, 2016) was conducted to independently test group assignments and verified strong support for two genetic groups with the same assignment of individuals (K = 2, probability 0.999, data not shown). The two genetic group STRUCTURE analysis (**Figure 3**) shows consistent differentiation between hemp-type and drug-type *Cannabis*. All hemp samples were assigned a genetic proportion of inferred ancestry (Q) greater than 0.92 (hemp mean group 1, Q = 0.96). All but two drug-type samples showed admixture associated with hemp <0.78 (range 0.03–0.78) with 31 of 38 (83%) samples <0.50 proportion of ancestry associated with hemp genetic signal.

Categorical Group Analysis

Principal coordinate analysis with 95% confidence interval ellipses around the major groups shows that there is clear separation of hemp samples from the drug types, with NIDA

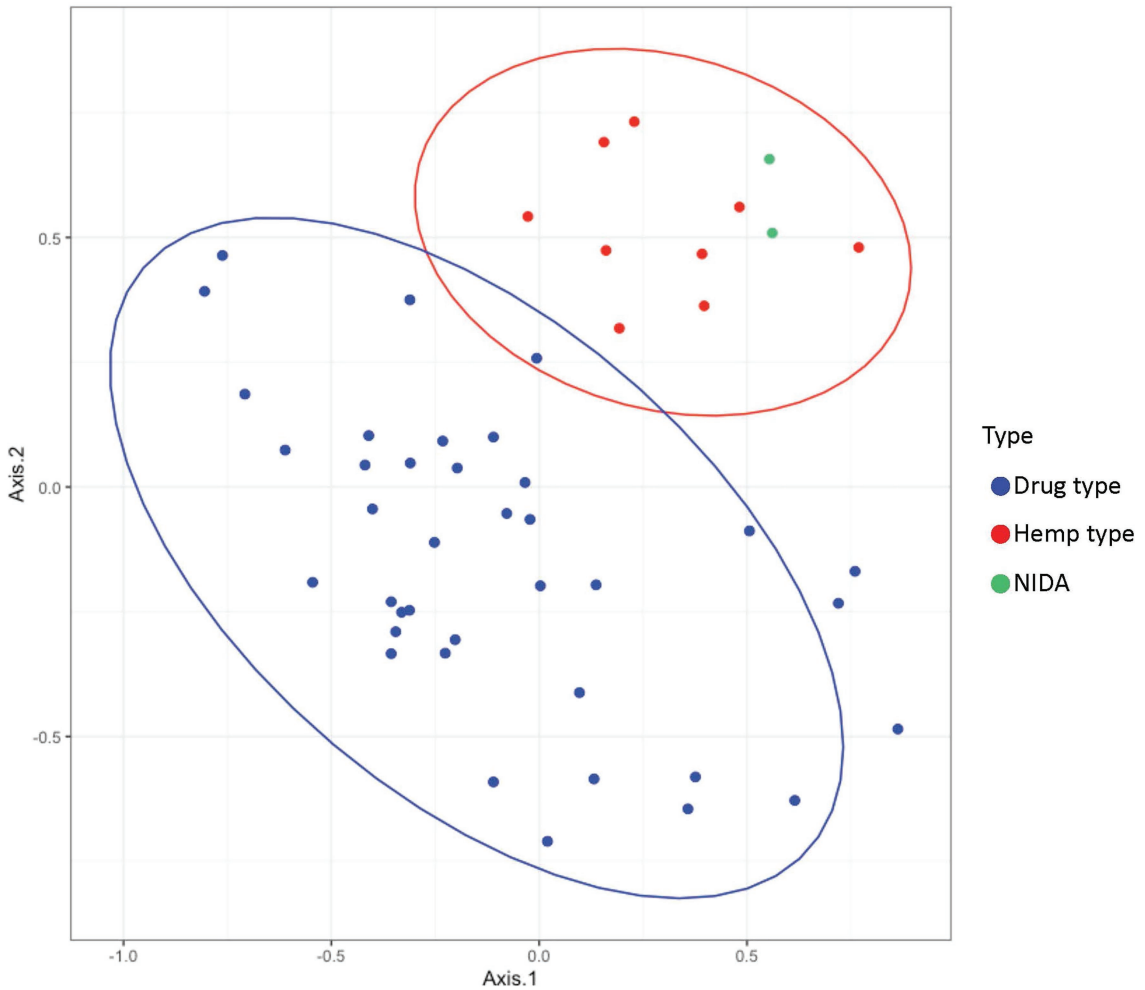

FIGURE 1 | Principal coordinates analysis of genetic distance among samples. Samples clustering together are more closely related. The ellipses represent 95% confidence intervals for each group (Cultivated hemp = orange, Wild hemp = yellow, NIDA = blue, High CBD = pink, Sativa = red, Hybrid = green, Indica = purple). Approximately 24% of the genetic variation in these groups is shown (Axis 1 = 13.02% and Axis 2 = 11.17%).

samples (green) clustering within the hemp confidence interval (**Figure 2**). The drug-type samples (Indica, Sativa, Hybrid, and high CBD) all occupy the same character space, distinct from hemp.

For the categorical group STRUCTURE analyses, the two genetic group STRUCTURE analysis (K2, **Figure 4**) shows consistent differentiation between hemp- and drug-type samples. All hemp samples were assigned to genetic group 1 (yellow) with a proportion of inferred ancestry (Q) greater than 0.93 (hemp mean group 1, Q = 0.96). High THC drug-type samples showed some admixture with 29 of 35 samples having the majority of the genetic signal assigned to genetic group 2 (green; high THC drug-type mean group 2, Q = 0.75). The three high CBD drug-type samples were assigned with a mean of 0.61 to group 1 and 0.39 to groups 2. NIDA samples were assigned to genetic group 1 (NIDA mean group 1, Q = 0.97), demonstrating a strong genetic association with hemp in this analysis.

Although not strongly supported, the three genetic group STRUCTURE analysis (K3, **Figure 4**) shows some additional genetic structure among drug-type samples. All hemp-type samples were assigned to genetic group 1 (yellow) with a proportion of inferred ancestry (Q) greater than 0.90 (hemp mean group 1, Q = 0.93). The high THC drug-type samples demonstrated some admixture with 12 of 35 samples assigned genetic signal Q = > 0.50 to group 2 (green; high THC drug-type mean group 2, Q = 0.33), and 21 of 35 samples assigned genetic signal Q = > 0.50 to group 3 (purple; high THC drug-type mean group 3, Q = 0.53). The three high CBD drug-type samples were assigned with a mean of 0.34 to group 1, 0.10 to group 2 and 0.58 to group 3. NIDA samples were assigned to genetic group 1 (NIDA mean group 1, Q = 0.95) with similarly low signal from groups 2 and 3 (0.03 and 0.02 respectively) demonstrating a strong genetic association with hemp. STRUCTURE analysis results are also presented from K = 2–10 (Supplementary Figure 1).

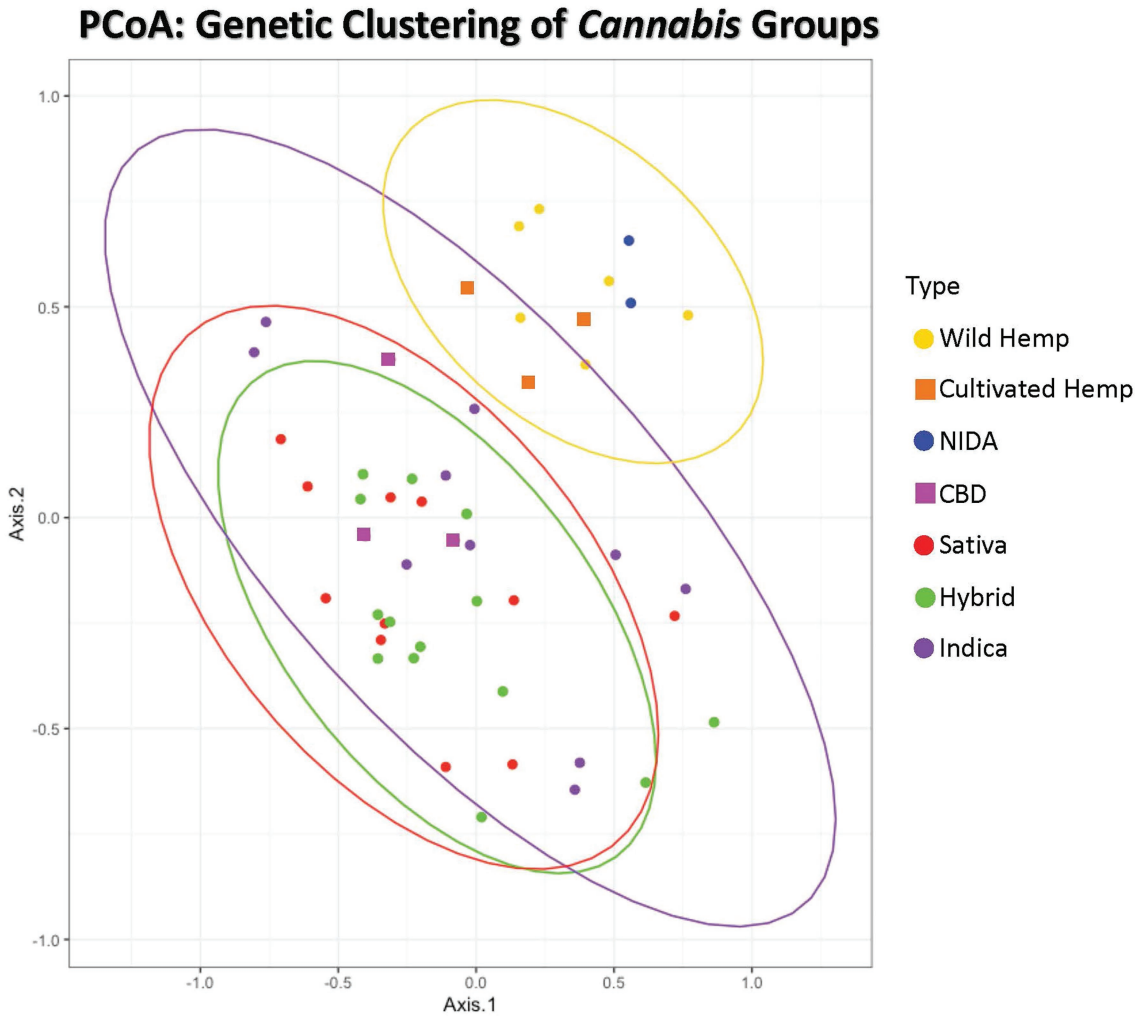

FIGURE 2 | Principal Coordinates Analysis of genetic distance among samples. Samples clustering together are more closely related. The ellipses represent 95% confidence intervals for each group (Cultivated hemp = orange, Wild hemp = yellow, NIDA = blue, High CBD = pink, Sativa = red, Hybrid = green, Indica = purple). Approximately 24% of the genetic variation in these groups is shown (coordinate 1= 13.02% and coordinate 2 = 11.17%). No confidence intervals were drawn for NIDA, High CBD, or Cultivated Hemp samples due to the small sample size (n = 2, n = 3, and n = 3, respectively).

Genetic Analyses: Population Level

Genetic Differentiation

Pairwise genetic differentiation (Fst and Nei's D) calculated in GENALEX ver. 6.4.1 [59, 60] found the highest level of divergence between NIDA and high CBD drug type (Fst = 0.394) and between hemp and Sativa high THC drug type (Nei's D = 1.026; **Table 1**). The least divergence was observed among the high THC drug types (Fst = 0.023–0.039; Nei's D = 0.066–0.102).

Private Alleles

Private alleles, alleles found only in a single group, are commonly used in population genetic studies to identify divergent groups. Eight of the ten utilized loci contained at least one private allele in one *Cannabis* group (**Table 2**). Wild hemp contained the most private alleles, 12, while the high CBD group contained only 1. Given that we only sampled two NIDA individuals, the four observed private alleles indicate that this group contains unique genetic signal.

DISCUSSION

The purpose of this study was to examine the genetic relationship of *Cannabis* samples from each of the common categories and subgroups and to determine where NIDA samples fall on the *Cannabis* genetic spectrum. The genetic regions used in this study were designed to target non-coding regions of the genome, and therefore less likely to reflect artifacts related to recent human selection. Our results clearly demonstrate that NIDA *Cannabis* samples are substantially genetically different from most commercially available drug-type strains and share a genetic affinity with hemp samples in several of the analyses. We do not claim that NIDA is supplying hemp for *Cannabis* research, rather we are confident that our analyses show that the "research grade marijuana" supplied by NIDA is genetically different from the retail drug-type samples analyzed in this study. Previous research has found that medical and recreational

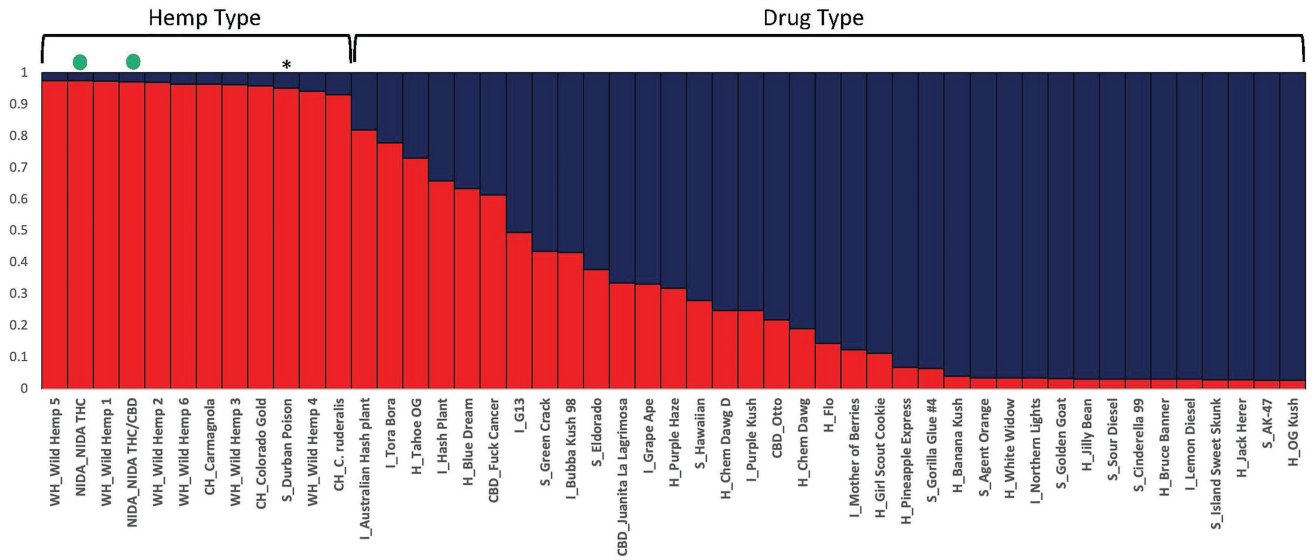

FIGURE 3 | Bayesian clustering analysis from STRUCTURE with the proportion of inferred ancestry for two genetic groups (K = 2) sorted by proportion of genotype assignment. Each individual is represented as a single bar in the graph. The NIDA samples are indicated by a green dot. * "Durban Poison" is a drug type assigned 0.95 to hemp ancestry. The letters preceding the sample name relate to the category the sample was place in (WH, wild hemp; CH, cultivated hemp; CBD, high CBD drug type; S, sativa drug type; H, hybrid drug type; I, Indica drug type).

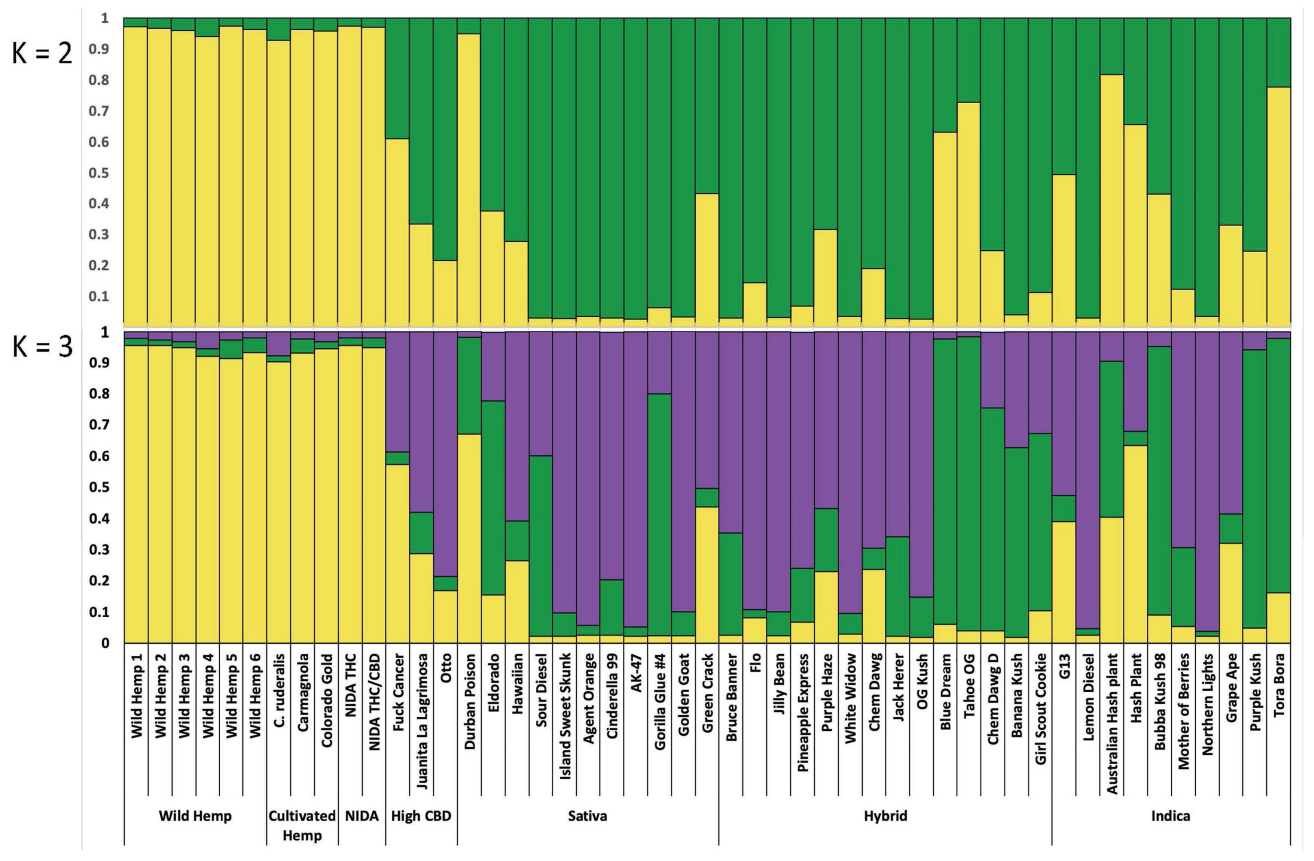

FIGURE 4 | Bayesian clustering analysis from STRUCTURE with the proportion of inferred ancestry for two genetic groups (K = 2, top), and for three genetic groups (K = 3, bottom), Each individual is represented as a single bar in the graph.

TABLE 1 | Pairwise Fst values (below the diagonal) and Nei's D (above the diagonal) for major *Cannabis* groups.

	NIDA	Wild Hemp	Cultivated Hemp	High CBD	Sativa	Hybrid	Indica
NIDA	-	0.738	1.018	0.911	1.026	0.918	0.808
Wild Hemp	0.245	-	0.386	0.500	0.606	0.605	0.475
Cultivated Hemp	0.324	0.086	-	0.532	0.652	0.614	0.518
High CBD	0.394	0.153	0.175	-	0.196	0.215	0.206
Sativa	0.319	0.117	0.143	0.092	-	0.098	0.102
Hybrid	0.310	0.122	0.147	0.096	0.039	-	0.066
Indica	0.268	0.083	0.109	0.092	0.033	0.023	-

TABLE 2 | Private alleles in each categorical group for ten loci. The number in parentheses after the locus name is number total number alleles for a locus.

	Total	Casa_02 (8)	Casa_06 (3)	Casa_14 (11)	Casa_18 (12)	Casa_22 (5)	Casa_26 (9)	Casa_27 (9)	Casa_28 (11)	Casa_29 (7)	Casa_30 (15)
NIDA	4				215		215		169		326
Wild Hemp	12	282		263			194, 239, 242	181	199	177, 180	267, 291, 294
Cultivated Hemp	3				203, 218				193		
High CBD	1	312									
Sativa	3						253	208			269
Hybrid	2			291	185						
Indica	3							187	196		297

Cannabis from California, Colorado, and Washington differs significantly in cannabinoid levels from the "research grade marijuana" supplied by NIDA (Vergara et al., 2017). This investigation adds to the previous research, indicating that the sampled NIDA *Cannabis* is also genetically distinctive from commercially available medical and recreational *Cannabis*. Given both this genetic and previous chemotypic investigations have concluded that NIDA is supplying product that does not align with what is available for consumers, our hope is that the NIH and NIDA will support the cultivation of *Cannabis* that is representative of what medical and recreational consumers are using. Medical practitioners, researchers and patients deserve access to *Cannabis* products that are comparable to products available on the legal market.

The genetic data collected in this study indicate that two major genetic groups exist within *Cannabis sativa* (**Figures 1, 3**). These results contribute to the growing consensus that hemp- and drug-type *Cannabis* can be consistently differentiated (Forapani et al., 2001; Datwyler and Weiblen, 2006; McPartland, 2006; Hakki et al., 2007; Sawler et al., 2015; Lynch et al., 2016; Dufresnes et al., 2017; Soler et al., 2017), but all *Cannabis* groups are currently considered a single species that has been selected for different uses. Some admixture of the hemp-type genetic signal is seen in many of the drug-type samples; this is not unexpected as the legal definition of hemp (0.3% total THC by dry weight) is not biologically significant and therefore holds no scientific basis for formal taxonomic separation. To our knowledge, this study and collaborative work investigating the genomic *Cannabis* data (Vergara et al., 2021) are the first to include "research grade marijuana" from NIDA. The placement of NIDA samples with hemp in multiple analyses was unexpected. However, it is important to note that some drug-type samples (e.g., "Durban Poison," **Figure 3**) are also placed in the hemp-type genetic group. This finding supports that although there are two distinct *Cannabis* genetic groups (hemp type and drug type), some strains within those groups have been selected to have the characteristics that we do not commonly associate with their specific genetic background. Crosses between hemp-type and drug-type strains may have been intentional, such as the recently developed high CBD drug strains that have low THC concentrations or the development of auto-flowering drug strains that flower as a function of age rather than photoperiod, which is a trait historically seen in some hemp varieties (Punja et al., 2017). Additionally, most *Cannabis* strains are a product of clandestine breeding in underground markets, so their presumed lineage may not match their actual genetic group. Hence, the finding that NIDA samples belong in the hemp-type genetic group in several analyses does not make these samples hemp, but it does demonstrate that they are different than the majority of drug-type *Cannabis* found in the marketplace.

Analyses were also conducted to examine how NIDA samples relate to traditionally recognized subgroups of *Cannabis*. It is important to note that some of the subgroups we assigned samples to are largely artificial and were based on information provided by online databases, which is the information that a recreational or medical consumer would have access to (Leafly, 2018; PotGuide.com, 2018; Wikileaf, 2018; Seedfinder, 2020). Although the categories Sativa, Indica and Hybrid are frequently used in the *Cannabis* industry and among consumers, researchers have yet to find consistent phenotypic and/or genotypic traits driving these widely referenced categories (Hillig, 2005; McPartland, 2017; McPartland and Guy, 2017; McPartland and Small, 2020). Given the high degree of intentional hybridization among drug-type *Cannabis*, it stands to reason that we would not see clear genetic separation among these categories. Additionally, the growing interest in *Cannabis* with alternative

combinations of cannabinoids other than THC has led to increased breeding efforts between hemp and drug types, further diluting any historical genetic distinctions that might have existed. Therefore, we did not expect the seven groups we used here to resolve as genetically unique. The analyses of genetic distance (**Table 1**) and private alleles (**Table 2**) support that NIDA samples are substantially diverged from all other *Cannabis* groups, including hemp, and contain a unique genetic profile. The high CBD drug-type samples are genetically more divergent from the hemp group than the high THC drug-type groups, suggesting that these are hybrids of hemp-type and high THC drug-type *Cannabis*. Additionally, the high CBD drug-type samples and several drug-type samples are admixed with some genetic signal assigned to both hemp and drug groups. Given the intentional breeding of different *Cannabis* groups and the fact that hemp-type and drug-type *Cannabis* are defined by total THC content, a trait under selection, the lack of genetic support for many distinct groups is not surprising.

The University of Mississippi National Center for Natural Products Research (NCNPR) produces research grade drug-type *Cannabis* for NIDA. NCNPR does not provide variety or strain information when filling *Cannabis* orders, so it is unclear what is currently grown for federally funded *Cannabis* research. Our data suggest that the NIDA *Cannabis* analyzed in this study was sourced from a single strain or two very closely related strains within the NCNPR stock. Without additional information about NCNPR *Cannabis* production, it is difficult to know how many strains are provided for federally funded research using *Cannabis* from NIDA. This study included only two *Cannabis* samples from NIDA which limits what we can conclude about the breadth of genetic diversity contained in NIDA collections. The inclusion of additional NIDA samples would be beneficial, but additional sampling would in no way change the genotypes of the samples included in this study, which was supplied to researchers conducting federally approved *Cannabis* research. Although the sample size of NIDA samples could impact their placement in group-based analyses of genetic distance (**Table 1**), all other analyses were carried out at an individual level (**Figures 1–4,** and **Supplemental Figure 1**) to avoid this issue. The exact cause of the genetic distinction in NIDA samples cannot be determined, but many factors could play a role such as directional selection, inbreeding, sourcing of ancestral strains not currently represented in the commercial market, and/or cross-pollination from wild or cultivated hemp. It is our hope that this study will inspire further investigation of additional material supplied by NIDA.

Our study indicates the need for additional research and refinement of our understanding of *Cannabis* genetic structure and how those differences might impact *Cannabis* consumers. As the demand for medical *Cannabis* increases, it is important that research examining the threats and benefits of *Cannabis* use accurately reflects the experiences of the general public.

Given the rapidly changing landscape of *Cannabis* regulation and consumption (ProCon, 2018a,b), it is not surprising that commercially available *Cannabis* contains a diversity of genetic types. Commercially available *Cannabis* has come to market through non-traditional means leading to many inconsistencies. We have previously documented (Schwabe and McGlaughlin, 2019) that there is substantial genetic divergence among samples within named strains, which only exacerbates questions about the impacts of *Cannabis* consumption. These results emphasize the need to increase consistency within the *Cannabis* marketplace, and the need for "research grade marijuana" to accurately represent what is accessible to consumers.

This study highlights the genetic difference between "research grade marijuana" provided by NIDA and commercial *Cannabis* available to medical and recreational users. Hence, research conducted with NIDA *Cannabis* may not be indicative of the effects that consumers are experiencing. Additionally, research has demonstrated that *Cannabis* distributed by NIDA has lower levels of the principal medicinal cannabinoids (THC and CBD) and higher levels of the THC degradation product cannabinol (CBN; Vergara et al., 2017). Taken together, these results demonstrate the need for there to be a greater diversity of *Cannabis* available for medical research and that the genetic provenance of those samples to be established to fully understand the implications of results.

DATA AVAILABILITY STATEMENT

The original contributions presented in the study are included in the article/**Supplementary Material**, further inquiries can be directed to the corresponding authors.

AUTHOR CONTRIBUTIONS

AS conceived the project, collected the samples, conducted DNA extractions, designed and optimized microsatellite primers, compiled and analyzed the data, and drafted manuscript content. CH conducted DNA extractions, compiled and analyzed the data, and prepared the first draft of the manuscript. RH provided DNA from the NIDA samples. MM directed the project, provided some funding, and contributed to statistical analysis and manuscript revisions. All authors contributed to the article and approved the submitted version.

FUNDING

The University of Northern Colorado Graduate Student Association and the Gerald Schmidt Memorial Biology Scholarship awarded grants providing partial funding for this project. Funding was also obtained from the University of Northern Colorado School of Biological Sciences. These funding sources did not play any roles in the development, design, execution, or analysis of this study, nor did they contribute to the writing of the manuscript and had no input in the decision to publish this research.

ACKNOWLEDGMENTS

The National Institute on Drug Abuse provided the Research Grade *Cannabis* samples from which DNA used in this study was extracted. We thank Matt Kahl and Caren Kershner for providing hemp samples for this project, Melissa Islam, Associate Director of Biodiversity Research at the Denver Botanic Gardens for access to wild collected hemp herbarium specimens (Kathryn Kalmbach Herbarium), and the Cannabis Genome Research Initiative for the sample of *Cannabis ruderalis*. Funding for this project was provided through research grants awarded to A. Schwabe by the University of Northern Colorado Graduate Student Association and the University of Northern Colorado College of Natural and Heath Sciences, and the McGlaughlin Lab, School of Biological Sciences, University of Northern Colorado. We appreciate and are grateful to Samantha Naibauer and Emily Schumacher for assisting with the figures. Many thanks to Nolan Kane who provided feedback and support for this research. Finally, thank you Daniela Vergara for providing feedback and support for this research, and on the manuscript preparation.

SUPPLEMENTARY MATERIAL

The Supplementary Material for this article can be found online at: https://www.frontiersin.org/articles/10.3389/fpls.2021.675770/full#supplementary-material

REFERENCES

Abel, E. L. (2013). *Marihuana: The First Twelve Thousand Years*. New York, NY: Springer Science & Business Media.

Backes, M., and Weil, A. (2014). Use of Medicinal *Cannabis*. In *Cannabis* Pharmacy: The Practical Guide to Medical Marijuana. Black Dog & Leventhal, 230. New York.

Baron, E. P. (2018). Medicinal properties of cannabinoids, terpenes, and flavonoids in *Cannabis*, and benefits in migraine, headache, and pain: an update on current evidence and *Cannabis* science. *Headache* 58, 1139–1186. doi: 10.1111/head.13345

Borgelt, L. M., Franson, K. L., Nussbaum, A. M., and Wang, G. S. (2013). The pharmacologic and clinical effects of medical cannabis. Pharmacotherapy: *The Journal of Human Pharmacology and Drug Therapy.* 33, 195–209. doi: 10.1002/phar.1187

Citti, C., Braghiroli, D., Vandelli, M. A., and Cannazza, G. (2018). Pharmaceutical and biomedical analysis of cannabinoids: a critical review. *J. Pharm. Biomed. Anal.* 147, 565–579. doi: 10.1016/j.jpba.2017.06.003

Clarke, R. C., and Merlin, M. D. (2013). *Cannabis: Evolution and Ethnobotany*. Berkeley: University of California Press.

Clarke, R. C., and Merlin, M. D. (2015). Letter to the editor: small, ernest. 2015. Evolution and classification of *Cannabis sativa* (marijuana, hemp) in relation to human utilization. *Bot. Rev.* 81, 295–305. doi: 10.1007/s12229-015-9158-2

Cousijn, J., Nunez, A. E., and Filbey, F. M. (2018). Time to acknowledge the mixed effects of cannabis on health: a summary and critical review of the NASEM 2017 report on the health effects of cannabis and cannabinoids. *Addiction* 113, 958–966. doi: 10.1111/add.14084

Datwyler, S. L., and Weiblen, G. D. (2006). Genetic variation in hemp and marijuana (*Cannabis sativa* L.) according to amplified fragment length polymorphisms. *J. Forensic Sci.* 51, 371–375. doi: 10.1111/j.1556-4029.2006.00061.x

de Meijer, E. P. M., Vanderkamp, H. J., and Vaneeuwijk, F. A. (1992). Characterization of *Cannabis* accessions with regard to cannabinoid content in relation to other plant characters. *Euphytica* 62, 187–200. doi: 10.1007/BF00041753

Doyle, J. J. (1987). A rapid DNA isolation procedure for small quantities of fresh leaf tissue. *Phytochemi. Bulletin* 4, 359–361.

Drug Enforcement Administration and Department of Justice (2016). Applications to become registered under the controlled substances act to manufacture marijuana to supply researchers in the United States. Policy statement. *Fed. Regist.* 81, 53846–53848.

Dufresnes, C., Jan, C., Bienert, F., Goudet, J., and Fumagalli, L. (2017). Broad-scale genetic diversity of *Cannabis* for forensic applications. *PLoS One* 12:e0170522. doi: 10.1371/journal.pone.0170522

Earl, D. A., and vonHoldt, B. M. (2012). STRUCTURE HARVESTER: a website and program for visualizing STRUCTURE output and implementing the Evanno method. *Conserv. Genet. Resour.* 4, 359–361. doi: 10.1007/s12686-011-9548-7

ElSohly, M.A. (2007). *Marijuana & the Cannabinoids*. Totowa, New Jersey: Humana Press.

Emboden, W. A. (1977). Taxonomy for *Cannabis*. *Taxon* 26:110. doi: 10.2307/1220203

Emboden, W. A. (1981). The genus *Cannabis* and the correct use of taxonomic categories. *J. Psychoactive Drugs* 13, 15–21. doi: 10.1080/02791072.1981.10471446

Evanno, G., Regnaut, S., and Goudet, J. (2005). Detecting the number of clusters of individuals using the software STRUCTURE: a simulation study. *Mol. Ecol.* 14, 2611–2620. doi: 10.1111/j.1365-294X.2005.02553.x

Ferber, S. G., Namdar, D., Hen-Shoval, D., Eger, G., Koltai, H., Shoval, G., et al. (2020). The "entourage effect:" terpenes coupled with cannabinoids for the treatment of mood disorders and anxiety disorders. *Curr. Neuropharmacol.* 18, 87–96. doi: 10.2174/1570159X17666190903103923

Forapani, S., Carboni, A., Paoletti, C., Cristiana, V. M., Ranalli, N. P., and Mandolino, G. (2001). Comparison of hemp varieties using random amplified polymorphic DNA markers. *Crop Sci.* 41, 1682–1689. doi: 10.2135/cropsci2001.1682

Gao, C. S., Xin, P. F., Cheng, C. H., Tang, Q., Chen, P., Wang, C. B., et al. (2014). Diversity analysis in *Cannabis sativa* based on large-scale development of expressed sequence tag-derived simple sequence repeat markers. *PLoS One* 9:e110638. doi: 10.1371/journal.pone.0110638

Hakki, E. E., Kayis, S. A., Pinarkara, E., and Sag, A. (2007). Inter simple sequence repeats separate efficiently hemp from marijuana (*Cannabis sativa* L.). *Electron. J. Biotechnol.* 10, 570–581. doi: 10.2225/vol10-issue4-fulltext-4

Hazekamp, A., and Fischedick, J. T. (2012). *Cannabis* - from cultivar to chemovar. *Drug Test. Anal.* 4, 660–667. doi: 10.1002/dta.407

Heilig, S. (2011). The pot book: a complete guide to *Cannabis*, its role in medicine, politics, science, and culture. *J. Psychoactive Drugs* 43, 76–77. doi: 10.1080/02791072.2011.566505

Hillig, K. W. (2005). Genetic evidence for speciation in *Cannabis* (Cannabaceae). *Genet. Resour. Crop. Evol.* 52, 161–180. doi: 10.1007/s10722-003-4452-y

Jaeger, K. (2018). Surgeon General Says Marijuana's Schedule 1 Status Hinders Research. Available at: https://www.marijuanamoment.net/surgeon-general-says-marijuanas-schedule-i-status-hinders-research/ (Accessed January 7, 2019).

Jikomes, N., and Zoorob, M. (2018). The cannabinoid content of legal cannabis in Washington state varies systematically across testing facilities and popular consumer products. *Sci. Rep.* 8:4519. doi: 10.1038/s41598-018-22755-2

Leafly (2018). Cannabis Strain Explorer. Available at: https://www.leafly.com/explore (Accessed September 12, 2018).

Lynch, R. C., Vergara, D., Tittes, S., White, K., Schwartz, C. J., Gibbs, M. J., et al. (2016). Genomic and chemical diversity in *Cannabis*. *Crit. Rev. Plant Sci.* 35, 349–363. doi: 10.1080/07352689.2016.1265363

Maa, E., and Figi, P. (2014). The case for medical marijuana in epilepsy. *Epilepsia* 55, 783–786. doi: 10.1111/epi.12610

McPartland, J. M. (2006). Commentary on: Datwyler SL, Weiblen GD. Weiblen. Genetic variation in hemp and marijuana (*Cannabis sativa* L.) according to amplified fragment length polymorphisms. *J. Forensic Sci.* 51:1405. doi: 10.1111/j.1556-4029.2006.00276.x

McPartland, J. M. (2017). "*Cannabis sativa* and *Cannabis indica* versus "Sativa" and "Indica"," in *Botany and Biotechnology*. eds. S. Chandra, H. Lata and M. ElSohly (Cham: Springer).

McPartland, J. M., and Guy, G. W. (2017). Models of *Cannabis* taxonomy, cultural bias, and conflicts between scientific and vernacular names. *Bot. Rev.* 83, 327–381. doi: 10.1007/s12229-017-9187-0

McPartland, J. M., and Small, E. (2020). A classification of endangered high-THC cannabis (*Cannabis sativa* subsp. *indica*) domesticates and their wild relatives. *Phytokeys* 144, 81–112. doi: 10.3897/phytokeys.144.46700

Nahler, G., Jones, T., and Russo, E. (2019). Cannabidiol and contributions of major hemp phytocompounds to the "entourage effect;" possible mechanisms. *J. Altern. Complement. Int. Med.* 5:070. doi: 10.24966/ACIM-7562/100066

National Institute on Drug Abuse (2016a). NIDA Research on Marijuana and Cannabinoids. Available at: https://www.drugabuse.gov/drug-topics/marijuana/nida-research-marijuana-cannabinoids (Accessed November 15, 2019).

National Institute on Drug Abuse (2016b). Marijuana Plant Material Available From the Nida Drug Supply Program. Available at: https://www.drugabuse.gov/research-training/research-data-measures-resources/nida-drug-supply-program-dsp/marijuana-plant-material-available-nida-drug-supply-program (Accessed June, 2020).

Peakall, R., and Smouse, P. E. (2006). GENALEX 6: genetic analysis in excel. Population genetic software for teaching and research. *Mol. Ecol. Notes* 6, 288–295. doi: 10.1111/j.1471-8286.2005.01155.x

Peakall, R., and Smouse, P. E. (2012). GENALEX 6.5: genetic analysis in excel. Population genetic software for teaching and research-an update. *Bioinformatics* 28, 2537–2539. doi: 10.1093/bioinformatics/bts460

Piluzza, G., Delogu, G., Cabras, A., Marceddu, S., and Bullitta, S. (2013). Differentiation between fiber and drug types of hemp (*Cannabis sativa* L.) from a collection of wild and domesticated accessions. *Genet. Resour. Crop. Evol.* 60, 2331–2342. doi: 10.1007/s10722-013-0001-5

Pisupati, R., Vergara, D., and Kane, N. C. (2018). Diversity and evolution of the repetitive genomic content in *Cannabis sativa*. *BMC Genomics* 19:156. doi: 10.1186/s12864-018-4494-3

PotGuide.com (2018). Marijuana Strain Profiles. Available at: https://potguide.com/strain-profiles/ (Accessed March, 2018).

Potter, D. J., Clark, P., and Brown, M. B. (2008). Potency of delta(9)-THC and other cannabinoids in *Cannabis* in England in 2005: implications for psychoactivity and pharmacology. *J. Forensic Sci.* 53, 90–94. doi: 10.1111/j.1556-4029.2007.00603.x

Pritchard, J. K., Stephens, M., and Donnelly, P. (2000). Inference of population structure using multilocus genotype data. *Genetics* 155, 945–959. doi: 10.1093/genetics/155.2.945

ProCon (2018a). Legal medical marijuana states and DC. Available at: https://medicalmarijuana.procon.org/view.resource.php?resourceID=000881 (Accessed February 2021).

ProCon (2018b). Number of legal medical marijuana patients (as of May 17 2018). Available at: https://medicalmarijuana.procon.org/view.resource.php?resourceID=005889 (Accessed February 2021).

Punja, Z. K., Rodriguez, G., and Chen, S. (2017). "Assessing genetic diversity in Cannabis sativa using molecular approaches," in *Cannabis sativa L. - Botany and Biotechnology*. eds. S. Chandra, H. Lata and M. A. ElSohly (Cham, Switzerland: Springer International Publishing AG), 395–418.

R Studio Team (2015). R Studio: integrated development for R,. RStudio, Inc., Boston, MA.

Russo, E. B. (2019). The case for the entourage effect and conventional breeding of clinical *Cannabis*: no 'strain,' no gain. *Front. Plant Sci.* 9:1969. doi: 10.3389/fpls.2018.01969

Sawler, J., Stout, J. M., Gardner, K. M., Hudson, D., Vidmar, J., Butler, L., et al. (2015). The genetic structure of marijuana and hemp. *PLoS One* 10:e0133292. doi: 10.1371/journal.pone.0133292

Schwabe, A. L., and McGlaughlin, M. E. (2019). Genetic tools weed out misconceptions of strain reliability in *Cannabis sativa*: implications for a budding industry. *J. Cannabis Res.* 1:332320. doi: 10.1186/s42238-019-0001-1

Seedfinder (2020). Seed-Finder. Available at: https://en.seedfinder.eu/ (Accessed January, 2020)

Small, E. (2015). Evolution and classification of *Cannabis sativa* (marijuana, hemp) in relation to human utilization. *Bot. Rev.* 81, 189–294. doi: 10.1007/s12229-015-9157-3

Small, E. (2016). *Cannabis: A Complete Guide*. Boca Raton, FL: CRC Press.

Small, E. (2017). "Classification of *Cannabis sativa* L. in relation to agricultural, biotechnological, medical and recreational utilization," in *Cannabis sativa L. - Botany and Biotechnology*. eds. S. Chandra, H. Lata and M. A. ElSohly (Cham, Switzerland: Springer International Publishing AG), 1–62.

Small, E., Jui, P. Y., and Lefkovitch, L. P. (1976). A numerical taxonomic analysis of *Cannabis* with special reference to species delimitation. *Syst. Bot.* 1, 67–84. doi: 10.2307/2418840

Smith, M. H. (2012). *Heart of Dankness: Underground Botanists, Outlaw Farmers, and the Race for the Cannabis Cup*. New York, NY: Broadway Books.

Soler, S., Gramazio, P., Figas, M. R., Vilanova, S., Rosa, E., Llosa, E. R., et al. (2017). Genetic structure of *Cannabis sativa* var. *indica* cultivars based on genomic SSR (gSSR) markers: implications for breeding and germplasm management. *Ind. Crop. Prod.* 104, 171–178. doi: 10.1016/j.indcrop.2017.04.043

United States Congress (1970). *Comprehensive Drug Abuse Prevention and Control Act of 1970*. United States: Public Law.

Vergara, D., Baker, H., Clancy, K., Keepers, K. G., Mendieta, J. P., Pauli, C. S., et al. (2016). Genetic and genomic tools for *Cannabis sativa*. *Crit. Rev. Plant Sci.* 35, 364–377. doi: 10.1080/07352689.2016.1267496

Vergara, D., Bidwell, L. C., Gaudino, R., Torres, A., Du, G., Ruthenburg, T. C., et al. (2017). Compromised external validity: federally produced cannabis does not reflect legal markets. *Sci. Rep.* 7:1. doi: 10.1038/srep46528

Vergara, D., Huscher, E. L., Keepers, K. G., Pisupati, R., Schwabe, A. L., McGlaughlin, M. E., et al. (2021). Genomic evidence that governmentally produced Cannabis sativa poorly represents genetic variation available in state markets. *Front. Plant Sci.* [Preprint]. doi: 10.3389/fpls.2021.668315

Verity, R., and Nichols, R. A. (2016). Estimating the number of subpopulations (K) in structured populations. *Genetics* 203, 1827–1839. doi: 10.1534/genetics.115.180992

Wikileaf (2018). *Cannabis* Strains: Strain Library. Available at: https://www.wikileaf.com/strains/ (Accessed March, 2018).

World Health Organization (2018). Management of Substance Abuse, *Cannabis*. Available at: http://www.who.int/substance_abuse/facts/cannabis/en/ (Accessed November 15, 2018).

Conflict of Interest: The authors declare that the research was conducted in the absence of any commercial or financial relationships that could be construed as a potential conflict of interest.

Publisher's Note: All claims expressed in this article are solely those of the authors and do not necessarily represent those of their affiliated organizations, or those of the publisher, the editors and the reviewers. Any product that may be evaluated in this article, or claim that may be made by its manufacturer, is not guaranteed or endorsed by the publisher.

frontiers in Plant Science

ORIGINAL RESEARCH
published: 01 November 2021
doi: 10.3389/fpls.2021.718092

Production of Feminized Seeds of High CBD *Cannabis sativa* L. by Manipulation of Sex Expression and Its Application to Breeding

*Marko Flajšman, Miha Slapnik and Jana Murovec**

Department of Agronomy, Biotechnical Faculty, University of Ljubljana, Ljubljana, Slovenia

The use of the cannabis plant as a source of therapeutic compounds is gaining great importance since restrictions on its growth and use are gradually reduced throughout the world. Intensification of medical (drug type) cannabis production stimulated breeding activities aimed at developing new, improved cultivars with precisely defined, and stable cannabinoid profiles. The effects of several exogenous substances, known to be involved in sex expressions, such as silver thiosulfate (STS), gibberellic acid (GA), and colloidal silver, were analyzed in this study. Various concentrations were tested within 23 different treatments on two high cannabidiol (CBD) breeding populations. Our results showed that spraying whole plants with STS once is more efficient than the application of STS on shoot tips while spraying plants with 0.01% GA and intensive cutting is ineffective in stimulating the production of male flowers. Additionally, spraying whole plants with colloidal silver was also shown to be effective in the induction of male flowers on female plants, since it produced up to 379 male flowers per plant. The viability and fertility of the induced male flowers were confirmed by fluorescein diacetate (FDA) staining of pollen grains, *in vitro* and *in vivo* germination tests of pollen, counting the number of seeds developed after hybridization, and evaluating germination rates of developed seeds. Finally, one established protocol was implemented for crossing selected female plants. The cannabinoid profile of the progeny was compared with the profile of the parental population and an improvement in the biochemical profile of the breeding population was confirmed. The progeny had a higher and more uniform total CBD (tCBD) to total tetrahydrocannabinol (tTHC) ratio (up to 29.6; average 21.33 ± 0.39) compared with the original population (up to 18.8; average 7.83 ± 1.03). This is the first comprehensive report on the induction of fertile male flowers on female plants from dioecious medical cannabis (*Cannabis sativa* L.).

Keywords: ***Cannabis sativa*** **L., sex manipulation, silver thiosulfate, cannabidiol, high CBD medical cannabis, feminized seed, cannabinoids**

OPEN ACCESS

Edited by:
Donald Lawrence Smith, McGill University, Canada

Reviewed by:
Zamir Punja, Simon Fraser University, Canada
Ayelign M. Adal, University of British Columbia Okanagan, Canada
Jordi Petit Pedró, Polytechnic University of Valencia, Spain

****Correspondence:***
Jana Murovec
jana.murovec@bf.uni-lj.si

Specialty section:
This article was submitted to Crop and Product Physiology, a section of the journal Frontiers in Plant Science

Received: *31 May 2021*
Accepted: *30 September 2021*
Published: *01 November 2021*

Citation:
Flajšman M, Slapnik M and Murovec J (2021) Production of Feminized Seeds of High CBD Cannabis sativa L. by Manipulation of Sex Expression and Its Application to Breeding. Front. Plant Sci. 12:718092. doi: 10.3389/fpls.2021.718092

INTRODUCTION

Cannabis (*Cannabis sativa* L.) naturally shows sexual dimorphism with a small proportion of monoecism. In the past, it was mostly cultivated for fiber and grain, but nowadays, the plant is gaining importance in the medicinal industry due to its production of unique cannabinoids (Andre et al., 2016). They are produced in the trichomes on flower bracts of female inflorescences

(Small, 2015; Andre et al., 2016). Most pharmaceutically important cannabinoids are cannabidiol (CBD) and the psychoactive tetrahydrocannabinol (THC) (Δ-9-THC) (Freeman et al., 2019). The relative content (in % of dry weight) of the latter divides cannabis genotypes into two groups: (i) industrial cannabis, commonly known as hemp or fiber-type hemp (defined as containing < 0.2% THC by dry weight in Europe) and commonly grown as a field crop and (ii) medical cannabis, marijuana or drug type cannabis (with > 0.2% THC) (The European Commission, 2014), cultivated under strict legal restrictions.

Sex of *C. sativa* L. (2n = 20) is genetically determined by one pair of sex chromosomes X and Y, where male gender of dioecious plants is determined by heterogametic XY chromosomes, while dioecious female and monoecious or hermaphrodite plants exhibit homogametic chromosomes XX (Moliterni et al., 2004; van Bakel et al., 2011; Divashuk et al., 2014; Faux et al., 2014). The ratio of female to male flowers in a single monoecious cannabis plant is highly variable and ranges from predominantly male flowers to predominantly female flowers (Faux et al., 2014). Moreover, dioecious cannabis plants can produce flowers of the opposite sex as determined by their sex chromosomes (Moliterni et al., 2004). Due to instability of the sexual phenotypes across generations of XX plants, and the quantitative nature of sex expression, it was hypothesized that sex expression is a polygenic trait (Faux et al., 2013, 2014; Faux and Bertin, 2014). A first association mapping study of sex determination was performed in 2016 (Faux et al., 2016) on three biparental hemp populations (two dioecious and one monoecious) using 71 amplified fragment length polymorphism (AFLP) markers. It identified five quantitative trait loci (QTLs) associated with sex expressions that were putatively located on sex chromosomes. Recently, Petit and colleagues (Petit et al., 2020) published the results of a GWAS (Genome-Wide Association Study) analysis for characterization of the genetic architecture underpinning sex determination in hemp. They used a set of 600 K single-nucleotide polymorphism (SNP) markers on a panel of 123 hemp accessions (monoecious and dioecious), tested in three contrasting environments across Europe with contrasting photoperiod regimes. They identified two QTLs for sex determination across locations that contained transcription factors and genes involved in regulating the balance of phytohormones, especially auxins and gibberellic acid (GA). Two auxin response factor genes (*arf2* and *arf5*), *bZIP* transcription factor 16-like, and gene *gibberellic acid insensitive* (GAI) that codes for the DELLA RGL1-like (repressor of giberellic acid-like) protein were identified in QTL*Sex_det1* for sex determination. These genes are involved in the balance of the phytohormones auxins and gibberellic acid (GA), which are known to play an active role in the sex expression (male or female) in many crops, such as hemp or spinach. The lack of a complete genome sequence did not allow to map of the QTL*Sex_det1* in any specific chromosome (Petit et al., 2020).

The findings confirmed previous reports that several factors, like sex-determining genes, sex chromosomes, epigenetic control by DNA methylation, and microRNAs, and physiological regulation with phytohormones influence sex expression of predetermined cannabis plants (Galoch, 1978; Dellaporta and Calderon-Urrea, 1993; Hall et al., 2012; Punja and Holmes, 2020). Several studies with hormonal manipulation confirmed gender reversal in *C. sativa* L. and proved bipotency of sexually predetermined dioecious cannabis plants. It has been shown that gibberellins induce maleness in plants, while ethylene, cytokinins, and auxins stimulate the formation of female flowers on genetically male plants (Ainsworth, 2000). Galoch (1978) showed that indole-3-acetic acid (IAA), kinetin (up to 100 μg/plant), and ethylene-releasing compound ethrel (up to 500 μg/plant) enhanced the feminization of male plants. Abscisic acid (ABA) was completely ineffective in sexing both male and female hemp when used alone. GA3 (up to 100 μg/plant) promoted masculinization of female plants while having no effect on sex change in male plants. Similarly, Ram and Jaiswal (1972) earlier found that male plants showed no change in sex expression when treated with gibberellins (up to 100 μg/plant), but female plants developed male flowers with normal stamens and viable pollen grains. Besides, environmental factors such as temperature, photoperiod, light conditions, nutrient deficiency, and mechanical stresses (e.g., damages) can influence sex expression and induce monoecism (Ram and Sett, 1979). As reviewed in Truta et al. (2007) and Petit et al. (2020), the ratio of different phytohormones plays a crucial role in the sex expression of hemp. External treatment of GA to spinach, for example, affects the expression of the *GAI* gene, which is a transcription factor of the DELLA family. It is highly expressed in female inflorescences and acts as a repressor of the expression of B-*class* homeotic genes, which are masculinizing factors. B-*class* genes stimulate male organ formation and simultaneously suppress the development of female organs in the flowers (Petit et al., 2020).

Cannabis sex determination could be modified by applying exogenous growth regulators or chemicals, which can influence the ratio of endogenous hormones and hence the incidence of sex organs (Truta et al., 2007). Silver compounds such as silver nitrate ($AgNO_3$) or silver thiosulfate ($Ag_2S_2O_3$; STS) have been found to have masculine effects in many plant species, e.g., in *Coccinia grandis* (Devani et al., 2017), *Cucumis sativus* (Den Nijs and Visser, 1980), *Silene latifolia* (Law et al., 2002), *Cucumis melo* (Owens et al., 1980), and also *Cannabis sativa*. Ram and Sett (1982) applied 50, 100, and 150 μg of silver nitrate and 25, 50, and 100 μg of STS to shoot tips of female cannabis plants. Both silver compounds successfully evoked the formation of male flowers, but STS was more effective than $AgNO_3$. 100 μg of STS caused the highest number of fully altered male flowers, which was significantly higher than the number of reduced male, intersexual, and female flowers. On the other hand, the treatment of shoot tip with 100 μg $AgNO_3$ resulted in more than half the lower number of male flowers, with the highest amount of $AgNO_3$ (150 μg) being ineffective in altering sex expression. Furthermore, pollen from all induced male flowers was viable *in vitro* and also successfully induced seed set. Lubell and Brand (2018) published the results of using 3 and 0.3 mM STS to induce male flowers in genetically female hemp plants of four strains. They sprayed three times at 7-day intervals and counted flowers (male and female) on terminal buds, not whole plants. They determined the percentage of male flowers to all flowers and the masculinization rate. The authors confirmed the

successful induction of male flowers in hemp strains. Regarding the percentage of inflorescences with male flowers, their best two hemp strains yielded up to ≈15% no male inflorescences, regardless of the STS concentration used. In the books by Green (2005) and Rosenthal (2010), the authors suggest a method for making 0.3 mM STS and spraying the entire female plant until the solution drips from the plant. There is no quantitative evidence of the success of the method used. More recently, two other studies have also successfully used STS to induce male flowers: DiMatteo et al. (2020) sprayed 3 mM of STS until runoff three times at 7-day intervals after exposing the plants to short-day conditions for 12 h. Adal et al. (2021) applied 20 ml of STS (2.5 μg/ml) to whole plants on the first and third day after the start of 12-h lighting and fertilization on a foliar basis. However, these studies aimed to investigate some other aspects of male sex induction in cannabis rather than the establishment of the sex induction protocol, so no detailed data on the success of the sex reversal were presented. As far as we know, no scientific study has used colloidal silver for sex reversal in cannabis and not in other plants species. However, this method is very well known in the cannabis industry and a lot of information is available on the internet. Several other chemicals have shown alteration of cannabis sex expression, e.g., female plants treated with 75 μg of aminoethoxyvinylglycine formed only male and no intersexual flowers (Ram and Sett, 1981). Foliar spraying of male cannabis plants with 960 ppm 2-chloroethanephosphonic acid caused the highest formation of the fertile female flower (Ram and Jaiswal, 1970). A total of 100 μg/plant of cobalt chloride applied to the shoot tip triggers male sex expression in the female plants of cannabis (Ram and Sett, 1979). The mode of action of these chemicals in plants is not yet entirely deciphered. Truta et al. (2007) hypothesized that these external factors probably indirectly affect the level of endogenous auxins, which have a regulatory role on factors controlling sexual organs differentiation. The authors concluded that sex determination genes balance endogenous hormonal levels *via* signal transduction mechanism and thus enable sex reversion in sexually bipotent floral primordia. A comprehensive study of gene expression during flower development in cannabis was recently published by Adal et al. (2021), who discovered approximately 200 genes that were potentially involved in the production of male flowers in female plants. Although the exact role of all these genes was not examined further, the study opened many possibilities for further studies of the genetic background of sex expression in cannabis.

Manipulation of sex expression is of paramount importance in breeding medical cannabis, since only genetically and phenotypically female plants are used in commercial cultivation. It enables self-pollination and crossing of female plants for obtaining pure lines and feminized seeds, respectively (Ram and Sett, 1982). Upon germination, the latter produce entirely female progeny that is used for the production of female flowers. Most cannabis sex manipulation studies are performed on fiber-type hemp (Ram and Sett, 1982; Lubell and Brand, 2018; DiMatteo et al., 2020), and knowledge about the efficiency of various exogenous factors and application methods for inducing sex conversion in medical cannabis is needed.

The aim of our investigation was to test different sex manipulation methods (chemical, hormonal, and physiological) for induction of male flowers on female plants of medical cannabis and to evaluate their efficiency based on the number of male inflorescences and male flowers, by evaluation of pollen viability, germination potential *in vitro* and *in vivo,* and seed set. In addition, the selected treatment was implemented in a breeding program for crossing a population of female plants of a high CBD breeding population of medical cannabis to verify the usefulness of such treatments in the high-valued medical cannabis industry.

MATERIALS AND METHODS

Plant Material and Growing Conditions

The experiment was carried out using plants of two breeding populations of medical cannabis, namely MX-CBD-11 and MX-CBD-707, owned by MGC Pharmaceuticals Ltd. and described in Mestinšek Mubi et al. (2020). They were grown as part of a joint research project between the Biotechnical Faculty of the University of Ljubljana and MGC Pharmaceuticals under license from the Slovenian Ministry of Health.

The mother plants (48 different genotypes of MX-CBD-707 and 31 different genotypes of MX-CBD-11) were grown from feminized seeds. Rooted cuttings were made from lateral shoots of mother plants. All plants were grown in 3.5 L pots (substrate Kekkila, Finland) in a step-in growth chamber under 24–26°C and 16/8 light/dark regime. The light was ensured by using 600-W high-pressure sodium (HPS) lamps (Phantom HPS 600W; Hydrofarm, Petaluma, CA, United States). At the vegetative stage, plants were fertilized with a mixture of vegetative fertilizer (NPK 4-1-2) and CalMag (N-Ca-Mg 2-5-2.5) + microelements in 1:1 proportion. After 31 (Experiment 1) or 60 (Experiment 2) days of vegetative growth, the plants were fertilized with a mixture of flowering fertilizer (NPK 1-3-5) and CalMag (N-Ca-Mg 2-5-2.5) + microelements in 1:1 proportion and subjected to a 12/12 photoperiod.

Design and Performance of the Experiments

In the first experiment, eight different treatments were applied using two different growth regulators in different concentrations and modes of application, along with one physiological treatment (cut) and control (no application) (**Table 1**). The concentrations (amounts) of STS and GA were chosen based on literature data (Ram and Sett, 1982; Green, 2005; Rosenthal, 2010) and the variant "cut" was based on the recommendations from the growers. The experiment was designed as a randomized complete block design with two factors: seven male induction treatments and control on two breeding populations, with six replicates (potted plants) for each combination of factors.

A total of 20 mM STS was prepared by mixing 0.1 M $AgNO_3$ and 0.1 M $Na_2S_2O_3$ in a molar ratio of 1:4. 0.7 mM STS was prepared by 30x dilution of 20 mM STS with water. GA3 (Duchefa) was dissolved in double-distilled water and applied in 0.01% concentration. Spraying with STS or GA3 (treatments 1, 2,

TABLE 1 | Treatments of the first experiment of male flowers induction on female plants of *Cannabis sativa*.

Variant	Treatments on whole plants (concentration of STS)	Treatments on shoot tips (amount of STS)
1	20 mM	
2	0.7 mM	
3		50 μg
4		100 μg
5		150 μg
6	Spraying whole plants with 0.01% gibberellic acid (GA3)	
7	Cutting plants to a height of two nodes	
8	Control (no application)	

and 6) was performed once at the beginning of the experiment until runoff. For treatments 3, 4, and 5, 10 μl of STS stock solutions (1, 2, and 3 μg/μl, respectively) were applied for five consecutive days on the apical shoot tip until final amounts of STS were reached (50, 100, and 150 μg of STS, respectively) (**Figure 1A**). For treatment 7, plants were cut down to the height of the first two nodes. Plants from the eighth treatment represented a control group and no treatment was performed. When the treatments were applied and the experiment began, the plants (age of 31 days) were put on under a 12/12 light/dark regime to induce flowering.

In the second experiment (**Table 2**), 45 plants of breeding population MX-CBD-707 were treated for male sex induction. After 60 days on vegetative growth, they were first exposed to three different lighting regimes (henceforth referred to as "pretreatments;" 15 plants per pretreatment), which was followed by four different treatments: spraying whole plants with STS (Green, 2005), spraying whole plants with colloidal silver once, or every day until anthesis (recommendation of grower), and control (non-treated plants).

After the application of silver solutions, the plants from almost all combinations of pretreatment and treatment were exposed to a 12/12 light/dark regime to induce flowering. After application of 0.3 mM STS on whole plants, a stress-inducing photoperiod with 96 h of light and 72 h of the dark was tested and compared with the results of the same STS treatment followed by a normal 12-h photoperiod.

Measurements of Response Variables

In the first experiment, five different response variables were analyzed, namely:

(1) Plant height.
(2) A number of nodes per plant, both expressed as a ratio between the final state (measurement/count at the end of the experiment) and the initial state (counted at the start of the experiment prior to (pre)treatments). In this way, not only the final morphology of the plants was taken into account, but also the initial state of the plants.
(3) Number of all inflorescences per plant.
(4) The number of inflorescences with one male flower or more per plant.
(5) The number of male flowers per plant. Variables were counted 31 days after the beginning of the experiment.

In the second experiment, the number of male flowers on breeding population MX-CBD-707 was counted 37 days after the beginning of the experiment.

Viability and Germination of Pollen

Several tests were performed to verify the viability of pollen developed in induced male flowers. Pollen was stained with FDA at a final concentration of 1 μg/ml and analyzed under an epi-fluorescent microscope (Nikon Eclipse 80i) with filter sets for the detection of green fluorescence. The germination of pollen was first tested *in vitro* on solidified germination medium composed of 170 g/l sucrose, 0.1 g/l H_3BO_3, 0.432 g/l $Ca(NO_3)_2{}^*4H_2O$, and pH 7.0. The Petri dishes were incubated in the dark at room temperature for 24 h and the results were detected under the microscope. Furthermore, *in vivo* germination of pollen was tested by pollinating female flowers of control, not treated, and plants. The stigmas of pollinated female flowers were collected after 24 h, stained with 1% aniline blue in 0.1 N Na_3PO_4, as described by Murovec and Bohanec (2013), and analyzed under the epi-fluorescent microscope with filter sets for the detection of blue fluorescence. Finally, pollen from some of the treatments was used for pollination of female control plants, and the number of developing seeds was counted 2 weeks after pollination.

Statistical Analysis

Both sex induction experiments were performed once and analyzed as a two-factorial experiment, where, the main effect of factors and their interaction was statistically quantified using ANOVA. Before analysis, each response variable was tested for assumptions about normal distribution and homogeneity of the treatment variances by Levene's test. In the case of non-homogeneity of variances, data were transformed to sqrt(y). Significant differences in mean values indicated by ANOVA were evaluated using Tukey's test ($\alpha = 0.05$). All statistical analyses were performed using the agricolae package in the statistical software program R version 3.2.5 (R Core Team, 2019). Data are presented as untransformed means ± SE. Graphs were drawn in the Microsoft Excel program.

Implementation of Sex Manipulation for Breeding Medical Cannabis

In order to verify the usefulness of our approach for breeding medical cannabis, we first analyzed the cannabinoid content in inflorescences of 48 mother plants of breeding population MX-CBD-707. The high performance liquid chromatography (HPLC) analysis was performed as described by Gul et al. (2015), with modifications described in Laznik et al. (2020).

Based on the results, 23 mother plants with high total CBD (tCBD) and low total THC (tTHC) content with a ratio of tCBD:tTHC > 13 were selected for further breeding. From each selected mother plant, two clones were produced and cultured under vegetative conditions in separate chambers. One clone per

FIGURE 1 | The induction of male flowers on female plants of medical cannabis. **(A)** Application of silver thiosulfate (STS) on shoot tip. **(B)** Yellow spots on the leaves 1 week after spraying with 20 mM STS. **(C)** Male inflorescence at full flowering. **(D)** *In vivo* germination of pollen. **(E)** *In vitro* germination of pollen. **(F)** The occurrence of male flowers on female plants of breeding population MX-CBD-707 after spraying with 30 ppm colloidal silver every day. **(G)** Viable pollen stained with fluorescein diacetate (FDA). **(H)** Developing seeds after pollination of a control plant.

mother plant was exposed to flowering conditions of light and fertilization and was sprayed with 30 ppm colloidal silver every day until the appearance of the male flower. The other clone was exposed to a flowering regime without any treatment in order to stimulate female flowering. The masculinized and non-treated plants were joined in the same flowering room upon the occurrence of male flowers on treated plants and left to cross-pollinate due to forced ventilation in the flowering chamber.

Mature seeds were collected, soaked in water for 12 h in the dark at room temperature, and then sown in polystyrene plates with 84 holes in the substrate Kekkila (Finland). The polystyrene plates were incubated at 25°C with a photoperiod of 16/8 days/nights and 60% humidity. The emerged seedlings were clonally propagated and the clones of 74 genetically different seedlings were analyzed for their cannabinoid content in inflorescences as described above. Plants from this breeding

TABLE 2 | Combinations of pretreatments, treatments, and growing photoperiods used in the second experiment of male flowers induction.

Variant	Pretreatment	Treatment	Photoperiod after treatment (light/dark)
9	1 week under constant light (168 h of light)	0.3 mM STS	12/12
10	1 week under constant light (168 h of light)	0.3 mM STS	96/72
11	1 week under constant light (168 h of light)	30 ppm colloidal silver once	12/12
12	1 week under constant light (168 h of light)	30 ppm colloidal silver every day until anthesis	12/12
13	1 week under constant light (168 h of light)	Control – not treated plants	12/12
14	1 week under constant dark (168 h of dark)	0.3 mM STS	12/12
15	1 week under constant dark (168 h of dark)	0.3 mM STS	96/72
16	1 week under constant dark (168 h of dark)	30 ppm colloidal silver once	12/12
17	1 week under constant dark (168 h of dark)	30 ppm colloidal silver every day until anthesis	12/12
18	1 week under constant dark (168 h of dark)	Control – not treated plants	12/12
19	1 week under 18/6 light/dark photoperiod	0.3 mM STS	12/12
20	1 week under 18/6 light/dark photoperiod	0.3 mM STS	96/72
21	1 week under 18/6 light/dark photoperiod	30 ppm colloidal silver once	12/12
22	1 week under 18/6 light/dark photoperiod	30 ppm colloidal silver every day until anthesis	12/12
23	1 week under 18/6 light/dark photoperiod	Control – not treated plants	12/12

Each variant was applied to three plants.

experiment were grown in the vegetative and flowering stages like the other plants in this study (described in section "Plant Material and Growing Conditions").

RESULTS

Experiment 1

Silver Thiosulfate Negatively Effects the Growth of Plants and Morphology

On the plants from treatment 1 (sprayed with 20 mM STS), yellow spots on the leaves were observed 1 week after application, and then the spots started to dry (**Figure 1B**). The plants began to lose leaves after 3 weeks of flowering. The plants from treatment 2 (sprayed with 0.7 mM STS) had fewer yellowish spots and dry leaves. Their growth and development were not as inhibited as those of plants from treatment 1.

Treatments 3, 4, and 5 (application of 50, 100, and 150 μg STS on shoot tip, respectively) also caused some physiological responses. Three weeks after application, the young leaves, which were not fully developed at the time of treatment, began to show injuries and deformations. The leaves began to dry throughout the plant, not only at the shoot tip, where STS was applied. The intensity of these injuries coincided with the amount of STS applied at the shoot tip. The higher the amount of STS applied to the shoot tip, the more severe effect it had to plant morphology and fitness. Plants from treatment 6 (sprayed with 0.01% GA) began to grow in length and intensive elongation of internodes was observed.

Male inflorescences began to appear 3 weeks after treating female plants. They were first observed in treatment 1 (20 mM STS, sprayed), followed by the appearance of male flowers on plants from treatments 2 (0.7 mM STS, sprayed), 5, 4, and 3 (application of 150, 100, and 50 μg STS on shoot tip, respectively) at intervals of 3 days as the treatments are listed. Male flowers began to open 4 weeks after treating the plants and pollen began to spread (**Figure 1C**). On the plants from treatments 6 (GA3), 7 (cut), and the control, only a few male flowers were observed. Plants from all treatments developed female flowers as well. No hermaphrodite flowers (i.e., pistillate flowers containing also anthers) were observed.

Different Treatments Induced the Formation of Male Flowers on Female Plants

The breeding population and the treatment had a statistically significant influence on the ratio of plants height, the ratio of the number of nodes, number of all inflorescences, and number of male inflorescences with only one exception (**Table 3**). No interaction between breeding population and treatment was found for mentioned variables.

The statistically significant breeding populations ($p < 0.001$) differed for all four measured response variables, where MX-CBD-707 exposed more intensive morphological growth (higher ratio for height and number of nodes) and formed more inflorescences compared with MX-CBD-11. But the breeding population MX-CBD-11 exhibited a higher number of male inflorescences.

Treatment had no influence on the height ratio, despite the fact that cut plants exhibited the least growth. On the contrary, the ratio of a number of nodes significantly differed among treatments ($p < 0.001$), where cut plants showed the smallest increase in a number of nodes. The same observation goes with the number of all inflorescences, where plants from this treatment developed the least inflorescences. The differences among treatments are more pronounced for the number of inflorescences with male flowers, where spraying with 20 mM STS stimulated the development of the highest number of male inflorescences, followed by spraying with 0.7 mM STS and application of 50 μg STS on shoot tip. Lower numbers of

TABLE 3 | Influence of breeding population and treatment on the ratio of plants height, the ratio of the number of nodes, number of all inflorescences, and number of male inflorescences.

	Height (ratio)	Number of nodes (ratio)	Number of all inflorescences	Number of inflorescences with male flowers
Breeding population (*n* = 48)				
MX-CBD-707	3.02 ± 0.15a	4.45 ± 0.26a	94.6 ± 2.7a	20.1 ± 2.7b
MX-CBD-11	1.85 ± 0.05b	3.26 ± 0.14b	79.3 ± 3.0b	28.4 ± 3.7a
p	***	***	***	***
Treatment (*n* = 12)				
1–20 mM STS	2.46 ± 0.26a	4.05 ± 0.41a	97.3 ± 3.7a	53.8 ± 3.4a
2–0.7 mM STS	2.39 ± 0.23a	4.01 ± 0.24a	92.0 ± 4.6a	50.9 ± 4.6a
3–50 μg STS	2.38 ± 0.21a	4.19 ± 0.39a	91.34.8 ± a	38.7 ± 4.6ab
4–100 μg STS	2.46 ± 0.28a	4.17 ± 0.41a	94.3 ± 4.7a	24.8 ± 2.7bc
5–150 μg STS	2.38 ± 0.28a	4.36 ± 0.65a	94.7 ± 4.6a	21.0 ± 3.7c
6–GA3	2.78 ± 0.39a	4.09 ± 0.37a	88.3 ± 5.2*a*	2.2 ± 0.7d
7–Cut	1.82 ± 0.28a	1.84 ± 0.15b	46.8 ± 3.0b	1.7 ± 0.7d
8–Control	2.82 ± 0.27a	4.09 ± 0.38a	91.4 ± 3.7a	1.0 ± 0.4d
p	ns	***	***	***

*Mean values are followed by SE. The ratio of height and number of nodes means a ratio between the final state (measurement/count at the end of the experiment) and the initial state (counted at the start of the experiment prior to (pre)treatments); STS, silver thiosulfate; GA3, gibberellic acid (0.01%); treatments 1, 2, and 6, spraying once with the chemical until runoff of the leaves; treatments 3, 4, and 5, application on shoot tip. Mean values followed by different letters are significantly different at the 5% level of probability (Tukey); ***p < 0.001; ns, not significant.*

inflorescences with male flowers with no statistical difference were observed in treatments 6 (GA3), 7 (cut), and the control.

The Number of Male Flowers Was Influenced by the Interaction Effect Between Both Factors

Statistically significant interaction (p = 0.0393) was found between main factors for the number of male flowers per plant (**Figure 2**). The highest number of male flowers (for both breeding populations) was observed after treatments 1 and 2 (sprayed with 20 and 0.7 mM STS), followed by treatments 3, 4, and 5 (application 50, 100, and 150 μg STS on shoot tip, respectively). The last three treatments (6 – GA3, 7 – cut, and control) produced a significantly lower number of male flowers. In all the eight tested treatments, the breeding population MX-CBD-11 developed a higher number of male flowers compared with MX-CBD-707 (**Figure 2**).

Experiment 2

Colloidal Silver Induced Formation of Fertile Male Flowers on Female Plants

In the second experiment, the effect of different pretreatments (168 h light, 168 h dark, and alternation of 18/6 light/dark) before application of 0.3 mM STS or 30 ppm colloidal silver was studied. After spraying the whole plants, they were exposed to a constant 12/12 light/dark photoperiod or to a stress-inducing photoperiod (one treatment). Pretreatment, as well as treatment, had a statistically significant influence on the number of male flowers, but their interaction was not observed (**Table 4**). The highest average number of male flowers per plant (339) was achieved after pretreating plants at the usual light regime for vegetative growth (18 h of light and 6 h of darkness), while incubation in darkness for 168 h caused the lowest appearance of male flowers. Among the tested treatments, 0.3 mM STS caused the highest formation of male flowers, followed by the same treatment and exposing plants to stress-inducing light regimes. In contrast to spraying of 0.3 mM STS, which induces male flowering after only one application, the colloidal silver had to be sprayed every day until the formation of male flowers and yielded on an average 293 male flowers per plant. Spraying plants with colloidal silver only once produced a negligible number of male flowers, the results being practically equal to the results of control plants, which were not sprayed with any silver solutions (**Tables 4**, **5**). The appearance of induced male flowers and the viability of pollen are shown in **Figures 1F,G**.

Pollen Successfully Germinated *in vitro* and *in vivo*

The *in vitro* germination test showed that the induced male flowers produced viable pollen that is able to germinate *in vitro* on solidified germination medium (**Figure 1E** and **Table 5**).

The germination ability of pollen was confirmed also with *in vivo* pollination of female flowers. After 24 h, the germinating pollen tubes were clearly visible on stigmas stained with aniline blue (**Figure 1D**).

In order to verify the ability of pollen to fertilize female flowers and produce feminized seeds, the pollen was collected from treated plants of breeding population MX-CBD-707 and used for pollination of different shoots of one control (non-treated) plant. Two weeks after pollination, the number of developing feminized seeds was counted, which is presented in **Table 6** and **Figure 1H**.

Breeding MX-CBD-707

Analysis of cannabinoid profile revealed that 48 plants of MX-CBD-707 contained between 3.47 and 11.70% and 0.41 to 9.91% of tCBD and tTHC, respectively. The ratios between tCBD and tTHC thus varied between 0.9 and 18.8, which represents an almost 21 fold difference. In order to stabilize CBD extraction

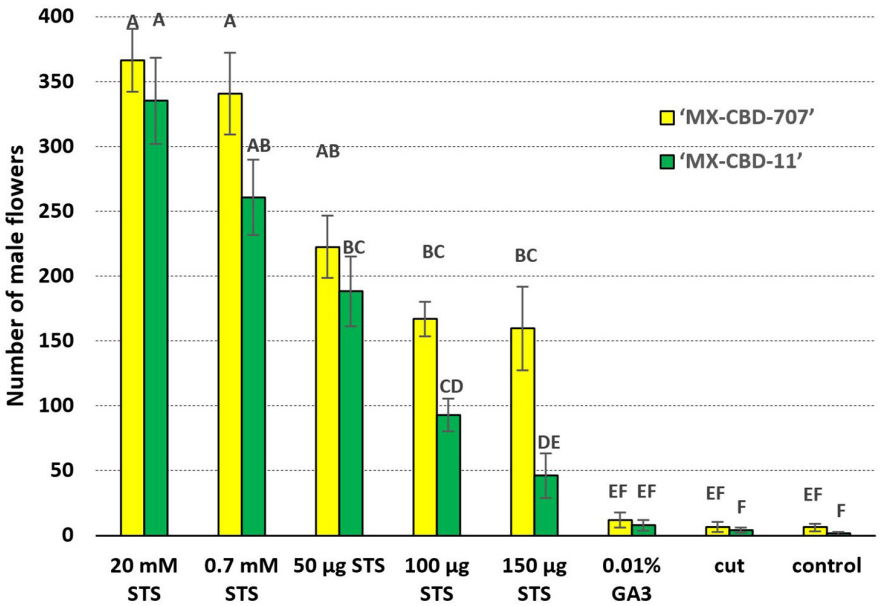

FIGURE 2 | The number of induced male flowers per plant is indicated by the interaction effect between breeding population and treatment. Mean values followed by different letters are significantly different at the 5% level of probability (Tukey). Horizontal bars represent SE (± SE).

TABLE 4 | Influence of pretreatment and treatment on a number of male flowers per plant of MX-CBD-707.

	Number of male flowers per plant
Pretreatment (*n* = 15)	
18/6 light/dark	339 ± 87a
168 h light	253 ± 70ab
168 h dark	155 ± 62b
p	*
Treatment (*n* = 9)	
1–0.3 mM STS, 12/12	497 ± 60a
2–0.3 mM STS, 96/72	448 ± 99a
3–30 ppm colloidal silver every day, 12/12	293 ± 91a
4–30 ppm colloidal silver once, 12/12	1 ± 1b
5–Control, 12/12	0 ± 0b
p	***

*Mean values are followed by SE. Pretreatments: 18/6 light/dark, incubation of plants 1 week under 18/6 light/dark photoperiod; 168 h light, incubation of plants 1 week under constant light; 168 h dark–incubation of plants 1 week under constant dark. Treatment denotes the use of silver solutions and control treatment (non-treated plants); treatments 1, 2, and 4, spraying once with the chemical until runoff of the leaves; treatment 3, spraying with the chemical until runoff of the leaves every day until anthesis. Photoperiod after treatment: 12/12, exposure to 12/12 light/dark regime; 96/72, exposure to photoperiod with 96 h of light and 72 h of dark. STS–silver thiosulfate. Mean values followed by different letters are significantly different at the 5% level of probability (Tukey); ***p < 0.001; *p < 0.05.*

from female flowers, we selected 23 plants with tCBD to tTHC ratios above 13.

These mother plants were cloned, induced to produce male flowers by spraying them with 30 ppm colloidal silver every day, and left to cross-pollinate in a contained flowering chamber. The colloidal silver treatment was chosen based on our results obtained in the above described experiments, which demonstrated the best performance in terms of the number of *in vitro* germinated pollen grains and of the number of developing seeds (**Tables 5**, **6**). Seeds were left on plants until maturity when they were sown, and a 64.3% germination rate was recorded. The cannabinoid analysis of 74 seedlings showed that their flowers contained from 1.77 to 24.34% and 0.09 to 0.85% of tCBD and tTHC, respectively. The ratio between tCBD and tTHC varied between 13.26 and 29.58 (**Figure 3**).

DISCUSSION

Alteration of the reproduction system in cannabis, in the form of the appearance of male flowers on female plants, is a useful phenomenon in cannabis breeding. It enables self-pollination and/or crossing plants that are genetically female. Moreover, it leads to offspring seeds that are entirely feminized. As such, they are highly valuable in medical cannabis production, which relies exclusively on phenotypically female plants (Soler et al., 2017).

Ethylene is a known gaseous plant hormone, which is involved in sex expression in plants. It promotes femaleness and inhibitors of ethylene biosynthesis or ethylene response suppress the development of female reproductive organs, thus promoting masculinity (Kumar et al., 2009). The mode of action was partly elucidated recently in cucumber and melon, where, Tao et al. (2018) demonstrated that ethylene signaling is directly involved in interaction among sex determination-related genes by controlling ethylene-responsive transcription factors CsERF110 and CmERF110 (Tao et al., 2018). Silver ions from STS and colloidal silver act as ethylene antagonists, thus blocking its function, and in this way probably enable male sex

TABLE 5 | Number of male flowers per plant and number of germinated pollen cells *in vitro* after the induction of male flowering on female plants of MX-CBD-707.

Pretreatment	Treatment	Average number of male flowers per plant ± SE	Percentage of pollen cells germinated *in vitro* ± SE
168 h light	0.3 mM STS, 12/12	577 ± 89	3.48 ± 0.99
168 h dark	0.3 mM STS, 12/12	431 ± 160	2.40 ± 1.48
18/6 light/dark	0.3 mM STS, 12/12	482 ± 66	7.18 ± 3.02
168 h light	0.3 mM STS, changing 96/72	497 ± 82	0.00
168 h dark	0.3 mM STS, changing 96/72	129 ± 11	0.00
18/6 light/dark	0.3 mM STS, changing 96/72	717 ± 100	0.00
168 h light	30 ppm colloidal silver once, 12/12	0	/
168 h dark	30 ppm colloidal silver once, 12/12	0	/
18/6 light/dark	30 ppm colloidal silver once, 12/12	0	/
168 h light	30 ppm colloidal silver every day, 12/12	285 ± 59	0.91 ± 0.91
168 h dark	30 ppm colloidal silver every day, 12/12	216 ± 182	2.66 ± 1.11
18/6 light/dark	30 ppm colloidal silver every day, 12/12	379 ± 190	4.34 ± 1.62
168 h light	–, 12/12	0	/
168 h dark	–, 12/12	0	/
18/6 light/dark	–, 12/12	0	/

Pretreatments: 18/6 light/dark, incubation of plants 1 week under 18/6 light/dark photoperiod; 168 h light, incubation of plants 1 week under constant light; 168 h dark, incubation of plants 1 week under constant dark. Treatment denotes the use of silver solutions and control treatment (non-treated plants); treatments 1, 2, and 4, spraying once with the chemical until runoff of the leaves; treatment 3, spraying with the chemical until runoff of the leaves every day until anthesis. Photoperiod after treatment: 12/12, exposure to 12/12 light/dark regime; 96/72, exposure to photoperiod with 96 h of light and 72 h of dark. STS, silver thiosulfate.

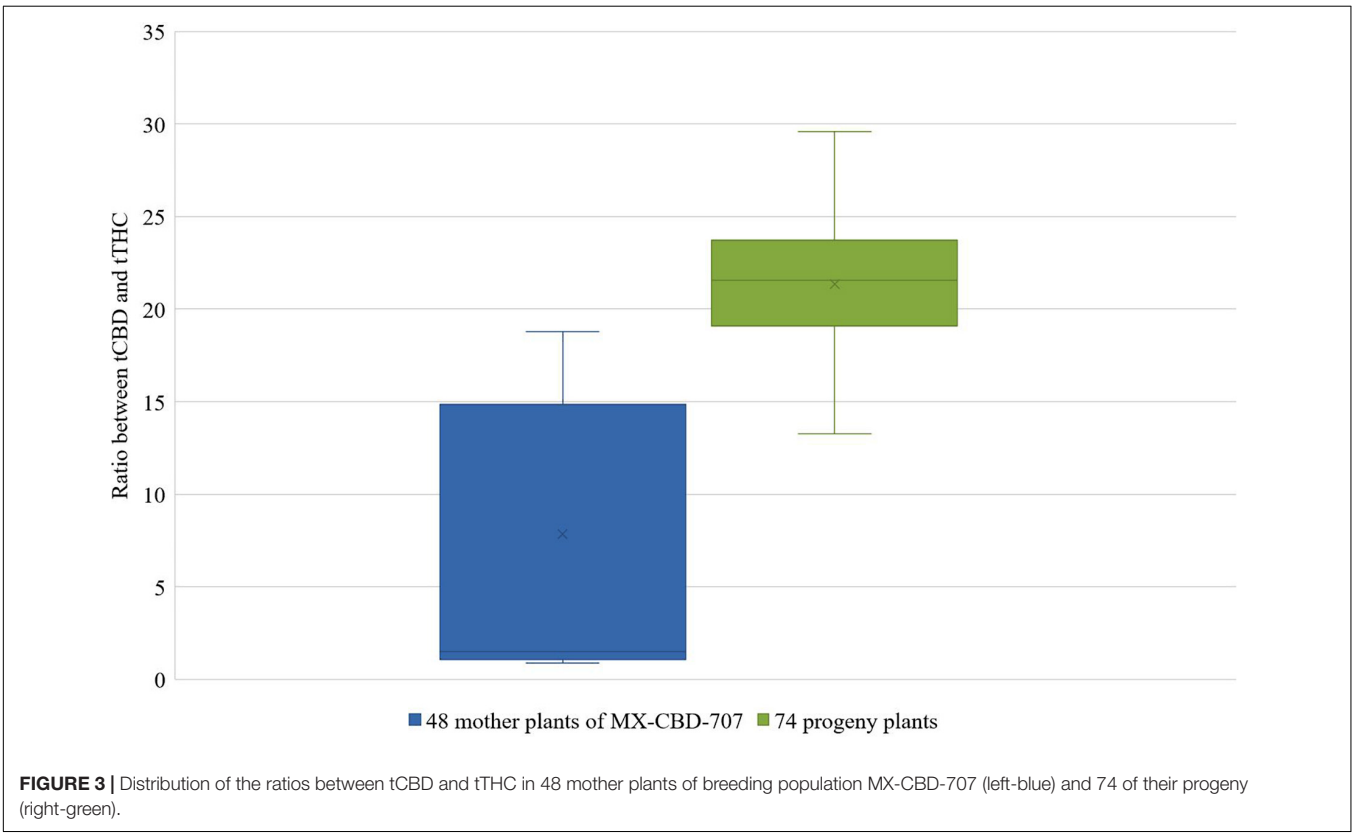

FIGURE 3 | Distribution of the ratios between tCBD and tTHC in 48 mother plants of breeding population MX-CBD-707 (left-blue) and 74 of their progeny (right-green).

induction (Ram and Sett, 1982). Ram and Sett (1982) showed for the first time that STS is capable of male sex induction on wild accession of *C. sativa* L. They also discovered that STS was more efficient compared to $AgNO_3$, probably due to the faster transport of STS through plants. Recently, Adal et al. (2021) used STS for the chemical induction of male flowers on

TABLE 6 | Number of developing seeds 2 weeks after pollination with pollen from plants MX-CBD-707 induced with different light (pre)treatments and silver applications.

Pretreatment	Treatment	No. of developing seeds
168 h light		12
168 h dark	0.3 mM STS, 12/12	7
18/6 light/dark		18
168 h light		12
168 h dark	0.3 mM STS, 96/72	3
18/6 light/dark		1
168 h light		39
168 h dark	30 ppm colloidal silver every day, 12/12	31
18/6 light/dark		11

Pretreatments: 18/6 light/dark, incubation of plants 1 week under 18/6 light/dark photoperiod; 168 h light, incubation of plants 1 week under constant light; 168 h dark, incubation of plants 1 week under constant dark. Treatment denotes the use of silver solutions and control treatment (non-treated plants); treatments 1, 2, and 4, spraying once with the chemical until runoff of the leaves; treatment 3, spraying with the chemical until runoff of the leaves every day until anthesis. Photoperiod after treatment: 12/12, exposure to 12/12 light/dark regime; 96/72, exposure to photoperiod with 96 h of light and 72 h of dark. STS, silver thiosulfate.

female plants. They identified over 10,500 differentially expressed genes, of which, around 200 are potentially responsible for male flower development on female plants. Their study confirmed that sex determination in cannabis flowers is controlled primarily at the genetic level. However, the expressed genes appeared to be involved in several pathways, such as phytohormone signaling, floral development, metabolism of lipids, sugar, and others, implying that the process of sex expression in cannabis plants occurs at multiple levels.

In our experiment, 23 different treatments (chemical using STS or colloidal silver; hormonal using GA; and physiological by intensive cutting) were used for induction of male flowers on female plants, in order to evaluate their influence on sex expression in medical cannabis. Plant height and number of nodes, which assessed the influence of treatments on plant growth, showed no negative influence as a result of our treatments. Although Ram and Sett (1982) reported that after application of STS on shoot tips the treated plants became black, the young leaves became decolorized, wilted, and deformed, etc., less pronounced effects of STS on plant growth and morphology were observed in our study. Even the highest amount of STS added on the shoot tip in our research (150 μg) had no negative influence on plant growth (**Table 3**), while application of 100 μg on the shoot tip in the study of Ram and Sett (1982) caused a total collapse of the shoot tip, decreased leaf area, and reduced plant growth in height after treatment. The number of male flowers per plant in our study was similar to the number they counted for the same treatment (application of 100 μg; up to 110 male flowers), but our research also showed that applying STS to whole plants is more efficient than the application of STS to the shoot tips.

The interaction effect between genotype and treatment on a number of male flowers in this study proved that genotype affects the success of male flower induction. Overall, we observed a higher number of male flowers developed per plant compared with the study of Ram and Sett (1982), who treated fiber-type hemp plants; while in our experiment, plants of medical cannabis were used. Besides, we applied STS by spraying whole plants, where Ram and Sett (1982) add STS to shoot tip only and this could also be the reason for the obtained variation. Differences in maleness induction were also observed by comparing our results with Lubell and Brand (2018), who used STS for the induction of male flowers on female hemp plants. Although the number of male flowers in their study was not exactly counted, they determined up to ≈85% of inflorescences with male flowers, where in our study, only approximately 55% of inflorescences contained male flowers. Lubell and Brand (2018) found that one (out of four tested) hemp strain was more prone to sex conversion and exhibited a higher level of masculinization. The phenomenon of genotype dependency on sex induction was also observed by Moliterni et al. (2004), who noticed that European hemp varieties exhibit different stages of resistance to sex reversion treatments.

The assumption about genotype specificity for sex reversion was confirmed by the results of our first experiment, in which breeding population MX-CBD-11 outperformed MX-CBD-707 in terms of male flower production after all seven different treatments. Since the treatments were identical for both breeding populations and performed simultaneously under the same flowering conditions, the results clearly demonstrate genotype dependency of physio-morphologic response to silver compounds.

Comparison of pollen from naturally male hemp plants and masculinized female ones showed that the latter produce a significantly higher number of irregular or misshapen pollen grains that are inefficient in dispersal from anthers and had a lower germination rate (DiMatteo et al., 2020). In our study, a comparison between pollen from masculinized female plants and male plants was not possible, because the medical breeding populations contained exclusively female plants. We, therefore, decided to test pollen viability and its germinability *in vitro* and *in vivo* and, finally, evaluated seed set after pollination of female plants with pollen from masculinized plants. Our results (**Figure 1** and **Tables 5**, **6**) confirmed the viability and functionality of the pollen developed on masculinized female plants. It demonstrated that colloidal silver is also very efficient for the induction of male flowers (as reported in **Table 5**), and this is the first report about the induction of male flowers on female plants of cannabis with colloidal silver.

On the other hand, spraying with hormone GA3 had no significant effects on male flower induction in our medical cannabis plants, as was also shown by Sarath and Ram (1978). Although, Chailakhyan (1979) demonstrated that GA3 has a strong effect on the appearance of male flowers, they applied the hormone through roots of very young cannabis plants, which is impractical for breeding purposes. In addition to chemical and hormonal triggers, physiological stress caused by mechanical damage was also expected to increase the likelihood of sex reversion (Clarke, 1999). However, intensive cut, which was one of our treatments, did not produce positive results in terms of induction of male flowers.

Some male flowers appeared on the control plants, where no staminate flowers were expected. It is possible that unwanted drift of STS from treated plants to the control plants occurred in the growing room since strong ventilation was used during growth. On the other hand, it has been recently shown by Punja and Holmes (2020) that male flowers can form spontaneously on up to 10% of female plants, therefore, the possibility of unwanted spontaneous sex conversion cannot be excluded.

Finally, the protocol using colloidal silver was successfully used for breeding female plants of medical cannabis breeding population MX-CBD-707. Entirely, the female progeny was obtained after crossing the parental population of females induced to form male flowers, thus confirming the theory of producing exclusively feminized seeds when crossing only XX plants (Green, 2005). Furthermore, a significant improvement of tCBD/tTHC ratio was observed (with a maximal tCBD content of 29.58% measured in a plant with a tTHC as low as 0.82%) after crossing only 23 selected parental plants. It shows that crossing plants selected based on their chemotype profile improves the genetic constitution of the breeding population and consequently enables the development of new varieties with improved cannabinoid profiles.

CONCLUSION

To the best of our knowledge, this is the first comprehensive scientific report on the induction of fertile male flowers on female plants of medical cannabis (*Cannabis sativa* L.). Previous reports on gender manipulation in cannabis were performed on fiber-hemp genotypes (Ram and Sett, 1982; Lubell and Brand, 2018; DiMatteo et al., 2020), while methods for medical cannabis have been shared among growers for years, but the information was not obtained in a manner based on scientific methodologies.

DATA AVAILABILITY STATEMENT

The original contributions presented in the study are included in the article/supplementary material, further inquiries can be directed to the corresponding author.

AUTHOR CONTRIBUTIONS

MF and JM conceived and designed the study and wrote the manuscript. MS performed the experiments. MF, MS, and JM analyzed the data. All authors read and approved the manuscript.

FUNDING

This work was carried out in the framework of the scientific-research project "Breeding medical cannabis (*Cannabis sativa* L.)" in collaboration between the Biotechnical Faculty of the University of Ljubljana, Slovenia, and MGC Pharmaceuticals Ltd. This study received funding from MGC Pharmaceuticals Ltd. The funder was not involved in the study design, collection, analysis, and interpretation of data, the writing of this article, or the decision to submit it for publication. The research was also supported by research programme P4-0077 and infrastructural centre IC RRC-AG (IO-0022-0481-001) of the Slovenian Research Agency.

ACKNOWLEDGMENTS

We thank Sinja Svetik, Špela Mestinšek Mubi, Liza Zavrl (from the Biotechnical Faculty), and Irena Pribošič (from MGC Pharmaceuticals Ltd.) for their technical assistance during the experiments.

REFERENCES

Adal, A. M., Doshi, K., Holbrook, L., and Mahmoud, S. S. (2021). Comparative RNA-Seq analysis reveals genes associated with masculinization in female *Cannabis sativa*. *Planta* 253, 1–17. doi: 10.1007/s00425-020-03522-y

Ainsworth, C. (2000). Boys and girls come out to play: the molecular biology of dioecious plants. *Ann. Bot.* 86, 211–221. doi: 10.1006/anbo.2000.1201

Andre, C. M., Hausman, J. F., and Guerriero, G. (2016). *Cannabis sativa*: the plant of the thousand and one molecules. *Front. Plant Sci.* 7:19. doi: 10.3389/fpls.2016.00019

Chailakhyan, M. K. (1979). Genetic and hormonal regulation of growth, flowering, and sex expression in plants. *Am. J. Bot.* 66, 717–736. doi: 10.1002/j.1537-2197.1979.tb06276.x

Clarke, R. C. (1999). "Botany of the genus Cannabis," in *Advances in Hemp Research*, ed. P. Ranalli (New York: Food Products Press), 1–19.

Dellaporta, S., and Calderon-Urrea, A. (1993). Sex determination in flowering plants. *Plant Cell* 5, 1241–1251. doi: 10.1105/tpc.5.10.1241

Den Nijs, A., and Visser, D. (1980). Induction of male flowering in gynoecious cucumbers (*Cucumis sativus* L.) by silver ions. *Euphytica* 29, 237–280. doi: 10.1007/BF00025124

Devani, R. S., Sinha, S., Banerjee, J., Sinha, R. K., Bendahmane, A., and Banerjee, A. K. (2017). De novo transcriptome assembly from flower buds of dioecious, gynomonoecious and chemically masculinized female Coccinia grandis reveals genes associated with sex expression and modification. *BMC Plant Biol.* 17:241. doi: 10.1186/s12870-017-1187-z

DiMatteo, J., Kurtz, L., and Lubell-Brand, J. D. (2020). Pollen appearance and in vitro germination varies for five strains of female hemp masculinized using silver thiosulfate. *HortScience* 55, 1–3. doi: 10.21273/HORTSCI14842-20

Divashuk, M. G., Alexandrov, O. S., Razumova, O. V., Kirov, I. V., and Karlov, G. I. (2014). Molecular cytogenetic characterization of the dioecious *Cannabis sativa* with an XY chromosome sex determination system. *PLoS One* 9:e85118. doi: 10.1371/journal.pone.0085118

Faux, A. M., Berhin, A., Dauguet, N., and Bertin, P. (2014). Sex chromosomes and quantitative sex expression in monoecious hemp (*Cannabis sativa* L.). *Euphytica* 196, 183–197. doi: 10.1007/s10681-013-1023-y

Faux, A. M., and Bertin, P. (2014). Modelling approach for the quantitative variation of sex expressions in monoecious hemp (*Cannabis sativa* L.). *Plant Breed.* 133, 782–787. doi: 10.1111/pbr.12208

Faux, A. M., Draye, X., Flamand, M. C., Occre, A., and Bertin, P. (2016). Identification of QTLs for sex expression in dioecious and monoecious hemp (*Cannabis sativa* L.). *Euphytica* 209, 357–376. doi: 10.1007/s10681-016-1641-2

Faux, A. M., Draye, X., Lambert, R., D'andrimont, R., Raulier, P., and Bertin, P. (2013). The relationship of stem and seed yields to flowering phenology and sex expression in monoecious hemp (*Cannabis sativa* L.). *Eur. J. Agron.* 47, 11–22. doi: 10.1016/j.eja.2013.01.006

Freeman, T. P., Hindocha, C., Green, S. F., and Bloomfield, M. A. P. (2019). Medicinal use of cannabis based products and cannabinoids. *BMJ* 365:l1141. doi: 10.1136/bmj.l1141

Galoch, E. (1978). The hormonal control of sex differentiation in dioecious plants of hemp (*Cannabis sativa*). The influence of plant growth regulators on sex expression in male and female plants. *Acta. Soc. Bot. Pol.* 47, 153–162. doi: 10.5586/asbp.1978.013

Green, G. (2005). *The Cannabis Breeder's Bible*. San Francisco: Green Candy Press.

Gul, W., Gul, S. W., Radwan, M. M., Wanas, A. S., Mehmedic, Z., Khan, I. I., et al. (2015). Determination of 11 cannabinoids in biomass and extracts of different varieties of Cannabis using high-performance liquid chromatography. *JAOAC Int.* 98, 1523–1528. doi: 10.5740/jaoacint.15-095

Hall, J., Bhattarai, S. P., and Midmore, D. J. (2012). Review of flowering control in industrial hemp. *J. Nat. Fibers* 9, 23–36. doi: 10.1080/15440478.2012.651848

Kumar, V., Parvatam, G., and Ravishankar, G. A. (2009). AgNO3: a potential regulator of ethylene activity and plant growth modulator. *Electron. J. Biotechnol.* 12, 8–9. doi: 10.4067/S0717-34582009000200008

Law, T. F., Lebel-Hardenack, S., and Grant, S. R. (2002). Silver enhances stamen development in female white campion (Silene latifolia [Caryophyllaceae]). *Am J Bot.* 89, 1014–20. doi: 10.3732/ajb.89.6.1014

Laznik, Ž, Košir, I. J., Košmelj, K., Murovec, J., Jagodič, A., and Trdan, S. (2020). Effect of *Cannabis sativa* L. root, leaf and inflorescence ethanol extracts on the chemotrophic response of entomopathogenic nematodes. *Plant Soil* 455, 367–379. doi: 10.1007/s11104-020-04693-z

Lubell, J. D., and Brand, M. H. (2018). Foliar sprays of silver thiosulfate produce male flowers on female hemp plants. *HortTechnology* 28, 743–747. doi: 10.21273/HORTTECH04188-18

Mestinšek Mubi, Š, Svetik, S., Flajšman, M., and Murovec, J. (2020). In vitro tissue culture and genetic analysis of two high-CBD medical cannabis (*Cannabis sativa* L.) breeding lines. *Genetika* 52, 925–941. doi: 10.2298/GENSR2003925M

Moliterni, V. M. C., Cattivelli, L., Ranalli, P., and Mandolino, G. (2004). The sexual differentiation of *Cannabis sativa* L.: a morphological and molecular study. *Euphytica* 140, 95–106. doi: 10.1007/s10681-004-4758-7

Murovec, J., and Bohanec, B. (2013). Haploid induction in Mimulus aurantiacus Curtis obtained by pollination with gamma irradiated pollen. *Sci. Hortic.* 162, 218–225. doi: 10.1016/j.scienta.2013.08.012

Owens, K. W., Peterson, C. E., and Tolla, G. E. (1980). Production of hermaphrodite flowers on gynoecious muskmelon by silver nitrate and aminoethyoxyvinylglycine. *Hortscience* 15, 654–655.

Petit, J., Salentijn, E. M. J., Paulo, M. J., Denneboom, C., and Trindade, L. M. (2020). Genetic architecture of flowering time and sex determination in hemp (*Cannabis sativa* L.): a genome-wide association study. *Front. Plant Sci.* 11:569958. doi: 10.3389/fpls.2020.569958

Punja, Z. K., and Holmes, J. E. (2020). Hermaphroditism in marijuana (*Cannabis sativa* L.) Inflorescences–impact on floral morphology, seed formation, progeny sex ratios, and genetic variation. *Front. Plant Sci.* 11:718. doi: 10.3389/fpls.2020.00718

R Core Team (2019). *R: A Language and Environment for Statistical Computing*. Vienna: R Foundation for Statistical Computing.

Ram, H. Y. M., and Sett, R. (1981). Modification of growth and sex expression in *Cannabis sativa* by aminoethoxyvinylglycine and ethephon. *Z. Pflanzenphysiol.* 105, 165–172. doi: 10.1016/s0044-328x(82)80008-1

Ram, H. Y. M., and Jaiswal, V. S. (1970). Induction of female flowers on male plants of *Cannabis sativa* L. by 2-chlorethanephosphoric acid. *Experientia* 26, 214–216.

Ram, H. Y. M., and Jaiswal, V. S. (1972). Induction of male flowers on female plants of *Cannabis sativa* by gibberellins and its inhibition by abscisic acid. *Planta* 105, 263–266. doi: 10.1007/BF00385397

Ram, H. Y. M., and Sett, R. (1979). Sex reversal in the female plants of *Cannabis sativa* by Cobalt ion. *Proc. Indian. Acad.* 2, 303–308. doi: 10.1007/BF03046194

Ram, H. Y. M., and Sett, R. (1982). Induction of fertile male flowers in genetically female *Cannabis sativa* plants by silver nitrate and silver thiosulphate anionic complex. *Theor. Appl. Genet.* 62, 369–375. doi: 10.1007/BF00275107

Rosenthal, E. (2010). *Marijuana Grower's Handbook*. Oakland: Quick American Archives.

Sarath, G., and Ram, H. Y. M. (1978). Comparative effect of silver ion and gibberellic acid on the induction of male flowers on female Cannabis plants. *Cell. Mol. Life Sci.* 3, 333–334. doi: 10.1007/BF01964334

Small, E. (2015). Evolution and classification of *Cannabis sativa* (marijuana, hemp) in relation to human utilization. *Bot. Rev.* 81, 189–294. doi: 10.1007/s12229-015-9157-3

Soler, S., Gramazio, P., Figàs, M. R., Vilanova, S., Rosa, E., Llosa, E. R., et al. (2017). Genetic structure of *Cannabis sativa* var. indica cultivars based on genomic SSR (gSSR) markers: implications for breeding and germplasm management. *Ind. Crops Prod.* 104, 171–178. doi: 10.1016/j.indcrop.2017.04.043

Tao, Q., Niu, H., Wang, Z., Zhang, W., Wang, H., Wang, S., et al. (2018). Ethylene responsive factor ERF110 mediates ethylene-regulated transcription of a sex determination-related orthologous gene in two Cucumis species. *J. Exp. Bot.* 69, 2953–2965. doi: 10.1093/jxb/ery128

The European Commission (2014). *Regulation (Eu) No 809/2014: Official Journal of the European Union*. Brussels: European Commission.

Truta, E., Olteanu, N., Surdu, S., Zamfirache, M. M., and Oprica, L. (2007). Some aspects of sex determinism in hemp. Analele Stiint ale Univ Alexandru Ioan Cuza" din Iasi Sec II. *Genet. Biol. Mol.* 8, 31–38.

van Bakel, H., Stout, J. M., Cote, A. G., Tallon, C. M., Sharpe, A. G., Hughes, T. R., et al. (2011). The draft genome and transcriptome of *Cannabis sativa*. *Genome Biol.* 12:R102. doi: 10.1186/gb-2011-12-10-r102

Conflict of Interest: The authors declare that the research was conducted in the absence of any commercial or financial relationships that could be construed as a potential conflict of interest.

Publisher's Note: All claims expressed in this article are solely those of the authors and do not necessarily represent those of their affiliated organizations, or those of the publisher, the editors and the reviewers. Any product that may be evaluated in this article, or claim that may be made by its manufacturer, is not guaranteed or endorsed by the publisher.

frontiers in Plant Science

ORIGINAL RESEARCH
published: 02 November 2021
doi: 10.3389/fpls.2021.725078

Cannabis Inflorescence Yield and Cannabinoid Concentration Are Not Increased With Exposure to Short-Wavelength Ultraviolet-B Radiation

*Victoria Rodriguez-Morrison, David Llewellyn and Youbin Zheng**

School of Environmental Sciences, University of Guelph, Guelph, ON, Canada

Before ultraviolet (UV) radiation can be used as a horticultural management tool in commercial *Cannabis sativa* (cannabis) production, the effects of UV on cannabis should be vetted scientifically. In this study we investigated the effects of UV exposure level on photosynthesis, growth, inflorescence yield, and secondary metabolite composition of two indoor-grown cannabis cultivars: 'Low Tide' (LT) and 'Breaking Wave' (BW). After growing vegetatively for 2 weeks under a canopy-level photosynthetic photon flux density (PPFD) of ≈225 $\mu mol \cdot m^{-2} \cdot s^{-1}$ in an 18-h light/6-h dark photoperiod, plants were grown for 9 weeks in a 12-h light/12-h dark "flowering" photoperiod under a canopy-level PPFD of ≈400 $\mu mol \cdot m^{-2} \cdot s^{-1}$. Supplemental UV radiation was provided daily for 3.5 h at UV photon flux densities ranging from 0.01 to 0.8 $\mu mol \cdot m^{-2} \cdot s^{-1}$ provided by light-emitting diodes (LEDs) with a peak wavelength of 287 nm (i.e., biologically-effective UV doses of 0.16 to 13 $kJ \cdot m^{-2} \cdot d^{-1}$). The severity of UV-induced morphology (e.g., whole-plant size and leaf size reductions, leaf malformations, and stigma browning) and physiology (e.g., reduced leaf photosynthetic rate and reduced F_v/F_m) symptoms intensified as UV exposure level increased. While the proportion of the total dry inflorescence yield that was derived from apical tissues decreased in both cultivars with increasing UV exposure level, total dry inflorescence yield only decreased in LT. The total equivalent Δ^9-tetrahydrocannabinol (Δ^9-THC) and cannabidiol (CBD) concentrations also decreased in LT inflorescences with increasing UV exposure level. While the total terpene content in inflorescences decreased with increasing UV exposure level in both cultivars, the relative concentrations of individual terpenes varied by cultivar. The present study suggests that using UV radiation as a production tool did not lead to any commercially relevant benefits to cannabis yield or inflorescence secondary metabolite composition.

Keywords: ***Cannabis sativa*, potency, ultraviolet, indoor, sole source, terpene**

OPEN ACCESS

Edited by:
Donald Lawrence Smith, McGill University, Canada

Reviewed by:
Juan Luis Valenzuela, University of Almería, Spain
Gianpaolo Grassi, CREA-CIN, Italy

***Correspondence:**
Youbin Zheng
yzheng@uoguelph.ca

Specialty section:
This article was submitted to Crop and Product Physiology, a section of the journal Frontiers in Plant Science

Received: *14 June 2021*
Accepted: *13 October 2021*
Published: *02 November 2021*

Citation:
Rodriguez-Morrison V, Llewellyn D and Zheng Y (2021) Cannabis Inflorescence Yield and Cannabinoid Concentration Are Not Increased With Exposure to Short-Wavelength Ultraviolet-B Radiation. Front. Plant Sci. 12:725078. doi: 10.3389/fpls.2021.725078

INTRODUCTION

Drug-type *Cannabis sativa* (i.e., genotypes grown for their high cannabinoid content; hereafter, cannabis) are short-day plants commonly cultivated for their unique secondary metabolites (e.g., cannabinoids) that are used both medicinally and recreationally (Small, 2017). Cannabis is often grown in controlled-environment facilities that are illuminated solely with electrical lighting to accommodate its photoperiod specificity and produce uniform plants by maintaining prescribed environmental parameters (Zheng, 2021). Popular sole-source lighting technologies used in the flowering stage of cannabis production include high-pressure sodium (HPS) and, increasingly, light-emitting diodes (LEDs) (Cannabis Business Times, 2020).

Both HPS and LED technologies normally have little or no ultraviolet (UV; 100 to 400 nm) radiation in their spectra (Radetsky, 2018). Conversely, cannabis plants in the natural environment are exposed to a small but significant fraction of UV radiation relative to the amount of photosynthetically active radiation (PAR; 400-700 nm) in sunlight (Nikiforos et al., 2011). While the relative spectral distribution of UV and PAR wavebands varies over time and space, the UV waveband normally comprises approximately 5% of the day-time PAR intensity at any given time and global location. The solar UV that reaches the earth's surface is comprised mostly of ultraviolet A (UVA; 315 to 400 nm) with the remainder being ultraviolet B (UVB; 280 to 315 nm) at an irradiance ratio of approximately 40:1 (Nikiforos et al., 2011), although reported UVA to UVB ratios range from 20:1 to 100:1, depending on time and place. The wavelength cutoff for solar UV reaching the earth's surface is approximately 290 nm (Nikiforos et al., 2011), meaning that outdoor-grown plants are not exposed to short-wavelength UVB (i.e., <290 nm) or UVC (100 to 280 nm) (McElroy and Fogal, 2008). While UVC is used in horticultural applications to inactivate microorganisms such as waterborne pathogens in recirculating irrigation systems (Younis et al., 2019), foliage is only rarely directly exposed UVC – normally to inactivate foliar pathogens through short-term exposures (Aarrouf and Urban, 2020) – since UVC can cause tissue damage (Stapleton, 1992).

Many studies have investigated the effects of stratospheric ozone depletion on plant exposure to UV radiation (Searles et al., 2001; Caldwell et al., 2003) either through ecological or controlled-environment type research. The ratios between UV and PAR in controlled-environment type investigations tend to be much higher than in the solar spectrum in terrestrial ecosystems (Robson et al., 2019). Therefore plants in these studies may have exhibited relatively amplified responses to UV radiation including increased secondary metabolite accumulation and reduced photosynthesis and growth relative to lower UV:PAR responses (Behn et al., 2010; Dou et al., 2019). The other spectra within the lighting environment have also been shown to influence plant sensitivity to UV radiation, including biomass accumulation (Palma et al., 2021). Some spectra, such as UVA, have even been shown to counteract UVB-induced damage (Krizek, 2004). Perhaps through serendipity, researchers have discovered some potential horticultural benefits for providing unnaturally stressful UV exposure conditions which can enhance pertinent traits in economically relevant crops, for example increasing secondary metabolite concentrations (Huché-Thélier et al., 2016).

Relative to the UVA and PAR in the solar spectrum, the higher-energy photons in the UVB waveband are disproportionately effective in evoking plant responses, including changes in morphology, physiology, and metabolism (Flint and Caldwell, 2003; Huché-Thélier et al., 2016; Jenkins, 2017; Robson et al., 2019). Plant responses to UVB exposure are induced through pathways mediated by UV resistance 8 (UVR8; a UV-specific photoreceptor) or by UV-induced oxidative cellular damage, including to DNA (Czégény et al., 2016; Tossi et al., 2019). Typical plant responses to UV exposure include stunted growth, reduced leaf area, increased leaf thickness (Robson et al., 2019), epicuticular wax accumulation (Cen and Bornman, 1993), and foliar necrosis (Klem et al., 2012; Torre et al., 2012). From an ecological standpoint, it has been speculated that production of Δ^9-tetrahydrocannabinol (Δ^9-THC), which is the most economically valuable psychoactive cannabinoid, may be upregulated in cannabis tissues under UV exposure to serve as photoprotection. This concept arose from studies that found comparatively higher Δ^9-THC concentrations in cannabis ecotypes that were grown in global regions with relatively high solar UV exposure, such as at low latitudes and high altitudes (Small and Beckstead, 1973; Pate, 1983). However, despite an apparent focus on interactions between UV and Δ^9-THC in the cannabis literature, other cannabinoids have similar UV absorbing properties (Hazekamp et al., 2005), which may challenge an ecological explanation for favoring the upregulation of Δ^9-THC over other cannabinoids in plants under UV stress.

Preliminary controlled-environment studies, that were done about three decades ago, also alluded to the potential for UV to increase Δ^9-THC concentration in cannabis foliar and floral tissues (Fairbairn and Liebmann, 1974; Lydon et al., 1987). However, the concentration of Δ^9-THC in mature female cannabis inflorescence tissues (hereafter, inflorescence) has increased substantially over the past decades, with contemporary genotypes having ≈10 times higher Δ^9-THC concentrations than the genotypes used in these older studies (Dujourdy and Besacier, 2017). Therefore, modern cannabis genotypes may function nearer to cannabis' maximum capacity for producing Δ^9-THC; which could impede their ability to further increase Δ^9-THC production under an abiotic stress such as UV exposure, relative to older genotypes. However, studies on modern cannabis genotypes have shown that various environmental stimuli can modify the cannabinoid composition. For example,

Abbreviations: NCER, net carbon dioxide exchange rate; PPFD, photosynthetic photon flux; PFD, photon flux density; CCI, chlorophyll content index; SLW, specific leaf weight; LED, light-emitting diode; DLI, daily light integral; PAR, photosynthetically active radiation; DW, dry weight; SD, standard deviation; Δ^9-THC, Δ^9-tetrahydrocannabinol; Δ^9-THCA, Δ^9-tetrahydrocannabinolic acid; CBD, cannabidiol; CBDA, cannabidiolic acid; CBG, cannabigerol; CBGA, cannabigerolic acid; CBN, cannabinol; UV, ultraviolet; UVA, ultraviolet-A; UVB, ultraviolet-B; UVC, ultraviolet-C; Fv/Fm, variable to maximum chlorophyll fluorescence; TLI, total light integral; LT, 'Low Tide'; BW, 'Breaking Wave'; CB, culture basin; NIE, no increase in extent; NI, not investigated; UDL, under detection limit; UV-PFD, photon flux density of ultra-violet radiation.

inflorescences of cannabidiol (CBD)-dominant genotypes had greater CBD concentrations when grown at high vs. low altitude, which may have been a response to increased UV exposure at higher elevation (Giupponi et al., 2020). Drought-stress, salt-stress, and PAR spectra have also been shown to alter the inflorescence cannabinoid composition in modern, indoor-grown genotypes (Mahlberg et al., 1983; Magagnini et al., 2018; Caplan et al., 2019; Yep et al., 2020; Westmoreland et al., 2021). Therefore, the potential for UV exposure to provoke changes in the secondary metabolite composition in inflorescences of modern cannabis genotypes grown in controlled environments merits scientific investigation. Evaluating the effects of UV on modern genotypes with relatively balanced concentrations of Δ^9-THC and CBD [i.e., chemotype II; a cultivar with a ratio of Δ^9-THC to CBD of ≈1 (Small and Beckstead, 1973)] may provide additional insight into cannabinoid-specificity of UV exposure responses.

The objectives of this study were to: (1) characterize morphological and physiological responses of indoor-grown cannabis to UV exposure, and (2) investigate the relationships between UV exposure levels applied during the flowering stage and inflorescence yield and secondary metabolite composition of modern chemotype II cannabis genotypes.

MATERIALS AND METHODS

Plant Culture

Clonal cuttings were taken from mother plants of indoor grown cultivars: 'Low Tide' and 'Breaking Wave' and allowed to root for 13 d under humidity domes and fluorescent light (F32T8/TL850; Philips, Amsterdam, Netherlands) providing a photosynthetic photon flux density (PPFD, 400 to 700 nm) of ≈100 $\mu mol \cdot m^{-2} \cdot s^{-1}$ at the canopy. Rooted cuttings were transferred to 3.79L pots (height: 18.4 cm, diameter: 16.2 cm) containing a peat-based substrate and grown for an additional 9 d under LED light comprised of a mixture of Pro-325 (Lumigrow; Emeryville, CA, United States) and generic (unbranded) white LEDs providing a PPFD of ≈225 $\mu mol \cdot m^{-2} \cdot s^{-1}$ at the canopy. The propagation and vegetative growth stages both had 18-h photoperiods. The potted plants were subsequently transferred to a single deep-water culture basin (CB), where they were placed in floating polystyrene rafts in an indoor cannabis production facility in southern Ontario, Canada (described in Rodriguez-Morrison et al., 2021a). There were 384 evenly-spaced plants in the CB at a density of 0.09 m^2/plant. The daily PAR photoperiod was reduced to 12 h (07:30 HR to 19:30 HR) on the day the plants were transferred to the CB.

PAR and UV LED Fixture Layout

Photosynthetically active radiation was supplied by 24 LED fixtures (Pro650; Lumigrow Inc.) arranged evenly over the CB in 2 rows of 12 fixtures. The LED composition and spectrum of the PAR fixtures were described in Rodriguez-Morrison et al. (2021a) and the relative spectral photon flux distribution is provided in **Figure 1A**. Single UV LED fixtures were centered between adjacent PAR fixtures (within each row), resulting in 2 rows of 11 UV fixtures. The 22 UV LED fixtures were a custom design (10 × 90 cm), comprised of UVB LEDs with a peak wavelength of 287 nm (**Figure 1B**) and adjustable intensity (with analog, constant current dimmers). According to the conventional definitions of the different UV wavebands, the photon flux ratio of UVB (280 to 315 nm) to UVC (100 to 280 nm) was UVB(93):UVC(7). Additionally, 30% of the UV photon flux was at wavelengths >290 nm and there was no photon flux between 310 and 400 nm or <270 nm. The UV treatments (described below) were applied daily, in the last 3.5 hours (16:00 HR to 19:30 HR) of the PAR photoperiod, for 60 d from the day that the plants were transferred to the CB and then harvested.

Experimental Setup

The experiment was arranged and carried out as a gradient design, which can outperform treatment × replication designs when evaluating biological responses along a continuous independent variable (Kreyling et al., 2018), such as radiation intensity (Rodriguez-Morrison et al., 2021a). With a gradient design, regression analyses are performed on the response variables (i.e., measured parameters) against all different levels of the independent variable.

For each cultivar, 44 uniform representative plants were selected from the larger populations to be experimentally evaluated. Plots, each consisting of 4 plants of a single cultivar, were arranged where 2 plants were positioned directly below each UV LED fixture, and 2 plants were adjacent. Three UV LED fixture settings were randomly assigned (within each cultivar) to each plot: off, half power, and full power. Within each plot, the 2 plants positioned below the UV LED fixtures had relatively higher UV exposure than the 2 adjacent treatment plants. This configuration allowed for each cultivar to be exposed to a wide array of UV photon flux densities (UV-PFD); evenly-distributed across the 0.01 to 0.8 $\mu mol \cdot m^{-2} \cdot s^{-1}$ range (**Figure 2**).

At the start of the UV treatments, experimental plants of LT had heights from the substrate surface to the shoot apex ranging from 14 to 23 cm and experimental plants of BW had heights ranging from 14 to 20 cm. Experimental plants were surrounded by plants of the same cultivar to maintain canopy uniformity. The LT cultivar populated the south half of the CB, while BW populated the north half.

The average distance from the bottom of the fixtures to the top of the treatment plants was maintained at 50.5 cm by adjusting the height of the light racks weekly using a system of pulleys and cables. Canopy-level PPFD and UV-PFD were measured at the apex of each plant weekly, after the light rack height adjustment, using a PAR meter (LI-180; LI-COR Biosciences, Lincoln, NE, United States) and a radiometrically calibrated spectrometer (UV-Vis Flame-S-XR, Ocean Optics, Dunedin, Florida), respectively. The UV-PFDs were measured with the PAR LEDs turned off. A MS Excel tool developed by Mah et al. (2019) was used to integrate spectrometer data into UV-PFD, biologically-effective UV-PFD (Flint and Caldwell, 2003), and daily biologically-effective UV dose ($kJ \cdot m^{-2} \cdot d^{-1}$)

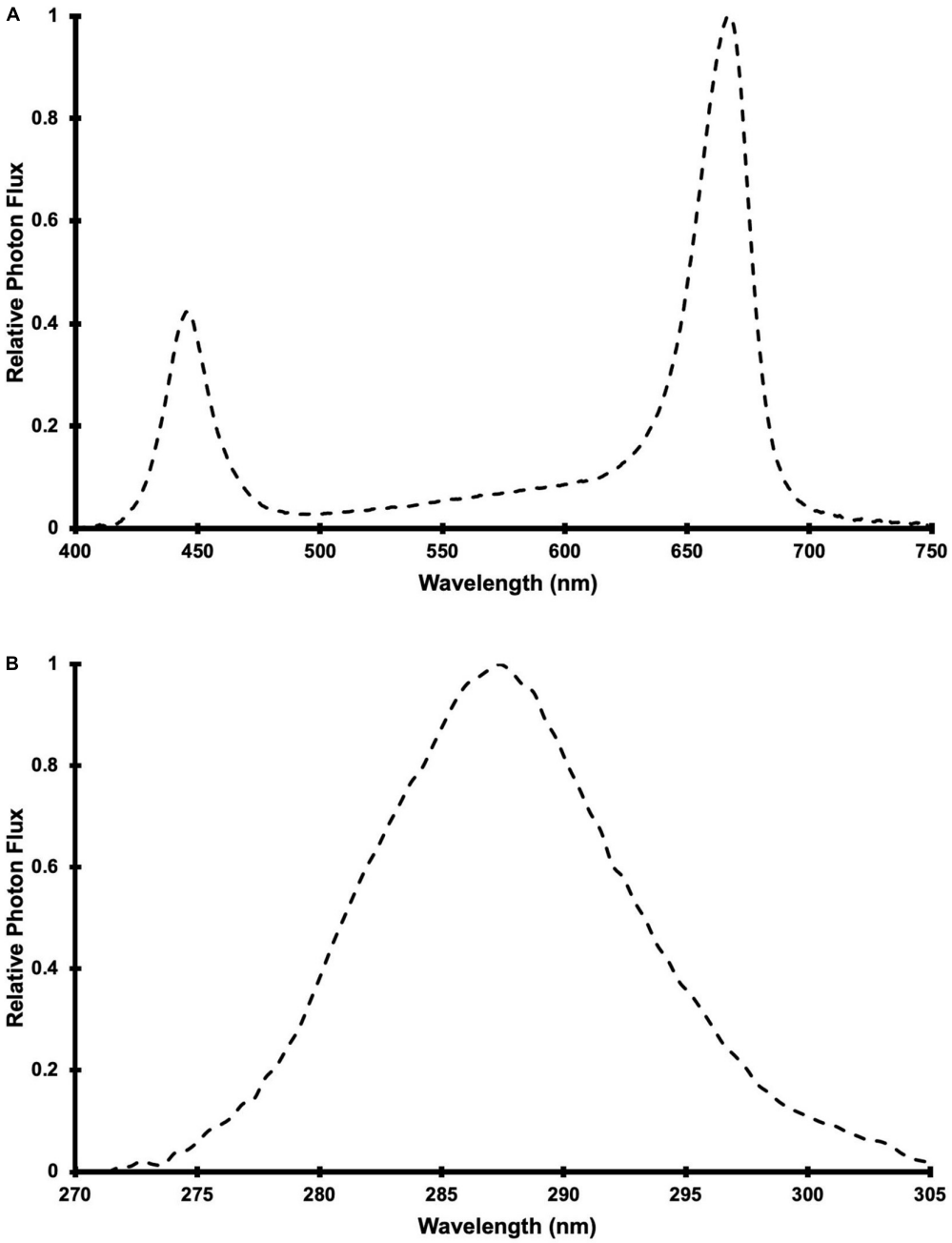

FIGURE 1 | Relative spectral photon flux distribution of **(A)** Pro-650 Lumigrow LED fixtures and **(B)** UV LED fixtures.

(**Table 1**). At the end of the trial, average PPFD and average UV-PFD were calculated for each treatment plant by determining the corresponding total light integrals (TLI; $mol \cdot m^{-2}$) and then dividing by accumulated time, as described in Rodriguez-Morrison et al. (2021a). The experiment-wise average (± SE, n = 88) PPFD was 408 ± 6.5 $\mu mol \cdot m^{-2} \cdot s^{-1}$. The average UV-PFD for each plant was used as the independent variable (i.e., x-axis) in regressions of UV exposure vs. the measured growth, yield and quality parameters.

Plant husbandry and environmental controls followed the cultivator's standard operating procedures except for the UV radiation. The air temperature and relative humidity set points were 25°C and 60%. There was no CO_2 supplementation, with typical concentrations of ≥400 ppm when the PAR lights were on. Air was continuously circulated throughout the room with wall-mounted axial fans and the HVAC circulation rate was ≈2 air changes per hour (ACH) with ≥25% refresh with pre-conditioned outside air. The aquaponic solution was maintained

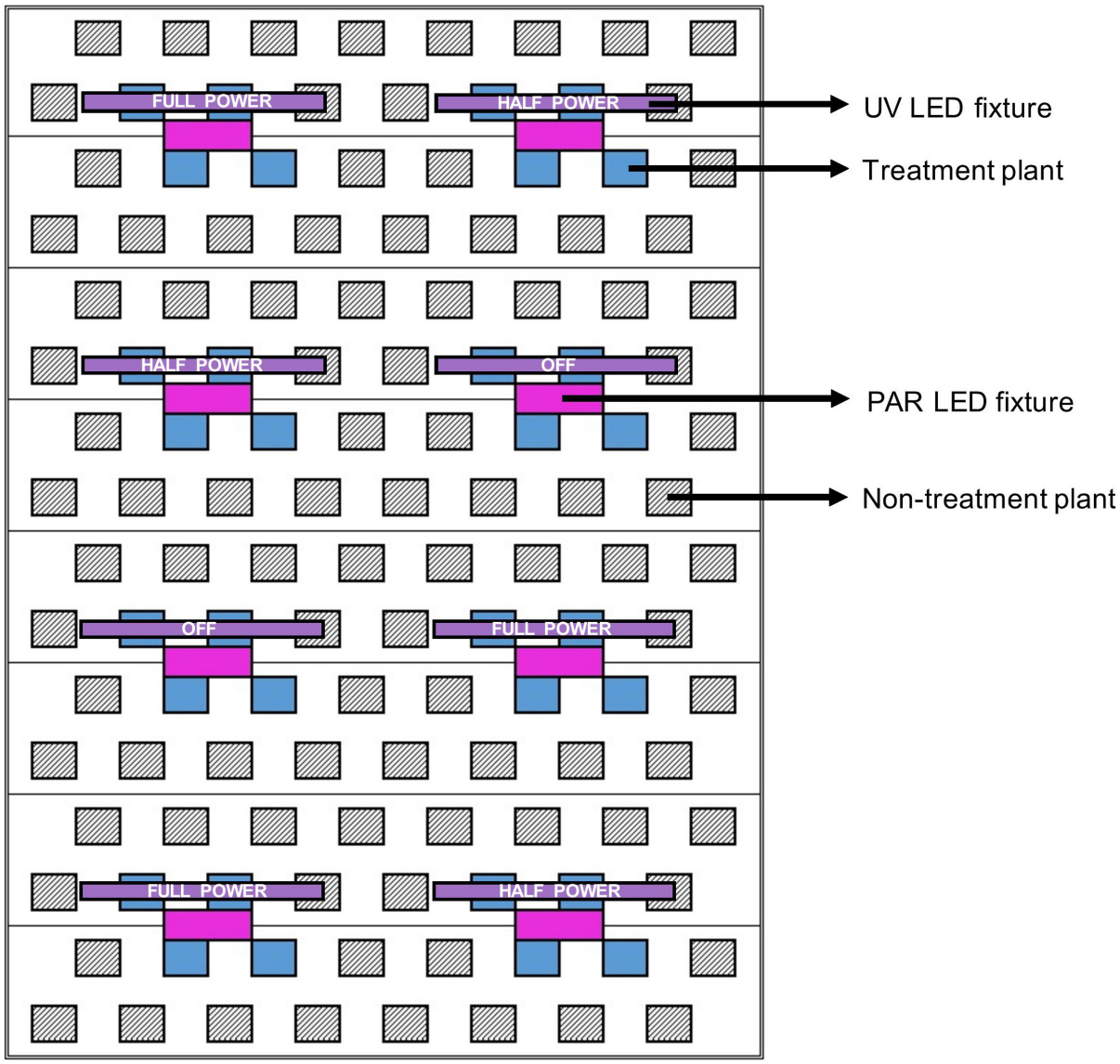

FIGURE 2 | Schematic of a single LED rack comprised of 8 PAR fixtures (in magenta) and 8 UV fixtures (in purple) above one third of the deep-water culture basin (CB). The entire growing area consisted of 3 light racks. The 3 UV LED settings (off, half power, full power) were randomly assigned to individual UV fixtures (i.e., plots). Each treatment plant (in blue, 4 per plot) was assigned a UV exposure level, reflecting its average canopy-level UV photon flux density (UV-PFD) measured throughout the trial. The UV-PFDs were used as the independent variable in analyses of plant growth, physiology and harvest metrics. Each plot was surrounded by non-treatment plants (hatched diagonal lines) to ensure uniform growing environment and normal planting density. The north half of the CB was populated with BW and the south half was populated with LT.

within normal levels of nutrient concentrations, pH, electrical conductivity, and dissolved oxygen; as described in Rodriguez-Morrison et al. (2021a).

Growth Measurements

The height (i.e., length of main stem from substrate surface to the highest point) and widths (i.e., the widest part and its perpendicular width) of each experimental plant were measured in week 6. Plant height and widths were used to calculate growth index [(height $\times$ width$_1$ $\times$ width$_2$)/300 (Ruter, 1992)] for each plant, where width$_1$ was the widest part of the plant and width$_2$ was perpendicular to width$_1$.

Leaf Chlorophyll and Fluorescence Measurements

Foliar chlorophyll content index [CCI; the ratio of % transmission 569 at 931 nm and % transmission at 653 nm (Parry et al., 2014)] was measured in upper and lower canopy leaves in week 3. Measurements of CCI were taken from the center leaflet of the three youngest fully-expanded fan leaves

TABLE 1 | Range of canopy-level UV photon flux density, UV biologically-effective photon flux density and daily UV biologically-effective dose from UV LEDs with a peak wavelength of 287 nm and a daily 3.5 h photoperiod.

UV exposure level	UV photon flux density ($\mu mol \cdot m^{-2} \cdot s^{-1}$)	UV biologically-effective[z] photon flux density ($\mu mol \cdot m^{-2} \cdot s^{-1}$)	Daily UV biologically-effective dose ($kJ \cdot m^{-2} \cdot d^{-1}$)
Minimum	0.01	0.032	0.16
Low	0.1	0.32	1.6
Moderate	0.5	1.6	8.0
Maximum	0.8	2.6	13

[z]*Weighted using the Biological Spectral Weighting Factor for Plant Growth by Flint and Caldwell (2003).*

and from three fan leaves at the bottom of each plant using a chlorophyll meter (CCM-200; Opti-Sciences, Hudson, NH, United States). The CCI measurements were averaged, for the upper and lower canopy leaves, respectively, on a per plant basis.

The ratio of variable to maximum fluorescence (F_v/F_m) emitted from photosystem II in dark-acclimated leaves exposed to a light-saturating pulse is an indicator of maximum quantum yield of photosystem II photochemistry (Murchie and Lawson, 2013). In week 5, during the first 8.5 h of the PAR photoperiod (i.e., before daily UV exposure), the middle leaflet of the youngest fully-expanded fan leaf from each plant was dark acclimated for 15 min and then F_v/F_m measurements were taken with a fluorometer (FluorPen FP 100; Drasov, Czech Republic).

Leaf Gas Exchange, Leaf Size and Specific Leaf Weight

Quantifications of leaf gas exchange of the middle leaflet of the youngest, fully-expanded fan leaf on each treatment plant was performed in week 5 during the first 8.5 h of the PAR photoperiod using a portable photosynthesis machine (LI-6400XT; LI-COR Biosciences, Lincoln, NE, United States) equipped with the B and R LED light source (6400-02B; LI-COR Biosciences). *In situ* net CO_2 exchange rate (NCER) was measured with the leaf cuvette environmental conditions set to: PPFD of 500 $\mu mol \cdot m^{-2} \cdot s^{-1}$, block temperature of 26.7°C, CO_2 concentration of 400 ppm, and air flow rate of 500 $\mu mol \cdot s^{-1}$. Because the leaflets were not wide enough to cover the entire cuvette, the section of each leaflet that was clamped in the cuvette gasket was marked along the outside of the gasket with a permanent marker so that leaf area inside the cuvette could be calculated *post hoc* (described below). After removing the leaflets from the cuvette, whole leaves were excised from the plant and scanned (CanoScan LiDE 25; Canon Canada Inc., Brampton, ON, Canada) at 600 dpi resolution. Each leaf was oven dried to constant weight at 65°C (Isotemp Oven 655G; Fisher Scientific, East Lyme, CT, United States). The scanned images were processed using ImageJ 1.42 software (National Institute of Health; https://imagej.nih.gov/ij/download.html) to determine the leaflet area within the gas exchange chamber (by subtracting the width of the chamber gaskets from the marks made during gas exchange measurements) and the total individual leaf size. The NCER for each leaf was corrected for measured leaf area inside the cuvette. The dry weight (DW) of each entire scanned leaf was measured using an analytical balance (MS304TS/A00; Mettler-Toledo, Columbus, OH, United States) to determine specific leaf weight [SLW; leaf DW/leaf size ($g \cdot m^{-2}$)].

Visual Observations

Weekly observations were performed on each entire plant to visually evaluate observable changes in morphological attributes, including: upward curling of the leaflet margins, leaf shine, browning of stigmas, leaf epinasty, leaf necrotic patches, and appearance of powdery mildew on the adaxial sides of the leaves. Except for week 1 observations, which occurred 4 d after the start of the UV treatments, all weekly observations occurred on 7-d intervals thereafter. The absence or presence of each respective parameter was evaluated for each plant weekly, except where noted in the results (**Table 2**). While these are observational data, the minimum UV-PFDs under which individual attributes were observed were reported, on per cultivar and per week bases, regardless of whether all plants exposed to higher UV-PFDs displayed the observed responses.

At various points throughout the trial, photos of representative whole plants and specific tissues of each cultivar growing under different UV exposure levels were taken with a digital camera (iPhone XR iOS 14.4.1; Cupertino, CA, United States) or flat bed scanner (CanoScan LiDE 25). Photos of whole plants grown under minimum and maximum UV exposure levels were taken in week 2. Photos of the inflorescences grown under minimum and maximum exposure levels, of each cultivar, were taken in week 3. Photos of whole plants grown under minimum, low, moderate and maximum UV exposure levels (described in **Table 1**) were taken in week 3. In week 5 [i.e., approximately when vegetative growth in cannabis ceases (Rodriguez-Morrison et al., 2021a)], fully-expanded leaves from plants under minimum, moderate, and high UV exposure were excised from the plants and scanned at 600 dpi resolution. Photos of whole plants and apical inflorescences grown under minimum, low, moderate, and maximum UV exposure levels were taken at harvest (i.e., week 9). All photos were processed using ImageJ 1.42 software to add appropriate scale bars.

Yield and Quality

After 60 d of UV exposure, all treatment plants were harvested by cutting the stems at substrate level. The LEDs were turned off prior to harvest and plants were harvested, randomly, one at a time to minimize any harvesting effects on fresh biomass assessments. The aboveground tissue of each plant was separated into stems, leaves, and inflorescences. The inflorescences were further subdivided into apical (i.e., grouping of terminal inflorescences at the top of the main stem, located above the uppermost side-branch) and non-apical groupings. All inflorescence tissues were trimmed of foliar materials, according to the cultivator's normal practices. The fresh weights (FW) of stems, leaves, and apical and non-apical inflorescence were separately recorded for each plant using a precision balance (EG 2200-2NM; Kern, Balingen,

TABLE 2 | Minimum UV-PFD ($\mu mol \cdot m^{-2} \cdot s^{-1}$) where symptoms were observed in *Cannabis sativa* 'Low Tide' (LT) and 'Breaking Wave' (BW) cultivars in each week after the initiation of UV treatments, regardless of whether all plants above the minimum UV-PFD presented the observed symptom.

		Foliar			Inflorescence
Week[z]	Cultivar	Upward curling	Epinasty	Necrotic patches	Stigma browning
1	LT	0.33	NI[y]	NI	NI
1	BW	0.37	NI	NI	NI
2	LT	NIE[x]	NI	NI	NI
2	BW	NIE	NI	NI	NI
3	LT	NIE	NI	NI	0.69
3	BW	NIE	NI	NI	0.30
4	LT	NIE	NI	NI	0.22
4	BW	NIE	NI	NI	0.14
5	LT	0.16	0.13	NI	0[w]
5	BW	0.34	0.14	NI	NIE
6	LT	0.13	NIE	NI	0
6	BW	0.33	NIE	NI	0
7	LT	NIE	0.10	0.12 to 0.69[v]	0
7	BW	NIE	0.13	0.32	0
8	LT	NIE	0.018	0.12 to 0.70	0
8	BW	NIE	0.034	0.20 to 0.51	0
9	LT	NIE	NIE	NIE	0
9	BW	NIE	NIE	NIE	0

[z] *All weekly observations occurred on 7-d intervals except for observations in week 1, which occurred 4 days after the start of the UV treatments.*
[y] *NI: symptom was not investigated.*
[x] *NIE: no increase in extent of crop sensitivity to UV exposure level was observed.*
[w] *Zero indicates that the symptom was observed at the lowest UV-PFD.*
[v] *Ranges are provided when the symptom was observed in only intermediate UV-PFDs.*

Germany). The apical inflorescences for 18 plants of each cultivar that were representative of the entire range of UV-PFD exposure levels were air dried at 15°C and 40% relative humidity for 7 d. Following air drying, ≈2 g sub-samples (actual weights were recorded) from each plant were submitted to an independent laboratory (RPC Science & Engineering; Fredericton, NB, Canada) for analysis of concentrations [reported in $mg \cdot g^{-1}_{(DW)}$] of cannabinoids using ultra-high-performance liquid chromatography and variable wavelength detection (HPLC-VWD), terpenes using gas chromatography and mass spectrometry detection (GC-MSD), and moisture content. The total equivalent (annotated with: *eq*) Δ^9-THC, CBD, and cannabigerol (CBG) concentrations were determined by assuming complete carboxylation of the acid-forms of the respective cannabinoids, whose concentrations were adjusted by factoring out the acid-moiety from the molecular weight of each respective compound [e.g., Δ^9-THC*eq* = (Δ^9-THCA × 0.877) + Δ^9-THC]. The remaining apical tissues from the air-dried samples and the entire apical inflorescences of the non-air-dried plants were re-combined with non-apical inflorescences to make up total inflorescence groupings, on a per-plant basis. All separated aboveground tissues of all plants were oven-dried at 65°C to constant weight (Isotemp Oven 655G) and the DW of the respective tissues were recorded. Moisture content of each separated aboveground tissue grouping was calculated as: [(FW – DW) / FW] × 100%. The sub-sampled apical tissues were accounted for in this calculation using their respective sample weight and moisture content measurements for each sample, provided by RPC.

Statistical Analysis

The UV-PFD in this experiment was a continuous, independent variable based on the weekly calculated UV-PFDs for each individual plant. On a per cultivar bases, the best-fit models (linear, quadratic, or cubic) for measured parameters vs. UV-PFD were selected based on the lowest value for the Akaike Information Criterion (AICc) using UV-PFD as the independent variable using the PROC NLMIXED procedure (SAS Studio Release 3.8; SAS Institute Inc., Cary, NC, United States). Analyses also revealed that each dataset had a normal distribution. For parameters that were measured prior to harvest, the average UV-PFD for each plant determined based on the weekly UV measurements made until the parameter was measured. If there were no UV-PFD treatment effects on a given parameter, then parameter means (± SD) were calculated.

RESULTS

The canopy-level average UV-PFDs ranged from 0.01 to 0.8 $\mu mol \cdot m^{-2} \cdot s^{-1}$ for both cultivars; therefore, this range was used to contextualize the models presented below (e.g., lowest vs. highest UV-PFD) for all measured parameters. The average (± SE, n = 44) increases in UV-PFD between adjacent UV-PFD levels was 2.3 ± 0.46% for LT and 2.3 ± 0.39% for BW. The

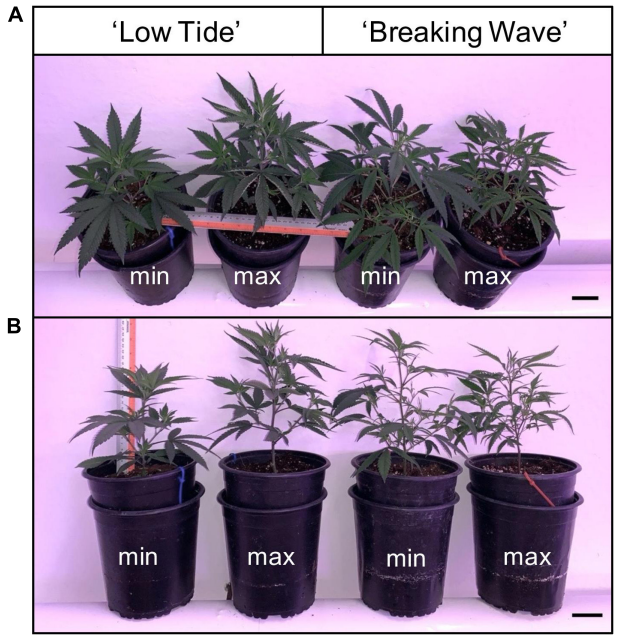

FIGURE 3 | (A) Side and **(B)** top views of representative *Cannabis sativa* plants of 'Low Tide' and 'Breaking Wave' under minimum (min) and maximum (max) UV exposure levels in week 2 after the initiation of the UV treatments. The black scale bar at the lower right of each image is 5.0 cm.

photon flux ratio of PAR to UV at the maximum UV-PFD was ≈500:1, which was within the range normally reported for PAR to UVB in the solar spectrum.

UV-Induced Cannabis Morphology and Physiology Changes

While the aboveground portions of each entire plant was observed for UV-induced changes in morphology, the recorded effects occurred primarily in recently-developed tissues. When UV effects were also seen in older tissues, this has been highlighted in the text. The data in **Table 2** are provided to show how the development of temporal trends in these observed parameters related to each other, and how crop sensitivity to UV exposure increased over time.

The first observed UV-induced changes in cannabis morphology appeared within the first few days of the initiation of the UV treatments where the leaflet margins on leaves that had developed in the vegetative stage (i.e., prior to the initiation of the UV exposure) curled upwards under UV-PFDs ≥0.33 and ≥0.37 $\mu mol \cdot m^{-2} \cdot s^{-1}$ in LT and BW, respectively during week 1 (**Table 2**). Leaves also appeared to accumulate epicuticular wax, as demonstrated by the increase in shiny appearance of adaxial surfaces, shortly after UV exposure began and persisted henceforth (data not shown). Leaf shine appeared to be more prevalent in plants exposed to higher UV-PFDs, and the prevalence appeared to be greater in BW vs. LT. In week 2 there were no changes in the extent of upward curling in mid-canopy foliage (i.e., leaves that had developed during the vegetative stage) however, newly expanded leaves did not appear to present this symptom with the same level of severity (**Figure 3**). In week 3, which was about one week after the presence of inflorescence tissues were readily apparent, stigmas of terminal inflorescences began to turn from white to brown on LT and BW plants exposed to UV-PFDs ≥0.69 and ≥0.30 $\mu mol \cdot m^{-2} \cdot s^{-1}$, respectively (**Figure 4** and **Table 2**). In week 3, early symptoms of foliar epinasty (i.e., interveinal tissues that were raised in the middle) started to appear in upper canopy leaves only of plants grown under higher UV-PFDs (**Figure 4**). Some leaves at the bottom of the plants started to become yellow and drop off in week 3 for both cultivars under higher UV-PFDs (data not shown). Fallen leaves appeared to be predominantly the same leaves that showed upward curling in week 1. There were no UV treatment effects on the CCI of the upper canopy leaves of LT in week 3, but the CCI of the upper canopy leaves of BW decreased linearly by 42% from the lowest to highest UV-PFD (**Figures 5A,B**). The CCI in the lower canopy leaves decreased linearly by 60% and 46% from the lowest to highest UV-PFD in LT and BW, respectively (**Figures 5C,D**). In week 4, the minimum UV-PFD at which plants exhibited stigma browning were lower than the previous week (**Table 2**). In week 5, the *in situ* NCER of the youngest fully-expanded leaves decreased linearly with increasing UV exposure, with 31% and 27% lower NCER at highest vs. lowest UV-PFD in LT and BW, respectively (**Figures 5E,F**). In week 5, the F_v/F_m values of the youngest fully-expanded leaves decreased linearly by 9% and 19% in LT and BW, respectively (**Figures 5G,H**). The severity of UV-induced epinasty was elevated in plants exposed to higher UV exposure levels, as shown in images of whole plants in week 3 (**Figure 6**) and single-leaf scans in week 5 (**Figure 7**) of representative plants grown under different UV exposure levels. In week 5, upper canopy leaves in particular showed upward curling under UV-PFDs ≥0.16 and ≥0.34 $\mu mol \cdot m^{-2} \cdot s^{-1}$ in LT and BW, respectively (**Table 2** and **Figure 7**). In week 5, brown stigmas were observed on plants grown under the lowest UV-PFD in LT and ≥0.14 $\mu mol \cdot s \cdot m^{-2}$ in BW (**Table 2**). In week 5, leaf epinasty was predominantly evident in youngest fully-expanded leaves in plants exposed to UV-PFDs ≥0.13 $\mu mol \cdot m^{-2} \cdot s^{-1}$ in LT and ≥0.14 $\mu mol \cdot m^{-2} \cdot s^{-1}$ in BW (**Table 2**). In week 5, the size of the youngest fully-expanded leaves decreased linearly with increasing UV-PFD, with ≈45% reductions in young leaf size in plants grown under highest vs. lowest UV-PFD (**Figures 8A,B**). There were corresponding linear increases in SLW with increasing UV exposure, with 27% and 21% increases in LT and BW, respectively, in plants grown under the highest vs. lowest UV-PFD (**Figures 8C,D**). Brown stigmas were observed in all experimental plants starting in week 6 (**Table 2**). Starting in week 7, upper canopy leaves on a few LT plants grown under intermediate UV-PFDs, ranging from 0.12 to 0.69 $\mu mol \cdot m^{-2} \cdot s^{-1}$, began to show brown (necrotic) patches (**Table 2**). The minimum UV-PFDs under which leaf epinasty was evident were marginally lower in week 7 vs. week 5, and substantially lower in week 8 vs. week 7 (**Table 2**) in both cultivars. The prevalence of leaves exhibiting necrotic patches increased in BW in week 8 vs. week 7 (**Table 2**). Investigating the effects of UV exposure on foliar powdery mildew was not one of

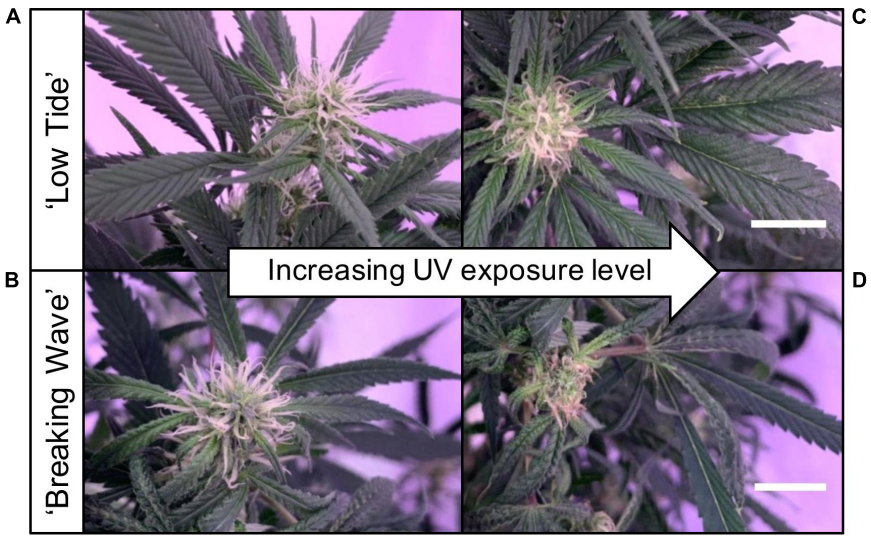

FIGURE 4 | Images of stigmas of representative **(A)** 'Low Tide' (LT) and **(B)** 'Breaking Wave' (BW) *Cannabis sativa* plants grown under minimum UV exposure levels and **(C)** LT and **(D)** BW under maximum UV exposure levels, in week 3 after the initiation of the UV treatments. The white scale bar at the lower right of **(C)** applies to **(A)**, and at the lower right of **(D)** applies to **(B)**. Both scale bars are 1.0 cm.

the objectives at the outset of this study, however, some potential treatment effects were observed. For example, evidence of powdery mildew was visible on the adaxial leaf surfaces on plants exposed to low UV-PFDs at harvest, but was not observed on any plants exposed to UV-PFDs $\geq$0.090 $\mu mol \cdot m^{-2} \cdot s^{-1}$ (**Figure 9**). By harvest, there also appeared to be greater incidences of foliar chlorosis in both cultivars, especially in the lower canopy, with increasing levels of ultraviolet exposure (**Figure 9**).

Growth Responses to UV

Exposure to UV generally suppressed plant growth, which was recorded as increase in height and growth index in week 6. The majority of vegetative growth had ceased by week 6 given that height only increased 1.76 $\pm$ 0.41 cm and 0.62 $\pm$ 0.48 cm (mean $\pm$ SE) for LT and BW respectively, between week 6 and harvest (data not shown). Both increase in height and growth index had negative linear relationships with increasing UV-PFD in both cultivars. Increases in height were 31% and 26% lower in plants grown under the highest vs. lowest UV-PFDs in LT and BW, respectively (**Figures 8E,F**). Growth indices were 61% and 33% lower in plants grown under the highest vs. lowest UV-PFDs in LT and BW, respectively (**Figures 8G,H**). There were no UV treatment effects on the moisture content of any aboveground tissues in either cultivar (**Table 3**).

Responses of Inflorescence Yield, Apparent Quality, Cannabinoid and Terpene Concentrations to UV

The most discernable UV exposure effects on inflorescences were differences in the size of the apical inflorescences (**Figure 10**). The apical inflorescence DW decreased linearly by 78% and 69% in LT and BW, respectively, from the lowest to highest UV-PFD (**Figures 11A,B**). However, the reduction in apical inflorescence DW under increasing UV exposure only translated to reductions in total inflorescence DW in LT (**Figures 11C,D**). Approximately 60% of the reduction of the total inflorescence DW in LT at the highest vs. lowest UV exposure levels (a 32% reduction) arose from decreases in the DW of the apical inflorescences. The leaf DW were 19% and 32% lower under highest vs. lowest UV-PFD in LT and BW, respectively (**Figures 11E,F**); and there were no UV treatment effects on stem DW in either cultivar (**Table 3**).

At the minimum UV exposure levels, the concentrations of the acid and neutral forms of both Δ^9-THC and CBD and the ratio of Δ^9-THC to CBD were within the normal range for each of these cultivars grown in the same production environment (without UV) according to the cultivator (personal communication). The effects of UV exposure on the apical inflorescence secondary metabolite composition varied between the two cultivars (**Table 3** and **Figure 12**). Graphical representations of the best fit models for minor cannabinoids and terpenes that had UV-exposure treatment effects in at least one cultivar are also presented **Supplementary Figures 1–12**. In LT, the concentrations of Δ^9-THCA, CBDA and CBGA decreased linearly by 15%, 21%, and 31%, respectively, as UV-PFD increased from lowest to highest; with concomitant reductions in Δ^9-THC*eq*, CBD*eq*, and CBG*eq*. As UV-PFD increased from lowest to highest, the concentrations of myrcene, limonene, fenchol all decreased in LT, resulting in a combined 41% decrease in the total terpene content. In BW, the Δ^9-THC concentration was 1.6 times higher and the ratio of Δ^9-THC*eq* to CBD*eq* was 10% higher under the highest vs. lowest UV-PFD. The myrcene and linalool concentrations decreased while caryophyllene and guaiol concentrations increased with increasing UV-PFD, resulting in a combined 24% decrease in the total terpene content in BW at the highest vs. lowest UV-PFD.

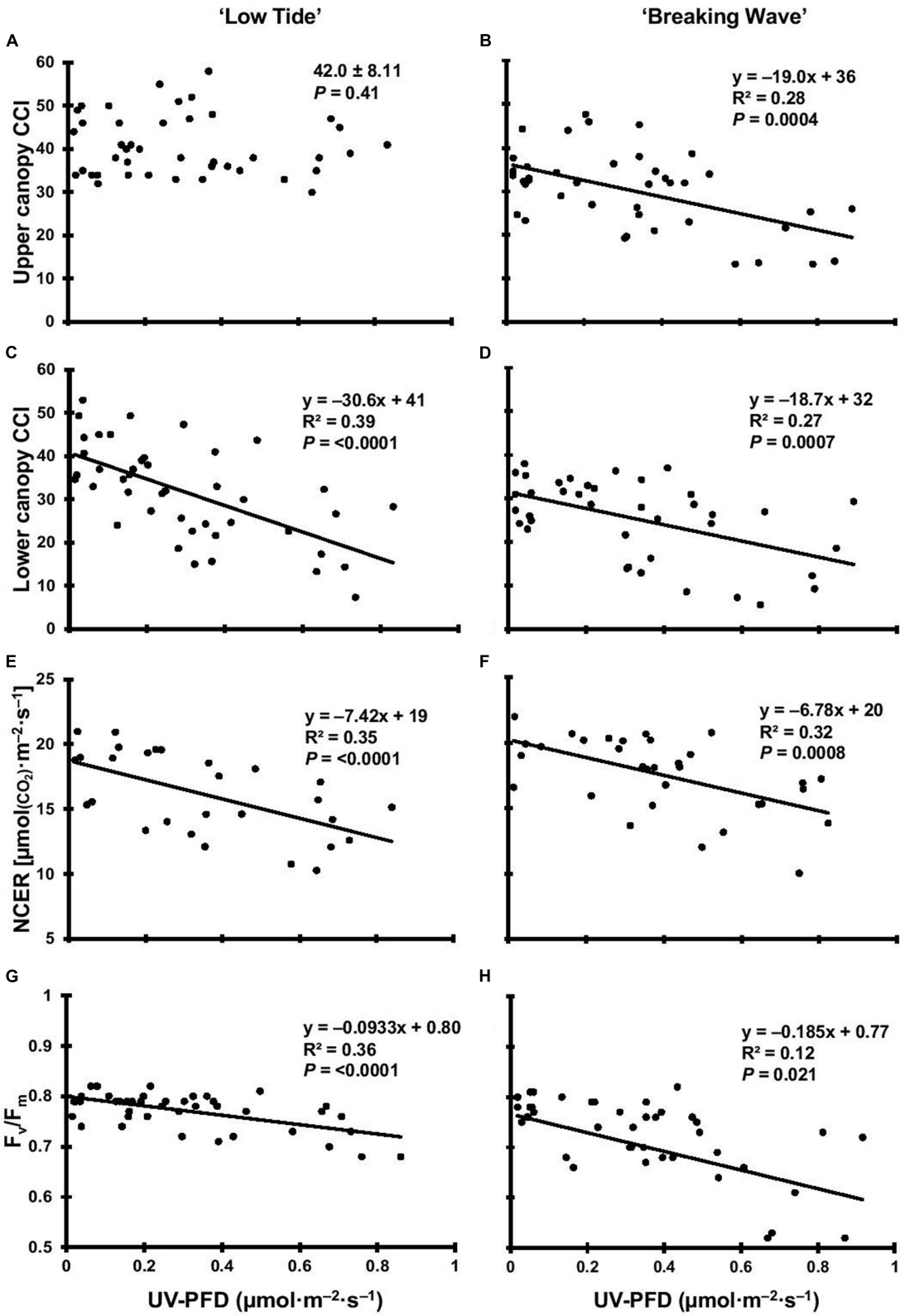

FIGURE 5 | The upper canopy leaf chlorophyll content index (CCI) of *Cannabis sativa* 'Low Tide' **(A)** and 'Breaking Wave' **(B)**, the lower canopy leaf CCI of 'Low Tide' **(C)** and 'Breaking Wave' **(D)**, the net CO_2 exchange rate (NCER) of 'Low Tide' **(E)** and 'Breaking Wave' **(F)**, and the F_v/F_m of 'Low Tide' **(G)** and 'Breaking Wave' **(H)** in response to increasing UV-PFD. Each datum is a single plant.

DISCUSSION

Both LT and BW cultivars would be categorized as chemotype II because they have relatively balanced ratio of Δ^9-THC to CBD (Small and Beckstead, 1973). However, they demonstrated disparate morphological attributes: LT had a relatively compact phenotype with wide leaflets and BW had a relatively spindly phenotype with narrow leaflets. Each cultivar responded to UV exposure with different magnitudes of severity but, in the majority of the parameters that had UV treatment effects, increasing UV exposure resulted in distress-type responses [i.e., damage to plant growth and health following a strong stress event (Hideg et al., 2013)] that would be generally unfavorable for commercial cannabis production.

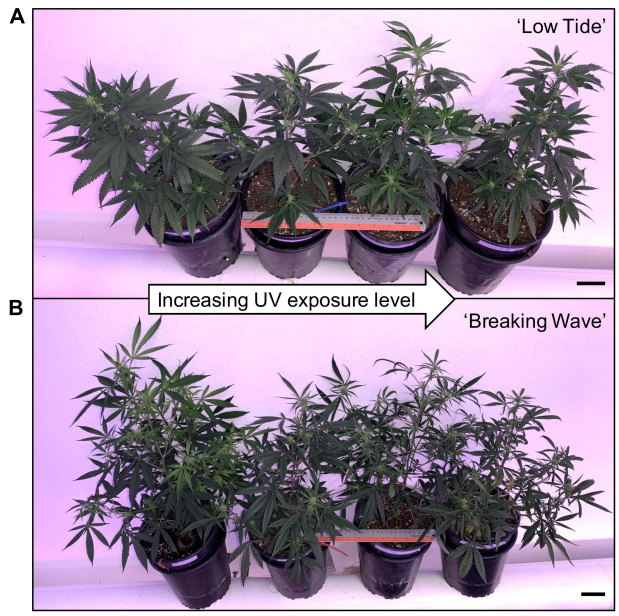

FIGURE 6 | Representative **(A)** 'Low Tide' and **(B)** 'Breaking Wave' *Cannabis sativa* plants demonstrating (from left to right) minimum, low, moderate, and high UV exposure levels. The images were taken in week 3 after the initiation of the UV treatments. The black scale bar at the lower right of each image is 5.0 cm.

UV Radiation Alters Cannabis Morphology and Physiology

Leaf morphology demonstrated substantial plasticity in response to UV radiation exposure throughout the 9-week flowering stage. The first observed morphological response to UV was upward curling of leaflet margins during the first week of UV exposure. Upward leaf curling was most evident under higher UV-PFDs, and it occurred primarily on the youngest leaves (i.e., that developed in the vegetative stage, just prior to UV exposure). Upward leaf curling under UV stress is not a commonly-reported morphological response, although it has been observed in cotyledons of canola (Wilson and Greenberg, 1993). Upward leaf curling has been a more commonly- reported response to pathogen infection in some crops (Taliansky et al., 2003; Halldorson and Keller, 2018) and to various physiological stresses in tomato, including light stress (Powell et al., 2014). The recently-developed leaves in the present study may also have lacked the acclimative plasticity of the leaves that later developed under UV exposure, which exhibited more typical UV-induced morphology responses such as epinasty, reduced leaf size and increased leaf thickness indicated by SLW (Wilson, 1998; Searles et al., 2001; Zlatev et al., 2012; Fierro et al., 2015). Further, the apparent increase in leaf shine shortly after the initiation of UV exposures indicates an accumulation of epicuticular wax, which is a common response to UV exposure in other crops (Steinmüller and Tevini, 1985; Cen and Bornman, 1993; Fukuda et al., 2008; Valenta et al., 2020). All of these observed morphological responses to UV exposure may reduce the potential for damage to the photosynthetic machinery.

UV radiation accelerated plant senescence (i.e., deterioration with age) symptoms in both inflorescence and foliar tissues. Female inflorescence maturation can normally be characterized by carpel swelling and the transition of stigmas from white to

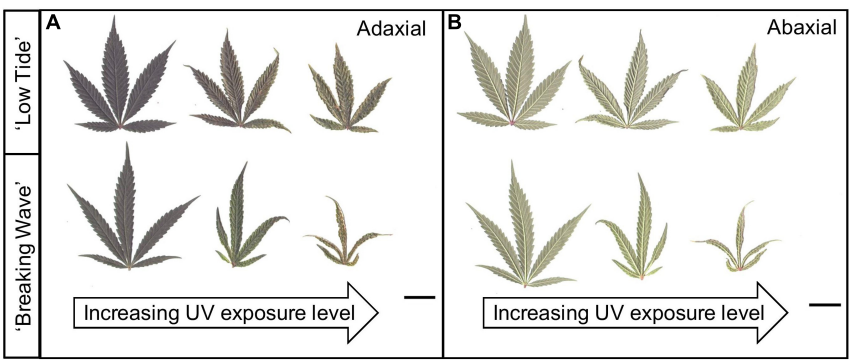

FIGURE 7 | (A) Adaxial and **(B)** abaxial sides of representative youngest, fully-expanded *Cannabis sativa* fan leaves of 'Low Tide' (top row in each image) and 'Breaking Wave' (bottom row in each image) demonstrating UV induced leaf morphology effects with increasing UV-PFD. Leaves from plants under minimum UV exposure are on the left, moderate UV exposure in the middle, and high UV exposure on the right. Scans were taken in week 5 after the initiation of UV treatments. The black scale bar at the lower right of each image is 2.0 cm.

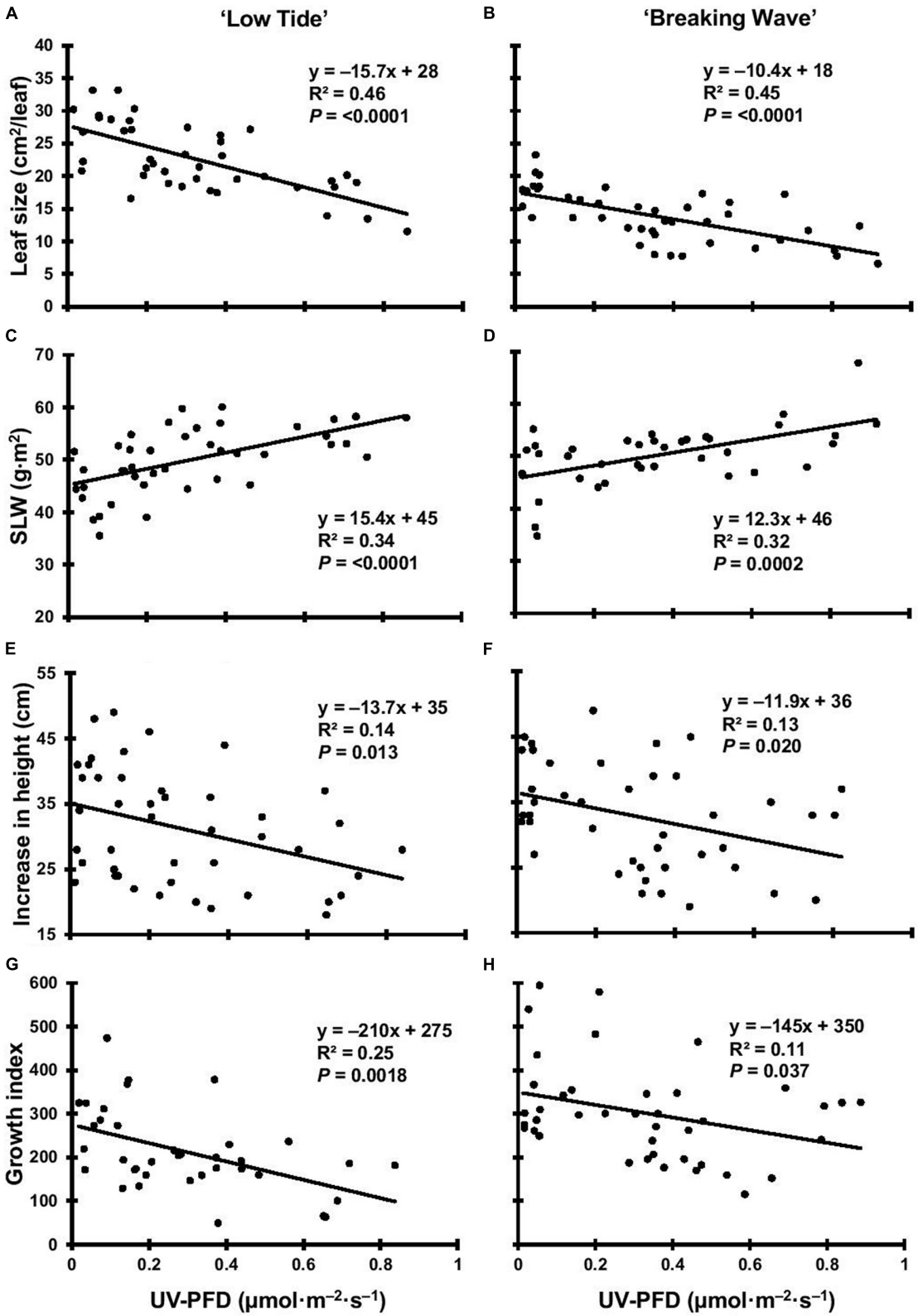

FIGURE 8 | The leaf size of *Cannabis sativa* 'Low Tide' **(A)** and 'Breaking Wave' **(B)**, the specific leaf weight (SLW) of 'Low Tide' **(C)** and 'Breaking Wave' **(D)**, the increase in height of 'Low Tide' **(E)** and 'Breaking Wave' **(F)** and the growth index of 'Low Tide' **(G)** and 'Breaking Wave' **(H)** in response to increasing UV-PFD. Each datum is a single plant.

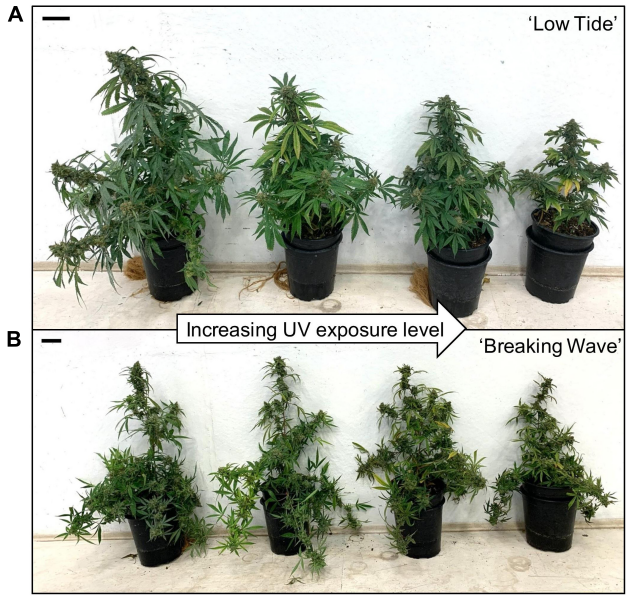

FIGURE 9 | Gross plant morphology of representative **(A)** 'Low Tide' and **(B)** 'Breaking Wave' *Cannabis sativa* plants grown under (from left to right) minimum, low, moderate, and high UV exposure levels. Images were taken just prior to harvest (i.e., 9 weeks after the initiation of UV treatments). Note the white spots (powdery mildew) on the adaxial sides of leaves on the far-left plants in both images. The black scale bar at the upper left of each image is 5.0 cm.

brown in the final days before harvest (Punja and Holmes, 2020). Although the number of days between the initiation of the 12-h photoperiod and appearance of inflorescences was unaffected by UV exposure (data not shown), plants exposed to higher UV-PFDs exhibited earlier stigma browning (**Figure 4**). It is unknown if premature stigma senescence has any knock-on effects on other inflorescence development parameters, such as production of secondary metabolites. However, since the rate of stigma browning depended on UV exposure levels, this attribute could not be used reliably to determine the "optimum harvest maturity" for the plants in this trial.

Foliar chlorophyll content is often negatively correlated to UV exposure level (Neugart and Schreiner, 2018). Both cultivars showed increasing SLW with increasing UV exposure; similar to cannabis exposed to high PAR intensity (Rodriguez-Morrison et al., 2021a). While the CCI levels measured in this study were within the ranges of cannabis leaves reported by others (Caplan et al., 2017; Yep et al., 2020; Rodriguez-Morrison et al., 2021a), there were only UV treatment effects on CCI in the upper canopy leaves of BW. However, LT showed relatively greater increases in SLW with increasing UV exposure. Since foliar thickness affects a leaf's optical properties, hence CCI measurements (Parry et al., 2014), LT's enhanced increases in leaf thickness may have offset any UV-induced reductions in chlorophyll concentration on a biomass basis (e.g., $mg{\cdot}g^{-1}$) in this cultivar. While lower vs. upper canopy leaves in indoor-grown cannabis may have lower CCI, regardless of plant age (Rodriguez-Morrison et al., 2021a), the reductions in lower-canopy chlorophyll content with increasing UV-PFD in both cultivars may be another indication of the UV damage done to young leaves at onset of UV exposure. This damage eventually manifested as higher rates of early leaf-drop and increased leaf chlorosis at harvest in plants exposed to higher UV-PFDs. Both of these phenomena have also been observed in UV-stressed sweet basil (Dou et al., 2019). Nitrogen from lower canopy leaves is normally remobilized to more active upper canopy foliage as plants age (Havé et al., 2017); this appeared to be accelerated by UV exposure given the reductions in lower-canopy CCI after only 3 weeks of exposure. Foliar necrosis is also a commonly-observed symptom of UV damage in many species (Maffei and Scannerini, 2000; Zhao et al., 2003; Dou et al., 2019). While the severity of most of the observed UV stress responses increased with increasing UV exposure, necrotic patches were observed on upper canopy leaves that were predominantly exposed to intermediate UV-PFDs (primarily in LT) in the latter weeks of the trial. The acclimation (e.g., epinasty, curling, reduced size) of leaves exposed to the highest UV-PFDs may have mitigated foliar damage, while the leaves grown under intermediate UV-PFDs may not have been sufficiently acclimated for long-term UV exposure. Unstressed leaves normally have F_v/F_m values of ≈0.8 (Björkman and Demmig, 1987). While the reductions in F_v/F_m in upper canopy leaves of both cultivars were similar to cannabis plants exposed high PAR intensity in Rodriguez-Morrison et al. (2021a), the opposite effects of increasing UV vs. PAR radiation on NCER is strongly indicative of UV-induced damage to the photosynthetic machinery.

Lydon et al. (1987) reported no UV treatment effects on the cannabis morphology and physiology parameters they measured, which is in stark contrast to the copious morphological and physiological UV-induced stress responses observed in the present study. Evidently, the plants in the present study were subjected to more efficacious UV radiation treatments than in Lydon et al. (1987) despite similar reported maximum biologically-effective UV doses in both studies. This may be partly due to the shorter-wavelength UV spectrum in the present study. Further, the plants in Lydon et al. (1987) may have experienced lower than reported doses due to rapid UV-induced reductions of UVB transmissivity of the cellulose acetate filters they used to eliminate UVA and PAR wavelengths from their UV spectrum treatments (Middleton and Teramura, 1993). Additionally, their plants grew for several months under greenhouse conditions (likely including some UV) prior to exposure to UV treatments, whereas there was no UV exposure of the plants prior to initiation of the UV treatments in the present study. Therefore, light history (e.g., spectrum and intensity) and plant age may affect how plants to acclimate to new UV stresses.

UV Radiation Suppresses Cannabis Growth and Yield

While increasing UV radiation exposure suppressed overall vegetative plant growth (e.g., height and growth index) in both cultivars, the responses were more severe in LT than BW.

TABLE 3 | The effects of UV-PFD ($\mu mol \cdot m^{-2} \cdot s^{-1}$) applied during the flowering stage on aboveground tissue moisture content (%), stem dry weight (DW; $g \cdot m^{-2}$), and cannabinoid and terpene concentrations [$mg \cdot g^{-1}{}_{(DW)}$] in the mature, air-dried apical inflorescence tissues of *Cannabis sativa* 'Low Tide' and 'Breaking Wave.'

Parameter	'Low Tide'		'Breaking Wave'	
	Regression equation[z], R^2 or mean ± SD[y]	*P*-value	Regression equation, R^2 or mean ± SD	*P*-value
Inflorescence moisture content	79.0 ± 1.27	0.14	79.3 ± 1.01	0.37
Leaf moisture content	69.5 ± 3.59	0.94	72.0 ± 2.31	0.28
Stem moisture content	72.4 ± 2.93	0.77	74.5 ± 2.17	0.41
Stem DW	49.2 ± 26.5	0.44	46.1 ± 21.6	0.16
Δ^9-tetrahydrocannabinol (Δ^9-THC)	1.66 ± 0.347	0.18	y = 1.02x + 1.4, 0.33	0.013
Δ^9-THC acid (Δ^9-THCA)	y = −15.9x + 84, 0.29	0.020	73.8 ± 12.2	0.91
Cannabidiol (CBD)	1.38 ± 0.447	0.56	1.47 ± 0.338	0.12
CBD acid (CBDA)	y = −33.9x + 130, 0.43	0.0032	93.8 ± 13.8	0.46
Cannabigerol (CBG)	0.657 ± 0.275	0.57	1.27 ± 0.217	0.85
CBG acid (CBGA)	y = −3.31x + 8.6, 0.58	0.0003	6.04 ± 1.07	0.82
Δ^9-THC*eq*:CBD*eq*[x]	0.678 ± 0.0387	0.18	y = 0.0980x + 0.76, 0.26	0.030
Cannabinol (CBN)	UDL[w]	–	UDL	–
Alpha pinene	UDL	–	0.214 ± 0.0593	0.91
Beta pinene	0.235 ± 0.0672	0.37	0.440 ± 0.124	0.067
Myrcene	y = −4.16x + 6.2, 0.38	0.0089	y = −2.47x + 3.5, 0.36	0.0082
Limonene	y = −0.788x + 1.3, 0.34	0.014	1.57 ± 0.423,	0.058
Linalool	0.274 ± 0.0703	0.27	y = −0.147x + 0.22, 0.53	0.0010
Terpineol	0.254 ± 0.0655	0.32	0.379 ± 0.108	0.26
Caryophyllene	2.42 ± 0.746	0.28	y = 0.520x + 1.1, 0.35	0.0092
Humulene	0.892 ± 0.324	0.42	0.403 ± 0.0842	0.39
Fenchol	y = −0.118x + 0.22, 0.32	0.018	0.257 ± 0.0653	0.52
Guaiol	0.801 ± 0.100	0.17	y = 0.251x + 0.46, 0.31	0.016
Alpha-bisabolol	0.677 ± 0.181	0.26	0.355 ± 0.104	0.14
Total terpenes	y = −7.25x + 14, 0.38	0.0081	y = −2.72x + 9.2, 0.22	0.049

[z] *Parameters with UV treatment effects ($P \leq 0.05$) are presented as equations and R^2.*
[y] *Means ± SD are presented for parameters without UV treatment effects.*
[x] *The total equivalent cannabinoids are annotated with: eq, where Δ^9-THCeq = (Δ^9-THCA × 0.877) + Δ^9-THC, CBDeq = (CBDA × 0.877) + CBD.*
[w] *Under detection limit of 0.5 $mg \cdot g^{-1}$ of inflorescence DW.*

However, these are in contrast with the UV-induced reductions in foliar biomass, which were substantially greater in BW. This was particularly surprising given that there were no consequent reductions in total inflorescence biomass in BW. In fact, despite some leaf senescence observed in both cultivars, harvest index – which is the ratio of inflorescence DW to total aboveground DW – went up by ≈10% in BW and went down by ≈10% in LT as UV-PFD increased from lowest to highest. Under low UV exposure, the harvest index for both cultivars was ≈0.6, which was similar to a different cultivar grown under the same PPFD in the same production system without UV (Rodriguez-Morrison et al., 2021a). Given that there were no UV exposure effects on inflorescence DW in BW, earlier and/or elevated foliar senescence in BW may have contributed to its relatively elevated harvest index.

Reduced aboveground biomass and lower yields are commonly observed effects of UV radiation on some other plant species (Teramura et al., 1990; Fiscus and Booker, 1995; Caldwell et al., 2003; Liu et al., 2005). The UV-induced alterations in leaf morphology and physiology probably contributed to the general reductions in growth and overall biomass in both cultivars. For example, reduced leaf area is a typical response to radiative stresses such as high PAR intensity and UV exposure (Wargent and Jordan, 2013; Poorter et al., 2019). In the present study, the reductions in individual leaf size, total foliar biomass, and leaf-level NCER with increasing UV exposure, would have limited the plants' capacity to convert PAR into biomass (Kakani et al., 2003; Zlatev et al., 2012).

Total inflorescence DW and the proportion of that DW which is comprised of apical tissues are two major considerations for commercial cannabis production. The apical proportion may be of particular interest since these tissues are normally considered premium quality due to their relatively large size and potentially higher cannabinoid concentrations compared to higher-order (i.e., on lower branches) inflorescences (Namdar et al., 2018). Despite the UV-induced limitations to biomass accumulation seen in both cultivars, increasing UV exposure only reduced inflorescence DW in LT. Within this context, the various growth habits of common indoor-grown cannabis cultivars may influence their yield responses to UV stress. In the present study, BW and LT had disparate whole-plant reproductive macro-morphology (i.e., the distribution of inflorescence biomass within the canopy) under normal indoor conditions. For example, under minimum UV exposure, the apical inflorescence comprised 24%

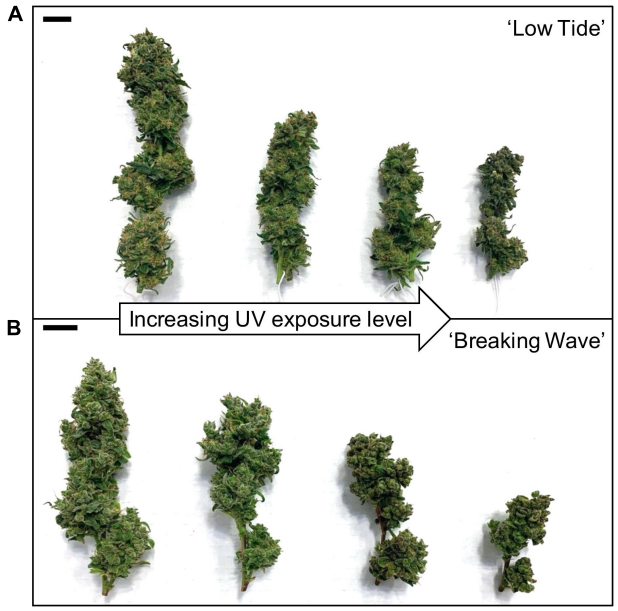

FIGURE 10 | The apical inflorescences of representative **(A)** 'Low Tide' and **(B)** 'Breaking Wave' *Cannabis sativa* plants grown under (from left to right) minimum, low, moderate, and high UV exposure levels. Images were taken at harvest (i.e., 9 weeks after the initiation of UV treatments). The black scale bar at the upper left of each image is 2.0 cm.

of the total inflorescence DW in LT compared to only 11% in BW. Apparently, growth habit may have predisposed BW's mitigation of UV-induced yield reductions by partitioning relatively more inflorescence biomass to positions farther away (i.e., more protected from the UV) from the top of the plant. However, while this may be a self-protective response to reduce UV exposure to reproductively important (from an ecological sense) tissues, it still came at commercially-objectionable reductions in inflorescence quality, such as visually unappealing morphology (**Figure 10**).

To prevent UV-induced yield losses, such as are reported in the present study, it is conceivable that cannabis plants could be exposed to UV only after the majority of vegetative growth has completed [i.e., a few weeks after the visual appearance of inflorescences (Potter, 2014)]. This strategy would shorten the accumulated period of exposure to UV stress and may minimize some UV-induced foliar acclimations that could inhibit biomass accumulation. However, there is a risk that later-term UV exposure might also sufficiently stress unacclimated foliar tissues to provoke rapid-onset whole-plant senescence before the inflorescences reach optimum maturity. This strategy warrants further exploration.

UV Radiation Alters the Secondary Metabolite Composition of Cannabis Inflorescences

The most economically relevant cannabinoids (i.e., Δ^9-THC and CBD) are predominantly found in their acid forms in mature female inflorescence tissues, which are converted to the psychoactive and medicinal neutral forms through decarboxylation (Eichler et al., 2012; Zou and Kumar, 2018). The neutral forms also exist in relatively low quantities in the fresh inflorescences and tend to increase in proportion to the acid forms as the inflorescences mature (Aizpurua-Olaizola et al., 2016). While the Δ^9-THC concentration increased in BW with increasing UV-PFD, it was a relatively small proportion of the Δ^9-THC*eq*; maximized at 3.3% at the highest UV-PFD. Further, CBN was undetectable in the inflorescences, which is an indicator that the crops were not past peak maturity at the time of harvest since Δ^9-THC naturally degrades to CBN (Russo, 2007). There were no UV-induced enhancements to Δ^9-THC*eq*, CBD*eq*, and CBG*eq* in either cultivar. These results are consistent with a recent study that found no UV treatment effects on Δ^9-THC*eq* content in a Δ^9-THC-dominant cultivar (Llewellyn et al., 2021), but contrast with studies on older genotypes (Pate, 1983; Lydon et al., 1987). For example, Lydon et al. (1987) found that inflorescence Δ^9-THC concentrations increased linearly from 32 to 25 mg·g^{-1} in greenhouse-grown cannabis as UV exposure increased from their no-UV control up to biologically-effective UV doses (based on Caldwell, 1971) of 13.4 kJ·m^{-2}·d^{-1}. These contrasting results may be due to the disparate growing conditions (both before and during UV exposure), plant age at the time of UV exposure, and the relative magnitude of cannabinoid concentrations. Further, while the proportional increases in Δ^9-THC content (28%) presented in Lydon et al. (1987) appeared to be substantial, the magnitude of their increase (i.e., only 7 mg·g^{-1}) is probably inconsequential in the context of cannabinoid composition in modern genotypes which can have Δ^9-THC concentrations that exceed 200 mg·g^{-1} (Dujourdy and Besacier, 2017).

Pate (1983) reported an increase in the ratio of Δ^9-THC to CBD in inflorescence tissues of cannabis ecotypes grown in global positions with naturally higher UV exposures, which suggests that the production of Δ^9-THC may be upregulated and CBD downregulated as adaptations (i.e., over multiple generations) to the localized environment. However, the results of the present study do not support this trend, at least as an acclimation response to UV stress of a single generation. Additionally, De Meijer et al. (2003) showed that cannabinoid profiles are largely genetically predetermined (e.g., a CBD-dominant cultivar is lacking the genetic predisposition to generate abundant Δ^9-THC). This favors the concept that the upregulation of Δ^9-THC under UV stress may be an adaptive response (i.e., over generations) rather than an acclimation response (i.e., during a single production cycle). Over the past few decades, there have been radical increases in inflorescence cannabinoid concentrations, which is often attributed to intensive breeding programs (Chouvy, 2015; Dujourdy and Besacier, 2017; Aliferis and Bernard-Perron, 2020) and the "sinsemilla" cultivation method that eliminates seeds and chiefly produces high potency female inflorescences (ElSohly et al., 2016). Thus, these factors may have a larger impact on cannabis inflorescence cannabinoid composition in indoor production than environmental factors such as UV stress.

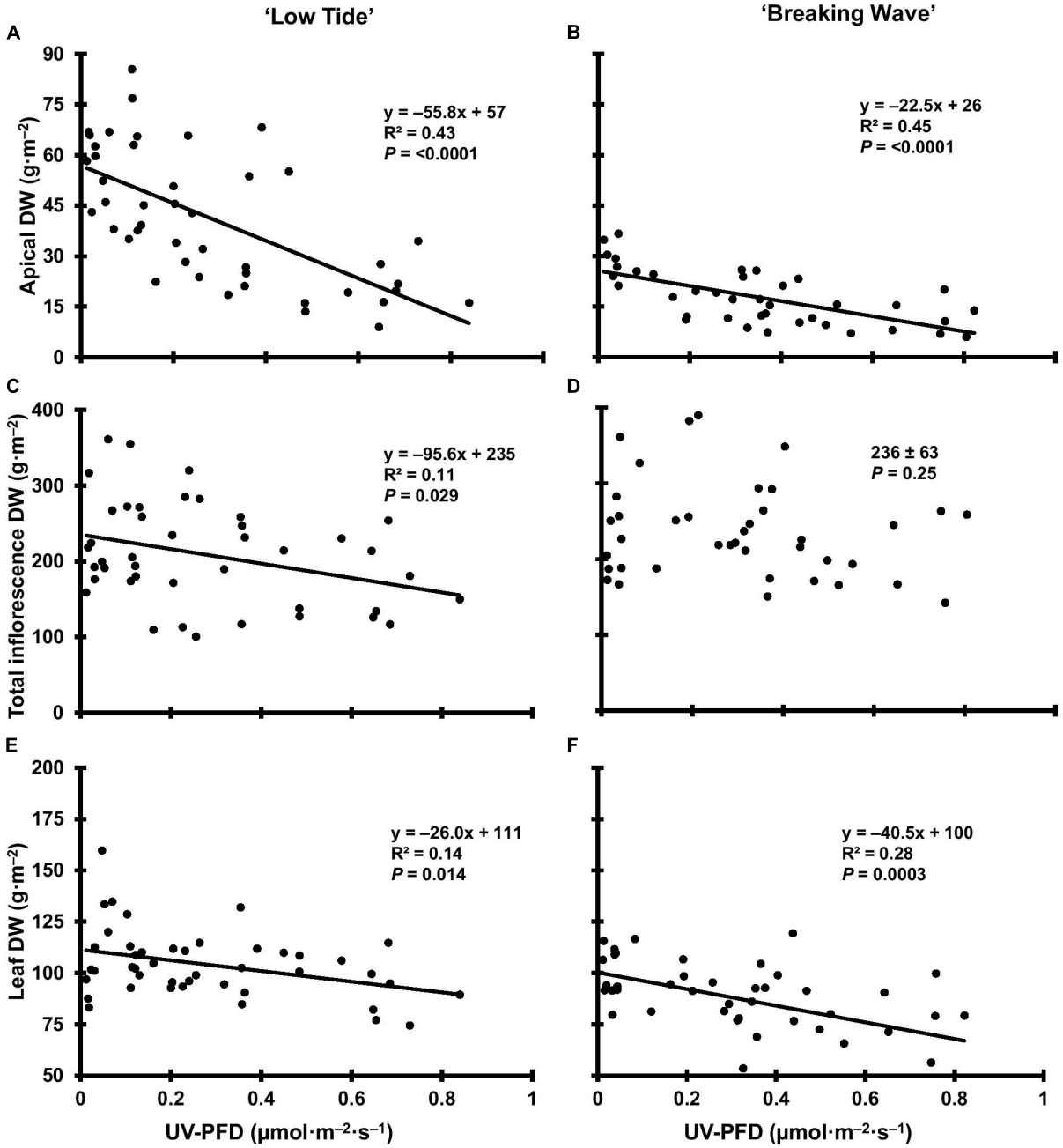

FIGURE 11 | The apical inflorescence dry weight (DW) of *Cannabis sativa* 'Low Tide' **(A)** and 'Breaking Wave' **(B)**, the total inflorescence DW of 'Low Tide' **(C)** and 'Breaking Wave' **(D)** and the leaf DW of 'Low Tide' **(E)** and 'Breaking Wave **(F)** in response to increasing UV-PFD. Each datum is a single plant.

While cannabinoids comprise the primary psychoactive and medicinal compounds in cannabis inflorescences, volatile terpenes are also economically valuable; both for the aromas that influence consumer preference and potential medicinal properties (Nuutinen, 2018; Booth and Bohlmann, 2019). UV exposure equivocally altered the terpene composition in the present study, with disparate responses within the different terpenes and between cultivars. However, total terpene concentrations in both cultivars decreased linearly with increasing UV exposure, which would tend to depreciate the overall quality of aromas and extracts (McPartland and Russo, 2001; Nuutinen, 2018).

While UV exposure did not result in any economically relevant increases in cannabinoid or terpene concentrations in cannabis inflorescences under the conditions of the present study, UV radiation has been shown to increase concentrations of UV-absorbing secondary metabolites (e.g., flavonoids and phenolic compounds) in many species (Huché-Thélier et al.,

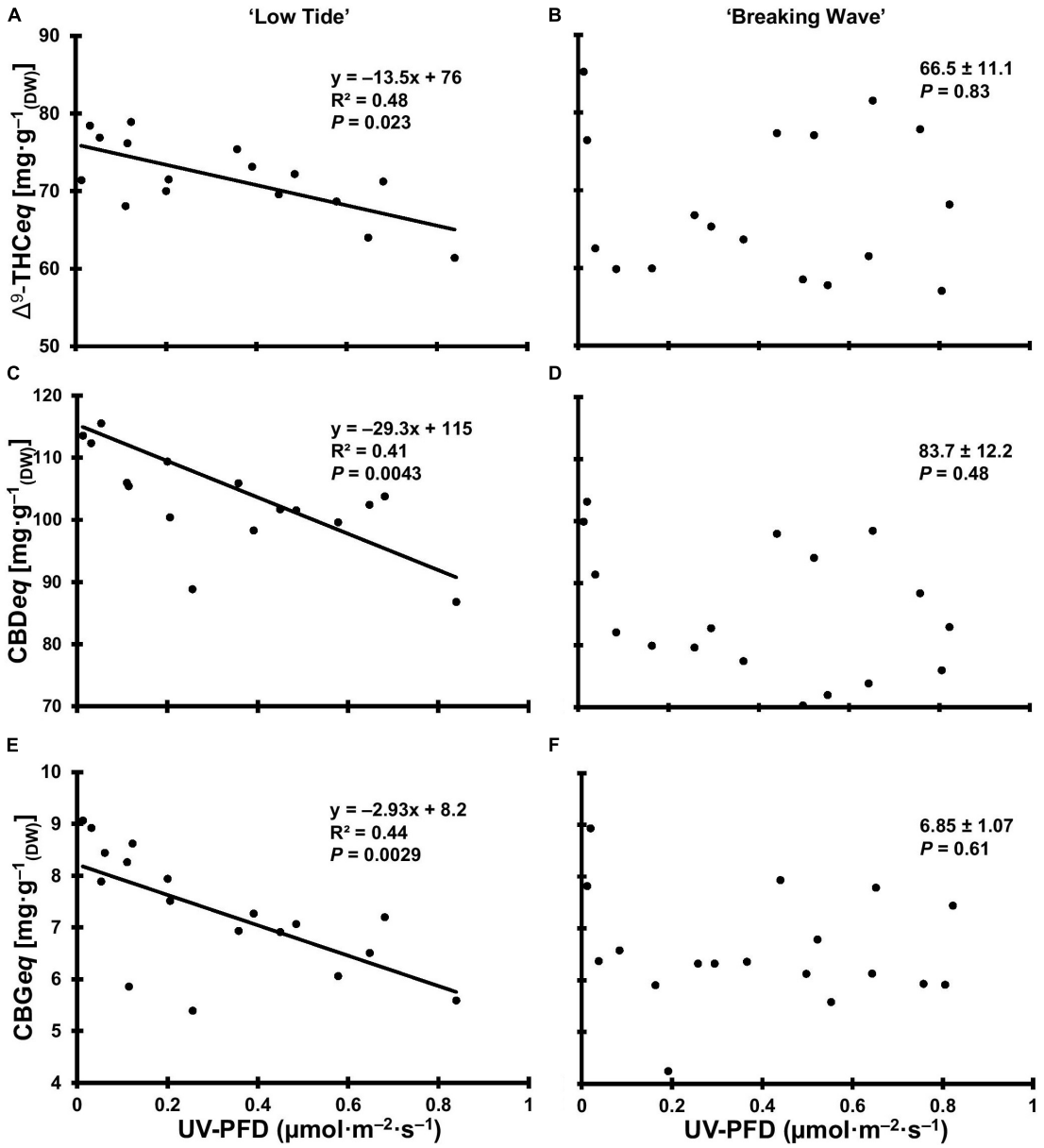

FIGURE 12 | The total equivalent cannabinoid concentrations of Δ^9-tetrahydrocannabinol (Δ^9-THC*eq*) of *Cannabis sativa* 'Low Tide' **(A)** and 'Breaking Wave' **(B)**, cannabidiol (CBD*eq*) of 'Low Tide' **(C)** and 'Breaking Wave' **(D)** and cannabigerol (CBG*eq*) of 'Low Tide' **(E)** and 'Breaking Wave' **(F)** in response to increasing UV-PFD. Each datum is a single plant.

2016; Robson et al., 2019), including economically important essential oil producing crops (Schreiner et al., 2012; Neugart and Schreiner, 2018). However, UV-induced increases in secondary metabolite concentrations are often concurrent with biomass reductions (Fiscus and Booker, 1995; Caldwell et al., 2003). This paradox must be evaluated when considering the use of UV radiation to manipulate secondary metabolite composition in indoor cannabis production, since the simultaneous yield reduction may offset any improvements in secondary metabolite composition.

Compared to the UV spectra employed in most other studies, the biologically effective doses in the present study were dramatically higher for a given photon flux density due to the very short peak wavelength of the UV LEDs. In fact, ≈70% of the UV photon flux were at wavelengths below 290 nm, and thus outside of the solar spectrum that plants would naturally be exposed and adapted to Nikiforos et al. (2011). Therefore, cannabis may respond dramatically differently to UV from slightly longer wavelength LEDs (e.g., 300 to 315 nm).

Implications for UV Use in Indoor Cannabis Production and Future Research Directions

This study provided insight into the sensitivity of cannabis to relatively short-wavelength UVB radiation (including a small proportion of UVC) and long-term UV exposure. Increasing UV exposure levels generally had negative impacts on cannabis plant growth, yield, quality, and secondary metabolite composition. The plants exhibited primarily distress-type responses to UV radiation, even at low exposure levels; no amount of UV exposure resulted in substantial increases of cannabinoid concentrations. While none of the UV exposure levels in the present study would have been commercially beneficial, results from studies in other species (Huché-Thélier et al., 2016; Neugart and Schreiner, 2018; Höll et al., 2019; Robson et al., 2019) indicate a strong potential for there being UV treatment protocols – as yet unidentified through rigorous scientific investigation and reporting – that could enhance secondary metabolite concentrations in cannabis. Further research is required to determine if there is a combination of UV spectrum, intensity and time of application that would have commercially beneficial effects in cannabis production. The range of tested cannabis cultivars should also be expanded to cover a broader range of chemotypes and growth habits.

When making the decision to utilize UV wavelengths (as with any production technology) in indoor cannabis production, the positive crop outcomes must outweigh factors related to the cost of deploying the technology including infrastructure and energy costs, fixture lifespan, and health risks that UV radiation could pose to employes. While UVB LEDs in particular (Kusuma et al., 2020) and UV lighting technologies in general are much less energy efficient than modern horticultural PAR fixtures (Nelson and Bugbee, 2014; Radetsky, 2018), UV fluence rates are also typically many times lower than the PAR spectrum. The functional lifespans of UVB LEDs are currently much lower (Kebbi et al., 2020) than common horticultural LEDs (Kusuma et al., 2020); potentially leading to relatively rapid degradation in fluence rates over time. Given that plant responses in the present study were closely tied to the UV exposure level, fixture degradation could lead to inconsistencies between sequential crops, which is an important parameter in the indoor cannabis production industry.

Overall, it is still possible that the alternate UV treatment protocols may have more positive results in the controlled environment production of modern, drug-type cannabis cultivars; for example: longer wavelength and less energetic spectra (Hikosara et al., 2010) and shorter-term (e.g., proximal to harvest maturity) exposure (Johnson et al., 1999; Martínez-Lüscher et al., 2013; Huarancca Reyes et al., 2018; Dou et al., 2019). Future research could seek to promote eustress responses in cannabis secondary metabolite concentrations while minimizing distress responses (e.g., yield reductions) by using less energetic UV spectra and/or different daily exposure protocols than were used in the present study. The effects of cannabis plants grown under different lighting histories should also be investigated to determine the ideal developmental stage for UV exposure to achieve the desired effects in both yield and quality.

CONCLUSION

Long-term exposure of various intensities of relatively short-wavelength UV radiation had generally negative impacts on cannabis growth, yield, and inflorescence quality. By studying two cultivars with similar cannabinoid profiles, we found some differences in phenotypic plasticity in the temporal dynamics in morphology, physiology, yield, and quality responses to UV exposure level. For the first time this paper described the visible symptoms caused by UVB stress on indoor cannabis plants. Importantly, as it was applied in this study, UV radiation provoked substantially reduced yield in one cultivar, reduced inflorescence quality in both cultivars, and had no commercially relevant benefits to inflorescence secondary metabolite composition. Therefore, potential for UV radiation to enhance cannabinoid concentrations must still be confirmed before UV can be used as a tool in cannabis production.

DATA AVAILABILITY STATEMENT

The raw data supporting the conclusions of this article will be made available by the authors, without undue reservation.

AUTHOR CONTRIBUTIONS

VR-M and DL performed the experiment and collected and analyzed the data. VR-M, DL, and YZ wrote and revised the manuscript. All authors contributed to the experimental design and approved the final manuscript.

FUNDING

This work was funded by Natural Sciences and Engineering Research Council of Canada (CRDPJ 533527 – 18). Green Relief Inc. provided the research facility, cannabis plants, experimental materials, and logistical support.

ACKNOWLEDGMENTS

We thank Derek Bravo, Tim Moffat, and Madeline Baker for technical support throughout the experiment. We also thank Angus Footman and Erica Emery for their logistical support. This article was first published as a preprint (Rodriguez-Morrison et al., 2021b).

SUPPLEMENTARY MATERIAL

The Supplementary Material for this article can be found online at: https://www.frontiersin.org/articles/10.3389/fpls.2021.725078/full#supplementary-material

REFERENCES

Aarrouf, J., and Urban, L. (2020). Flashes of UV-C light: An innovative method for stimulating plant defences. *PLoS One* 15:3235918. doi: 10.1371/journal.pone.0235918

Aizpurua-Olaizola, O., Soydaner, U., Öztürk, E., Schibano, D., Simsir, Y., Navarro, P., et al. (2016). Evolution of the cannabinoid and terpene content during the growth of *Cannabis sativa* plants from different chemotypes. *J. Nat. Prod.* 79, 324–331. doi: 10.1021/acs.jnatprod.5b00949

Aliferis, K. A., and Bernard-Perron, D. (2020). Cannabinomics: Application of metabolomics in cannabis (*Cannabis sativa* L.) research and development. *Front. Plant Sci.* 11:554. doi: 10.3389/fpls.2020.00554

Behn, H., Albert, A., Marx, F., Noga, G., and Ulbrich, A. (2010). Ultraviolet-B and photosynthetically active radiation interactively affect yield and pattern of monoterpenes in leaves of peppermint (*Mentha x piperita* L.). *J. Agric. Food Chem.* 58, 7361–7367. doi: 10.1021/jf9046072

Björkman, O., and Demmig, B. (1987). Photon yield of O_2 evolution and chlorophyll fluorescence characteristics at 77 K among vascular plants of diverse origins. *Planta* 170, 489–504. doi: 10.1007/BF00402983

Booth, J. K., and Bohlmann, J. (2019). Terpenes in *Cannabis sativa* – From plant genome to humans. *Plant Sci.* 284, 67–72. doi: 10.1016/j.plantsci.2019.03.022

Caldwell, M. M. (1971). Solar UV irradiation and the growth and development of higher plants. *Photophysiology* 6, 131–177. doi: 10.1016/b978-0-12-282606-1.50010-6

Caldwell, M. M., Ballaré, C. L., Bornman, J. F., Flint, S. D., Björn, L. O., Teramura, A. H., et al. (2003). Terrestrial ecosystems, increased solar ultraviolet radiation and interactions with other climatic change factors. *Photochem. Photobiol. Sci.* 2, 29–38. doi: 10.1039/b211159b

Cannabis Business Times (2020). *2020 State of the Industry Report*. Valley View, OH: GIW Media Inc.

Caplan, D., Dixon, M., and Zheng, Y. (2017). Optimal rate of organic fertilizer during the flowering stage for cannabis grown in two coir-based substrates. *HortScience.* 52, 1796–1803. doi: 10.21273/HORTSCI12401-17

Caplan, D., Dixon, M., and Zheng, Y. (2019). Increasing inflorescence dry weight and cannabinoid content in medical cannabis using controlled drought stress. *HortScience.* 54, 964–969. doi: 10.21273/HORTSCI13510-18

Cen, Y., and Bornman, J. F. (1993). The effect of exposure to enhanced UV-B radiation on the penetration of monochromatic and polychromatic UV-B radiation in leaves of *Brassica napus*. *Physiol. Plant.* 87, 249–255. doi: 10.1111/j.1399-3054.1993.tb01727.x

Chouvy, P.-A. (2015). *The Supply of Hashish to Europe Report Prepared for the EMCDDA*. Paris, France: European Monitoring Centre for Drugs and Drug Addiction.

Czégény, G., Mátai, A., and Hideg, É (2016). UV-B effects on leaves-Oxidative stress and acclimation in controlled environments. *Plant Sci.* 248, 57–63. doi: 10.1016/j.plantsci.2016.04.013

De Meijer, E. P. M., Bagatta, M., Carboni, A., Crucitti, P., Moliterni, V. M. C., Ranalli, P., et al. (2003). The inheritance of chemical phenotype in *Cannabis sativa* L. *Genetics* 163, 335–346. doi: 10.1093/genetics/163.1.335

Dou, H., Niu, G., and Gu, M. (2019). Pre-harvest UV-B radiation and photosynthetic photon flux density interactively affect plant photosynthesis, growth, and secondary metabolites accumulation in basil (*Ocimum Basilicum*) plants. *Agronomy* 9:434. doi: 10.3390/agronomy9080434

Dujourdy, L., and Besacier, F. (2017). A study of cannabis potency in France over a 25 years period (1992–2016). *Forensic Sci. Int.* 272, 72–80. doi: 10.1016/j.forsciint.2017.01.007

Eichler, M., Spinedi, L., Unfer-Grauwiler, S., Bodmer, M., Surber, C., Luedi, M., et al. (2012). Heat exposure of cannabis sativa extracts affects the pharmacokinetic and metabolic profile in healthy male subjects. *Planta Med.* 78, 686–691. doi: 10.1055/s-0031-1298334

ElSohly, M. A., Mehmedic, Z., Foster, S., Gon, C., Chandra, S., and Church, J. C. (2016). Changes in cannabis potency over the last 2 decades (1995-2014): Analysis of current data in the United States. *Biol. Psychiatry* 79, 613–619. doi: 10.1016/j.biopsych.2016.01.004

Fairbairn, J. W., and Liebmann, J. A. (1974). The cannabinoid content of *Cannabis sativa* L. grown in England. *J. Pharm. Pharmacol.* 26, 413–419. doi: 10.1111/j.2042-7158.1974.tb09306.x

Fierro, A. C., Leroux, O., De Coninck, B., Cammue, B. P. A., Marchal, K., Prinsen, E., et al. (2015). Ultraviolet-B radiation stimulates downward leaf curling in *Arabidopsis thaliana*. *Plant Physiol. Biochem.* 93, 9–17. doi: 10.1016/j.plaphy.2014.12.012

Fiscus, E. L., and Booker, F. L. (1995). Is increased UV-B a threat to crop photosynthesis and productivity? *Photosynth. Res.* 43, 81–92. doi: 10.1007/BF00042965

Flint, S. D., and Caldwell, M. M. (2003). A biological spectral weighting function for ozone depletion research with higher plants. *Physiol. Plant.* 117, 137–144.

Fukuda, S., Satoh, A., Kasahara, H., Matsuyama, H., and Takeuchi, Y. (2008). Effects of ultraviolet-B irradiation on the cuticular wax of cucumber (*Cucumis sativus*) cotyledons. *J. Plant Res.* 121, 179–189. doi: 10.1007/s10265-007-0143-7

Giupponi, L., Leoni, V., Pavlovic, R., and Giorgi, A. (2020). Influence of altitude on phytochemical composition of hemp inflorescence: A metabolomic approach. *Molecules* 25:1381. doi: 10.3390/molecules25061381

Halldorson, M. M., and Keller, M. (2018). Grapevine leafroll disease alters leaf physiology but has little effect on plant cold hardiness. *Planta* 248, 1201–1211. doi: 10.1007/s00425-018-2967-x

Havé, M., Marmagne, A., Chardon, F., and Masclaux-Daubresse, C. (2017). Nitrogen remobilization during leaf senescence: Lessons from Arabidopsis to crops. *J. Exp. Bot.* 68, 2513–2529. doi: 10.1093/jxb/erw365

Hazekamp, A., Peltenburg, A., Verpoorte, R., and Giroud, C. (2005). Chromatographic and spectroscopic data of cannabinoids from *Cannabis sativa* L. *J. Liq. Chromatogr. Relat. Technol.* 28, 2361–2382. doi: 10.1080/10826070500187558

Hideg, É, Jansen, M. A. K., and Strid, Å (2013). UV-B exposure, ROS, and stress: Inseparable companions or loosely linked associates? *Trends Plant Sci.* 18, 107–115. doi: 10.1016/j.tplants.2012.09.003

Hikosara, S., Ito, K., and Goto, E. (2010). Effects of ultraviolet light on growth, essential oil concentration, and total antioxidant capacity of Japanese mint. *Environ. Control Biol.* 48, 185–190. doi: 10.2525/ecb.48.185

Höll, J., Lindner, S., Walter, H., Joshi, D., Poschet, G., Pfleger, S., et al. (2019). Impact of pulsed UV-B stress exposure on plant performance: How recovery periods stimulate secondary metabolism while reducing adaptive growth attenuation. *Plant Cell. Environ.* 42, 801–814. doi: 10.1111/pce.13409

Huarancca Reyes, T., Scartazza, A., Castagna, A., Cosio, E. G., Ranieri, A., and Guglielminetti, L. (2018). Physiological effects of short acute UVB treatments in *Chenopodium quinoa* Willd. *Sci. Rep.* 8:371. doi: 10.1038/s41598-017-18710-2

Huché-Thélier, L., Crespel, L., Le Gourrierec, J., Morel, P., Sakr, S., and Leduc, N. (2016). Light signaling and plant responses to blue and UV radiations: Perspectives for applications in horticulture. *Environ. Exp. Bot.* 121, 22–38. doi: 10.1016/j.envexpbot.2015.06.009

Jenkins, G. I. (2017). Photomorphogenic responses to ultraviolet-B light. *Plant Cell. Environ.* 40, 2544–2557. doi: 10.1111/pce.12934

Johnson, C. B., Kirby, J., Naxakis, G., and Pearson, S. (1999). Substantial UV-B-mediated induction of essential oils in sweet basil (*Ocimum basilicum* L.). *Phytochemistry* 51, 507–510. doi: 10.1016/S0031-9422(98)00767-5

Kakani, V. G., Reddy, K. R., Zhao, D., and Sailaja, K. (2003). Field crop responses to ultraviolet-B radiation: A review. *Agric. For. Meteorol.* 120, 191–218. doi: 10.1016/j.agrformet.2003.08.015

Kebbi, Y., Muhammad, A. I., Sant'Ana, A. S., do Prado-Silva, L., Liu, D., and Ding, T. (2020). Recent advances on the application of UV-LED technology for microbial inactivation: Progress and mechanism. *Compr. Rev. Food Sci. Food Saf.* 19, 3501–3527.

Klem, K., Ač, A., Holub, P., Kováč, D., Špunda, V., Robson, T. M., et al. (2012). Interactive effects of PAR and UV radiation on the physiology, morphology and leaf optical properties of two barley varieties. *Environ. Exp. Bot.* 75, 52–64. doi: 10.1016/j.envexpbot.2011.08.008

Kreyling, J., Schweiger, A. H., Bahn, M., Ineson, P., Migliavacca, M., Morel-Journel, T., et al. (2018). To replicate or not to replicate – that is the question: How to tackle nonlinear responses in ecological experiments. *Ecol. Lett.* 21, 1629–1638. doi: 10.1111/ele.13134

Krizek, D. T. (2004). Influence of PAR and UV-A in determining plant sensitivity and photomorphogenic responses to UV-B radiation. *Photochem. Photobiol.* 79, 307–315. doi: 10.1562/2004-01-27-ir.1

Kusuma, P., Pattison, P. M., and Bugbee, B. (2020). From physics to fixtures to food: Current and potential LED efficacy. *Hortic. Res.* 7:56. doi: 10.1038/s41438-020-0283-7

Liu, L. X., Xu, S. M., and Woo, K. C. (2005). Solar UV-B radiation on growth, photosynthesis and the xanthophyll cycle in tropical acacias and eucalyptus. *Environ. Exp. Bot.* 54, 121–130. doi: 10.1016/j.envexpbot.2004.06.006

Llewellyn, D., Golem, S., Foley, E., Dinka, S., Maxwell, A., Jones, P., et al. (2021). *Cannabis Yield Increased Proportionally With Light Intensity, but Additional Ultraviolet Radiation Did Not Affect Yield or Cannabinoid Content*. [Preprint]. doi: 10.20944/preprints202103.0327.v1

Lydon, J., Teramura, A. H., and Coffman, C. B. (1987). UV-B radiation effects on photosynthesis, growth and cannabinoid production of two *Cannabis sativa* chemotypes. *Photochem. Photobiol.* 46, 201–206. doi: 10.1111/j.1751-1097.1987.tb04757.x

Maffei, M., and Scannerini, S. (2000). UV-B effect on photomorphogenesis and essential oil composition in peppermint (*Mentha piwperita* L.). *J. Essent. Oil Res.* 12, 523–529. doi: 10.1080/10412905.2000.9712150

Magagnini, G., Grassi, G., and Kotiranta, S. (2018). The effect of light spectrum on the morphology and cannabinoid content of *Cannabis sativa L. Med. Cannabis Cannabinoids* 1, 19–27. doi: 10.1159/000489030

Mah, J. J., Llewellyn, D., and Zheng, Y. (2019). *Protocol for Converting Spectrometer Radiometric Data to Photon Flux Units [Microsoft Excel Spreadsheet]*. Guelph: University of Guelph.

Mahlberg, P. G., John, K., and Hemphill. (1983). Effect of light quality on cannabinoid content of *Cannabis sativa L.* (Cannabaceae). *Bot. Gazette.* 144, 43–48.

Martínez-Lüscher, J., Morales, F., Delrot, S., Sánchez-Díaz, M., Gomés, E., Aguirreolea, J., et al. (2013). Short- and long-term physiological responses of grapevine leaves to UV-B radiation. *Plant Sci.* 213, 114–122. doi: 10.1016/j.plantsci.2013.08.010

McElroy, C. T., and Fogal, P. F. (2008). Ozone: From discovery to protection. *Atmos. Ocean* 46, 1–13. doi: 10.3137/ao.460101

McPartland, J. M., and Russo, E. B. (2001). Cannabis and cannabis extracts: greater than the sum of their parts? *Cannabis Ther. HIV/AIDS* 1, 103–132. doi: 10.1300/J175v01n03_08

Middleton, E. M., and Teramura, A. H. (1993). Potential Errors in the use of cellulose acetate and Mylar filters in UV-B radiation studies. *Photochem. Photobiol.* 57, 744–751.

Murchie, E. H., and Lawson, T. (2013). Chlorophyll fluorescence analysis: A guide to good practice and understanding some new applications. *J. Exp. Bot.* 64, 3983–3998. doi: 10.1093/jxb/ert208

Namdar, D., Mazuz, M., Ion, A., and Koltai, H. (2018). Variation in the compositions of cannabinoid and terpenoids in *Cannabis sativa* derived from inflorescence position along the stem and extraction methods. *Ind. Crops Prod.* 113, 376–382. doi: 10.1016/j.indcrop.2018.01.060

Nelson, J. A., and Bugbee, B. (2014). Economic analysis of greenhouse lighting: Light emitting diodes vs. high intensity discharge fixtures. *PLoS One* 9:e99010. doi: 10.1371/journal.pone.0099010

Neugart, S., and Schreiner, M. (2018). UVB and UVA as eustressors in horticultural and agricultural crops. *Sci. Hortic.* 234, 370–381. doi: 10.1016/j.scienta.2018.02.021

Nikiforos, K., Eduardo, R., and Robert, S. (2011). The value of the ratio of UVA to UVB in sunlight. *Photochem. Photobiol.* 87, 1474–1475. doi: 10.1111/j.1751-1097.2011.00980.x

Nuutinen, T. (2018). Medicinal properties of terpenes found in *Cannabis sativa* and *Humulus lupulus*. *Eur. J. Med. Chem.* 157, 198–228. doi: 10.1016/j.ejmech.2018.07.076

Palma, C. F. F., Castro-Alves, V., Morales, L. O., Rosenqvist, E., Ottosen, C.-O., and Strid, Å (2021). Spectral composition of light affects sensitivity to UV-B and photoinhibition in cucumber. *Front. Plant Sci.* 11:11. doi: 10.3389/fpls.2020.610011

Parry, C., Blonquist, J. M., and Bugbee, B. (2014). *In situ* measurement of leaf chlorophyll concentration: Analysis of the optical/absolute relationship. *Plant Cell Environ.* 37, 2508–2520. doi: 10.1111/pce.12324

Pate, D. W. (1983). Possible role of ultraviolet radiation in evolution of cannabis chemotypes. *Econ. Bot.* 37, 396–405.

Poorter, H., Niinemets, Ü, Ntagkas, N., Siebenkäs, A., Mäenpää, M., Matsubara, S., et al. (2019). A meta-analysis of plant responses to light intensity for 70 traits ranging from molecules to whole plant performance. *New Phytol.* 223, 1073–1105. doi: 10.1111/nph.15754

Potter, D. J. (2014). A review of the cultivation and processing of cannabis (*Cannabis sativa L.*) for production of prescription medicines in the UK. *Drug Test. Anal.* 6, 31–38. doi: 10.1002/dta.1531

Powell, M., Gundersen, B., Cowan, J., Miles, C. A., and Inglis, D. A. (2014). The effect of open-ended high tunnels in western Washington on late blight and physiological leaf roll among five tomato cultivars. *Plant Dis.* 98, 1639–1647. doi: 10.1094/PDIS-12-13-1261-RE

Punja, Z. K., and Holmes, J. E. (2020). Hermaphrodism in marijuana (*Cannabis sativa* L.) inflorescences – Impact on floral morphology, seed formation, progeny sex ratios, and genetic variation. *Front. Plant Sci.* 11:718. doi: 10.3389/fpls.2020.00718

Radetsky, L. C. (2018). *LED and HID Horticultural Luminaire Testing Report Prepared for Lighting Energy Alliance Members and Natural Resources Canada*. Troy, NY: Lighting Research Center, Rensselaer Polytechnic Institute.

Robson, T. M., Aphalo, P. J., Banaś, A. K., Barnes, P. W., Brelsford, C. C., Jenkins, G. I., et al. (2019). A perspective on ecologically relevant plant-UV research and its practical application. *Photochem. Photobiol. Sci.* 18, 970–988. doi: 10.1039/c8pp00526e

Rodriguez-Morrison, V., Llewellyn, D., and Zheng, Y. (2021a). Cannabis yield, potency, and leaf photosynthesis respond differently to increasing light levels in an indoor environment. *Front. Plant Sci.* 12:456. doi: 10.3389/fpls.2021.646020

Rodriguez-Morrison, V., Llewellyn, D., and Zheng, Y. (2021b). *Cannabis Inflorescence Yield and Cannabinoid Concentration Are Not Improved With Long-Term Exposure to Short-Wavelength Ultraviolet-B Radiation*. [Preprint]. doi: 10.20944/preprints202106.0317.v1

Russo, E. B. (2007). History of cannabis and its preparations in saga, science, and sobriquet. *Chem. Biodivers.* 4, 1614–1648. doi: 10.1002/cbdv.200790144

Ruter, J. M. (1992). Influence of source, rate, and method of applicating controlled release fertilizer on nutrient release and growth of "Savannah" holly. *Fertil. Res.* 32, 101–106. doi: 10.1007/BF01054399

Schreiner, M., Mewis, I., Huyskens-Keil, S., Jansen, M. A. K., Zrenner, R., Winkler, J. B., et al. (2012). UV-B-induced secondary plant metabolites - Potential benefits for plant and human health. *CRC. Crit. Rev. Plant Sci.* 31, 229–240. doi: 10.1080/07352689.2012.664979

Searles, P. S., Flint, S. D., and Caldwell, M. M. (2001). A meta-analysis of plant field studies simulating stratospheric ozone depletion. *Oecologia* 127, 1–10. doi: 10.1007/s004420000592

Small, E. (2017). *Cannabis: A Complete Guide*. Boca Raton, FL: CRC Press.

Small, E., and Beckstead, H. D. (1973). Cannabinoid phenotypes in *Cannabis sativa*. *Nature* 245, 147–148. doi: 10.1038/245147a0

Stapleton, A. E. (1992). Ultraviolet radiation and plants: burning questions. *Plant Cell.* 4, 1353–1358. doi: 10.1105/tpc.4.11.1353

Steinmüller, D., and Tevini, M. (1985). Action of ultraviolet radiation (UV-B) upon cuticular waxes in some crop plants. *Planta* 164, 557–564. doi: 10.1007/BF00395975

Taliansky, M., Mayo, M. A., and Barker, H. (2003). *Potato leafroll virus*: a classic pathogen shows some new tricks. *Mol. Plant Pathol.* 4, 81–89. doi: 10.1046/j.1364-3703.2003.00153.x

Teramura, A. H., Sullivan, J. H., and Lydon, J. (1990). Effects of UV-B radiation on soybean yield and seed quality: a 6-year field study. *Physiol. Plant.* 80, 5–11.

Torre, S., Roro, A. G., Bengtsson, S., Mortensen, L. M., Solhaug, K. A., Gislerød, H. R., et al. (2012). Control of plant morphology by UV-B and UV-B-temperature interactions. *Acta Hortic.* 956, 207–214. doi: 10.17660/ActaHortic.2012.956.22

Tossi, V. E., Regalado, J. J., Iannicelli, J., Laino, L. E., Burrieza, H. P., Escandón, A. S., et al. (2019). Beyond arabidopsis: Differential UV-B response mediated by UVR8 in diverse species. *Front. Plant Sci.* 10:780. doi: 10.3389/fpls.2019.00780

Valenta, K., Dimac-Stohl, K., Baines, F., Smith, T., Piotrowski, G., Hill, N., et al. (2020). Ultraviolet radiation changes plant color. *BMC Plant Biol.* 20:253. doi: 10.1186/s12870-020-02471-8

Wargent, J. J., and Jordan, B. R. (2013). From ozone depletion to agriculture: Understanding the role of UV radiation in sustainable crop production. *New Phytol.* 197, 1058–1076. doi: 10.1111/nph.12132

Westmoreland, F. M., Kusuma, P., and Bugbee, B. (2021). Cannabis lighting: Decreasing blue photon fraction increases yield but efficacy is more important

for cost effective production of cannabinoids. *PLoS One.* 16:e0248988. doi: 10.1371/journal.pone.0248988

Wilson, M. I. (1998). *Photomorphological and Photochernical Effects of UV-B radiation on Brassica napus* (L.) and *Arabidopsis thaliana* (L.) Heynh: Morphological, Cellular and Structural Biological Changes. [Thesis]. Waterloo, ON: University of Waterloo.

Wilson, M. I., and Greenberg, B. M. (1993). Specificity and photomorphogenic nature of ultraviolet-B- induced cotyledon curling in *Brassica napus* L. *Plant Physiol.* 102, 671–677. doi: 10.1104/pp.102.2.671

Yep, B., Gale, N. V., and Zheng, Y. (2020). Aquaponic and hydroponic solutions modulate NaCl-induced stress in drug-type *Cannabis sativa* L. *Front. Plant Sci.* 11:1169. doi: 10.3389/fpls.2020.01169

Younis, B. A., Mahoney, L., Schweigkofler, W., and Suslow, K. (2019). Inactivation of plant pathogens in irrigation water runoff using a novel UV disinfection system. *Eur. J. Plant Pathol.* 153, 907–914. doi: 10.1007/s10658-018-01608-8

Zhao, D., Reddy, K. R., Kakani, V. G., Read, J. J., and Sullivan, J. H. (2003). Growth and physiological responses of cotton (*Gossypium hirsutum* L.) to elevated carbon dioxide and ultraviolet-B radiation under controlled environmental conditions. *Plant Cell Environ.* 26, 771–782. doi: 10.1046/j.1365-3040.2003.01019.x

Zheng, Y. (2021). Soilless production of drug-type *Cannabis sativa*. *Acta Hortic.* 1305, 375–382. doi: 10.17660/ActaHortic.2021.1305.49

Zlatev, Z. S., Lidon, F. C., and Kaimakanova, M. (2012). Plant physiological responses to UV-B radiation. *Emirates J. Food Agric.* 24, 481–501. doi: 10.9755/ejfa.v24i6.481501

Zou, S., and Kumar, U. (2018). Cannabinoid receptors and the endocannabinoid system: Signaling and function in the central nervous system. *Int. J. Mol. Sci.* 19:833. doi: 10.3390/ijms19030833

Conflict of Interest: The authors declare that the research was conducted in the absence of any commercial or financial relationships that could be construed as a potential conflict of interest.

Publisher's Note: All claims expressed in this article are solely those of the authors and do not necessarily represent those of their affiliated organizations, or those of the publisher, the editors and the reviewers. Any product that may be evaluated in this article, or claim that may be made by its manufacturer, is not guaranteed or endorsed by the publisher.

frontiers in Plant Science

ORIGINAL RESEARCH
published: 05 November 2021
doi: 10.3389/fpls.2021.753847

Fertilization Following Pollination Predominantly Decreases Phytocannabinoids Accumulation and Alters the Accumulation of Terpenoids in Cannabis Inflorescences

Carni Lipson Feder[1†], Oded Cohen[2†], Anna Shapira[1], Itay Katzir[2], Reut Peer[2], Ohad Guberman[1], Shiri Procaccia[1], Paula Berman[1], Moshe Flaishman[2] and David Meiri[1]*

[1] The Laboratory of Cancer Biology and Cannabinoid Research, Faculty of Biology, Technion-Israel Institute of Technology, Haifa, Israel, [2] Agricultural Research Organization (ARO), Volcani Center, Institute of Plant Sciences, Rishon LeZion, Israel

OPEN ACCESS

Edited by:
Orazio Taglialatela-Scafati, University of Naples Federico II, Italy

Reviewed by:
Dinesh Adhikary, University of Alberta, Canada
Roberto Berni, University of Liège, Belgium

***Correspondence:**
David Meiri
dmeiri@technion.ac.il

[†] *These authors have contributed equally to this work*

Specialty section:
This article was submitted to Plant Metabolism and Chemodiversity, a section of the journal Frontiers in Plant Science

Received: *05 August 2021*
Accepted: *04 October 2021*
Published: *05 November 2021*

Citation:
Lipson Feder C, Cohen O, Shapira A, Katzir I, Peer R, Guberman O, Procaccia S, Berman P, Flaishman M and Meiri D (2021) Fertilization Following Pollination Predominantly Decreases Phytocannabinoids Accumulation and Alters the Accumulation of Terpenoids in Cannabis Inflorescences. Front. Plant Sci. 12:753847. doi: 10.3389/fpls.2021.753847

In the last decades, growing evidence showed the therapeutic capabilities of *Cannabis* plants. These capabilities were attributed to the specialized secondary metabolites stored in the glandular trichomes of female inflorescences, mainly phytocannabinoids and terpenoids. The accumulation of the metabolites in the flower is versatile and influenced by a largely unknown regulation system, attributed to genetic, developmental and environmental factors. As *Cannabis* is a dioecious plant, one main factor is fertilization after successful pollination. Fertilized flowers are considerably less potent, likely due to changes in the contents of phytocannabinoids and terpenoids; therefore, this study examined the effect of fertilization on metabolite composition by crossbreeding (-)-Δ^9-*trans*-tetrahydrocannabinol (THC)- or cannabidiol (CBD)-rich female plants with different male plants: THC-rich, CBD-rich, or the original female plant induced to develop male pollen sacs. We used advanced analytical methods to assess the phytocannabinoids and terpenoids content, including a newly developed semi-quantitative analysis for terpenoids without analytical standards. We found that fertilization significantly decreased phytocannabinoids content. For terpenoids, the subgroup of monoterpenoids had similar trends to the phytocannabinoids, proposing both are commonly regulated in the plant. The sesquiterpenoids remained unchanged in the THC-rich female and had a trend of decrease in the CBD-rich female. Additionally, specific phytocannabinoids and terpenoids showed an uncommon increase in concentration followed by fertilization with particular male plants. Our results demonstrate that although the profile of phytocannabinoids and their relative ratios were kept, fertilization substantially decreased the concentration of nearly all phytocannabinoids in the plant regardless of the type of fertilizing male. Our findings may point to the functional roles of secondary metabolites in *Cannabis*.

Keywords: *Cannabis*, cannabinoids, terpenoids, secondary metabolites, chromatography/mass spectrometry, analytical—methods, gas chromatography, high pressure liquid chromatography

SUMMARY

Fertilization of Cannabis decreases phytocannabinoids accumulation and alters the accumulation of terpenoids from distinct families.

INTRODUCTION

Cannabis sativa L. (*Cannabis*) has been known as a medicinal plant since ancient times (Bonini et al., 2018). During the last two decades, many studies added to the growing evidence for its therapeutic effects in a wide range of conditions such as neurodegenerative disorders (Fernández-Ruiz, 2019; Cassano et al., 2020), pain (Starowicz and Finn, 2017), epilepsy (Franco et al., 2021), multiple sclerosis (Rice and Cameron, 2017), and others (for review, see Gonçalves et al., 2019). These therapeutic abilities have been attributed to the secondary metabolites biosynthesized in *Cannabis* (Andre et al., 2016). Around 500 different secondary metabolites have been identified (ElSohly and Slade, 2005; Flores-Sanchez and Verpoorte, 2008). These belong to several groups of compounds including phytocannabinoids, terpenoids and flavonoids. The most characterized to date are the phytocannabinoids, lipophilic compounds made of isoprene units (five-carbon building blocks) (Hanuš et al., 2016), which are almost exclusive to *Cannabis* (Gülck and Møller, 2020). More than 140 different phytocannabinoids are accumulated to various extents in glandular trichomes that are located in the aerial parts of the plant and mostly on the female flowers, which are arranged in a cluster on the stem of the inflorescence (Hanuš et al., 2016). The phytocannabinoids can be classified into several subclasses according to their chemical structures, including the (-)-Δ^9-*trans*-tetrahydrocannabinol (THC) and cannabidiol (CBD) families as well as cannabinol (CBN), cannabigerol (CBG), cannabichromene (CBC), and others (Flores-Sanchez and Verpoorte, 2008; Berman et al., 2018). A second large group of metabolites is the terpenoids, which are also found in many other plants. These metabolites are closely related to phytocannabinoids, sharing the same isoprenoid precursor and built up by branched isoprene units (Booth et al., 2020). Terpenoids are responsible for the fragrance and taste of the plant and are suggested to also have defensive roles. They also contribute to the therapeutic effects attributed to *Cannabis* (Russo and Marcu, 2017). Another group of metabolites worth mentioning is flavonoids. Among this group, which is widespread in the plant kingdom, there are three specific prenylated flavonoids, termed Cannflavins A–C, which are unique to *Cannabis* and show potent anti-inflammatory abilities (Radwan et al., 2008; Rea et al., 2019; Erridge et al., 2020).

Ongoing research is focused on matching specific metabolites found in the plant and their therapeutic capabilities. To this end, specialized analytical methods have been developed in order to obtain precise knowledge on all the components of the plant and the effects they are responsible for. Currently, more than 90 phytocannabinoids and 100 terpenoids are routinely identified and quantified to obtain an overall chemical profile of each chemovar used for a medicinal purpose (Berman et al., 2018; Shapira et al., 2019). In parallel to the search for specific biological activities of the secondary metabolites, broad ongoing research is focused upon the elucidation of *in planta* metabolites' biosynthesis, transport and accumulation pathways. Genome, transcriptome and proteome data have been published since 2011 (van Bakel et al., 2011; Laverty et al., 2019; Vincent et al., 2019; Livingston et al., 2020; McGarvey et al., 2020), and have been integrated into a genomic database for *Cannabis* (CannabisGDB) (Cai et al., 2021). Biosynthetic pathways are being unraveled, and recently more than 30 *Cannabis* specific terpenoid synthases have been characterized (Booth et al., 2017, 2020; Allen et al., 2019; Zager et al., 2019; Livingston et al., 2020). In addition, the environmental and developmental factors that affect metabolite accumulation are also studied, such as light (Hawley et al., 2018; Magagnini et al., 2018; Namdar et al., 2019), soil and harvest time (Meier and Mediavilla, 1998; Bernstein et al., 2019; Chandra et al., 2020). The increasing information on the impact of these different factors on metabolite accumulation has the prospect of developing specific chemovars harboring a pre-planned group of metabolites (Romero et al., 2020).

This study examined the effect of an additional factor, the fertilization of *Cannabis* flowers following pollination of the pistil. Fertilization of flowers is a key step in the plant life cycle. Successful pollination activates a series of events followed by fertilization and embryogenesis. This includes the development of an ovary on one hand, together with senescence and abscission of floral organs, degradation of macromolecules, and recycling of different nutrients on the other hand (O'Neill, 1997; Tripathi and Tuteja, 2007; Borghi and Fernie, 2020). *Cannabis* is a dioecious plant, harboring either female or male reproductive organs. It is also a wind-pollinated plant, in which the pollination of flowers is not dependent on specific animal pollinators. Phytocannabinoids are most abundant in the female flower inflorescences (Flores-Sanchez and Verpoorte, 2008). Fertilized flowers, harboring seeds, are considerably less potent. Hence the term "sinsemilla," Spanish for "without seed," that defines plants associated with high psychoactive effects (Potter et al., 2018). In addition, it is a common work practice by *Cannabis* growers to eliminate male plants growing in a field to maintain the unfertilized inflorescences and maximize the phytocannabinoid concentrations. Therefore, it is likely that the content of secondary metabolites such as phytocannabinoids and terpenoids changes following the pollination and fertilization of *Cannabis* inflorescences. However, although mentioned in a few studies (Meier and Mediavilla, 1998; Potter, 2009; Russo and Marcu, 2017), this phenomenon was not studied in depth. In the last few years, an increasing number of *Cannabis* growers are moving from using cuttings from female "mother plants" to seeds. Even though the seeds are usually feminized, around 5–10% will be males, and thus the question about the effect of pollination on the phytocannabinoids and terpenoids expression becomes critical.

Abbreviations: For a list of full and abbreviated names of the 95 phytocannabinoids (see **Supplementary Table 1**). ESI, Electrospray ionization; GC, Gas chromatography; LC, Liquid chromatography; MS, Mass spectrometry; PPM, Parts per million; SHS, Static headspace; UHPLC, Ultra-high-performance liquid chromatography; w/w, Weight for weight.

In order to gain more insight into the *Cannabis* metabolite regulation pathway, this work studied the effect of flower fertilization on the plant's secondary metabolite accumulation. We used indoor growing methods together with analytical procedures in order to investigate the effect of fertilization on metabolite composition and concentration in *Cannabis* inflorescences, and specify which metabolites are affected and to what extent.

MATERIALS AND METHODS

Chemicals and Reagents

Liquid chromatography-mass spectrometric (LC/MS) grade acetonitrile (catalog number 1.00029), methanol (1.06035), and water (1.15333); and gas chromatography (GC) headspace grade dimethyl sulfoxide (DMSO) (1.01900) were purchased from Mercury Scientific and Industrial Products Ltd. (Rosh Haayin, Israel). Ethanol, (catalog number 052541), acetic acid (010778) and n-Hexane (091484) were obtained from BioLab Ltd. (Jerusalem, Israel). Phytocannabinoid analytical standards (>98%) CBG, THC, CBD, CBC, CBN, Cannabigerolic acid (CBGA), Tetrahydrocannabinolic acid (THCA), Cannabidiolic acid (CBDA), Cannabinolic acid (CBNA), Cannabichromenic Acid (CBCA), (-)-Δ8-trans-tetrahydrocannabinol (Δ^8-THC), tetrahydrocannabivarin (THCV), Cannabidivarin (CBDV), Cannabidivarinic acid (CBDVA) and Cannabicyclol (CBL) were purchased from Sigma-Aldrich (Rehovot, Israel); Cannabichromevarin (CBCV) was purchased from Cayman Chemical (Ann Arbor, MI, United States). Terpenoid analytical standards (>95% unless stated otherwise) were purchased from Sigma-Aldrich (Rehovot, Israel); valencene (>80% pure), α- and β-curcumene (>90% pure), α-phellandrene, and sabinene were purchased from Extrasynthese (Genay, France); a mixture of n-alkanes was purchased from Sigma R 769 (40 mg/mL, C8-C20, Saint Louis, MO, United States) for semi-quantitative analysis.

Experimental Design

The effect of fertilization was tested on two *Cannabis sativa* L. female plants. Female strains 333 THC-rich (15% THCA, 0.07% CBDA) and 423 CBD-rich (0.33% THCA, 9% CBDA) were subjected to fertilization and two male plants strains, 319 THC-rich (progeny of high THC landrace Highland Thai, Seedsman seeds) and 405 CBD-rich (progeny of Cherry CBD), were used as pollen donors. In addition, the female plants were subjected to a sex conversion treatment (Mohan Ram and Sett, 1982; Small and Naraine, 2016) and these induced males were also used as pollen donors to fertilize the two female plants. In order to achieve pollen sacs, 45 days old rooted cutting, 30 cm size female plants were sprayed daily until completely moist with ethylene inhibitor (Sodium Thiosulfate 0.5%) for 5 days prior to transferring to short day conditions. The female plants that were sex changed are referred to as males or induced-males. The female *Cannabis* plants were grown, three plants for each treatment, under an 18/6 light/dark regime (800 μmol), 23–27°C for 30 days before being transferred to flowering chambers with a 12/12 light/dark regime (500 μmol), 23–27°C for up to either 42 (6 weeks) or 56 (8 weeks) days before some inflorescences were removed for chemical analysis. Female plants were grown in small flowering chambers (1 m^2) in the presence of a single pollen donor. All plants were grown in 1 L pots on a mixture of pit/coconut 70%/30% soil, respectively.

Extraction and Sample Preparation of Phytocannabinoids

The inflorescences of the treated plants, 3–4 apical inflorescences per plant, were harvested and dried for 24–48 h at 40°C until they reached a moisture content of 12% weight for weight (w/w). The inflorescences were ground to a fine powder using an electric grinder, then 98–103 mg were weighed and extracted with 1 mL ethanol. Samples were sonicated in an ultrasonic bath for 30 min, agitated in an orbital shaker at 25°C for 20 min, centrifuged at 20,000 x g for 5 min, then the samples were dissolved and diluted x20 in ethanol and filtered through a 0.22 μm Polytetrafluoroethylene syringe filter (Lumitron Ltd., Petah Tikva, Israel) prior to analysis.

Phytocannabinoid Identification and Quantification

Phytocannabinoid analyses for high concentrations of THC and CBD were performed using a Thermo Scientific UltiMate 3000 ultra-high-performance liquid chromatography coupled with an ultraviolet-visible diode array detector (UHPLC/UV) system. All other phytocannabinoids were identified and quantified by a similar UHPLC instrument coupled with a Q Exactive™ Focus Hybrid Quadrupole-Orbitrap MS (Thermo Scientific, Bremen, Germany), as previously described (Berman et al., 2018; Milay et al., 2020). In short, chromatographic separation was achieved using a HALO C18 Fused-Core column (2.7 μm, 150 × 2.1 mm), with a HALO guard column (2.7 μm, 5 × 2.1 mm), and a ternary A/B/C multistep gradient (solvent A: water with 0.1% acetic acid, solvent B: acetonitrile with 0.1% acetic acid, and solvent C: methanol). Identification and absolute quantification of phytocannabinoids were performed by external calibrations, as previously described (Berman et al., 2018). Sixteen analytical standards (CBDVA, CBDA, CBCA, CBNA, CBGA, THCA, CBDV, CBD, CBC, CBN, CBG, THC, Δ8-THC, CBL, THCV, CBCV) were used for direct quantification and semi-quantification of additional phytocannabinoids. All extracted samples were injected and analyzed by electrospray ionization (ESI)-LC/MS analysis, diluted at ratios of 1:9, 1:99, and 1:999 v/v *Cannabis* extract to ethanol.

Terpenoids Identification and Quantification

Profiling of terpenoids was performed using a modification of the static headspace gas chromatography tandem MS (SHS-GC/MS/MS) method by full evaporation technique (Shapira et al., 2019). SHS-injections were performed by PAL RTC robotic tool (CTC Analytics, Swaziland) with 30 min incubation time, temperature of 140°C and 1,000 μL injection volume of the gas phase. Gas chromatographic separation was achieved in 74 min using a TRACE 1310 GC (Thermo Fisher Scientific, Bremen,

Germany) equipped with a 30 m × 0.25 mm × 0.25 μm capillary DB-35MS UI column (Agilent Technologies, United States). MS/MS compounds detection was performed by a TSQ 8000 Evo triple quadrupole mass spectrometer (Thermo Fisher Scientific, Bremen, Germany). For the terpenoids analyses, 10 mg of each ground *Cannabis* sample was weighed in duplicates in a 20 mL HS amber vial with 1.2 g of glycerol and sealed by a magnetic cap. Solutions for the construction of the calibration curves were prepared in hexane and then 10 μL for each calibration level was added to amber vials with 1.2 g of glycerol in the same manner as the samples.

Some of the terpenoids were calculated semi-quantitatively based on the calibration curves of terpenoids with commercially available analytical standards with similar MS spectral characteristics and retention times. Identification of these terpenoids was performed by spectral searching against the NIST library (version 2.2) and relative Kovats retention indexes using a mixture of n-alkanes run under the same chromatographic conditions (for full details see **Supplementary Tables 2, 3**).

Statistical Analysis

Statistical analyses were conducted using GraphPad Prism software version 8.2.1 (GraphPad Inc.). Differences between samples in phytocannabinoid and terpenoid concentrations were analyzed using two-way ANOVA followed by Dunnett's multiple comparison test. *P*-values were corrected for multiple testing using the Tukey *post hoc* test. A value of at least $p \leq 0.05$ was considered significant for all tests ($^{*}p \leq 0.05$, $^{**}p \leq 0.01$, $^{***}p \leq 0.001$, $^{****}p \leq 0.0001$). Outliers were defined as data points greater than two standard deviations from the mean (9.6 for THCA and 9.5 for CBDA).

RESULTS

Phytocannabinoids Quantity Predominantly Decreases After Fertilization

Mature inflorescences (6 or 8 weeks post flower induction) from female *Cannabis* plants of two distinct chemovars (**Figures 1A,B**), THC-rich (Type I) and CBD-rich (Type III), were subjected to fertilization by three different male *Cannabis* plants: THC-rich (**Figures 1C,D**), CBD-rich (**Figures 1E,F**) or the original female plant induced to develop male pollen sacs by application of ethylene inhibitor (**Figure 1**). Induced-male plants (**Figures 1G,H**) were genetically identical to the female plants, had a distinct change in the sex of the flowers after treatment and a larger number of inflorescences compared to males (**Figure 1I**). Specific fertilization was achieved by incubation of the individual plants (**Figure 1J**).

Fertilization resulted in a predominantly significant decrease of overall total phytocannabinoids concentration in inflorescences for both the THC-rich and CBD-rich females, by all three types of males (**Figure 2A**). The concentration of the phytocannabinoids was analyzed by UHPLC/UV and electrospray ionization-liquid chromatography/mass spectrometry (ESI-LC/MS). The full list of the 95 phytocannabinoids quantified is displayed in **Supplementary Table 1** (as named by Berman et al., 2018). A sharper decrease was detected in the THC-rich chemovar female, exhibiting an average 75% decrease, while CBD-rich females showed a 60% decrease in phytocannabinoid contents after fertilization. Next, we investigated changes in quantities of individual phytocannabinoids (**Figures 2B–E**). For the THC-female, fertilization caused a reduction in the abundant phytocannabinoids, whose concentrations in the plant were above 0.02%, except for the phytocannabinoid (CBCA), which had an increase of about 50% when the plant was fertilized with an induced male (**Figure 2B**). Additional phytocannabinoids, whose concentrations in the plant were 0.001–0.2%, were also mostly reduced upon fertilization. The concentrations of CBC, cannabichromevarinic acid (CBCVA) and 373-15c were increased when fertilized by the induced male (**Figure 2C**). When THCA was excluded as an outlier as its concentration is 15-fold higher, the less abundant phytocannabinoids 331-18b, CBG, CBDA and 331-18d were significantly reduced upon fertilization. Similarly, for the CBD-female, fertilization caused a reduction in both the abundant (**Figure 2D**) and additional phytocannabinoids when CBDA is excluded as an outlier (**Figure 2E**), except for the concentrations of THCA and THC that increased after fertilization with the induced male.

Terpenoids Quantity Decreases After Fertilization in the Cannabidiol-Rich Female Plant but Varies in the THC-Rich Female Plant

In addition to assessing the phytocannabinoid contents, we quantified over 100 terpenoid compounds. The THC- and CBD-rich female plants differed in their profile of terpenoids before fertilization (**Supplementary Figure 1**). About half of the quantified terpenoids had pure analytical standards available and were analyzed as previously described (Shapira et al., 2019). However, out of a total of 113 terpenoids detected using (SHS-GC/MS/MS), 63 terpenoids in either the THC-rich or the CBD-rich plants did not have commercially available standards (for a full list see **Supplementary Table 4**). Some of these terpenoids demonstrated significant changes after fertilization, therefore, we assessed them with a newly developed semi-quantitative analysis (**Figure 3**). In this manner, we quantified terpenoids such as δ-Guaiene and *trans*-α-Bisabolene (denoted as 81 and 93, respectively). The semi-quantitative analysis is based on the calibration curves of terpenoids with commercially available analytical standards, relying primarily on similar MS spectral characteristics and also on retention times (**Supplementary Figure 2**).

The total amount of terpenoids in the inflorescences was found to be chemovar specific (**Figure 4A**). The high-CBD female plants exhibited two to threefold higher concentrations of terpenoids, both in the unfertilized and all three types of fertilized plants, compared to the THC-rich female plants. Upon fertilization, there were no significant changes in terpenoid accumulation in the THC-rich female. In the CBD-rich female

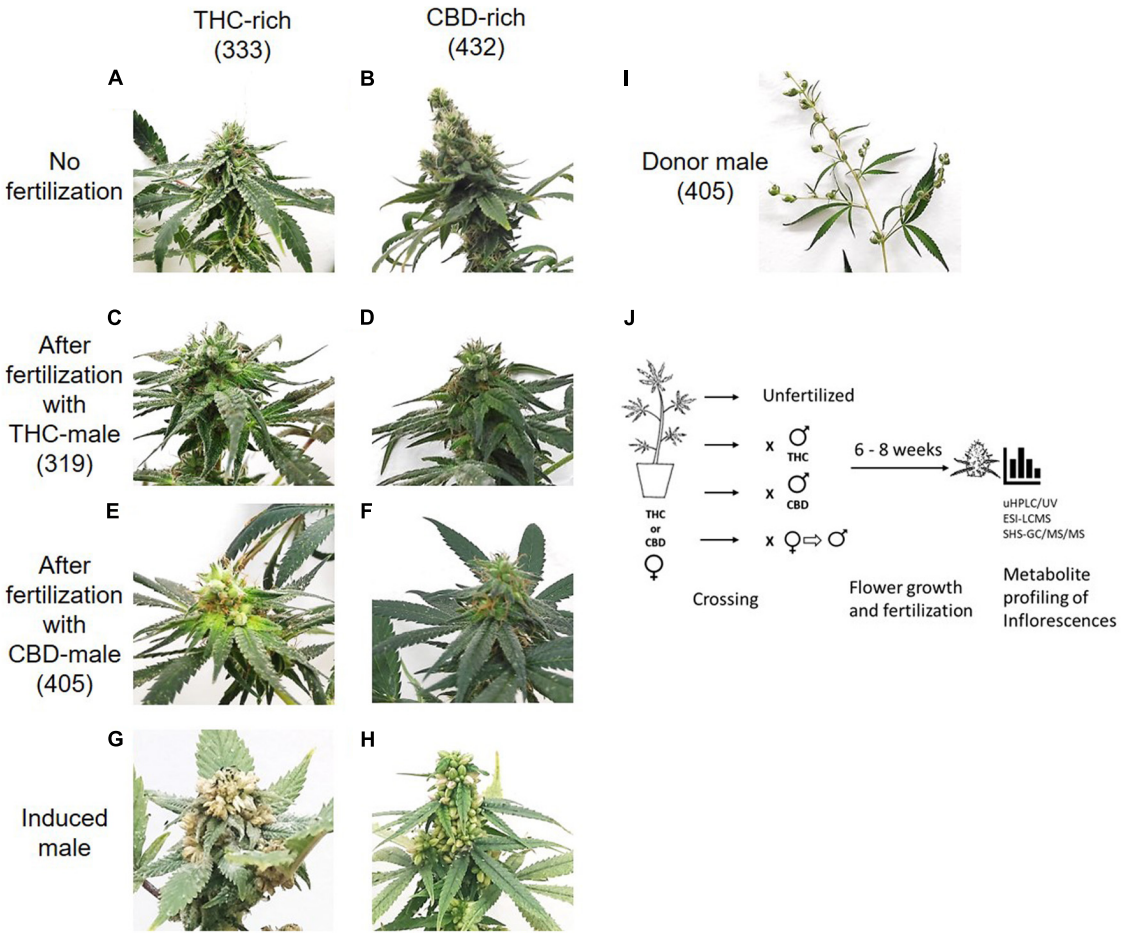

FIGURE 1 | Study design. Differences in inflorescences between THC-rich and CBD-rich plants without **(A,B)** and after fertilization with either THC-rich male (strain 319) **(C,D)** or CBD-rich male (strain 405) **(E,F)** and their respective induced-male plants **(G,H)**. **(I)** Representative image of a male donor plant (strain 405). To capture images, the plants were placed on the same white background and photographed individually. **(J)** Experimental design. Female *Cannabis* plants of two distinct types, THC- or CBD-rich chemovars, were subjected to fertilization by three different male *Cannabis* plants: THC- or CBD-rich plants, and an induced-male plant achieved by application of ethylene inhibitor. Female and male plants were incubated together for 6–8 weeks. The profile of their secondary metabolites was analyzed by UHPLC/UV and ESI-LC/MS for phytocannabinoids and SHS-GC/MS/MS for terpenoids.

plants, there was no significant change when fertilized with a THC-rich male plant, but fertilization with a CBD-rich male or an induced male resulted in a significant reduction in total terpenoids. The profile of terpenoids in plants is highly variable (Booth et al., 2020), and being mostly volatile compounds, they are also more susceptible to changes due to sample preparation procedure, e.g., the freshness of samples (Livingston et al., 2020). We detected an overall fertilization-dependent decrease in total terpenoid accumulation only in the CBD-rich plant, while the THC-rich plant showed a mixed trend of changes, either reduction or no significant change.

Out of 113 terpenoids detected, 31 were monoterpenoids, built up by two isoprene units (10 carbons) and the rest were sesquiterpenoids, built up by three isoprene units (15 carbons) (Shapira et al., 2019). To further evaluate the influence of fertilization on terpenoid accumulation after fertilization, we analyzed these two distinct subgroups. Monoterpenoid concentrations were significantly reduced for the THC-rich female by 60–80% upon fertilization with all three types of males; for the CBD-rich female, there was a significant 50% reduction except for when fertilized by the induced-male, which left the concentrations unchanged (**Figure 4B**). The concentration of sesquiterpenoids was unchanged for the THC-rich female, but there was a trend of reduced concentrations in the CBD-rich fertilized female, which was statistically significant when fertilized with the CBD-rich or the induced male (**Figure 4C**).

Individual Terpenoid Concentrations Are Differentially Affected by Fertilization

Next, we set out to examine the accumulation of individual terpenoids in the plants (**Figure 5**) and found chemovar-specific differences. For the THC-rich female, the most abundant terpenoid was β-caryophyllene and its concentration was reduced upon fertilization (**Figures 5A,B**). For the CBD-rich female, the most abundant terpenoid was α-bisabolol, its concentration

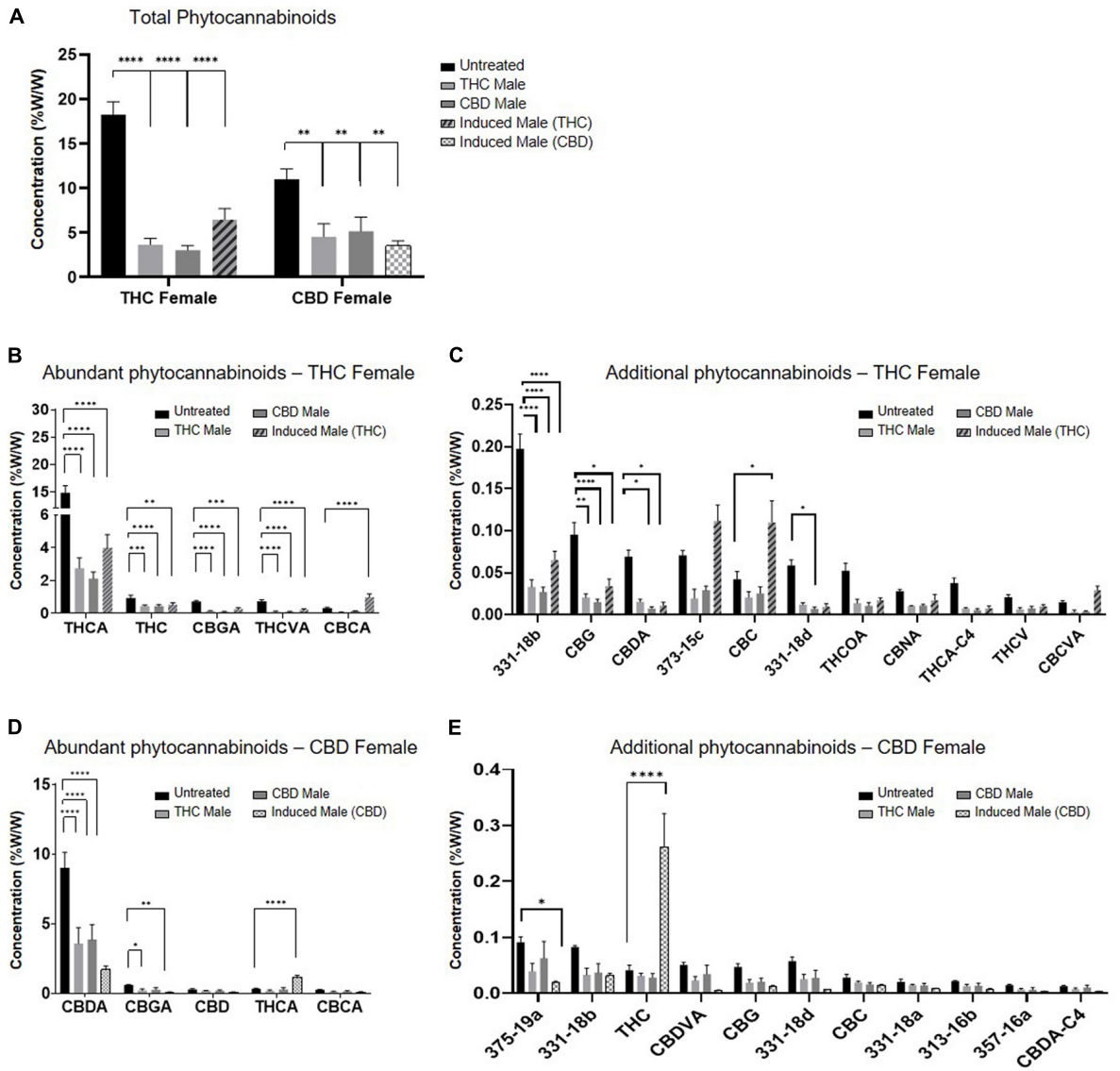

FIGURE 2 | Phytocannabinoids quantity predominantly decreases after fertilization with all types of males. **(A)** Total phytocannabinoid concentrations and **(B–E)** Individual phytocannabinoid concentrations after fertilization relative to unfertilized control. Abundant phytocannabinoid concentrations were considered > 0.2% **(B,D)** and additional phytocannabinoid concentrations were 0.001–0.2% **(C,E)** in the unfertilized plants. Data are presented as mean ± SEM (n = 4–6, %w/w) and statistically analyzed by two-way ANOVA followed by Dunnett's multiple comparison test (*$p \leq 0.05$; **$p \leq 0.01$; ***$p \leq 0.001$; ****$p \leq 0.0001$). Significance in C, E was calculated after excluding THCA and CBDA, respectively, from the data.

was above detection limit both before and after fertilization (**Figures 5C,D**). Moreover, we noticed that the terpenoid profile changed during the length of the flowering time, between 6–8 weeks after fertilization. This was in contrast to the phytocannabinoids profile, which was more consistent between these two time-points (data not shown). For example, for the CBD-rich female, the sesquiterpenoid Caryophyllene oxide had a very low concentration in the 6-week flowering plant but became highly abundant in the 8-week plant (**Figures 5C,D**). Hence, in addition to chemovar-specific differences, differential accumulation was observed between 6- and 8-week growth in the same chemovar.

As seen in **Figure 5**, numerous terpenoids significantly decreased following fertilization. However, several specific terpenoids showed an interesting increase in concentration after fertilization. For example, in the THC-rich female, members of the Eudesmol family of sesquiterpenoids (α-, β-, and γ-Eudesmol) were mostly undetected in the unfertilized plant, but their concentrations were significantly increased upon fertilization by the THC male plant only, both at 6 and 8 weeks after fertilization (**Figure 6A**). Interestingly, the levels of these terpenoids were either reduced or unchanged in the CBD-rich female due to fertilization processes. In contrast, in the CBD-rich female, the monoterpenoid Linalool significantly

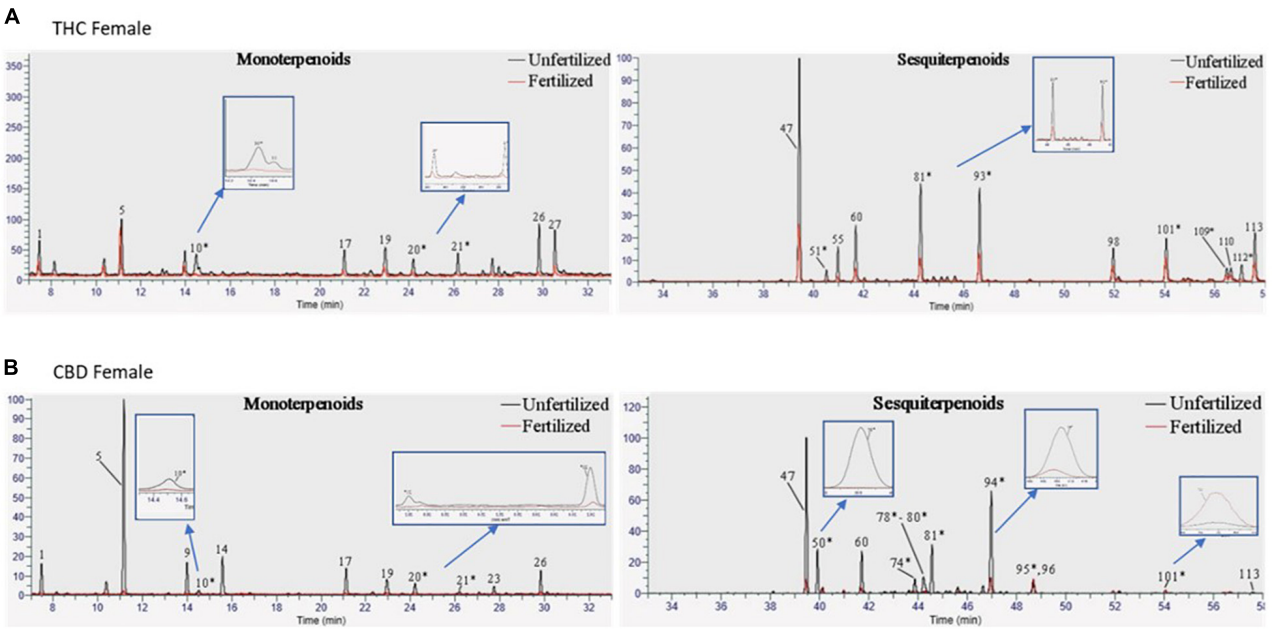

FIGURE 3 | Terpenoid profiles of *Cannabis* strains before and after fertilization. Overlay of chromatograms of the unfertilized and fertilized samples of **(A)** THC-rich and **(B)** CBD-rich female plants were performed by the same scales [retention time (RT); relative abundance of the signal intensity; weight of the samples (10 mg)], showing monoterpenoids on the left and sesquiterpenoids on the right. * Terpenoids that were semi-quantified.

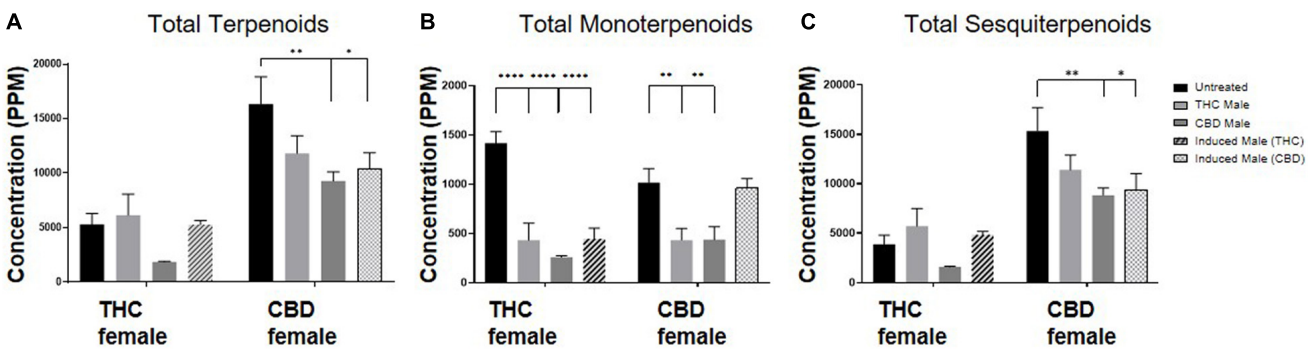

FIGURE 4 | Terpenoid quantity varies after fertilization. Terpenoid concentrations as quantified by SHS-GC/MS/MS of **(A)** total identified terpenoids, **(B)** total monoterpenoids and **(C)** total sesquiterpenoids. Data are reported as mean ± SEM of terpenoid concentrations (n = 3–4, ppm). Statistically significant differences between treatments and control (unfertilized) were calculated by two-way ANOVA followed by Dunnett's multiple comparison test (*$p \leq 0.05$; **$p \leq 0.01$; ****$p \leq 0.0001$).

increased upon fertilization by the induced male, but was reduced or unchanged following all other fertilization processes in both plant chemovars (**Figure 6B**).

DISCUSSION

The present study was designed to examine the influence of flower fertilization on the accumulation of *Cannabis* secondary metabolites. The primary outcome is the significant overall decrease in phytocannabinoid metabolites upon fertilization. This decrease was evident in almost all phytocannabinoids measured, regardless if those were the abundant ones or the relatively low accumulating components (**Figure 2**). Though the altogether amount of phytocannabinoids is drastically reduced, the ratio between the different compounds is kept and their profile in the plant remains principally unchanged.

Terpenoid concentrations mostly decreased but varied. While monoterpenoids had a similar decrease as portrayed by the phytocannabinoids, sesquiterpenoids exhibited a more diverse pattern, some of which increased and some decreased upon fertilization (**Figure 3**). However, examining specific metabolites can point to several phytocannabinoids or terpenoids that have an

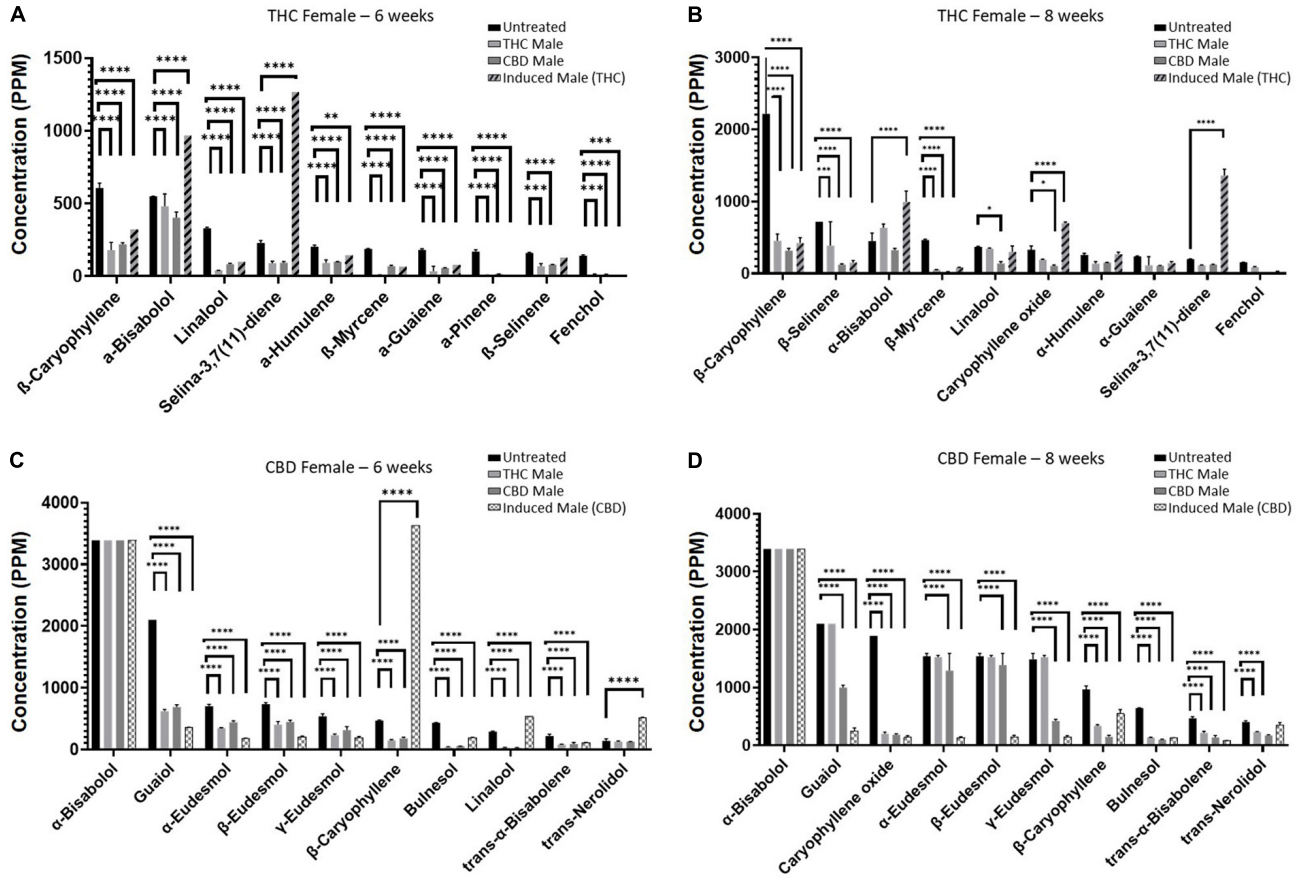

FIGURE 5 | Individual terpenoid concentrations in THC- and CBD-rich female plants at 6 or 8 weeks. Abundant terpenoids in the unfertilized female flowers and their concentrations at 6 weeks **(A,C)** and 8 weeks **(B,D)**. Data are reported as mean ± SEM of terpenoid concentration (n = 2–3, except THC-female fertilized by induced male (THC) at 6 weeks). Statistically significant differences between treatments and control (unfertilized) were calculated by two-way ANOVA followed by Dunnett's multiple comparison test (*$p \leq 0.05$; **$p \leq 0.01$; ***$p \leq 0.001$; ****$p \leq 0.0001$). Values presented without SEM exceeded the maximal detection limit (maximum limits of detection for terpenoids appear in **Supplementary Table 5**).

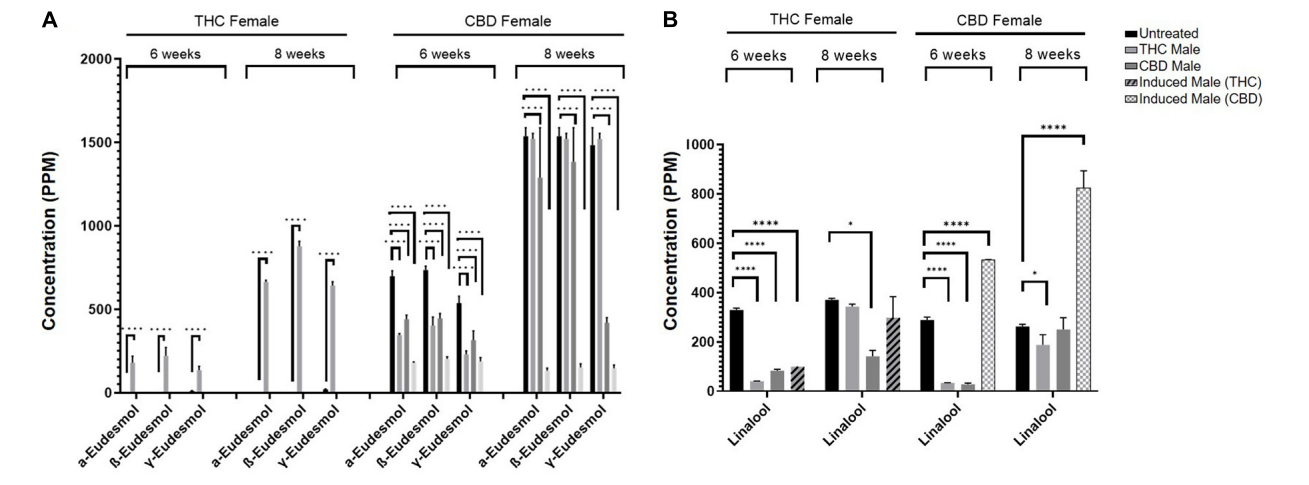

FIGURE 6 | Specific terpenoids are increased following fertilization. **(A)** α-, β-, and γ-Eudesmol and **(B)** Linalool concentrations in THC-rich and CBD-rich females at 6-weeks and 8-weeks after fertilization (n = 2–3, except THC-female fertilized by induced male (THC) at 6 weeks). Statistically significant differences between treatments and control (unfertilized) were calculated by two-way ANOVA followed by Dunnett's multiple comparison test (*$p \leq 0.05$; ****$p \leq 0.0001$).

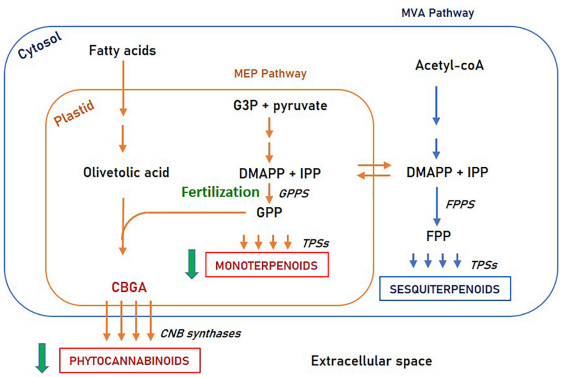

FIGURE 7 | Phytocannabinoids and terpenoids biosynthesis pathways. Fertilization affects the MEP pathway in an enzymatic step upstream to GPP synthase. MEP, Methylerythritol phosphate; MVA, Mevalonate; G3P, Glyceraldehyde 3-phosphate; DMAPP, Dimethylallyl diphosphate; IPP, Isopentenyl diphosphate; GPP, Geranyl diphosphate; FPP, Farnesyl diphosphate; GPPs, GPP synthase; FPPS, FPP synthase; TPSs, Terpene synthases.

individual trend, suggesting a more complex regulatory network (**Figures 4**, **5**).

First, these results confirm that when the objective is to maintain high levels of phytocannabinoids, fertilization must be avoided. Apart from a physical separation between female and male flowers or vegetative reproduction, this goal could be achieved using advanced genetic manipulations that target female fertilization pathways (Huang et al., 2016; Jung et al., 2020; Zhu et al., 2020).

Second, this study revealed the resemblance between monoterpenoids and phytocannabinoids accumulation patterns. Both secondary metabolite species are decreased upon fertilization, while sesquiterpenoids are differently influenced. Possible explanations for this similarity are common intracellular regulation pathways or shared morphological structures. From a cellular perspective, monoterpenoids and phytocannabinoids share the common biosynthetic precursor Geranyl diphosphate (GPP) and are both biosynthesized in the plastid (Booth et al., 2020; Romero et al., 2020). In contrast, sesquiterpenoids are synthesized in the cytosol from a different precursor (Farnesyl pyrophosphate—FPP). This suggests that phytocannabinoids and monoterpenoids may share a common regulation mechanism, involving an enzymatic step upstream to GPP, such as GPP synthase (illustrated in **Figure 7**).

Alternatively, from a morphological perspective, previous studies have shown that although phytocannabinoids, monoterpenoids, and sesquiterpenoids are all biosynthesized and accumulated in the glandular trichomes, their distribution differentiates during trichome development and between trichome types. A recent study by Booth et al. (2020) showed an increase in the ratio of monoterpenoids relative to sesquiterpenoids when flowers are maturing. Another study (Livingston et al., 2020) showed that monoterpenoids are accumulated in both pre-stalked and stalked trichomes, while sesquiterpenoids are abundant in sessile trichomes. Phytocannabinoids are accumulated in both types of trichomes, but the stalked type composed 80–90% of the total trichomes in the mature flower. A common accumulation pattern of monoterpenoids and phytocannabinoids during flower development was also previously demonstrated (Aizpurua-Olaizola et al., 2016). Parallel accumulation and decrease of phytocannabinoids and monoterpenoids in contrast to sesquiterpenoids may suggest that trichome types are differently affected by fertilization, and hence the diversity in metabolite accumulation.

An additional major finding depicted in this study is the somewhat dependent outcome of the fertilization process on the pollen donor plant. Both THC- or CBD-rich male plants, whether naturally occurring or female-induced, had a different impact on the metabolite concentration in the female after fertilization. For instance, fertilization by the induced-male led to an increase of specific phytocannabinoids (**Figure 2**): THC and THCA in the CBD female and CBC, CBCA, CBCVA, and 373-15C in the THC female. The exact mechanism by which these phytocannabinoids are increased is not yet clear. It may be the result of altered regulation of synthesis enzymes, for example the upregulation of THCA synthase or CBCA synthase (Laverty et al., 2019). A previous study found over 10,000 genes are differentially expressed upon masculinization of female plants (Adal et al., 2021), but it is not clear how these genes are related to phytocannabinoid expression in the fertilized female plant. A donor-dependent effect was also detected in the specific increase in the Eudesmol family (α-, β-, and γ-Eudesmol) components, which were highly increased in the THC-rich female upon fertilization by the THC-rich male plant (**Figure 6A**) and a parallel specific increase in Linalool in the CBD-rich female fertilized by the induced male (**Figure 6B**). However, regardless of the type of male plant used for fertilization, the overall profile of the phytocannabinoids in the fertilized female plant remained unaltered, i.e., no new phytocannabinoids that were not expressed in the unfertilized plant were discovered and the relative ratio between the different phytocannabinoids was mostly kept. Interestingly, though the density of phytocannabinoids and terpenoids in males is minor (data not shown) compared to the female flowers, with high potency female plants showing 10–20-times more THC than corresponding males (Clarke and Merlin, 2016), male plants also possess a distinct profile of these compounds.

CONCLUSION

Here, we used highly advanced analytical methods to thoroughly assess the composition of 95 phytocannabinoids and 113 terpenoids in the inflorescences of female plants fertilized by different males, including the female plant itself induced to develop male pollen sacs. We found that fertilization significantly decreased phytocannabinoids content, while terpenoids were differentially affected. To further elucidate the effect of fertilization on the secondary metabolite accumulation, future studies that follow the gene expression of enzymes upstream to

GPP after fertilization may allow exposing master regulators of the biochemical pathways. In addition, better characterization of the morphological changes following fertilization may shed light on how different trichome types are affected by fertilization. Finally, the variance in metabolites observed by fertilization with different male plants may suggest that the pollen itself or the developing embryo influence the female sporophyte.

Altogether, one must remember that these specialized secondary metabolites have an important role *in planta*, increasing the plant fitness to the environment (Huchelmann et al., 2017). The substantial decrease in phytocannabinoids and terpenoids after fertilization may point to their functional roles in the plant. The actual functions of phytocannabinoids and terpenoids in *Cannabis* were only sparsely studied, mainly suggesting roles in defense against biotic or abiotic factors (Potter, 2009), protection from UV radiation (Eichhorn Bilodeau et al., 2019), prevention of desiccation (Gülck and Møller, 2020), or induction of cell death in leaves (Morimoto et al., 2007). The observed dynamics of the accumulation of these metabolites during flower development and fertilization may point to their different roles along the plant's life cycle.

DATA AVAILABILITY STATEMENT

The raw data supporting the conclusions of this article will be made available by the authors, without undue reservation.

AUTHOR CONTRIBUTIONS

PB, MF, and DM: conception and design. OC, IK, and RP: plant maintenance, manipulations, fertilization, and harvest. CL: acquisition and ESI-LC/MS analysis and interpretation of data. AS: acquisition of GC data and development of semi-quantitative GC methodology. OG: extraction and sample preparation of Cannabis samples and UHPLC/UV analysis. CL, AS, and SP: figure preparation. CL, SP, PB, MF, and DM: writing, review, and revision of the manuscript. MF and DM: study supervision. All authors contributed to the article and approved the submitted version.

ACKNOWLEDGMENTS

We thank Dr. Ari Feder for helpful discussions and insights.

SUPPLEMENTARY MATERIAL

The Supplementary Material for this article can be found online at: https://www.frontiersin.org/articles/10.3389/fpls.2021.753847/full#supplementary-material

REFERENCES

Adal, A. M., Doshi, K., Holbrook, L., and Mahmoud, S. S. (2021). Comparative RNA-Seq analysis reveals genes associated with masculinization in female *Cannabis sativa*. *Planta* 253, 1–17. doi: 10.1007/S00425-020-03522-Y

Aizpurua-Olaizola, O., Soydaner, U., Öztürk, E., Schibano, D., Simsir, Y., Navarro, P., et al. (2016). Evolution of the cannabinoid and terpene content during the growth of *Cannabis sativa* plants from different chemotypes. *J. Nat. Prod.* 79, 324–331. doi: 10.1021/acs.jnatprod.5b00949

Allen, K. D., McKernan, K., Pauli, C., Roe, J., Torres, A., and Gaudino, R. (2019). Genomic characterization of the complete terpene synthase gene family from *Cannabis sativa*. *PLoS One* 14:e0222363. doi: 10.1371/journal.pone.0222363

Andre, C. M., Hausman, J. F., and Guerriero, G. (2016). *Cannabis sativa*: the plant of the thousand and one molecules. *Front. Plant Sci.* 7:19. doi: 10.3389/fpls.2016.00019

Berman, P., Futoran, K., Lewitus, G. M., Mukha, D., Benami, M., Shlomi, T., et al. (2018). A new ESI-LC/MS approach for comprehensive metabolic profiling of phytocannabinoids in *Cannabis*. *Sci. Rep.* 8:14280. doi: 10.1038/s41598-018-32651-4

Bernstein, N., Gorelick, J., Zerahia, R., and Koch, S. (2019). Impact of N, P, K, and humic acid supplementation on the chemical profile of medical cannabis (*Cannabis sativa* L). *Front. Plant Sci.* 10:736. doi: 10.3389/fpls.2019.00736

Bonini, S. A., Premoli, M., Tambaro, S., Kumar, A., Maccarinelli, G., Memo, M., et al. (2018). Cannabis sativa: a comprehensive ethnopharmacological review of a medicinal plant with a long history. *J. Ethnopharmacol.* 227, 300–315. doi: 10.1016/j.jep.2018.09.004

Booth, J. K., Page, J. E., and Bohlmann, J. (2017). Terpene synthases from *Cannabis sativa*. *PLoS One* 12:e0173911. doi: 10.1371/journal.pone.0173911

Booth, J. K., Yuen, M. M. S., Jancsik, S., Madilao, L. L., and Page, A. J. E. (2020). Terpene synthases and terpene variation in cannabis sativa1[OPEN]. *Plant Physiol.* 184, 130–147. doi: 10.1104/PP.20.00593

Borghi, M., and Fernie, A. R. (2020). Outstanding questions in flower metabolism. *Plant J.* 103, 1275–1288. doi: 10.1111/tpj.14814

Cai, S., Zhang, Z., Huang, S., Bai, X., Huang, Z., Zhang, Y. J., et al. (2021). CannabisGDB:a comprehensive genomic database for *Cannabis sativa* L. *Plant Biotechnol. J.* 19, 857–859. doi: 10.1111/pbi.13548

Cassano, T., Villani, R., Pace, L., Carbone, A., Bukke, V. N., Orkisz, S., et al. (2020). From *Cannabis sativa* to cannabidiol: promising therapeutic candidate for the treatment of neurodegenerative diseases. *Front. Pharmacol.* 11:124. doi: 10.3389/fphar.2020.00124

Chandra, S., Lata, H., and ElSohly, M. A. (2020). Propagation of *Cannabis* for clinical research: an approach towards a modern herbal medicinal products development. *Front. Plant Sci.* 11:958. doi: 10.3389/fpls.2020.00958

Clarke, R., and Merlin, M. (2016). *Cannabis: Evolution and Ethnobotany*. Berkeley, CA: University of California Press.

Eichhorn Bilodeau, S., Wu, B. S., Rufyikiri, A. S., MacPherson, S., and Lefsrud, M. (2019). An update on plant photobiology and implications for cannabis production. *Front. Plant Sci.* 10:296. doi: 10.3389/fpls.2019.00296

ElSohly, M. A., and Slade, D. (2005). Chemical constituents of marijuana: the complex mixture of natural cannabinoids. *Life Sci.* 78, 539–548. doi: 10.1016/j.lfs.2005.09.011

Erridge, S., Mangal, N., Salazar, O., Pacchetti, B., and Sodergren, M. H. (2020). Cannflavins – From plant to patient: a scoping review. *Fitoterapia* 146:104712. doi: 10.1016/j.fitote.2020.104712

Fernández-Ruiz, J. (2019). The biomedical challenge of neurodegenerative disorders: an opportunity for cannabinoid-based therapies to improve on the poor current therapeutic outcomes. *Br. J. Pharmacol.* 176, 1370–1383. doi: 10.1111/bph.14382

Flores-Sanchez, I. J., and Verpoorte, R. (2008). Secondary metabolism in cannabis. *Phytochem. Rev.* 7, 615–639. doi: 10.1007/s11101-008-9094-4

Franco, V., Bialer, M., and Perucca, E. (2021). Cannabidiol in the treatment of epilepsy: current evidence and perspectives for further research. *Neuropharmacology.* 185:108442. doi: 10.1016/j.neuropharm.2020.108442

Gonçalves, J., Rosado, T., Soares, S., Simão, A., Caramelo, D., Luís, Â, et al. (2019). *Cannabis* and its secondary metabolites: their use as therapeutic drugs, toxicological aspects, and analytical determination. *Medicines* 6:31. doi: 10.3390/medicines6010031

Gülck, T., and Møller, B. L. (2020). Phytocannabinoids: origins and biosynthesis. *Trends Plant Sci.* 25, 985–1004. doi: 10.1016/j.tplants.2020.05.005

Hanuš, L. O., Meyer, S. M., Muñoz, E., Taglialatela-Scafati, O., and Appendino, G. (2016). Phytocannabinoids: a unified critical inventory. *Nat. Prod. Rep.* 33, 1357–1392. doi: 10.1039/c6np00074f

Hawley, D., Graham, T., Stasiak, M., and Dixon, M. (2018). Improving *Cannabis* bud quality and yield with subcanopy lighting. *HortScience* 53, 1593–1599. doi: 10.21273/HORTSCI13173-18

Huang, J., Smith, A. R., Zhang, T., and Zhao, D. (2016). Creating completely both male and female sterile plants by specifically ablating microspore and megaspore mother cells. *Front. Plant Sci.* 7:30. doi: 10.3389/fpls.2016.00030

Huchelmann, A., Boutry, M., and Hachez, C. (2017). Plant glandular trichomes: natural cell factories of high biotechnological interest. *Plant Physiol.* 175, 6–22. doi: 10.1104/pp.17.00727

Jung, Y. J., Kim, D. H., Lee, H. J., Nam, K. H., Bae, S., Nou, I. S., et al. (2020). Knockout of slms10 gene (Solyc02g079810) encoding bhlh transcription factor using crispr/cas9 system confers male sterility phenotype in tomato. *Plants* 9:1189. doi: 10.3390/plants9091189

Laverty, K. U., Stout, J. M., Sullivan, M. J., Shah, H., Gill, N., Holbrook, L., et al. (2019). A physical and genetic map of *Cannabis sativa* identifies extensive rearrangements at the THC/CBD acid synthase loci. *Genome Res.* 29, 146–156. doi: 10.1101/gr.242594.118

Livingston, S. J., Quilichini, T. D., Booth, J. K., Wong, D. C. J., Rensing, K. H., Laflamme-Yonkman, J., et al. (2020). *Cannabis* glandular trichomes alter morphology and metabolite content during flower maturation. *Plant J.* 101, 37–56. doi: 10.1111/tpj.14516

Magagnini, G., Grassi, G., and Kotiranta, S. (2018). The effect of light spectrum on the morphology and cannabinoid content of *Cannabis sativa* L. *Med. Cannabis Cannabinoids* 1, 19–27. doi: 10.1159/000489030

McGarvey, P., Huang, J., McCoy, M., Orvis, J., Katsir, Y., Lotringer, N., et al. (2020). *De novo* assembly and annotation of transcriptomes from two cultivars of *Cannabis* sativa with different cannabinoid profiles. *Gene* 762:145026. doi: 10.1016/j.gene.2020.145026

Meier, C., and Mediavilla, V. (1998). Factors influencing the yield and the quality of hemp (*Cannabis sativa* L.) essential oil. *J. Int. Hemp Assoc.* 5, 16–20.

Milay, L., Berman, P., Shapira, A., Guberman, O., and Meiri, D. (2020). Metabolic profiling of *Cannabis* secondary metabolites for evaluation of optimal postharvest storage conditions. *Front. Plant Sci.* 11:583605. doi: 10.3389/fpls.2020.583605

Mohan Ram, H. Y., and Sett, R. (1982). Induction of fertile male flowers in genetically female *Cannabis sativa* plants by silver nitrate and silver thiosulphate anionic complex. *Theor. Appl. Genet.* 62, 369–375. doi: 10.1007/BF00275107

Morimoto, S., Tanaka, Y., Sasaki, K., Tanaka, H., Fukamizu, T., Shoyama, Y., et al. (2007). Identification and characterization of cannabinoids that induce cell death through mitochondrial permeability transition in cannabis leaf cells. *J. Biol. Chem.* 282, 20739–20751. doi: 10.1074/jbc.M700133200

Namdar, D., Charuvi, D., Ajjampura, V., Mazuz, M., Ion, A., Kamara, I., et al. (2019). LED lighting affects the composition and biological activity of *Cannabis sativa* secondary metabolites. *Ind. Crops Prod.* 132, 177–185. doi: 10.1016/j.indcrop.2019.02.016

O'Neill, S. D. (1997). Pollination regulation of flower development. *Annu. Rev. Plant Biol.* 48, 547–574. doi: 10.1146/annurev.arplant.48.1.547

Potter, D. J. (2009). *The Propagation, Characterisation and Optimisation of Cannabis sativa L. as a Phytopharmaceutical.* Ph.D. Thesis. London: King's College London.

Potter, D. J., Hammond, K., Tuffnell, S., Walker, C., and Di Forti, M. (2018). Potency of Δ9–tetrahydrocannabinol and other cannabinoids in cannabis in England in 2016: implications for public health and pharmacology. *Drug Test. Anal.* 10, 628–635. doi: 10.1002/dta.2368

Radwan, M. M., ElSohly, M. A., Slade, D., Ahmed, S. A., Wilson, L., El-Alfy, A. T., et al. (2008). Non-cannabinoid constituents from a high potency *Cannabis sativa* variety. *Phytochemistry* 69, 2627–2633. doi: 10.1016/j.phytochem.2008.07.010

Rea, K. A., Casaretto, J. A., Al-Abdul-Wahid, M. S., Sukumaran, A., Geddes-McAlister, J., Rothstein, S. J., et al. (2019). Biosynthesis of cannflavins A and B from *Cannabis sativa* L. *Phytochemistry* 164, 162–171. doi: 10.1016/j.phytochem.2019.05.009

Rice, J., and Cameron, M. (2017). Cannabinoids for treatment of MS symptoms: state of the evidence. *Curr. Neurol. Neurosci. Rep.* 18:50. doi: 10.1007/s11910-018-0859-x

Romero, P., Peris, A., Vergara, K., and Matus, J. T. (2020). Comprehending and improving cannabis specialized metabolism in the systems biology era. *Plant Sci.* 298:110571. doi: 10.1016/j.plantsci.2020.110571

Russo, E. B., and Marcu, J. (2017). Cannabis pharmacology: the usual suspects and a few promising leads. *Adv. Pharmacol.* 80, 67–134. doi: 10.1016/bs.apha.2017.03.004

Shapira, A., Berman, P., Futoran, K., Guberman, O., and Meiri, D. (2019). Tandem mass spectrometric quantification of 93 terpenoids in *Cannabis* using static headspace injections. *Anal. Chem.* 91, 11425–11432. doi: 10.1021/acs.analchem.9b02844

Small, E., and Naraine, S. G. U. (2016). Expansion of female sex organs in response to prolonged virginity in *Cannabis sativa* (marijuana). *Genet. Resour. Crop Evol.* 63, 339–348. doi: 10.1007/s10722-015-0253-3

Starowicz, K., and Finn, D. P. (2017). Cannabinoids and pain: sites and mechanisms of action. *Adv. Pharmacol.* 80, 437–475. doi: 10.1016/bs.apha.2017.05.003

Tripathi, S. K., and Tuteja, N. (2007). Integrated signaling in flower senescence: an overview. *Plant Signal. Behav.* 2, 437–445. doi: 10.4161/psb.2.6.4991

van Bakel, H., Stout, J. M., Cote, A. G., Tallon, C. M., Sharpe, A. G., Hughes, T. R., et al. (2011). The draft genome and transcriptome of *Cannabis sativa*. *Genome Biol.* 12:R102. doi: 10.1186/gb-2011-12-10-r102

Vincent, D., Rochfort, S., and Spangenberg, G. (2019). Optimisation of protein extraction from medicinal cannabis mature buds for bottom-up proteomics. *Molecules* 24:659. doi: 10.3390/molecules24040659

Zager, J. J., Lange, I., Srividya, N., Smith, A., and Markus Lange, B. (2019). Gene networks underlying cannabinoid and terpenoid accumulation in *cannabis*. *Plant Physiol.* 180, 1877–1897. doi: 10.1104/pp.18.01506

Zhu, H., Li, C., and Gao, C. (2020). Applications of CRISPR–Cas in agriculture and plant biotechnology. *Nat. Rev. Mol. Cell Biol.* 21, 661–677. doi: 10.1038/s41580-020-00288-9

Conflict of Interest: The authors declare that the research was conducted in the absence of any commercial or financial relationships that could be construed as a potential conflict of interest.

Publisher's Note: All claims expressed in this article are solely those of the authors and do not necessarily represent those of their affiliated organizations, or those of the publisher, the editors and the reviewers. Any product that may be evaluated in this article, or claim that may be made by its manufacturer, is not guaranteed or endorsed by the publisher.

frontiers in Plant Science

ORIGINAL RESEARCH
published: 17 November 2021
doi: 10.3389/fpls.2021.764103

Optimisation of Nitrogen, Phosphorus, and Potassium for Soilless Production of *Cannabis sativa* in the Flowering Stage Using Response Surface Analysis

Lewys Bevan[1], *Max Jones*[2] *and Youbin Zheng*[1]*

[1] School of Environmental Sciences, University of Guelph, Guelph, ON, Canada, [2] Department of Plant Agriculture, University of Guelph, Guelph, ON, Canada

Following legalisation, cannabis has quickly become an important horticultural crop in Canada and increasingly so in other parts of the world. However, due to previous legal restrictions on cannabis research there are limited scientific data on the relationship between nitrogen (N), phosphorus (P), and potassium (K) supply (collectively: NPK) and the crop yield and quality. This study examined the response of a high delta-9-tetrahydrocannabinol (THC) *Cannabis sativa* cultivar grown in deep-water culture with different nutrient solution treatments varying in their concentrations (mg L^{-1}) of N (70, 120, 180, 250, 290), P (20, 40, 60, 80, 100), and K (60, 120, 200, 280, 340) according to a central composite design. Results demonstrated that inflorescence yield responded quadratically to N and P, with the optimal concentrations predicted to be 194 and 59 mg L^{-1}, respectively. Inflorescence yield did not respond to K in the tested range. These results can provide guidance to cultivators when formulating nutrient solutions for soilless cannabis production and demonstrates the utility of surface response design for efficient multi-nutrient optimisation.

Keywords: cannabis, cannabinoids, nutrient, nitrogen, phosphorus, potassium

OPEN ACCESS

Edited by:
Donald Lawrence Smith, McGill University, Canada

Reviewed by:
Francesco Di Gioia, The Pennsylvania State University (PSU), United States
Ada Baldi, Department of Agriculture, Food, Environment and Forestry, Italy

***Correspondence:**
Youbin Zheng
yzheng@uoguelph.ca

Specialty section:
This article was submitted to Crop and Product Physiology, a section of the journal Frontiers in Plant Science

Received: *25 August 2021*
Accepted: *20 October 2021*
Published: *17 November 2021*

Citation:
Bevan L, Jones M and Zheng Y (2021) Optimisation of Nitrogen, Phosphorus, and Potassium for Soilless Production of Cannabis sativa in the Flowering Stage Using Response Surface Analysis. Front. Plant Sci. 12:764103. doi: 10.3389/fpls.2021.764103

INTRODUCTION

Drug-type cannabis (*Cannabis sativa*) is an important horticultural crop grown for medicinal and recreational purposes. Historically, many countries have prohibited the cultivation of drug-type cannabis which consequently provided a significant barrier to research on this crop. However, change in social attitudes towards consumption of cannabis has led to the repeal of cannabis prohibition in several countries/regions around the world. Following the 2018 repeal of cannabis prohibition in Canada, production of cannabis has quickly become an important part of the Canadian horticulture industry worth billions of dollars annually (Zheng, 2021). However, cannabis cultivators still lack scientific information about optimal growing conditions, such as supply of mineral nutrients, to help maximise crop yields, quality, and profits while minimising environmental impacts.

Proper supply of mineral nutrients is essential for efficient and sustainable cultivation of any crop. Among the most important nutrients for plants are nitrogen (N), phosphorus (P),

and potassium (K). However, few studies have investigated the response of cannabis to these nutrients. As a result, cannabis cultivators often rely on nutrient recipes developed by fertiliser companies, or by community consensus based on previously clandestine production. This poses a problem because deficient or excessive supply of nutrients may reduce yield (Caplan et al., 2017a,b) or lead to environmental pollution from runoff of excess nutrients (Beerling et al., 2014; Zheng, 2018). Nutrient runoff is an issue in many agricultural areas of the world because excess nutrients, specifically P, can lead to the eutrophication of water bodies (Schindler et al., 2016). In Ontario (the Canadian province in which this study was conducted) disposal of waste greenhouse nutrient solution, including from cannabis production facilities, is regulated by law at considerable cost to the cultivators (Ontario Ministry of Agriculture Food and Rural Affairs, 2019). An understanding of cannabis' mineral nutrient requirements can help us better synchronise nutrient supply and demand to maximise production while reducing nutrient waste and resulting environmental impacts.

Recent peer-reviewed studies have started to examine the response of *Cannabis* to mineral nutrients, but this area of research remains largely unexplored. These studies indicate the optimal N supply for both vegetative and flowering stages of cannabis production using conventional fertilisers is approximately 160 mg L^{-1} (Saloner and Bernstein, 2021). Plants supplied with N below 160 mg L^{-1} during the vegetative stage saw reduced photosynthetic capacity and plant growth, and during the flowering stage saw reduced inflorescence yield, though cannabinoid concentrations (not total production) were greater at extremely low N rates. The optimal N supply for plants grown with liquid organic fertilisers seems to be higher, with the highest yields being achieved with an organic N supply of approximately 390 and 260 mg L^{-1} for the vegetative and flowering stages, respectively (Caplan et al., 2017a,b). Given the limited number of studies and the relative importance of N on plant growth and development, collecting more information about cannabis response to N are needed to establish more accurate recommendations.

Phosphorus nutrition has long been a focus in cannabis cultivation. Growers often supply plants with relatively high P concentrations (up to 200 mg L^{-1}) during the flowering stage based on a belief that high P promotes flower development. However, there is little evidence to support this practice. A recent study found that cannabis plants in the vegetative stage supplied with 100 mg L^{-1} P performed similar to those supplied with 30 mg L^{-1} P (Shiponi and Bernstein, 2021). High P concentration in the nutrient solution creates a situation where environmental pollution from excess P is more likely. Clearly, the practice of supplying cannabis with high concentrations of P needs to be evaluated.

While there are no published studies examining the effect of K on inflorescence quality, some recent studies have looked at how K impacts inflorescence yield. Yield of aquaponically grown cannabis (g/plant) increased linearly with increasing nutrient solution K concentration in the range of 15–150 mg L^{-1} (Yep and Zheng, 2020). The nitrogen concentration (75 mg L^{-1}) used by Yep and Zheng (2020) reflects that of a typical aquaponic solution, but this N concentration is fairly low compared to conventional hydroponic nutrient solutions and may have been a limiting factor for plant growth and yield (Yep et al., 2020b). For the vegetative stage, cannabis plants supplied with 15 mg L^{-1} K had reduced growth and displayed foliar symptoms characteristic of K deficiency, while plants that received 60–240 mg L^{-1} K produced substantially more biomass and did not display K deficiency symptoms (Saloner et al., 2019). Although there is a lack of recommendations based on scientific research, some fertiliser companies are recommending 300–400 mg L^{-1} K. More research is needed to determine the optimal nutrient solution K concentration during cannabis flowering in soilless production systems when other nutrient elements are not limiting.

A challenge in developing fertiliser recommendations is that the number of combinations of nutrient concentrations that can be empirically tested is limited due to logistical and statistical considerations. As a result, most nutrient studies have a limited range of nutrient compositions that can overlook potential nutrient interactions across a broad range of nutrient compositions. Studies on cannabis response to nutrients so far have either investigated different concentrations of one nutrient while holding the others constant (Saloner et al., 2019; Saloner and Bernstein, 2020, 2021; Shiponi and Bernstein, 2021), or provided different concentrations of NPK in a set ratio (Caplan et al., 2017a,b; Bernstein et al., 2019). Neither of these approaches can evaluate nutrient interactions, which could have substantial impacts on the recommendations of optimum application rates.

Response surface methodology (RSM) is an alternative experimental design capable of concurrently optimising multiple factors over a wide range of levels using fewer experimental units compared to traditional designs (Myers et al., 2016). The efficiency of this design is achieved by using fewer experimental units which conserves space, time, and resources. Nutrient solution optimisation has been approached by some researchers as a "mixture system" which is a type of multifactor optimisation similar to response surface analysis (De Rijck and Schrevens, 1998, 1999a). However, the experimental design of a mixture system only optimises the nutrient composition of the solution but not the overall nutrient concentration as the design maintains a constant total nutrient supply in the solution. RSM allows the optimisation of both the nutrient solution composition and the concentrations of individual components without this limitation. Given the high cost of cannabis and growing space being limited to government-approved production facilities, the reduced number of experimental units required for a RSM approach is an advantage over conventional experimental designs.

The objective of this study was to determine the optimal concentrations of NPK for the flowering stage of cannabis in a soilless production system using the RSM approach.

MATERIALS AND METHODS

Plant Material and Growing Conditions

The experiment was conducted in a controlled-environment growth room at a Health Canada approved cannabis production facility located in Southern Ontario. A clonal selection of a high

FIGURE 1 | Rows of deep-water culture units containing trial plants at the end of the 3-week vegetative stage.

delta-9-tetrahydrocannabinol (THC), low cannabidiol (CBD) *C. sativa* cultivar "Gelato" was used for this trial. Plants were grown in deep-water culture (DWC) systems. Each DWC unit used a 19 L white plastic bucket (36 cm height × 30.5 cm top outside diameter × 26.4 cm bottom outside diameter) as the nutrient solution reservoir. DWC units were placed on the floor in five double rows of ten DWCs each (i.e., 100 DWCs total), each with one plant, spaced ten cm between adjacent units, 15 cm within the rows, and a one metre aisle-space between rows (**Figure 1**). Uniform 2-week-old cuttings (∼15 cm tall, 5–6 nodes trimmed to 3–4 leaves) rooted in rockwool cubes were transplanted into each DWC unit using a mesh pot (FHD Plastics, 0.62 L, 10.3 cm height × 12.5 cm diameter) filled with 8–16 mm expanded clay pebbles (Liapor, Hallerndorf, Germany) and inserted flush to the top of the bucket lids, with the bottom three cm of the mesh pot submerged in the nutrient solution. Each DWC bucket was supplied with nutrient solution and had an air-stone (Pawfly ASC030, 30 mm height × 18 mm diameter) providing 1.5 litres of air per minute to continuously mix and aerate the solution. The nutrient solutions in all DWC units were drained and replaced with 17 L of fresh nutrient solution weekly.

Plants were grown in the DWC systems vegetatively, under 18/6-h light/dark conditions, for 3 weeks before switching to a 12/12-h light/dark (i.e., short-day) photoperiod, to induce flowering. Plants were grown under short-day conditions for 7 weeks before being harvested. Light was provided by 1000 W metal halide bulbs at an average canopy-level photosynthetically photon flux density of 570 μmol m^{-2} s^{-1}. The air temperature and relative humidity were set at 25°C and 65%, respectively. There was no CO_2 supplementation.

Experimental Design and Treatments

A three-factor (i.e., N, P, and K), second order central rotatable composite design was used to model cannabis responses to these mineral nutrients. Following a response surface design (**Table 1**), treatments combinations were defined by their concentrations of N (70, 120, 180, 250, and 290 mg L^{-1}), P (20, 40, 60, 80, and 100 mg L^{-1}), and K (60, 120, 200, 280, and 340 mg L^{-1}) (**Table 2**) achieved by using different amounts of varies straight fertilisers (**Table 3**). The experimental unit (replicate) was one plant grown in an individual DWC unit. There were 15 different treatments, with at least five replicates per treatment. Plants were randomly assigned to each nutrient solution treatment by generating a random sequence of numbers from 1 to 100 arranged in ten columns and ten rows (matching DWC unit arrangement). For the first 3 weeks following transplant (vegetative growth), all plants received the same nutrient solution containing (mg L^{-1}): 112.8 N-NO_3, 7.2 N-NH_4, 40 P, 180 K, 110 Ca, 45 Mg, and 60 S. Once switched to short-day conditions, plants received their respective treatment nutrient solutions for the remainder of the experiment. Rainwater was used to make the nutrient solutions. The major cation and anion compositions of the treatment nutrient solutions are detailed in **Table 4**. All treatments were formulated to have the same N-NH_4/N-NO_3 ratio (1:16). All plants received the same concentration of a commercial ethylenediaminetetraacetate (EDTA) and diethylenetriamine pentaacetate (DTPA) chelated micronutrient mix throughout both vegetative and flowering stages (Plant-Prod Chelated Micronutrient Mix; Master Plant-Prod Inc., Brampton, Ontario, Canada) containing (mg L^{-1}): 2.1 Fe, 0.6 Mn, 0.12 Zn, 0.03 Cu, 0.39 B, and 0.018 Mo.

TABLE 1 | Coded and un-coded factors for each treatment of the response surface analysis experiment investigating the effect of nitrogen (N), phosphorus (P), and potassium (K) rates on cannabis production in deep-water culture.

	Coded factors			Un-coded factors (mg L^{-1})		
Treatment	**A**	**B**	**C**	**N[a]**	**P**	**K**
1	−1	−1	−1	120	40	120
2	+1	-1	−1	250	40	120
3	−1	+1	−1	120	80	120
4	+1	+1	−1	250	80	120
5	−1	−1	+1	120	40	280
6	+1	−1	+1	250	40	280
7	−1	+1	+1	120	80	280
8	+1	+1	+1	250	80	280
9	−1.682	0	0	70	60	200
10	+1.682	0	0	290	60	200
11	0	−1.682	0	180	20	200
12	0	+1.682	0	180	100	200
13	0	0	−1.682	180	60	60
14	0	0	+1.682	180	60	340
15	0	0	0	180	60	200
16	0	0	0	180	60	200
17	0	0	0	180	60	200
18	0	0	0	180	60	200
19	0	0	0	180	60	200
20	0	0	0	180	60	200

[a]*N-NH_4 + N-NO_3.*

TABLE 2 | Range and levels of the experimental factors according to three-factor central rotatable composite design.

	Range and levels				
Element	**–1.68[b]**	**–1**	**0**	**1**	**1.68[b]**
N[a]	70	120	180	250	290
P	20	40	60	80	100
K	60	120	200	280	340

[a] *$N\text{-}NH_4 + N\text{-}NO_3$.*
[b] *Radius adjustment factor for a three-factor design to make the design rotatable.*

The initial pH of the nutrient solutions was adjusted to 5.6 with 1 M sulphuric acid or 1 M sodium hydroxide, as needed. DWC units were topped up with pH-adjusted (5.6) rainwater 3–4 days after each weekly nutrient solution replacement to replace water lost due to evapotranspiration. Nutrient solution pH and electrical conductivity (EC, mS cm^{-1}) were measured using a hand-held metre (BLU2300E Combo Metre, Bluelab Corporation, New Zealand). EC and pH of treatment feed solution and of the final drained solution are listed in **Table 5**.

Plant Measurements

Aboveground Growth

Plant height and spread of the first three plants in each treatment were measured during the fifth week of the flowering stage. Plant height (cm) was measured from the lid of the DWC unit to the top of the apical inflorescence, and plant spread (cm) was measured at the widest point on the plant and then perpendicular to this measurement. Growth index (GI) was then calculated using the formula [GI = (height × $width_1$ × $width_2$)/300] (Caplan et al., 2017a). Plants were destructively harvested during the eighth week of flowering. To assess aboveground (including inflorescence) fresh weight (FW), plants were cut at substrate level and individually weighed on a digital balance.

Root Weight

During harvest, roots from the first three replicates of each treatment were cut from around the outer surface of the mesh pot and air dried for several days and then oven-dried at 92°C for 72 h and weighed (EG2200-2NM, KERN & SOHN, Balingen, Germany) to obtain root dry weight (DW).

Inflorescence Yield

Inflorescence material was trimmed of leaf tissue, removed from the stem, and then weighed to obtain inflorescence fresh weight (g/plant). To determine inflorescence dry weight (i.e., yield), ∼25 g samples of fresh inflorescence material from the first three plants in each treatment were weighed, dried at 70°C for 72 h, and then re-weighed to obtain dry weight (DW). Yield was computed on a per-plant basis as the total inflorescence FW × (sample DW/sample FW). Cured "whole-bud" cannabis inflorescence sold commercially normally contains 10 to 15% water. Therefore, the marketable yield can be calculated from inflorescence DW by factoring in the appropriate water content.

TABLE 3 | Amount of each straight fertiliser compound used to make treatment nutrient solutions.

	Fertiliser compound concentration (mg L^{-1})								
Treatment	**$Ca(NO_3)_2$**	**KNO_3**	**NH_4NO_3**	**KH_2PO_4**	**$(NH_3)H_2PO_4$**	**K_2SO_4**	**KCl**	**$MgSO_4{\cdot}7H_2O$**	**$CaCl_2{\cdot}2H_2O$**
1	650	180	–	180	–	–	–	450	–
2	1400	200	20	180	–	–	–	450	–
3	700	60	–	350	–	–	–	450	–
4	1550	60	–	350	–	–	–	450	–
5	600	200	–	180	–	–	300	450	50
6	1000	600	40	180	–	–	–	450	–
7	600	250	–	375	–	–	150	450	50
8	1100	500	30	350	–	–	–	450	–
9	150	350	–	250	20	–	–	450	300
10	1550	350	–	250	–	–	–	450	–
11	800	400	10	90	–	–	40	450	–
12	950	220	–	400	40	–	–	450	–
13	1100	–	–	220	–	–	–	450	–
14	450	700	40	260	–	–	–	450	150
15	800	400	–	200	50	–	–	450	–
16	800	400	–	200	50	–	–	450	–
17	800	400	–	200	50	–	–	450	–
18	800	400	–	200	50	–	–	450	–
19	800	400	–	200	50	–	–	450	–
20	800	400	–	200	50	–	–	450	–

TABLE 4 | Composition of major anions and cations in the treatment nutrient solutions.

	Nutrient concentrations (mg L^{-1})						
Treatment	**N**	**P**	**K**	**Ca**	**Mg**	**S[a]**	**Cl**
1	120	40	120	130	45	180	5.0
2	250	40	120	260	45	180	5.0
3	120	80	120	130	45	180	5.0
4	250	80	120	260	45	180	5.0
5	120	40	280	130	45	180	190
6	250	40	280	190	45	180	5.0
7	120	80	280	130	45	180	120
8	250	80	280	190	45	180	5.0
9	70	60	200	130	45	180	190
10	290	60	200	260	45	180	5.0
11	180	20	200	130	45	180	20
12	180	100	200	160	45	180	5.0
13	180	60	60	190	45	180	5.0
14	180	60	340	130	45	180	95
15	180	60	200	130	45	180	5.0
16	180	60	200	130	45	180	5.0
17	180	60	200	130	45	180	5.0
18	180	60	200	130	45	180	5.0
19	180	60	200	130	45	180	5.0
20	180	60	200	130	45	180	5.0

[a]*Includes sulphur added by the sulphuric acid used to adjust pH of the nutrient solution.*

TABLE 5 | Electrical conductivity (EC) and pH of feed and drain nutrient solutions.

Treatment	**Feed EC (mS cm^{-1})**	**Drain EC (mS cm^{-1})**	**Feed pH**	**Drain pH**
1	1.5	1.1	5.6	6.5
2	2.4	2.3	5.6	5.6
3	1.5	1.2	5.6	6.2
4	2.5	2.2	5.6	5.6
5	2.1	2.0	5.6	6.5
6	2.5	2.5	5.6	5.9
7	2.1	1.9	5.6	6.2
8	2.5	2.2	5.6	6.1
9	1.8	1.8	5.6	6.5
10	2.8	2.8	5.6	5.6
11	2.0	1.9	5.6	6.6
12	2.1	2.0	5.6	5.6
13	1.8	1.6	5.6	5.3
14	2.3	2.4	5.6	6.4
15	1.9	1.9	5.6	5.9
16	1.9	1.8	5.6	6.0
17	1.9	1.8	5.6	5.6
18	1.9	1.8	5.6	6.1
19	1.9	1.8	5.6	5.9
20	1.9	1.9	5.6	5.9

Cannabinoid Content

Representative samples (∼50 g) of fresh inflorescence from three plants per treatment were dried at 18°C and 50% relative humidity until inflorescence material reached ∼10% moisture. Composite sub-samples (∼10 g) of air-dried inflorescence material from the first three replicates in each treatment were vacuum-sealed and sent to HEXO Corp's in-house laboratory to determine cannabinoid concentration, including delta-9-tetrahydrocannabinol (Δ^9-THC), tetrahydrocannabinolic acid (THCA), cannabidiol (CBD), cannabidiolic acid (CBDA), cannabigerol (CBG), cannabigerolic acid (CBGA), cannabichromene (CBC), cannabinol (CBN), and delta-8-tetrahydrocannabinol (Δ^8-THC).

The cannabinoid analysis was conducted using ultra performance liquid chromatography (UPLC) separation. The composite sub-sample of dried cannabis was milled to a fine powder; from which1.0 g was extracted with an Acetontrile/H_2O mixture with sonication and agitation for 20 min at ambient temperature. A 1.5 mL aliquot was diluted and filtered into a HPLC vial and analysed as per 7020006509EN (Layton and Aubin, 2019).

Statistical Design and Analysis

RStudio software (RStudio Team, 2020) was used for data analysis. Normality and homoscedasticity of the data were assessed, and the data met these assumptions. The RStudio package "rsm" (Lenth, 2009) was used to analyse inflorescence yield and to generate three-dimensional and contour plots to represent the response surface. To improve the precision of yield estimates, the average yield of the five replicates in each treatment was used. Two sets of three surface and contour plots were created, each while holding one of the nutrient concentrations fixed at its centre point. These surface and contour plots, along with canonical analysis, were then used to determine the optimal rate of all three factors. Correlation analysis of yield and vegetative parameters was performed using the RStudio software package "ggplot2" (Wickham, 2016). To determine if there were differences in inflorescence cannabinoid content attributable to treatment, data from cannabinoid analysis was tested with a one-way ANOVA followed by Tukey's HSD *post hoc* test.

Statistical Model

$$yield = \mu + n + n^2 + p + p^2 + k + k^2 + (n \times p) + (n \times k) + (p \times k) + (n \times p \times k)$$

yield = dry inflorescence weight (g/plant)

μ = overall mean inflorescence weight (g/plant)

n = linear nitrogen component (fixed effect)

n^2 = quadratic nitrogen component (fixed effect)

p = linear phosphorus component (fixed effect)

p^2 = quadratic phosphorus component (fixed effect)

k = linear potassium component (fixed effect)

k^2 = quadratic potassium component (fixed effect)

n × p = nitrogen and phosphorus interaction (fixed interaction effect)

n × k = nitrogen and potassium interaction (fixed interaction effect)

p × k = phosphorus and potassium interaction (fixed interaction effect)

n × p × k = nitrogen and phosphorus and potassium interaction (fixed interaction effect).

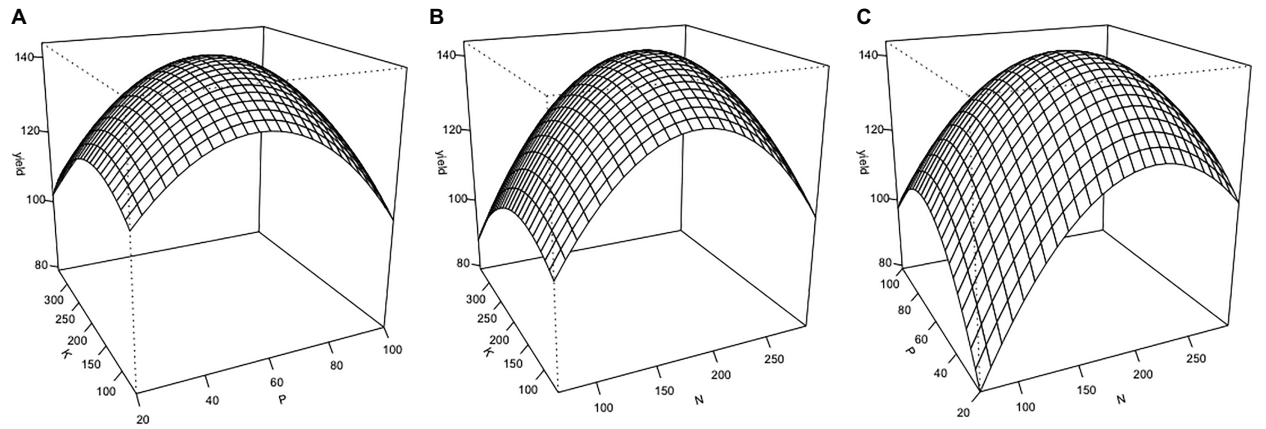

FIGURE 2 | Three-dimensional response surfaces for inflorescence yield (g/plant) at a range of nutrient solution N, P, and K concentrations (mg L^{-1}) of *Cannabis sativa* grown in deep water culture ($P \leq 0.05$, $R^2 = 0.57$). **(A)** Surface plot of K vs. P at N = 180 mg L^{-1}. **(B)** Surface plot of K vs. N at P = 60 mg L^{-1}. **(C)** Surface plot of P vs. N at K = 200 mg L^{-1}.

RESULTS

Inflorescence Yield Response

Cannabis inflorescence yield responded to increasing N and P supply but did not respond to K within the tested range (**Figures 2**, **3**). Based on the surface response model, the estimated highest average yield of 144 g/plant would be achieved with N and P concentrations of 194 and 59 mg L^{-1}, respectively. Visual analysis of contour graphs (with a 5 g resolution) show that yield responded to N best in the range of 160–230 mg L^{-1}, and P in the range of 40–80 mg L^{-1} (**Figure 2**).

Cannabinoid Content

There were no nutrient treatment effects on the inflorescence cannabinoid content. The average cannabinoid contents are listed in **Table 6**. In addition to those cannabinoids listed, the following were below the detection limits (i.e., <0.5 mg/g): CBC, CBD, CBDA, CBN, Δ^8THC.

Relationships Between Inflorescence Yield and Vegetative Growth Attributes

No nutrient deficiency or toxicity symptoms were observed on any plants. Inflorescence yield was linearly and positively correlated with the measured vegetative growth attributes. Inflorescence yield had significant correlations with aboveground plant fresh weight (**Figure 4**), plant growth index (**Figure 5**), and root dry weight (**Figure 6**).

DISCUSSION

The goal of this study was to determine the optimal concentration of N, P, and K in the nutrient solution for the flowering stage of soilless cannabis production using RSM. The optimal concentrations of nutrient solution N and P was predicted to be approximately 194 mg L^{-1} N, and 59 mg L^{-1} P, respectively. Based on analysis of the response surface model, it was found N and P were the most important factors in predicting inflorescence yield. Inflorescence yield decreased markedly outside of the range of 160–230 mg L^{-1} N, and 40–80 mg L^{-1} P. These findings suggest that drug-type cannabis responds well to nitrogen and phosphorus during the flowering stage. Inflorescence yield did not respond to nutrient solution K concentration within the tested range, indicating the K currently supplied (300–400 mg L^{-1}) by some commercial cultivators are likely too high.

Inflorescence yield had a strong positive correlation with a number of vegetative growth attributes. The strong correlation between inflorescence yield and plant growth index indicates that larger plant size can result in higher inflorescence yield. Nutrient supply, especially N, can determine cannabis plant size as N is an essential component of plant chlorophyll and ribulose-1,5-bisphosphate carboxylase-oxygenase (Rubisco). Low levels of N can reduce plant photosynthetic capacity and limit plant growth (Saloner and Bernstein, 2020). For flowering drug-type cannabis in soilless culture, supply of 30 and 80 mg L^{-1} N restricted whole plant and inflorescence growth, but plants performed optimally with supply of 160–320 mg L^{-1} N (Saloner and Bernstein, 2021). The optimal N supply (194 mg L^{-1}) found in our study is within their range, despite the two studies using two different growing methods and plants with different genetic backgrounds. For drug-type cannabis during the flowering stage in an organic-based soilless production system, the optimal N supply was slightly higher (212–261 mg L^{-1}; Caplan et al., 2017a) than the optimal level found in the present study. A possible explanation for the higher optimal N supply in the organic fertiliser study is that N from organic-based fertilisers may not always be readily available, as the release of N from organic fertilisers depends on the speed and extent of the mineralisation process (Hartz et al., 2010; Dion et al., 2020). Though it is unclear what source of organic nitrogen was used in their study, factoring in organic N availability of around 60% would put our findings in line with those by Caplan et al. (2017a). Along with aboveground growth, root growth also contributes to overall plant size. We found that inflorescence yield had a strong positive correlation with root

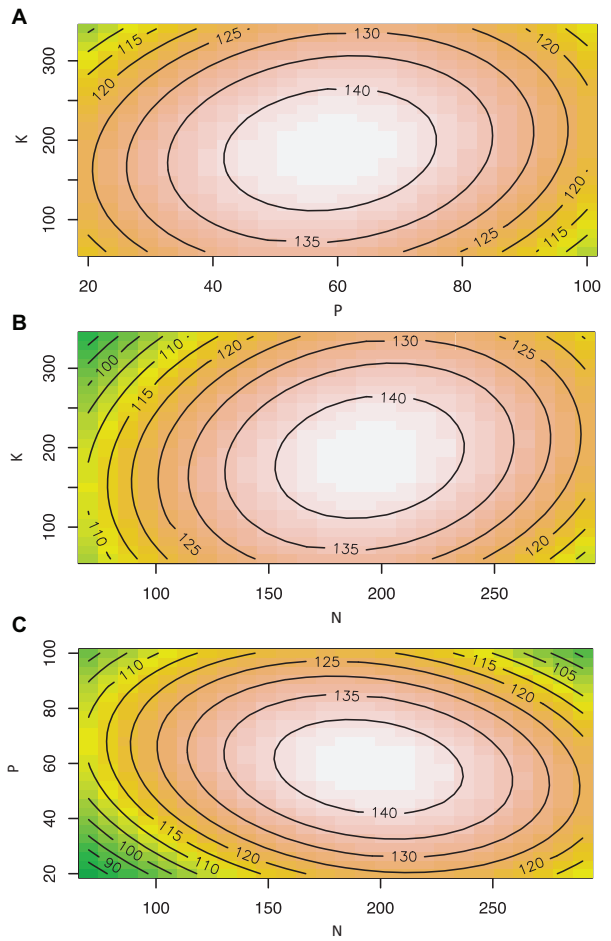

FIGURE 3 | Contour plots showing the effect of nutrient solution N, P, and K concentrations (mg L^{-1}) on inflorescence yield (g/plant) of *Cannabis sativa* grown in deep water culture ($P \leq 0.05$, $R^2 = 0.57$). **(A)** Contour plot of P vs. K at N = 180 mg L^{-1}. **(B)** Contour plot of N vs. K at P = 60 mg L^{-1}. **(C)** Contour plot of N vs. P at K = 200 mg L^{-1}.

TABLE 6 | Dry inflorescence average cannabinoid contents of *Cannabis sativa* grown in the deep-water culture system with different NPK concentrations in the solution.

Cannabinoid	Concentration in inflorescence (mg g^{-1})[b]
CBG	0.86 ± 0.01
CBGA	3.9 ± 0.08
THC	4.4 ± 0.09
THCA	161 ± 2.32
Total THC[a]	146 ± 2.06

[a] *Total THC = [THC] + 0.877[THCA].*
[b] *Mean ± SE (n = 60).*

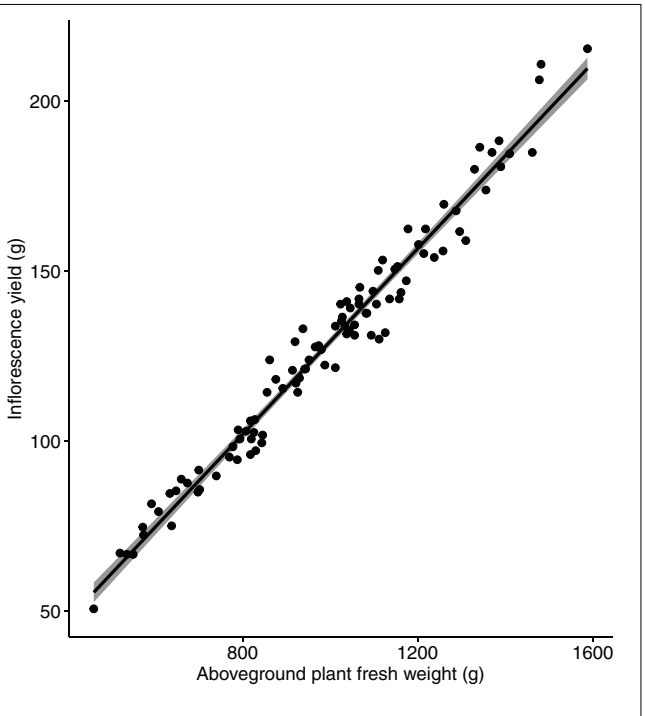

FIGURE 4 | Correlation between inflorescence yield (g/plant) and aboveground plant fresh weight (g/plant) of *Cannabis sativa* ($r = 0.98$, $P < 0.001$). Shaded area represents 95% confidence interval.

dry weight, supporting our conclusion that larger plants produce higher yields. The context of where plants spend their energy is important. For industrial hemp, increasing N supply increased plant growth, but this growth was partitioned more towards stem material rather than valuable inflorescence material (Campiglia et al., 2017). Further investigations of cannabis response to nitrogen should consider product quality, and the distribution of biomass to various plant organs to maximise inflorescence growth and quality.

While modelling of cannabis inflorescence yield response to N, P, and K with surface analysis accounts for interaction between nutrients, the surface response model demonstrated that K, within the tested range of 60–340 mg L^{-1}, had no effect on inflorescence yield. This lack of response may suggest that 60 mg L^{-1} K is not low enough to cause nutrient deficiency, and 340 mg L^{-1} K is not high enough to cause toxicity. Moreover, cannabis responses to K may be genotype specific. Plants of one cannabis genotype Royal Medic supplied with 240 mg L^{-1} K had 25% reduced fresh shoot and root biomass by compared to those fed with 175 mg L^{-1}, while plants of genotype Desert Queen had up to 40% increased shoot and root biomass (Saloner et al., 2019). Plant height, number of nodes on the main stem, and stem diameter of these two genotypes remained similar, so this difference in biomass was caused by one genotype becoming "bushier" than the other under high K supply. These differences in the response to K supply may be due to differences in plant tissue (e.g., main stem vs. side branch) sensitivity to K. Plant phenological stage (i.e., vegetative or flowering stage) may also be a factor in cannabis response to K supply. In a previous study of flowering aquaponic cannabis response to K, inflorescence yield increased when plants were provided with K up to 150 mg L^{-1} (Yep and Zheng, 2020). Genotype and plant phenological stage should be considered in future studies looking at cannabis response to nutrients, especially K.

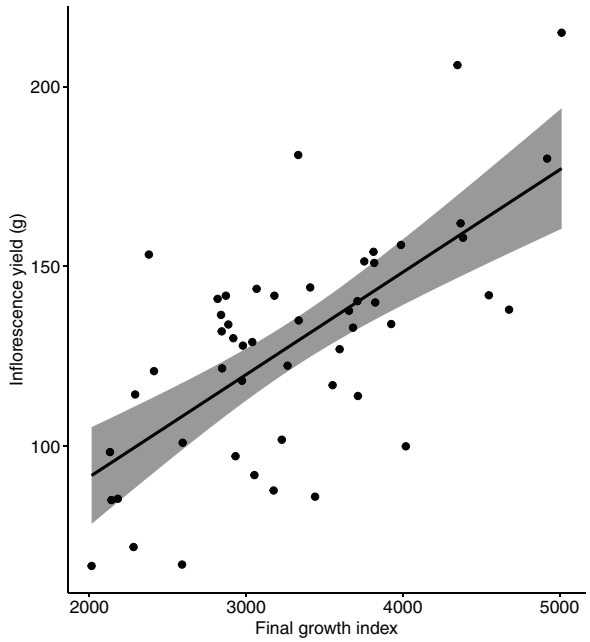

FIGURE 5 | Correlation between inflorescence yield (g/plant) and plant growth index of *Cannabis sativa* ($r = 0.67$, $P < 0.001$). Shaded area represents 95% confidence interval.

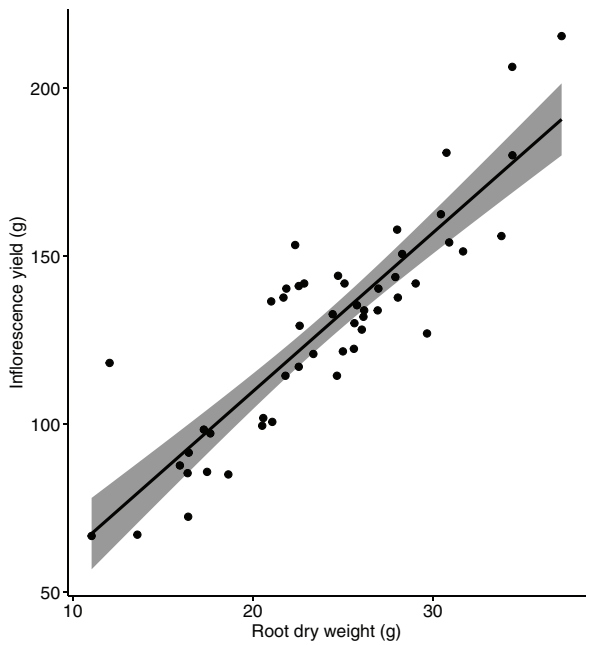

FIGURE 6 | Correlation between inflorescence yield and root dry weight of *Cannabis sativa* ($r = 0.9$, $P < 0.001$). Shaded area represents 95% confidence interval.

Many commercial cannabis cultivation operations currently use fertiliser formulations that contain very high levels of P (more than 200 mg L^{-1} P in some cases). This practice is based on anecdotal evidence that P enhances inflorescence production. These concentrations are much higher than the optimal rate of 60 mg L^{-1} P found in our study, and at the higher range could cause reduction of both plant growth and inflorescence yield. In addition to reducing plant growth and yield, excessive supply of nutrients is a potential source of environmental pollution. Though, cannabis does appear to have the ability to store and mobilise certain amount of P when required. When provided with P higher than 30 mg L^{-1} in the vegetative stage, cannabis sequestered excess P in root tissue to prevent excess accumulation in the shoots (Shiponi and Bernstein, 2021). A greater understanding of what cannabis P requirements are, and whether there is any truth to the practice of supplying high concentrations of P, should be a priority for making cannabis production more sustainable. However, based on existing data it appears that the levels of P found in many cannabis specific commercial fertilisers are far higher than needed and could lead to negative environmental impacts.

While the cannabinoid concentrations in the floral tissues in our study did not respond to nutrient solution NPK concentrations, other studies indicate that plant mineral nutrition can affect production of secondary metabolites in cannabis (Caplan et al., 2017a; Saloner and Bernstein, 2021). There appears to be an inverse relationship between cannabis yield and potency, with cannabinoid concentrations decreasing as plant inflorescence yield increases. Inflorescence from plants supplied with 160 mg L^{-1} N had approximately 30 and 20% lower concentrations of THCA and CBDA than plants supplied with 30 mg L^{-1} N (Saloner and Bernstein, 2021). However, while nutrient stress and deficiency may enhance inflorescence cannabinoid content, this method is not ideal for optimising overall plant productivity as plants supplied with 160 mg L^{-1} N yielded twice that of those supplied with 30 mg L^{-1} N. Cannabis grown in two organic growing media with different organic fertiliser rates (i.e., 57, 113, 170, 226, and 283 mg L^{-1} N) had negative linear relationships between the concentrations of inflorescence THCA and CBGA and the fertiliser application rate for some of the treatment combinations (i.e., growing media and fertiliser rate) (Caplan et al., 2017a). However, for the most of the treatment combinations, fertiliser rates from 57 to 226 mg L^{-1} N did not have any effects on THCA or CBGA concentrations; and the cannabinoid concentrations only dropped when the fertiliser rate increased to the highest level of 283 mg L^{-1} N. The context of yield is again important when analysing differences in cannabinoid content as THCA concentrations dropped by ∼20% in the highest fertiliser rate, but inflorescence yield almost doubled vs. lowest fertiliser rate. As noted by Bernstein et al. (2019), an understanding of how nutrient supply influences cannabinoid concentrations would be an important step towards controlling and standardising the cannabinoid contents of medical cannabis. Cannabinoid concentrations are also important to recreational consumers, who rank THC and CBD concentrations among the most important factors when making purchasing decisions (Zhu et al., 2020). Given that cannabinoids are the compounds that make cannabis so uniquely valuable, more work needs to be done to investigate the effect of mineral nutrition on cannabis yield,

and the relationship between yield and potency. Further work should also evaluate other compounds that are known to impact product quality.

The use of central-composite design allows experimenters to account for potential interactions between the different nutrients. This is important as nutrient interactions have been shown to affect plant nutrient uptake (Fageria, 2001; Rietra et al., 2017). A recent study found that high K supply decreased concentrations of Ca and Mg in cannabis leaf tissue, indicating antagonistic relationships between these positively charged ions (Saloner et al., 2019). An understanding of how combinations of nutrients at different concentrations affect crop growth, yield, and quality is important for the development of recommendations for the commercial cannabis industry. Had the same number of nutrients and nutrient levels as were included in this study been investigated with a traditional full-factorial design, many more nutrient solution treatment groups would have been required, compared to the number of treatment groups used in this study. The difference in number of treatment groups needed can be more pronounced as more factors (i.e., Ca, Mg) are included. Considering the high cost of cannabis and growing space in controlled environments, the response surface approach allowed us to complete this study where another experimental design may have been prohibitive.

No matter the experimental design used, an inherent problem in nutrient solution experiments is that nutrients cannot be added individually but must be added as a compound containing both anions and cations. Further, the ionic balance constraint requires the sum of the charges of cations and anions in solution to be equal (De Rijck and Schrevens, 1999b). The implication for formulating experimental treatment solutions is that it is practically impossible to change the level of one nutrient while keeping concentrations of all other nutrients the same. In this study, we focused on N, P, and K concentrations while attempting to keep all other nutrients at reasonable levels using commonly available horticultural fertiliser compounds. For example, potassium nitrate and calcium nitrate usually contribute to the bulk of nitrogen, potassium, and calcium in horticultural nutrient solutions (Resh, 2012). Formulating a high N, low K nutrient solution with these fertilisers results in higher levels of Ca than other nutrient solution treatments. Likewise, a low N, high K nutrient solution necessitates an additional source of K such as KCl, which would increase solution Cl concentration. Higher concentrations of nutrients such as Ca and Cl bring the potential for nutrient interactions which may affect experimental results. The lack of response to K in the range of 60–340 mg L^{-1} observed in our trial may be partially due to competition for uptake from Ca. Regarding experimental Cl levels, hydroponic cannabis has been shown to tolerate rates of 180 mg L^{-1} Cl with no impact on yield or potency (Yep et al., 2020a) so it is unlikely Cl levels limited plant growth in this trial. Though less than ideal in an experimental setting, there is no perfect solution for the problem of keeping all nutrient concentrations the same when formulating treatment solutions.

While this trial determined the theoretical optimum levels of N and P for the DWC growing method, these levels may not be definitive for all production methods or genotypes. Our trial was conducted in solution culture with weekly nutrient solution changes, and the EC and pH dynamics of our DWC units are likely different than other growing methods, meaning that plant nutrient availability and overall salinity of the nutrient solution would also likely be considerably different. Many commercial cannabis operations utilise substrate-based soilless cultivation systems, such as coir in containers, that may offer more nutrient and pH buffering capacity (Zheng, 2020). Having said that, our trial does represent or closely resemble some common soilless production practices, such as growing cannabis in rockwool, in the current cannabis production industry (Zheng, 2021). The treatments were applied only during the short-day period (i.e., flowering stage), and considering that plant nutrient requirement may vary at different development stages, the same experiment may also need to be conducted for the vegetative stage. Another limitation of our study was that we only used a single cannabis cultivar. Similar experiments should be performed on different cultivars, with disparate growth habits and cannabinoid compositions to investigate how individual cultivars may respond to NPK treatment levels. Additionally, this study only looked at inflorescence yield and cannabinoid composition and did not evaluate the impact of NPK on inflorescence terpene content or organoleptic properties.

Drug-type cannabis is still a relatively new crop in the legal setting, especially for large-scale commercial production, and many aspects of its cultivation are relatively unknown. We found that response surface methodology was a suitable experimental approach for investigation of cannabis responses to NPK, and that modelling of yield response to these nutrients aided us in achieving our experimental objective. Based on the results of this study, we recommend providing plants with a nutrient solution containing N and P at approximately 194 and 59 mg L^{-1}, respectively, to achieve maximal inflorescence yield. Future studies should investigate the inflorescence yield and vegetative growth response of genetically diverse cultivars to macronutrients and include more quality parameters to ensure that plant yields do not compromise product quality. Improving our understanding of cannabis responses to mineral nutrients is an essential step towards the effective and sustainable cultivation of this high-value horticultural crop.

DATA AVAILABILITY STATEMENT

The original contributions presented in the study are included in the article/supplementary material, further inquiries can be directed to the corresponding author.

AUTHOR CONTRIBUTIONS

All authors designed the experiment and wrote the manuscript. LB conducted the trial and processed the data.

FUNDING

We thank the Ontario Centres of Excellence and HEXO Co., for their financial support.

ACKNOWLEDGMENTS

This study would not have been possible without the support from Steve Dinka, Scott Golem, Liz Foley, and the other growing facility staff at HEXO Co. We thank David Llewellyn for his technical on-site research support, aid in data collection, resourcefulness in provisioning materials, and his informative discussions. We thank Simon Bourque for performing the laboratory cannabinoid analysis. We also thank Master Plant Prod. Inc. for their support and providing the straight fertiliser compounds used in this study. In addition, we thank Bluelab Corporation for providing pH/EC metre parts and calibration solution for this trial.

REFERENCES

Beerling, E. A. M., Blok, C., van der Maas, A. A., and van Os, E. A. (2014). Closing the water and nutrient cycles in soilless cultivation systems. *Acta Hortic.* 1034, 49–55. doi: 10.17660/ActaHortic.2014.1034.4

Bernstein, N., Gorelick, J., Zerahia, R., and Koch, S. (2019). Impact of N, P, K, and humic acid supplementation on the chemical profile of medical cannabis (*Cannabis sativa* L.). *Front. Plant. Sci.* 10:736. doi: 10.3389/fpls.2019.00736

Campiglia, E., Radicetti, E., and Mancinelli, R. (2017). Plant density and nitrogen fertilization affect agronomic performance of industrial hemp (Cannabis sativa L.) in Mediterranean environment. *Ind. Crop. Prod.* 100, 246–254. doi: 10.1016/j.indcrop.2017.02.022

Caplan, D., Dixon, M., and Zheng, Y. (2017b). Optimal rate of organic fertilizer during the vegetative-stage for cannabis grown in two coir-based substrates. *HortScience* 52, 1307–1312. doi: 10.21273/hortsci11903-17

Caplan, D., Dixon, M., and Zheng, Y. (2017a). Optimal rate of organic fertilizer during the flowering stage for cannabis grown in two coir-based substrates. *HortScience* 52, 1796–1803. doi: 10.21273/hortsci12401-17

De Rijck, G., and Schrevens, E. (1998). Multifactorial optimisation of the nutrient solution for hydroponically grown chicory plants. *Sci. Hortic.* 76, 149–159. doi: 10.1016/S0304-4238(98)00126-125

De Rijck, G., and Schrevens, E. (1999a). Application of mixture theory for the optimisation of the composition of nutrient solutions for hydroponic cropping: practical use. *Acta Hortic.* 481, 205–212. doi: 10.17660/ActaHortic.1999.481.21

De Rijck, G., and Schrevens, E. (1999b). Chemical feasibility region for nutrient solutions in hydroponic plant nutrition. *J. Plant Nutr.* 22, 259–268. doi: 10.1080/01904169909365624

Dion, P.-P., Jeanne, T., Thériault, M., Hogue, R., Pepin, S., and Dorais, M. (2020). Nitrogen release from five organic fertilizers commonly used in greenhouse organic horticulture with contrasting effects on bacterial communities. *Can. J. Soil. Sci.* 100, 120–135. doi: 10.1139/cjss-2019-2056

Fageria, V. D. (2001). Nutrient interactions in crop plants. *J. Plant Nutr.* 24, 1269–1290. doi: 10.1081/pln-100106981

Hartz, T. K., Smith, R., and Gaskell, M. (2010). Nitrogen availability from liquid organic fertilizers. *HortTechnology* 20, 169–172. doi: 10.21273/horttech.20.1.169

Layton, C., and Aubin, A. J. (2019). *UPLC Separation for the Analysis of Cannabinoid Content in Cannabis Flowers and Extracts*. Available online at: https://www.waters.com/webassets/cms/library/docs/720006509en.pdf (accessed October 25, 2021).

Lenth, R. V. (2009). Response-surface methods in R, using rsm. *J. Stat. Softw.* 32, 1–17.

Myers, R. H., Montgomery, D. C., and Anderson-Cook, C. M. (2016). *Response Surface Methodology: Process and Product Optimization using Designed Experiments*, 4th Edn. Hoboken, NJ: Wiley.

Ontario Ministry of Agriculture Food and Rural Affairs (2019). *Nutrient Management- Greenhouse Nutrient Feedwater Regulation*. Guelph, ONT: OMAFRA.

Resh, H. M. (2012). *Hydroponic Food Production: a Definitive Guidebook for the Advanced Home Gardener and the Commercial Hydroponic Grower*, 7th Edn. Boca Raton, FL: CRC Press, Taylor & Francis Group.

Rietra, R. P. J. J., Heinen, M., Dimkpa, C. O., and Bindraban, P. S. (2017). Effects of nutrient antagonism and synergism on yield and fertilizer use efficiency. *Commun. Soil. Sci. Plant Anal.* 48, 1895–1920. doi: 10.1080/00103624.2017.1407429

RStudio Team (2020). *RStudio: Integrated Development Environment for R*. Boston, MA: RStudio.

Saloner, A., and Bernstein, N. (2020). Response of medical cannabis (*Cannabis sativa* L.) to nitrogen supply under long photoperiod. *Front. Plant Sci.* 11:572293. doi: 10.3389/fpls.2020.572293

Saloner, A., and Bernstein, N. (2021). Nitrogen supply affects cannabinoid and terpenoid profile in medical cannabis (*Cannabis sativa* L.). *Ind. Crop. Prod.* 167:113516. doi: 10.1016/j.indcrop.2021.113516

Saloner, A., Sacks, M. M., and Bernstein, N. (2019). Response of medical cannabis (*Cannabis sativa* L.) genotypes to K supply under long photoperiod. *Front. Plant Sci.* 10:1369. doi: 10.3389/fpls.2019.01369

Schindler, D. W., Carpenter, S. R., Chapra, S. C., Hecky, R. E., and Orihel, D. M. (2016). Reducing phosphorus to curb lake eutrophication is a success. *Environ. Sci. Technol.* 50, 8923–8929. doi: 10.1021/acs.est.6b02204

Shiponi, S., and Bernstein, N. (2021). Response of medical cannabis (*Cannabis sativa* L.) genotypes to P supply under long photoperiod: functional phenotyping and the ionome. *Ind. Crop. Prod.* 161:113154. doi: 10.1016/j.indcrop.2020.113154

Wickham, H. (2016). *ggplot2: Elegant Graphics for Data Analysis*. New York, NY: Springer-Verlag.

Yep, B., Gale, N. V., and Zheng, Y. (2020b). Comparing hydroponic and aquaponic rootzones on the growth of two drug-type *Cannabis sativa* L. cultivars during the flowering stage. *Ind. Crop. Prod.* 157:112881. doi: 10.1016/j.indcrop.2020.112881

Yep, B., Gale, N. V., and Zheng, Y. (2020a). Aquaponic and hydroponic solutions modulate NaCl-induced stress in drug-type *Cannabis sativa* L. *Front. Plant Sci.* 11:1169. doi: 10.3389/fpls.2020.01169

Yep, B., and Zheng, Y. (2020). Potassium and micronutrients fertilizer addition in aquaponic solution for drug-type *Cannabis sativa* L. cultivation. *Can. J. Plant Sci.* 101, 341–352. doi: 10.1139/cjps-2020-2107

Zheng, Y. (2018). Current nutrient management practices and technologies used in North American greenhouse and nursery industries. *Acta Hortic.* 1227, 435–442. doi: 10.17660/ActaHortic.2018.1227.54

Zheng, Y. (2020). Integrated rootzone management for successful soilless culture. *Acta Hortic.* 1273, 1–8. doi: 10.17660/ActaHortic.2020.1273.1

Zheng, Y. (2021). Soilless production of drug-type *Cannabis sativa*. *Acta Hortic.* 1305, 376–382. doi: 10.17660/ActaHortic.2021.1305.49

Zhu, B., Guo, H., Cao, Y., An, R., and Shi, Y. (2020). Perceived importance of factors in cannabis purchase decisions: a best-worst scaling experiment. *Int. J. Drug Policy* 91:102793. doi: 10.1016/j.drugpo.2020.102793

Conflict of Interest: The authors declare that the research was conducted in the absence of any commercial or financial relationships that could be construed as a potential conflict of interest.

Publisher's Note: All claims expressed in this article are solely those of the authors and do not necessarily represent those of their affiliated organizations, or those of the publisher, the editors and the reviewers. Any product that may be evaluated in this article, or claim that may be made by its manufacturer, is not guaranteed or endorsed by the publisher.

frontiers in Plant Science

ORIGINAL RESEARCH
published: 24 February 2022
doi: 10.3389/fpls.2022.786161

Analysis of Morphological Traits, Cannabinoid Profiles, *THCAS* Gene Sequences, and Photosynthesis in Wide and Narrow Leaflet High-Cannabidiol Breeding Populations of Medical Cannabis

Jana Murovec, Jan Jurij Eržen, Marko Flajšman and Dominik Vodnik*

Department of Agronomy, Biotechnical Faculty, University of Ljubljana, Ljubljana, Slovenia

OPEN ACCESS

Edited by:
Derek Stewart, The James Hutton Institute, United Kingdom

Reviewed by:
Antonio Giovino, Council for Agricultural and Economics Research (CREA), Italy
Robert D. Hancock, The James Hutton Institute, United Kingdom

***Correspondence:**
Jana Murovec
jana.murovec@bf.uni-lj.si

Specialty section:
This article was submitted to Plant Metabolism and Chemodiversity, a section of the journal Frontiers in Plant Science

Received: *29 September 2021*
Accepted: *14 January 2022*
Published: *24 February 2022*

Citation:
Murovec J, Eržen JJ, Flajšman M and Vodnik D (2022) Analysis of Morphological Traits, Cannabinoid Profiles, THCAS Gene Sequences, and Photosynthesis in Wide and Narrow Leaflet High-Cannabidiol Breeding Populations of Medical Cannabis. Front. Plant Sci. 13:786161. doi: 10.3389/fpls.2022.786161

Cannabis sativa L. is one of the oldest cultivated crops, used in medicine for millennia due to therapeutic characteristics of the phytocannabinoids it contains. Its medicinal properties are highly influenced by the chemotype, that is, the ratio of the two main cannabinoids cannabidiol (CBD) and Δ-9-tetrahydrocannabinol (THC). Based on published data, the chemotype should correlate with plant morphology, genetics, and photosynthetic properties. In this work, we investigated leaf morphology, plant growth characteristics, cannabinoid profiles, *THCAS* gene sequences, and plant photosynthetic traits in two breeding populations of medical cannabis (MX-CBD-11 and MX-CBD-707). The populations differed significantly in morphological traits. The MX-CBD-11 plants were taller, less branched, and their leaves had narrower leaflets than the bushier, wideleaved MX-CBD-707 plants, and there were significant differences between populations in the dry biomass of different plant parts. Based on these morphological differences, MX-CBD-11 was designated as a narrow leaflet drug type or vernacular "Sativa" type, while MX-CBD-707 was classified as wide leaflet drug type or "Indica" type. Chemical characterisation revealed a discrepancy between the expected chemotypes based on plant morphology; although both populations have high CBD, within each Type II (CBD/THC intermediate) and Type III (CBD dominant) plants were detected. The *THCAS* gene sequence analysis clustered the plants based on their chemotypes and showed high similarity to the *THCAS* sequences deposited in NCBI. *In silico* complementary analysis, using published molecular markers for chemotype determination, showed their low discrimination power in our two populations, demonstrating the genotype dependence of the molecular markers. Basic photosynthetic traits derived from light and CO_2 response curves were similar in the populations. However, measurements of gas exchange under chamber conditions revealed higher stomatal conductivity and photosynthesis in MX-CBD-707 plants, which were also characterised by higher day respiration. The results of this study showed that based on visual appearance and some morphological measurements, it is not possible to determine a plant's chemotype. Visually homogenous plants had different cannabinoid profiles and, vice versa, morphologically distinct plants

contained similar CBD and THC content. The two chemotypes identified in our experimental plants therefore did not correlate with plant visual appearance, leaf morphometry, and photosynthetic properties of the populations studied. Correlation was only demonstrated with the respect to *THCAS* sequences, which showed great discrimination power between the chemotypes.

Keywords: *Cannabis sativa* L., high CBD medical cannabis, cannabinoids, photosynthesis, respiration, *THCA synthase*, morphometry

INTRODUCTION

Cannabis (*Cannabis sativa* L.) is gaining popularity in the modern world through industrial, food, cosmetic, and medicinal uses. It is one of the oldest cultivated crops, having been grown worldwide for a plethora of purposes for millennia. This has led to the development of numerous groups of plants that, although genetically and phenotypically diverse, can interbreed and are therefore difficult to classify based on standard botanical nomenclature. Hence, various types of classifications have been introduced over the past century.

A generally accepted classification of cannabis plants is based on their primary agronomic purpose, which determines the traits to be selected and consequently profoundly affects the phenotypes of registered varieties. The most widely cultivated group is "hemp" ("fibre-type hemp," "industrial cannabis"), which was once an important crop for the production of raw materials for textiles and ropes and which is currently experiencing a revival after a steady decrease in its acreage after World War II (Tang et al., 2017). It is grown for seeds and fibre, food and beverage production, substances for cosmetic use, animal feed, and other industrial uses. It can be cultivated as a field crop of registered varieties that contain no more than a legally defined, country-specific threshold level of the psychoactive substance Δ-9-tetrahydrocannabinol (THC). In European countries, for example, the threshold is set at 0.2% or 0.3% THC in the upper third of the dried plant or in an upper 30 cm of dried plants shoots containing at least one female inflorescence (Regulation EU No. 809/2014).

Although hemp can also be used for pharmaceutical purposes, it contains small amounts of cannabinoids. Higher relative (in per cent of inflorescence dry weight) and absolute (in g per cultivated m^2) amounts of cannabinoids can be produced in cannabis varieties popularly known as "medical cannabis" ("marijuana," "drug type cannabis"). They contain high levels of plant cannabinoids, of which cannabidiol (CBD) and THC are the most abundant and pharmaceutically most important (Friedman et al., 2019). They are produced in secretory cells within glandular trichomes as carboxylic acids cannabidiolic acid (CBD-A) and Δ9-tetrahydrocannabinolic acid (Δ9-THC-A) that are decarboxylated to their corresponding neutral forms CBD and THC, respectively, upon heating (Salami et al., 2020; Tanney et al., 2021). Medical cannabis varieties contain higher amounts of THC than the legal national limits for hemp and can be grown indoors or outdoors only in compliance with strict national legal restrictions.

The relative abundance and ratio of CBD and THC has led to the second most widely used cannabis nomenclature, which divides cannabis plants into three discrete groups: "THC dominant" or "high THC" (CBD/THC ratio 0.00–0.05), "intermediate" (CBD/THC ratio 0.5–3), and "CBD dominant" or "high CBD" (CBD/THC ratio 15–25) (Staginnus et al., 2014). These three chemical phenotypes (chemotypes) have been named Type I (THC dominant), Type II (CBD/THC balanced) and Type III (CBD dominant) (Small and Beckstead, 1973; de Meijer et al., 1992, 2003).

The first systematic genetic analyses of chemotype inheritance, performed by crossing and self-pollination of different chemotypes, indicated simple codominant inheritance through a single locus B with two alleles: the B_T allele for THCA synthase (THCAS) and the B_D allele for CBDA synthase (CBDAS). Based on this model, Type II plants would be heterozygous B_DB_T, while the plants of pure chemotypes Type I and III would be homozygous for B_TB_T and B_DB_D, respectively (de Meijer et al., 2003; Mandolino et al., 2003; Toth et al., 2019). A more complex model of inheritance now prevails. The genetic basis of chemotypes is thought to be determined by at least two closely linked loci, one encoding CBDAS and the other encoding THCAS, in medical and hemp cultivars (de Meijer et al., 2003; Kojoma et al., 2006; van Bakel et al., 2011; Onofri et al., 2015; Weiblen et al., 2015; Grassa et al., 2021) and/or by variation in gene copy number (Weiblen et al., 2015; Vergara et al., 2019). The cannabinoid profile is thought to be determined by the presence of *THCAS* and *CBDAS* with normal, weak, or no expression, resulting in Type I plants containing only functional *THCAS* gene, Type II plants containing functional genes for both synthases, and Type III plants lacking functional copies of *THCAS* and containing functional *CBDAS* (van Bakel et al., 2011; Weiblen et al., 2015). However, as shown by Zirpel et al. (2018a,b), both the *THCAS* and *CBDAS* genes are capable of producing THCA, CBCA and CBDA, as well as five other unknown products, which may explain the occurrence of low THCA levels in Type III cultivars (such as the hemp cultivar "Finola") carrying only one functional *CBDAS* allele (van Bakel et al., 2011).

The third level of differentiation between cannabis plants is based on their morphology, which is the oldest marker. It was used for plant classification by the pioneers in this field. As comprehensively reviewed by Jin et al. (2021b), Linneaeus described *C. sativa* L. in 1753 in *Species Plantarum* as a plant with loose inflorescences covered with sparse trichomes and resembling a northern European fibre-type landrace. Later, in 1785, de Lamarck described a second (or sub-) species, *Cannabis*

indica Lam. collected in India, with dense trichomes, narrower leaflets, a branching habitus, poorer fibre quality, a harder stem, and a thinner cortex, but stronger psychoactive effects. Schultes travelled to Afghanistan in 1971 and described *C. indica* as having wide leaflets, densely branched with very dense inflorescences for hashish (resin) production, departing from Lamarck's original taxonomic concept. Anderson drew illustrations of *C. indica* and *C. sativa* in 1980. The former was depicted as short, conical, densely branched, and with wide leaflets; the latter as relatively tall, laxly branched, and with narrow leaflets, which agreed with Schultes but diverged from Lamarck. Later, Hilling performed extensive analyses on 157 accessions of different geographic origins, classifying them into two species, *C. sativa* and *C. indica*, and seven putative taxa, including the narrow leaflet drug (NLD) biotype of *C. indica*, the wide leaflet drug (WLD) biotype of *C. indica*, the hemp biotype of *C. indica*, the feral *C. indica* biotype, the hemp biotype of *C. sativa*, the feral *C. sativa* biotype, and putative ruderal populations. The NLD biotype included landraces of Indian heritage (including cultivars from the Indian subcontinent, Africa, and other drug-producing regions) corresponding to Lamarck's *C. indica*. The WLD biotype included landraces from Afghanistan and Pakistan corresponding to Schultes'*C. indica*. The *C. indica* hemp biotype included landraces from South and East Asia, while the *C. sativa* hemp biotype included landraces from Europe, Asia Minor, and Central Asia.

Because of its complexity, the above classification has not been adopted for everyday use in the cannabis industry and recreational cultivation; therefore, the vernacular expressions "Sativa" and "Indica" have become accepted to describe cultivars with narrow leaflets and broad or wide leaflets, respectively. They were based on illustrations by Anderson, which differed from the original botanical nomenclature. "Sativa" plants produce much more THC than CBD, while "Indica" plants produce almost equal amounts of THC and CBD, with a CBD/THC ratio of around 1 (McPartland, 2017). However, as McPartland also reported, these vernacular categories are unreliable for distinguishing between different chemotypes and/or cannabis end uses due to extensive cross-breeding and incomplete labelling during hybridisation (McPartland, 2017). In addition, in most classification studies, samples had come from different sources and had been exposed to inconsistent environmental factors during growth phases, postharvest treatment, sample preparation, and extraction procedures during laboratory analysis (Jin et al., 2020, 2021a,b). Jin et al. (2021b) recently addressed these drawbacks. They analysed phenotypic variation in 21 cannabis cultivars covering three chemical phenotypes (THC dominant, intermediate, and CBD dominant) by measuring 30 morphological traits at the vegetative, flowering, and harvest stages on live plants and harvested inflorescences. Significant morphological differences were found between plants and chemotypes. Among others, leaflets characteristics were found to be usable as phenotypic markers to distinguish THC dominant, intermediate, and CBD dominant cultivars included in their study. Canonical correlation analysis assigned the experimental plants to the corresponding chemotypes with 92.9% accuracy (Jin et al., 2021b).

The physiological distinction of cannabis morphotypes/chemotypes is not clear. In an early study by Bazzaz et al. (1975), differences in the photosynthetic rate and THC content were found in four populations of *C. sativa* from temperate and warm climatic regions. Drug-type and fibre-type cannabis ecotypes tested by Lydon et al. (1987) had similar photosynthetic properties. Chandra et al. (2011) reported considerable variation in the temperature response of photosynthesis in different drug and fibre types of cannabis. However, the variations were more varietal specific compared with the types (drug and fibre). Overall, the photosynthetic response of cannabis types and varieties mainly reflects their inherited prevalence to specific growing conditions, that is adaptation to the particular environment at the sites of origin.

The relationship between photosynthesis and cannabinoid profile/content is not clear-cut. Photosynthesis interferes with secondary metabolism and some researchers have found that the accumulation of secondary metabolites is directly related to the rate of photosynthesis (Mosaleeyanon et al., 2005). However, this relationship was not demonstrated in cannabis when photosynthesis was assessed by measurements of gas exchange. Khajuria et al. (2020) reported a strong negative correlation between THC content and photochemical efficiency and a weak zeaxanthin-dependent component of non-photochemical quenching (NPQ). The authors even suggested that measuring chlorophyll *a* fluorescence could be used as a rapid tool for high-throughput screening of cannabis for its cannabinoid content, as cannabis plants with a higher CBD than THC content offer better protection of the photosynthetic machinery.

Cannabidiol (CBD) has been shown to have therapeutic effects on humans and animals and no psychoactive effects; it even abolishes the psychoactivity and some adverse effects of THC, such as anxiety, tachycardia, and sedation (Romero et al., 2020). As a result, there has been a dramatic increase in CBD-containing supplements in the food and cosmetic industries in recent years, and even greater potential for its pharmaceutical use has been reported (Glivar et al., 2020; Salami et al., 2020). This has encouraged breeding programmes aimed at developing new varieties of medical cannabis with increased and stable CBD content, as well as basic research into the inheritance of specific chemical profiles.

Two breeding populations (MX-CBD-11 and MX-CBD-707) of medical cannabis were included in this study, both showing high CBD yield in industrial production and contrasting phenotypes based on visual examination. The breeding population MX-CBD-11 resembles a narrow leaflet phenotype, while MX-CBD-707 has a wide leaflet phenotype based on the descriptions of Schultes and Anderson. Our first aim was to analyse precisely the morphological characteristics and cannabinoid content of these populations at the individual plant level. This comprehensive characterisation of the gene pool within our breeding programme enabled us to examine the intra- and inter-population variability of our plants and to verify the correlation between morphotype and chemotype. Because the results showed a uniform morphology within the populations alongside contrasting cannabinoid contents (chemotypes), we further analysed the genetic basis of the observed chemical

differences by sequencing their *THCAS* genes. In addition, we measured the photosynthetic characteristics of the breeding populations and analysed them with respect to morphological, chemotype and, genetic differences.

MATERIALS AND METHODS

The reported research was conducted on two breeding populations (MX-CBD-11 and MX-CBD-707) of medical cannabis (*C. sativa* L.) owned by MGC Pharma Ltd. (United Kingdom). They were studied as part of the project 'Breeding medical cannabis (*Cannabis sativa* L.)', which is a collaboration between the Biotechnical Faculty of the University of Ljubljana and MGC Pharma Ltd. (United Kingdom). Plants were grown in a growth room under controlled temperature, humidity, and illumination at the Agronomy Department of the Biotechnical Faculty, University of Ljubljana, Slovenia. The medical cannabis plants were grown in accordance with a research licence granted by the Ministry of Health of the Republic of Slovenia.

Our breeding programme started with two groups of cannabis plants, which differed in morphological appearance. Plants of each group were crossed within the group in separate rooms and at different times to avoid crossing plants from different groups. The obtained progenies were selected for morphological and growth uniformity within each population and for high CBD content at the industrial production level. Only genetically female plants were cultivated, which were crossed and propagated with feminised seeds obtained by manipulating sex expression, as reported in our recent publication (Flajšman et al., 2021). This approach enabled us to develop two feminised high CBD breeding populations of medical cannabis, one corresponding to the "narrow leaflet drug type" (named MX-CBD-11) and the other one to the "wide leaflet drug type" (named MX-CBD-707) phenotype based on plant morphology according to McPartland (2017, 2018).

Ninety-five plants of the MX-CBD-11 and MX-CBD-707 breeding populations were analysed for genetic (di)similarity with microsatellite markers, as reported in our previous study (Mestinšek Mubi et al., 2020). Twelve genetically distinct plants were randomly selected from each population and included in this study. Each of them was obtained from a germinated feminised seed, therefore representing a unique genotype labelled with a code: 11/02, 11/03, 11/05, 11/06, 11/08, 11/13, 11/20, 11/23, 11/24, 11/25, 11/35, 11/40, 707/03, 707/04, 707/06, 707/08, 707/12, 707/14, 707/31, 707/33, 707/36, 707/39, 707/41, and 707/47. A total of 24 plants were grown in 7 L pots filled with fertilised peat substrate Brown 540 W (Kekkilä, Finland). The culturing conditions in the growth chamber were maintained at: 26°C, 55–60% relative humidity (RH), a photoperiod of 18 h light/6 h dark, and a photosynthetic photon flux density (PPFD) of 350–400 μmol m^{-2} s^{-1} (at canopy level) by using 600-W high-pressure sodium (HPS) lamps (Phantom HPS 600W; Hydrofarm, Petaluma, CA, United States). At the vegetative stage, plants were fertilised with a mixture of vegetative fertilizer (NPK 4-1-2) and CalMag (N-Ca-Mg 2-5-2.5) + microelements in a 1:1 proportion. After 15 weeks of vegetative growth, the photoperiod was changed to 12 h light/12 h dark and fertilisation to flowering fertiliser (NPK 1-3-5) and CalMag (N-Ca-Mg 2-5-2.5) + microelements in a 1:1 proportion in order to induce flowering. Plants from the different populations were randomly distributed in the growth chamber.

Phenotypic Characterisation of the Breeding Populations

Ten weeks after the beginning of the flowering phase, the plants were harvested. The whole aboveground part of the plants (in our experiment consisting of stems, leaves and inflorescences) was separated from the root system and weighted ("Shoot FW"). After drying the plant material to constant weight, the roots were weighted ("Root DW") and the dried shoots separated into stems and leaves with inflorescences. They were weighted and the sum of "Stem DW" and "Leaf + inflorescences DW" represented the dry mass of the shoot ("Shoot DW"), while the "Plant DW" was calculated as the sum of "Root DW" and "Shoot DW". These analyses were performed on five plants per breeding population ($N = 5$).

The herbarised leaves of all 12 plants per population ($N = 12$) were scanned and several leaf parameters were measured by using CellSense software (Olympus): the number of leaflets per leaf, the length of the central leaflet, the width of the central leaflet, the distance from the base of the central leaflet to the widest point of the leaflet, the petiole length, the petiole width, the number of primary serrations on the central leaflet, and the number of secondary serrations on the central leaflet. **Figure 1** shows leaf traits measured on the leaves and their central leaflets.

Analysis of Cannabinoid Content

The inflorescences were collected 10 weeks after the induction of flowering. Their stems and supporting leaves were removed, and the remaining inflorescences were dried at 40°C to a constant weight. High-performance liquid chromatography (HPLC) analysis was performed in the laboratory of MGC Pharma (Ljubljana, Slovenia) according to Gul et al. (2015) with minor modifications described by Laznik et al. (2020) as follows. Inflorescences were ground at 15,000 rpm for 11 s; then, the cannabinoids were extracted from the plant material by mixing 1 g of powder in 50 mL of methanol (JT Baker) with 0.1% formic acid (Sigma Aldrich) for 30 min at room temperature. The extracts were filtered through 0.45 μm filters (Chromafil® AO -45/25, Macherey-Nagel) and three dilutions were prepared for HPLC analyses. Extracts were analysed by using an Agilent 1260 Infinity quaternary HPLC system with a Poroshell 120 SB -C18 (4.6 × 150 mm, 2.7 μm; Agilent) column. The injection volume was 10 μL and the flow rate was 1,200 mL min^{-1}. The oven temperature was 28.0°C and the detection signal wavelength (λ) was 276.0 nm. Mobile phase A was H_2O (HPLC grade, JT Baker) with 0.1% v/v formic acid, and mobile phase B was acetonitrile (HPLC grade, JT Baker) with 0.1% v/v formic acid. The cannabinoid content of each plant was determined by measuring seven cannabinoids: cannabidiolic acid (CBDA), cannabidiol

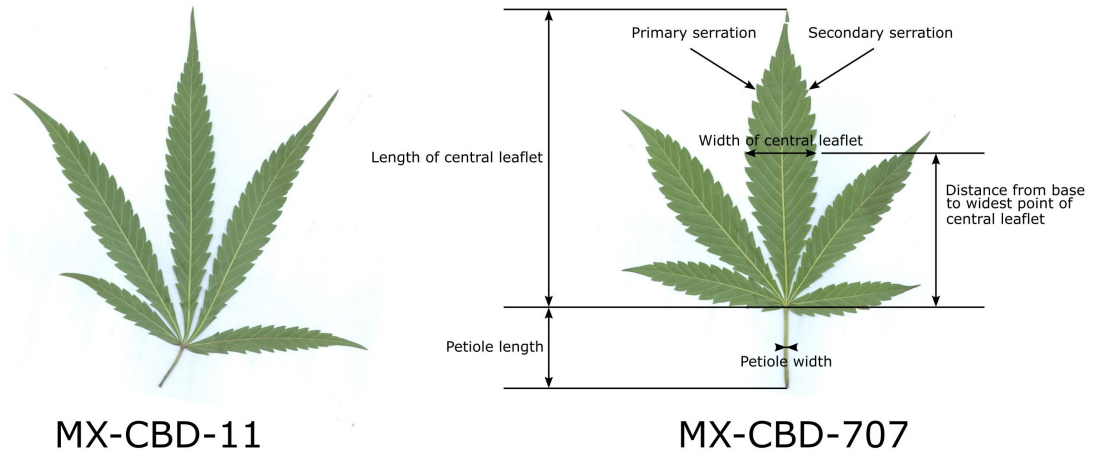

FIGURE 1 | Characteristic leaves of breeding populations MX-CBD-11 (left) and MX-CBD-707 (right) with marked leaf and central leaflet traits that were measured for all the experimental plants included in this study.

(CBD), cannabigerolic acid (CBGA), cannabigerol (CBG), Δ8-tetrahydrocannabinol (d8-THC), Δ9-tetrahydrocannabinol (d9-THC), and tetrahydrocannabinolic acid (THCA), using standards specific for each cannabinoid (Cerilliant). A calibration curve was constructed with concentrations ranging from 2 to 75 mg L^{-1} ± 0.006 mg ml^{-1}. The concentrations of total CBD, THC, and CBG in % (w/w) were calculated as the sum of the carboxylic acid forms (CBDA, THCA, and CBGA) with the non-carboxylic acid derivatives (CBD, d8-THC, d9-THC, and CBG) using the conversion factor of 0.877 for CBDA and THCA and the conversion factor of 0.878 for CBGA.

Sequencing the *THCA Synthase* Gene

Genomic DNA was extracted from leaves of each of the 24 mother plants (genotypes) included in this study by using a modified cetyltrimethylammonium bromide (CTAB) method. The full-length *THCA synthase* gene was amplified with the primers THCAsynF (GGA CTG AAG AAA AAT GAA TTG CTC AG) and THCAsynR (GGG AAA TAT ATC TAT TTA AAG ATA ATT AAT GAT) published by Weiblen et al. (2015). Polymerase chain reaction (PCR) was performed in a total volume of 15 μL and contained 25 ng of isolated DNA, 1 × KAPA2G buffer A, 0.8 mM dNTP, 0.5 mM of forward and reverse primers, and 0.3 U Taq DNA polymerase (KAPA2G Fast PCR Kit). The temperature profile was: initial denaturation at 95°C for 3 min; 35 cycles at 95°C for 15 s, 55°C for 15 s, and 72°C for 30 s; and a final extension at 72°C for 10 min. Amplified products were verified on a 1.2% agarose gel electrophoresis and then purified using the GenElute PCR Clean-Up Kit (Sigma-Aldrich Co. LLC). The purified products were cloned into the pGEM®-T Easy Vector (Promega), and the plasmids containing full-length *THCAS* sequences Sanger sequenced using BigDye™ Terminator v3.1 Cycle Sequencing Kit (Applied Biosystems™) according to the manufacturer's instructions. The sequences were analysed by using CodonCode Aligner (CodonCode Corporation), CLC Genomics (Quiagen) and BLAST algorithm at NCBI. The sequences were first aligned in CLC with default settings and then a genetic distance tree was constructed with Clustal W implemented in CLC.

The obtained *THCAS* sequences were further aligned with primer sequences for published chemotype molecular markers with CodonCode Aligner and CLC Genomics. The aim of this analysis was to determine whether the published molecular markers are suitable to discriminate between Type II and III plants in our breeding populations. The results were scored as complementary or not. To distinguish between different chemotypes, the primers have to be complementary to the *THCAS* gene of only one chemotype of a population. If primers were to anneal to both or none of the chemotypes, such a chemotype marker would be considered non-informative for our breeding populations.

Photosynthetic Measurements

Gas exchange measurements were performed on the middle leaflet of the first fully developed leaf from the apex (6th or 7th leaf) during the week 15 of the experiment by using the Li-6400xt measuring system (LiCor, Lincoln, NE, United States). Net photosynthesis (A), transpiration (E), stomatal conductance (g_s), leaf intercellular CO_2 concentration (C_i), and photochemical efficiency (F_v'/F_m') were measured by setting Li6400xt controls to growth chamber conditions [PPFD = 400 μmol m^{-2} s^{-1}, water pressure deficit for leaf (VPDL) 0.9–1.2. kPa; T = 26°C], with reference CO_2 maintained at 400 μmol mol^{-1}. The measurements were done on five plants per breeding population ($N = 5$).

Light response curves of photosynthesis (AQ curves; Ögren and Evans, 1993) were measured. The PPFD was varied, keeping the temperature (26°C) and CO_2 concentration (1000 μmol mol^{-1}) constant and controlling the VPDL (1–1.2 kPa). Initially, the measured leaf was acclimated at 1000 μmol m^{-2} s^{-1}, and after recording the photosynthetic parameters, the light was reduced to 800 μmol m^{-2} s^{-1} and later gradually to 600, 400,

200, 100, 50, 0 μmol m^{-2} s^{-1}. A fast transition of PPFD was used to avoid stomatal closure (Li6400xt manual). Five plants of each line were measured.

The photosynthetic response to CO_2 (photosynthetic AC_i curves; Sharkey et al., 2007) was evaluated by measuring photosynthetic rates at fixed saturating PPFD (1000 μmol m^{-2} s^{-1}), a temperature of 26°C, and VPDL of 1–1.2 kPa. The CO_2 reference concentration was set at 50, 100, 200, 400, 800, 1200, 1400, and 1600 μmol mol^{-1}. At each concentration, it took 15–20 min to reach steady-state conditions. Five plants of each line were measured.

Chlorophyll was measured by using the SPAD -502 m (Minolta, Japan) on the leaves sampled for photosynthetic measurements. Six measurements per leaf blade were taken and then averaged. Subsequently, the leaves were sampled and herbarised for morphometry.

Statistical Analysis

For the basic photosynthetic parameters and those related to leaf morphology and growth, the *t*-test and two-way analysis of variance (ANOVA) were used. We tested the significance of the breeding population only (*t*-test) or in combination with the chemotype and their interaction (two-way ANOVA). AQ_i curves were fitted by using a polynomial quadratic equation (Ögren and Evans, 1993). Photosynthetic light saturation and the light compensation point can be derived from the obtained non-rectangular hyperbolic curve. CO_2 response curves were fitted and analysed as described by Sharkey et al. (2007), estimating V_{cmax}, J, TPU, R_d and g_m -the maximum rate of carboxylation of Rubisco, the maximum rate of electron transport for the given light intensity, the maximum rate of triose phosphate use, day respiration, and mesophyll conductance for CO_2 transfer, respectively). For these parameters, differences between breeding populations were tested by using the *t*-test.

A significance level of 0.05 was used for all tests. Data were analysed by using the R environment (packages nlme and agricola; R Core Team, 2018).

RESULTS

Morphological Characterization of MX-CBD-11 and MX-CBD-707

The tested breeding populations differed significantly in growth habitus. The MX-CBD-11 plants were taller, less branched, had longer internodes, and had leaves consisting of an average of 5.00 ± 0.21 narrow leaflets. The average length of the central leaflet was 111.59 ± 4.47 mm and the average width was 20.06 ± 0.93 mm.

The MX-CBD-707 plants were shorter, bushier and had shorter internodes. Their leaves had on average 5.08 ± 0.34 leaflets. The average length of the central leaflet was 127.64 ± 6.44 mm, which was not significantly different ($p = 0.053$) from that of breeding population MX-CBD-11. There was a significant difference ($p \leq 0.001$) for the average width of the central leaflet, which was 26.59 ± 0.71 mm and therefore wider in MX-CBD-707 than in MX-CBD-11 (**Figure 1** and **Table 1**). As a result, the populations differed significantly in the length/width ratio ($p = 0.038$) and the width/length ratio ($p = 0.020$). Besides, the distance from the base of the central leaflet to the widest point of the leaflet was significantly longer in MX-CBD-707 than in MX-CBD-11 ($p = 0.032$) and the petiole width was also significantly wider in MX-CBD-707 than in MX-CBD-11 ($p = 0.039$). Leaf traits were measured for all 24 plants included in our study on fully expanded leaves and their central leaflets, as shown in **Figure 1**.

Differences in plants habitus were reflected in yield parameters. For all biomass parameters [shoot dry weight (DW), DW of leaves and inflorescences, stem DW, and root DW], the values were higher in MX-CBD-11 than in MX-CBD-707 (**Table 1**). Our results of leaf morphology and growth confirmed the assumption that MX-CBD-11 resembles the "narrow leaflet" type of cannabis, while MX-CBD-707 resembles the "wide leaflet" type of cannabis.

Cannabinoid Profiles of MX-CBD-11 and MX-CBD-707 Breeding Populations

High-performance liquid chromatography (HPLC) analysis (**Figure 2A**) revealed that the cannabinoid content in inflorescences of breeding population MX-CBD-11 varied from 4.11 to 11.66% for tCBD (total CBD) and from 0.31 to 5.39% for tTHC (total THC), while in breeding population MX-CBD-707, the tCBD content varied from 2.99 to 8.01% and the tTHC content varied from 0.42 to 4.49%, as shown in **Figure 2B** and **Table 2**.

Within each breeding population, two types of plants were identified based on the tCBD/tTHC ratio: plants with a ratio around 1 (average values 1.52 ± 0.09 in MX-CBD-11 and 1.12 ± 0.01 in MX-CBD-707) and plants with a ratio > 11 (average values 20.09 ± 0.70 in MX-CBD-11 and 14.41 ± 0.44 in MX-CBD-707). The two defined groups of each breeding population were characterised as Type II (CBD/THC balanced) and Type III (CBD dominant) cannabis, respectively.

The tCBG content ranged from 0.05 to 0.27% and from 0.03 to 0.78% in MX-CBD-11 and MX-CBD-707, respectively.

Based on the results obtained from cannabinoid content measurements, a two-way ANOVA of leaf morphological parameters was carried out, considering the breeding population and chemotype as factors. The analysis showed that both the breeding population ($p < 0.001$) and the chemotype ($p = 0.017$) had a significant effect only on the central leaflet width (26.59 ± 0.71 mm for MX-CBD-707 and 20.06 ± 0.93 mm for MX-CBD-11; 25.23 ± 1.00 mm for the CBD/THC balanced chemotype and 21.42 ± 1.29 mm for the CBD-dominant chemotype). For all the other measured parameters listed in **Table 1**, the chemotype did not have a significant influence. Therefore, a *t*-test was used to analyse the measured parameters.

The tTHC content measured in experimental plants of MX-CBD-11 and MX-CBD-707 demonstrated that they can all be

TABLE 1 | Growth and morphological parameters of two breeding populations of medical cannabis, namely MX-CBD-11 and MX-CBD-707.

		MX-CBD-11	MX-CBD-707	p
Plant growth parameters (*N* = 5)	Plant DW [g]	93.2 ± 6.7	59.7 ± 11.2	**0.039**
	Shoot FW [g]	297.6 ± 14.4	198.8 ± 40.1	0.069
	Shoot DW [g]	89.5 ± 6.4	57.5 ± 10.7	**0.039**
	Stem DW [g]	31.9 ± 1.4	14.9 ± 3.4	**0.004**
	Leaf + inflorescence DW [g]	57.6 ± 5.1	42.5 ± 7.6	0.145
	Root DW [g]	3.8 ± 0.5	2.3 ± 0.5	**0.072**
	Shoot/root DW ratio	25.1 ± 3.3	26.8 ± 1.8	0.673
Leaf morphological parameters (*N* = 12)	Number of leaflets per leaf	5.00 ± 0.21	5.08 ± 0.34	0.836
	Length of central leaflet [mm]	111.59 ± 4.47	127.64 ± 6.44	0.053
	Width of central leaflet [mm]	20.06 ± 0.93	26.59 ± 0.71	**< 0.001**
	Length/width ratio of central leaflets	5.65 ± 0.25	4.83 ± 0.27	**0.038**
	Width/length ratio of central leaflets	0.18 ± 0.01	0.21 ± 0.01	**0.020**
	Distance from base to widest point of central leaflet [mm]	56.47 ± 2.71	65.08 ± 2.60	**0.032**
	Distance from base of central leaflet to widest point/total length ratio	0.50 ± 0.01	0.51 ± 0.01	0.521
	Number of primary serrations on central leaflet	28.67 ± 1.11	26.50 ± 1.07	0.174
	Number of secondary serrations on central leaflet	3.08 ± 1.25	2.08 ± 0.54	0.471
	Petiole length [mm]	23.60 ± 2.73	29.47 ± 2.44	0.123
	Petiole width [mm]	0.88 ± 0.05	1.06 ± 0.07	**0.039**

The data are presented as the mean ± standard error (N = 5 or 12). The p values of the t-tests are shown, with statistically significant p values in bold. DW, dry weight; FW, fresh weight.

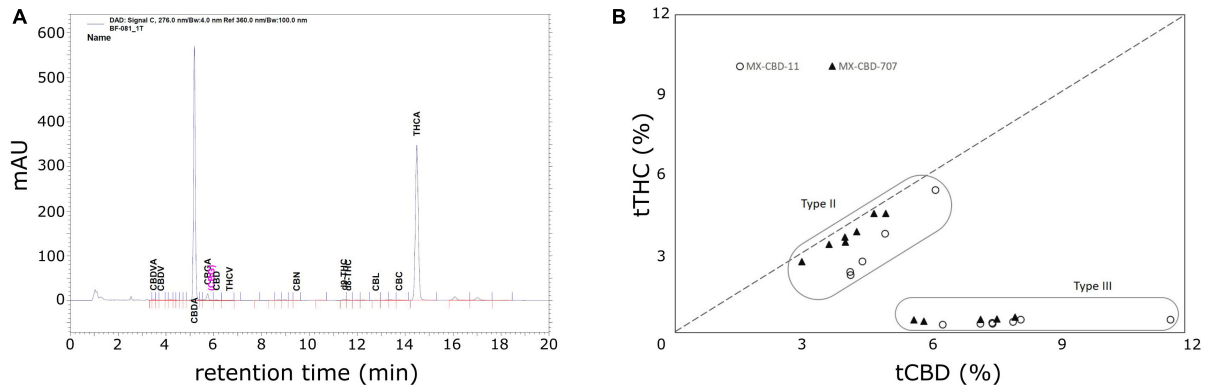

FIGURE 2 | The results of high-performance liquid chromatography (HPLC) analysis of dried inflorescences of breeding populations MX-CBD-11 and MX-CBD-707: **(A)** A representative HPLC chromatogram showing the retention times of various cannabinoids from MX-CBD-707/plant 41; **(B)** total cannabidiol (tCBD) and total tetrahydrocannabinol (tTHC) contents (in % w/w) in all 24 analysed cannabis plants. Each dot represents the measurements of one inflorescence per plant.

characterised as drug-type cannabis, as none of them contained less than 0.3% tTHC in inflorescence dry weight.

Sequence Analysis of the *THCAS* Gene in MX-CBD-11 and MX-CBD-707 Breeding Populations

Amplification with the primer pair THCAsynF and THCAsynR resulted in a single approximately 1,676 base pair (bp) PCR product from plants of breeding populations MX-CBD-11 and MX-CBD-707 (**Supplementary Figure 1**). PCR products were cloned in the pGEM-T-Easy Vector and isolated plasmids were sequenced with the primer pair SP6 and T7, which annealed to the vector backbone. Backbone sequences were removed in CodonCode Aligner and the remaining *THCAS* sequences was aligned in CLC Genomics with standard settings. Alignment of the sequences obtained from MX-CBD-11 revealed several single nucleotide substitutions among the sequences of different plants and clearly grouped the 12 analysed plants into two distinct groups: five Type II plants (CBD/THC balanced) in one group and the remaining seven Type III plants (CBD dominant) in the second group. A consensus sequence from each group was extracted by using CLC and compared with BLASTN to the sequences deposited in NCBI. The consensus sequence of the Type II plants of MX-CBD-11 breeding population showed similarities with several *THCAS* sequences

TABLE 2 | Concentrations of CBDA, CBD, tCBD, THCA, d8-THC, d9-THC, and tTHC (in % w/w) measured in dried inflorescences of breeding populations MX-CBD-11 and MX-CBD-707.

Breeding population	Cannabinoid	Min [%]	Max [%]	Average retention time [s] ± standard error
MX-CBD-11	CBDA	4.521	12.910	5.185 ± 0.002
(*N* = 12)	CBD	0.125	0.344	6.097 ± 0.002
	tCBD	4.114	11.657	/
	d9-THC	0.029	0.273	11.424 ± 0.002
	d8-THC	0.033	0.175	11.596 ± 0.002
	THCA	0.308	5,631	14.467 ± 0.002
	tTHC	0.310	5.386	/
MX-CBD-707	CBDA	3.293	8.468	5.193 ± 0.002
(*N* = 12)	CBD	0.102	0.582	6.108 ± 0.003
	tCBD	2.990	8.008	/
	d9-THC	0.065	0.363	11.443 ± 0.003
	d8-THC	0.040	0.150	11.606 ± 0.003
	THCA	0.358	4.726	14.487 ± 0.003
	tTHC	0.424	4.492	/

CBDA, Cannabidiolic Acid; CBD, Cannabidiol; tCBD, total CBD; THCA, Tetrahydrocannabinolic acid; d8-THC, Delta-8-Tetrahydrocannabinol; d9-THC, Delta-9-Tetrahydrocannabinol; tTHC, total THC; / – information non-relevant.

deposited in NCBI and 100% identity with the complete coding DNA sequences (cds) of accessions AB057805, MW382908 and the partial cds of accessions AB212832, KT875984, and MG996418. The consensus sequence of the III chemotype plants was 100% identical and showed 98% overlap with the *tetrahydrocannabinolic acid synthase (THCA2)* gene of the Skunk #1 cultivar (KJ469379, complete cds) and more than 99% identity with several other deposited THCAS sequences [KJ469380 (high CBD cultivar Carmen), MG996405 (high CBD cultivar Ermes1), AB212830, etc.].

We obtained similar results by aligning *THCAS* sequences from MX-CBD-707. The consensus sequences of the Type II and III plants were also compared with the sequences deposited in NCBI. The Type II plants showed 100% identity with five *THCAS* (AB057805, MW382908, AB212832, KT875984, and MG996418), while the Type III plants showed almost complete identity with *THCAS* accessions MT338560, MW504064 (high-THC cultivar Animal Cookies), MW504063 (high-THC cultivar Cake Breath), KT876015, KT875987, and MG996417.

ClustalW analysis of all 24 *THCAS* sequences grouped the Type III MX-CBD-11 and MX-CBD-707 plants in two separate clusters, while almost all sequences of Type II plants of both breeding populations were grouped in the same cluster (**Figure 3**). The only exception was plant 707/33.

To determine whether a PCR and electrophoresis analysis with published molecular markers could be used to distinguish between Type II and III MX-CBD-11 and MX-CBD-707 plants, we performed an *in silico* complementary analysis. It was based on sequence alignment of primers for published chemotype molecular markers to our *THCAS* sequences with CodonCode Aligner and CLC Genomics (**Supplementary Figure 1**). The results are shown in **Table 3** in which "Yes" indicates that the primers are complementary to *THCAS* sequences of the concerned group of plants (e.g., primers D589 to MX-CBD-11 Type II), while "No" indicates that the primers are not complementary due to INDELs or substitutions in the annealing region of the gene. To distinguish between different chemotypes, the primers have to be complementary (should anneal to *THCAS* during PCR) to the DNA of only one chemotype of the population. Primers that are complementary to the DNA of both chemotypes of a population, would amplify a fragment of *THCAS* in both and therefore would not be informative. On the other hand, a primer pair that is not complementary to the DNA of any chemotype is also not informative for the distinction between chemotypes. Such results are marked with an asterisk in **Table 3**. The chemotypes of MX-CBD-11 could be distinguished by using markers D589 and B1080/B1192, but not THCA583-For/THCA1034-Rev, as these were complementary to the *THCAS* genes of both chemotypes. In contrast, only the primer pair THCA583-For/THCA1034-Rev could be used to distinguish Type II or III MX-CBD-707 plants, whereas the other two (D589, and B1080/B1192) were complementary to all *THCAS* sequences and were therefore not suitable for discrimination between plants of different chemotypes. Primers for marker B190/B200 were not complementary to any of our *THCAS* sequences.

Photosynthetic Parameters

Most photosynthetic parameters differed significantly between breeding populations, while they were not dependent on chemotype (**Table 4**). Stomatal conductance (g_s), transpiration (E), and net photosynthesis (A) measured under chamber conditions were higher in MX-CBD-707 than in MX-CBD-11 (**Figure 4**). However, intrinsic water use efficiency (*WUE*), calculated as the ratio of A to E, was higher in MX-CBD-11 than in MX-CBD-707. There was no difference in chlorophyll content (SPAD).

Plants from both populations did not differ in photosynthesis dependence on light (**Figure 5**). The *AQ* curves showed a similar photosynthetic light compensation point, similar light use efficiency (the slope of the initial linear part of the curve), and similar light saturation. Photosynthesis of both populations was light saturated above 600 $\mu mol\ m^{-2}\ s^{-1}$.

Regarding CO_2 response curves, the maximum photosynthetic rates were measured at 2000 $\mu mol\ CO_2\ mol^{-1}$ (under saturating PPFD of 1000 $\mu mol\ m^{-2}\ s^{-1}$), and were 37.1 and 36.7 $\mu mol\ m^{-2}\ s^{-1}$ for MX-CBD-11 and MX-CBD-707, respectively. Analysis of the AC_i curves (**Figure 6**) showed that plants from the two populations did not differ in the maximum carboxylation rate of Rubisco (V_{cmax}), the maximum rate of electron transport (J), and the maximum rate of triose phosphate utilisation (TPU) (**Table 5**). However, differences in day respiration (R_d) were pronounced, with MX-CBD-707 ($R_{dS707} = 3.9 \pm 0.6\ \mu mol\ m^{-2}\ s^{-1}$) having significantly higher respiration than that of the MX-CBD-11 breeding population ($R_{dS11} = 1.9 \pm 0.5\ \mu mol\ m^{-2}\ s^{-1}$).

Comparison of cannabinoid content (expressed as the THC content or the CBD/THC ratio) and photosynthesis [net photosynthetic rate (A), assessed by gas exchange] or photochemical efficiency (F_v'/F_m', assessed by fluorescence measurements) revealed no clear relationship (**Figure 7**).

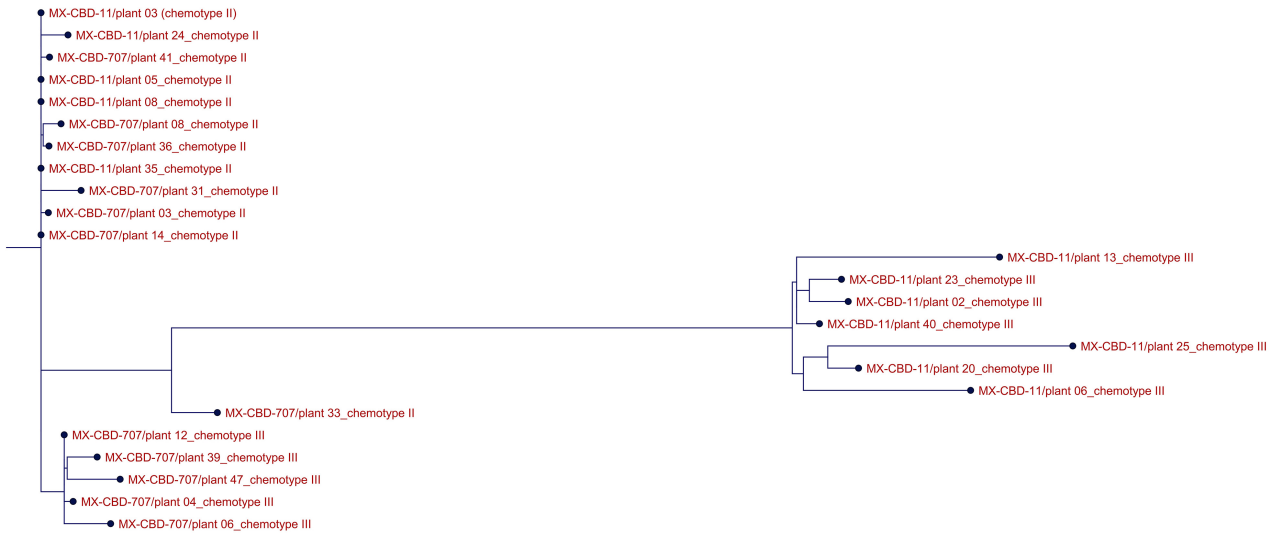

FIGURE 3 | Alignment of *THCAS* sequences from 24 cannabis plants of the MX-CBD-11 and MX-CBD-707 breeding populations with ClustalW. The provenances of the sequences are indicated with the name of the breeding population, the plant's unique code, and the plant's chemotype.

TABLE 3 | Published DNA molecular markers developed for determination of cannabis chemotypes and their applicability to discriminate between different chemotypes of MX-CBD-11 and MX-CBD-707.

Marker	Reference	Primer sequence	MX-CBD-11		MX-CBD-707	
			Type II	Type III	Type II	Type III
D589	Staginnus et al. (2014)	For CCTGAATTCGACAATACAAAATCTTAGATTCAT	Yes	No	Yes	Yes*
		Rev ACTGAATATAGTAGACTTTGATGGGACAGCAACC	Yes	No	Yes	Yes*
B1080/B1192	Pacifico et al. (2006)	For AAGAAAGTTGGCTTGCAG	Yes	No	Yes	Yes*
		THCAS-specific-Rev TTAGGACTCGCATGATTAGTTTTTC	Yes	No	Yes	Yes*
B190/B200	de Meijer et al. (2003)	For TGCTCTGCCCAAAGTATCAA	No*	No*	No*	No*
		Rev CCACTCACCACTCCACCTTT	No*	No*	No*	No*
THCA583-For	Weiblen et al. (2015)	For GTG GAG GAG GCT ATG GAG C	Yes	Yes*	Yes	Yes*
THCA1034-Rev		Rev CCC AAC TCA GGA AAG CTC TTG	Yes	Yes*	Yes	No

Asterisks (*) mark discrepancies in the expected versus obtained results, because primers D589, B1080/B1192, and THCA583-For/THCA1034-Rev should amplify parts of the functional THCAS gene, while marker B190/B200 should amplify parts of the THCAS (190 bp) and CBDAS (200 bp) genes.

DISCUSSION

The chemical profiles of CBD-dominant (Type III) and intermediate (Type II) cannabis chemotypes are gaining increased attention due to the therapeutic potential without psychoactive effects of CBD (Avraham et al., 2011). As a result, numerous breeding programmes are underway aimed at increasing CBD content and stabilising this trait in breeding populations intended for varietal registration. Plant genetic resources are searched for accessions suitable for introgression of this valuable trait in breeding programmes, and plant phenotypes are often used as morphological markers.

It has long been assumed that cannabis plants can be divided into a few groups/ecotypes whose specific phenotypes correlate with the plant's chemotypes. Since the early work of Linnaeus in 1753, several contrasting classifications of cannabis have been proposed. Fossil pollen studies suggest that genetic drift initiated allopatric differences between European *C. sativa* and Asian *C. indica*. *C. sativa* and *C. indica* could thus be separated by morphology (*C. sativa* is taller with a fibrous stalk, whereas *C. indica* is shorter with a woody stalk) and, by phytochemistry (*C. sativa* with THC > CBD, whereas *C. indica* with THC < CBD). DNA barcode analysis supports

TABLE 4 | The results of two-way analysis of variance (ANOVA) (factors: breeding population, chemotype) for stomatal conductance (g_s), transpiration (E), net photosynthesis (A), intrinsic water use efficiency ($WUE_i = A/E$), photochemical efficiency, and chlorophyll content (SPAD) ($N = 5$).

ANOVA (p-value)	g_s	E	A	WUE	F_v'/F_m'	Chlorophyll (SPAD)
Breeding population	**0.004**	**0.008**	**0.025**	**0.001**	0.052	0.467
Chemotype	0.210	0.446	0.716	0.971	0.999	0.105
Breeding population × chemotype	0.821	0.633	0.715	0.357	0.941	0.523

Statistically significant p values are presented in bold.

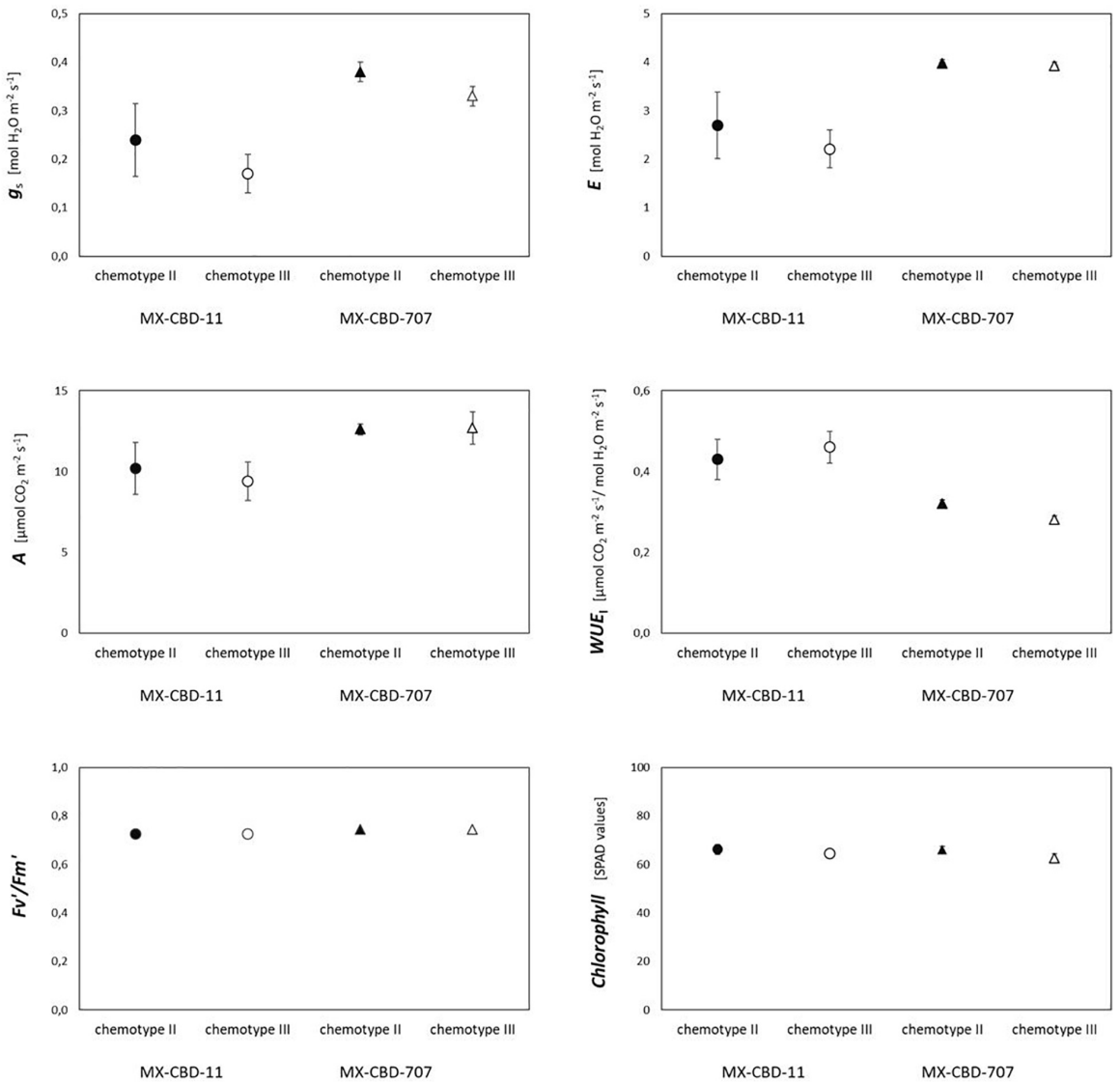

FIGURE 4 | Photosynthetic traits of two breeding populations of medical cannabis MX-CBD-11 and MX-CBD-707. The data are presented as the mean ± standard error ($N = 5$).

the separation of these taxa at a subspecies and not species level, recognising the formal nomenclature of *C. sativa* subsp. *sativa* and *C. sativa* subsp. *indica* (McPartland, 2018). In the same publication, a diverse description of the (sub)species is listed (subsp. *sativa* containing < 0.3% of THC and subsp. *indica* containing > 0.3% THC in dried inflorescences). When considering other authors, the classification/nomenclature and descriptions of cannabis are even more confusing. As pointed out by McPartland (2017), the ubiquitous interbreeding and hybridisation of cannabis species, subspecies, and ecotypes in recent decades renders their distinction almost meaningless. As a result, vernacular taxonomy of drug-type plants "Sativa" and "Indica" prevails today: cannabis plants are classified primarily on the basis of leaf morphology. The narrow leaflet drug-type plants (the "Sativas") can be identified by their narrow and light green leaves and should produce more THC than CBD, while deep green and wide leaflet drug-type plants ("Indicas") should produce more CBD than "Sativa," with a THC/CBD ratio closer to 1. "Indica" refers to plants with broad leaflets, compact habitus, and early maturation, typified by plants from Afghanistan. "Sativa" refers to plants with narrow leaflets, slender and tall habitus, and late maturation, typified by plants from India and their descendants in Thailand, South and East Africa, Colombia, and Mexico (Figure 4 in McPartland, 2018). The author emphasised that conflating formal and vernacular taxonomy has resulted in the confusion of otherwise excellent studies that used "Sativa" but latinised the taxon as *C. sativa*.

We therefore decided to study the morphology, chemotype, genotype, and physiology of two cannabis breeding populations that based on visual appearance showed characteristics of NLD

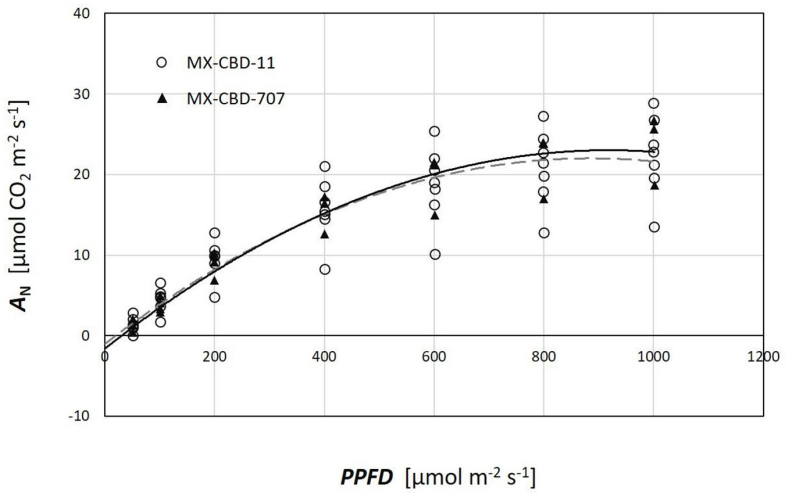

FIGURE 5 | Photosynthetic light response (*AQ*) curves of two breeding populations of medical cannabis: MX-CBD-11 and MX-CBD-707. The data points indicate measurements on individual plants (5 plants of each population).

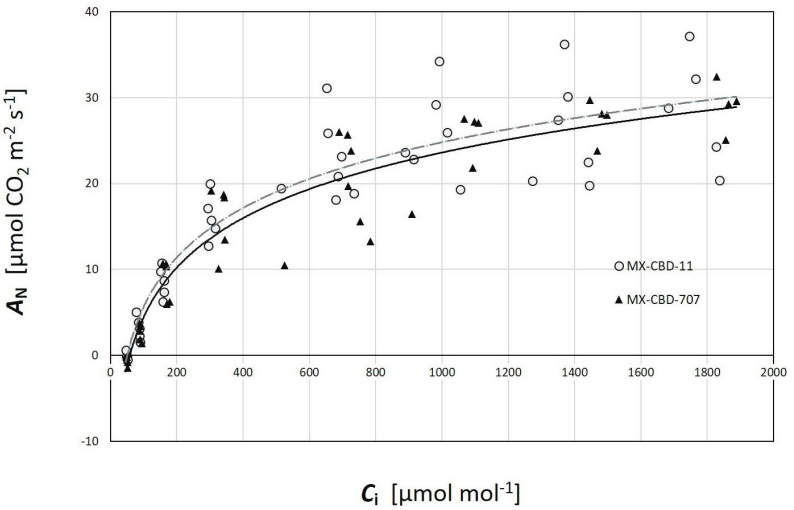

FIGURE 6 | Photosynthetic CO_2 response (AC_i) curves of two breeding populations of medical cannabis MX-CBD-11 and MX-CBD-707. The data points indicate measurements on individual plants (5 plants of each population).

and WLD plants. Furthermore, we wanted to determinate the linkage between morphological and chemical traits and to use the obtained data to classify our cannabis populations based on literature data. As recently reported in an excellent study in which Jin et al. (2021b) phenotypically characterised 21 cannabis cultivars covering three chemical phenotypes, morphological traits can be used reliably to distinguish among cannabis chemotypes, which facilitates taxonomic classification.

We first measured plant growth and leaf parameters, which confirmed uniformity within populations and showed significant differences between populations. Among the measured parameters, plant, shoot, stem, and root dry weights showed statistically significant differences between MX-CBD-11 and MX-CBD-707, with clear differences in biomass distribution and a higher biomass accumulation in MX-CBD-11. Interestingly, there were no significant differences in dry weights of inflorescences and leaves.

A detailed analysis of leaf morphology showed statistically significant differences in the average width of central leaflets ($p < 0.001$), the distance from the base of the central leaflet to the widest point of leaflets ($p = 0.032$), and the petiole width ($p = 0.039$) between the two studied populations. These differences were reflected in the calculated ratios of central leaflet width to length and distance from the base to the widest point divided by the total length, which were further compared with the results reported by Jin et al. (2021b). The calculated mean value of the central leaflet width/length ratio of MX-CBD-11 was 0.18 ± 0.01, which is identical to the value measured by

TABLE 5 | Maximum carboxylation rate of Rubisco (V_{cmax}), maximum rate of electron transport (J), maximum rate of triose phosphate utilization (TPU), and day respiration (R_d) of two breeding populations of medical cannabis MX-CBD-11 and MX-CBD-707.

	V_{cmax}	J	TPU	R_d
MX-CBD-11	100.2 ± 24.4	122.3 ± 12.0	9.9 ± 0.9	1.9 ± 0.5
MX-CBD-707	133.5 ± 15.7	137.2 ± 11.4	11.0 ± 0.9	3.9 ± 0.6
t-test	ns	ns	ns	$p = 0.0338$

The data are presented as the mean ± standard error (N = 5).

Jin et al. (2021b) for CBD-dominant cultivars (0.18 ± 0.02), while MX-CBD-707 had a wider average central leaflet width with a higher width/length ratio of 0.21 ± 0.01. The calculated ratio was between their parameters for CBD dominant (0.18 ± 0.02) and THC dominant (0.25 ± 0.03) cultivars, most similar to the ratio of intermediate plants (0.20 ± 0.02). Moreover, Jin et al. (2021b) demonstrated that the CBD-dominant cultivars have more leaflets per leaf (4.45–5.39, average 4.92 ± 0.47) compared with the intermediate and THC-dominant cultivars. In our study, both breeding populations had a similar average number of leaflets per leaf, namely 5.0 for MX-CBD-11 and 5.1 for MX-CBD-707, both resembling CBD-dominant cultivars. Our results confirmed the ones reported by Jin et al. (2021b), because our breeding populations were considered high CBD at an industrial production scale.

The calculated ratio of distance from the base of the central leaflet to the widest point divided by the total length was 0.50 ± 0.01 and 0.51 ± 0.01 for MX-CBD-11 and MX-CBD-707, respectively, and did not differ significantly ($p = 0.521$). Jin et al. (2021b) obtained nearly identical results: 0.50 and 0.51 for all three chemotype groups of cultivars, without a significant difference among them ($p = 0.9282$). Absolute values of measured leaf parameters were less comparable between our study and Jin et al. (2021b) and therefore less applicable for chemotype determination.

Because there was a discrepancy in some leaf (leaflet) traits, we could not fully rely on morphological classification by Jin et al. (2021b) to deduce the cannabinoid profile of the plants. Moreover, on the basis of plant habitus, we would classify MX-CBD-11 as "Sativa" because the plants were taller, had longer internodes, and had light green narrow leaflets, while MX-CBD-707 would be classified as "Indica" because the plants were shorter, bushier, and had deep green wide leaflets. Based on vernacular classifications, MX-CBD-11 should contain higher THC than CBD ("Sativa") and MX-CBD-707 more CBD than MX-CBD-11, with a THC/CBD ratio closer to 1.

We proceeded with the analysis of cannabinoids to verify their content in the narrow leaflet MX-CBD-11 and the wide leaflet MX-CBD-707 breeding populations. We sampled and processed inflorescences from each experimental plant separately to obtain results at the individual plant level rather than as population averages presented in other publications and our

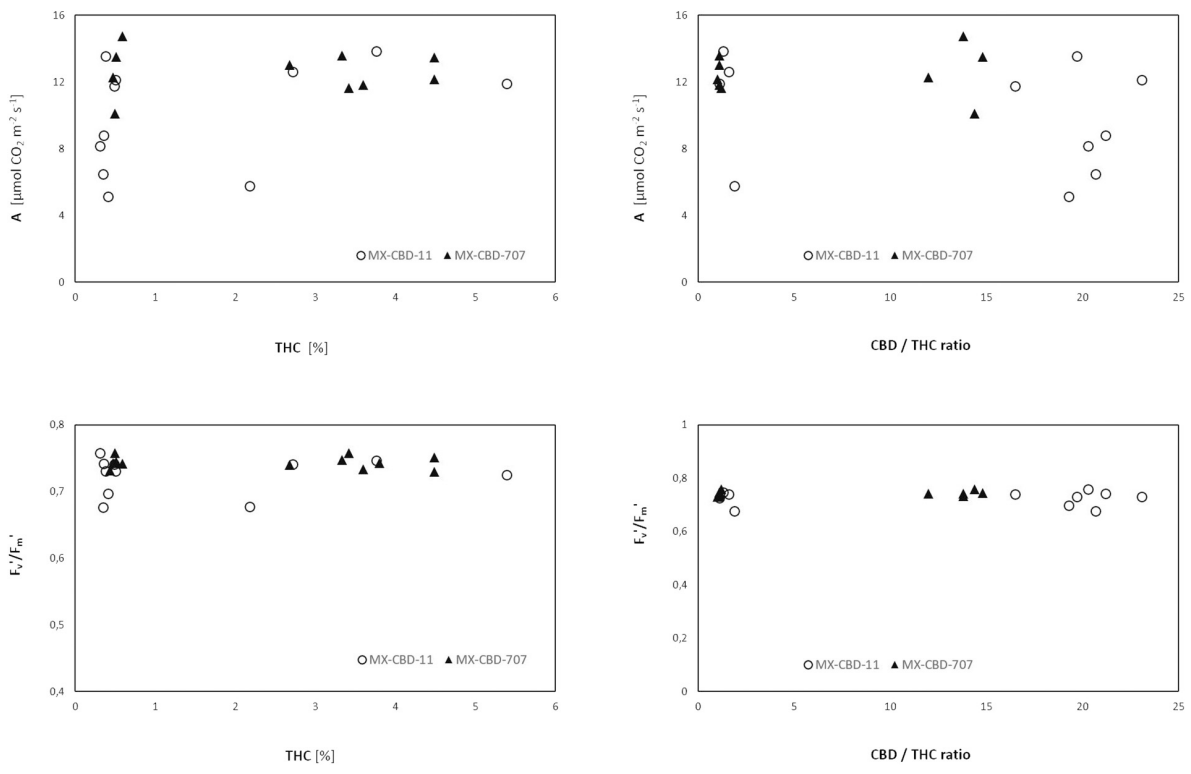

FIGURE 7 | Net photosynthesis (*A*) and photochemical efficiency F_v'/F_m' of two breeding populations of medical cannabis MX-CBD-11 and MX-CBD-707 as a function of cannabinoid content.

previous analyses of these two populations. HPLC measurements of the main cannabinoids revealed that plants within both populations differed significantly in their cannabinoid content. Within the MX-CBD-11, the minimum and maximum values of total CBD and total THC varied by 2.84- and 18.35-fold, respectively. A 3.87- and 16.26-fold difference in tCBD and tTHC was observed in MX-CBD-707 plants (**Figure 2B**). Calculating the tCBD/tTHC ratio allowed us to identify plants of two different chemotypes within each population. The tCBD/tTHC ratios varied from 1.04 to 23.14 and classified the plants of both breeding populations into Type II (CBD/THC intermediate) with an average ratio of 1.52 ± 0.09 (MX-CBD-11), and 1.12 ± 0.01 (MX-CBD-707), and Type III (CBD dominant), with an average ratio of 20.09 ± 0.70 (MX-CBD-11) and 14.41 ± 0.44 (MX-CBD-707) (**Figure 2B**). In contrast to the reports by Welling et al. (2016), higher variability in cannabinoid composition was observed in Type III plants compared with Type II plants in our study. The cannabinoid contents in our breeding populations were unexpected because plants within populations had consistent phenotypes based on visual inspection and leaf measurements. At least for our NLD and WLD populations, the results obtained disprove the theory about the correlation between plant morphology and cannabinoid content. This was further analyzed with a two-way analysis of variance in which we tested the influence of the breeding population, the chemotype and their interaction on leaf morphology. The analysis showed that the chemotype had a significant effect only on the average width of the central leaflet ($p = 0.017$), while not to the other measured or calculated leaf parameters presented in **Table 1**. It also confirmed a significant effect of the breeding population to the width of the central leaflet ($p < 0.001$), the length to width ratio of the central leaflets ($p = 0.044$), the width to length ratio of the central leaflets ($p = 0.021$), the distance from the base of the central leaflet to the widest point of the leaflet ($p = 0.023$) and the petiole width ($p = 0.048$), like it was already shown with the *t*-test (**Table 1**). The chemotype ($p = 0.292$) or the interaction ($p = 0.502$) did not have a significant effect on the ratio of central leaflet width to length, as was also reported by Jin et al. (2021b). In our experiment, the average value was larger in Type II (CBD/THC intermediate) plants than in Type III (CBD dominant) ones (0.21 ± 0.01 and 0.19 ± 0.01, respectively), which was also in accordance with the results of Jin et al. (2021b; 0.20 ± 0.02 for Type II and 0.18 ± 0.02 for Type III). Similarly, like reported in Jin et al. (2021b), our average values of distances from the base to the widest point divided by the total length were not significantly different between the two chemotypes ($p = 0.056$).

Because both populations had similar ranges of tCBD and tTHC and both contained Type II and III plants, we wanted to determine whether the chemotypes from different populations were determined by the same alleles. We sequenced the *THCAS* gene because, according to the literature, both Type II and III plants contain functional alleles for *CBDAS*, so we did not expect to find differences in that gene. Type II plants should also contain a functional *THCAS*, while Type III plants should be caused by non-functionality of *THCAS*. The genes for *THCAS* were amplified from all 24 plants that were included in our study and sequenced using classical Sanger sequencing. Alignment of the obtained sequences correlated with their tCBD/tTHC ratios (**Figure 3**), with Type III MX-CBD-11 and MX-CBD-707 plants clustering in two distinct groups and all but one Type II plant from both breeding populations clustering together as one group. BLASTN analysis of *THCAS* gene sequences showed high (up to 100%) similarity with *THCAS* sequences deposited in NCBI. Interestingly, we found 100% similarity between the consensus sequence of MX-CBD-11-chemotype III plants and the *THCAS* gene from cultivar Skunk #1 (KJ469379). This was unexpected because previous findings suggest that Type III plants contain non-functional alleles for *THCAS*, while Skunk #1 is a hybrid cultivar with high THC content (Type I). The same consensus sequence showed > 99% identity with several other deposited *THCAS* sequences, two of which were from high-CBD cultivars of both drug and fibre types (KJ469380 drug type Carmen and MG996405 fibre type Ermes1). One of our *THCAS* sequences was outside its group based on chemotype (**Figure 3**). This ambiguity was due to poorer sequence quality, with gaps and unknown nucleotides caused by sequencing errors.

Molecular markers are also widely used to determine the chemotypes of cannabis. In recent years, several molecular DNA markers based on the analysis of bulk segregants of *THCAS* and *CBDAS* gene sequences have been developed to allow rapid and accurate determination of plant chemotypes in marker-assisted selection. They relied on the model of simple genetic determinism of chemotypes based on a gene with two alleles encoding two isoforms (*THCAS,* and *CBDAS*) of the same enzyme, as described by de Meijer et al. (2003). Two dominant (D589, THCA583-For/THCA1034-Rev) and two codominant (B1080/B1192, B190/B200) markers have been described in the literature (**Table 3**) and have been used successfully to determine chemical types. For B190/B200, de Meijer et al. (2003) showed 88% correct identification of Type I chemotypes, 95% for Type II, and 98% for Type III, while Pacifico et al. (2006) used the B190/B200 marker to determine the chemotypes of 148 plants and obtained only 20% accuracy for Type I, 0% for Type II, and 93% for Type III. They developed a new codominant marker B1080/B1192 that gave 100% correct identification. Welling et al. (2016) used a combination of two markers (D589 and B1080/B1192) and accurately predicted the chemotype of > 98% of plants (65 of 66). Our *in silico* complementary analysis showed that the published molecular markers were not equally effective in unrelated plant material with different genetic backgrounds. As shown in **Table 3**, only the THCA583-For/THCA1034-Rev marker could be used to discriminate between Type II and III MX-CBD-707 plants, whereas the other three could amplify parts of the *THCAS* genes in all MX-CBD-707 plants. For MX-CBD-11, markers D589 and B1080/B1192 could be used, but not THCA583-For/THCA1034-Rev and B190/B200. This simple analysis clearly demonstrated genotype dependence of the developed molecular markers.

There was no clear relationship between biomass yield and photosynthesis in either breeding line. High maximum photosynthetic rates indicate that the plants were grown under suitable conditions. The higher photosynthesis (*A*) and transpiration (*E*) measured in MX-CBD -707 plants can be

attributed to higher stomatal conductance (g_s). As a result, plants in this line operated at a slightly lower water use efficiency compared with MX-CBD-11 plants. In general, the results of gas exchange measurements indicate a different stomatal regulation of the two lines under growth chamber conditions. The values for V_{cmax}, J, and TPU derived from the and AC_i curves were within the range reported by Tang et al. (2017) for moderately nitrogen-supplied hemp. There were no differences between the breeding populations, even when comparing the light response curves. However, leaf photosynthetic performance under chamber conditions was better in MX-CBD-707 than in MX-CBD-11, which, in contrast, had a higher biomass yield. This discrepancy could be explained by differences in carbon allocation. The different plant habitus and biomass accumulation patterns of the tested populations suggest differences in the distribution of photosynthates to different sinks, plant parts, ephemeral, and long-lived tissues. In addition, a significant fraction of carbohydrates may be used for respiration. The twofold higher day respiration (R_d) of the MX-CBD-707 population could reduce photosynthetic gain of carbohydrates and, consequently, lead to lower biomass accumulation. Significant differences in leaf respiration between different cannabis cultivars (fibre and drug type) were previously reported by Lydon et al. (1987). More detailed analyses would be required for a deeper understanding of allocation, including analyses of mechanical tissue (fibre content) and non-structural carbohydrates.

Neither chlorophyll content (i.e., greenness) nor photochemical efficiency, which have been reported as possible indicators of cannabinoid profile (Khajuria et al., 2020; Jin et al., 2021b), were associated with the CBD/THC ratio. This calls into question the use of physiological parameters for chemical screening of cannabis.

CONCLUSION

The species *C. sativa* L. exhibits an astonishing diversity of morphological, physiological, and chemical characteristics, all of which could be attributed to the species great genetic diversity and adaptation to different growing conditions. Previously published scientific data have shown correlations between chemotype categories and traits of the plant phenotype, genes encoding cannabinoid synthesising enzymes, and physiology. However, our study has shown that the reported correlations are genotype dependent and apply to the genotypes included in the reported studies. The two chemotypes identified in our experimental plants did not differ in plant visual appearance, leaf morphology, and photosynthetic traits in the populations studied. Correlation was only demonstrated with the respective *THCAS* sequences, which showed great discrimination power between the chemotypes, whereas previously published molecular markers for chemotype determination were not found to be equally reliable in a different genetic background.

DATA AVAILABILITY STATEMENT

The raw data supporting the conclusions of this article will be made available by the authors, without undue reservation.

AUTHOR CONTRIBUTIONS

JM, JJE, MF, and DV conceived and designed this study. JJE, MF, and JM performed the experiments. DV and JM analysed the data and wrote the manuscript. All authors have read and approved this manuscript.

FUNDING

This work was conducted as part of the scientific research project "Breeding medical cannabis (*Cannabis sativa* L.)," a collaboration between the Biotechnical Faculty of the University of Ljubljana, Slovenia (project leader JM), and MGC Pharmaceuticals Ltd. This study was funded by MGC Pharmaceuticals Ltd. The funder was not involved in the study design; the collection, analysis, and interpretation of the data; the writing of this article; or the decision to submit it for publication. The research was also funded by Research Programmes P4-0077 and P4-0085, and the Infrastructure Centre IC RRC-AG (IO-0022-0481-001) of the Slovenian Research Agency.

ACKNOWLEDGMENTS

We thank Miha Slapnik, Sinja Svetik, and Špela Mestinšek Mubi (from the Biotechnical Faculty) and Irena Pribošič (from MGC Pharmaceuticals Ltd.) for their technical assistance during the experiments.

SUPPLEMENTARY MATERIAL

The Supplementary Material for this article can be found online at: https://www.frontiersin.org/articles/10.3389/fpls.2022.786161/full#supplementary-material

Supplementary Figure 1 | Alignment of 24 Sanger sequences of *THCAS* from plants of breeding populations MX-CBD-11 and MX-CBD-707.

REFERENCES

Avraham, Y., Grigoriadis, N., Poutahidis, T., Vorobiev, L., Magen, I., Ilan, Y., et al. (2011). Cannabidiol improves brain and liver function in a fulminant hepatic failure-induced model of hepatic encephalopathy in mice. *Br. J. Pharmacol.* 162, 1650–1658. doi: 10.1111/j.1476-5381.2010.01179.x

Bazzaz, F. A., Dusek, D., Seigler, D. S., and Haney, A. W. (1975). Photosynthesis and cannabinoid content of temperate and tropical populations of *Cannabis sativa*. *Biochem. Syst. Ecol.* 3, 15–18. doi: 10.1016/0305-1978(75)90036-8

Chandra, S., Lata, H., Khan, I. A., and ElSohly, M. A. (2011). Temperature response of photosynthesis in different drug and fiber varieties of (*Cannabis sativa* L.). *Physiol. Mol. Biol. Plants* 17, 297–303. doi: 10.1007/s12298-011-0068-4

de Meijer, E. P. M., Baggata, M., Carboni, A., Crucitti, P., Moliterni, V. M., Rannali, P., et al. (2003). The inheritance of chemical phenotype in *Cannabis sativa* L. *Genetics* 163, 335–346.

de Meijer, E. P. M., Van der Kamp, H. J., and Euwjik, F. A. (1992). Characterisation of *Cannabis* accessions with regard to cannabinoid content in relation to other plant characters. *Euphytica* 62, 187–200. doi: 10.1007/BF00041753

Flajšman, M., Slapnik, M., and Murovec, J. (2021). Production of feminised seeds of high CBD *Cannabis sativa* L. by manipulation of sex expression and its application to breeding. *Front. Plant Sci.* 12:718092. doi: 10.3389/fpls.2021.718092

Friedman, D., French, J. A., and Maccarrone, M. (2019). Safety, efficacy, and mechanisms of action of cannabinoids in neurological disorders. *Lancet Neurol.* 18, 504–512. doi: 10.1016/S1474-4422(19)30032-8

Glivar, T., Eržen, J., Kreft, S., Eržen, M., Čerenak, A., Čeh, B., et al. (2020). Cannabinoid content in industrial hemp (*Cannabis sativa* L.) varieties grown in Slovenia. *Ind. Crops Prod.* 145:112082. doi: 10.1016/j.indcrop.2019.112082

Grassa, C. J., Weiblen, G. D., Wenger, J. P., Dabney, C., Poplawski, S. G., Motley, S. T., et al. (2021). A new *Cannabis* genome assembly associates elevated cannabidiol (CBD) with hemp introgressed into marijuana. *New Phytol.* 230, 1665–1679. doi: 10.1111/nph.17243

Gul, W., Gul, S. W., Radwan, M. M., Wanas, A. S., Mehmedic, Z., Khan, I. I., et al. (2015). Determination of 11 cannabinoids in biomass and extracts of different varieties of *Cannabis* using high-performance liquid chromatography. *J. AOAC Int.* 98, 1523–1528. doi: 10.5740/jaoacint.15-095

Jin, D., Dai, K., Xie, Z., and Chen, J. (2020). Secondary metabolites profiled in cannabis inflorescences, leaves, stem barks, and roots for medicinal purposes. *Sci. Rep.* 10:3309. doi: 10.1038/s41598-020-60172-6

Jin, D., Henry, P., Shan, J., and Chen, J. (2021b). Identification of phenotypic characteristics in three chemotype categories in the genus *Cannabis*. *Hortscience* 56, 481–490. doi: 10.21273/HORTSCI15607-20

Jin, D., Henry, P., Shan, J., and Chen, J. (2021a). Identification of chemotypic markers in three chemotype categories of cannabis using secondary metabolites profiled in inflorescences, leaves, stem bark, and roots. *Front. Plant Sci.* 12:699530. doi: 10.3389/fpls.2021.699530

Khajuria, M., Prakash Rahul, V., and Vyas, D. (2020). Photochemical efficiency is negatively correlated with the Δ9 tetrahydrocannabinol content in *Cannabis sativa* L. *Plant Physiol. Biochem.* 151, 589–600. doi: 10.1016/j.plaphy.2020.04.003

Kojoma, M., Seki, H., Yoshida, S., and Muranaka, T. (2006). DNA polymorphisms in the tetrahydrocannabinolic acid (THCA) synthase gene in "drug-type" and "fiber-type" *Cannabis sativa* L. *Forensic Sci. Int.* 159, 132–140. doi: 10.1016/j.forsciint.2005.07.005

Laznik, Ž, Košir, I. J., Košmelj, K., Murovec, J., Jagodič, A., and Trdan, S. (2020). Effect of *Cannabis sativa* L. root, leaf and inflorescence ethanol extracts on the chemotrophic response of entomopathogenic nematodes. *Plant Soil* 455, 367–379. doi: 10.1007/s11104-020-04693-z

Lydon, J., Teramura, A. H., and Coffman, C. B. (1987). UV-B radiation effects on photosynthesis, growth and cannabinoid production of two *Cannabis sativa* chemotypes. *Photochem. Photobiol.* 46, 201–206. doi: 10.1111/j.1751-1097.1987.tb04757.x

Mandolino, G., Bagatta, M., Carboni, A., Ranalli, P., and de Meijer, E. (2003). Qualitative and quantitative aspects of the inheritance of chemical phenotype in *Cannabis*. *J. Ind. Hemp* 8, 51–72. doi: 10.1300/J237v08n02_04

McPartland, J. M. (2017). "*Cannabis sativa* and *Cannabis indica* versus 'sativa' and 'indica'," in *Cannabis sativa L.-Botany and Biotechnology*, eds S. Chandra, H. Lata, and M. A. ElSohly (Cham: Springer), 101–121.

McPartland, J. M. (2018). *Cannabis* systematics at the levels of family, genus, and species. *Cannabis Cannabinoid Res.* 3, 203–212. doi: 10.1089/can.2018.0039

Mestinšek Mubi, Š, Svetik, S., Flajšman, M., and Murovec, J. (2020). *In vitro* tissue culture and genetic analysis of two high-CBD medical cannabis (*Cannabis sativa* L.). *Genet. Belgrade* 42, 925–940. doi: 10.2298/GENSR2003925M

Mosaleeyanon, K., Zobayed, S. M. A., Afreen, F., and Kozai, T. (2005). Relationships between net photosynthetic rate and secondary metabolite contents in St. John's wort. *Plant Sci.* 169, 523–531.

Ögren, E., and Evans, J. R. (1993). Photosynthetic light-response curves I. The influence of CO_2 partial pressure and leaf inversion. *Planta* 189, 182–190. doi: 10.1007/BF00195075

Onofri, C., de Meijer, E. P. M., and Mandolino, G. (2015). Sequence heterogeneity of cannabidiolic- and tetrahydrocannabinolic acid-synthase in *Cannabis sativa* L. and its relationship with chemical phenotype. *Phytochemistry* 116, 57–68. doi: 10.1016/j.phytochem.2015.03.006

Pacifico, D., Miselli, F., Micheler, M., Carboni, A., Ranalli, P., and Mandolino, G. (2006). Genetics and marker-assisted selection of the chemotype in *Cannabis sativa* L. *Mol. Breed.* 17, 257–268. doi: 10.1007/s11032-005-5681-x

R Core Team (2018). *R: A Language and Environment for Statistical Computing*. Vienna: R Foundation for Statistical Computing.

Romero, P., Peris, A., Vergara, K., and Matus, J. T. (2020). Comprehending and improving cannabis specialized metabolism in the systems biology era. *Plant Sci.* 298:110571. doi: 10.1016/j.plantsci.2020.110571

Salami, S. A., Martinelli, F., Giovino, A., Bachari, A., Arad, N., and Mantri, N. (2020). It is our turn to get cannabis high: put cannabinoids in food and health baskets. *Molecules* 25:4036. doi: 10.3390/molecules25184036

Sharkey, T. D., Bernacchi, C. J., Farquhar, G. D., and Singsaas, E. L. (2007). Fitting photosynthetic carbon dioxide response curves for C_3 leaves. *Plant Cell Environ.* 30, 1035–1040. doi: 10.1111/j.1365-3040.2007.01710.x

Small, E., and Beckstead, H. D. (1973). Common cannabinoid phenotypes in 350 stocks of *Cannabis*. *Lloydia* 36, 144–165.

Staginnus, C., Zörntlein, S., and de Meijer, E. (2014). A PCR marker linked to a THCA synthase polymorphism is a reliable tool to discriminate potentially THC-rich plants of *Cannabis sativa* L. *J. Forensic Sci.* 59, 919–926. doi: 10.1111/1556-4029.12448

Tang, K., Struik, P. C., Amaducci, S., Stomph, J. T., and Yin, X. Y. (2017). Hemp (*Cannabis sativa* L.) leaf photosynthesis in relation to nitrogen content and temperature: implications for hemp as a bio-economically sustainable crop. *GCB Bioenergy* 9, 1573–1587. doi: 10.1111/gcbb.12451

Tanney, C. A. S., Backer, R., Geitmann, A., and Smith, D. L. (2021). *Cannabis* glandular trichomes: a cellular metabolite factory. *Front. Plant Sci.* 12:721986. doi: 10.3389/fpls.2021.721986

Toth, J. A., Stack, G. M., Cala, A. R., Carlson, C. H., Wilk, R. L., Crawford, J. L., et al. (2019). Development and validation of genetic markers for sex and cannabinoid chemotype in *Cannabis sativa* L. *GCB Bioenergy* 12, 213–222. doi: 10.1111/gcbb.12667

van Bakel, H., Stout, J. M., Cote, A. G., Tallon, C. M., Sharpe, A. G., Hughes, T. R., et al. (2011). The draft genome and transcriptome of *Cannabis sativa*. *Genome Biol.* 12:R102. doi: 10.1186/gb-2011-12-10-r102

Vergara, D., Huscher, E. L., Keepers, K. G., Givens, R. M., Cizek, C. G., Torres, A., et al. (2019). Gene copy number is associated with phytochemistry in *Cannabis sativa*. *AoB Plants* 11:plz074. doi: 10.1093/aobpla/plz074

Weiblen, G. D., Wenger, J. P., Craft, K. J., ElSohly, M. A., Mehmedic, Z., Treiber, E. L., et al. (2015). Gene duplication and divergence affecting drug content in *Cannabis sativa*. *New Phytol.* 208, 1241–1250. doi: 10.1111/nph.13562

Welling, M. T., Shapter, T., Rose, T. J., Liu, L., Stanger, R., and King, G. J. (2016). A belated green revolution for *Cannabis*: virtual genetic resources to fast-track cultivar development. *Front. Plant Sci.* 7:1113. doi: 10.3389/fpls.2016.01113

Zirpel, B., Degenhardt, F., Zammarelli, C., Wibberg, D., Kalinowski, J., Stehle, F., et al. (2018a). Optimization of Δ9-tetrahydrocannabinolic acid synthase production in *Komagataella phaffii via* post-translational bottleneck identification. *J. Biotechnol.* 272–273, 40–47. doi: 10.1016/j.jbiotec.2018.03.008

Zirpel, B., Kayser, O., and Stehle, F. (2018b). Elucidation of structure-function relationship of THCA and CBDA synthase from *Cannabis sativa* L. *J. Biotechnol.* 284, 17–26. doi: 10.1016/j.jbiotec.2018.07.031

Conflict of Interest: The authors declare that the research was conducted in the absence of any commercial or financial relationships that could be construed as a potential conflict of interest.

Publisher's Note: All claims expressed in this article are solely those of the authors and do not necessarily represent those of their affiliated organizations, or those of the publisher, the editors and the reviewers. Any product that may be evaluated in this article, or claim that may be made by its manufacturer, is not guaranteed or endorsed by the publisher.

frontiers | Frontiers in Plant Science

ORIGINAL RESEARCH
published: 29 September 2022
doi: 10.3389/fpls.2022.713481

Too Dense or Not Too Dense: Higher Planting Density Reduces Cannabinoid Uniformity but Increases Yield/Area in Drug-Type Medical Cannabis

*Nadav Danziger and Nirit Bernstein**

Institute of Soil Water and Environmental Sciences, Volcani Center, Rishon LeZion, Israel

A major challenge for utilizing cannabis for modern medicine is the spatial variability of cannabinoids in the plant, which entail differences in medical potency. Since secondary metabolism is affected by environmental conditions, a key trigger for the variability in secondary metabolites throughout the plant is variation in local micro-climates. We have, therefore, hypothesized that plant density, which is well-known to alter micro-climate in the canopy, affects spatial standardization, and concentrations of cannabinoids in cannabis plants. Canopy density is affected by shoot architecture and by plant spacing, and we have therefore evaluated the interplay between plant architecture and plant density on the standardization of the cannabinoid profile in the plant. Four plant architecture modulation treatments were employed on a drug-type medicinal cannabis cultivar, under a density of 1 or 2 plants/m^2. The plants were cultivated in a naturally lit greenhouse with photoperiodic light supplementation. Analysis of cannabinoid concentrations at five locations throughout the plant was used to evaluate treatment effects on chemical uniformity. The results revealed an effect of plant density on cannabinoid standardization, as well as an interaction between plant density and plant architecture on the standardization of cannabinoids, thus supporting the hypothesis. Increasing planting density from 1 to 2 plants/m^2 reduced inflorescence yield/plant, but increased yield quantity per area by 28–44% in most plant architecture treatments. The chemical response to plant density and architecture modulation was cannabinoid-specific. Concentrations of cannabinoids in axillary inflorescences from the bottom of the plants were up to 90% lower than in the apical inflorescence at the top of the plant, considerably reducing plant uniformity. Concentrations of all detected cannabinoids in these inflorescences were lower at the higher density plants; however, cannabinoid yield per cultivation area was not affected by neither architecture nor density treatments. Cannabigerolic acid (CBGA) was the cannabinoid least affected by spatial location in the plant. The morpho-physiological response of the plants to high density involved enhanced leaf drying at the bottom of the plants, increased plant elongation, and reduced cannabinoid concentrations, suggesting an involvement of chronic light deprivation at the bottom of the plants. Therefore, most importantly, under high density growth, architectural

OPEN ACCESS

Edited by:
Donald Lawrence Smith, McGill University, Canada

Reviewed by:
Youbin Zheng, University of Guelph, Canada
Pavel Tlustos, Czech University of Life Sciences Prague, Czechia

***Correspondence:**
Nirit Bernstein
Nirit@agri.gov.il

Specialty section:
This article was submitted to Crop and Product Physiology, a section of the journal Frontiers in Plant Science

Received: *23 May 2021*
Accepted: *15 June 2022*
Published: *29 September 2022*

Citation:
Danziger N and Bernstein N (2022) Too Dense or Not Too Dense: Higher Planting Density Reduces Cannabinoid Uniformity but Increases Yield/Area in Drug-Type Medical Cannabis. Front. Plant Sci. 13:713481. doi: 10.3389/fpls.2022.713481

modulating treatments that facilitate increased light penetration to the bottom of the plant such as "Defoliation", or that eliminated inflorescences development at the bottom of the plant such as removal of branches from the lower parts of the plant, increased chemical standardization. This study revealed the importance of plant density and architecture for chemical quality and standardization in drug-type medical cannabis.

Keywords: architecture, cannabis, cannabinoids, density, stand, pruning, yield, light

INTRODUCTION

Drug-type cannabis (*Cannabis sativa L.*) is utilized by mankind for thousands of years for religious rituals and for its' medicinal and inebriant properties (Andre et al., 2016). At the last decade, the use of cannabis sharply increased due to awareness of the plants medicinal potential and benefits for life quality, facilitated by changes in its legal status. The emerging global-markets stimulate large-scale production of cannabis, which created a need for modern agri-practices. A major challenge for quality and safe production for the pharmaceutical and recreational markets is the lack of science-based knowledge on cannabis plant biology and agronomy (Bernstein et al., 2019a).

The medical effects of cannabis are based on biologically active secondary metabolites, including terpenes, flavonoids, and cannabinoids. More than 100 cannabinoids have been identified in cannabis (Berman et al., 2018); the most abundant are the pentyl type Δ^9-tetrahydrocannabinolic acid (THCA), cannabidiolic acid (CBDA), cannabichromenic acid (CBCA), and cannabigerolic acid (CBGA). The precursors for the cannabinoid biosynthesis are derived from the deoxyxylulose phosphate/methyl-erythritol phosphate (DOXP/MEP) pathway and the polyketide pathway (Flores-Sanches and Verpoorte, 2008). CBGA is the direct precursor for THCA, CBDA, and CBCA, and it originates from prenylation of geranyl diphosphate to olivetolic acid (Gülck and Møller, 2020). Δ^9-tetrahydrocannabivarinic acid (THCVA) and cannabidivarinic acid (CBDVA), propyl analogs of THCA and CBDA, are minor cannabinoids originating from geranyl diphosphate and divarinic acid (Sarma et al., 2020). The biological activity is attributed to the decarboxylated forms of the cannabinoids and is affected by concentrations and interactions between cannabinoids as well as with other secondary metabolites in the plant.

Plant development and function are considerably affected by environmental conditions. Optimization of production quantity and quality, therefore, requires understanding of plant responses to environmental factors that determine the plant's phenotypic expression. Drug-type cannabis is often cultivated in greenhouses or growing rooms under environment-controlled conditions, which are needed to satisfy quality demands for the new standards defined for the highly regulated medical market (Potter, 2014). To improve growers' success and patient welfare, growing protocols that enhance yield quantity, chemical quality, and reproducibility are being developed (Bernstein et al., 2019b; Saloner et al., 2019; Eaves et al., 2020; Saloner and Bernstein, 2020, 2021, 2022a,b; Shiponi and Bernstein, 2021a,b) based on recently accumulated information on the plant responses. Recent findings demonstrate that numerous factors, including light intensity (Eaves et al., 2020; Rodriguez-Morrison et al., 2021), light quality (Magagnini et al., 2018; Danziger and Bernstein, 2021a), salt concentration (Yep et al., 2020), mineral nutrition (Saloner and Bernstein, 2021, 2022a,b; Shiponi and Bernstein, 2021b), pests and pathogens (Punja et al., 2019), affect phenotypic expression of cannabinoids in cannabis.

Plant density, or stand (Semira and Bikila, 2018), is among the main factors affecting plant development and function. It is defined as the number of plants cultivated per unit area, but could also be described by the distance, i.e., spacing between plants. Planting density affects micro-climate aspects in the plant shoot, including light availability/shading, humidity, and temperature (Yang et al., 2014). Higher plant density is therefore used to increase crop yield by increasing leaf coverage and as a result light interception (Chapepa et al., 2020). An ideal density maximizes light interception by the foliage, optimizing resource usage and growth, and too dense planting results in resource competition for light (Singh et al., 1992; Jarecki and Bobrecka-Jamro, 2011) that can compromise plant function and production.

Increased plant density was indeed documented to increase yield in a range of crops, including cotton (*Gossipium hirsutum*) (Mao et al., 2014), vine-spinach (*Basella Alba* L) (Masombo et al., 2018), and watermelon (*Citrullus lanatus*) (Akintoye et al., 2009), and the response can be cultivar-dependent (Akintoye et al., 2009). Above optimal density was reported to reduce production of individual plants as reviewed by Postma et al. (2020). One study (Campiglia et al., 2017) evaluated effects of plant density on *cannabis sativa*. It targeted industrial hemp cultivars grown for seed and stem fiber production, and reported reduced stem biomass and increased seed yield per area under increased plant density. Since industrial hemp is cultivated under different agro-techniques and density than drug-type cannabis and it targets different plant organs as yield, this information cannot directly contribute to the understanding of the drug-type crop response. Understanding responses of drug-type cannabis to plant density are needed to direct optimization of the crop morpho-development.

Plant density is known to affect the physiological and molecular state of plant tissues and therefore also primary and secondary metabolisms, and the nutritional value of crops. Various trends were noted for effects of plant density on metabolism, and increased density was reported to increase, decrease, or to have no effect on production of various metabolites. For example, carotenoid concentration of paprika (*Capsicum annuum*) (Cavero et al., 2001) and tarragon (*Artemisia dracunculus*) (Nurzyńska-Wierdak and Zawiślak,

2014) decreased with the increase in plant density; essential oil production in tarragon increased with the increase in plant density (Nurzyńska-Wierdak and Zawiślak, 2014); and in hydroponic-cultivated tomatoes (*Solanum lycopersicum*) plant spacing did not affect carotenoids, lycopene, and citric acid production (Cardoso et al., 2018). We know of no other study that evaluated effects of plant density on secondary metabolism in drug-type - medical cannabis.

Tight interrelations exist between plant spacing and shoot architecture. Architecture development of plants can be considerably affected by exogenous factors, especially microclimate parameters in the shoot. The reduced area available for the shoot under high plant density induces morphological adaptations such as elongation or retarded growth (Xiao et al., 2006). In agricultural practices, to optimize growth under higher densities, plant architecture is often altered, aiming at achieving an optimal ratio of shoot-size/yield, and reduced shading, to facilitate sufficient light penetration to the canopy (Kool, 1997; Maboko et al., 2011; Oga and Umekwe, 2016; Cardoso et al., 2018; Ayala-tafoya and Yáñez-juárez, 2019). Ideal plant density is, therefore, closely related to shoot architecture.

In the present study, we therefore focused on the interplay between plant density, plant architecture and yield quantity, and chemical standardization in medical (drug-type) cannabis. The hypotheses leading the workplan were: (i) High plant density affects chemical quality and compromises chemical uniformity in the plant, but increases inflorescence biomass per m^2. (ii) Manipulation of the plant canopy architecture (by removal of leaves or branches, thus decreasing canopy density; or by pruning for removal of apical dominance, thus increasing branching and canopy density) affects plant responses to plant density. To test these hypotheses, we analyzed morphological, physiological, and chemical profiling of medical (drug-type) cannabis plants under two plant densities of 1 or 2 plants/m^2 and four plant architecture manipulation treatments. The architectural treatments included defoliation, pruning and the removal of the bottom leaves, branchlets, and inflorescences, compared to a non-treated control. The study was aimed at achieving understanding required for directing horticultural practices to increase chemical quality and standardization.

MATERIALS AND METHODS

Plant Material and Growing Conditions

A type III cultivar, i.e., containing high CDB (8–16%) and low THC (<1%) levels medical (drug-type) cannabis (*Cannabis sativa* L.) cultivar ("Topaz", BOL Pharma, Israel), was used as a model plant in this study. The plants were propagated from cuttings, in coconut fiber plugs (Jiffy international AS, Kristiansand, Norway). The rooted cuttings were planted in 13 L pots in a peat-moss potting mixture (Kekkila-BVB, the Netherlands) and cultivated under 2 plants/m^2. Uniform plants were randomly divided into groups of 12 plants, and each group was randomly assigned a treatment (detailed in section experimental treatments). The experiment consisted of six replicated groups per treatment. Plants of each replicated group were grown together as a single plot. The replicated plots were randomly arranged in a commercial cannabis cultivation farm in Israel (BOL Pharma, Israel), in a naturally lit greenhouse with photoperiodic light supplementation. During the vegetative stage under long photoperiod cultivation, illumination was supplied by fluorescent lamps 24 h a day. The density treatments were initiated 27 days after the rooted cuttings were transplanted to the experimental plants (during the vegetative stage). At that time, the plants were 90–100 cm in height, except the plants from the pruning treatment that due to the nature of the treatment, and were 55–65 cm shorter in height. After a total of 62 days of vegetative growth (i.e., 62 days post-transplanting), the plants were transferred to a flowering-induced short-day photoperiod of 12:12 h of light: darkness. Fertilizers were supplied by fertigation at each irrigation event, i.e., dissolved in the irrigation solution. The fertigation solution contained in ppm: N (200), P (25), K (180), Ca (30), Mg (30), S (25), Fe (0.842), Mn (0.421), Zn (0.211), Cu (0.031), Mo (0.225), and B (0.202). pH was adjusted to 6.0 with H_2SO_4 and the amount of S added is included in the reported concentration of S in the fertigation solution. Irrigation was supplied with 1.2 L h^{-1} discharge-regulated drippers (Plastro Gvat, Israel), four drippers per pot. The volume of irrigation water in each irrigation event was 500–800 mL pot^{-1} day^{-1}, adjusted to generate ∼30% of drainage. The experiment was terminated at chemical maturity of the plants, 69 days after the transfer to the short photoperiod (131 days after the rooted cuttings were transplanted to the experimental pots), following the agronomic practice for this cultivar.

Experimental Treatments

The plants were exposed to two plant densities, and four plant architecture modulation treatments, for a total of eight treatments, in a completely randomized experimental design. The four architectural treatments studied included (i) A non-treated control [Control]; (ii) Removal of all fan leaves on the plants except very small leaves at the top of branches 3 weeks prior to harvest (69 days after the transfer to the short photoperiod), [Defoliation]; (iii) At the beginning of the vegetative growth phase (at the time of transplanting), the top of the rooted cuttings was pruned, leaving the six bottom branches [Pruning]; (iv) Removal of the branches and leaves from the lower one-third part of the plants at the transition to the short photoperiod, 62 days post-transplanting (we named this treatment "Bottom branches and leaves removal") [BBLR]; this treatment is also known as "Lollipoping" in the cannabis industry jargon. Plants of each architecture treatment were evaluated under two plant densities of either 1 or 2 plants/m^2. The plants in each replicated plot were arranged in four rows with three plants per row, and a central plant from a central rows was used for the measurements. The remaining plants in the plot received the same treatment and served as margins.

Plant Growth and Development

Plant height was measured non-destructively biweekly as the difference from the plant base to the top of the apical meristem on the main stem, or on the tallest branch in the pruning treatments. Stem diameter was measured with a digital caliper (Signet tools international co., LTD., Shengang District, Taiwan),

at the middle of the first internode from the plant base. Fresh biomass of inflorescences, stems, and fan leaves was measured for each plant by destructive sampling at the termination of the experiment. Inflorescences were trimmed by an industrial trimmer T2 twister (Keirton inc. Ferndale, WA, USA) and the trimmed inflorescences were weighted again for the calculation of the trimmed inflorescence leaves biomass. Dry inflorescences yield was determined following drying in the dark for 20 days at 45% air humidity and 19°C, to ∼10% humidity.

Physiological Responses

The measurements were conducted 1 week after the initiation of the leaf removal treatment (2 weeks prior to harvest), i.e., 69 days after the transfer to the short photoperiod. Following the experimental design, all measurements were conducted with six biological repeats (i.e., for six plants).

Pigment Concentrations, Gas Exchange Parameters, Water Use Efficiency, and PAR

Concentrations of the photosynthetic pigments chlorophyll *a*, chlorophyll *b*, and carotenoids were measured as previously described (Ignat et al., 2013; Saloner et al., 2019). In short, five discs with diameter of 0.6 cm were severed from the youngest mature leaf on the main stem (or alternatively from the highest primary branch in the pruning treatments) after it was washed twice in distilled water and blotted dry. Pigment extraction was conducted as described by Gorelick et al. (2015), and pigment concentrations were calculated according to Lichtenthaler and Wellburn (1983).

Stomatal conductance, photosynthesis and transpiration rates, and intercellular CO_2 concentration were measured with LI-COR 6400XT (LI-COR, Lincoln, NE, USA). The measurements were performed on the youngest mature leaf on the main stem (or alternatively on the highest primary branch in the pruning treatments), at 8–10 am [CO_2 concentration: 400 mgL^{-1} and PPFD: 500 $\mu mol\ (m^2s)^{-1}$]. Leaves temperature was kept at 25°C and relative humidity at 60%. Water use efficiency (WUE) was calculated from Equation 1.

$$Water\ use\ efficieancy\ (\%) = \frac{Photosynthesys\ rate}{Transpiration\ rate} * 100 \qquad (1)$$

Photosynthetic active radiation (PAR) was measured at four heights along the plant (0, 0.5, 1.2, and 2 m from the plant base) using an Apogee quantum sensor MQ-500 (Apogee Instruments, Logan, UT, USA).

Membrane Leakage and Osmotic Potential

The youngest mature leaf on the main stem (or on the tallest branch in the pruning treatments) was washed twice in distilled water and blotted dry. For membrane leakage analysis, the middle leaflet was then separated and submerged in 30 mL of double distilled water. After 24 h of shaking in a horizontal shaker, electric conductivity (EC) of the sample was measured using an EC-meter (Cyberscan CON 1500, Eutech Instruments Europe B.V., Nijkerk, The Netherlands). Following autoclaving (30 min at 121°C) (Shoresh et al., 2011) and 30 min of cooling at room temperature, EC was measured again. Membrane leakage was calculated as the percentage of the first EC measurement value from the value of the second measurement (Kravchik and Bernstein, 2013).

For osmotic potential measurements, ∼150 mg of leaf tissue was inserted into a 1.7-mL Eppendorf tube and immediately frozen in liquid N and kept in −20°C until further analysis. For expression of the cell-sap from the tissue, the sample was partially thawed and macerated inside the tube with a pestle and centrifuged (Sigma Laboratory Centrifuges, Germany) at 4°C and 6,000 rpm for 5 min. A 50 μL aliquot of the supernatant was measured in a cryo-osmometer (Gonotec, Berlin, Germany) to determine the osmotic potential of the leaf tissue sap.

Cannabinoid Analyses

For evaluation of the effect of the treatments on the cannabinoid profile and its' standardization in the plant, inflorescences were sampled for cannabinoid analyses from five locals along the plants, illustrated in **Supplementary Figure 1**: (1) The top most inflorescence; (2) The apical inflorescence of a high branch (the 4th highest branch); (3) The apical inflorescence of a low branch (4th from plant base); (4) An inflorescence located close to the stem (an axillary inflorescence) at the top area of the plant (2nd branch from the top); (5) The bottom most inflorescence located closest to the stem (an axillary inflorescent, from the 1st branch from the plant base). Trimmed inflorescences were dried in the dark for 20 days at 45% air humidity and 19°C to 10% humidity in an environment-controlled chamber. Cannabinoid analysis was conducted for six replicated plants per treatment.

The dried inflorescences were ground using a manual herb grinder. Fifty mg of the ground tissue was placed with 10 mL of ethanol in a 20-mL glass vial and was shaken in a reciprocal shaker for 1 h at room temperature. The extract was filtered through PVDF (a polyvinylidene difluoride membrane filter) of 0.22-μm pore size (Bar-Naor ltd, Ramat Gan, Israel). Concentrations of cannabinoids in the filtered extracts were analyzed with a Jasco 2000 Plus series HPLC system that consist of an autosampler, column compartment, quaternary pump, and a PDA detector (Jasco, Tokyo, Japan). Chromatographic separation was performed with a Luna Omega 3 μm Polar C18 column (Phenomenex, Torrance, CA USA) with acetonitrile: water 75:25 (v/v) with 0.1% (v/v) formic acid, at the isocratic mode. The flow rate was 1.0 mL min^{-1}. Calculation of cannabinoid concentrations was based on pure analytical standards that were purchased from Sigma-Aldrich (Germany): cannabichromene (CBC), cannabichromenic acid (CBCA), cannabichromevarin (CBCV), cannabigerol (CBG), cannabigerolic acid (CBGA), cannabinol (CBN), cannabinolic acid (CBNA), cannabidiol (CBD), cannabidiolic acid (CBDA), cannabicyclol (CBL), cannabidivarin (CBDV), cannabidivarinic acid (CBDVA), Δ^9-tetrahydrocannabivarinic acid (THCVA); from Cayman chemical company (Pennsylvania, USA) cannabicitran (CBT); and from Restek (Pennsylvania, USA) Δ^9-tetrahydrocannabinolic acid (THCA), Δ^9-tetrahydrocannabinol (THC), Δ^8-tetrahydrocannabinol (Δ^8-THC), Δ^9-tetrahydrocannabivarin

(THCV). R^2 values for linear regressions of the calibrations curves of all cannabinoid standards were >0.994 (Saloner and Bernstein, 2021); Concentrations of CBD were small (<0.21%) and are, therefore, presented together with the CBDA concentrations. Concentrations of CBC, CBG, CBN, CBNA, CBL, CBDV, CBT, THC, Δ^8-THC, and THCV were lower than the detection limits. Cannabinoid yield per cultivation area (mg/m^2) was calculated from the plant average concentration of the cannabinoids.

Evaluation of Spatial Uniformity of the Cannabinoid Profile in the Plant

Two scores were developed to evaluate the uniformity of cannabinoid concentrations within a plant: "Cannabinoid Variation Score" (CVS) evaluates the variability of an individual cannabinoid in the plant, and "Plant Variation Score" (PVS) evaluates an integration of variability of all identified cannabinoids in the plant. These scores were developed from two indexes ("Cannabis uniformity" and "plant uniformity score") that were suggested and applied by Danziger and Bernstein (2021b) for the evaluation of treatments' effects on uniformity of compounds in plants. The evaluation is based on the enumeration of the percentage of inflorescences in a treatment having a concentration of a secondary metabolite that varies by more than a defined percentage from the plant average concentration. In the present study, we used variation of 15% for the calculations of CVS. For the calculations, first, the average concentration of each identified cannabinoid (CAC) is calculated as of Equation 2 (30 samples were used for the calculations). Second, the concentration of the cannabinoid in each sample was compared to the generated average, and the number of samples that varied by more than 15% from the average were counted (denotes by the numerator in Equation 3). This number was divided by the number of samples which contained the specific cannabinoid (as not all samples had detectable concentrations of all cannabinoids) and multiplied by 100 to receive the CVS value (Equation 3). The CSV value, therefore, has units of %; it is the percentage of samples with a concentration of a specific cannabinoid varying by up to 15% from the average. It, therefore, represents variability for a specific cannabinoid (or any other evaluated plant compound). In order to receive an integrated value for uniformity of all the identified cannabinoids, the calculated CVS values for all individual cannabinoids were averaged to receive the PVS (Equation 4). The

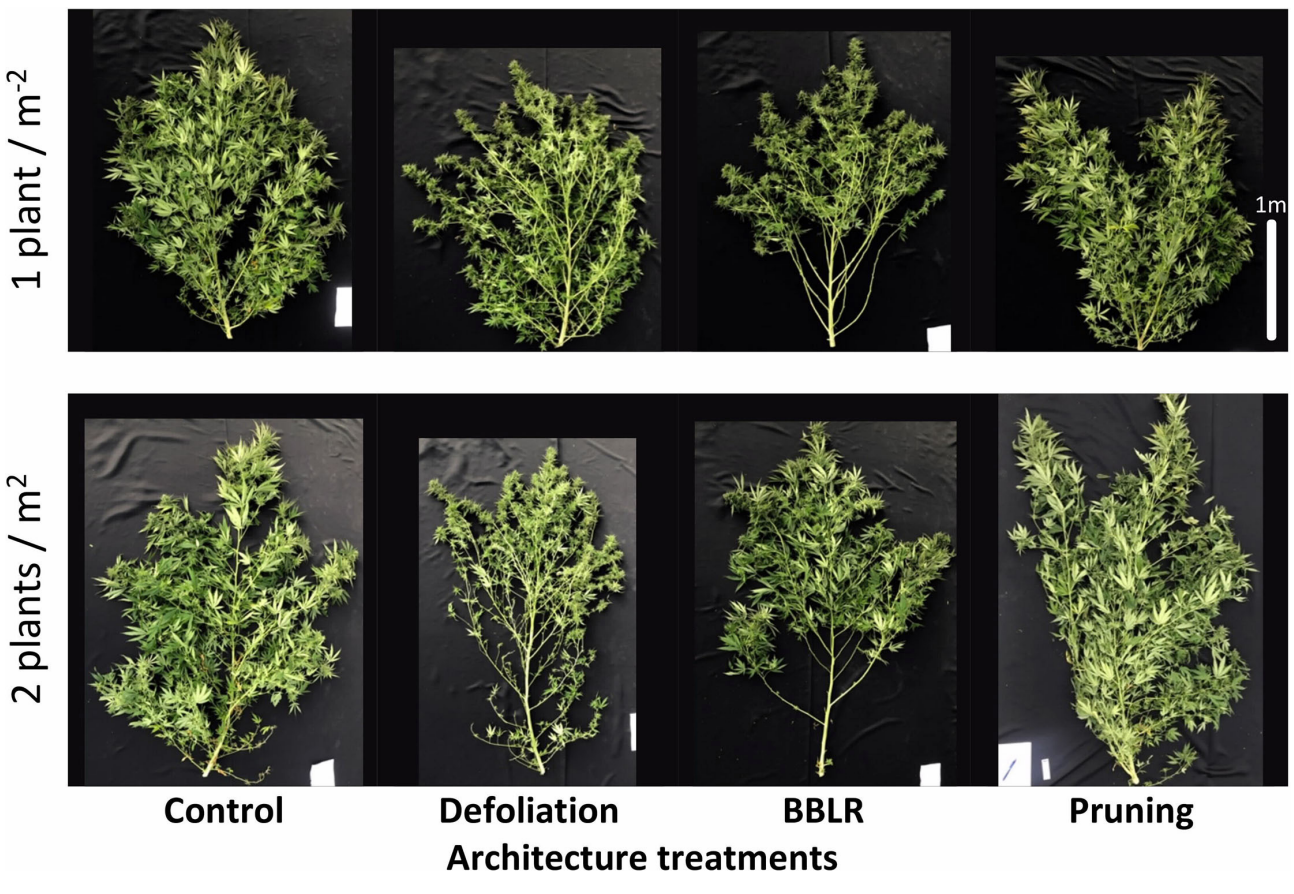

FIGURE 1 | Effect of planting density (1 or 2 plants m^{-2}) on visual appearance of medical cannabis plants, subjected to four plant architecture modulation treatments. Control, Defoliation, removal of leaves and branches from the bottom part of the plant [BBLR] at the transition to the flowering stage, and pruning at the beginning of the vegetative growth stage. The images were taken 69 days following the transition to the short photoperiod, at the time of harvest.

higher the PVS score, the more variable is the treatment. These variation scores can be applied for the evaluation of uniformity in the plant concentrations of secondary metabolites, as well as other chemical compounds.

$$Cannabinoid\ average\ concentration\ (CAC) = \frac{\sum cannabinoid\ concentration\ in\ the\ individual\ samples}{No.\ of\ samples\ that\ contained\ the\ cannabinoid} * 100 \quad (2)$$

$$Cannabinoid\ Variation\ Score\ (CVS)\ [\%] = \frac{\left|(No.\ of\ samples\ with\ conc. < CAC * 0.85) \cup (No.\ of\ samples\ with\ conc. > CAC * 1.15)\right|}{No.\ of\ samples\ that\ contained\ the\ identified\ cannabinoid} * 100 \quad (3)$$

$$Plant\ Variation\ Score\ (PVS)[\%] = \frac{\sum CVS\ for\ each\ of\ the\ identified\ cannabinoids}{The\ number\ of\ identified\ cannabinoids} \quad (4)$$

Statistical Analysis

The data were subjected to a one-way and two-way analysis of variance (ANOVA) ($\alpha < 0.05$) followed by Tukey's HSD *post-hoc* test. The data met the assumption of homogeneity of variances. Comparison of relevant means was performed using Fisher's LSD test at 5% level of significance. The analysis was performed with the Jump software (version 9, SAS 2015, Cary, NC, USA).

RESULTS

Plant Development

Plant density as well as the architectural manipulation treatments affected plant development and the visual appearance of the plants (**Figure 1**). Plants from the higher density treatments were taller and slightly narrower in appearance compared to the plants from the lower density treatments. The "BBLR" plants had no leaves or inflorescences at the bottom part of the plant since these were removed as part of the treatment, and the "Pruning" treatment caused the plant to develop two main stalks rather than the natural one main stem form. Additionally, in the "Control" and the "Defoliation" treatments, lower leaves and branches in the higher density treatment (2 plants/m^2) were senescing. The taller stature of the higher density plants is also seen in **Figure 2A** that shows the plants of all high-density treatments were significantly higher compared with their low-density counterparts.

Fresh weight of the plant was significantly reduced by the increase in plant density across all the architecture treatments, with a 22–37 and 28–36% decrease in total plant fresh weight, and inflorescence yield, respectively (**Figure 2B**). The least-affected organ was the stem, with a 5–32% less fresh weight compared with the lower density treatments, whereas both fan leaves and inflorescence leaves were highly susceptible to planting density, demonstrating 48–74% fresh weight compared with the low-density treatments. In the "Defoliation" treatments as well, that involve an inherent reduction of leaf tissue biomass, a significant reduction in leaf tissue biomass was induced by the increase in cultivation density.

The diameter of the stem (**Figure 2C**) was not affected significantly by plant density; and neither did the number of branches that were developed on the plants (**Figure 2D**). The number of branches on the main stem was significantly lower for the "pruning" treatments compared with all other treatments (**Figure 2D**), representing the six bottom branches that were kept on the plants during decapitation. Following the decapitation, the plant body developed mainly from two main stalks (i.e., secondary branches) (**Figure 1**).

Inflorescence yield production per cultivation area (gDW/m^2) was higher (by 28–78%) in the higher density treatment than in the lower density treatments in the control, "BBLR" and "defoliation" treatments, but was not significantly affected by plant density in the "Pruning" treatment (**Table 1**).

Chemical Profile

Cannabinoid concentrations were determined in five defined locals in the plants, including (1) The top most inflorescence; (2) The apical inflorescence of a high branch (the 4th highest branch); (3) Apical inflorescence of a low branch (4th from plant base); (4) An axillary inflorescence located close to the stem at the top area of the plant (2nd branch from the top); (5) The bottom most inflorescence located closest to the stem (an axillary inflorescence from the lowest branch closest to the stem (**Supplementary Figure 1**).

Cannabinoid concentrations in the highest inflorescence on the plant (location 1), which is the representative inflorescence commonly sampled for cannabinoid analysis, are presented in **Figure 3**. The concentrations in this location were overall not affected by the treatments, with only small changes ($p < 0.05$) induced by some treatments. Specifically, CBDA (**Figure 3B**) levels were higher in the closely spaced plants of the "BBLR" and "Defoliation" treatments compared with the less dense treatments; and under the high density, CBDA concentrations in these treatments were also higher than in the "Control" and "Pruning" treatments. At the lower density, THCA (**Figure 3A**) and CBCA (**Figure 3D**) levels were higher in the "Defoliation" treatment compared with all other treatments, and CBCA of the defoliation low-density treatment was higher than all other architecture treatments also under the higher density. The concentration of CBGA (**Figure 3C**), the precursor of all the above-mentioned cannabinoids, was similar across all treatments

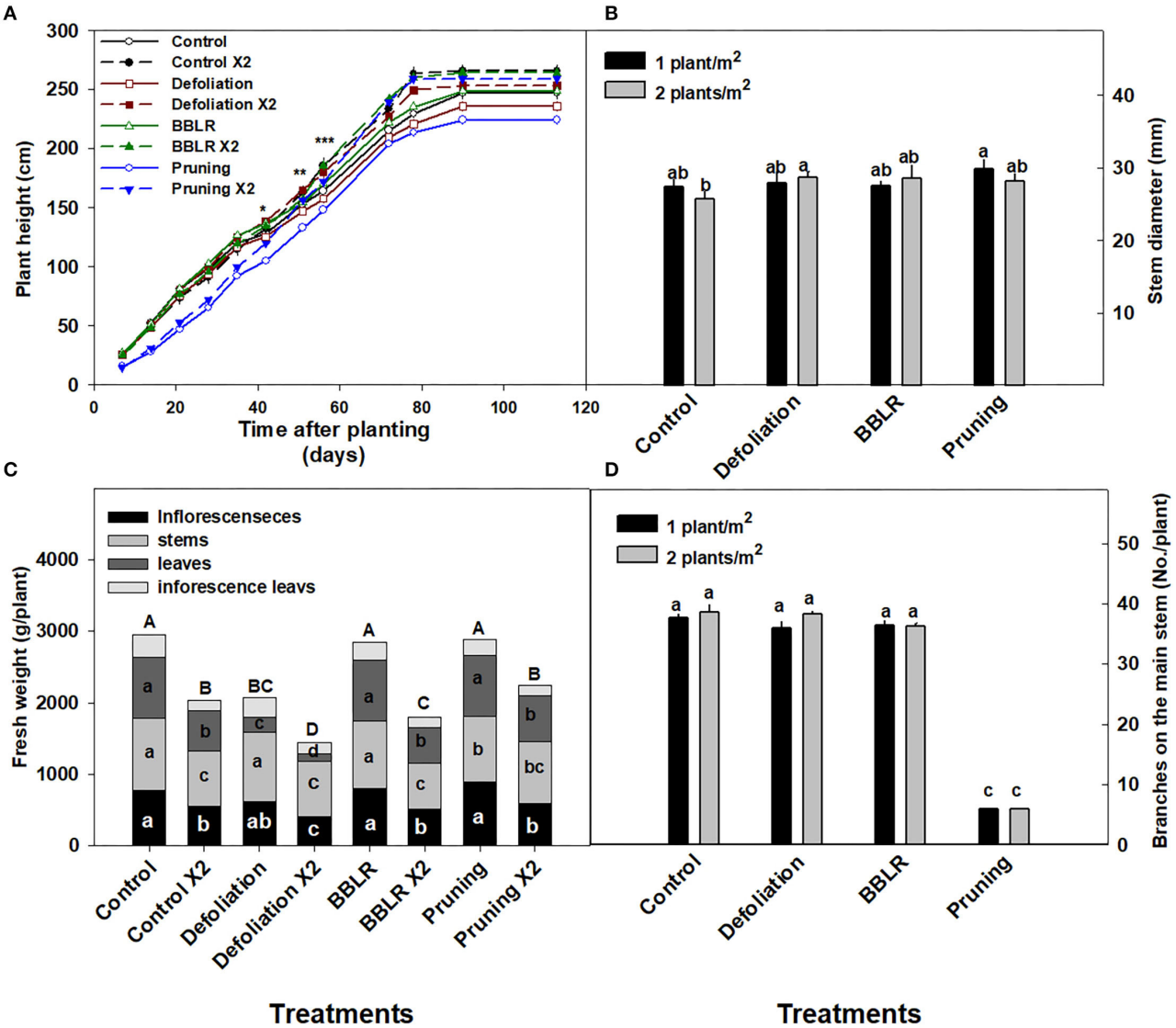

FIGURE 2 | Effects of plant density and architecture modulation treatments on plant morphology. Plant height **(A)**, biomass of plant organs and of the whole plant (bars) **(B)**, Stem diameter **(C)**, and number of branches **(D)** at harvest. The results are mean ($n = 6$) and SE (in **C,D**). Different letters above the bars represent significant differences between treatments by Tukey HSD test at $\alpha = 0.05$. In **(A)**, asterisks represent the day significant differences were first identified between density treatments within an architecture treatment (*-"Pruning", **-"Control," and "Defoliation," ***-"BBLR"). In **(B)**, different letters within the bars across a plant organ, represent significant differences between treatments. x 2 represents the density of 2 plants/m^2.

except for the "Pruning" higher density treatment that had a lower concentration. For both THCVA and CBDVA, no significant changes between the density treatments were seen except for the "BBLR" treatment that had higher levels in the high-density plants (**Figures 4E,F**).

Unlike the inflorescences from the top of the plant from location 1, cannabinoid concentrations in axillary inflorescences from low branches of location 5 (**Figure 4**) were considerably affected by plant density. Several trends were observed: (i) Most important is the overall decrease in cannabinoid concentrations, up to 90% reduction compared with the top inflorescence. (ii) In all treatments, except "BBLR," concentrations of all detected cannabinoids were considerably lower in the higher density treatment. The treatment that was affected the most by plant density is the "Control," with a decline of 71–76% in the concentrations of all six detected cannabinoids with the increase in plant density. (iii) In the "BBLR" treatment, cannabinoid concentrations were 25–90% higher in the high-density plants. (iv) In this location (location 5), concentrations of all identified cannabinoids, except for CBGA, were lower in the "Control" treatment than in both the "Pruning" and "Defoliation" treatments when comparing similar

TABLE 1 | Effect of plant density on inflorescence yield per cultivation area (g DW/m^2)[B].

Treatment	1 plant/m^2	2 plants/m^2
Control	222 ± 14.9^b	321 ± 19.3^a
Defoliation	180 ± 17.3^b	320 ± 29.3^a
BBLR[A]	229 ± 12.5^b	295 ± 27.3^a
Pruning	255 ± 10.6^a	232 ± 12.9^a

[A]*Removal of branches and leaves from the bottom of the plant.*
[B]*Different lowercase letters by the averages within a row signifies significant differences between the two density treatments according to Tukey HSD test, at* $\alpha = 0.05$ *(*$n = 6$*).*

densities. Cannabinoid yield per cultivation area (mg/m^2) were not affected by neither architecture nor density treatments (**Table 2**).

To visualize chemical uniformity across the plant, the concentrations of each cannabinoid at the five evaluated locations throughout the plant were divided by the concentrations in location 1 of the "Control" treatment (the highest inflorescence on the plant) under the 1 plant/m^2 density. These ratios were plotted to a radar chart (**Figure 5**). This normalization facilitates comparison of trends between locations, and across treatments that are presented in the sub-charts of **Figure 5**. The results reveal three major trends: (i) Axillary inflorescences from the bottom of the plants (location 5) accumulated significantly lower concentrations of cannabinoids across all treatments. (ii) For three treatments "Control" (**Figure 5B**), "Defoliation" (**Figure 5D**), and "Pruning" (**Figure 5H**), the double density hampered cannabinoid synthesis at location 4 (an inner axillary inflorescence at the top part of the plant). (iii) Treatments effects on specific cannabinoids. The outer perimeter shape of each radar chart represents the chemical profile, and a "misshaped" hexagon, therefore, indicates a change in ratios between all cannabinoids. For example, in all treatments (**Figures 5A–H**), the CBGA corner of location 5 is closer to the outer perimeter than the corners of all other cannabinoids showing that CBGA is the cannabinoid least affected by the spatial location.

To further evaluate how spatial uniformity of cannabinoid concentration in the plants was affected by the treatments, an index previously developed by Danziger and Bernstein (2021b) was used to rate plant uniformity by comparing each inflorescence to the plant average, allowing various rates of deviation from it (**Table 3**). Both the "*Plant Variation Score*" and the "*Cannabinoid Variation Score*" were higher in the densely grown plants for all cannabinoids and under all levels of acceptance (with the exception of CBGA of BBLR), indicating that higher density impairs cannabinoid uniformity under these growing conditions. For the higher plant density, at all acceptance rates (excluding 5%), the plant variation score of "BBLR" was lowest demonstrating the best chemical uniformity, and "Control" was ranked to have the lowest chemical uniformity.

Physiological Response

Plant gas-exchange parameters of the youngest mature leaf on the main stem (or alternatively on the highest primary branch in the pruning treatments) were significantly affected by both the architecture modulation treatments and plant density (**Figure 6**). Increased density stimulated photosynthesis and stomatal conductance in both "Control" and "Defoliation" plants (**Figures 6A,C**), but reduced photosynthesis and stomatal conductance in "BBLR" plants and photosynthesis in pruned plants. Transpiration rate (**Figure 6B**) was unaffected by plant density except for an inhibition in the double density "BBLR" treatment, which showed 55% decline compared with the less dense treatment. The reduced transpiration in this treatment, which implies reduced stomatal opening, reduced also tissue aeration and concentration of CO_2 in the leaf mesophyll (**Figure 6D**).

The plants water management strategy was measured using two indicators (**Figure 7**): Water Use Efficiency (WUE) and osmotic potential; and membrane leakage was measured as an indicator of plant stress representing cell membrane damage. Under all architecture altering treatments, membrane leakage was higher under higher density (**Figure 7A**), and under the lower density all plant architecture treatments showed a lower stress response than the "Control." The plants WUE (**Figure 7B**) was calculated using the CO_2 assimilation rate, and it presents three different responses according to the plant architecture treatments: higher density increased WUE in the "BBLR" treatments, reduced WUE in the "Pruning" treatment but had no effect in both the "Control" and "Defoliation" treatments. The osmotic potential (**Figure 7C**) was affected by both plant density and plant architecture modulation treatments. In the "Defoliation," "BBLR," and "Pruning" plants, the osmotic potential was lower under higher density, whereas no difference was seen in the "Control." In addition, "Defoliation" reduced the osmotic potential compared to the "Control."

Overall, the effects of the treatments on accumulation of photosynthetic pigments were small, with some statistically significant trends (**Figures 7D–F**). Pigment accumulation had a varied response to plant density (**Figures 7D–F**). For both "Control" and "Defoliation," no difference between densities was apparent in neither chlorophyll *a*, chlorophyll *b* nor carotenoids. However, "BBLR" and "Pruning" plants usually had higher pigment concentrations in the low-density plants (**Figures 7D,F**). Plant architecture and planting density affected light penetration to the plant (**Supplementary Figure 3**), and under all plant architecture treatments, increasing density reduced light penetrance. Light intensity along the plants in both defoliation-density treatments was higher for all other treatments (**Supplementary Figure 3**).

DISCUSSION

Cultivation and environmental conditions considerably affect secondary metabolism in plants, which is of importance for the medical and recreational product of drug-type cannabis (Gorelick and Bernstein, 2017). In the fast-growing world of cannabis pharmaceuticals, agronomic knowhow for production of high-quality, safe, and chemically standardized plant material needs to rapidly develop. To keep up with demand, various

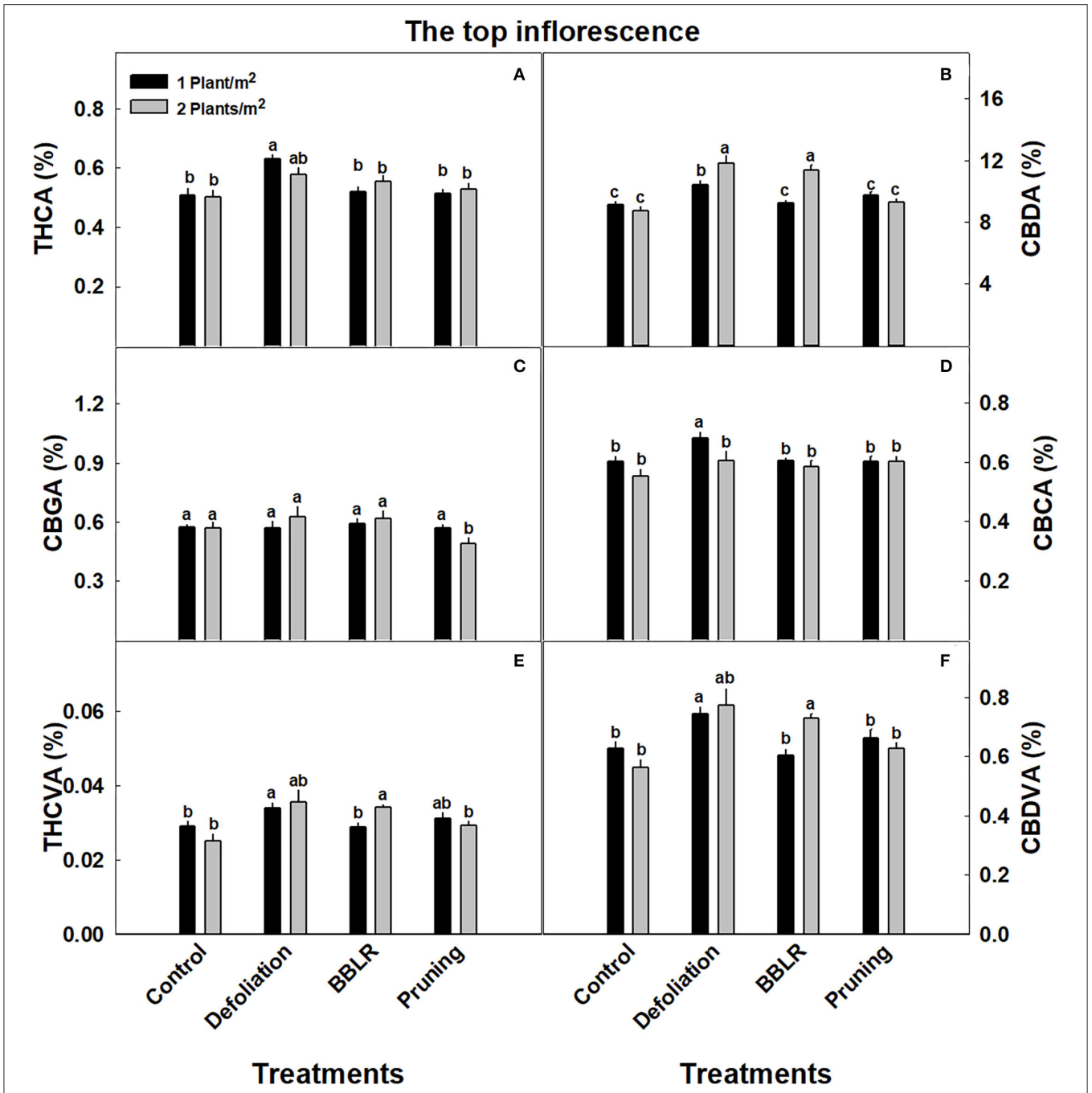

FIGURE 3 | Cannabinoid concentrations at the top inflorescence of cannabis plants grown under two densities and four architectural modulation treatments. The results are means and SE ($n = 6$). THCA **(A)**, CBDA **(B)**, CBGA **(C)**, CBCA **(D)**, THCVA **(E)**, and CBDVA **(F)**. Different letters above the bars represent significant differences between treatments by Tukey HSD test at $\alpha = 0.05$. "BBLB" removal of leaves and branches from the bottom part of the plant.

agricultural practices are used by the growers, but the effects of these newly adopted cultivation practices on product quality were usually not tested. Some agronomic practices such as mineral nutrition (Bernstein et al., 2019b; Bevan et al., 2021; Saloner and Bernstein, 2021, 2022a,b; Shiponi and Bernstein, 2021b), light quality (Magagnini et al., 2018; Danziger and Bernstein, 2021a; Westmoreland et al., 2021), light intensity (Potter and Duncombe, 2012), and manipulation of the canopy architecture (Danziger and Bernstein, 2021b,c) were recently shown to change yield quantity and chemical quality in drug-type medical cannabis, and to affect the physiological state of the plant. Spatial variabilities in environmental conditions within

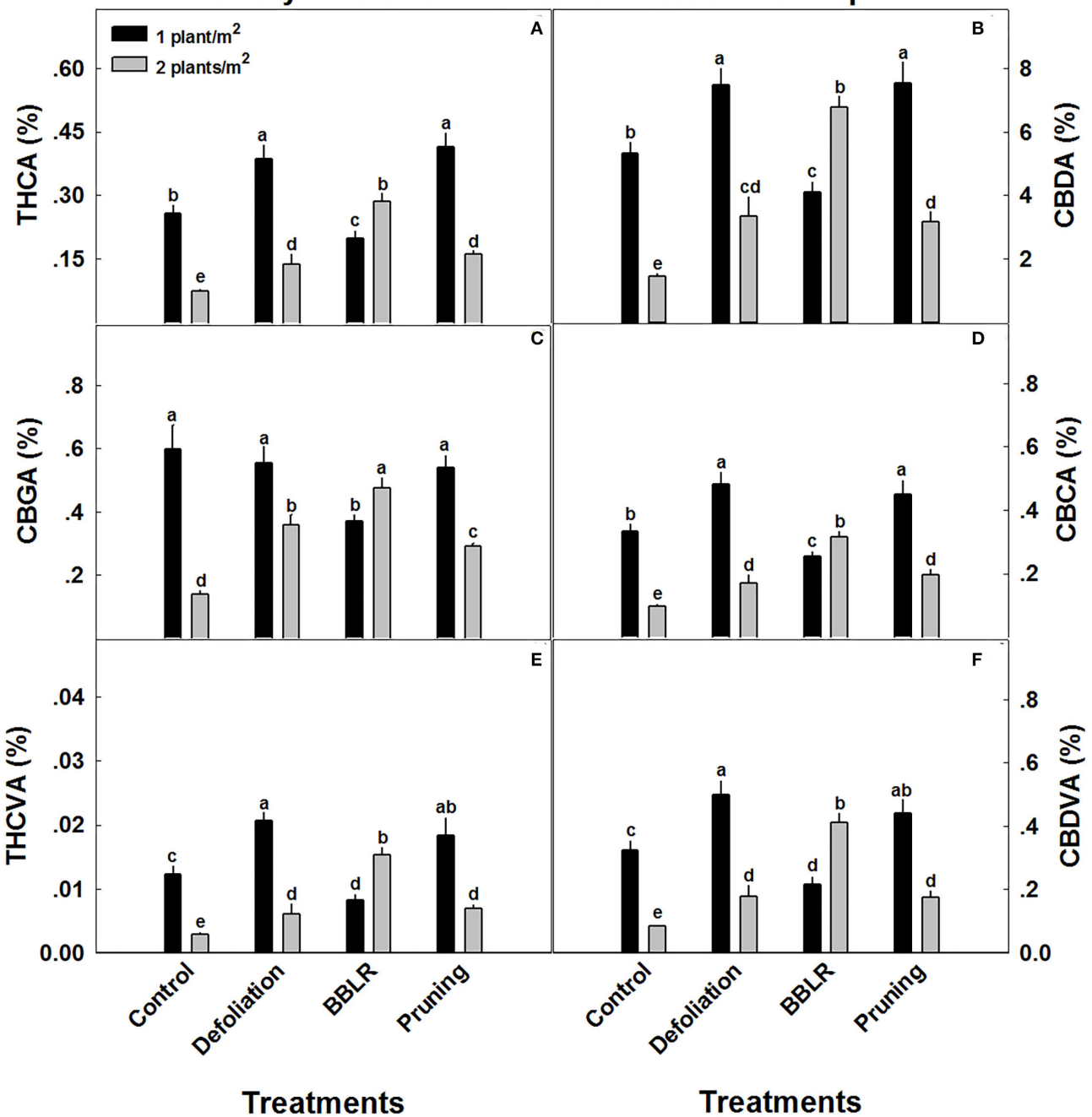

FIGURE 4 | Cannabinoid concentrations in axillary inflorescences from the lowest branch on the plant, close to the point of emergence from the main stem. The cannabis plants were grown under two densities (1 or 2 plants m^{-2}) and four architectural modulation treatments. Cannabinoids detected include THCA **(A)**, CBDA **(B)**, CBGA **(C)**, CBCA **(D)**, THCVA **(E)**, and CBDVA **(F)**. The results are mean and SE ($n = 6$). Different letters above the bars represent significant differences between treatments by Tukey HSD test at $\alpha = 0.05$. "BBLB" removal of leaves and branches from the bottom part of the plant.

the canopy are directly related to canopy density via effects on shading and air circulation (Morales et al., 2000; Boulard et al., 2017) and are considered to be a key to the lack of chemical standardization in cannabis cultivation. Crop plants depend on light radiation for their growth and development and hence for yield production (Yang et al., 2014). Plant density and plant architecture affect light penetration through the canopy and are, therefore, important crop growth parameters. A common method to increase yield per cultivation area is to increase plant stand, i.e., to grow under higher densities (Bekhradi et al.,

TABLE 2 | Cannabinoid yield per cultivation area (mg/m^2) as affected by plant density and architecture modulation treatments[B].

	CBDVA (mg/m^2)	CBGA (mg/m^2)	THCVA (mg/m^2)	THCA (mg/m^2)	CBCA (mg/m^2)	CBDA (mg/m^2)
Treatment			**1 plant /m^2**			
Control	0.94 ± 0.06[a]	0.93 ± 0.06[a]	0.043 ± 0.003[a]	0.80 ± 0.04[a]	0.95 ± 0.05[a]	14.27 ± 0.79[a]
Defoliation	0.90 ± 0.10[a]	0.79 ± 0.10[a]	0.041 ± 0.004[a]	0.76 ± 0.08[a]	0.87 ± 0.09[a]	13.31 ± 1.40[a]
BBLR[A]	0.91 ± 0.08[a]	0.92 ± 0.08[a]	0.042 ± 0.004[a]	0.79 ± 0.07[a]	0.93 ± 0.07[a]	13.99 ± 1.08[a]
Pruning	1.08 ± 0.05[a]	0.94 ± 0.03[a]	0.050 ± 0.002[a]	0.87 ± 0.04[a]	1.01 ± 0.05[a]	16.51 ± 0.78[a]
Treatment			**2 plant /m^2**			
Control	1.02 ± 0.19[a]	0.94 ± 0.17[a]	0.048 ± 0.009[a]	0.85 ± 0.15[a]	0.98 ± 0.17[a]	15.08 ± 2.64[a]
Defoliation	1.03 ± 0.21[a]	0.94 ± 0.17[a]	0.047 ± 0.009[a]	0.73 ± 0.12[a]	0.80 ± 0.13[a]	15.72 ± 2.55[a]
BBLR[A]	1.24 ± 0.16[a]	1.07 ± 0.14[a]	0.055 ± 0.007[a]	0.87 ± 0.12[a]	0.95 ± 0.13[a]	19.04 ± 2.62[a]
Pruning	1.00 ± 0.19[a]	0.89 ± 0.17[a]	0.046 ± 0.009[a]	0.84 ± 0.16[a]	0.98 ± 0.19[a]	15.31 ± 3.00[a]

[A]*Removal of branches and leaves from the bottom of the plant.*

[B]*Data followed by the same small letter within a column that includes both density treatments, signifies that the cannabinoid concentration did not differ significantly between treatments according to Tukey HSD test, at* $\alpha = 0.05$ *(*$n = 5$*).*

2014; Nurzyńska-Wierdak and Zawiślak, 2014). An increase of plant density changes numerous micro-climatic conditions in the plant canopy, which can alter floral development and chemical profile (Khorshidi et al., 2009; El-Zaeddi et al., 2016). We have, therefore, hypothesized that the concentrations and spatial standardization of cannabinoids in drug-type cannabis plants could be affected by plant density, and that the response will be an interplay with architecture manipulations. The results identified that the cannabinoids profile is indeed highly affected by plant density and by architectural manipulations thus supporting the hypothesis; and furthermore, highlighting the importance of plant density and canopy structure for the standardization of the chemical profile. Our results thus expand the ability to regulate cannabinoid metabolism and yield in medical cannabis, and therefore direct researchers and growers to improve the chemical quality.

Yield and Yield Components

Cannabis-based therapeutics use inflorescences or their extracts for patients' care, and the cannabis inflorescence is the marketable yield in medical cannabis. A wide range of cultivation practices is utilized in the production industry, and cultivation is based on growth of plants that vary dramatically in size, architecture, and plant density. For economic considerations, a growers' yield is best considered as the output harvest for cultivation area (g/m^2), rather than for a single plant (g/plant). In all plant architecture treatments evaluated in this study, inflorescence biomass yield production per m^2 was higher in the higher density treatment compared with the lower density treatment, except for the "Pruning" treatment that was not significantly affected by plant density (**Table 1**). In many crop species, changing plant density was reported to affect yield biomass/m^2 as well as yield quality (Islam et al., 2011; Maboko et al., 2011; Hozayn et al., 2013). Increased density was found to increase yield (Hozayn et al., 2013) but also to reduce yield quality (Maboko et al., 2011), suggesting the existence of an optimum density that needs to be determined for each production goal. As cannabis is prized for its chemical components, it could be compared to aromatic herbs, as their value is defined mostly by the secondary metabolites rather than solely by yield biomass. Similar to our results for cannabis, in basil (*Ocimum basilicum*), parsley (*Petroselinum crispum*) and chamomile (*Matricaria chamomilla*), leaves and floral yield increased with the increase in plant density (Pirzad et al., 2011; Bekhradi et al., 2014; El-Zaeddi et al., 2016) but not in dill (*Anethum graveolens*) (Callan et al., 2007). The interplay between plant density and architectural manipulation was seen in tomatoes where total yield increased with increased density and with reduced stem pruning (Maboko et al., 2011).

Several studies involving planting density were conducted on hemp-type cannabis in the past, but the yield tested in those studies was biomass for animal feed, fibers, or seeds (Amaducci et al., 2002; Grabowska and Koziara, 2006), under cultivation practices that vary considerably from drug-type cannabis agrotechniques. A study by Campiglia et al. (2017) did however test inflorescence yield and found that higher plant density resulted in improved floral yield in seven genotypes, but the effect on inflorescence chemical composition was not tested. A meta-analysis of *Cannabis sativa* yield for data reported by previous studies, point at the use of low plant density, $\leq$12 plants per square meter, for increased cannabis yield per square meter (Backer et al., 2019).

In the present study, cannabinoid concentrations in the plant, calculated as the plant average concentration (**Supplementary Figure 2**) were mostly reduced (by up to 24%) or not affected by the increase in density (excluding "BBLR" CBDA and CBDVA, which were increased by up to 18%). However, the increase in inflorescence yield biomass per cultivation area under dense plant cultivation compensated for the reduced concentrations, and the cannabinoid yield per cultivation area (mg/m^2) (**Table 2**) was, therefore, not affected.

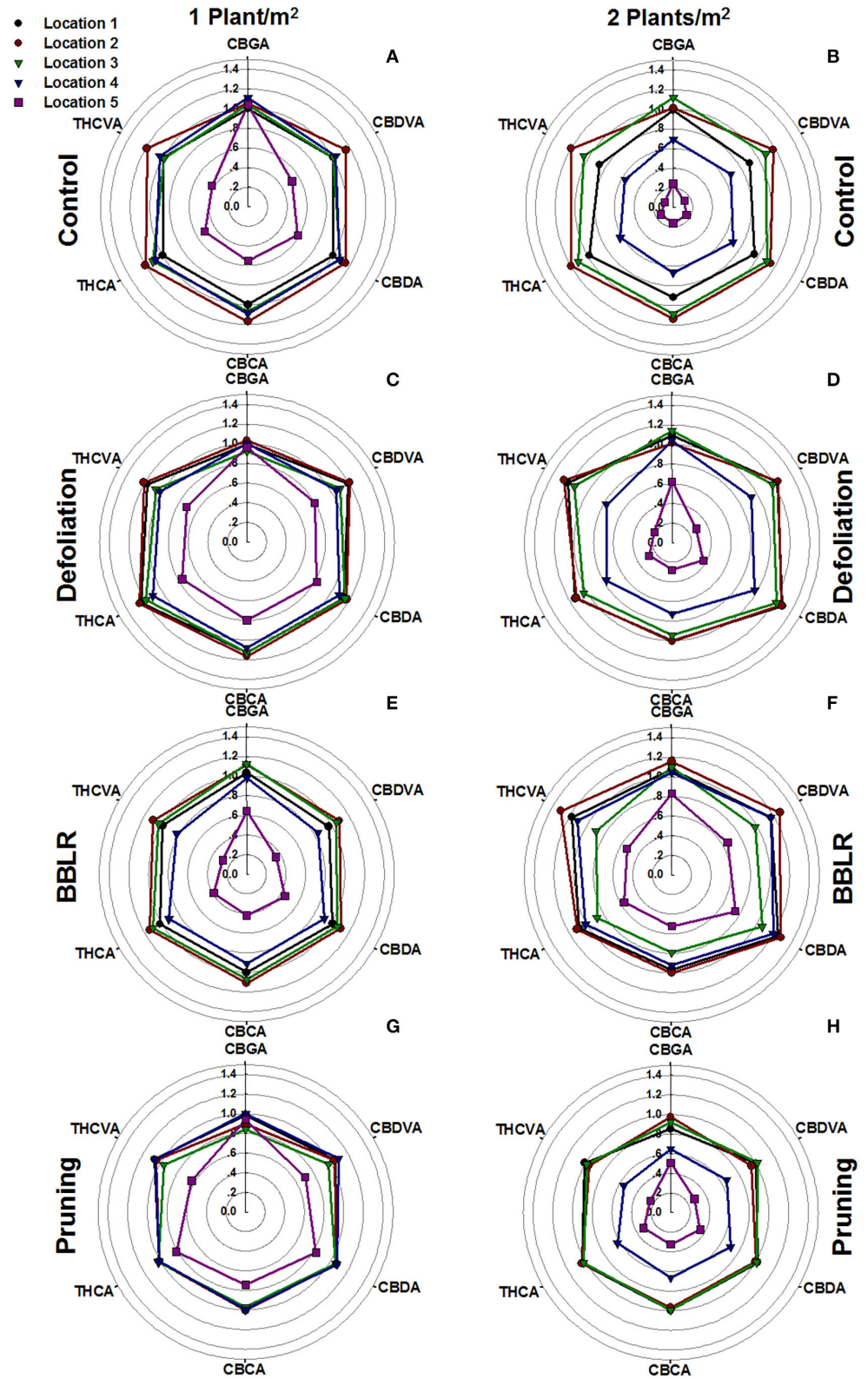

FIGURE 5 | Effect of plant density and plant architecture treatments on cannabinoid concentrations in inflorescences from five locations in the plant. The data presented are concentration of each cannabinoid, relative to its concentration in the apical inflorescence of the main stem of the "Control" at the 1 plant/m^2 treatment (location1). 1 plant/m^2 density **(A,C,E,G)**, 2 plants/m^2 density **(B,D,F,H)**. Architecture manipulation treatments: "Control" **(A,B)**, "Defoliation" **(C,D)**, Removal of leaves and branches from the bottom part of the plant ["BBLR"] **(E,F)** and "Pruning" **(G,H)**. The results are mean ($n = 6$).

TABLE 3 | Effect of plant density (1 and 2 plants/m^2) and architectural modulation treatments on chemical uniformity of cannabinoids in *Cannabis sativa* plants[D].

	Cannabinoid variation score (%)[A]						Plant variation score (%)[B]				
	CBDVA	CBGA	THCVA	THCA	CBCA	CBDA	5%	10%	15%	25%	50%
Treatment					**1 plant /m^2**						
Control	37^{f}	40^{d}	43^{f}	47^{e}	40^{e}	33^{e}	79^{c}	59^{e}	41^{d}	22^{e}	^{e}
Defoliation	43^{e}	27^{e}	47^{e}	43^{e}	43de	33^{e}	77^{d}	56^{f}	39^{e}	18^{f}	2^{e}
BBLR[C]	47^{d}	53^{b}	57^{d}	53^{d}	47^{d}	40^{d}	79^{c}	66^{d}	49^{d}	30^{d}	8^{d}
Pruning	43^{e}	27^{e}	47^{e}	33^{f}	40^{e}	37^{d}	77^{d}	54^{f}	38^{e}	17^{f}	4^{e}
					2 plants /m^2						
Control	76^{a}	72^{c}	76^{b}	90^{a}	76^{a}	72^{a}	95^{a}	87^{a}	77^{a}	60^{a}	19^{a}
Defoliation	73^{a}	40^{d}	77^{b}	70^{c}	70^{b}	67^{ab}	88^{b}	76^{b}	66^{b}	49^{b}	17^{b}
BBLR	60^{c}	47^{c}	73^{c}	80^{b}	60^{c}	43^{c}	94^{a}	73^{c}	61^{c}	38^{c}	9^{d}
Pruning	66^{b}	72^{a}	83^{a}	69^{c}	66^{bc}	62^{b}	90^{b}	80^{b}	70^{b}	43^{b}	13^{c}

[A] *"Cannabinoid variation score" represents the percentage of inflorescences deviating by more than 15% from the average cannabinoid concentration in the plant.*
[B] *"Plant variation score" represent the percentage of inflorescences having concentrations similar to the treatment average across all cannabinoids. It is presented for five levels of variation acceptance: 5, 10, 15, 25, and 50% variation from the treatments average.*
[C] *"BBLB"-removal of leaves and branches from the bottom part of the plant.*
[D] *Different lowercase letters near the means within a column represent significant differences between treatments for each cannabinoid by Tukey HSD test, $\alpha = 0.05$.*

Effect of plant density on secondary metabolites production per cultivation area may vary between crops; in lavender (*Lavandula hybrida*), decreased intra-plant spacing increased secondary metabolite production (Arabaci et al., 2007).

Cannabis inflorescence is a rather unique plant-remedy since it is used today by western medicine mainly as an intact plant material or its extract. While other plant-based medicinal compounds are extracted from plants (if synthetic production is not possible or is less economical) and are dosed at a well-defined concentration into modern drugs with known specific effects. As such, it is still not fully known how varying amounts and ratios of the cannabis components affect the treatments' efficacy. In this study, a larger variability in concentrations and ratios between identified cannabinoids was identified in the densely grown plants compared with the more spaced stand. In the treatments of this density, 9–19% of the inflorescences in a plant varied in concentration by more than 50% from the average plant concentration (**Table 3**). This alarmingly large variation might impose a problem for inflorescence-based therapy, but less so for mass production of extracts which allows standardization of some of the compounds. According to a previous study (Danziger and Bernstein, 2021b), with smaller plants cultivated at a similar (1 plant/m^2) density, the chemical variation in the smaller plants was generally lower. Until further studies evaluating the effects of varying inflorescence chemical profile on cannabis-treated patients will be conducted, it will not be possible to determine whether the added value of increased yield outweighs the reduced uniformity under higher density.

Light Effects

Light is a key factor effecting plant growth and development (Kami et al., 2010). Higher light irradiance is connected to faster growth and higher yields (Eaves et al., 2020). However, even under high irradiance, some high-intensity crops suffer from insufficient light levels when dense canopy prevents sufficient light from reaching lower parts of the plant (Fowler and Reta-sanchez, 2002). Under higher density growth, cannabis inflorescences showed decreased cannabinoids synthesis at the lower parts of the plants, leading to an increase in spatial chemical variability (**Figure 5**). This decrease could be attributed to lower light penetration through the denser canopy (**Supplementary Figure 3**). In numerous crops, including cotton, light penetration to the canopy was found to have a profound effect on yield (Chapepa et al., 2020), and a similar reduction in yield was observed in this study (**Figure 2B**). The chronic lack of light at the bottom of the highly dense plants is suggested also by the increased degradation of leaves and branches in the high-density treatments (**Figure 1**), as was formerly described for a range of plants including *Arabidopsis thaliana* (Weaver and Amasino, 2001). Such degradation is reported to be highly localized, which explain why only the bottom-most branches senesced, while branches from higher and more external locations showed little variance. The earlier senescence of the lower leaves and branches corresponds also with the localized effect on the chemical profile of inflorescence from the lower parts of the plant (**Figure 5**).

Plants have developed various mechanisms to cope with the reduction of light penetration through the canopy. According to Slattery et al. (2017), reduced leaf chlorophyll contents lowers photosynthetic rate at the upper leaves but increases light penetrance to the canopy without reducing yield. Our results reveal a trend for similar adaptation mechanism in cannabis, with significant reductions in most pigments in the BBLR and pruning treatments in the more densely grown plants (and a similar albeit not significant trend in the control treatment) (**Figure 7**). A similar trend was reported also for pepper and

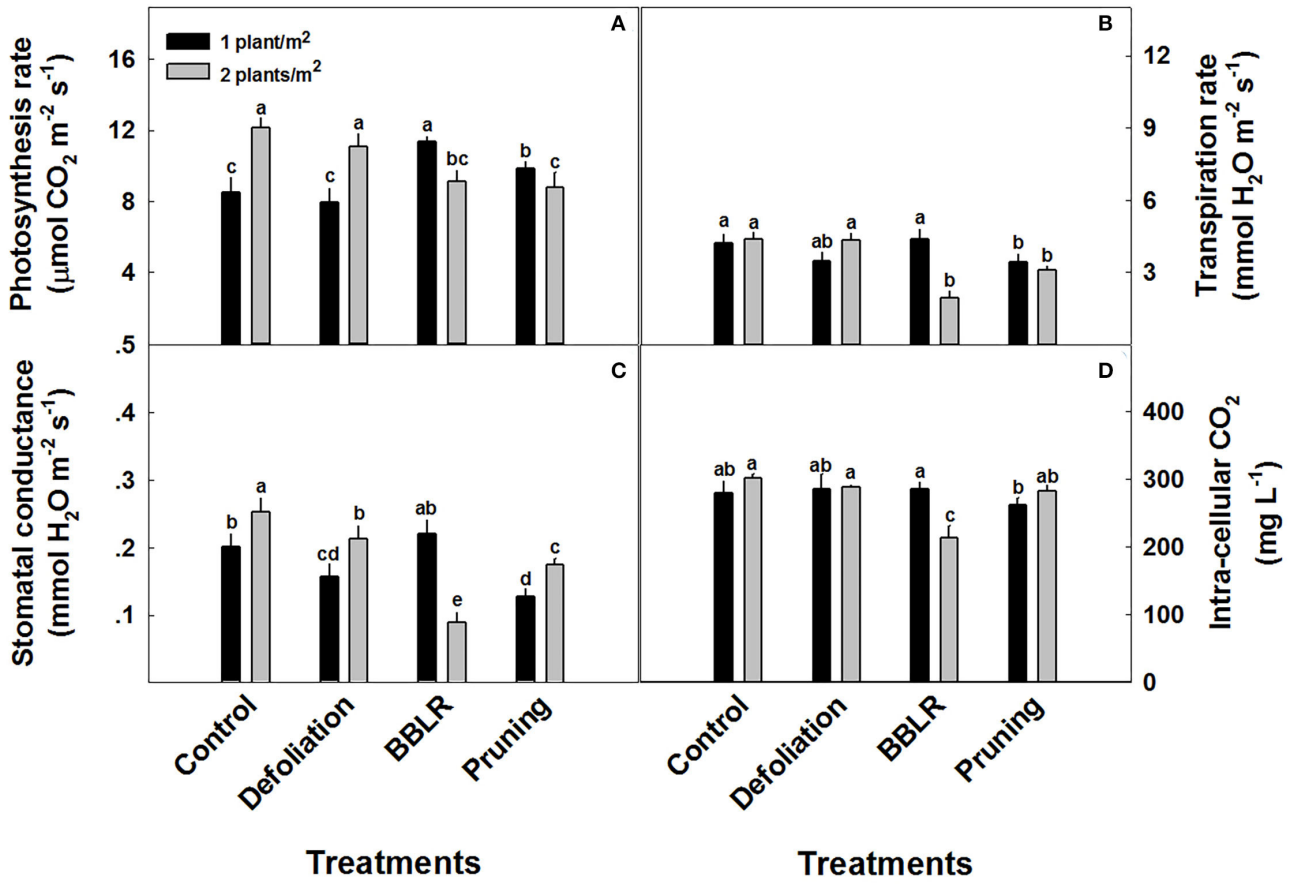

FIGURE 6 | Response of gas-exchange parameters to planting density (1 and 2 plants/m^2) and plant architecture treatments in medical cannabis plants. Photosynthesis **(A)**, Stomatal conductance **(B)**, Transpiration **(C)**, and intracellular CO_2 **(D)**. The results are mean and SE ($n = 6$). Different letters above the bars represent significant differences between treatments by Tukey HSD test at $\alpha = 0.05$.

basil, as high-density planting reduced leaf chlorophyll contents (Aminifard et al., 2010; Abdou et al., 2017). Since the leaves analyzed for pigment quantification in our study were located at the upper third of the canopy, shading could not have influenced pigment biosynthesis. This suggests that other elicitors induced these observed changes in chlorophyll accumulation. Possible effectors are hormonal changes such as gibberellin, which stimulates plant elongation under low light but whose presence is also associated with lower chlorophyll content per area (Liu et al., 2017; Yan et al., 2020). This reasoning is strengthened by the elongated plants that developed under the high-density cultivation, as was previously seen in many crops such as tomatoes (Ohta et al., 2018) and corn (*Zea mays*) (Maddonni et al., 2001). Results for membrane leakage and osmotic potential in leaves from the upper 3rd of the plants reflect as well impact of planting density on the physiological status of the plants. Membrane leakage and osmotic potential were generally higher and lower, respectively, in upper leaves of the higher density plants, presenting a negative effect of high density on the physiological state (**Figure 7**). It should be noted that very high plant densities (>20 plants/m^2) reduced cannabis hemp-type plant height as was described previously (Amaducci et al., 2002; Bhattarai and Midmore, 2014). However, since industrial fiber-hemp morphology differs from drug-type medical cannabis, and the growth patterns were bred for different production goals, developmental and physiological responses are expected to differ. It is, therefore, not possible to predict responses of medical cannabis plants from industrial fiber-hemp results.

In our study, two treatments changed light penetration to the canopy, "Defoliation," by removing most of the leaves obscuring the light, and "BBLR" that involved removal of all leaves, branches, and inflorescences from the bottom of the plant thus eliminating tissue that receive insufficient light levels (**Supplementary Figure 3**). Light penetrance to the canopy was substantially higher in the "Defoliation" treatments compared to all other treatments, though this change was made late in development and its effect was, therefore, limited. This is unlike the "BBLR" treatment, which eliminated growth in the shaded lower parts of the plant altogether throughout the growing season. Defoliating the plants resulted in reduced yield biomass per plant under the high density, but increased cannabinoid concentrations at the bottom of the plants compared to the

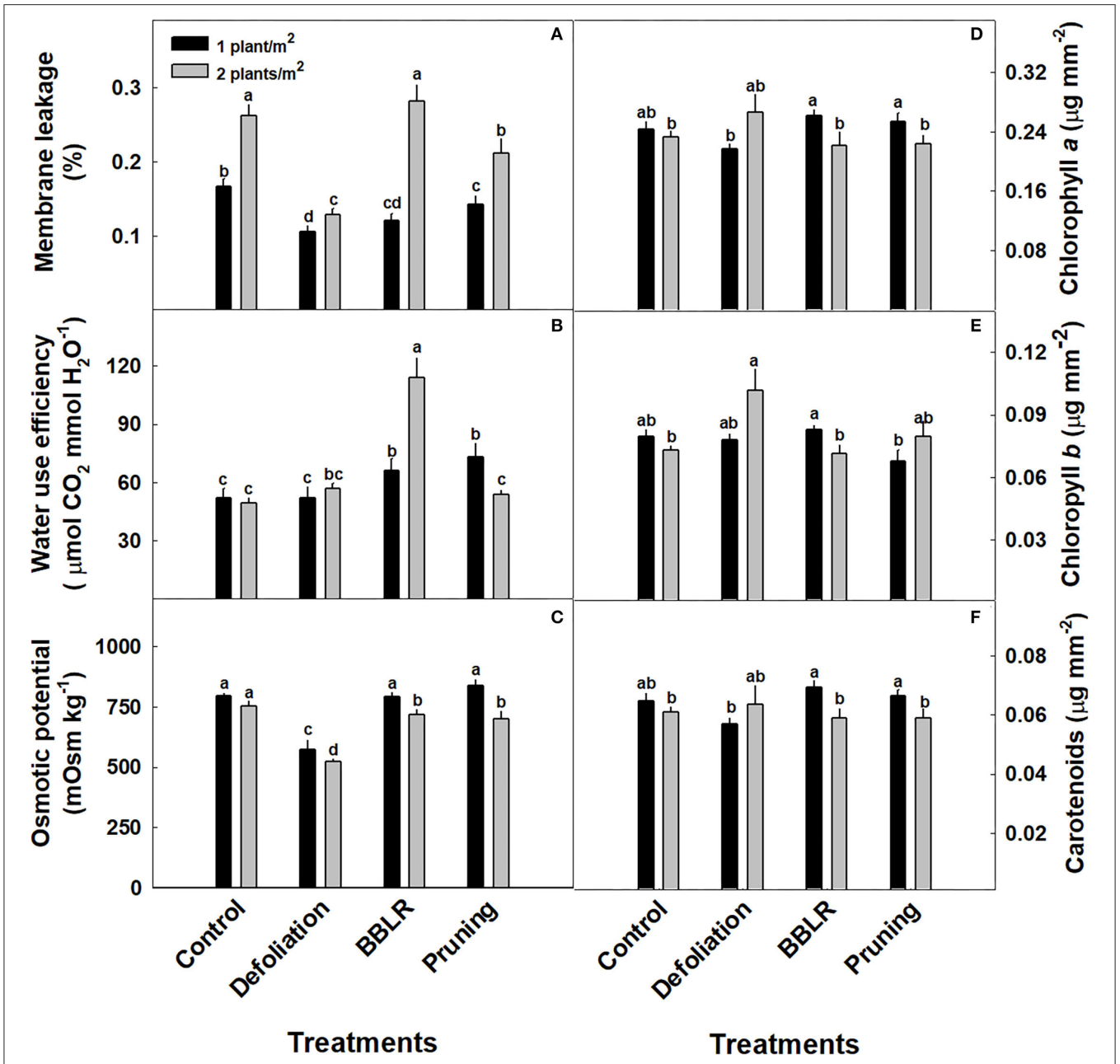

FIGURE 7 | Effects of plant density (1 or 2 plants/m^2) and plant architecture modulating treatments on medical cannabis plants. Membrane leakage **(A)**, Water use efficiency **(B)**, Osmotic potential **(C)**, Chlorophyll *a* **(D)**, Chlorophyll *b* **(E)**, carotenoids **(F)**. The results are mean and SE ($n = 6$). Different letters above the bars represent significant differences between treatments by Tukey HSD test at $\alpha = 0.05$.

"Control." It is possible that the yield reduction results from inhibition of inflorescence growth by a chronic lack of light throughout the season prior to the defoliation, similar to the effect on the "control," and that the loss of leaves that was imposed at the end of the season occurred too late in development to compensate for the reduction in inflorescence yield by the chronic lack of light. However, cannabinoid synthesis was improved by the added light at the end of the season following defoliation, during chemical maturation. Unlike the "Defoliation" treatment, "BBLR" has not caused a decrease in yield compared to the control under both density treatments, which could be explained by the timing of the treatment that was imposed on the plants early at the flowering stage thus preventing inhibition of floral development due to lack of light.

To mitigate yield loss and reduction of secondary metabolites, it is possible to introduce artificial light into the canopy. The use of intra-canopy lights is becoming more prevalent to increase yield at the lower sun-deprived parts of plants

(Davis and Burns, 2016). In cannabis, a single study used sub-canopy LED lights that were shown to increase yield quantity as well as the cannabinoid contents at the bottom third of the plant (Hawley et al., 2018). In addition, several studies evaluated different spectral properties on cannabis development, yield and its components showing differential response to light quality (Magagnini et al., 2018; Eaves et al., 2020; Bevan et al., 2021; Danziger and Bernstein, 2021a) as well light intensity (Potter and Duncombe, 2012). As light travels through the plant canopy, different wavelengths are absorbed by the plant organs altering its spectrum as well as intensity (Kasperbauer, 1971). We therefore suggest that a combined approach of spectral quality optimization inside the canopy, and increased light intensity by architectural modulation treatments or sub-lighting illumination can be utilized to improve yield components in cannabis grown in high density.

CONCLUSIONS

In this study, we evaluated the effects of plant architecture and plant density on growth, development and chemical properties of medical drug-type) *Cannabis sativa* plants. We tested the hypotheses that an increase in plant density will increase inflorescence yield per area while reducing chemical quality and uniformity, and furthermore, that manipulating plant architecture will interact with such variations. The results indicated that an increase in plant density decreased inflorescence yield per plant but increased yield per area (except in the pruning treatment that was not affected significantly) thus supporting the hypotheses. In addition, cannabinoid concentrations were reduced in the lower part of the plant by the increase in plant density (except in the BBLR treatment that did not have true lower branches), but were generally unchanged (or much less affected) in the top apical inflorescence- thus highly reducing the cannabinoid uniformity across the plant. Plant biomass was reduced by the higher plant density, while plant height was increased. The information gained in this study can direct cannabis growers to customize cultivation practices to target the final product goals, in terms of yield quantity vs. chemical quality.

DATA AVAILABILITY STATEMENT

The original contributions presented in the study are included in the article/**Supplementary material**, further inquiries can be directed to the corresponding authors.

AUTHOR CONTRIBUTIONS

NB conceptualization, Funding acquisition, supervision, and planning the experiments. ND carried out the experiments. NB and ND wrote the manuscript. Both authors contributed to the article and approved the submitted version.

FUNDING

This work was funded by the Chief scientist fund of the Israeli Ministry of Agriculture, Israel, Grant No. 20-03-0049.

ACKNOWLEDGMENTS

The study was conducted at the commercial facility of BOL Pharma, a certified commercial cultivation farm in Israel. We are grateful for the cooperation and assistance of Hagay Helman, Dr. Dvir Taler and the farm staff. We thank Yael Sade for guidance concerning the cannabinoid analyses and for technical support, Uri Hochberg for advice concerning the Licor measurements, and Sivan Shiponi, Dalit Morad, Ayana Neta, Eliav Shtul-Trauring, and Jecki Shoef, for technical support.

SUPPLEMENTARY MATERIAL

The Supplementary Material for this article can be found online at: https://www.frontiersin.org/articles/10.3389/fpls.2022.713481/full#supplementary-material

REFERENCES

Abdou, M., El-Sayed, A., Taha, R., and Marzok, Z. (2017). Effect of plant density and some vitamins, as well as, active yeast on sweet basil (*Ocimum Basilicum*) plant. B- Essential oil production and chemical constituents. *Sci. J. Flowers Ornam. Plants* 4, 101–120. doi: 10.21608/sjfop.2017.5398

Akintoye, H. A., Kintomo, A. A., and Adekunle, A. A. (2009). Yield and fruit quality of watermelon in response to plant population. *Int. J. Veg. Sci.* 15, 369–380. doi: 10.1080/19315260903012110

Amaducci, S., Errani, M., and Venturi, G. (2002). Plant population effects on fibre hemp morphology and production. *J. Ind. Hemp* 7, 33–60. doi: 10.1300/J237v07n02_04

Aminifard, M. H., Aroiee, H., Karimpour, S., and Nemati, H. (2010). Growth and yield characteristics of paprika pepper (*Capsicum annum* L.) in response to plant density. *Asian J. Plant Sci.* 9, 276–280. doi: 10.3923/ajps.2010.276.280

Andre, C. M., Hausman, J. F., and Guerriero, G. (2016). Cannabis sativa: the plant of the thousand and one molecules. *Front. Plant Sci.* 7:19. doi: 10.3389/fpls.2016.00019

Arabaci, O., Bayram, E., Baydar, H., Savran, A. F., Karadogan, T., and Ozay, N. (2007). Chemical composition, yield and contents of essential oil of *Lavandula hybrida reverchon* grown under different nitrogen fertilizer, plant density and location. *Asian J. Chem.* 19, 2184–2192.

Ayala-tafoya, F., and Yáñez-juárez, M. G. (2019). Plant density and stem pruning in greenhouse cucumber production. *Rev. Mex. Ciencias Agrícolas* 10, 79–90. doi: 10.29312/remexca.v10i1.1211

Backer, R., Schwinghamer, T., Rosenbaum, P., McCarty, V., Eichhorn Bilodeau, S., Lyu, D., et al. (2019). Closing the yield gap for cannabis: a meta-analysis of factors determining cannabis yield. *Front. Plant Sci.* 10:495. doi: 10.3389/fpls.2019.00495

Bekhradi, F., Delshad, M., Kashi, A., Babalar, M., and Ilkhani, S. (2014). Effect of plant density in some basil cultivars on yield and radiation use efficiency. *J. Biodiversity Environ. Sci.* 5, 91–96.

Berman, P., Futoran, K., Lewitus, G. M., Mukha, D., Benami, M., Shlomi, T., et al. (2018). A new ESI-LC/MS approach for comprehensive metabolic profiling of phytocannabinoids in Cannabis. *Sci. Rep.* 8:14280. doi: 10.1038/s41598-018-32651-4

Bernstein, N., Gorelick, J., and Koch, S. (2019a). Interplay between chemistry and morphology in medical cannabis (*Cannabis sativa* L.). *Ind. Crops Prod.* 129, 185–194. doi: 10.1016/j.indcrop.2018.11.039

Bernstein, N., Gorelick, J., Zerahia, R., and Koch, S. (2019b). Impact of N, P, K, and humic acid supplementation on the chemical profile of medical cannabis (*Cannabis sativa* L). *Front. Plant Sci.* 10:736. doi: 10.3389/fpls.2019.00736

Bevan, L., Jones, M., and Zheng, Y. (2021). Optimisation of nitrogen, phosphorus, and potassium for soilless production of *Cannabis sativa* in the flowering stage using response surface analysis. *Front. Plant Sci*. 17:764103. doi: 10.3389/fpls.2021.764103

Bhattarai, J. H. S. P., and Midmore, D. J. (2014). Effect of industrial hemp (*Cannabis sativa* L) planting density on weed suppression, crop growth, physiological responses, and fibre yield in the subtropics. *Renew. Bioresour.* 2:1. doi: 10.7243/2052-6237-2-1

Boulard, T., Roy, J. C., Pouillard, J. B., Fatnassi, H., and Grisey, A. (2017). Modelling of micrometeorology, canopy transpiration and photosynthesis in a closed greenhouse using computational fluid dynamics. *Biosyst. Eng.* 158, 110–133. doi: 10.1016/j.biosystemseng.2017.04.001

Callan, N. W., Johnson, D. L., Westcott, M. P., and Welty, L. E. (2007). Herb and oil composition of dill (*Anethum graveolens* L.): Effects of crop maturity and plant density. *Ind. Crops Prod.* 25, 282–287. doi: 10.1016/j.indcrop.2006.12.007

Campiglia, E., Radicetti, E., and Mancinelli, R. (2017). Plant density and nitrogen fertilization affect agronomic performance of industrial hemp (*Cannabis sativa* L.) in Mediterranean environment. *Ind. Crops Prod.* 100, 246–254. doi: 10.1016/j.indcrop.2017.02.022

Cardoso, F. B., Martinez, H. E. P., da Silva, D. J. H., Milagres, C. D. C., and Barbosa, J. G. (2018). Yield and quality of tomato grown in a hydroponic system, with different planting densities and number of bunches per plan. *Pesqui. Agropecu. Trop.* 48, 340–349. doi: 10.1590/1983-40632018v4852611

Cavero, J., Gil Ortega, R., and Gutierrez, M. (2001). Plant density affects yield, yield components, and color of direct-seeded paprika pepper. *Hortscience* 36, 76–79. doi: 10.21273/HORTSCI.36.1.76

Chapepa, B., Mudada, N., and Mapuranga, R. (2020). The impact of plant density and spatial arrangement on light interception on cotton crop and seed cotton yield: an overview. *J. Cott. Res.* 3:18. doi: 10.1186/s42397-020-00059-z

Danziger, N., and Bernstein, N. (2021a). Light matters: effect of light spectra on cannabinoid profile and plant development of medical cannabis (*Cannabis sativa* L.). *Ind. Crops Prod.* 164:113351. doi: 10.1016/j.indcrop.2021.113351

Danziger, N., and Bernstein, N. (2021b). Plant architecture manipulation increases cannabinoid standardization in 'drug-type' medical cannabis. *Ind. Crops Prod.* 167:113528. doi: 10.1016/j.indcrop.2021.113528

Danziger, N., and Bernstein, N. (2021c). Shape matters: plant architecture affects chemical uniformity in large-size medical cannabis plants. *Plants*. 10, 1834. doi: 10.3390/plants10091834

Davis, P. A., and Burns, C. (2016). Photobiology in protected horticulture. *Food Energy Secur.* 5, 223–238. doi: 10.1002/fes3.97

Eaves, J., Eaves, S., Morphy, C., and Murray, C. (2020). The relationship between light intensity, cannabis yields, and profitability. *Agron. J.* 112, 1466–1470. doi: 10.1002/agj2.20008

El-Zaeddi, H., Calín-Sánchez, Á., Martínez-Tomé, J., Noguera-Artiaga, L., Burló, F., and Carbonell-Barrachina, Á. A. (2016). Irrigation dose and plant density affect the essential oil content and sensory quality of parsley (*Petroselinum sativum*). *Sci. Hortic.* 206, 1–6. doi: 10.1016/j.scienta.2016.04.028

Flores-Sanches, J., and Verpoorte, R. (2008). Secondary metabolism in cannabis. *Phytochem. Rev.* 7, 615–639. doi: 10.1007/s11101-008-9094-4

Fowler, J. L., and Reta-sanchez, D. G. (2002). Canopy light environment and yield of narrow-row cotton as affected by canopy architecture. *Agron. J.* 94, 1317–1323. doi: 10.2134/agronj2002.1317

Gorelick, J., and Bernstein, N. (2017). "Chemical and physical elicitation for enhanced cannabinoid production in cannabis," in *Cannabis sativa L. - Botany and Biotechnology*, eds S. Chandra, H. Lata, M. ElSohly (Cham: Springer), 439–456. doi: 10.1007/978-3-319-54564-6_21

Gorelick, J., Rosenberg, R., Smotrich, A., Hanuš, L., and Bernstein, N. (2015). Hypoglycemic activity of withanolides and elicitated *Withania somnifera*. *Phytochemistry* 116, 283–289. doi: 10.1016/j.phytochem.2015.02.029

Grabowska, L., and Koziara, W. (2006). The effect of nitrogen dose, sowing density and time of harvest on development and yields of hemp cultivar bialobrzeskie. *J. Nat. Fibers* 2, 1–17. doi: 10.1300/J395v02n04_01

Gülck, T., and Møller, B. L. (2020). Phytocannabinoids: origins and biosynthesis. *Trends Plant Sci.* 25, 985–1004. doi: 10.1016/j.tplants.2020.05.005

Hawley, D., Graham, T., Stasiak, M., and Dixon, M. (2018). Improving Cannabis bud quality and yield with subcanopy lighting. *Hortscience* 53, 1593–1599. doi: 10.21273/HORTSCI13173-18

Hozayn, M., Tawfik, M. M., Abd El-Ghany, H. M., and Korayem, A. M. (2013). Effect of plant density on yield and sugar quality characteristics of sugar beet. *J. Appl. Sci. Res.* 9, 1004–1009.

Ignat, T., Schmilovitch, Z., FefÖldi, J., Bernstein, N., Steiner, B., Egozi, H., et al. (2013). Nonlinear methods for estimation of maturity stage, total chlorophyll, and carotenoid content in intact bell peppers. *Biosyst. Eng.* 114, 414–425. doi: 10.1016/j.biosystemseng.2012.10.001

Islam, M., Saha, S., Akand, H., and Rahim, M. A. (2011). Effect of spacing on the growth and yield of sweet pepper (*Capsicum annuum* L.). *J. Cent. Eur. Agric.* 12, 328–335. doi: 10.5513/JCEA01/12.2.917

Jarecki, W., and Bobrecka-Jamro, D. (2011). Reaction of spring wheat CV. PARABOLA to diversified sowing density. *Acta Sci. Pol.* 10, 79–86.

Kami, C., Lorrain, S., Hornitschek, P., and Fankhauser, C. (2010). Light-regulated plant growth and development. *Curr. Top. Dev. Biol.* 91, 29–66. doi: 10.1016/S0070-2153(10)91002-8

Kasperbauer, M. J. (1971). Spectral distribution of light in a tobacco canopy and effects of end-of-day light quality on growth and development. *Plant Physiol.* 47, 775–778. doi: 10.1104/pp.47.6.775

Khorshidi, J., Fakhr Tabatabaie, M., Omidbaigi, R., and Sefidkon, F. (2009). Effect of densities of planting on yield and essential oil components of Fennel (*Foeniculum vulgare* Mill Var. Soroksary). *J. Agric. Sci.* 1, 152–157. doi: 10.5539/jas.v1n1p152

Kool, M. T. N. (1997). Importance of plant architecture and plant density for rose crop performance. *J. Hortic. Sci.* 72, 195–203. doi: 10.1080/14620316.1997.11515506

Kravchik, M., and Bernstein, N. (2013). Effects of salinity on the transcriptome of growing maize leaf cells point at cell-age specificity in the involvement of the antioxidative response in cell growth restriction. *BMC Genomics* 14:24. doi: 10.1186/1471-2164-14-24

Lichtenthaler, H. K., and Wellburn, A. R. (1983). Determinations of total carotenoids and chlorophylls a and b of leaf extracts in different solvents. *Biochem. Soc. Trans.* 11, 591–592. doi: 10.1042/bst0110591

Liu, X., Li, Y., and Zhong, S. (2017). Interplay between light and plant hormones in the control of arabidopsis seedling chlorophyll biosynthesis. *Front. Plant Sci.* 8:1433. doi: 10.3389/fpls.2017.01433

Maboko, M. M., Du Plooy, C. P., and Chiloane, S. (2011). Effect of plant population, fruit and stem pruning on yield and quality of hydroponically grown tomato. *Afr. J. Agric. Res.* 6, 5144–5148.

Maddonni, G. A., Otegui, M. E., and Cirilo, A. G. (2001). Plant population density, row spacing and hybrid effects on maize canopy architecture and light attenuation. *F. Crop. Res.* 71, 183–193. doi: 10.1016/S0378-4290(01)00158-7

Magagnini, G., Grassi, G., and Kotiranta, S. (2018). The effect of light spectrum on the morphology and cannabinoid content of *cannabis sativa* L. *Med. Cannabis Cannabinoids* 1, 19–27. doi: 10.1159/000489030

Mao, L., Zhang, L., Zhao, X., Liu, S., van der Werf, W., Zhang, S., et al. (2014). Crop growth, light utilization and yield of relay intercropped cotton as affected by plant density and a plant growth regulator. *F. Crop. Res.* 155, 67–76. doi: 10.1016/j.fcr.2013.09.021

Masombo, B., Rop, N., Omami, E., and Waswa, W. (2018). Influence of intra-row spacing, training and pruning on performance of vine spinach (*Basella Alba* L) in Western Kenya. *Afr. J. Educ.* 4, 79–91.

Morales, P., Davies, F. S., and Littell, R. C. (2000). Pruning and skirting affect canopy microclimate, yields, and fruit quality of "Orlando" tangelo. *Hortscience* 35, 30–35. doi: 10.21273/HORTSCI.35.1.30

Nurzyńska-Wierdak, R., and Zawiślak, G. (2014). Herb yield and bioactive compounds of tarragon (*Artemisia dracunculus* L.) as influenced by plant density. *Acta Sci. Pol. Hortorum Cultus* 13, 207–221.

Oga, I. O., and Umekwe, P. N. (2016). Effects of pruning and plant spacing on the growth and yield of watermelon (*Citrullus lanatus* L.) in Unwana-Afikpo. *Int. J. Sci. Res.* 5, 110–115. doi: 10.21275/v5i4.NOV161890

Ohta, K., Makino, R., Akihiro, T., and Nishijima, T. (2018). Planting density influence yield, plant morphology and physiological characteristics

of determinate "suzukoma" tomato. *J. Appl. Hortic.* 20, 3–10. doi: 10.37855/jah.2018.v20i01.01

Pirzad, A., Shakiba, M. R., Zehtab-Salmasi, S., Mohammadi, S. A., Hadi, H., and Darvishzadeh, R. (2011). Effects of irrigation regime and plant density on harvest index of German chamomile (*Matricaria chamomilla* L.). *Aust. J. Agric. Eng.* 2, 120–126. doi: 10.1080/10496475.2011.584824

Postma, J. A., Hecht, V. L., Hikosaka, K., Nord, E. A., Pons, T. L., and Poorter, H. (2020). Dividing the pie: a quantitative review on plant density responses. *Plant Cell Environ.* 44, 1072–1094. doi: 10.1111/pce.13968

Potter, D. J. (2014). A review of the cultivation and processing of cannabis (*Cannabis sativa* L.) for production of prescription medicines in the UK. *Drug Test. Anal.* 6, 31–38. doi: 10.1002/dta.1531

Potter, D. J., and Duncombe, P. (2012). The effect of electrical lighting power and irradiance on indoor-grown cannabis potency and Yield. *J. Forensic Sci.* 57, 618–622. doi: 10.1111/j.1556-4029.2011.02024.x

Punja, Z. K., Collyer, D., Scott, C., Lung, S., Holmes, J., and Sutton, D. (2019). Pathogens and molds affecting production and quality of *Cannabis sativa* L. *Front. Plant Sci*. 10:1120. doi: 10.3389/fpls.2019.01120

Rodriguez-Morrison, V., Llewellyn, D., and Zheng, Y. (2021). Cannabis yield, potency, and leaf photosynthesis respond differently to increasing light levels in an indoor environment. *Front. Plant Sci.*12:456. doi: 10.3389/fpls.2021.646020

Saloner, A., and Bernstein, N. (2020). Response of medical cannabis (*Cannabis sativa* L.) to nitrogen supply under long photoperiod. *Front. Plant Sci.* 11:572293. doi: 10.3389/fpls.2020.572293

Saloner, A., and Bernstein, N. (2021). Nitrogen supply affects cannabinoid and terpenoid profile in medical cannabis (*Cannabis sativa* L.). *Ind. Crop. Prod.* 167:113516. doi: 10.1016/j.indcrop.2021.113516

Saloner, A., and Bernstein, N. (2022a). Nitrogen source matters: High NH4/NO3 ratio reduces cannabinoids, terpenoids, and yield in medical cannabis. *Front. Plant Sci.* 13, 830224. doi: 10.3389/fpls.2022.830224

Saloner, A., and Bernstein, N. (2022b). Effect of potassium (K) supply on cannabinoids, terpenoids and plant function in medical cannabis. *Agronomy*. 12, 1242. doi: 10.3390/agronomy12051242

Saloner, A., Sacks, M. M., and Bernstein, N. (2019). Response of medical cannabis (*Cannabis sativa* L.) genotypes to K supply under long photoperiod. *Front. Plant Sci.* 10:1369. doi: 10.3389/fpls.2019.01369

Sarma, N. D., Waye, A., Elsohly, M. A., Brown, P. N., Elzinga, S., Johnson, H. E., et al. (2020). Cannabis inflorescence for medical purposes: USP considerations for quality attributes. *J. Nat. Prod.* 83, 1334–1351. doi: 10.1021/acs.jnatprod.9b01200

Semira, N., and Bikila, A. (2018). Review on effect of population density and tuber size on yield components and yield of potato (*Solanum tuberosum* L.). *Afr. J. Plant Sci.* 12, 319–323. doi: 10.5897/AJPS2018.1701

Shiponi, S., and Bernstein, N. (2021a). Phosphorus sensitivity of medical cannabis at the vegetative growth stage: impact on functional phenotyping and the ionome. *Ind. Crop Prod.* 161:113154. doi: 10.1016/j.indcrop.2020.113154

Shiponi, S., and Bernstein, N. (2021b). The highs and lows of P supply in medical cannabis: effects on cannabinoids, the ionome and morpho-physiology. *Front. Plant Sci*. 12:657323. doi: 10.3389/fpls.2021.657323

Shoresh, M., Spivak, M., and Bernstein, N. (2011). Involvement of calcium-mediated effects on ROS metabolism in the regulation of growth improvement under salinity. *Free Radic. Biol. Med.* 51, 1221–1234. doi: 10.1016/j.freeradbiomed.2011.03.036

Singh, S. P., Singh, N. P., and Pandey, R. K. (1992). *Performance of faba bean varieties at different plant densities (Vicia faba)*. Faba Bean Inf. Serv.

Slattery, R. A., Vanloocke, A., Bernacchi, C. J., Zhu, X. G., and Ort, D. R. (2017). Photosynthesis, light use efficiency, and yield of reduced-chlorophyll soybean mutants in field conditions. *Front. Plant Sci.* 8:549. doi: 10.3389/fpls.2017.00549

Weaver, L. M., and Amasino, R. M. (2001). Senescence is induced in individually darkened Arabidopsis leaves, but inhibited in whole darkened plants. *Plant Physiol.* 127, 876–886. doi: 10.1104/pp.010312

Westmoreland, F. M., Kusuma, P., and Bugbee, B. (2021). Cannabis lighting: decreasing blue photon fraction increases yield but efficacy is more important for cost effective production of cannabinoids. *PLoS ONE* 16:e0248988. doi: 10.1371/journal.pone.0248988

Xiao, S., Chen, S. Y., Zhao, L. Q., and Wang, G. (2006). Density effects on plant height growth and inequality in sunflower populations. *J. Integr. Plant Biol.* 48, 513–519. doi: 10.1111/j.1744-7909.2006.00265.x

Yan, J., Xiang, F., Yang, P., Li, X., Zhong, M., He, R., et al. (2020). Overexpression of BnGA2ox2, a rapeseed gibberellin 2-oxidase, causes dwarfism and increased chlorophyll and anthocyanin accumulation in Arabidopsis and rapeseed. *Plant Growth Regul.* 93, 1–13. doi: 10.1007/s10725-020-00665-6

Yang, G. Z., Luo, X. J., Nie, Y. C., and Zhang, X. L. (2014). Effects of plant density on yield and canopy micro environment in hybrid cotton. *J. Integr. Agric.* 13, 2154–2163. doi: 10.1016/S2095-3119(13)60727-3

Yep, B., Gale, N. V., and Zheng, Y. (2020). Aquaponic and hydroponic solutions modulate NaCl-Induced stress in drug-type *Cannabis sativa* L. *Front. Plant Sci.* 11:1169. doi: 10.3389/fpls.2020.01169

Conflict of Interest: The authors declare that the research was conducted in the absence of any commercial or financial relationships that could be construed as a potential conflict of interest.

Publisher's Note: All claims expressed in this article are solely those of the authors and do not necessarily represent those of their affiliated organizations, or those of the publisher, the editors and the reviewers. Any product that may be evaluated in this article, or claim that may be made by its manufacturer, is not guaranteed or endorsed by the publisher.

Advantages of publishing in Frontiers

OPEN ACCESS
Articles are free to read for greatest visibility and readership

FAST PUBLICATION
Around 90 days from submission to decision

HIGH QUALITY PEER-REVIEW
Rigorous, collaborative, and constructive peer-review

TRANSPARENT PEER-REVIEW
Editors and reviewers acknowledged by name on published articles

Frontiers
Avenue du Tribunal-Fédéral 34
1005 Lausanne | Switzerland

Visit us: www.frontiersin.org
Contact us: frontiersin.org/about/contact

REPRODUCIBILITY OF RESEARCH
Support open data and methods to enhance research reproducibility

DIGITAL PUBLISHING
Articles designed for optimal readership across devices

FOLLOW US
@frontiersin

IMPACT METRICS
Advanced article metrics track visibility across digital media

EXTENSIVE PROMOTION
Marketing and promotion of impactful research

LOOP RESEARCH NETWORK
Our network increases your article's readership